

Open Research Online

The Open University's repository of research publications and other research outputs

Geochemical and isotopic characteristics of palaeo-hydrothermal fluids related to granite magmatism, S W England

Thesis

How to cite:

Miller, Martin Fitzhardinge (1994). Geochemical and isotopic characteristics of palaeo-hydrothermal fluids related to granite magmatism, S W England. PhD thesis The Open University.

For guidance on citations see [FAQs](#).

© 1994 The Author

Version: Version of Record

Copyright and Moral Rights for the articles on this site are retained by the individual authors and/or other copyright owners. For more information on Open Research Online's data [policy](#) on reuse of materials please consult the policies page.

oro.open.ac.uk

DX181452
UNRESTRICTED

Geochemical and isotopic characteristics of palæo-hydrothermal
fluids related to granite magmatism, S W England

by

Martin Fitzhardinge Miller
B.Sc. (Hons.) *Bristol*

A thesis submitted in partial fulfilment of the requirements for
the degree of Doctor of Philosophy

Author number: M7023576
Date of submission: 16 May 1994
Date of award: 5 August 1994

Department of Earth Sciences,
The Open University

May 1994

Abstract

An assessment of stepped heating procedures for the extraction and isolation of carbonaceous species from fluid inclusions resulted in the development of low-blank procedures which permitted $\delta^{13}\text{C}$ characterisation of palaeofluid CO_2 (down to nanomole quantities) with an accuracy approaching that of the corresponding analytical precision. Similar procedures were successfully applied to the $\delta^{15}\text{N}$ measurement of palaeofluid nitrogen at the sub-nanomole level.

An investigation into the origin of fluids which characterised the earliest episodes of palaeohydrothermal activity associated with the granites of SW England indicates that the abundance of trace carbon species (CO_2 , CH_4) and nitrogen in the fluids was correlated with the metasedimentary contribution to the respective granite source. Furthermore, $\delta^{15}\text{N}$ and $\delta^{13}\text{C}$ data (obtained on fluid components and local Palaeozoic metasediments, in conjunction with published $\delta^{15}\text{N}$ values of Cornubian granites), indicate that carbon and nitrogen in the hydrothermal systems were derived from the granite magmas.

The chemical composition of the early hydrothermal fluids, together with geochemical and isotopic constraints from the characterisation of Palaeozoic metasedimentary country rocks, support the view that the fluids were genetically associated with the granites. Fluid interaction with the local metasedimentary rocks at a high level crustal appears to have been very limited. The incorporation of sedimentary matter into granitic protoliths during anatexis, with subsequent transfer to an exsolved hydrous phase during pluton cooling, is the most probable route by which palaeofluid solutes entered the early hydrothermal systems.

Hydrogen stable isotope data, measured on the extracted palaeowaters, indicate that meteoric water was not a significant component of early hydrothermal systems associated with either the Dartmoor granite or the nearby Hemerdon Ball intrusive, if sub-solidus isotopic exchange was significant. In contrast, comparable data from early fluids associated with other component intrusives of the batholith (as characterised by $\text{W} \pm \text{Sn}$ oxide paragenesis) are consistent with the progressive dilution of a magmatic-hydrothermal component by local groundwaters.

Acknowledgements

It is a truism that little if any progress is achieved in science (or in most other fields of academic endeavour) in the absence of a supportive infrastructure, both in a material and intellectual sense. With respect to the latter in particular, I owe a debt of gratitude to many colleagues, both personally and professionally, who have contributed in various ways during the course of this work.

First and foremost, my thanks are due to Professor Colin Pillinger FRS for permitting someone outside of the extraterrestrial isotope cosmochemistry research community to participate in the activities of the OU Planetary Sciences Unit. And for a project involving terrestrial palæofluids. I hope that the ends have justified the means. It has indeed been both a pleasure and a privilege to have experienced life in a laboratory at the scientific 'front-end', and my thanks are extended to past and present members of the PSU who contributed to the stimulating working environment during my irregular visits over the period 1986-1990. In particular, appreciation is expressed to Dr Monica Grady for tuition and assistance with laboratory facilities during the early stages of this study. Dr Ian Wright is thanked for numerous lengthy discourses on a variety of subjects, largely of a geopolitical nature, and for kindly providing a thorough and constructive review of an earlier draft of the carbon isotope work (Chapter 3). The nitrogen isotope data (Chapter 4) could not have been obtained without the laboratory facilities and techniques developed by Dr Stuart Boyd, who also contributed training, advice and useful discussions, as well as favourable comments on a draft of Chapter 4.

This work was undertaken whilst the author was on the staff of the British Geological Survey (a component body of the Natural Environment Research Council) and I am grateful to the many colleagues whose assistance contributed towards the completion of the project. Dr Tom Shepherd deserves special mention for introducing the author to the study of ancient hydrothermal fluids in the first place, for supporting the research proposal, and for general project supervision. Truly, it has been a long road. Dr Richard Scrivener kindly organised and led several excursions into the field on the author's behalf for sampling purposes; supplied numerous specimens from collections held at the Exeter office of the British Geological Survey; reviewed a draft of Chapter 5, and contributed greatly to my understanding of the regional geology.

An especially large debt of gratitude is owed to Dr Baruch Spiro, for generosity in providing access to the stable isotope facilities of the NERC Isotope Geosciences Laboratory on request; for invaluable advice and encouragement over the years with regard to the direction of the research, and for thorough and constructive reviews of several of the draft chapters.

Peter Greenwood and Dr Mike Fowler are thanked for comprehensive training in the use of silicate fluorination facilities, for congenial company during long days in the fluorination lab, and for a seemingly inexhaustible supply of anecdotes. Fiona Darbyshire supervised the strontium isotope analytical work reported in Chapter 6 and kindly provided access to unpublished data. Dr Jane Evans reviewed sections of Chapter 6 and suggested several helpful improvements to the presentation. Dr Adrian Boyce (SURRC) generously measured the oxygen stable isotopic compositions of a batch of quartz samples on the author's behalf, during the period in which the NERC silicate fluorination facility was unavailable because of laboratory relocation out of London.

The sampling of Devonian metasediments from a traverse across the Dartmoor granite aureole (Chapter 6) was arranged and supervised by Tony Goode (BGS Exeter), whose expertise and local knowledge enabled a comprehensive suite of suitable material to be collected. Don Bradley (BGS) and Dr Tim Heaton (NERC Isotope Geosciences Lab) advised on ammonium extraction from the metasedimentary rocks and subsequent $\delta^{15}\text{N}$ measurements, respectively.

Fluid inclusion crush-leach analyses reported in Chapter 5 were undertaken at the University of Leeds. The procedures were developed largely by Dr David Banks, who provided training to the author and also performed many of the analyses reported herein, besides reading through a draft of the resulting text. I am especially indebted for the patience displayed whilst manuscript preparation has awaited completion of the present work. Also at the University of Leeds, Dr Simon Bottrell, a source of much scientific wisdom on a wide range of subjects over the years, kindly read and indicated approval of Chapter 4.

Dr John Chesley (currently at the University of Arizona) contributed with humour and enthusiasm to much discussion about the Cornubian batholith and associated hydrothermal phenomena, and was responsible for a considerable proportion of my e-mail correspondence over recent years. Thanks are also due for advice and assistance in the field during June '89.

Throughout the duration of the project, funding was provided in part by the British Geological Survey, for which I am grateful.

Last, but by no means least, without the encouragement, good humour and unstinting support of my spouse and soulmate, Dr Helen Glenny, who shouldered an unreasonable share of parental responsibility during what seemed like an interminable period of writing-up, this work would probably never have been completed. To her I owe my heartfelt thanks.

Geochemical and isotopic characteristics of palæo-hydrothermal fluids related to granite magmatism, SW England

Table of contents

Title page	i
Abstract	ii
Acknowledgements	iii
Contents	v
List of Figures	xii
List of Tables	xvi

Chapter 1 General Introduction

1.1	The Cornubian batholith, S W England	1
1.1.1	Geological setting	1
1.1.2	Stages of hydrothermal mineralisation	4
1.2	Fluid inclusions as tracers of palæo-hydrothermal processes	6
1.2.1	Overview	6
1.2.2	The chemical composition of fluid inclusions: representative of entrapment composition?	7
1.2.3	Modelling of chemical equilibria and redox conditions	9
1.3	Stable isotope fractionations: terminology	12
1.4	Thesis structure	13

Chapter 2 Hydrogen and oxygen stable isotope constraints on the source of palæo-waters associated with protracted hydrothermal activity, SW England

2.1	Synopsis	15
2.2	Introduction	15
2.2.1	Hydrogen and oxygen isotope natural abundances	15
2.2.2	The combined δD and $\delta^{18}O$ approach to the characterisation of natural waters: application to palæofluids	17
2.2.3	Modelling of water-rock interaction	21
2.2.4	Hydrothermal fluids associated with mineralisation in the Cornubian province: previous investigations of the stable isotope hydrology	22
2.2.5	Palæogeographic considerations, S W England	24
2.2.5.1	Palæolatitude	24
2.2.5.2	Palæoaltitude	25

2.2.6	Experimental considerations	25
2.2.6.1	D/H measurements on natural waters	25
2.2.6.1.1	Water reduction methods	26
2.2.6.2	$^{18}\text{O}/^{16}\text{O}$ determinations of fluid inclusion water	27
2.2.6.3	The effect of dissolved electrolytes on the oxygen and hydrogen stable isotope activities of water	28
2.2.7	Sampling localities	28
2.3	Research objectives	29
2.4	Experimental	30
2.4.1	Sample preparation	30
2.4.2	D/H analysis of fluid inclusion waters	30
2.4.3	Quartz $^{18}\text{O}/^{16}\text{O}$ determinations	33
2.5	Results	34
2.6	Discussion	38
2.6.1	Problems to be addressed	38
2.6.2	The isotopic composition of magmatic water during batholith evolution: implications for the source of early-stage hydrothermal fluids, S W England	39
2.6.2.1.	The effect of fluid boiling on the isotopic characteristics of the waters	40
2.6.2.2	pH effects	41
2.6.3	Pegmatitic and early mineralising fluids of the Dartmoor granite	42
2.6.4	Early-stage fluids characterised by $\text{W}\pm\text{Sn}$ oxide association	43
2.6.5	'Main-stage' (sulphide-associated) hydrothermal fluids	45
2.6.6	Low temperature, 'cross-course' fluids	45
2.7	Summary and conclusions	46
Chapter 3	The occurrence and stable isotope characterisation of carbon in palæo-hydrothermal fluids, S W England	
3.1	Synopsis	49
3.2	Introduction	50
3.2.1	Carbon reservoirs and geochemical cycles	50
3.2.2	Stable isotopic characteristics of near-surface carbon reservoirs	51
3.2.3	Carbon in the mantle: isotopic characterisation	52
3.2.4	Carbon abundance and stable isotope ratio measurements: experimental problems highlighted by oceanic basalt analyses	53
3.2.5	Carbonaceous matter - an indigenous component of magmatic rocks?	55
3.2.6	Carbon solubility and speciation in silicate melts	56

3.2.7	The speciation of oxidised carbon in hydrothermal fluids	57
3.2.8	The occurrence and sources of methane in crustal fluids: stable isotope considerations	57
3.2.9	CO ₂ -CH ₄ carbon isotope exchange equilibria in hydrothermal systems: an unresolved problem	60
3.2.10	Carbonaceous volatiles in palæo-hydrothermal fluids associated with the Cornubian batholith, S W England	62
3.3	Research objectives	62
3.4	Experimental	63
3.4.1	The extraction of palæofluid inclusions for carbon stable isotope ratio analysis	63
3.4.1.1	Fluid extraction by crushing <i>in vacuo</i>	64
3.4.1.2	Fluid extraction by thermal decrepitation <i>in vacuo</i>	64
3.4.2	Palæofluid δ ¹³ C measurements: previous studies	65
3.4.3	Preliminary δ ¹³ C _{CO₂} results from fluid inclusions (this study)	67
3.4.4	Carbon stable isotope ratio analysis of small samples	67
3.4.4.1	Contamination removal: the application of stepped heating	67
3.4.4.2	Static vacuum mass spectrometry: application to carbon stable isotope ratio analysis	70
3.4.4.3	Sample preparation for the measurement of carbon stable isotope ratios at the nanomole level by static vacuum mass spectrometry:	73
3.4.4.3.1	The protocol of Carr <i>et al.</i> (1986)	73
3.4.4.3.2	The protocol of Ash <i>et al.</i> (1990)	77
3.4.5	Dynamic vacuum mass spectrometry and associated sample preparation lines used in the present study	81
3.4.6	The development of an experimental protocol appropriate to fluid inclusion extraction for small sample δ ¹³ C analysis	83
3.4.6.1	Initially-adopted procedures for the removal of 'contaminant' carbon	83
3.4.6.2	Preliminary δ ¹³ C results using static vacuum mass spectrometry	84
3.4.6.3	Investigation strategy: towards an 'optimised' stepped heating procedure	92
3.4.6.4	An assessment of procedures based on Swart <i>et al.</i> (1983) as applied to quartz grains used for fluid inclusion δ ¹³ C analysis	93
3.4.6.5	The experimental protocol of Jackson <i>et al.</i> (1988b)	108
3.4.7	Application of the optimised stepped heating procedure to δ ¹³ C analysis of inclusion CO ₂ by static vacuum mass spectrometry	110
3.4.7.1	Experimental details	110
3.4.7.2	Results: comparison with data obtained by 'conventional' mass spectrometry	112

3.4.8	Carbon stable isotope analysis of fluid inclusion methane	117
3.4.8.1	Methane oxidation catalyst	117
3.4.8.2	Experimental protocol adopted for $\delta^{13}\text{C}$ analysis of fluid inclusion methane	117
3.5	Results of the palaeofluid $\delta^{13}\text{C}$ analyses	119
3.5.1	Hydrothermal fluids characterised by W \pm Sn oxide association	119
3.5.2	'Transitional' (pegmatitic - pneumatolytic) fluids	119
3.5.3	The Dartmoor hydrothermal system	125
3.5.4	Comparative data: examples from NW England and S China	129
3.5.4.1	Carrock Fell (NW England): wolframite-associated quartz veins	129
3.5.4.2	S China: Transitional stages of hydrothermal evolution in the Yanshanian granites	132
3.6	Discussion	137
3.6.1	Salient features of the Cornubian palaeofluid carbon data	137
3.6.2	CO ₂ in the Cornubian hydrothermal system: a primary magmatic component?	137
3.6.3	Controls on carbon speciation and ^{13}C distribution in the Cornubian palaeofluids	138
3.6.3.1	Carbon sources, fluxes and redox reactions	138
3.6.3.2	Carbon stable isotope systematics	141
3.7	Summary and conclusions	145
3.8	Suggestions for further research	147

Chapter 4 Nitrogen stable isotope characterisation of palaeohydrothermal fluids, SW England

4.1	Synopsis	149
4.2	Introduction	149
4.2.1	Nitrogen stable isotope abundances the terrestrial environment	149
4.2.2	Biological processes affecting the distribution of nitrogen isotopes	152
4.2.3	Kinetic isotope effects	153
4.2.4	The oceanic environment	153
4.2.5	Diagenesis of nitrogen in sediments	153
4.2.6	Nitrogen stable isotope distributions in igneous rocks	155
4.2.7	Atmospheric nitrogen	156
4.2.8	Nitrogen stable isotope distributions in metamorphic rocks	156
4.2.9	Ammonium in igneous and sedimentary rocks	157
4.2.10	Nitrogen in crustal fluids - the fluid inclusion evidence	159
4.2.11	Nitrogen stable isotope ratio analysis of crustal fluids	161

4.2.12	The speciation of nitrogen in hydrothermal fluids	162
4.3	Objectives of the research	165
4.4	Location of samples	166
4.5	Experimental	168
4.5.1	Nitrogen stable isotope ratio analysis - from micrograms to nanograms	168
4.5.2	The development of an appropriate experimental protocol	170
4.6	Results of the palæofluid $\delta^{15}\text{N}$ analyses	180
4.7	$\delta^{15}\text{N}$ of the Cornubian granites and metasedimentary rocks	184
4.7.1	The granites	184
4.7.2	The Palaeozoic metasediments	185
4.8	Discussion	185
4.8.1	Fluid inclusion nitrogen stable isotope data	185
4.8.2	Ammonium contents and the 'S'-type characteristics of the S W England granites	186
4.8.3	Palæo-atmospheric nitrogen in the fluid inclusions? Argon isotope evidence	188
4.8.4	Sources of the palæofluid nitrogen - isotopic considerations	189
4.8.5	The oxidation of ammonia by C^0 and C^{IV} components - potential mechanisms for the release of nitrogen to the fluid phase	191
4.9	Summary and conclusions	195
4.10	Suggestions for further work	197
Chapter 5	The chemical composition of early mineralising fluids of the Cornubian batholith	
5.1	Synopsis	198
5.2	Introduction	199
5.2.1	Procedures for the extraction and electrolyte analysis of aqueous fluid inclusions	199
5.2.2	The chemical composition of granite-hosted thermal groundwaters in S W England: evidence for (low-temperature) hydrothermal alteration of the granite?	201
5.2.3	Hydrothermal alteration of the granite at higher temperature: evidence from model experiments	202
5.2.4	The Dartmoor granite: magmatic activity and early hydrothermal alteration	203
5.2.4.1.	Chronology of magmatic activity	203
5.2.4.2.	Paragenetic stages of hydrothermal mineralisation	204
5.2.5	Sampling localities	205

5.3	Research objectives	206
5.4	Experimental	206
5.5	Results - fluid inclusion leachate analyses	207
5.5.1	Dartmoor hydrothermal quartz	207
5.5.2	Hydrothermal quartz associated with W±Sn oxide mineralisation	216
5.6	Discussion	226
5.6.1	Hydrothermal fluids associated with early mineralisation of the Dartmoor granite.	226
5.6.1.1	Chemical characteristics: salient features	226
5.6.1.2	Cation ratio geothermometry and fluid-rock interaction	228
5.6.1.3	Halogen ion ratios: evidence for a magmatic origin?	229
5.6.1.4	Sr and Pb isotopes in the hydrothermal fluids hosted by the Dartmoor granite	235
5.6.2	Chemical characteristics of fluids associated with W±Sn oxide mineralisation of the Cornubian batholith	235
5.6.2.1	Ionic charge imbalance of leachates: possible explanations	235
5.6.2.2	Comparative overview: constraints on the origins of component elements	236
5.6.2.3	Palaeofluid Pb concentrations at Hemerdon: comparison with an earlier study	241
5.7	Summary and conclusions	242
5.8	Suggestions for further research	245
Chapter 6	Palaeozoic metasediments of SW England: geochemical and isotopic constraints on the effects of granite emplacement. An exploratory study, with reference to the Dartmoor granite	
6.1	Synopsis	248
6.2	Research objectives	249
6.3	Salient features of the regional metasedimentary rocks, with reference to the thermal aureole of the Dartmoor granite	249
6.3.1	General observations	249
6.3.2	Kate Brook Slate	250
6.3.3	Crackington Formation shales	251
6.4	An investigation of selected characteristics of metasedimentary rocks sampled across the thermal aureole of the Dartmoor granite	251
6.4.1	Samples used in the present study	251
6.4.2	Chemical compositions of the metasedimentary rocks	252
6.4.3	Strontium, carbon and nitrogen isotopic behaviour during contact metamorphism of metasediments by the Dartmoor granite	258

6.4.3.1	Strontium isotope studies	258
6.4.3.1.1	Introduction: Sr isotope systematics	258
6.4.3.1.2	Experimental	260
6.4.3.1.3	Results and discussion	260
6.4.3.2	Carbon stable isotope compositions of the metasediments	267
6.4.3.2.1	Scope of the investigation	267
6.4.3.2.2	Experimental	268
	6.4.3.2.2.1 Carbonate analysis	268
	6.4.3.2.2.2 'Organic' carbon analysis	268
6.4.3.2.3	Results and discussion	269
6.4.3.3	Nitrogen stable isotope compositions of the metasediments	273
6.4.3.3.1	Scope of the investigation	273
6.4.3.3.2	Experimental	273
6.4.3.3.3	Results and discussion	275
6.5	Summary and conclusions	278
Chapter 7	Synthesis and concluding remarks	
7.1	Overview	281
7.2	Experimental procedures	281
7.3	Principal findings of the research	282
7.4	Concluding remarks	286
Appendices		
A	Sample catalogue	289
B	Stepped heating data: Carbon yields and $\delta^{13}\text{C}$ results as a function of the analytical protocol	295
C	Analytical protocol for the extraction, purification and stable isotope ratio analysis by static vacuum mass spectrometry, of fluid inclusion nitrogen	301
References		302
Addenda		333

List of Figures

Chapter 1

- 1.1 Simplified map of the geology of S W England, illustrating the setting of the Cornubian batholith 2
- 1.2 Redox field (as $\log_{10} f_{O_2}$ versus temperature) characteristic of hydrothermal fluids associated with Sn-W oxide mineralisation, together with the graphite stability curve 8
- 1.3 Temperature variation (at constant pressure) of mole fractions X_i of the principal fluid components resulting from reaction between equimolar quantities of water and graphite at thermodynamic equilibrium 11

Chapter 2

- 2.1 Plot of δD versus $\delta^{18}O$ showing meteoric waters, the field for ocean waters, and generalised fields for magmatic and metamorphic waters 18
- 2.2 Schematic diagram of the vacuum line used for the extraction and isolation of fluid inclusion water (together with carbon dioxide and methane), for stable isotope ratio analysis 32
- 2.3 δD versus $\delta^{18}O$ characteristics of quartz-hosted palaeo-hydrothermal fluids, S W England 37

Chapter 3

- 3.1 $\delta^{13}C$ and δD characteristics of some naturally-occurring methanes 58
- 3.2 The variation of combustion temperature as a function of atomic H/C ratio of the kerogen component, for a variety of sedimentary rocks 68
- 3.3 Typical yield profiles of CO_2 obtaining by stepped heating of kerogen, amorphous carbon, calcite and graphite in excess of pure oxygen 69
- 3.4 Schematic diagram illustrating the difference in principle between static vacuum and dynamically pumped mass spectrometer configurations as used for carbon stable isotope ratio analysis 71
- 3.5 Schematic diagram of the extraction line used for stepped combustion or pyrolysis, in conjunction with carbon stable isotope ratio analysis by static vacuum mass spectrometry, as described by Carr *et al.* (1986) 74
- 3.6 The variable volume aliquotter as described by Carr *et al.* (1986), illustrating also the construction of J Young[®] type 'PSU' valves 75
- 3.7 The typical yield and isotopic composition of carbon blank released during a stepped combustion experiment using the sample preparation protocol of Carr *et al.* (1986) 76

3.8	The sample extraction and combustion section described by Ash <i>et al.</i> (1990), substituting for that of Carr <i>et al.</i> (1986) in the gas preparation system used in conjunction with carbon stable isotope ratio analysis at the nanomole level	78
3.9	Stability fields of copper and copper oxides as a function of temperature and oxygen partial pressure	79
3.10	Schematic diagram of the extraction line used for stepped combustion/pyrolysis in conjunction with carbon stable isotope ratio analysis by VG [®] SIRA 24 mass spectrometer	82
3.11	Preliminary results obtained for stepped heating release and isolation of palæofluid carbon $\Sigma C_{(CO_2, CH_4)}$ from hydrothermal fluid inclusions in quartz, with ¹³ C/ ¹² C ratio determination at the nanomole level by static vacuum mass spectrometry	85
3.12	Stepped heating release of palæofluid carbon $\Sigma C_{(CO_2, CH_4)}$ from hydrothermal fluid inclusions in quartz single grain (~20mg) replicates (sample HEM-80-1), with ¹³ C/ ¹² C ratio determination by static vacuum mass spectrometry using the protocol of Carr <i>et al.</i> (1986)	88
3.13	Variation in measured yield and $\delta^{13}C$ of released carbon-bearing volatiles as a function of quartz sample size, using stepped heating in excess of pure oxygen to 350°C, followed by stepped heating <i>in vacuo</i> to 600°C. Released gases exposed to Pt foil catalyst at ~1050°C during extraction procedure	94
3.14	Carbon yield and $\delta^{13}C$ results of 'high resolution' stepped heating of sample HEM-80-1 in the absence of supplied oxygen and with the on-line Pt catalyst at room temperature	96
3.15	Carbonaceous volatiles released from fluid inclusion-bearing quartz: further examples of the $\delta^{13}C$ discrepancy between measurements using combined stepped 'combustion' and 'pyrolysis' in the presence of a Pt catalyst at ~1050°C, <i>versus</i> data obtained by stepped heating <i>in vacuo</i> , with the Pt catalyst at room temperature	97
3.16	The concentration of components A, B and C as a function of time in series first-order reactions, for a typical case where $k_1=0.25\text{sec}^{-1}$ and $k_2=0.025\text{sec}^{-1}$	102
3.17	Carbon yield and $\delta^{13}C$ results of stepped heating of sample SW-84-27, in the absence of supplied oxygen and with the Pt catalyst at room temperature	104
3.18	The effect of hydrogen sulphide as a contaminant species during stable isotope ratio analysis of CO ₂ by VG [®] SIRA 24 mass spectrometer	106
3.19	Carbon yield and $\delta^{13}C$ results of stepped heating of incipient charnockite quartz sample TR10D, as reported by Jackson <i>et al.</i> (1988 a)	109

3.20	Yield profiles, together with $\delta^{13}\text{C}$ as measured by static vacuum mass spectrometry, of CO_2 released by stepped heating of quartz samples using the optimised extraction procedure	113
3.21	Yield profile, together with $\delta^{13}\text{C}$ as measured by static vacuum mass spectrometry, of CO_2 released by optimised stepped heating of quartz sample CD-88-1	115
3.22	Simplified map of S W England, indicating the location of samples included in the investigation of palaeofluid carbon species associated with early-stage granite-related hydrothermal processes	120
3.23	The yield and $\delta^{13}\text{C}$ of carbon dioxide extracted from quartz associated with early-stage hydrothermal activity, S W England	123
3.24	Carbon yield and $\delta^{13}\text{C}$ values of carbon dioxide released by stepped heating of quartz sample SW-88-3 (South Crofty mine) in the absence of supplied oxygen and with the on-line Pt foil at room temperature	124
3.25	Yield profiles, together with $\delta^{13}\text{C}$ as measured by static vacuum mass spectrometry, of CO_2 released during stepped heating of quartz associated with hydrothermal mineralisation of the Dartmoor granite	126
3.26	Yield profiles and corresponding $\delta^{13}\text{C}$ values of CO_2 released during stepped heating of hydrothermal vein quartz, Carrock Fell	131
3.27	Yield profiles and $\delta^{13}\text{C}$ of CO_2 released by stepped heating of quartz associated with W-Mo-bearing transitional vein systems in the Yanshanian granites of S China	134
3.28	Carbon stable isotope ratios in hydrothermal palaeofluid methane <i>versus</i> carbon dioxide, S W England and Carrock Fell	142

Chapter 4

4.1	Fractionation factors (α) for equilibria involving the exchange of nitrogen	150
4.2	Aqueous redox equilibria involving stable nitrogen species at 25°C, 1 atm.	163
4.3	The predicted speciation of nitrogen in hydrothermal fluids	164
4.4	Simplified map of S W England, indicating the location of samples included in the investigation of palaeofluid nitrogen associated with early-stage hydrothermal mineralisation in the region	167
4.5	Schematic diagram of the vacuum line used for thermal extraction (incremental heating) and subsequent purification of fluid inclusion nitrogen for isotope ratio analysis by static vacuum mass spectrometry	172
4.6	Procedural nitrogen blank during stepped thermal extraction	173
4.7	Equilibrium compositions predicted by thermodynamic modelling for initial reactants N_2 and O_2 at 850 and 1150°C, pressure 10^{-2} atm., as a function of initial O_2/N_2 mole ratio	176

4.8	Stepwise thermal release of nitrogen <i>in vacuo</i> from quartz sample HEM-80-1	178
4.9	Nitrogen yield and $\delta^{15}\text{N}$ data for S W England palæo-hydrothermal fluids extracted from quartz	182
4.10	Predicted equilibrium compositions (mole fractions) resulting from the reaction between $8\text{NH}_3 + 3\text{CO}_2$ under a range of temperatures and pressures corresponding to crustal environments	193

Chapter 5

5.1	Ca/Na and K/Na molar ratios: comparison between palæofluids of the Dartmoor hydrothermal system and fluids characterised by association with early W±Sn oxide mineralisation in S W England	227
5.2	Br/Cl and I/Cl molar ratios: Dartmoor pegmatitic and mineralising palæofluids	230
5.3	Br/Cl and I/Cl molar ratios: comparison between palæofluids of the Dartmoor hydrothermal system and fluids characterised by association with early W±Sn oxide mineralisation in S W England	231
5.4	Br/Cl and I/Cl molar ratios in volcanic fumarole condensates: comparison with early hydrothermal palæofluids, S W England	232

Chapter 6

6.1	$^{87}\text{Sr}/^{86}\text{Sr}$ and $^{87}\text{Rb}/^{86}\text{Rb}$ ratios in Kate Brook Slate sampled across the thermal aureole (south-west) of the Dartmoor granite	263
6.2	$^{87}\text{Sr}/^{86}\text{Sr}$ and $^{87}\text{Rb}/^{86}\text{Rb}$ ratios in Crackington Formation rocks samples across the thermal aureole (north-east) of the Dartmoor granite	264
6.3	$^{87}\text{Sr}/^{86}\text{Sr}$ and $^{87}\text{Rb}/^{86}\text{Rb}$ ratios from Figures 6.1 and 6.2, back-corrected to an age of 280Ma on the basis of closed-system behaviour	265
6.4	Carbon content and corresponding stable isotope variations of the 'organic' component of metasedimentary rocks from the vicinity of the Dartmoor granite	271

List of Tables

Chapter 2

- 2.1 Results of δD and $\delta^{18}O$ analyses, quartz-hosted palæo-hydrothermal fluids, S W England 35

Chapter 3

- 3.1 Preliminary results obtained for carbon stable isotope ratio analysis of CO_2 extracted from fluid inclusions in vein quartz, Carrock Fell and Hemerdon, by thermal decrepitation *in vacuo* after initial outgassing 66
- 3.2 The distribution of carbon in gaseous pyrolysis products resulting from *in vacuo* heating to 440°C of various biological materials 100
- 3.3 Comparison of carbon procedural blank yields (± 0.2 ngC) resulting from stepped heating in the presence/absence of supplied oxygen, using the extraction system described by Ash *et al.* (1990) 111
- 3.4 The yield and $\delta^{13}C$ values of fluid inclusion carbon-bearing species extracted from quartz associated with early hydrothermal mineralisation and 'transitional' processes, S W England 121
- 3.5 Carbon yield and isotopic composition of fluid inclusion components, Carrock Fell vein quartz 130
- 3.6 Carbon yield and $\delta^{13}C$ data of fluid inclusion CO_2 extracted from quartz samples associated with wolframite-molybdenite vein mineralisation hosted by the Yanshanian granites of southern China 133
- 3.7 Comparison of carbon isotope equilibrium fractionation factors $\alpha_{CO_2-CH_4}$ compatible with Rayleigh distillation *versus* batch equilibration models for closed-system CO_2 reduction as the origin of fluid inclusion methane, measured CO_2/CH_4 ratios and associated ^{13}C distributions 143

Chapter 4

- 4.1 Nitrogen stable isotope ratios in some common components of the oceanic reservoir 154
- 4.2 Nitrogen yield and $\delta^{15}N$ data for S W England quartz samples 181
- 4.3 Nitrogen yield and $\delta^{15}N$ data for Carrock Fell quartz samples 183

Chapter 5

- 5.1 Dartmoor hydrothermal quartz: fluid inclusion leachate data 209
- 5.2 Estimated concentration limits of electrolytes in quartz-hosted aqueous inclusion fluids associated with hydrothermal mineralisation of the Dartmoor granite 212
- 5.3 S W England quartz samples associated with W±Sn oxide mineralisation: fluid inclusion leachate data 219

5.4	Estimated concentration limits of electrolytes in quartz-hosted aqueous inclusion fluids associated with hydrothermal W±Sn oxide mineralisation: Hemerdon	221
5.5	Estimated concentration limits of electrolytes in quartz-hosted aqueous inclusion fluids associated with hydrothermal W±Sn oxide mineralisation: Cligga Head, South Crofty and minor occurrences in the Gunnislake-Hingston Down area	223
5.6	Leachate analysis of quartz associated with W±Sn oxide, Castle-an-Dinas mine (St. Austell district)	225
5.7	Fluid inclusion leachate analysis, as reported by Bottrell and Yardley (1988), of a granite-hosted topaz-quartz-tourmaline rock from St. Mewan's Beacon, St. Austell district	243
Chapter 6		
6.1	X-ray fluorescence analyses of metasedimentary rocks from S W England	253
6.2	C, N and S analyses of metasedimentary rock samples from S W England	257
6.3	Rubidium and strontium concentrations, together with ⁸⁷ Sr/ ⁸⁶ Sr and ⁸⁷ Rb/ ⁸⁶ Rb isotope ratios, in metasedimentary rocks from S W England	261
6.4	Metasedimentary rocks from S W England: ⁸⁷ Sr/ ⁸⁶ Sr isotopic ratios back-corrected to an age of 280Ma, assuming closed-system behaviour	262
6.5	Carbon content and corresponding stable isotopic compositions of metasedimentary rocks from S W England	270
6.6	'Extractable' ammonium contents of metasedimentary rocks from the vicinity of the Dartmoor granite	276
6.7	Nitrogen stable isotopic composition of 'extractable' ammonium in metasedimentary rocks sampled across the thermal aureole of the Dartmoor granite	277

Chapter 1

General Introduction

1.1 The Cornubian batholith, SW England

1.1.1 Geological setting

The granites of SW England and their associated mineralisation are the subject of an extensive literature, as reviewed by Stone and Exley (1985) and summarised in the bibliography of Halls *et al.* (1985). More recent studies of relevance to the present work include those of Darbyshire and Shepherd (1985, 1987, 1994), Leat *et al.* (1987), Hall (1988, 1990), Willis-Richards and Jackson (1989), Lin (1989), Jackson *et al.* (1989), Boyd *et al.* (1993), Chesley *et al.* (1993) and Chen *et al.* (1993). Five major granite masses outcrop in the province, together with several smaller intrusions, emplaced into upper Palaeozoic metasedimentary and metavolcanic rocks. The sedimentary succession is of Devonian and Carboniferous age and was subjected to low-grade (generally sub-greenschist) regional metamorphism and folding prior to granite intrusion. The basement on which the sediments were deposited was inferred by Hampton and Taylor (1983) to be of late Proterozoic age (~800Ma) with an upper limit of 1200Ma; recent work suggests that it may be considerably older (Darbyshire and Shepherd, 1994).

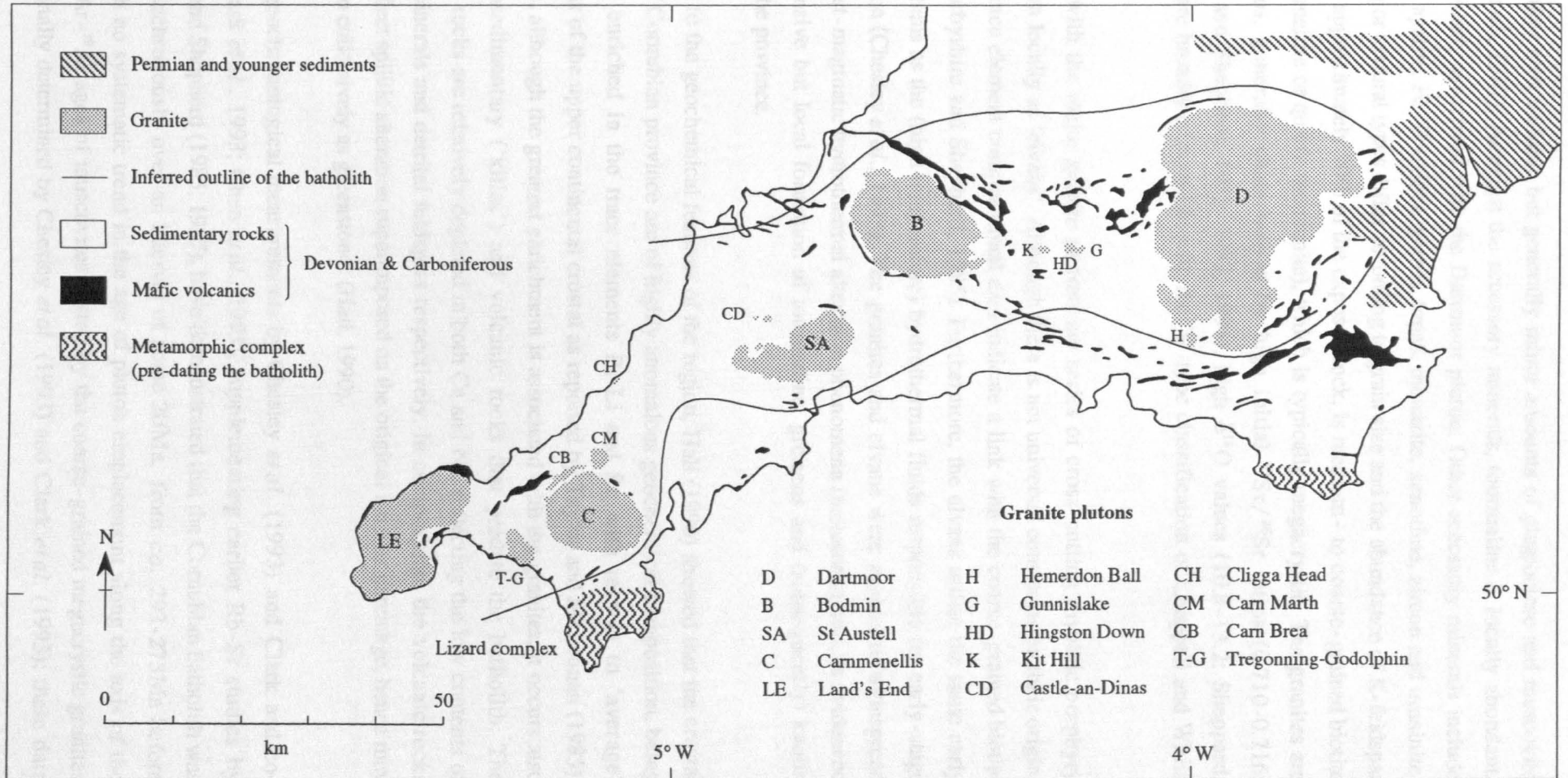
Geophysical data (Bott *et al.*, 1958) indicate that the granites are linked at depth, being the surface expression of a batholith which extends from the eastern contacts of the Dartmoor pluton to beyond the Isles of Scilly (Figure 1.1). On this basis, the batholith is some 250km in length and 40-60km wide, with a thickness that reduces from ~20km in the east to ~10km beneath the Isles of Scilly (Brooks *et al.*, 1984). Tectonically, the Cornubian province lies on the northern edge of the Hercynian (Variscan) orogenic belt; the batholith represents the most voluminous igneous manifestation of the Hercynian orogeny in the British Isles.

The batholith hosts extensive hydrothermal mineralisation and, as such, has provided a stimulus for the development of theories of granite emplacement and of the relation between granites and associated hydrothermal fluids. Despite detailed isotopic investigations during recent years, however, the origin of the granites is still not well understood (Darbyshire and Shepherd, 1994), nor is there a general consensus on the source and timing of the major episodes of hydrothermal activity in the region (Chesley *et al.*, 1993; Chen *et al.*, 1993).

With the exception of certain lithium-rich varieties, notably associated with the St Austell pluton, the Cornubian granites at outcrop consist predominantly of K-feldspar, quartz and

Figure 1.1

Simplified map of the geology of S W England, illustrating the setting of the Cornubian batholith.
 (Adapted from Hall, 1990, and Chesley *et al.*, 1993)



biotite, together with variable but generally minor amounts of plagioclase and muscovite (*e.g.* Leat *et al.*, 1987). Amongst the accessory minerals, tourmaline is locally abundant, being particularly associated with the Dartmoor pluton. Other accessory minerals include amphiboles, apatite, Fe-Ti oxides, garnet, topaz, monazite, xenotime, zircon and uraninite. Whereas major textural types differ according to grain size and the abundance of K-feldspar megacrysts, approximately 90% of the exposed rock, is medium- to coarse-grained biotite granite (adamellite or quartz monzonite), which is typically megacrystic. The granites are peraluminous, generally characterised by high initial $^{87}\text{Sr}/^{86}\text{Sr}$ ratios (0.710-0.716; Darbyshire and Shepherd, 1985, 1987, 1994), high $\delta^{18}\text{O}$ values (10.8-13.2; Sheppard, 1977), and are broadly compatible with the 'S'-type classification of Chappell and White (1974).

Associated with the major granite plutons are series of cross-cutting rhyolitic porphyry dykes, known locally as 'elvans'. Although there is not universal consensus on their origin, minor and trace element compositional data indicate a link with the coarse-grained biotite granites (Darbyshire and Shepherd, 1985). Furthermore, the elvans utilise the same early fracture systems as the (high temperature) hydrothermal fluids responsible for early-stage mineralisation (Chesley *et al.*, 1993). The granites and elvans were subject to widespread late- and post-magmatic hydrothermal alteration phenomena (metasomatism), as evidenced by the extensive but local formation of tourmaline, greisens and (subsequently) kaolin deposits in the province.

With regard to the geochemical features of the region, Hall (1990) showed that the crustal rocks of the Cornubian province are of highly anomalous geochemical composition, being particularly enriched in the trace elements B, Li and Sn with respect to 'average' compositions of the upper continental crustal as reported by Taylor and McLennan (1985). Furthermore, although the greatest enrichment is associated with the granites, it occurs also in the metasedimentary ('killas') and volcanic rocks that predate the batholith. The argillaceous rocks are relatively depleted in both Ca and Na, reflecting the low contents of carbonate minerals and detrital feldspars respectively. In composition, the volcanic rocks generally reflect spilitic alteration superimposed on the original igneous parentage, hence may be referred to collectively as greenstones (Hall, 1990).

^{235}U - ^{207}Pb geochronological measurements by Chesley *et al.* (1993) and Clark and co-workers (Clark *et al.*, 1993; Chen *et al.*, 1993), supplementing earlier Rb-Sr studies by Darbyshire and Shepherd (1985, 1987), have demonstrated that the Cornubian batholith was emplaced diachronously over an interval of some 20Ma, from *ca.* 293-275Ma before present, with no systematic trend in the age of pluton emplacement along the axis of the batholith. ^{40}Ar - ^{39}Ar ages of muscovites hosted by the coarse-grained megacrystic granites were additionally determined by Chesley *et al.* (1993) and Clark *et al.* (1993); these data

represent the timing of closure to Ar loss (~325°C), thereby permitting cooling rates to be established. Whereas there is some disagreement between Chesley *et al.* (1993) and Clark *et al.* (1993) regarding the early cooling history of the individual plutons and the timing of associated hydrothermal events, what is undisputed is that long-lived multiple intrusive episodes are implied, at least in the case of the Dartmoor and Land's End plutons, with emplacement having occurred over periods of *ca.* 3-5Ma (Chen *et al.*, 1993). All the plutons are essentially of a composite nature (Chesley *et al.*, 1993).

With regard to the origin of the batholith, there has been disagreement about whether the granites are of purely crustal origin, or were derived from a mixed crustal-mantle source (see Stone and Exley, 1985; Leat *et al.*, 1987; Willis-Richards and Jackson, 1989). Advocates of a crustal melting hypothesis have suggested that anatexis may have occurred in response to crustal thickening and radiogenic heating during the Hercynian orogeny (Shackleton *et al.*, 1982; Pearce *et al.*, 1984; Willis-Richards and Jackson, 1989). Watson *et al.* (1984), on the other hand, suggested that the most probable source of the parent magmas was mantle material, previously enriched in volatile and incompatible elements. The idea that an injection of mantle-derived mafic melts into the lower and intermediate-level crust provided the thermal energy to initiate crustal melting was suggested by Leat *et al.* (1987) and has found favour in recent studies, *e.g.* Chesley *et al.* (1993); Chen *et al.* (1993). Leat *et al.* (1987) proposed that potassic magmas assimilated pelitic material during intrusion into the lower crust; fractionation of the resulting large magma body subsequently led to granite formation. Nd and Sr isotopic data presented by Darbyshire and Shepherd (1994) indicate that the granites were derived from a composite lower crustal source, of which only a relatively minor basaltic magma component was extracted from a (slightly enriched) mantle source.

1.1.2 Stages of hydrothermal mineralisation

The term 'transitional processes' was introduced by Burnham and Ohmoto (1980) in the context of late-stage processes associated with felsic magmatism. It can be equated broadly with the pegmatitic and pneumatolytic stages defined by Niggli (1929) and is adopted in later sections of the present work. Field observations by Lin (1989) relating to transitional processes associated with the St Austell and Land's End granites illustrate the continuum linking the pegmatitic and pneumatolytic stages of hydrothermal evolution.

Mineralised pegmatites and greisen-bordered quartz vein swarms enriched in wolframite rather than tin or copper-bearing minerals generally constituted the earliest major stage of hydrothermal mineralisation associated with each pluton (Beer and Ball, 1987; Jackson *et al.*, 1989). Many such occurrences are located close to the periphery of the host granite, or indeed extend into the adjacent metasedimentary rocks. Associated fluid inclusion homogenisation temperatures generally range from 300-500°C (*e.g.* Chesley *et al.*, 1993).

The Dartmoor granite is distinctive, however, in that wolframite is unknown; the initial stage of mineralisation is represented by tourmaline, followed by assemblages of quartz, tourmaline and cassiterite (Scrivener, 1982). In all cases, the early veins are considered to have been controlled by the development of fracture systems closely related to granite intrusion and initial cooling. According to Clark *et al.* (1993), the formation of these early hydrothermal vein systems was synchronous with cooling of the host intrusive rocks to *ca.* 320°C, as indicated by the coincidence with muscovite cooling ages where comparative data were available. This is compatible with an origin based on retrograde boiling of magma in the upper regions of the associated intrusions, as proposed by Jackson *et al.* (1989).

The major ('main-stage') episode of mineralisation in the Cornubian region is represented by polymetallic (predominantly copper) sulphide-quartz fissure veins, with chlorite and minor tourmaline. Cassiterite may also be present. The veins trend predominantly east-west and are associated with fluid inclusion homogenisation temperatures generally ranging from 200-480°C (Chesley *et al.*, 1993, and references therein). Rb-Sr radiometric dating by Darbyshire and Shepherd (1985) indicated that chalcophile-element mineralisation at South Crofty mine may have post-dated emplacement of the nearby Carnmenellis granite by 20Ma, suggesting a significant hiatus between magmatism and main-stage hydrothermal activity. A consensus view subsequently developed (*e.g.* Jackson *et al.*, 1989; Chesley *et al.*, 1993) that the major Sn-Cu-bearing lodes in the province formed some 15-20Ma after granite emplacement and were essentially the result of geothermal processes (involving fluids of meteoric derivation) relating to the protracted cooling history inferred for the granites. Recent work has cast doubt on this interpretation, however. In particular, Clark *et al.* (1993)[†] concluded that, on the basis of ⁴⁰Ar-³⁹Ar incremental heating measurements on hydrothermal and primary muscovites, major Sn(±Cu) lode formation at South Crofty commenced within 1-3Ma of the immediate host rocks cooling to ~320°C. This corresponds to 5-9Ma since initial emplacement of the granite, on the basis of cooling rates proposed by these authors, and coincides with the attainment of ~320°C at (present) depths of 2-3km within the cooling granite. On this basis, the chalcophile mineralisation in the province is genetically related to the granites.

If the scenario advocated by Clark *et al.* (1993) and Chen *et al.* (1993) is correct, then protracted hydrothermal activity in the region resulted from the disparate timing of individual pluton emplacement. A corollary of this is that all lithophile and chalcophile element mineralisation associated with the older plutons of the batholith (such as the Carnmenellis granite) was completed before emplacement of the youngest (Land's End) pluton. This is in contrast to the view advocated by *e.g.* Jackson *et al.* (1989), whereby slow cooling on a batholith-wide scale (caused by high concentrations of uranium, thorium and potassium in the granitic rocks) was largely responsible for long-lived hydrothermal mineralisation.

[†] The same results were subsequently reported by Chen *et al.* (1993)

A significantly later stage of mineralisation in the region is represented by 'cross-courses', which trend north-south, are generally located at some distance from the granitic outcrops, and consist of quartz-fluorite-barite veins hosting Pb, Zn and Ag sulphides, together with minor amounts of uraninite. Fluid inclusion homogenisation temperatures generally range from 105-180°C (Shepherd and Scrivener, 1987). Rb-Sr radiometric dating of examples from the Tamar valley region (Darbyshire and Shepherd, 1990) indicates an early Triassic age (~235Ma). Such fluids are therefore not directly linked to the intrusion and cooling of the batholith. The compositional similarity of these fluids to deep sedimentary basin brines has led to the suggestion that the fluids were actually derived from Mesozoic sedimentary basins (Alderton, 1978; Shepherd and Scrivener, 1987; Alderton and Harmon, 1991). Alternatively, Durrance *et al.* (1982) considered that convective circulation of Mesozoic seawater, driven by the high heat production of the batholith, was a more likely scenario. In either case, tectonic reactivation of fracture systems may have aided an influx of external fluids.

The alteration of feldspar to kaolinite in the Cornubian granites, although widespread, was particularly intensive in the lithionite granites of the St Austell pluton and also in southern parts of the Dartmoor granite. The source and age of the kaolinisation, however, is still subject to debate. Whereas the isotopic data of Sheppard (1977) are compatible with kaolinite formation through weathering action, the idea that convective, post-magmatic hydrothermal circulation was primarily responsible (Durrance *et al.*, 1982) has probably gained more widespread acceptance.

1.2 Fluid inclusions as tracers of palæo-hydrothermal processes

1.2.1 Overview

The recognition and understanding of geochemical processes involving crustal fluids requires detailed information about the nature and composition of the fluids. Except for present-day geothermal areas and submarine hydrothermal vents, however, the fluid phase cannot be sampled directly. In the case of ancient fluids, information may be inferred from thermodynamic analysis of the associated mineral assemblages (*e.g.* Eugster, 1981). Although progress in this area continues (Sverjensky and Molling, 1992; Sverjensky, 1992), such an indirect approach is generally hampered by poorly-constrained variables and/or a lack of pertinent thermodynamic data (Dubessy *et al.*, 1989). Furthermore, many hydrothermal fluids contain volatile constituents and dissolved electrolytes which may not be recorded in the precipitated minerals (except in the fluid inclusions thereof). Fluid inclusions provide a unique source of information about the composition, temperature and pressure of fluids that once formed or traversed the host rock. They also allow the only possibility of sampling, and analysing directly, ancient fluids from a wide range of crustal environments.

According to Roedder (1984), inclusions in the size range 1-10 μm generally outnumber all inclusions >10 μm by a factor of 10² or 10³ for most naturally-occurring samples; a size continuum presumably exists down to the scale of individual water molecules either trapped along grain boundaries or structurally bound in the host crystal lattice. The development of techniques for fluid inclusion analysis has been reviewed by Roedder (1990); more recent work of relevance to the present study is referred to in the appropriate sections.

1.2.2 The chemical composition of fluid inclusions: representative of entrapment composition?

The value of fluid inclusions as samples of ancient fluids rests on the assumptions that: (i) the inclusions have remained closed since the time of formation; (ii) post-entrapment chemical re-equilibration of fluid composition during the cooling history of geological samples has not significantly changed the composition of the original fluid. With the exception of some metamorphic terranes, evidence for bulk fluid leakage has not been detected in samples from many geological environments (Roedder, 1984, pp.75-77 and references therein). However, the diffusion of water (Heggie, 1992; Bakker and Jansen, 1990; Hollister, 1990) and hydrogen (Mavrogenes and Bodnar, 1994, and references therein) into or out of inclusions may also occur in high-grade metamorphic environments, in response to the respective partial pressure gradients. Calculations by Kreulen (1987) and Hall and Bodnar (1990) indicate that water-deficient fluid compositions of the C-O-H system are only stable at very high or very low CO₂/CH₄ ratios, in contrast to many experimental findings on inclusions in medium- and high-grade metamorphic terranes.

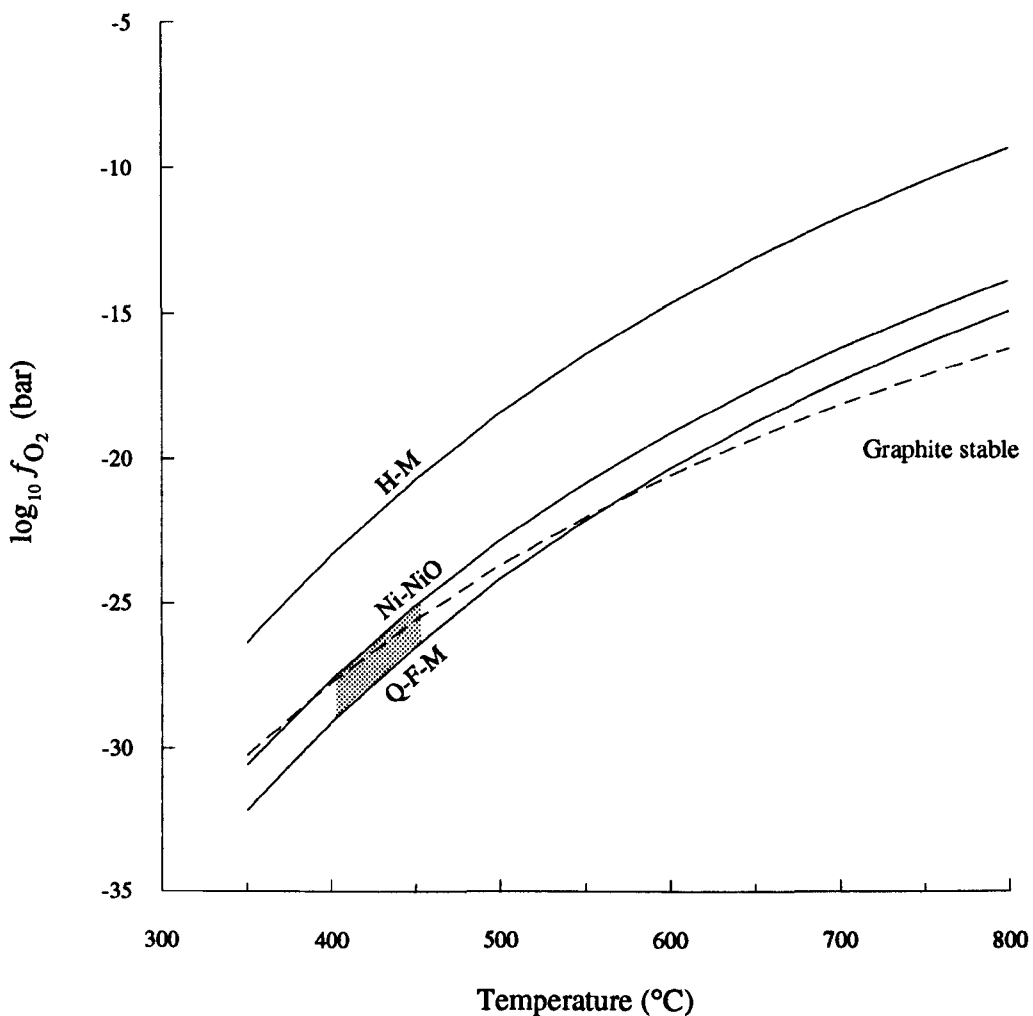
The question of whether post-entrapment chemical re-equilibration of fluid composition is of significance was addressed by Dubessy (1984) by equilibrium thermodynamic modelling of the C-O-H system; the results were subsequently extended to the C-O-H-N-S system by Dubessy *et al.* (1989). It was concluded from these studies that, over the temperature range 900 to 300°C,[†] and in the absence of graphite, relative variations of the mole fractions of CO₂, CH₄, H₂O, N₂ and H₂S are typically only around 10⁻² (as an order of magnitude). This type of modelling necessarily neglects kinetic considerations (and thus metastable assemblages), however, and as such represents the maximum potential change in chemical composition since trapping.

For fluids in the presence of graphite, a similar analysis by Dubessy (1984) indicated that the potential for chemical change is dependent on the initial composition: in hydrothermal systems containing CO₂ and CH₄, mole fraction variations with respect to initial values were predicted to be potentially of the order of tens of percent, if equilibrium was maintained.


[†] Kinetic considerations probably preclude attainment of equilibrium at lower temperatures (Sheppard, 1981).

Figure 1.2

Redox field (as $\log_{10} f_{O_2}$ versus temperature) characteristic of hydrothermal fluids associated with Sn-W oxide mineralisation (after Dubessy *et al.*, 1987), together with the graphite stability limit curve. (All curves refer to 1 kbar total pressure)



Notes:

1. H-M, Ni-NO and Q-F-M refer to hæmatite-magnetite, nickel-nickel oxide and quartz-fayalite-magnetite, respectively. Other commonly-quoted redox buffers, such as wüstite-magnetite, iron-quartz-fayalite, iron-magnetite and iron-wüstite, all correspond to more reducing conditions than the systems illustrated.
2. Mineral buffer redox curves were generated from the data of Ohmoto and Kerrick (1977).
3. The stability limit curve of graphite refers to the reaction: $C + O_2 \rightleftharpoons CO_2$, assuming equilibrium in the C-H-O system and using the equation of state of Holloway (1981). The computational routine of Dubessy (1984) was used to perform the calculations.
4.  indicates the redox field of palæo-hydrothermal fluids associated with Sn-W oxides.

1.2.3 Modelling of chemical equilibria and redox conditions

The parameter most commonly used to define the redox state of a fluid in high temperature geochemical systems is the oxygen fugacity, f_{O_2} , after Eugster (1957). The use of fluid inclusion analysis in combination with thermodynamic modelling of chemical equilibria in the C-O system was shown by Bergman and Dubessy (1984) to permit an estimate to be made of the f_{O_2} of a primary basaltic system (CO_2 -CO inclusions in a composite peridotite xenolith) at 1200°C. This technique was subsequently extended to the calculation of palaeofluid redox states of (lower temperature) hydrothermal systems (Ramboz *et al.*, 1985; Dubessy *et al.*, 1987; Dubessy *et al.*, 1989), on the basis that H_2O , CO_2 and CH_4 are close to chemical equilibrium under geothermal systems (Giggenbach, 1980) down to ~320°C (Sheppard, 1981). Figure 1.2 shows the resulting redox field attributed by Dubessy *et al.* (1987) to granite-associated palaeo-hydrothermal fluids associated with Sn-W oxide mineralisation; their study included samples from Cligga Head, Cornwall, as does the present work. From Figure 1.2, it is seen that coexistence between such fluids and graphite is thermodynamically feasible.

Oxygen is a 'virtual' species in geochemically relevant systems below ~600°C, hence the use of f_{O_2} to evaluate redox reactions in hydrothermal environments is questionable. For example, simple calculation shows that a fluid phase at 400°C, 1 kbar total pressure, with redox state defined by the Q-F-M buffer (f_{O_2} value of $10^{-29.09}$ bar) theoretically contains one molecule of O_2 in a volume of $\sim 1.1 \times 10^7$ litres (assuming ideal gas behaviour). Giggenbach (1987) persuasively argued that it is preferable to assess geochemical systems on the basis of actual reaction participants, or at least directly measurable quantities, and hence that the use of 'master variables' such as f_{O_2} should be avoided when discussing hydrothermal systems. As an endorsement of this viewpoint, thermodynamic modelling undertaken for the present work is confined to assessing the viability of potential reactions involving 'non-virtual' reactants.

There are in principle two approaches to the calculation of chemical equilibrium (van Zeggeren and Storey, 1970; Holub and Voňka, 1976). The more widely-used method for a system defined by a relatively small number of chemical species is the so-called method of equilibrium constants - mass balance. This describes the system in terms of a set of linearly-independent chemical reactions and the corresponding equilibrium constants, together with the constraint that the mole fractions of the species considered must sum to unity. Details of this technique as applied to calculate the composition of C-H-O fluids at high temperatures and pressures are given by *e.g.* French (1966), Ohmoto and Kerrick (1977), Dubessy (1984), Holloway (1987), and Hall and Bodnar (1990). An advantage of this approach is that the equilibrium composition may be calculated relatively easily for a specified redox state (as f_{O_2}) at fixed values of temperature and pressure (or density).

The second approach to the computation of chemical equilibrium is to calculate the Gibbs free-energy of the system and thence determine the composition that minimises this function, subject to satisfying the mass balance requirement. Formally, this involves (van Zeggeren and Storey, 1970) finding the set of n_i values which minimises

$$G = \sum_i \mu_i n_i \quad \text{subject to the conditions} \quad \sum_i a_{ie} n_i = B_e \quad \text{and} \quad n_i \geq 0$$

where μ_i is the chemical potential of species i , n_i is the number of moles of species i in the system, a_{ie} is the number of moles of element e in one mole of species i , and B_e is the total number of moles of element e present.

This method has much greater generality of application; a large number of species may be considered, providing that data are available on the respective standard free energies of formation at the temperature and pressure considered. Furthermore, condensed phases may be considered as an integral part of the calculation procedure. For the present study, the free-energy minimisation procedure developed by Gordon and McBride (1971) was used for the calculation of chemical equilibria.[†] Initial reactant composition and two thermodynamic state variables (generally temperature and pressure) specify the system under consideration.

The main application of thermodynamic modelling in the present work was to a consideration of the origin of palæofluid nitrogen, present as a trace constituent of hydrothermal fluids associated with the earliest stage of mineralisation of the Cornubian batholith (Chapter 4), together with the validation of related experimental procedures. For the sake of comparison with published work on the distribution of molecular species in fluids of the C-H-O system under (shallow) crustal conditions, however, the equilibrium compositions resulting from reaction between graphite and water at 1 kbar total pressure, 400-900°C, were calculated and are illustrated in Figure 1.3. As the Gordon and McBride (1971) computational routine uses the ideal gas equation of state, it was adapted by the present author to incorporate fugacity coefficients of all major species of the C-H-O system, as obtained from the modified Redlich-Kwong equation of state of Holloway (1981). Ideal mixing of fluid components was assumed. Figure 1.3 indicates that, in the absence of modification by wall-rock reactions, such fluids are predominantly aqueous with approximately equimolar quantities of methane and carbon dioxide as the minor constituents (assuming that equilibrium is maintained); this is largely in accord with the findings of Kreulen (1987).[‡]

[†] Adaptations of the Gordon and McBride (1971) routine, for application to the study of crustal fluids, have also been reported by Holloway and Reese (1974) and Mathez *et al.* (1989).

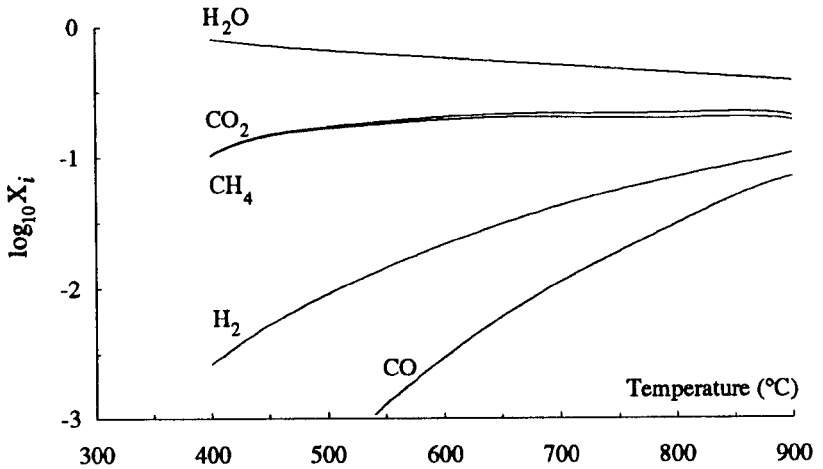
[‡] A major difference is that Kreulen (1987) additionally constrained the redox state of the system by specifying f_{O_2} values.

Figure 1.3

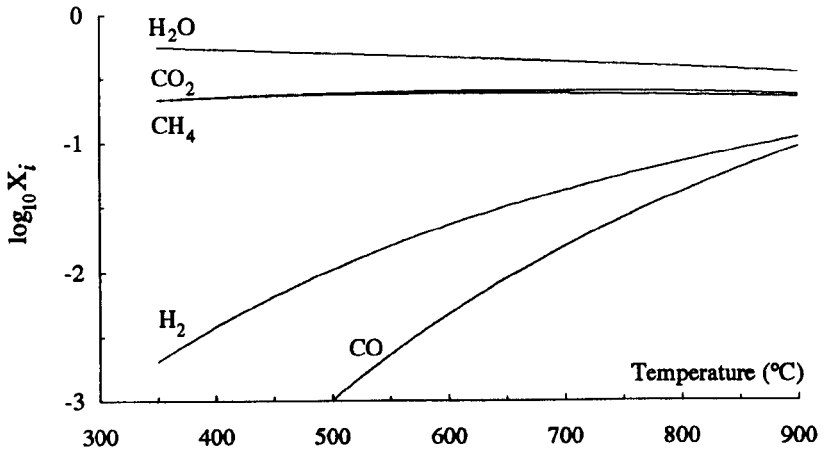
Temperature variation (at constant pressure) of mole fractions X_i of the principal fluid components resulting from reaction between equimolar quantities of water and graphite at thermodynamic equilibrium. The computational method of Gordon and McBride (1971) was used to perform the calculations. (Graphite was present in the product mixture in all cases.)

(a) Pressure = 1kbar.

Modified Redlich-Kwong equation of state of Holloway (1981) used to model non-ideal behaviour:

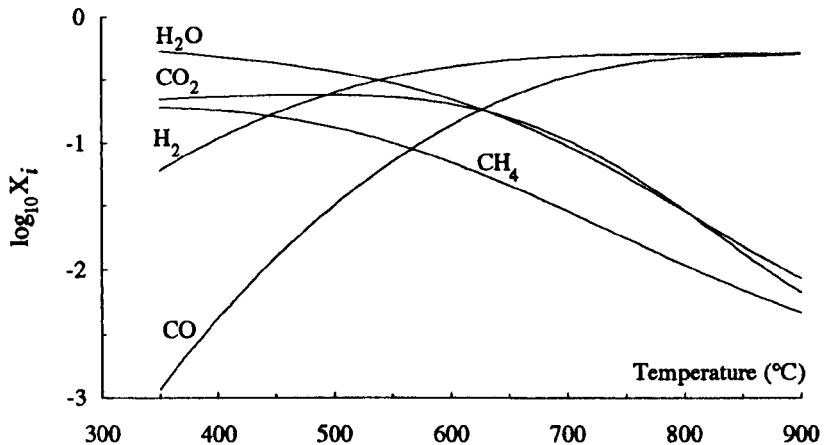


Calculations performed assuming ideal mixing of ideal gases:



(b) Pressure = 1bar.

Ideal mixing of ideal gases assumed:



The substantial solubility of carbon-bearing species in hydrothermal C-H-O(-Si) fluids and the possibility of graphite deposition from such fluids is well documented (*e.g.* Rumble *et al.*, 1986; Rumble and Hoering, 1986). What is less clear is the extent to which thermodynamic models provide a reliable description of the evolution of 'real' systems. For example, kinetic inhibition of graphite precipitation, giving rise to metastable assemblages at up to 700°C (Ziegenbein and Johannes, 1980); evidence for disequilibrium at ≤400°C between graphite and coexisting hydrothermal fluids (Ramboz *et al.*, 1985), together with the experimental findings of Morgan *et al.* (1992) provide a salutary reminder that the application of closed system, equilibrium modelling to hydrothermal fluids is not without limitation.

1.3 Stable isotope fractionations: terminology

As much of the present work is concerned with the measurement and interpretation of light-element stable isotope ratios in hydrothermal fluid constituents, a brief review of the relevant definitions and notation is presented here. Further details are to be found in many 'standard' works, such as Gonfiantini (1981), O'Neil (1986), Faure (1986) and Hoefs (1987). Most published work referring to stable isotope ratio analysis adopts the δ notation (after Urey, 1948), which reports the difference, in parts per thousand (per mil, ‰), of the rare isotope with respect to its abundance in a reference material:

$$\delta = 10^3 \left(\frac{R_{\text{sample}} - R_{\text{standard}}}{R_{\text{standard}}} \right) \text{‰}$$

where $R = (\text{D}/\text{H}), (^{13}\text{C}/^{12}\text{C}), (^{15}\text{N}/^{14}\text{N}), (^{18}\text{O}/^{16}\text{O}), (^{34}\text{S}/^{32}\text{S}), \text{etc.}$

This notation avoids calibration problems associated with absolute abundance ratio measurements and the instability of individual instruments over extended periods of time. For small enrichments of either isotope, the delta scale is effectively linear. It is of interest to note, however, that the limits of the delta scale are -1000‰ and +∞. Although of little consequence in most terrestrial studies, this is a significant consideration with respect to the analysis of many extraterrestrial samples, where much wider ranges of stable isotopic ratios have been recorded. A useful property of the δ notation is that, for two samples measured with respect to the same reference, the δ value of the first sample with respect to the second is given by:

$$\delta_{1-2} = \delta_1 - \delta_2 \left(\frac{1000 + \delta_1}{1000 + \delta_2} \right) \cong \delta_1 - \delta_2 \quad \text{for } |\delta_1|, |\delta_2| \ll 1000\text{‰}$$

Furthermore, for a mixture of n components, where x_i is the mole fraction characterised by isotopic composition δ_i , the isotopic composition of the mixture is given by:

$$\delta = \sum_{i=1}^n x_i \delta_i$$

To convert the δ value of a sample (A) relative to a reference (B) into the corresponding value relative to another reference (C), use is made of the relationship:

$$\delta_{A-C} = \delta_{A-B} + \delta_{B-C} + [10^{-3} \times \delta_{A-B} \times \delta_{B-C}]$$

where δ_{B-C} is the value of reference B with respect to reference C.

The isotopic fractionation factor between two substances A and B is defined as $\alpha_{A-B} = \frac{R_A}{R_B}$

In terms of δ values:

$$\alpha_{A-B} = \left[1 + \frac{\delta_A}{1000}\right] / \left[1 + \frac{\delta_B}{1000}\right] = \frac{1000 + \delta_A}{1000 + \delta_B}$$

Furthermore, as $\log_e \alpha_{A-B} = \log_e \left[1 + \frac{\delta_A}{1000}\right] - \log_e \left[1 + \frac{\delta_B}{1000}\right]$, and $\log_e(1 + \epsilon) \approx \epsilon$ if $\epsilon \ll 1$,

$$\text{then, } 10^3 \log_e \alpha_{A-B} \approx \delta_A - \delta_B = \Delta_{A-B} \quad \text{This is a good approximation if } |\delta| \leq 10$$

α_{A-B} is a function of the absolute temperature (T), but not generally a function of pressure. A detailed consideration of the temperature dependence of isotopic fractionation factors is given by Criss (1991).

1.4 Thesis structure

The present study is essentially concerned with the relation between ancient hydrothermal fluids (particularly those associated with early-stage lithophile mineralisation and pegmatite development) and granite magmatism, with reference to the Cornubian batholith, SW England. Of particular interest is the extent to which fluid constituents reflect high-level crustal processes involving regional metasedimentary and metavolcanic rocks, or whether they were essentially granite-derived.

A comparison is made between hydrothermal fluids associated with early tourmaline-dominated and greisen mineralisation of the Dartmoor granite, on the one hand, and comparable (early-stage) processes hosted diachronously by other component intrusives of the batholith, where the earliest stage is characterised by association with W±Sn oxides.

Chapters 2, 3 and 4 are primarily concerned with the measurement and interpretation of isotopic compositions of specific volatile constituents of the fluids. Fluids associated with the earliest stages of hydrothermal activity hosted diachronously by the batholith were at many localities characterised by the presence of carbon-bearing species and molecular nitrogen, albeit at trace levels. Because of their low absolute abundance in the fluids, it was necessary to develop appropriate low-blank experimental techniques to extract these components, ultimately down to sub-nanomole quantities, from fluid inclusions. The application of high-sensitivity, static vacuum mass spectrometry to these isotopic determinations is described.

Chapter 5 documents an investigation of the corresponding electrolyte compositions of the fluids, as determined using crush-leach analytical techniques. Chapter 6 considers geochemical and isotopic characteristics of Palæozoic metasedimentary rocks from the region, for comparison with the palæofluid data and hence to assess whether direct assimilation from the metasediments at a high crustal level was likely to have been a significant source of the fluid constituents.

Principal findings of particular aspects of this study are summarised in individual Chapters, whereas Chapter 7 additionally attempts to integrate the various results into a consistent framework and assesses the overall implications for the origin of early hydrothermal mineralisation in the Cornubian region.

Chapter 2

Hydrogen and oxygen stable isotope constraints on the source of palæo-waters associated with protracted hydrothermal activity, S W England

2.1 Synopsis

The hydrogen stable isotopic composition of waters associated with various stages of hydrothermal alteration and mineralisation of the Cornubian batholith was determined by the direct analysis of water extracted from quartz-hosted fluid inclusions. Corresponding palæofluid $^{18}\text{O}/^{16}\text{O}$ ratios were calculated from analyses of the respective quartz hosts, by application of appropriate fractionation factors in conjunction with estimated temperatures of fluid entrapment.

The combined δD and $\delta^{18}\text{O}$ results were used to assess the relative contributions of various water sources associated with protracted hydrothermal activity in the region. Particular emphasis was given to the early-stage (high temperature) fluids associated with oxide mineralisation in the region, both with regard to a possible link with pegmatite-associated fluids and also to assess the factors responsible for any variation of the isotopic data with locality, in the case of fluids characterised by a similar paragenetic assemblage.

A comparative assessment was undertaken of the δD and $\delta^{18}\text{O}$ characteristics of hydrothermal fluids associated with tourmaline-dominated and greisen mineralisation of the Dartmoor granite. The results were compared with those obtained for fluids associated with early $\text{W}\pm\text{Sn}$ oxide assemblages of the Hemerdon Ball granite, a minor pluton located to the south-west and within the metamorphic aureole of the Dartmoor intrusive. In view of the apparent 'magmatic' character of early fluids at both localities (Shepherd *et al.*, 1985), the isotopic data provide a reference point for the evaluation of waters from other comparable-stage fluids elsewhere in S W England. The investigation also includes a preliminary comparison with fluids characterised by association with sulphide assemblages in the region.

2.2 Introduction

2.2.1 Hydrogen and oxygen isotope natural abundances

Hydrogen, the most abundant element in the solar system, has two stable isotopes: ^1H and ^2H (or deuterium, D). The latter was discovered by Urey *et al.* (1932) and has an abundance of 155.76 ± 0.10 ppm (Hagemann, 1970) in the SMOW international standard. A third

naturally-occurring isotope, ^3H or tritium, is radioactive and is produced in the stratosphere by the interaction of ^{14}N with cosmic ray neutrons. Tritium has a half-life of 12.43 ± 0.05 a (IAEA, 1983) and decays by β^- emission to ^3He .

Oxygen is the most abundant terrestrial element. There are three stable isotopes, with approximate atomic abundances, in percentage terms, of $^{16}\text{O}=99.763$, $^{17}\text{O}=0.0375$ and $^{18}\text{O}=0.1995$ (Garlick, 1969). Because of the greater difference in mass, coupled with the higher natural abundance, it is the $^{18}\text{O}/^{16}\text{O}$ ratio that is usually determined in isotopic tracer studies.

D/H and $^{18}\text{O}/^{16}\text{O}$ ratios are generally reported using the conventional δ -notation (see Section 1.3) as shifts, in parts per thousand (per mil, ‰) from the SMOW ('Standard Mean Ocean Water') international standard, a hypothetical substance defined by Craig (1961 b) in terms of its relation to NBS-1, a distilled water standard. To improve inter-laboratory calibration of ^{18}O and deuterium measurements in natural waters, two water standards were introduced by the International Atomic Energy Agency in 1968 (Gonfiantini, 1978). These are V-SMOW (Vienna SMOW), obtained by mixing distilled ocean water with small amounts of other waters in order to obtain an isotopic composition as close as possible to SMOW, and SLAP (Standard Light Antarctic Precipitation). V-SMOW has the same $^{18}\text{O}/^{16}\text{O}$ ratio as SMOW (2005.20 ± 0.45) ppm (Baertschi, 1976), but a D/H ratio that is 0.2‰ lower (Gonfiantini, 1978); in reality this discrepancy is negligible for most applications and in many cases is less than the analytical precision of the measurements.

The use of normalised δ -scales for D/H and $^{18}\text{O}/^{16}\text{O}$ measurements was recommended by Gonfiantini (1978) - see also Coplen (1988) and references therein - with V-SMOW adopted as the zero points, and δ -values of SLAP relative to V-SMOW defined as: $\delta\text{D}=-428\text{‰}$, $\delta^{18}\text{O}=-55.5\text{‰}$, on the basis of inter-laboratory comparisons. Normalisation, *i.e.* the expansion or contraction of an isotope scale so that a second reference material is set to a defined δ -value relative to the first reference material, improves data reproducibility by reducing errors such as those arising from instrumentation effects (*e.g.* H_3^+ corrections during D/H ratio measurement) and 'memory effects' during the preparation of hydrogen gas samples. Thus, for hydrogen:

$$\delta\text{D}_{\text{V-SMOW/SLAP}} = 10^3 \times \left[\left[\frac{(\text{D}/\text{H})_{\text{sample}}}{(\text{D}/\text{H})_{\text{V-SMOW}}} \right] - 1 \right] \times R \quad (\text{‰})$$

where R is the ratio of the defined δ -value for SLAP (-428‰) to the actual measured value.

As the relative mass difference between the two stable isotopes of hydrogen is considerably greater than occurs in any other element, the range of D/H ratios encountered in naturally-occurring terrestrial samples is greater than that of any other isotopic system. Values range from about -500‰ to $+300\text{‰}$ (Magaritz and Gat, 1981), whereas the corresponding

variation of $\delta^{18}\text{O}$ is approximately $\pm 50\%$ about the value for SMOW (Magaritz and Gat, 1981; Hoefs, 1987).

Basaltic magmas throughout Earth's history back to the Archean appear to have had uniform $\delta^{18}\text{O}$ composition of about $+6.0 \pm 0.5\%$, which corresponds to the primordial isotope ratio according to Taylor and Sheppard (1986). These authors also suggested that the δD of primordial water is likely to have been obscured or obliterated by subduction-related cycling processes, but may have been not far removed from the values (-80 to -85%) obtained from basalts that contain high abundances of mantle-derived helium. In contrast, the present bulk Earth mean δD value is probably in the region of -15 to -20% (Taylor and Sheppard, 1986), with the corresponding value for the hydrosphere being *ca.* -10% .

2.2.2 The combined δD and $\delta^{18}\text{O}$ approach to the characterisation of natural waters: application to palaeofluids

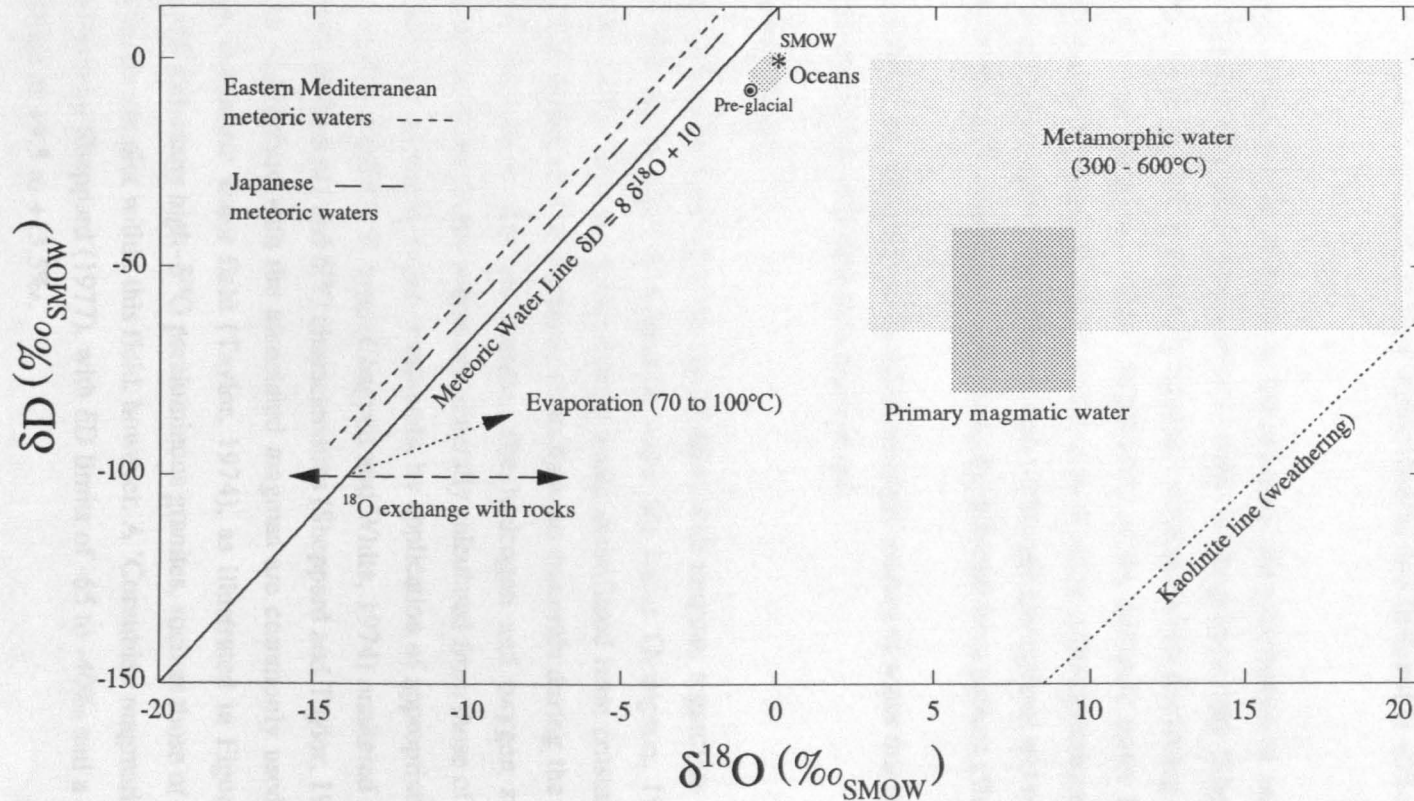
As noted by Sheppard (1986), the chemical composition of a natural, subaerial water cannot in general be used to identify the origin of the water, as this primarily records the nature and extent of water-rock reactions. In contrast, the combined use of hydrogen and oxygen stable isotopic compositions of the waters and coexisting minerals can potentially provide information about the source and history of the water, on the basis of comparisons with the principal water types (particularly meteoric[†] water and seawater, which are relatively well characterised) and established isotopic fractionation processes. In contrast to oxygen, hydrogen is generally a trace constituent in most rock types, the predominant reservoir being hydroxyl groups in silicate minerals. Hence, although water-rock interaction may involve both hydrogen and oxygen isotope exchange, the D/H ratio of an external water source is generally retained, except under conditions of very low water-to-rock ratios. In contrast, the ^{18}O composition of the water may undergo substantial modification as a result of exchange with minerals. Under equilibrium conditions, the resulting fractionation is temperature controlled and may be determined by established fractionation factors.

The δD and $\delta^{18}\text{O}$ values of present-day meteoric waters that have not undergone extensive evaporation are linearly related and generally plot very close to the so-called meteoric water line of Craig (1961 a), which is represented by: $\delta\text{D} = 8 \delta^{18}\text{O} + 10$, as shown in Figure 2.1. Minor deviations on a regional scale are principally the result of relative humidity effects. The extent of D and ^{18}O depletion of meteoric waters, relative to ocean water, increases with latitude and altitude; this effect is accentuated in continental interiors (*e.g.* Dansgaard, 1964).

[†] Meteoric waters are defined as those resulting from atmospheric precipitation, although ultimately derived from ocean water through atmospheric circulation.

Figure 2.1

Plot of δD versus $\delta^{18}O$ showing meteoric waters, the field for ocean waters, and generalised fields for magmatic and metamorphic waters
(Adapted from Sheppard, 1986)



The meteoric water line is from Craig (1961a). Regional variations as shown are related primarily to mean relative humidity effects. The mean annual isotopic composition of precipitation is also related approximately to the mean annual air temperature (Dansgaard, 1964). On this basis, the ordinate axis shown also corresponds linearly to a mean annual air temperature range of -10 to +20°C.

The primary magmatic water field is from Taylor (1974); that of metamorphic water is from Sheppard (1986), which differs slightly from that of Taylor (1974). The kaolinite line is from Savin and Epstein (1970).

With reference to ancient systems involving aqueous fluids of seawater or meteoric origin, interpretation is limited by uncertainties of how the contemporaneous oceanic-meteoric water system differed, in terms of isotopic composition, from that of the present day. On the basis of studies of palaeo-hydrothermal systems believed to be derived from seawater, Muehlenbachs and Clayton (1976) and Muehlenbachs (1986) suggested that the oxygen isotopic composition of seawater during the Phanerozoic was buffered at $\sim 0\%$ by exchanges with oceanic crust.

In the absence of compelling evidence to the contrary, the systematics of ancient meteoric waters are considered to have been similar to those of the present-day (Sheppard (1986), hence the meteoric water line is generally used as a reference when discussing palaeo systems (see also Taylor and Sheppard, 1986). Application of the meteoric water line to ancient systems may be inappropriate, however, if factors such as the contemporaneous atmospheric circulation system, temperature distribution (both within the atmosphere and over the Earth's surface) and/or humidity conditions, were radically different from present (Sheppard, 1986).

Apart from seawater or meteoric waters, other principal sources of water that have potentially contributed to ancient hydrothermal fluid regimes are:

(i) *'Magmatic' water*

This is defined as water that has equilibrated with magma, regardless of its ultimate origin. Possible sources of magmatic water are (after Thompson, 1992): shallow, 'recycled' water from the hydrosphere; water assimilated from crustal rocks; stored primordial water, or water derived from hydrous minerals during the subduction of oceanic lithosphere into the mantle. The hydrogen and oxygen stable isotopic compositions of magmatic waters are generally calculated from those of the associated unaltered igneous whole-rocks or minerals, by application of appropriate fractionation factors at 700-1200°C. 'T'-type (Chappell and White, 1974) unaltered plutonic rocks have well-defined δD and $\delta^{18}O$ characteristics (Sheppard and Taylor, 1986); waters in isotopic equilibrium with the associated magmas are commonly used to define the primary magmatic water field (Taylor, 1974), as illustrated in Figure 2.1. Waters associated with many high- $\delta^{18}O$ peraluminous granites, such as those of the Cornubian batholith, do not plot within this field, however. A 'Cornubian magmatic waters' field was defined by Sheppard (1977), with δD limits of -65 to -40‰ and a corresponding $\delta^{18}O$ range of +9.5 to +13.5‰.

(ii) *'Metamorphic' water*

Water that was equilibrated with, or released from, metamorphic rocks undergoing dehydration is referred to as metamorphic water. A generalised metamorphic waters field was described by Taylor (1974), based on D/H values of metamorphic minerals

in conjunction with tentative water-mineral fractionation curves. Metamorphosed sedimentary rocks and constituent minerals have a wide range of $\delta^{18}\text{O}$ values, as the original sedimentary $\delta^{18}\text{O}$ values are largely retained during metamorphism. Shales, limestones and cherts tend to be relatively enriched in ^{18}O , with $\delta^{18}\text{O}$ values generally ranging from +15 to +35‰. In contrast, rocks such as sandstones, graywackes, arkoses and volcanogenic sediments tend to be relatively depleted in ^{18}O ($\delta^{18}\text{O} \sim +8$ to +13‰); consequently, the $\delta^{18}\text{O}$ range in metamorphic waters is wide: +5 to +25‰ (Taylor, 1974). The range shown in Figure 2.1 is a subsequent modification (Sheppard, 1986, and references therein). Clearly, the boundaries are not absolute. Primmer (1985) reported hydrogen and oxygen stable isotopic compositions of mineral separates (illites and chlorites) from regionally-metamorphosed (diagenetic to greenschist facies) slates and shales from localities in north Cornwall. The isotopic composition of the coexisting metamorphic water, at appropriately lower temperatures of crystallisation (150-450°C, compared to the 300-600°C range used by Taylor, 1974) was also given. The field defined by Primmer (1985) is particularly relevant to the present study.

(iii) *'Formation' water*

This is water residing in the interstices or pores of sediments, but not necessarily trapped contemporaneously with sedimentation. If the water is ancient seawater, and was therefore trapped during sedimentation, the term 'connate water' is often used in the literature. Meteoric waters are generally major components of formation waters, with enrichment in ^{18}O abundance relative to the meteoric water line caused by isotopic exchange with sedimentary minerals, particularly carbonates. Diagenetically-modified seawater may also be a component of formation waters, as may water of metamorphic origin. The hydrothermal phase of carbonate-hosted Mississippi Valley type Pb-Zn-(F-Ba) deposits have δD values and salinities virtually identical to nearby formation waters (Hall and Friedman, 1963) and is therefore believed to involve fluids of formation water origin. During magma emplacement in sedimentary sequences, formation waters may migrate and become a source of hydrothermal fluids (Sheppard, 1986).

(iv) *'Juvenile' water:*

This is pristine water derived from mantle degassing; it has consequently never been in contact with the hydrosphere. As the initial D/H ratio may have been modified by crustal contamination and subduction processes, or mixing with other water sources, juvenile water has never knowingly been recognised and its isotopic composition is speculative. A general range of -50 to -80‰ has been suggested by several authors (Hoefs, 1987, and references therein).

In most present-day hydrothermal systems, the waters are almost exclusively of meteoric origin (Sheppard, 1986), on the basis of the δD values being essentially identical to those of local meteoric waters, although water-rock reaction may have resulted in ^{18}O -enrichment with respect to the meteoric water line.[†] Interpretation of the results for palæo systems is often complicated, however, because of factors such as limited knowledge of local palæo-geographic conditions (latitude and altitude) which, in turn, controlled the δD value of the associated meteoric water. A further complication is that, whereas meteoric water and seawater have reasonably well-characterised isotopic compositions, waters from other sources are less easily distinguished, as the composition fields are less well defined and may partially overlap. Modification of isotopic composition by exchange and/or mixing processes may serve to further obscure the origin of ancient fluids (see *e.g.* Welhan, 1987b; Taylor, 1987; Hoefs, 1987; Sheppard, 1986).

2.2.3 Modelling of water-rock interaction

The use of oxygen isotopes in attempts to quantify water/rock ratios during geochemical interaction was initially proposed by Taylor and associates (Taylor, 1974, and references therein; Taylor, 1977, 1979). The ideas and methodology have subsequently been widely applied, with varying degrees of success.[‡] Two 'end member' models may be considered:

- (i) In situations where the water reservoir is effectively infinite, such as submarine basalts altered by seawater interaction, the oxygen isotopic composition of the rock is modified whereas that of the water is buffered.
- (ii) In geothermal waters, by contrast, the opposite situation usually exists (^{18}O reservoir of rock \gg that of the fluid), resulting in modification of the $\delta^{18}O$ value of the water whereas that of the rock system remains effectively constant.

For cases where neither of the ^{18}O reservoirs is sufficiently overwhelming in size to permit buffering of the corresponding $\delta^{18}O$ value, simplified models based on either open or closed systems have been proposed, as summarised below, to estimate water-rock ratios in the case of meteoric-hydrothermal systems. However, a complication is that the oxygen isotope systematics are also (independently) a function of the temperature of alteration.

[†] Waters that plot to the left of the meteoric water line, *i.e.* exhibiting relative ^{18}O -depletion, are unusual. Examples are known, such as Canadian shield brines; also pore waters in oceanic sediments at depths of ~100m or more. Possible explanations for the ^{18}O compositions are discussed by Sheppard (1986).

[‡] According to N B W Harris (*pers. comm.*), the water/rock ratio is a meaningless parameter; the use of chemical shifts to trace fluid penetration into a rock is much more informative.

The usual closed system model, which assumes continuous circulation of fluid, is (after Taylor, 1977; Criss and Taylor, 1986):

$$(w/r)_{Closed} = \frac{\delta_{rock}^f - \delta_{rock}^i}{\delta_{water}^i - (\delta_{rock}^f - \Delta)} \left(\frac{C_{rock}^i}{C_{water}^i} \right)$$

where w/r is the water:rock mass ratio; superscripts i and f refer to initial and final values; $\Delta = \delta_{Rock}^f - \delta_{Water}^f$; C_{Rock}^i and C_{Water}^i are the initial proportions (by mass) of the element oxygen in the rock and in water, respectively. Ohmoto (1986) argued that this model is a poor analogue to natural systems and that water/rock ratios calculated on this basis rarely reflect the true values.

Taylor (1979) acknowledged that, in reality, some of the heated water would be lost from the system, such as by escape to the surface. In the extreme case in which there is no recirculation of the water, *i.e.* an open system, in which infinitesimal aliquots of water equilibrate with the rock and then move out of the system, the water:rock mass ratio is given by Taylor (1977) and Criss and Taylor (1986) as:

$$(w/r)_{Open} = \left(\frac{C_{rock}^i}{C_{water}^i} \right) \log_e \left\{ \left(\frac{C_{water}^i}{C_{rock}^i} \right) (w/r)_{Closed} + 1 \right\}$$

The open system scenario is also an unrealistic representation of actual hydrothermal systems (Taylor, 1977) and in reality the behaviour is likely to be somewhere in between the limits represented by these two models (Hoefs, 1987). Further complications are that such models only relate to minimum (w/r) values, as appreciable quantities of water may move through fractures without oxygen isotope exchange occurring (Taylor, 1977). Also, the attainment of equilibrium conditions may be inhibited by kinetic considerations (Criss and Taylor, 1986). The principal value of such modelling as applied to meteoric-hydrothermal systems, as noted by Taylor (1979), is probably that a wide range of water:rock ratios is predicted, from ~ 0 to >1 (in terms of atom% of oxygen). Values significantly in excess of unity, however, are generally incompatible with the energy available to drive the associated convection systems.

2.2.4 Hydrothermal fluids associated with mineralisation in the Cornubian province: previous investigations of the stable isotope hydrology

From δD and $\delta^{18}O$ measurements on minerals and whole-rock samples of unaltered granites, associated greisenised granites and modern meteoric waters, Sheppard (1977) concluded that vein-controlled greisenisation of the Cornubian batholith was primarily attributed to the action of meteoric-hydrothermal fluids. No fluid inclusion measurements were undertaken; the data for hydrothermal fluids were calculated from results obtained on minerals.

Jackson *et al.* (1982) concluded that the fluids responsible for main-stage hydrothermal activity associated with the Land's End granite were also overwhelmingly meteoric in origin and were of low to moderate salinity. Jackson *et al.* (1982) did, however, report isotopic evidence for a magmatic-hydrothermal fluid associated with the earliest stages of mineralisation. No isotopic measurements were made directly on fluid inclusions.

Primmer (1985) reported that regional metamorphic water had similar isotopic composition to that proposed for hydrothermal fluids associated with main-stage mineralisation (Sn-Cu, sulphides) in the province. Although Jackson *et al.* (1982) had accepted that dehydration of low-grade country rocks might have been a source of water for the hydrothermal fluid systems, lack of data on the isotopic characteristics of metamorphic waters in the Cornubian province, together with the consistency of interpretation based on a meteoric water source, led Jackson *et al.* (1982) to favour a meteoric-hydrothermal model. Sheppard (1977), on the other hand, argued that if metamorphic waters were a significant component of the Cornubian hydrothermal fluids, the associated metamorphic dehydration reactions must have occurred at depths considerably below the present levels of exposure, because of the very low metamorphic grade of the country rocks. Sheppard (1977) also suggested that the major part of any connate or formation water originally present in the sediments was probably lost during regional metamorphism, *i. e.* prior to emplacement of the Cornubian granites.

On the basis of microthermometric studies, Shepherd *et al.* (1985) proposed that early-stage hydrothermal fluids associated with $W \pm Sn$ oxide assemblages at Hemerdon and quartz \pm tourmaline \pm cassiterite mineralisation of the Dartmoor granite at Birch Tor were essentially of magmatic origin.[†] Dilution and mixing with local groundwaters was proposed as the possible origin of fluids responsible for the subsequent extensive development of sulphide (main-stage) mineralisation in the region.

Preceding pneumatolytic hydrothermal activity in the Cornubian region were higher temperature fluids associated with granitic pegmatite development. Both the pegmatitic and pneumatolytic stages were essentially transitional processes, linking the orthomagmatic evolution of silicate melts with the subsequent hydrothermal stage in which aqueous fluids and solid phases coexisted under supercritical conditions (Lin, 1989, and references therein). The pegmatitic fluids are more likely to be representative of a primary, exsolved 'magmatic' fluid (Burnham, 1979) than are later stage examples. In a study by Lin (1989) of pegmatitic and pneumatolytic evolution associated with the St Austell and Land's End granites, the present author collaborated by undertaking δD analyses of quartz-hosted fluid inclusion waters, for comparison with the fluids that are the focus of the present work.

[†] Preliminary, direct measurement of D/H ratios in the water component of quartz-hosted hydrothermal fluid inclusions from the Cornubian region was undertaken by the present author during that investigation.

It was found that the pegmatitic fluids ranged from -25 to -41‰, whereas those associated with quartz+tourmaline veins ranged from -21 to -32‰ (Lin, 1989). Only one of the seven samples plotted within Cornubian magmatic waters field as defined by Sheppard (1977); all the others showed relative enrichment of deuterium. A discussion of these data, and comparisons with the results of the present study, is deferred to Section 2.6.2.

Since completion of the experimental work for the present study, Alderton and Harmon (1991) published the results of their investigation of fluid inclusion and stable isotope characteristics of fluids associated with various stages of hydrothermal alteration and mineralisation in S W England. Although there is clearly a considerable degree of overlap with the investigation reported herein, there are significant differences in terms of both focus and interpretation, as discussed below.

2.2.5 Palaeogeographic considerations, S W England

As the isotopic composition of local meteoric water is dependant on latitude and altitude, estimates of the isotopic composition of S W England meteoric water during early hydrothermal alteration and mineralisation of the Cornubian batholith are dependant on palaeogeographic reconstructions of the region during the Permian and Triassic periods. A discussion of the associated palaeoclimate is given by Laming (1982), who suggested that the evidence is compatible with semi-arid conditions, comparable with present-day savannah zones (except for the absence of grasses, which evolved during the Cretaceous period).

2.2.5.1 Palaeolatitude

Laming (1982) summarised evidence on the geographical position of Devon during the Permian and Triassic, primarily obtained from measurements of the remanent magnetism of igneous and sedimentary rocks. Cornwell (1967) reported that palaeomagnetic measurements of Exeter volcanics (age 280Ma) placed the corresponding palaeomagnetic pole at 46°N and 165°E, agreeing with the results of an earlier investigation of the lavas (see also Zijdeveld, 1967). Together with Phanerozoic world maps (Smith *et al.*, 1973; Briden *et al.*, 1974), the evidence indicates that S W England was within 10 degrees of the equator during the late Palaeozoic and moving northwards to a position of 30°N by the middle of the Mesozoic. As noted by Jackson *et al.* (1982), locations within about 30° of the equator and at low elevations experience little fluctuation of mean annual air temperature; consequently, the isotopic composition of associated meteoric waters is not very variable and not particularly sensitive to changes in latitude, as long as the altitude remains low.

2.2.5.2 Palæoaltitude

A comprehensive consideration of the altitude of the Dartmoor region during emplacement of the granite was given by Worth (1953, pp. 17-20), who reasoned that: 'at few points can the present surface be far below the original surface of the granite, when it cooled as a plutonic rock'. Dangerfield and Hawkes (1969) also concluded from detailed field observations that the Dartmoor granite was exposed, at least locally, before the end of the Permian.

The finding of small outliers of acid volcanic rocks such as the Exeter volcanic series, and outcrops of rhyolite interbedded with basal New Red Sandstone sediments at Kingsand near Plymouth (R A Edwards, *pers. comm.*), may be interpreted as remnants of Permian volcanism. This supports the hypothesis that the current land surface is close to the Permo-Triassic land surface over much of the region. Extensive Permo-Triassic evaporites and red-beds throughout western Europe indicate that major areas of the region were at sea level during that time (Sheppard, 1986). With regard to S W England, only where basal New Red Sandstone sediments are actually preserved, or where there is extensive red staining of pre-Permian rocks (related to the former presence of New Red Sandstone cover), can it be confidently assumed that the present land surface is close to that of Permo-Triassic times.† The effects of post-Triassic faulting, tilting and erosion would have resulted in the basal New Red Sandstone land surface being preserved in relatively few places. Possible examples of the latter are to be found at Slapton, Kingsand and Thurlestone (BGS Salcombe and Kingsbridge memoir, pp.63-65).

2.2.6 Experimental considerations

2.2.6.1 D/H measurements on natural waters

It is salutary to consider that Friedman (1953), in a pioneering study of the deuterium content of natural waters, measured the D/H ratio by mass spectrometry to a precision of $\pm 1\%$; samples prepared from as little as 1 μ l of water could be analysed. The problems associated with the manipulation of water (primarily loss through adsorption) prior to its conversion to hydrogen for isotope ratio analysis, have seriously hampered attempts to significantly reduce the minimum size of water sample which can be considered for isotopic analysis with acceptable precision. Recent investigations into the problems of water adsorption (Morse *et al.*, 1993), together with a radically different approach to D/H determinations, based on the analysis of methane by static vacuum mass spectrometry (Morse, 1991) are making progress in this direction. Unlike $\delta^{13}\text{C}$ and $\delta^{15}\text{N}$ measurements (as discussed in Chapters 3

† Local red-staining of sedimentary rocks of Carboniferous age (Culm) has been recorded in central Devon (BGS Okehampton memoir, pp.54-55 and 152-153).

and 4 of the present work), improvements in analytical sensitivity during the last forty years have not been spectacular.

Hydrogen isotope ratio analysis of water samples is conventionally undertaken by first reducing the water to hydrogen and then measuring the HD^+/H_2^+ ratio by mass spectrometry. Alternative procedures have been reported, but these have not been widely used. Examples include the use of Fourier transform nuclear magnetic resonance (FT-NMR) spectrometry to measure the deuterium abundance on 2ml of water directly (Tse *et al.*, 1980). Methods based on the reduction of water to methane or ethane prior to isotope ratio analysis by mass spectrometry have also been proposed; a review is given by Morse (1991). A different approach is to equilibrate the water samples with hydrogen gas under temperature-controlled conditions in the presence of a Pt catalyst (Horita, 1988, and references therein; Coplen *et al.*, 1991). As noted by Horita (1988), the prime advantage of the H_2 -water equilibration method is that isotope activity ratios are determined, whereas water reduction methods give the corresponding concentration ratios.

With regard to D/H ratio measurements on water extracted from fluid inclusions, the published literature reporting such analyses is not very extensive, primarily because of the technical difficulties associated with obtaining one to several milligrams of water for each determination. Kokubu *et al.* (1961) were probably the first to report such data; subsequent investigations up to the early 1980s have been reviewed by Roedder (1984).

2.2.6.1.1 Water reduction methods

Although in theory the reduction of water to hydrogen can be achieved by any metal which is more electropositive than hydrogen in the electrochemical series, practical considerations (including the requirement for complete conversion, to prevent isotopic fractionation) have resulted in the use of uranium at 400-700°C (Bigeleisen *et al.*, 1952) or zinc at ~400°C (Graff and Rittenberg, 1952) as the preferred reagents for this reaction. The original methods were designed for continuous flow conditions, whereby water vapour is passed over the heated metal, with recirculation (usually by Toepler pump). Subsequent variations have been reported; a comprehensive summary is given by Morse (1991). The principal difficulty with such techniques, however, is that water vapour strongly adsorbs to internal surfaces of vacuum lines during transfer to the reduction furnace, unless adequate precautions are taken. This results in a 'memory effect' whereby the measured D/H ratio is displaced from its true value, towards that of the previous sample in the case of consecutive analyses.

The development of 'batch' methods during the 1980s, using zinc shot in sealed glass tubes, greatly facilitated sample preparation and throughput. Each water sample is reduced in a separate vessel with a quantity of fresh zinc. Sample preparation may be carried out on a

dedicated line separate from the mass spectrometer and many samples can be prepared simultaneously. Although such methods are suited to the preparation and reduction of small quantities of water, and were indeed originally developed to facilitate isotopic analysis of waters thermally extracted from fluid inclusions in natural and synthetic crystals[†] (Coleman *et al.*, 1982), the principal advantage of batch methods is that memory effects are eliminated. In the case of fluid inclusion analysis, however, adsorption of water onto internal surfaces of the vacuum line used to perform the extraction is a major potential source of isotopic fractionation. As noted by Morse *et al.* (1993), appropriately-designed continuous flow methods actually permit smaller quantities of water to be analysed than do sealed-tube reduction techniques. For the present investigation, however, practical considerations dictated that the batch method be used.

2.2.6.2 ¹⁸O/¹⁶O determinations of fluid inclusion water

The direct analysis of oxygen stable isotope ratios in water extracted from fluid inclusions is technically possible, using direct reaction with BrF₃ (O'Neil and Epstein, 1966) followed by conversion of the liberated oxygen to CO₂ for isotope ratio measurement. Direct reaction of natural water samples with guanidine hydrochloride to produce CO₂ has also been reported (Dugan *et al.*, 1985), although the method was optimised for a sample size of 10 μl samples and as such is inappropriate to fluid inclusion analysis. A micro CO₂-water equilibration technique for application to ¹⁸O/¹⁶O analysis of a few milligrams of water, with specific reference to fluid inclusions, was developed by Kishima and Sakai (1980); their procedure was subsequently modified by Ohba (1987), who reported achieving δ¹⁸O precision of ±0.42‰ (1σ) on ~100 μg of water.

Direct measurement of fluid inclusion water ¹⁸O/¹⁶O ratios has been reported in relatively few studies (see Taylor, 1987, and references therein; also Vityk *et al.*, 1993). For inclusions in quartz, Rye and O'Neil (1968) reported that post-entrapment ¹⁸O exchange between the fluid and the host occurs, rendering such measurements of limited value. Recent experimental work by Vityk *et al.* (1993) challenges this view, at least in the case of an epithermal environment. The usual procedure, however, is to analyse the ¹⁸O/¹⁶O ratio of the quartz, then apply the appropriate equilibrium isotopic fractionation factor for the estimated temperature of entrapment, to calculate the corresponding ¹⁸O/¹⁶O ratio of the original hydrothermal water. The conventional method (Clayton and Mayeda, 1963) for determining oxygen isotope abundances in quartz (and silicates in general) involves reaction with BrF₃ or ClF₃ to liberate O₂ for subsequent conversion to CO₂. Recent techniques using laser-induced

[†] As a guide, the quartz samples used for the present study generally yielded ~500-2000 ppm (by weight) of water during *in vacuo* thermal extraction. The minimum size requirement for subsequent reduction and D/H isotope ratio analysis at precision within ±1‰ is ~1 μl water.

fluorination (Mattey and Macpherson, 1993, and references therein) have permitted a reduction in mineral sample size from ~5mg to as little as 20µg, for the determination of $\delta^{18}\text{O}$ values to better than $\pm 0.2\%$.

2.2.6.3 The effect of dissolved electrolytes on the oxygen and hydrogen stable isotope activities of water

The effect of dissolved electrolytes on the oxygen and hydrogen isotope activities of water (the so-called isotope salt effect) is not well understood (see Horita *et al.*, 1993, and references therein) and is a matter of some controversy. Few studies have been undertaken on solutions at elevated temperatures ($>250^\circ\text{C}$), however. Zhang *et al.* (1989) reported that the ^{18}O equilibrium fractionation factor between water and quartz is independent of salinity (5-40 wt% investigated) and electrolyte composition (NaCl, KCl or NaF) over the temperature range 250-550°C and pressure 0.7-0.8 kbar. On the basis of their experiments, the salt effect on oxygen isotopic composition may not be important in natural hydrothermal systems at temperatures higher than 250°C. Similarly, from the results of Graham and Sheppard (1980), it is concluded that the effect of solute-water interactions on hydrogen stable isotope activities is probably negligible at the temperature (600°C) used to extract fluid inclusions during the present work.

2.2.7 Sampling localities

The samples (all quartz) used in the present investigation were considered to be representative of the associated stage of hydrothermal alteration or mineralisation in the following regions. Further information, including sample locations and descriptions, is given in Appendix A.

- (i) Dartmoor granite-hosted mineralisation, through early quartz+tourmaline±cassiterite±hæmatite association (high-temperature oxide assemblages), to an example of late-stage, lower temperature mineralisation characterised by quartz+hæmatite+pyrite, located on the north-eastern contact of the granite with local metasediments and greenstones.
- (ii) Early-stage, high temperature mineralisation characterised by occurrences of quartz coexisting with W±Sn oxides throughout the province. These were all associated with minor granite intrusives; some of the quartz veins were hosted by metasediments.
- (iii) Main-stage, sulphide-associated mineralisation, as characterised by E-W-trending veins from localities between the Dartmoor and Bodmin Moor granites, including examples from the eastern margin of the Bodmin Moor granite.

- (iv) Lower temperature, later mineralising events characterised by N-S-trending 'cross course' veins of Pb and Zn sulphides in a fluorite/quartz gangue. Present examples were from locations in the Tamar Valley (Bull, 1982; Shepherd and Scrivener, 1987).

2.3 Research objectives

Whether hydrothermal fluids associated with mineralisation of the Cornubian batholith were exsolved during crystallisation of magma (Burnham, 1979), or were largely comprised of local meteoric waters circulating in convection systems driven by the granites (*e.g.* Jackson *et al.*, 1982), is still largely unresolved. The controversy is compounded by Rb-Sr radiometric data indicating that main-stage hydrothermal activity at South Crofty mine post-dated emplacement of the adjacent Carnmenellis granite by ~20Ma (Darbyshire and Shepherd, 1985). The earliest stage of hydrothermal mineralisation in the region is generally linked to the presence of W±Sn oxide assemblages (Beer and Ball, 1987). A major objective of the present work was to characterise the isotopic composition of palæo-waters associated with such occurrences, thereby providing the basis for an assessment of the origin of these fluids. In conjunction with the associated fluid salinities and estimated trapping temperatures, derived from the literature, it was hoped that the relative roles of magmatically-derived and external fluids might be clarified. A complementary investigation of the chemical composition of the early-stage fluids is presented in Chapter 5.

Whereas the presence of wolframite is usually characteristic of 'transitional' pegmatitic-pneumatolytic fluids in SW England, this is not associated with the Dartmoor granite. Instead, the abundance of early tourmaline+quartz veins in the marginal and roof zones of this pluton is recognised, together with cassiterite±hæmatite (Scrivener, 1982). An objective of the present work was to determine whether the δD and $\delta^{18}O$ values of fluids associated with recognised stages of early hydrothermal mineralisation of the Dartmoor granite support the idea of a progressive influx of external fluids into early fracture systems of the pluton. A related objective was to compare the isotopic characteristics of the Dartmoor hydrothermal system with those of the W±Sn oxide-associated fluids.

The stable isotope hydrology of fluids associated with earliest stages of pegmatitic and pneumatolytic evolution of the St Austell and Land's end granites was jointly investigated by the present author and Lin (1989). These fluids represent high-temperature hydrothermal phenomena that preceded the development of early oxide mineralisation in the region. As such, they provide a link with the processes that are the focus of the present work. An objective of this study was therefore to incorporate the data reported by Lin (1989) into the framework of a general interpretation for the origin of granite-related fluids in the region.

The major episodes of hydrothermal mineralisation in S W England are characterised by association with sulphide assemblages, which are generally of a complex nature. A continuum probably existed between these fluids and the earlier, oxide-associated regimes (Bull, 1982). For comparative purposes, an exploratory assessment was undertaken of sulphide-associated fluids, primarily from the Gunnislake-Kit Hill area. The final stage of hydrothermal activity in the region is characterised by low-temperature (~ 120-170°C) killas-hosted quartz-fluorite-sulphide veins, trending in a north-south direction and located at some distance from the granite cupolas. Potential sources of these fluids, which have hitherto been attributed to sedimentary brines (*e.g.* Shepherd and Scrivener, 1987) or Mesozoic seawater (Durrance *et al.*, 1982), are assessed on the basis of δD and $\delta^{18}O$ determinations.

2.4 Experimental

2.4.1 Sample preparation

The quartz samples prepared for fluid inclusion D/H analysis were also required for other determinations of the fluid characteristics in most cases, such as carbon speciation and associated stable isotope ratio measurements; also, crush-leach analysis for the determination of electrolyte compositions. For this reason, it was ensured that no preparation procedure was adopted that was incompatible with the requirements of complementary analyses. Thus, the use of nitric acid to remove mineral impurities was avoided, as the nitrate ion adsorbs strongly to quartz and its thermal decomposition products subsequently give rise to isobaric interference effects during carbon stable isotope ratio analysis of extracted CO₂. For similar reasons, the use of halogenated alkanes ('heavy liquids'), as commonly used to separate minerals of differing densities, was avoided. Quartz samples (hand specimens) were initially crushed and sieved to produce a grain size fraction of 0.5-1.0mm. Further preparation was restricted to acid washing with hot, 6M HCl to remove any traces of carbonates, oxides or sulphides, followed by washing in doubly-distilled water. Samples were subsequently examined under a low-powered binocular microscope and individual grains visibly associated with mineral impurities were removed.

2.4.2 D/H analysis of fluid inclusion waters

All experimental work was undertaken solely by the author. During the course of the study, mass spectrometry facilities in three different laboratories were used, and minor modifications to analytical procedures adopted. Essentially, the batch method of Coleman *et al.* (1982) was used to reduce the water samples to hydrogen. Fluid inclusion water was extracted from quartz samples in a purpose-built glass line of low internal volume. One of the lines designed by the author and used during the present study is shown schematically in Figure 2.2; this was also used for the preparation of co-existing fluid inclusion carbon

dioxide and methane (Chapter 3) in the case of analyses performed at the NERC Isotope Geosciences Laboratory. Sections involved in the transfer of water from the extraction chamber through to the collection vessels were maintained at $\sim 80^{\circ}\text{C}$ by the use of insulated electrical heating tapes.

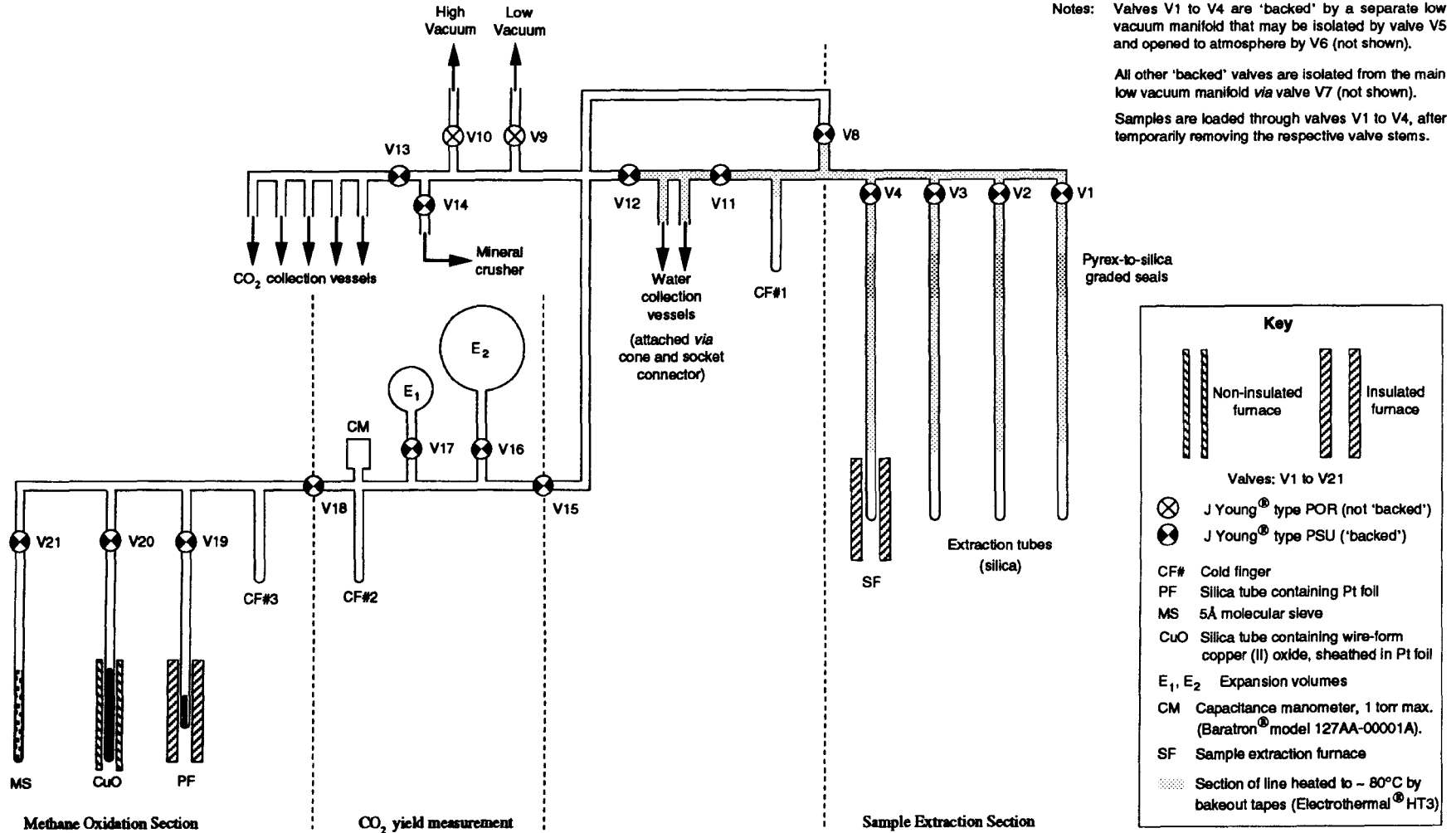
Quartz grain samples (total mass $\sim 1\text{g}$) were loaded into a silica tube (extraction vessel), which formed an integral component of the line, and evacuated to $< 5 \times 10^{-6}$ mbar (generally overnight). During this period, the sample was heated to 100°C to aid the removal of any adsorbed water vapour. The extraction vessel was then isolated from the pumping system and heated to 600°C ; this temperature was subsequently maintained for 30 minutes. At higher temperatures, there is the possibility of some water being reduced to hydrogen during the extraction process (with attendant isotopic fractionation). It is considered unlikely that hydrogen isotope fractionation from the hydrolysis of alkaline earth element chlorides (in the inclusion fluids) would have been of significance during extraction at 600°C , on the basis of data published by Horita (1989).

During extraction into the closed vacuum line, a cold finger maintained at liquid nitrogen temperature (-196°C) was used to freeze down released fluid components such as water and CO_2 . At the end of the 30 minute extraction period, the extraction tube was isolated from the cold finger section of the line; any non-condensed gases (primarily nitrogen and methane) were pumped away. Exchanging the liquid nitrogen for a n-pentane/liquid nitrogen slush bath (-130°C) released any CO_2 component, which was also subsequently removed. Transfer of the water component to an adjacent, evacuated stopcock vessel, the end of which was immersed in liquid nitrogen, was accomplished by aid of a hot air gun. Each stopcock vessel contained $\sim 250\text{mg}$ of Analar[®] zinc shot, as recommended by Coleman *et al.* (1982), or $\sim 80\text{mg}$ of specially-developed zinc laths supplied by the Biogeochemical Laboratory of the University of Indiana, USA. The latter reagent was used for analysis of all samples associated with early hydrothermal mineralisation of the Dartmoor granite, together with sample CD-88-1 (from Castle-an-Dinas mine); Analar[®] zinc shot was used in all other cases.

Sealed stopcock vessels containing water samples and zinc were subsequently removed from the extraction line and the water converted to hydrogen by standing the vessels in a temperature-controlled heating block for 30 minutes. A temperature of either 450°C (for Analar[®] zinc shot) or 500°C (for 'Indiana zinc' laths) was used for the water reduction. During the course of reaction, a small amount of zinc volatilises to form a ring on the cooler part of the tube. After reaction, vessels were allowed to cool to ambient temperature before D/H analysis was undertaken, using either a VG[®] 602 or SIRA Series II mass spectrometer.

Figure 2.2

Schematic diagram of the vacuum line used for extraction and isolation of fluid inclusion water (together with carbon dioxide and methane), for stable isotope ratio analysis



Vennemann and O'Neil (1993) reported that hydrogen isotope exchange with borosilicate glass reaction tubes during the water reduction procedure (as suggested by Kendall and Coplen, 1985; Sudzuki, 1987) was effectively eliminated when the water sample size was ~1 mg or greater. The same authors also noted that no significant differences in results were observed when using either Analar® zinc shot (0.5-2mm grain size), or zinc laths from the Biogeochemical Laboratory of the University of Indiana, as the water reduction reagent.

2.4.3 Quartz ¹⁸O/¹⁶O determinations

Analytical work was largely undertaken by the author, using a purpose-built fluorination line at the (then) London-based NERC Isotope Geosciences Laboratory. The principal exception was the analysis of a batch of samples (10, all with SW-89 reference codes) collected from the Dartmoor granite, together with a sample from Cligga Head (CH-88-1); these were undertaken on the author's behalf by Dr A Boyce at the SURRC facility, East Kilbride, during a period when the NERC facility was temporarily unavailable. The following description refers to the procedure undertaken in the London laboratory.

A small quantity of cleaned quartz grains (prepared as described in Section 2.4.1) was heated at 600°C *in vacuo* for 30 minutes, to expel fluid inclusion water. After cooling, the grains were ground to a fine powder, using an agate mortar and pestle, and 6-10mg of weighed (± 0.01 mg) sample transferred to a nickel tube reaction vessel. Twelve samples, including a reference material (generally NBS-28 quartz sand, or a laboratory standard periodically calibrated against NBS-28) were loaded into separate reaction tubes for analysis. Standard fluorination procedures, based on reaction with BrF₃ as described by Clayton and Mayeda (1963), were used to liberate oxygen from the quartz. The reaction conditions adopted, as recommended by P B Greenwood (*pers. comm.*) were as follows:

Samples were outgassed at 250°C overnight (14 hours). After cooling to ambient temperature, a 'pre-fluorination' routine was undertaken, whereby samples were reacted with BrF₃ at ambient temperature for ~2 hours, to remove any surficial contamination. Fluorination was subsequently undertaken at 450°C overnight (14 hours) to release molecular oxygen. This was then 'cleaned' from reaction products such as SiF₄ that may be removed cryogenically by a liquid nitrogen trap, before reaction with a platinised graphite rod, heated to ~625°C. CO₂ thus produced was isolated by a liquid nitrogen trap and remaining 'non-condensable' gases pumped out. The CO₂ yield was measured by capacitance manometer, as a check of conversion efficiency, prior to isotopic analysis using a VG® SIRA Series II mass spectrometer.

2.5 Results

Fluid inclusion δD values were generally reproducible to within $\pm 2\%$. The precision of the $\delta^{18}O$ results, being related to the magnitude of the associated procedural 'blank' during fluorination, was largely dependant on the nature of samples reacted earlier and the overall 'conditioning' of the line. Ultimately, variation of $<0.1\%$ between replicates could be obtained; overall reproducibility, however, was generally to within $\pm 0.2\%$.

Results of the δD and $\delta^{18}O$ analyses, characterising various stages of palæo-hydrothermal activity in the Cornubian region, are shown in Table 2.1. For conversion of the quartz $\delta^{18}O$ values to those of the coexisting water at the estimated temperature of fluid trapping, the equilibrium fractionation curve of Matsuhisa *et al.* (1979) was used. With the usual notation,

$$1000 \log_e \alpha \approx \delta_1 - \delta_2 = A (10^6 T^{-2}) + B, \quad \text{where } A = 3.34, B = -3.31$$

These coefficients are for the temperature range 250-500°C. It may be noted that the water $\delta^{18}O$ values obtained are consistently 0.5‰ enriched in ^{18}O compared to the equivalent data determined using values of the A and B coefficients given by Friedman and O'Neil (1977) or by Zhang *et al.* (1989).[†] Furthermore, the accuracy of the water $\delta^{18}O$ values is necessarily dependant on the reliability of fluid trapping temperatures as estimated from microthermometric data. For an error of $\pm 25^\circ C$ at 300°C, the corresponding difference in $\delta^{18}O$ of the water is $\pm 0.9\%$, using the data of Matsuhisa *et al.* (1979).

For fluids associated with N-S-trending veins, the $\delta^{18}O$ values given in Table 2.1 were determined by extrapolation of the fractionation data of Matsuhisa *et al.* (1979) beyond their range of validity, so appropriate caution needs to be exercised in the use of these data. Furthermore, the values were also consistently ^{18}O -enriched compared to equivalent data determined by the extrapolation of alternative fractionation factors. At the lowest temperature (120°C), the ^{18}O enrichment was 0.7‰ over that obtained from the data of Friedman and O'Neil, and 0.4‰ enriched with respect to values calculated from Zhang *et al.* (1989).

[†] The exact coincidence between the water $\delta^{18}O$ data calculated using the fractionation factors of either Friedman and O'Neil (1977) or Zhang *et al.* (1989) over the temperature range 250-500°C is surprising, given that the respective values of the A and B coefficients differ. The respective ranges of validity of the fractionation factors are 200-500°C for Friedman and O'Neil (1977); 180-550°C for Zhang *et al.* (1989).

Table 2.1

Results of δD and $\delta^{18}O$ analyses, quartz-hosted palæo-hydrothermal fluids, S W England

a) Quartz±tourmaline±cassiterite±haematite assemblages hosted by the Dartmoor granite

Sample reference	Paragenetic Stage [†]	$\delta^{18}O$ quartz (‰)	Estimated T(°C) of fluid trapping	$\delta^{18}O$ water (‰)	δD water (‰)
<i>Golden Dagger mine</i>					
SW-89-159	I	13.9	325 ^a	7.9	-26
SW-89-160	I	13.1	"	7.1	-24
SW-89-163	II (III)	13.1	"	7.1	-31
SW-89-162	II (III)	13.6	"	7.6	-24
SW-89-161	III (II)	10.6	"	4.6	-30
<i>East Vitifer mine</i>					
SW-89-156	II	14.1	325 ^a	8.1	-27
SW-89-155	II	13.6	"	7.6	-24
SW-89-154	III (II)	14.1	"	8.1	-33
<i>Barracott mine</i>					
SW-89-164	II	14.1	325 ^a	8.1	-31
<i>Birch Tor & Vitifer mine</i>					
SW-81-14	II	14.0	325 ^a	8.0	-
<i>Great Rock mine</i>					
SW-89-157	III	20.8	180 ^b	7.8	-29

b) Early-stage fluids characterised by associated with W±Sn oxide occurrence

Sample reference	Locality	$\delta^{18}O$ quartz (‰)	Estimated T(°C) of fluid trapping	$\delta^{18}O$ water (‰)	δD water (‰)
<i>Hemerdon area</i>					
HEM-80-1	<i>Hemerdon mine</i>	14.6	400 ^a	10.5	-24
HEM-80-39	"	15.0	"	10.9	-25
HEM-80-44	"	15.0	"	10.9	-30
HEM-80-47	"	14.6	"	10.5	-24
<i>Cligga Head</i>					
CH-88-1	<i>Cligga Head cliffs</i>	13.9	360 ^c	8.9	-15
<i>Gunnislake - Kit Hill region (E-W-trending veins)</i>					
SW-84-18	<i>Old Gunnislake mine</i>	10.0	380 ^d	5.5	-17
OG-88-1	"	9.8	"	5.3	-18
SW-84-15	<i>Drakewalls mine</i>	13.6	340 ^d	8.0	-16
SW-84-16	"	11.9	"	6.3	-11
SW-84-20	<i>South Bedford mine</i>	12.2	350 ^d	6.9	-16
SW-84-25	<i>Prince of Wales mine</i>	12.6	320 ^d	6.4	-
SW-84-27	"	12.9	"	6.7	-14
<i>Carnmenellis granite vicinity (Carn Brea granite)</i>					
SC-88-2	<i>South Crofty mine</i>	11.6	320 ^e	5.4	
SC-88-3	"	14.6	"	8.4	-17
<i>St Austell region</i>					
CD-88-1	<i>Castle-an-Dinas mine</i>	9.5	500 ^f	7.2	-10

† See note (2) overleaf

Table 2.1 (continued)

c) Fluids characterised by association with sulphide-stage mineralisation

Sample reference	Locality	$\delta^{18}\text{O}$ quartz (‰)	Estimated T(°C) of fluid trapping	$\delta^{18}\text{O}$ water (‰)	δD water (‰)
<i>Gunnislake - Kit Hill region (E-W-trending veins)</i>					
SW-84-19	Wheal Arthur mine	12.9	310 ^d	6.4	-14
SW-84-23	Okeltor mine	13.0	310 ^g	6.5	-21
SW-84-22	Cotehele Consols	15.0	305 ^d	8.3	-
SW-84-17	Wheal Emma mine	15.1	280 ^d	7.5	-32
<i>Eastern margin of the Bodmin Moor granite</i>					
SW-84-1	South Caradon mine	13.5	310 ^g	7.0	-22
SW-84-2	West Caradon mine	15.1	300 ^g	8.2	-28

d) Late-stage fluids associated with N-S-trending veins (Pb, Zn sulphides in quartz/fluorite gangue)

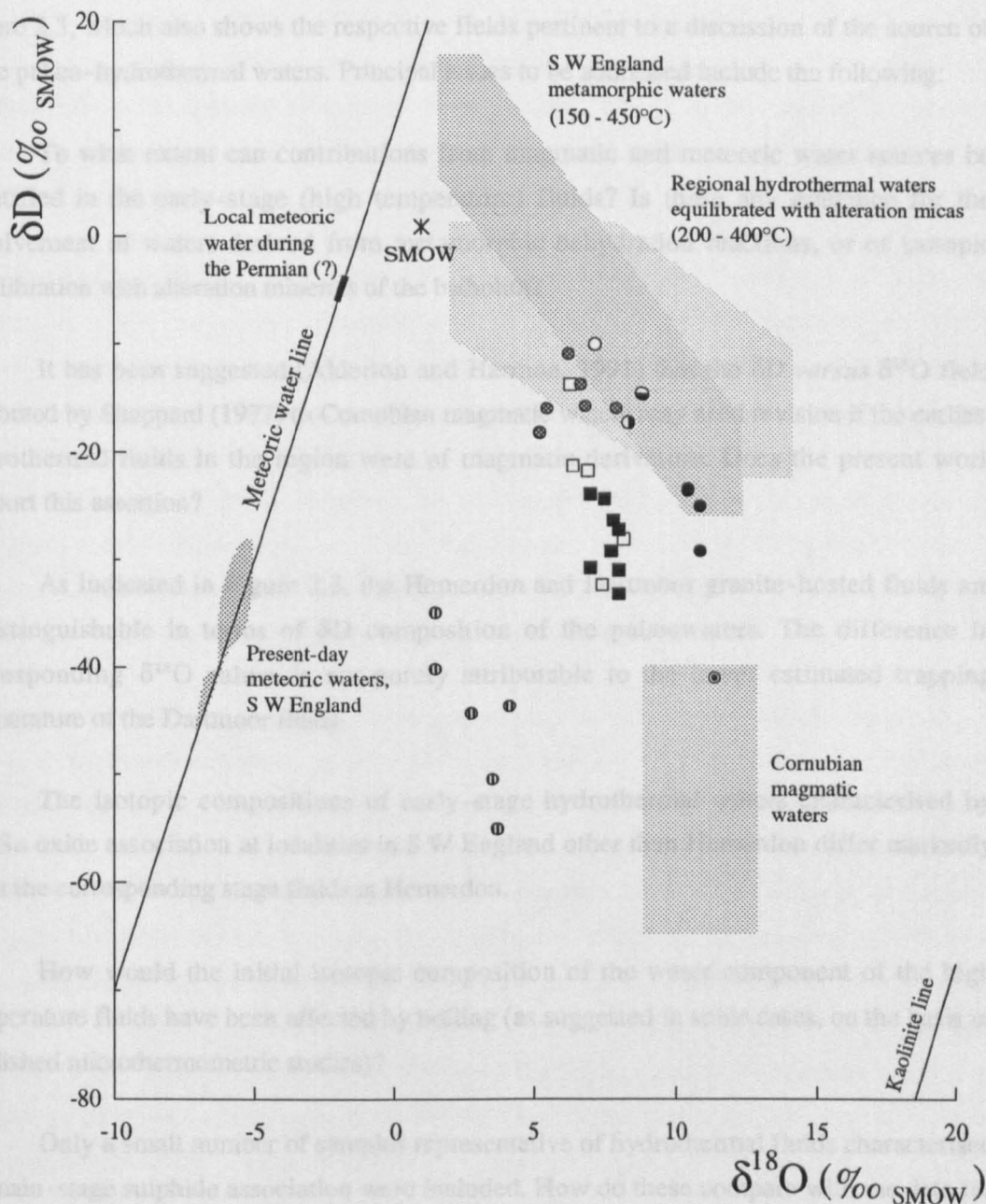
Sample reference	Locality	$\delta^{18}\text{O}$ quartz (‰)	Estimated T(°C) of fluid trapping	$\delta^{18}\text{O}$ water (‰)	δD water (‰)
<i>Tamar valley region</i>					
SW-88-4	Lockridge mine	17.9	170 ^h	4.2	-44
SW-88-5	North Hooe mine	23.0	120 ^h	4.7	-
SW-88-6	Buttspill mine	16.0	160 ^h	1.5	-40
SW-88-8	South Tamar Consols	15.2	170 ^h	1.5	-35
SW-88-9	"	16.5	170 ^h	2.8	-44
SW-84-9	Wheal Wrey mine	20.8	130 ⁱ	3.6	-51
SW-84-10	"	17.4	170 ⁱ	3.7	-55
SW-84-12	Wheal Mary Ann mine	18.9	160 ⁱ	4.4	-

Notes:

- 1). All isotopic results are with respect to SMOW. Hydrogen isotope data were normalised to the SMOW-SLAP scale.
- 2). The Dartmoor granite-hosted fluids are classified by paragenetic association, using the stages defined by Scrivener (1982). Stage I fluids were the earliest. Where a stage is shown in parentheses, this indicates minor veining (overprinting) by the associated fluid.
- 3). $\delta^{18}\text{O}$ values of the palæo-waters were calculated from those of the coexisting quartz by use of the fractionation data of Matsuhisa *et al.* (1979) in conjunction with fluid trapping temperatures estimated from published fluid homogenisation temperatures, where available. In several cases, polished wafers of the samples used for the present study had previously been investigated microthermometrically by other workers. Sources of reference for the estimated trapping temperatures were as follows:
 - (a) Shepherd *et al.* (1985)
 - (b) R C Scrivener, unpublished data
 - (c) Jackson *et al.* (1982)
 - (d) Bull (1982)
 - (e) Scrivener *et al.* (1986)
 - (f) See text, Section 2.6.4
 - (g) Estimated from data (Bull, 1982) on comparable-stage fluids from the Gunnislake - Kit Hill region
 - (h) T J Shepherd, *pers. comm.* (cf. data on coexisting fluorites: Shepherd and Scrivener, 1987)
 - (i) Estimate based on the assumption of similarity to comparable-stage fluids from this region

Figure 2.3

δD versus $\delta^{18}O$ characteristics of quartz-hosted palaeo-hydrothermal fluids, SW England



Key

Early-stage fluids associated with oxide assemblages

- Dartmoor granite-hosted system, associated with quartz \pm tourmaline \pm cassiterite \pm hæmatite
- W \pm Sn oxide-associated quartz :*
- Hemerdon
 - ⊙ Gunnislake - Kit Hill area (E-W-trending veins)
 - ⊖ South Crofty
 - ⊙ Cligga Head
 - Castle-an-Dinas (St Austell area)

- Sulphide-associated (main stage) fluids from the Gunnislake - Kit Hill vicinity (E-W-trending veins) and eastern margin of the Bodmin Moor granite
 - ⊖ Late stage (N-S-trending) fluids, associated with Pb-Zn sulphides and fluorite, Tamar valley region
 - ⊙ Pegmatite pod, Gunheath, St Austell area (Lin, 1989)
- Fields for Cornubian magmatic water and regional hydrothermal waters are from Sheppard (1977)
 Present-day meteoric waters from Edmunds *et al.* (1984)
 SW England metamorphic waters from Primmer (1985)
 Kaolinite (weathering) line from Savin and Epstein (1970)

2.6 Discussion

2.6.1 Problems to be addressed

The results given in Table 2.1 are presented in a conventional δD versus $\delta^{18}O$ diagram in Figure 2.3, which also shows the respective fields pertinent to a discussion of the source of these palæo-hydrothermal waters. Principal issues to be addressed include the following:

- (i) To what extent can contributions from magmatic and meteoric water sources be identified in the early-stage (high temperature) fluids? Is there any evidence for the involvement of waters derived from metamorphic dehydration reactions, or of isotopic equilibration with alteration minerals of the batholith?
- (ii) It has been suggested (Alderton and Harmon, 1991) that the δD versus $\delta^{18}O$ field attributed by Sheppard (1977) to Cornubian magmatic waters may need revision if the earliest hydrothermal fluids in the region were of magmatic derivation. Does the present work support this assertion?
- (iii) As indicated in Figure 2.3, the Hemerdon and Dartmoor granite-hosted fluids are indistinguishable in terms of δD composition of the palæowaters. The difference in corresponding $\delta^{18}O$ values is not purely attributable to the lower estimated trapping temperature of the Dartmoor fluids.
- (iv) The isotopic compositions of early-stage hydrothermal waters characterised by $W\pm Sn$ oxide association at localities in S W England other than Hemerdon differ markedly from the corresponding stage fluids at Hemerdon.
- (v) How would the initial isotopic composition of the water component of the high temperature fluids have been affected by boiling (as suggested in some cases, on the basis of published microthermometric studies)?
- (vi) Only a small number of samples representative of hydrothermal fluids characterised by main-stage sulphide association were included. How do these compare with the data for oxide-stage fluids?
- (vii) Explanations proposed for the origin of fluids associated with later hydrothermal events in the region, as represented by cross-course quartz examples from the Tamar valley region, are considered in the light of the present stable isotope data.

2.6.2 The isotopic composition of magmatic water during batholith evolution: implications for the source of early-stage hydrothermal fluids, S W England

The D/H isotopic composition of granite magma is generally determined by the nature of the associated protolith source, together with any crustal material assimilated during emplacement. For most felsic magmas, magmatic water represents 'recycled' water, derived primarily from the melting of hydrous crust (Taylor, 1987). In the case of the granite intrusives of the Cornubian batholith, a significant proportion may be derived from the melting of sedimentary rocks.

Considering initially the early-stage (W±Sn oxide-associated) hydrothermal fluids at Hemerdon, which on the basis of published microthermometric data (Shepherd *et al.*, 1985) are believed to have been trapped at higher temperatures than other comparable-stage fluids included in the present investigation, it is apparent from Figure 2.3 that these fluids are significantly enriched in deuterium compared to Cornubian primary magmatic waters as defined by Sheppard (1977). However, the estimated trapping temperatures, high salinity (Shepherd *et al.*, 1985; Kelley *et al.*, 1986) and chemical composition (this work, Chapter 5) of these fluids are compatible with their derivation (at least in part) from an aqueous phase such as that which separates from crystallising magma (Burnham, 1979).

Further support for a magmatic-hydrothermal component in the system at Hemerdon is provided by the observation that the D/H composition of waters from several early transitional (pegmatitic and pneumatolytic stage) fluids associated with the St Austell granite (Lin, 1989), as determined by the present author during the course of the work described herein, falls within the same range as that of the Hemerdon fluids.[†] The similarity, in terms of hydrogen isotopic composition, with early-stage hydrothermal fluids (including those hosted by pegmatitic quartz) in the Dartmoor granite (Figure 2.3) is also notable. As shown on Figure 2.3, isotopic equilibration at ≤400°C of meteoric water with hydrogen-bearing minerals in the granites is not compatible with the palæowater D/H characteristics. An alternative explanation, invoking waters derived from metamorphic dehydration reactions at temperatures up to 450°C (Primmer, 1985) is considered separately (Section 2.6.4).

The validity of the boundaries of the isotopic composition field for Cornubian primary magmatic water, as derived by Sheppard (1977), has been called into question during recent studies. In particular, it has been suggested that the δD range be extended to -30‰ (Lin,

[†] The pegmatitic and pneumatolytic fluids from the St Austell region were of lower salinity (10-25 wt % NaCl equivalent) according to Lin (1989), who suggested that these hydrous fluids are representative of a phase which separated from the associated lithium mica granite during crystallisation of the latter.

1989) or even -15‰ (Alderton and Harmon, 1991). The suggestion offered here, however, is that such an appeal is unnecessary, on the basis of the following arguments:

(i) The primary magmatic water field represents waters equilibrated with a granitic melt (*i.e.* at temperatures \geq ~700°C), whereas hydrothermal fluids associated with early mineralisation of the Cornubian batholith were generally trapped at temperatures within the range 300-450°C.

(ii) Recent measurements by Alderton and Harmon (1991) of fluid inclusion δ D in granitic quartz from the Dartmoor, Bodmin Moor and St Austell granites, plot within the primary magmatic waters field as defined by Sheppard (1977).

(iii) As noted by Taylor (1987), the δ D value of magmatic water varies during magma degassing, resulting in a positive correlation between δ D and residual water content of igneous rocks. The δ D value of the initial exsolved aqueous phase will be enriched in deuterium by approximately 20-25‰, relative to the bulk magma. Consequently, the δ D value of water exsolved from many felsic melts is in the range -30 to -60‰, but the associated magmatic rocks may be significantly depleted in deuterium. The temperatures at which initial exsolution occurred are considerably higher than the inferred trapping temperatures of the early-stage hydrothermal fluids presently considered.

(iv) Late-stage magmatic water derived from a cooling cryptobatholith should be characterised by enrichment in deuterium, relative to the magmatic water exsolved during earlier stages, on the basis of isotopic equilibration with hydrous silicates formed during cooling. For example, assuming that the crystallisation temperature of biotite and hornblende in a granitic melt is ~700°C, reference to the fractionation factors of Suzuoki and Epstein (1976) shows that the associated hydrous phase should be approximately 30-40‰ enriched in deuterium, depending on the Fe/Mg ratio of the silicates. Hydrogen isotopic fractionation between magma and aqueous vapour in a crystallising pluton (open and closed systems) was modelled by Brigham and O'Neil (1985), who showed that primary hydrogen isotopic compositions were generally preserved in plutonic micas.

For these reasons, it is argued that the D/H characteristics of early-stage hydrothermal waters associated with high temperature alteration and mineralisation of the Cornubian batholith is not incompatible with a magmatic origin.

2.6.2.1 The effect of fluid boiling on the isotopic characteristics of the waters

The coexistence of liquid-rich and vapour-rich inclusions may be assumed to represent a boiling assemblage if there is additional evidence that the inclusions are contemporaneous,

are characterised by the same homogenisation temperatures (Roedder, 1984), and have compositions consistent with end-member phases. With regard to the S W England palaeo-hydrothermal systems, Shepherd *et al.* (1985) suggested that such evidence for fluid boiling is present at Hemerdon. Boiling of early transitional fluids associated with the St Austell lithium mica granite magma was reported by Lin (1989), who also noted a correlation between the extent of boiling and deuterium enrichment. Bull (1982), in a comprehensive study of hydrothermal mineralisation in the Gunnislake-Kit Hill region, reported that no boiling assemblages were found in any E-W-trending sulphide-associated veins and that all inclusions homogenised into the liquid phase. For the earlier, quartz±cassiterite±wolframite veins in the region, boiling assemblages were evident in only a single specimen (from the Prince of Wales mine).

For pure water at saturated vapour pressure, the compilation of Friedman and O'Neil (1977) documents D/H and $^{18}\text{O}/^{16}\text{O}$ fractionations between liquid and vapour. For pure water, $\alpha_{\text{L-V}}(\text{D}/\text{H})$ is greater than unity at $<\sim 220^\circ\text{C}$ and becomes less than unity above this 'cross-over' temperature.† The value of the cross-over temperature for NaCl solutions decreases with increasing salt concentration, being 205°C for 1 molal NaCl and 165°C for 4 molal solutions, under vapour-saturated conditions (Kazahaya, 1986). For the trapping temperature range of the early-stage hydrothermal fluids considered in the present work, *i. e.* well above the associated $\alpha_{\text{L-V}}(\text{D}/\text{H})$ cross-over temperatures, any isotopically-equilibrated separation of a vapour phase through boiling results in deuterium enrichment of the vapour and corresponding deuterium depletion of the residual liquid phase. Deuterium enrichment of the fluids by separation from a liquid phase during boiling (as favoured by Alderton and Harmon, 1991) would require that the high salinities of early hydrothermal fluids hosted by the Dartmoor and Hemerdon Ball granites were the result of interaction with wall-rocks, rather than the expression of a primary magmatic component.

2.6.2.2 pH effects

An aqueous fluid separating from crystallising magma is likely to be saline and relatively acidic (Burnham, 1979; Bottrell and Yardley, 1988). As the dissociation constant of D_2O is significantly lower than that of H_2O under the same conditions, a consequence is that OH^- and H_3O^+ ions have very much lower deuterium concentrations (at isotopic equilibrium) than the water from which they were derived (Deines, 1979). Consequently, hydrogen isotope fractionation between hydrogen-bearing minerals and coexisting water may be significantly affected under strongly acidic (or alkaline) solutions. Appropriate fractionation data are

† The vapour pressure ratio $p(\text{H}_2\text{O})/p(\text{D}_2\text{O})$ exhibits a similar cross-over point near 220°C , as does the corresponding $p(\text{H}_2^{18}\text{O})/p(\text{H}_2^{16}\text{O})$ ratio.

unknown to the present author, however, so the magnitude of any such effect under magmatic-hydrothermal conditions cannot be assessed.

2.6.3 Pegmatitic and early mineralising fluids of the Dartmoor granite

Figure 2.3 shows that the Dartmoor granite-hosted hydrothermal fluids plot in a distinctive field on the δD vs. $\delta^{18}O$ diagram, away from early-stage fluids characterised by W±Sn oxide association in the region. The δD values coincide with those of W±Sn oxide-associated fluids at Hemerdon, however. There is no apparent dependence of the isotopic characteristics on associated paragenetic stage at Dartmoor (see Table 2.1), at least for the examples investigated in the present study, indicating that the corresponding fluids were derived from a common source.†

The difference in $\delta^{18}O$ characteristics between the Dartmoor-hosted fluids and those at Hemerdon is largely due to trapping temperature differences, estimated from the fluid inclusion microthermometric data of Shepherd *et al.* (1985) and Alderton and Harmon (1991). For example, if the Dartmoor Stage I and Stage II examples are recalculated to a quartz-water fractionation temperature of 400°C (as used for the Hemerdon fluids) rather than 325°C, the $\delta^{18}O$ values are increased by 1.9‰. There remains, however, a systematic discrepancy of <1‰, which is possibly attributable to the notably lower 'S'-type character (Chappell and White, 1974) of the Dartmoor granite, as discussed elsewhere in the present work and as referred to by Darbyshire and Shepherd (1985, 1987).

On the basis of the above discussion, and with reference to Table 2.1 and data reported in Lin (1989), it is suggested that the δD range of ancient magmatic-hydrothermal fluids in the Cornubian province is from *ca.* -21 to -33‰. This refers to fluids exsolved during the late stages of crystallisation of granitic magma, and which probably continued to undergo equilibrated isotopic exchange with hydrogen-bearing minerals in the granite during subsequent cooling, possibly down to the temperature of fluid trapping (quartz crystallisation). A continuum is presumed to exist between the magmatic-hydrothermal fluids trapped at 300-400°C and those fluids related to the formation of higher temperature rocks such as are associated with granitic pegmatites in the region.

† Table 2.1 shows that sample SW-89-161, from Golden Dagger mine, is anomalously depleted in ^{18}O compared to all other Dartmoor granite-hosted samples investigated. This sample was also characterised by a highly anomalous fluid electrolyte composition (Chapter 5). On these grounds, it is considered justified to exclude this sample from the complete data set illustrated in Figure 2.3.

2.6.4 Early-stage fluids characterised by W±Sn oxide association

Figure 2.3 illustrates the distinctive nature of the Hemerdon fluids, in terms of isotopic composition of the waters, compared to fluids of the same paragenetic association at other localities in SW England. As noted in Section 2.6.3, the relative enrichment in ^{18}O at Hemerdon is largely a reflection of the higher trapping temperature assumed for these fluids, with a minor component possibly deriving from the high degree of sedimentary material incorporated in the parent magma.[†] At other localities in the province, however, the fluids are notably more enriched in deuterium and are unlikely to be exclusively of magmatic origin.

Further evidence for the involvement of non-magmatic fluids at localities other than Hemerdon is provided by salinity estimates of the respective fluid inclusions, as determined by microthermometric analysis. Sources of the salinity data, together with the actual values, are discussed in detail in Section 5.5.2. A primary feature is that many of the fluids (excluding those at Hemerdon) were shown to be of relatively low salinity. An explanation for the observed δD versus $\delta^{18}\text{O}$ characteristics of early-stage fluids at localities such as Cligga Head and the Gunnislake-Kit Hill area is therefore that an initial magmatic-hydrothermal component was diluted by mixing with low salinity groundwaters. Considering the hypothesis that meteoric (rather than 'metamorphic') water was the source of this second fluid, there are several issues to be addressed:

- (i) At what stage did meteoric water enter the system, *i.e.* during early fracturing of the host rock, or during subsequent hydrothermal circulation?
- (ii) What were the respective temperatures immediately prior to fluid mixing? This has a direct bearing on the extent of water-rock interaction that the meteoric component would have experienced.
- (iii) Related to the above, it would seem unreasonable to postulate that a mixing line be drawn on Figure 2.3 between the presumed value of contemporaneous meteoric water and an 'end member' magmatic-hydrothermal component, the latter being represented by an area on Figure 2.3 that includes the Hemerdon and Dartmoor samples. Such a mixing line would only be valid if the isotopic composition of the original meteoric component was not modified by water-rock interaction.

If isotopic exchange between meteoric water and the country rocks occurred, in the vicinity of the hydrothermal system, it is likely that the isotopic characteristics of the meteoric water

[†] Darbyshire and Shepherd (1987) showed that the Hemerdon Ball granite has significantly greater 'S'-type character than the adjacent Dartmoor pluton, on the basis of Nd isotopic composition.

would have been modified by ^{18}O enrichment, as shown in Figure 2.1. On this basis, the mixing line referred to above would connect the proposed magmatic-hydrothermal 'end member' with a modified meteoric water component, the latter being represented by a box shifted to the right (on Figure 2.3) from the position shown for Permian meteoric water. This indeed provides a plausible explanation for the experimental data. The degree of $\delta^{18}\text{O}$ scatter for fluids associated with $\text{W}\pm\text{Sn}$ oxide assemblages other than at Hemerdon is then related to the variation in fluid trapping temperature, degree of sedimentary character of the associated parent granite, and the extent of prior interaction between the meteoric fluid component and the country rocks.

As an alternative (or in addition) to dilution of the magmatic-hydrothermal fluid by meteoric water, the possibility of 'metamorphic' water involvement needs to be considered. On the basis of the data available, it is not possible to distinguish unambiguously between 'metamorphic' water and that derived from a meteoric fluid which has subsequently become enriched in ^{18}O through reaction with the local country rocks. As noted by Sheppard (1977), however, the sedimentary country rocks had been regionally metamorphosed (albeit at very low grade, at the present level of exposure) prior to the emplacement of the Cornubian granites; much of any formation water or connate water would probably have been removed during this period. A significant input of metamorphic water to the hydrothermal fluids would therefore have required that the associated dehydration reactions occurred at depths substantially below those of the current level of exposure.

An important additional consideration is whether the early hydrothermal fluid systems were contemporaneous with granite emplacement, or whether the hydrothermal activity and related mineralisation is significantly younger. Each component intrusive of the batholith needs to be considered independently (Chesley *et al.*, 1993). For example, the suggestion that main-stage mineralisation at South Crofty mine post-dates the host (Carn Brea) granite by ~20Ma (Darbyshire and Shepherd, 1985) indicates that there may have been scope for an influx of local groundwaters into early fracture systems of the cooling pluton. Possibly, the extent of dilution of the initial magmatic-hydrothermal fluid is directly related to the magnitude of any hiatus between granite emplacement and the initial stages of associated hydrothermal activity.

The unusual nature of the early hydrothermal system at Castle-an-Dinas (St Austell region) is discussed elsewhere in the present work (Sections 4.8.2 and 5.5.2). The hydrothermal system at this locality pre-dates the existing Castle-an-Dinas granite (Dines, 1956) and was therefore derived from an unidentified intrusive of unknown age (Beer and Ball, 1987). Subsequent intrusion of the Castle-an-Dinas granite may have resulted in heating of the early quartz veins to temperatures higher than those associated with initial vein formation.

2.6.5 'Main-stage' (sulphide-associated) hydrothermal fluids

The limited data presented in Figure 2.3 and Table 2.1 for fluids associated with chalcophile-element assemblages generally refer to higher-temperature episodes from a relatively small area of the Cornubian region. As such, they must be regarded as somewhat cursory, permitting only tentative conclusions to be drawn. Compared to the earliest oxide-associated episode of hydrothermal activity in the Gunnislake-Kit Hill vicinity, the stage characterised by association with sulphide assemblages was of considerable complexity (Bull, 1982), as evident from the corresponding mineral paragenesis and wide range of fluid salinities and trapping temperatures. A hydrothermal continuum probably occurred, resulting in some overprinting of earlier fluids. The salient feature of the isotopic data is that the δD range of these fluids appears to encompass the various fields presented for early-stage oxide-associated fluids throughout S W England. The results are therefore compatible with the idea of an initial magmatic-hydrothermal fluid component diluted to varying degree by mixing with local meteoric water, as suggested by Shepherd *et al.* (1985).

2.6.6 Low temperature, 'cross-course' fluids

The δD and $\delta^{18}O$ characteristics of the water component of these late-stage fluids (age ~235Ma according to Darbyshire and Shepherd, 1990) are quite distinct from those of the higher temperature hydrothermal regimes, as shown in Figure 2.3. Emphasis has hitherto been placed on the possible involvement of formation waters derived from sedimentary basinal brines (Alderton and Harmon, 1991; Shepherd and Scrivener, 1987; Scrivener *et al.*, 1986; Shepherd *et al.*, 1985; Bull, 1982), largely on the basis of microthermometric evidence that the low-temperature fluids are enriched in calcium. Such an origin for these waters is hard to reconcile with the present stable isotope data, however, as is the Mesozoic seawater explanation of Durrance *et al.* (1982).

Fluid inclusion leachate analysis (Chapter 5, this work) has revealed that calcium enrichment is by no means confined to the cross-course fluids. Indeed, for early hydrothermal fluids hosted by the Dartmoor granite, all investigated samples contained higher molar abundances of calcium than potassium, even in the case of the earliest pegmatitic fluids. Clearly, geological considerations dictate that such fluids were not directly derived from sedimentary rocks. The relative abundance of calcium in the Cornubian hydrothermal fluids is therefore not necessarily a reliable guide to whether the fluid composition was primarily derived in a high or low temperature regime. Furthermore, the range of bulk salinity values of cross-course fluids from the Tamar valley, at 19-27 weight % NaCl equivalent (Shepherd and

Scrivener, 1987)[†], is comparable to that found in higher-temperature hydrothermal fluids associated with early pegmatite formation and oxide assemblages in S W England.

The isotopic variations of formation waters in sedimentary basins have received much investigation, as reviewed by *e.g.* Longstaffe (1987). Formation waters from various basins follow a linear trend away from the meteoric water line, towards enrichment in D and ¹⁸O. Furthermore, for a given basin, those waters trapped at higher temperatures (and with higher salinities) are generally the most enriched in D and ¹⁸O. Formation waters from high latitudes tend to plot along trends that intersect the meteoric water line at lower δD and $\delta^{18}O$ values than do formation waters from basins located at lower latitudes. The implication is that meteoric water comprises a significant fraction of the formation waters in such basins. With regard to the present results, the isotopic data (in particular, the low δD values) are not consistent with either a metamorphic water or Permo-Triassic meteoric water source. The only mechanism known to the author whereby significant deuterium depletion may be achieved in a formation water is that proposed by Knauth and Beeunas (1986), which invokes conditions of extreme evaporation of seawater, such as associated with halite formation. In Devon during Permo-Triassic times, however, conditions were not appropriate to salt formation (unlike in adjacent Somerset), as salt deposits and halite are virtually unknown in the region (Laming, 1982).

Towards an explanation of the present isotopic data, it is noted that the δD values lie within the field of the unaltered Cornubian granites and earliest hydrothermal alteration. It is therefore tentatively proposed here that the late-stage fluids from the Tamar valley region may be derived from fluid inclusions in an unidentified granite (probably deeply-buried, rather than one of the outcrops of the Gunnislake-Kit Hill vicinity), released by a changing tectonic stress regime. Mobilisation of these fluids in a low-temperature hydrothermal system, together with extended low-temperature interaction with the country rocks (such as proposed elsewhere to explain the notable ¹⁸O-depletion in Canadian Shield brines) could conceivably account for the present experimental findings.

2.7 Summary and conclusions

The isotopic evidence presented here is consistent with the view that hydrothermal fluids associated with tourmaline-dominated and greisen mineralisation of the Dartmoor granite were of magmatic derivation. This is also in accord with the relatively high salinities and

[†] The fluid salinity measurements reported by Shepherd and Scrivener (1987) were actually made on fluorite, rather than coexisting quartz, as the quartz collected for that study was too fine-grained to support inclusions of size >2mm (Shepherd *et al.*, 1985).

trapping temperatures (Shepherd *et al.*, 1985). The relative enrichment in deuterium compared to Cornubian primary magmatic waters (Sheppard, 1977) may be explained on the basis that the primary magmatic waters field represents equilibration with a granitic melt (*i. e.* at temperatures $\geq \sim 700^\circ\text{C}$), whereas the hydrothermal systems were generally trapped at temperatures within the range $300\text{-}450^\circ\text{C}$. Isotopic exchange between the fluids and hydrous silicates of the host granite at sub-solidus temperatures is the most probable explanation for the deuterium enrichment.

The uniformity and values of δD and $\delta^{18}\text{O}$ characteristics of the palæowaters associated with early mineralisation of the Dartmoor granite, from quartz \pm tourmaline \pm cassiterite \pm hæmatite mineralisation, to later fluids as characterised by quartz+hæmatite deposition, supports the idea of protracted magmatic-hydrothermal activity. Furthermore, the relative invariance of the isotopic data is in good agreement with the similarity of the solute electrolyte compositions associated with the different parageneses (this work, Chapter 5).

A comparative assessment of hydrothermal fluids characterised by association with early-stage W \pm Sn oxide assemblages in S W England has shown that, whereas the total δD range is *ca.* 20‰, a clear distinction may be made between the Hemerdon system and those elsewhere in the province. The similarity in δD values between the Hemerdon fluids and those of the Dartmoor system, together with thermometric evidence (Shepherd *et al.*, 1985; Kelley *et al.*, 1986), supports the hypothesis that these fluids were derived from an aqueous phase that separated from granite magma and that meteoric waters were not of significance. For other localities in the region, the isotopic data (and generally lower salinities) are consistent with the dilution of a magmatic-hydrothermal phase by local meteoric water that had experienced ^{18}O enrichment through water-rock interaction at elevated temperatures. It is tentatively proposed that there may be a correlation between the length of the hiatus by which the earliest hydrothermal activity post-dated granite emplacement, and the amount of meteoric water that entered the hydrothermal system. More data are needed, particularly with regard to the relative timing of hydrothermal events, to establish the viability of this proposal. Recent thermo-chronological studies by Chesley *et al.* (1993) and Chen *et al.* (1993) suggest that early-stage oxide mineralisation was contemporaneous with the time at which the respective host granite had cooled to $300\text{-}400^\circ\text{C}$, although the cooling rates of individual plutons are a matter of dispute.

The limited isotopic data obtained for hydrothermal fluids characterised by association with (main-stage) sulphide assemblages shows a relatively wide range of δD values that may also be interpreted as the result of dilution, to varying degree, of a magmatic-hydrothermal fluid. Such a scenario has been proposed elsewhere (*e.g.* Shepherd *et al.*, 1985). A hydrothermal continuum probably exists, extending from the earliest pegmatitic fluids to those

characterised by sulphide assemblages.† Chen *et al.* (1993) support the view that some chalcophile element mineralisation was coeval with the lithophile stage.

Waters derived from metamorphic dehydration reactions of *e.g.* chlorite or illite at high crustal levels are not considered to have made a significant contribution to the hydrothermal system. Evidence for this is provided by the narrow range of δD values at Hemerdon: the fluids are characterised by relatively high trapping temperatures (hence are the most likely to have incorporated metamorphic water) and yet fluids from killas-hosted quartz veins are indistinguishable from those hosted by the granite, in terms of δD value of the palæowater. That the values are also indistinguishable from those of the early hydrothermal system of the central region of the Dartmoor granite, where little or no direct contact with sedimentary rocks can have occurred, further supports this case.

The suggestion is offered that the δD and $\delta^{18}O$ characteristics of palæowaters associated with later N-S-trending structures in the Tamar valley region are compatible with a fluid origin based on the release of water from fluid inclusions in an unidentified (probably deeply buried) granite component of the underlying batholith. This may have occurred as a result of changes in the regional tectonic stress field. Subsequent oxygen isotopic exchange between the fluid and the country rocks, under low temperature conditions, could conceivably account for the relatively low $\delta^{18}O$ values.

† Arsenopyrite is actually one of the earliest minerals in the paragenetic sequence (Stone and Exley, 1985).

Chapter 3

The occurrence and stable isotope characterisation of carbon in palæo-hydrothermal fluids, SW England.

3.1 Synopsis

Carbon occurs locally in both oxidised and (to a lesser extent) reduced form as a trace component of ancient fluids associated with the earliest stages of hydrothermal mineralisation of the Cornubian batholith, SW England, being particularly associated with the occurrence of W±Sn oxide assemblages. Reported here is an investigation of regional and local variations in the associated fluid inclusion carbon abundance, speciation and stable isotope characteristics. Such information may be used to constrain models relating to the source of this component in terms of crustal carbon reservoirs and ultimately to further understanding of the origin of fluids that contributed to the large-scale hydrothermal evolution of the batholith.

A preliminary comparison with examples of 'transitional' pegmatitic and pneumatolytic fluids that preceded hydrothermal mineralisation in the region was undertaken. The purpose was to establish whether, on the basis of carbon abundance and $^{13}\text{C}/^{12}\text{C}$ isotopic characteristics, hydrothermal activity associated with the initial stages of oxide mineralisation could be linked to earlier processes characteristic of magmatic differentiation, in view of hypotheses advocating that a continuum relates pegmatitic and subsequent stages of (high temperature) hydrothermal evolution in the region.

The speciation and stable isotope characteristics of carbon in pegmatitic and early hydrothermal oxide-associated fluids of the Cornubian batholith are summarily compared with corresponding data, obtained during the present investigation, from (i) fluids associated with quartz-wolframite mineralisation at Carrock Fell, NW England, where the presence of carbon-bearing fluid components is well established and where quartz-wolframite deposition similarly occurred predominantly in close proximity to the margin of the associated granite pluton; (ii) fluids associated with early hydrothermal mineralisation of the Yanshanian granites of southern China, where carbon dioxide has been shown to be a significant palæofluid component and where recent studies have highlighted similarities with early evolution of the Cornubian batholith.

A critical assessment of experimental techniques used for the extraction of fluid inclusion carbonaceous volatiles for subsequent $^{13}\text{C}/^{12}\text{C}$ isotope ratio analysis at the sub-micromole level was of fundamental importance to the present investigation. In particular, the application

of stepped heating procedures to release carbon dioxide and coexisting methane from vesicles in quartz was investigated, with particular reference to the problems of associated adventitious contamination. An 'optimised' stepped heating procedure was devised, which was then also applied in conjunction with high-sensitivity, static vacuum mass spectrometry, to a preliminary investigation of fluid inclusion carbon stable isotope ratio analysis at the sub-nanomole level.

An attempt was made to apply the advantages conferred by this high sensitivity approach to address the question of whether carbon present at very low abundances in early-stage hydrothermal fluids, as found on a regional scale associated with the earliest pegmatitic quartz and tourmaline+quartz±cassiterite mineralisation of the Dartmoor granite, could be shown to be isotopically similar to (and therefore probably derived from a similar source as) the more abundant palæofluid carbon characterised by association with W±Sn oxide minerals elsewhere within the batholith.

3.2 Introduction

3.2.1 Carbon reservoirs and geochemical cycles

The terrestrial geochemistry of carbon has been inextricably linked with biological processes operating on a global scale throughout Earth's history. That life forms have been identified in Archean rocks of age 3.5×10^9 a (Schopf and Klein, 1992, and references therein) is testament to the existence and ubiquity of life almost as far back as the surviving rock record. Indeed, the sedimentary rocks that in general cover the continents of the present-day Earth contain a substantial amount of carbon-bearing compounds of biogenic origin. Estimates of the relative sizes of present-day major crustal reservoirs of carbon indicate that sedimentary carbonate rocks constitute ~73% of the total inventory, with most of the remainder being in the form of coal, petroleum and natural gas, oil shales and tar sands, together with disseminated amorphous carbon in sedimentary rocks (Faure, 1986).

Despite the fundamental role of the atmosphere, hydrosphere and biosphere in the carbon geochemical cycle, the total amount of carbon contained by these reservoirs presently amounts to only 0.046% of that stored in the Earth's crust (Holland, 1984, Table 3.5). This indicates that, unlike Ne or Ar, nearly all of the carbon degassed (as CO₂) from the Earth's interior over geological time has been transferred from the atmosphere to the crust (to reside primarily as a constituent of organic compounds, graphite, and carbonates of calcium and magnesium) and has been recycled by weathering and by CO₂ release during the metamorphism of sedimentary rocks (Holland, 1984). An analysis of the carbon cycle by Holland (1978) suggested that present-day degassing of 'juvenile' CO₂ accounts for probably no greater than a few percent of the rate at which carbon is being recycled by the

metamorphism of sedimentary rocks. Zhang and Zindler (1993) estimated that the CO₂ content of present-day degassed mantle amounts to (72±10)% of the total 'degassable' CO₂ reservoir, consistent with the idea that most CO₂ has been recycled from the Earth's surface into the degassed mantle, by subduction. The same authors suggested that recycling of N₂ back into the mantle occurs on a much smaller scale. It has even been suggested (Wood, 1993) that the Earth's core may contain approximately 2-4 wt% carbon (as Fe₃C); substantially more than in iron meteorites.

3.2.2 Stable isotopic characteristics of near-surface carbon reservoirs

The pioneering work of Craig (1953) and later Wickman (1956) heralded the beginning of carbon stable isotope geochemistry. Subsequent extensive examination of the carbon isotopic composition of naturally-occurring terrestrial matter has served to extend the range of values reported, whilst establishing well-defined fields for specific carbon reservoirs.[†] Carbon stable isotope ratios are, by convention, usually presented in terms of a shift in parts per thousand (per mil) from an internationally-agreed standard; results are thus reported in the 'delta' notation, where:

$$\delta^{13}\text{C} = 10^3 \times \left[\left[\left(\frac{^{13}\text{C}/^{12}\text{C}}{\text{sample}} \right) / \left(\frac{^{13}\text{C}/^{12}\text{C}}{\text{standard}} \right) - 1 \right] \right] \text{‰}$$

The standard (international reference), as first used at the University of Chicago by Craig and co-workers in the 1950's, is CO₂ prepared from a Cretaceous belemnite (*Belemnitella Americana*) sample from the Peedee Formation of South Carolina, USA. The supply of this belemnite, referred to as PDB, has been exhausted for many years, so working standards calibrated against PDB are used nowadays. The currently-accepted value for the absolute abundance (¹³C/¹²C) ratio in PDB is 0.0112372 (Craig, 1957).

Estimates for the average δ¹³C value of crustal carbon are generally in the range -5 to -7‰ (Fuex and Baker, 1973; Javoy *et al.*, 1986; Holser *et al.*, 1988), similar to the consensus value for the upper mantle.

One of the primary processes giving rise to changes in the isotopic composition of carbon is its abstraction from the atmospheric CO₂ reservoir (δ¹³C = -7‰) and surface waters by photosynthetic fixation. The overall fractionation associated with this process produces ¹³C-depletion in the resulting metabolites.

[†] Terrestrial ¹²C/¹³C values generally occur within the limits 89±4, similar to the range characterising bulk stony meteorites (Pillinger, 1984; Ash, 1990), in contrast to the large range discovered in extraterrestrial material (see *e.g.* Zinner and Epstein; 1987; Zinner *et al.*, 1987; Stone *et al.*, 1990; Amari *et al.*, 1990).

Between the time of photosynthetic fixation and eventual incorporation into sediment, the organic carbon reservoir is exposed to many oxidative processes, with the result that only a very small fraction of the total inventory is retained in the sediments. The marine and continental environments reflect limiting ('end member') conditions under which organic matter may be incorporated into sediments. Under marine conditions, the primary source is autochthonous plankton; this consists largely of proteins, carbohydrates and lipids, characterised by relatively high H/C ratios and the predominance of aliphatic structures. In contrast, organic matter in a continental environment is derived mainly from the detritus of higher plants and consists largely of lignin, cellulose and sclero-proteins, resulting in lower H/C ratios and a greater proportion of aromatic compounds. Diagenesis does not appear to drastically alter the isotopic composition of sedimentary organic carbon (see the comprehensive reviews by Deines, 1980, and Tissot and Welte, 1984).

Analyses of carbon stable isotope ratios in Recent (age $<10^4$ a) sediments of marine origin indicate that more than 90% of the $\delta^{13}\text{C}$ values lie within the range -20 to -27‰ (Deines, 1980), with a mean of -25‰ (Hoefs, 1987). The $\delta^{13}\text{C}$ range of older sediments and metasediments is comparable, although notably displaced towards ^{12}C enrichment (Deines, 1980; Arthur *et al.* 1986). With regard to the $\delta^{13}\text{C}$ values of carbonate rocks, those of marine origin have values close to 0‰. Furthermore, it has been shown that, almost as far back as the geological record exists, marine carbonates (and organic matter) have carbon isotopic compositions not dissimilar to their present-day counterparts (Junge *et al.*, 1975; Schidlowski *et al.*, 1983).

Freshwater carbonates are generally more depleted in ^{13}C than those of marine origin and show greater variation in $\delta^{13}\text{C}$ values (Hoefs, 1987, and references therein; Clark and Lauriol, 1992). Cryogenic calcites, formed by expulsion during the freezing of bicarbonate-enriched groundwaters, may also have high $\delta^{13}\text{C}$ values (up to +17‰ reported by Clark and Lauriol, 1992). The widest range of $\delta^{13}\text{C}$ values in carbonate rocks, however, from -60 to +21‰, is found in diagenetic dolomitic limestones in the deep-sea environment (Deuser, 1970; Murata *et al.*, 1967).

3.2.3 Carbon in the mantle: isotopic characterisation

The majority of measurements of the carbon isotopic composition of the mantle have been obtained on oceanic basaltic glasses, carbonatites, kimberlites, diamonds and mantle diopsides. The earliest isotopic measurements were by Craig (1953) and Wickman (1956), who analysed carbon stable isotope ratios in diamonds and showed that the $\delta^{13}\text{C}$ values clustered around -5‰. Since then, a wealth of data has been produced, stimulating a degree of controversy regarding mantle carbon isotope systematics. The subject has been reviewed by Javoy *et al.* (1986), Matthey (1987) and Boyd (1988); a more recent discussion with

reference to diamond formation is to be found in Galimov (1991). Although $\delta^{13}\text{C}$ values ranging from +2.8 to -34.5‰ have been recorded for diamonds globally, the majority range from -2 to -9‰, with a mode at -4.6‰ (Galimov, 1991). Vesicular CO_2 from oceanic basaltic glasses has $\delta^{13}\text{C}$ within the range -2 to -9‰, coinciding with the majority of measurements from carbonatites, kimberlitic carbonates and mantle diopsides.

Whereas the dominant present-day flux of carbon from the Earth's mantle is probably that associated with the outgassing of CO_2 at mid-ocean ridges (Mattey, 1987), carbon may also be returned to the mantle *via* subduction of oceanic crust (Mattey *et al.*, 1984; Boyd, 1988); this has been suggested as a viable mechanism for generating carbon isotopic heterogeneity in the mantle and hence explaining the origin of some ^{13}C -depleted diamonds. However, as noted by Javoy *et al.* (1986) and Deines *et al.* (1987), what is not explained by this hypothesis is why the recycled component is derived predominantly from kerogen (as required to produce ^{13}C -depletion), rather than marine carbonate ($\delta^{13}\text{C} \approx 0\text{‰}$). Indeed, the question of whether and how significant amounts of carbonate are returned into the mantle by subduction is still largely unresolved (Green *et al.*, 1993).

3.2.4 Carbon abundance and stable isotope ratio measurements: experimental problems highlighted by oceanic basalt analyses

'One of the problems with carbon isotope measurements is that the number obtained is very strongly dependant on the technique which is applied to measure it.' ... D P Mattey, Third International Symposium of Experimental Mineralogy, Petrology and Geochemistry, Edinburgh UK, 1990.

As noted by DesMarais (1986), large systematic discrepancies exist among carbon abundance and isotope data reported for aliquots of the same oceanic basalt samples by different laboratories. Stepped heating, entailing either combustion, pyrolysis, or a combination of the two, has been used in many investigations to release carbon from oceanic basalt glasses (Pineau and Javoy, 1983; Des Marais and Moore, 1984; Mattey *et al.*, 1984; Sakai *et al.*, 1984; Exley *et al.*, 1986, 1987). As variations of these experimental procedures were also adopted in the present study, the problems highlighted by the work on oceanic basalts are of considerable significance here.

A ubiquitous feature of the stepped heating analysis of basaltic glasses is the release by low temperature combustion (<600°C) of carbon (as CO_2) characterised by isotopic composition $\delta^{13}\text{C} \approx -25$ to -30‰ . Although there is not universal agreement on the origin of this carbon component, Des Marais and Moore (1984), Mattey *et al.* (1984) and Exley *et al.* (1986, 1987) suggested that surficial organic contamination, introduced in the marine environment and/or during sample handling, is the most probable source. This interpretation is supported by several lines of evidence (as summarised by Des Marais, 1986):

(i) During analyses of lunar basalts (Des Marais 1978, 1983), where little or no indigenous carbon was released upon melting, combustion at temperatures $<600^{\circ}\text{C}$ yielded carbon of similar isotopic characteristics (and sometimes in quantities as large) as reported for the low-temperature component obtained from oceanic basalts. (ii) The 'low-temperature' carbon component may be removed by combustion at 600°C , but will return if the glass is subsequently re-exposed to the atmosphere, thereby indicating the prevalence of airborne contaminants (dust and microbiological matter). (iii) Acid treatment of basaltic glasses, as often used in sample cleaning procedures, creates very active surfaces (Pineau and Javoy, 1984). (iv) The 'low-temperature' carbon is evolved at temperatures where the glass interior still retains its volatiles. (v) Small samples (greater surface area to volume ratio) yield proportionately more of this low-temperature component, as do weathered glasses compared to freshly-exposed chips. (vi) The carbon released below 600°C is isotopically characteristic of organic matter and, furthermore, combusts in the same temperature range.

Exley *et al.* (1986) and Matthey *et al.* (1989) showed that chemical pre-cleaning can be effective in minimising the carbon contribution from surficial organic contamination. In particular, Matthey *et al.* (1989) showed that up to 95% of the component derived from atmospheric exposure may be removed by a short period of ultrasonic cleaning in dichloromethane, followed by immediately loading the sample into a high-vacuum extraction line.

With regard to the origin of ^{13}C -depleted carbon ($\delta^{13}\text{C} \approx -27\text{‰}$) released during stepped combustion below 600°C , Nadeau *et al.* (1990), in an investigation of carbon concentrations and isotopic ratios in fluid inclusion-bearing upper-mantle xenoliths along the north-western margin of North America, preferred the explanation that it is due to complex carbon compounds condensed on mineral surfaces and in cracks (based on the work of Mathez, 1987), rather than arising through biological contamination (Matthey, 1987, and references therein). Nadeau *et al.* (1990) also noted that the ^{13}C -depleted component persisted, at low levels, up to 1450°C (the maximum temperature of their experiments). A typical CO_2 'blank' reported by these authors was equivalent to $0.96\mu\text{gC}$ at 1200°C , with a reproducible $\delta^{13}\text{C}$ value of $-27.6 \pm 0.2\text{‰}$. Although Nadeau *et al.* (1990) reported cleaning their samples by ultrasonic agitation in a 50:50 mixture of high purity dichloromethane and methanol, the minimum exposure procedure recommended by Matthey *et al.* (1989) was not used; samples were instead dried overnight at 75°C in an oven and subsequently outgassed at 200°C in a high-vacuum system for several hours. Of particular relevance (as discussed below) is that the extraction section comprised a Pt-10%Rh crucible in a silica tube; the precious metal crucible was presumably incorporated to catalyse the oxidation of low molecular weight alkanes.

3.2.5 Carbonaceous matter - an indigenous component of magmatic rocks?

Until relatively recently, elemental carbon was regarded as an incompatible element in oxide and silicate lattices. In a series of papers, Freund and co-workers (Freund *et al.*, 1980; Oberhauser *et al.*, 1983; Freund, 1986) reported that olivine, $(\text{Mg,Fe})_2\text{SiO}_4$, the most abundant mineral in the upper mantle, contains elemental carbon at concentrations of between 100 and 10,000 ppm. These reports have not been substantiated by more recent studies, however (Tsong and Knipping, 1986; Mathez *et al.*, 1987; Tingle *et al.*, 1988), indicating that surficial contamination may have been responsible. Carbonaceous films have been observed in olivines (from mantle nodules), however, which are obviously not the result of biological contamination (Tingle *et al.*, 1990). Mathez (1987) reported similar findings for peridotite xenoliths, and suggested that the carbonaceous films possibly derived from Fischer-Tropsch synthetic reactions of volcanic gases on chemically active (fractured) surfaces during cooling of the xenoliths.†

Tingle *et al.* (1991) considered whether organic-bearing carbonaceous films are unique to olivine crystals or whether any silicate mineral or glass surface might be suitable for the formation of such films; also, whether they are exclusive to volcanic rocks or might additionally be formed in plutonic environments, where the cooling is on a longer timescale and the source of the carbon is a supercritical fluid rather than a volcanic gas. Samples of gabbro, the intrusive equivalent of basalt, from the Stillwater (Montana, USA) and Bushveld (South Africa) layered intrusions, were analysed for this purpose. The presence of graphite, and evidence for the presence of carbon-bearing fluids during crystallisation at these localities, is documented (*e.g.* Mathez *et al.*, 1989). However, none of the samples analysed by Tingle *et al.* (1991) yielded organic components in excess of the procedural blank levels, which was surprising.

The question of the isotopic composition of carbon in films on crack surfaces of olivine, and whether it might be related to the ^{13}C -depleted carbon released below 600°C as reported for stepped heating experiments of basalts and mantle xenoliths (*e.g.* Matthey *et al.*, 1989; Matthey, 1990) was also addressed by Tingle *et al.* (1991). Preliminary stepped combustion analysis using the procedures of Matthey *et al.* (1989), but without sample pre-cleaning, and also incorporating corrections for the system blank and 'adventitious' carbon contamination, indicated that carbonaceous films in San Carlos olivine corresponded to $\sim 4\text{ppmC}$, with an associated $\delta^{13}\text{C}$ value of approximately -32% . An abiogenic origin was suggested, as advocated by Mathez (1987), although as the carbon isotopic composition of hydrocarbons in

† Mathez and Delaney (1981) had indicated that ill-defined C, or carbonaceous matter, was ubiquitous in submarine basalt glasses and mantle-derived peridotite nodules from alkali basalts.

volcanic gases and hydrothermal fluids approaches -30‰ (e.g. DesMarais, 1981), deposition directly from volcanic gas of organic compounds having a crustal biogenic origin could not be excluded.

In summary, the work of Tingle *et al.* (1991) showed that some (but not all) erupted materials may contain amorphous carbonaceous films on microcrack surfaces, associated with Si, alkali metals, halogens, nitrogen and transition metals (as characteristic of magmatic vapours and in accord with a catalytic, abiogenic origin for the carbonaceous films). Furthermore, the films may in some instances be associated with organic matter. An important finding was that the association of organic matter with carbonaceous films on crack surfaces appeared to be restricted to extrusive rocks.

3.2.6 Carbon solubility and speciation in silicate melts

As noted by Taylor (1986), many magmas are emplaced in close proximity to the hydrosphere and biosphere, thereby enhancing the probability of contamination from these sources. For this reason, recent studies on the concentration and speciation of magmatic volatiles have largely focused on investigations of volcanic glasses. With regard to the speciation of carbon dissolved in basaltic melts, infra-red absorption analysis has confirmed the presence of carbonate complexes in natural basaltic glasses (Fine and Stolper, 1985; Stolper and Holloway, 1988). There are few experimental data on the behaviour of CO₂ in igneous systems at kilobar and lower pressures. However, because of the low (but finite) solubility of CO₂ in granitic melts (Eggler and Kadik, 1979), CO₂ is usually a major component of gases exsolving from magmas during ascent through the crust (Stolper and Holloway, 1988); CO₂-bearing magmas are also implicated in granulite formation (Farquhar and Chacko, 1991). Matthey *et al.* (1989) estimated the solubility of carbon in tholeiitic melts from the data of Stolper and Holloway (1988) as 0.05 to 0.10 wt% carbon. Experiments by Blank *et al.* (1993) showed that the solubility of CO₂ (and water) in rhyolitic melts at 850°C, 750 bars (*i.e.* conditions appropriate to degassing of silicic magma near the Earth's surface) follows Henry's law.

Carbon in tholeiitic melts is present in oxidised form, on the basis of measurements of the carbon isotopic fractionation factor between coexisting CO₂ and 'dissolved' carbon species in natural basalt melts (Matthey *et al.*, 1989; Matthey *et al.*, 1990). Matthey *et al.* (1990) reported $\alpha_{\text{CO}_2\text{-melt}}$ to be less than 2.4‰, significantly lower than value of 4.4‰ as determined experimentally by Javoy *et al.* (1978). As noted by Matthey *et al.* (1989), a fractionation factor of 4.4‰ is consistent with dissolved carbon being in reduced form, whereas theoretical considerations suggest that, for carbon present as carbonate ionic complexes in natural silicate melts, isotopic fractionation between dissolved CO₃²⁻ and exsolved CO₂ should be nearer 2‰ at magmatic temperatures.

3.2.7 The speciation of oxidised carbon in hydrothermal fluids.

Under hydrothermal conditions below ~600°C, the principal oxidised carbon species consist of $\text{CO}_{2(\text{aq})}$, H_2CO_3 , HCO_3^- and CO_3^{2-} , as is the case for surface waters at ambient temperature. As noted by Ohmoto (1986), for most geologic fluids at temperatures greater than ~100°C (and $\text{pH} < \sim 6$) the activity of bicarbonate is negligible compared to that of $\text{CO}_{2(\text{aq})} + \text{H}_2\text{CO}_3$. Furthermore, at 1 kbar, the equilibrium constant for: $\text{H}_2\text{O} + \text{CO}_{2(\text{aq})} \rightleftharpoons \text{HCO}_3^- + \text{H}^+$ is $10^{-7.20}$ at 300°C, $10^{-10.43}$ at 550°C (Stein and Walther, 1987); the values increase with increasing pressure. With increasing pH, HCO_3^- becomes dominant up to $\text{pH} \sim 10$, beyond which CO_3^{2-} is the major species (see Faure, 1986). The corresponding activity coefficients are regulated by ionic strength effects, whilst the temperature determines the magnitudes of the respective equilibrium constants.

By way of comparison, in present-day seawater ($\text{pH} = 8.1$) bicarbonate predominates: the respective global molar quantities ($\times 10^{18}$) of oceanic carbon as $\text{CO}_{2(\text{aq})} + \text{H}_2\text{CO}_3$, HCO_3^- and CO_3^{2-} are 0.019, 2.9 and 0.36 (Stumm and Morgan, 1981). Low-salinity geothermal fluids are typically near-neutral, or slightly alkaline, under which circumstances the concentration of HCO_3^- is again significant (Heinrich, 1990). In contrast, electrolyte analysis of a primary granite-derived palaeo-hydrothermal fluid from the St Austell district, SW England, by Bottrell and Yardley (1988) has confirmed that such fluids were highly acidic chloride brines. If such a composition typified the pegmatitic-pneumatolytic transitional fluids and also those associated with early hydrothermal mineralisation in SW England, the levels of HCO_3^- and CO_3^{2-} species in those fluids would have been negligible.

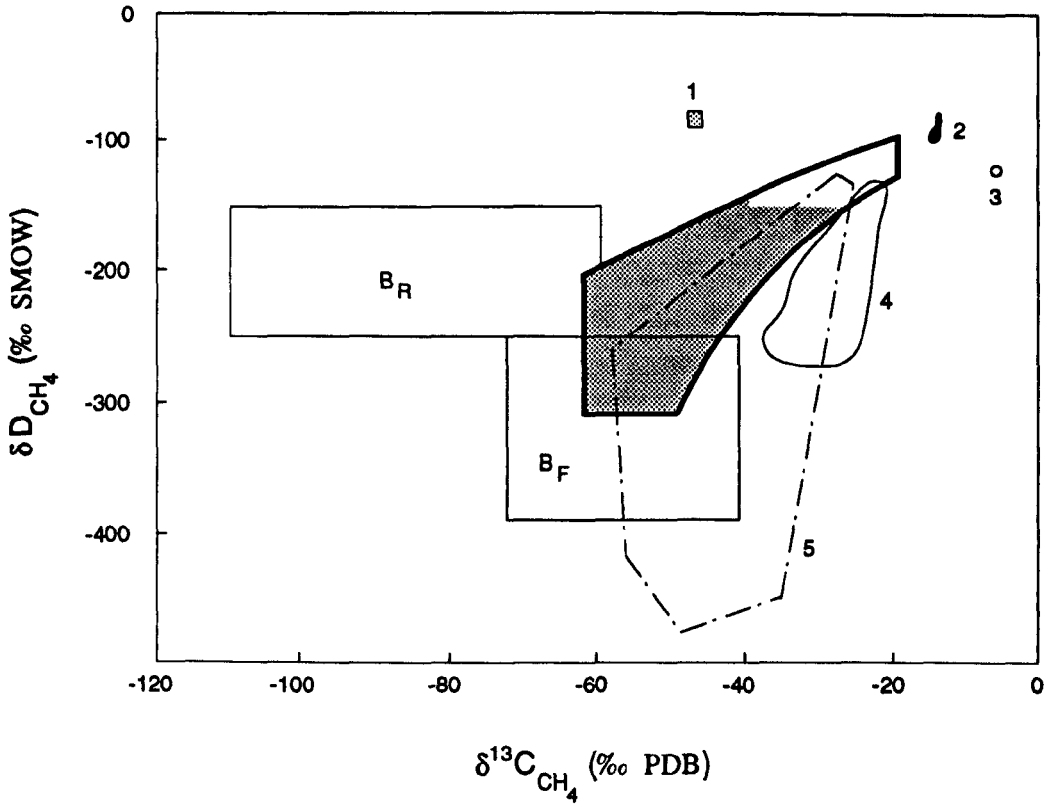
3.2.8 The occurrence and sources of methane in crustal fluids: stable isotope considerations

Methane is an important component of many geochemical processes in the Earth's crust. For example, early stages of the diagenesis of recent sediments are affected by bacterial processes which act as sources and sinks for methane fluxes. The pyrolysis of organic matter at elevated temperatures deeper in the crust leads to methane formation (Galimov, 1988); high grade metamorphic rocks may contain methane-rich fluid inclusions (Kreulen and Schuiling, 1982). In present-day geothermal systems, methane is a notable component in both continental (Lyon and Hulston, 1984; Des Marais *et al.*, 1988) and oceanic environments (Welhan, 1988). Methane from other sources in the marine environment has $\delta^{13}\text{C}$ values ranging from -35 to -90‰ (Fisher *et al.*, 1990, and references therein). The characterisation of methanes by the combined use of $\delta^{13}\text{C}$ and δD isotope parameters was shown by Schoell (1980, 1983) to be of diagnostic value in identifying their origin. Figure 3.1 (after Schoell, 1988) indicates the range of ^{13}C and deuterium abundances in naturally-occurring methanes from a variety of environments.

Figure 3.1

$\delta^{13}\text{C}$ and δD characteristics of some naturally-occurring methanes.

(Adapted from Schoell, 1988)



Key

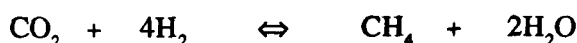
Fields B_R and B_F represent the isotopic characteristics of bacterial methanes, formed by CO₂ reduction and fermentation respectively. Methane of thermogenic origin is denoted by the area bounded by bold outline; the shaded part therein depicts methane associated with oils. Other fields are as follows:

- 1 Atmospheric methane (present day). Data from Wahlen *et al.* (1987);
- 2 East Pacific Rise methane (Welhan, 1981);
- 3 Methane associated with Zambales ophiolite, Philippines (Abrajano *et al.*, 1988);
- 4 Geothermal methane (Welhan, 1988; Lyon and Hulston, 1984; Des Marais *et al.*, 1981);
- 5 Canadian Shield methane (Sherwood *et al.*, 1988).

In hydrothermal fluids, there are two principal alternative sources of methane:

(i) Thermal breakdown (at temperatures $>100^{\circ}\text{C}$) of complex hydrocarbons of presumed biogenic origin.[†] The associated $\delta^{13}\text{C}$ ranges from about -60 to -20‰ (Schoell, 1988).

(ii) Inorganic (abiogenic) synthesis at relatively high temperature ($>300\text{-}400^{\circ}\text{C}$) through *e. g.* Fischer-Tropsch type mechanisms (Hulston and McCabe, 1962; Giggenbach, 1980):



The discovery of methane in mid-ocean ridge hydrothermal systems, involving only basaltic rock and seawater, is undoubtedly abiogenic and is characterised by $\delta^{13}\text{C}$ values in the range -18 to -15‰ (Welhan, 1987a; 1988). Welhan (1987) suggested that the $\delta^{13}\text{C}$ data represent isotopic equilibration with mantle-derived CO_2 ($\delta^{13}\text{C}$ -5 to -7‰) at $500\text{-}800^{\circ}\text{C}$ within the basalt, with effectively no carbon isotope exchange occurring during cooling to $<500^{\circ}\text{C}$. Methane of $\delta^{13}\text{C}$ $-7.0 \pm 0.4\text{‰}$ has been recorded in serpentinised ultramafic rock of the Zambales ophiolite, Philippines (Abrajano *et al.*, 1988; Abrajano *et al.*, 1990); hydrolysis of the ultramafic rocks, with concomitant reduction of deep-seated CO_2 , has been postulated to explain these results.

Metcalf *et al.* (1992) reported evidence for the presence of abiogenic methane in an ancient (Ordovician age) hydrothermal system in the British Isles, at Builth Wells, Wales. These authors argued that the methane, characterised by a $\delta^{13}\text{C}$ value of $\approx -13\text{‰}$, was possibly mantle-derived (consistent with the location of the fossil hydrothermal system on the Pontesford Lineament, a long-lived zone of crustal weakness which was a locus of strike-slip movement in Ordovician times). As fluid inclusion evidence suggests that the temperature of the hydrothermal vein system did not exceed 450°C , alternative explanations invoking inorganic synthesis through a Fischer-Tropsch type mechanism necessarily require that methane production occurred at some greater crustal depth than the host Builth Volcanic Group.

Outgassing of primordial methane from the Earth's mantle has been suggested by Gold (1979) and Gold and Soter (1982). Although there is at present no unambiguous evidence for this, it has been suggested on the basis of theoretical models that methane is probably stable under primitive mantle conditions (Saxena, 1989).

[†] Recent work (Mango *et al.*, 1994) has indicated that catalysis by transition metals of reaction at $\sim 200^{\circ}\text{C}$ between hydrogen and n-alkenes (formed during thermal decomposition of kerogen) is a more probable source of methane than is direct thermal decomposition of sedimentary organic matter.

There is little evidence to suggest that bacterially-produced methane (involving CO₂ reduction or fermentation - see Schoell, 1988) is a significant component in hydrothermal systems. Methane derived from bacterially-mediated CO₂ reduction is most common in older sediments and is characterised by δ¹³C < -60‰ (Schoell, 1980; 1988).

3.2.9 CO₂-CH₄ carbon isotope exchange equilibria in hydrothermal systems: an unresolved problem

Craig (1953) first advanced the possibility that equilibrium isotopic exchange of carbon between coexisting CO₂ and CH₄ molecules in geothermal fluids might form the basis of a geothermometer:



where the equilibrium constant $K(T) = \alpha(T)_{\text{CO}_2\text{-CH}_4} = \frac{[(^{13}\text{C}/^{12}\text{C})_{\text{CO}_2}]}{[(^{13}\text{C}/^{12}\text{C})_{\text{CH}_4}]}$

α is the equilibrium fractionation factor, and is related to the respective delta values through:

$$\delta^{13}\text{C}_{\text{CO}_2} - \delta^{13}\text{C}_{\text{CH}_4} = \Delta^{13}\text{C}_{\text{CO}_2\text{-CH}_4} \cong 10^3 \log_e \alpha_{\text{CO}_2\text{-CH}_4} \quad (\text{see Section 1.3})$$

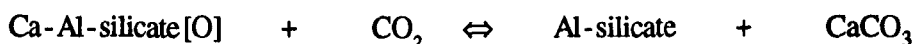
Nearly four decades later, and with refinement of the equilibrium fractionation factors (Bottinga, 1969; Richet *et al.*, 1977), the issue is still a matter of some controversy. Carbon isotope exchange between CO₂ and CH₄ at high temperatures was investigated experimentally by Sackett and Chung (1979), who found no evidence for this exchange under any of the following conditions: (i) dry gases at 500°C for up to 136 hours; (ii) in the presence of water-bearing montmorillonite at 200°C for up to 32 days and also at 500°C over an equilibration period of up to 10.5 days; (iii) the pyrolysis of natural lignite at 500°C for up to 180 hours. Harting and Maass (1980) provided the first reported experimental evidence for carbon exchange between CO₂ and CH₄, using equilibration temperatures from 500 to 680°C over a period of 16 hours: rates of exchange were found to be very slow, corresponding to a reaction half-time of 2.86 years at 610°C (Giggenbach, 1982). As noted by Hulston (1986), extrapolation of these data indicates that at 400°C tens of thousands of years would be required for isotopic equilibrium to be attained, although such conditions may be satisfied in the case of a cooling magma body beneath a geothermal system. For lower temperature geothermal fluids (<300°C), Giggenbach (1982) suggested that carbon isotope exchange between CO₂ and CH₄ was unlikely to ever reach equilibrium.

Lyon and Hulston (1984), in an attempt to measure the rate of carbon isotope exchange between CO₂ and CH₄, reported that no change in the isotopic composition of either component was detectable after a period of 210 days at temperatures up to 350°C, when both components were contained in the presence of H₂ and liquid water in a stainless steel vessel. The same authors also found that Fischer-Tropsch synthesis of methane from CO₂ and H₂ at

400°C (in the presence of a platinised asbestos catalyst) gave a $\Delta^{13}\text{C}_{\text{CO}_2\text{-CH}_4}$ value of -35.9‰ in 40 days, equivalent to an equilibrium temperature of only 180°C on the basis of fractionation factors calculated from the data of Richet *et al.* (1977). Furthermore, no significant change was detected during a further 150 days.

Sheppard (1981) compiled carbon isotope data from several published studies of geothermal systems and showed that in all cases, the temperature derived on the basis of carbon isotopic equilibration between CO_2 and CH_4 was higher (by between ~40 and 350°C) than the actual value measured in the well or at the surface of the spring or fumarole. These differences had in earlier studies been interpreted either as (i) equilibrium isotopic exchange, but with the isotope geothermometer recording a temperature appropriate to a deeper part of the system than where the measurements were taken; alternatively (ii) isotopic disequilibrium conditions. Sheppard (1981) noticed, however, that about two thirds of the compiled data points recorded an apparent isotopic exchange temperature of $320 \pm 20^\circ\text{C}$ and on this basis proposed that isotopic exchange below about 320°C was inhibited ('blocked') by kinetic considerations. As acknowledged by Sheppard (1981), this hypothesis is not supported by the experimental findings of Sackett and Chung (1979), although such experiments may well be inappropriate to the modelling of geothermal conditions on a geological timescale.

With regard to chemical equilibration between CO_2 and CH_4 , which has been reported as proceeding some two orders of magnitude faster than isotopic equilibration (Giggenbach, 1982), it has been suggested (Giggenbach, 1980; Arnorsson and Gunnlaugsson, 1985) that in continental hydrothermal systems, CO_2 abundance is controlled (buffered) primarily by mineral-fluid reactions, of the type:



As noted by Hulston (1986), loss of CO_2 from the system through calcite deposition should not significantly affect calculated $\text{CO}_2\text{-CH}_4$ isotopic equilibration temperatures, as carbon isotopic fractionation between CO_2 and calcite is small (2-3‰) for temperatures in the range 300-700°C. The same author suggested that isotopic exchange with CO_2 at depth over a timescale of $> 10^3\text{a}$ satisfactorily explained the presence of ^{13}C -enriched methane in the Mokai geothermal area of New Zealand ($\delta^{13}\text{C}$ -13.9‰), without the need to invoke an abiogenic origin for the methane.

In contrast, Marty *et al.* (1991) found during their investigation of a geothermal reservoir in the south-west rift zone of Iceland that CO_2 partial pressures were *not* controlled by fluid-mineral equilibria. The CO_2 in this example appeared to derive from mixing between a mantle source and atmosphere; it was suggested that the flux of mantle-derived CO_2 was too large to be controlled by mineral phases.

3.2.10 Carbonaceous volatiles in palæo-hydrothermal fluids associated with the Cornubian batholith, S W England

The presence of CO₂ in the Cornubian palæo-hydrothermal system has only been reported at a limited number of localities, all of which are associated with the transitional stage from metasomatism to vein hydrothermalism, characterised by association with wolframite (Beer and Ball, 1987). With a single exception, involving a sample from Old Gunnislake mine included in the present study (Bannon, 1989; also reported in Turner and Bannon, 1992), no evidence for a discrete (liquid) CO₂ phase at ambient temperature was found during any published optical microthermometric studies (see Chapter 4) undertaken of quartz associated with hydrothermal mineralisation in the region[†]. The presence of CO₂ in the aqueous phase was detected, however, through CO₂-hydrate (clathrate) formation at sub-ambient temperatures by Bull (1982), Shepherd *et al.* (1985), Scrivener *et al.* (1986) and Bannon (1989) in a limited number of cases. The presence of methane as a trace constituent of the hydrothermal fluids, associated with enhanced CO₂ levels, was indicated by preliminary mass spectrometric analyses of extracted fluids by the present author (Shepherd *et al.*, 1985).

3.3 Research objectives

The primary objective of the present work was to examine the occurrence, speciation and stable isotopic characteristics of carbon in ancient (late Palæozoic) hydrothermal fluids associated with syn/post-magmatic events in S W England. Such information may be applied to constrain models relating to the origin of these components in terms of crustal carbon reservoirs and in assessing the source of fluids which contributed to the evolution of the Cornubian batholith, from the initial pegmatitic and pneumatolytic stages through to the early hydrothermal mineralisation characterised by W±Sn oxide assemblages.

For comparative purposes, a small number of selected samples from the Yanshanian granites of southern China (age 185-67Ma) were also included, as transitional phenomena in the evolution of the granites of S China and S W England are similar in many aspects (Lin, 1989). Also for comparison were included examples of vein quartz associated with wolframite from the Carrock Fell deposit (age ~395Ma), located on the boundary of the Skiddaw granite in the northern region of the English Lake District. The Carrock Fell veins occur, as do many examples of wolframite mineralisation in S W England, across the granite-country rock contact. The country rock comprises shales and volcanics of Ordovician

[†] It should be noted that a significant amount of CO₂ can be present without the appearance of a separate liquid phase. For such a phase to form in an aqueous inclusion at room temperature, the associated vapour bubble must contain CO₂ at a pressure in excess of the critical pressure, *i. e.* ~70atm. (Roedder, 1984, p.356). The aqueous phase will also be CO₂-saturated.

(500-435Ma) age. Levels of carbon dioxide, nitrogen and methane in the aqueous palaeofluids at Carrock Fell are comparable to those associated with W±Sn oxide mineralisation in S W England (Shepherd and Miller, 1988).

The critical re-appraisal of experimental procedures used for the extraction and determination of carbon stable isotope ratios in both carbon dioxide and (coexisting) methane from fluid inclusions, where one or both of these components is present at trace levels, was an essential preliminary requirement, in the light of controversies regarding the extent of contamination by 'adventitious' carbon during the stepped heating release of carbon for stable isotope ratio measurement.

In view of the low absolute abundance of carbon species in even the relatively CO₂-enriched (wolframite-associated) early-stage mineralising fluids of the ancient Cornubian hydrothermal system, a further objective was to investigate the application to fluid inclusion ¹³C/¹²C analysis of high-sensitivity, static vacuum mass spectrometry, developed for the measurement of carbon stable isotope ratios at the nanomole level (Carr *et al.*, 1986). The aims of this aspect of the work were twofold: firstly, a reduction in sample size conferred the advantages of reduced sample preparation time whilst allowing better lithological control of sample purity. Secondly, the high sensitivity permitted the investigation to be extended to determinations of the isotopic composition of carbon species present at very low levels in palaeofluids, thereby obtaining information inaccessible by other means. Thus, the question could be addressed as to whether carbon (in whatever form) is a ubiquitous primary constituent of the initial magmatic-hydrothermal fluids, with local abundance possibly reflecting the degree of 'S'-type character of the associated granite pluton.

3.4 Experimental

3.4.1 The extraction of palaeofluid inclusions for carbon stable isotope ratio analysis

The literature referring to the direct analysis of fluid inclusion components for carbon isotopic composition is not extensive, largely because of the analytical problems associated with the extraction and measurement of the small volumes of fluid involved. In recent years, progress has been made with the application of Raman spectroscopy, using a laser radiation source, to *in situ* non-destructive analysis of individual inclusions for carbon stable isotopic composition: Rosasco and Roedder (1979) reported measurements on CO₂ to a precision of ±20‰, whereas more recent investigations have improved this figure to ≈±7‰ (J Dubessy, unpublished data) using optimum examples. Such measurements are far from being commonplace, however, besides being of insufficient precision for most investigations, and require the presence of a discrete non-aqueous gas phase in the inclusion.

More conventionally, the direct measurement of carbon stable isotope ratios of fluid inclusion components is performed by gas-source mass spectrometry on CO₂ (and/or CH₄, oxidised to CO₂) extracted from the host mineral by the mass opening of individual inclusions *in vacuo*. The type of bulk extraction techniques currently employed preclude, to a large degree, any discrimination between different inclusion types and/or generations. Furthermore, limitations imposed by the instrumentation sensitivity during isotope ratio analysis ultimately dictate the minimum quantity of gas required, which may critically influence the degree of lithological control of sample material in some applications. Procedures for releasing the fluid trapped in inclusions for stable isotope analysis are essentially based either on crushing or thermal decrepitation techniques.

3.4.1.1 Fluid extraction by crushing *in vacuo*

Mechanical crushing of the host mineral grains offers the advantage that gas release from sources other than the fluid inclusions will be minimised, at the expense of a low yield. Methods that have been reported include mechanical crushing of a stainless steel pipe attached to the vacuum line (Kreulen, 1980); ball milling, using an alumina ball (Kazahaya and Matsuo, 1985), and a low-volume stainless steel screw press (Mattey *et al.*, 1989). The relatively low yield obtained, together with the requirement to prepare sufficient gas for isotope ratio analysis by conventional mass spectrometry, necessitates the use of greater quantities of mineral or whole-rock sample than does thermal extraction. Also, extended crushing/grinding creates a large increase in surface area, which may cause significant gas adsorption (Wahler, 1956; Piperov and Penchev, 1973). Barker and Torkelson (1975) reported that CO₂ is particularly prone to adsorption onto powdered quartz produced during this process. Kazahaya and Matsuo (1985), however, found that CO₂ was readily desorbed from fine-grained quartz at 200-280°C and, furthermore, detected no carbon isotopic fractionation for the overall extraction process.

3.4.1.2 Fluid extraction by thermal decrepitation *in vacuo*

The principle of the method is to increase the internal pressure of the trapped fluid by heating of the sample. If the difference between the internal and external pressures exceeds the mechanical strength of the mineral, deformation or fracture propagation will ensue, to allow fluid expansion and consequently relieve the pressure difference. If fracturing occurs, the process is referred to as decrepitation.

The internal pressure required to cause decrepitation is strongly dependent on inclusion volume (Leroy, 1979; Bodnar *et al.*, 1989); larger inclusions decrepitate at lower internal pressures than smaller inclusions. Experiments by Bodnar *et al.* (1989), using synthetic

inclusions of pure water in quartz, established the following empirical relation between the inclusion volume and the internal pressure required to cause decrepitation:

$$\text{internal pressure (kbar)} = 3.89V^{-0.141}$$

where V is the inclusion volume in μm^3 . As well as inclusion size, the density and chemical composition of the inclusion fluids critically influence the temperature at which decrepitation occurs, as the internal pressure generated is a function of these (see *e.g.* Roedder, 1984). The phase transition of quartz from α to β polymorph occurs at 573°C (1 atm.) and is pressure dependent, increasing by $\sim 25^\circ\text{C}/\text{kbar}$ (Koster van Groos and Ter Heege, 1973); this transition is often accompanied by fluid release (see Bodnar *et al.*, 1989).

Reported disadvantages of the thermal decrepitation method of fluid inclusion release are related to the potential occurrence of chemical reactions at the elevated temperatures required. For example, it has been postulated that reactions between the released gas phase components at high temperature may alter the composition from that occurring *in situ*. The complementary problem of post-entrapment chemical re-equilibration of fluid composition during the long cooling history of geological samples is considered in Chapter 1. On the basis of empirical studies by Sackett and Chung (1979) and Harting and Maass (1980), as discussed above, carbon isotope exchange between CO_2 and CH_4 should not be detectable up to at least 680°C (and probably not detectable at much higher temperatures also) during thermal extraction of fluid inclusion components on the timescale of a typical stepped heating experiment.

Gas release from sources other than the fluid inclusions is probably the major potential problem with the thermal decrepitation method. Examples include the thermal breakdown of carbonates, pyrolysis/combustion of organic contamination and oxidation of graphite. Quartz was used almost exclusively throughout this study, after careful preparation to minimise attendant contamination.

3.4.2 Palaeofluid $\delta^{13}\text{C}$ measurements: previous studies

Previous studies involving the extraction, for stable isotope analysis, of fluid inclusion carbon components from hydrothermal vein quartz associated with $\text{W}\pm\text{Sn}$ oxide mineralisation include: Landis and Rye (1974), Kelly and Rye (1979), Bussink *et al.* (1984) and Kazahaya and Matsuo (1985). Few details of the respective experimental procedures were published. Only Kazahaya and Matsuo (1985), who extracted the fluid volatiles by ball milling, reported carbon stable isotope analyses of coexisting CH_4 and CO_2 ; further details are given by Kazahaya (1986). Kazahaya and Matsuo (1985), using vein quartz from the Takatori wolframite deposit, Japan, obtained identical $\delta^{13}\text{C}$ results (-7.7‰) for fluid inclusion CO_2 extracted from quartz either by thermal decrepitation ($\sim 300\text{--}600^\circ\text{C}$) or by alumina ball-milling, if the sample was pre-heated in the ball mill to 280°C .

Table 3.1

Preliminary results obtained for carbon stable isotope ratio analysis of CO₂ extracted from fluid inclusions in vein quartz, Carrock Fell and Hemerdon, by single-step thermal decrepitation *in vacuo* after initial outgassing at 100°C. 2 g of sample (grain size 0.5-1 mm) used in every case.

Sample	$\delta^{13}\text{C}_{\text{PDB}}\text{‰}$
CF-76-25	-13.2*
CF-76-7	-11.1
CF-77-39B	-11.5
CF-77-77A	-12.0
CF-77-79B	-12.0
CF-77-98	-11.4
HEM-80-1	-9.8
HEM-80-39	-9.0

Note: * mean of four replicate analyses; $1\sigma = 0.22\text{‰}$

3.4.3 Preliminary $\delta^{13}\text{C}_{\text{CO}_2}$ results from fluid inclusions (this study)

Initial experiments were conducted by the present author using wolframite-associated vein quartz samples from Carrock Fell, NW England. Mineralogically, the veins are similar to those at Panasqueira, Portugal, for which fluid inclusion carbon isotope data have been reported by Kelly and Rye (1979) and Bussink *et al.* (1984). Sample preparation was minimal and is described in Section 2.4.1. Thermal decrepitation *in vacuo* was used to release the inclusion fluids from 2g of quartz grains, after outgassing at 100°C. The CO_2 fraction was isolated by cryogenic separation (after Sakai *et al.*, 1976). Isotopic measurements were performed using a VG[®]903 mass spectrometer. For comparison, two samples from Hemerdon, S W England, were analysed. The results are given in Table 3.1.

3.4.4 Carbon stable isotope ratio analysis of small samples

3.4.4.1 Contamination removal: the application of stepped heating

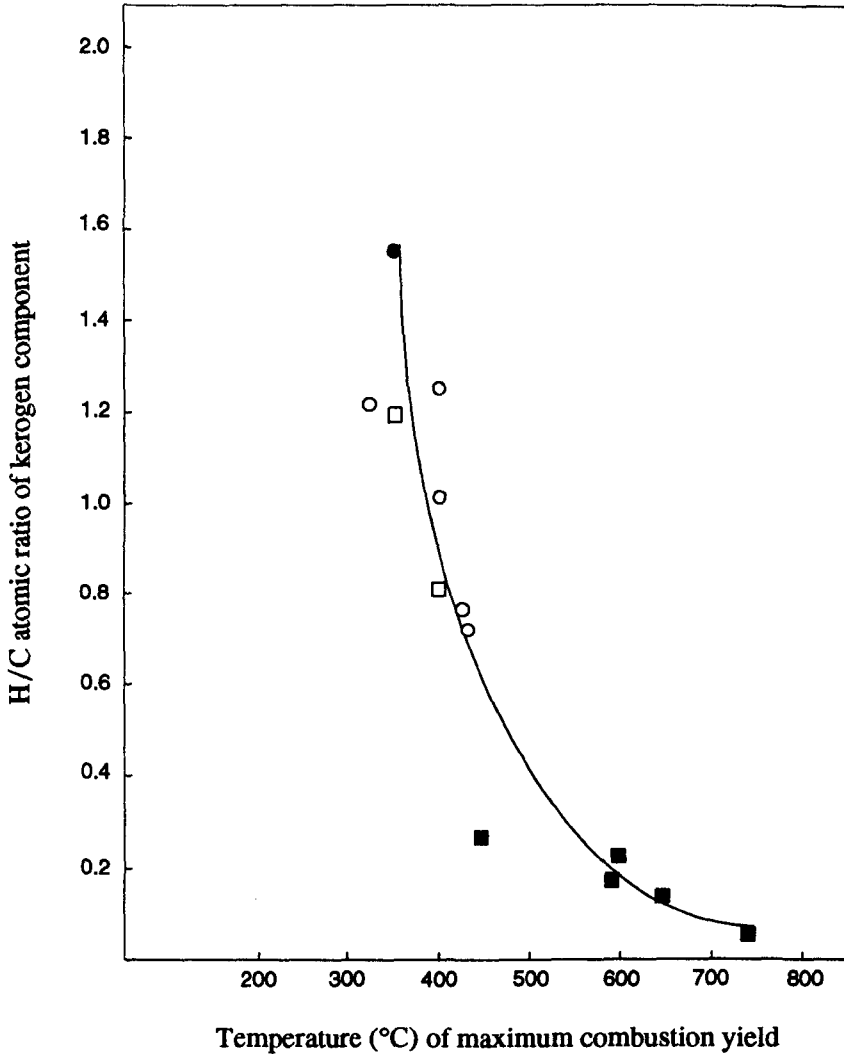
The principle of stepped combustion for resolving indigenous carbon from contamination, either 'organic' or weathering products, was proposed by Swart *et al.* (1983) for carbon isotopic analysis of extraterrestrial samples. Similar experimental procedures had been used earlier by Des Marais (1978), Frick and Pepin (1981a,b) and Becker and Epstein (1981), although the applications differ in detail. Essentially, the method of Swart *et al.* (1983) involved multi-step combustion, with heating increments generally of 100°C and for 30 minutes duration, in an attempt to distinguish between airborne and surficial organic contaminants, on the one hand, and indigenous carbon on the other hand; also to resolve different carbon-bearing phases present in the sample, on the basis of their respective combustion temperatures.

For the most part, organic contamination burns at relatively low temperature ($<425\pm 25^\circ\text{C}$; Swart *et al.*, 1983). Studies on oil shale and kerogen by Gilmour and Pillinger (1985) indicated that organic carbon generally burns at 200-400°C in these components, the combustion temperature being a function of the H/C ratio (Gilmour, 1986) as illustrated in Figure 3.2. Biological contaminants, such as spores, dust and fibres, combust over the temperature range similar to that of kerogen (Des Marais, 1983). At higher temperatures (400-700°C), combustion of amorphous carbon occurs (Grady, 1982), as does the thermal decomposition of carbonates. Milodowski and Morgan (1980) investigated the latter and found a temperature range from 300 to $>800^\circ\text{C}$, depending on chemical composition. Figure 3.3 illustrates the characteristics during stepped combustion of various carbon-containing species pertinent to the present investigation.

Figure 3.2

The variation of combustion temperature (defined as that at which maximum CO₂ release is obtained during stepped heating in excess of pure oxygen, using increments of typically 25-35°C) as a function of atomic H/C ratio of the indigenous kerogen component, for a variety of sedimentary rocks.

(After Gilmour, 1986; Wright and Pillinger, 1989)



Key

● Green River shale	□ Bakken shale
○ Deep-sea sediments	■ Archean sediments

Notes: Green River shale is referred to in the text.

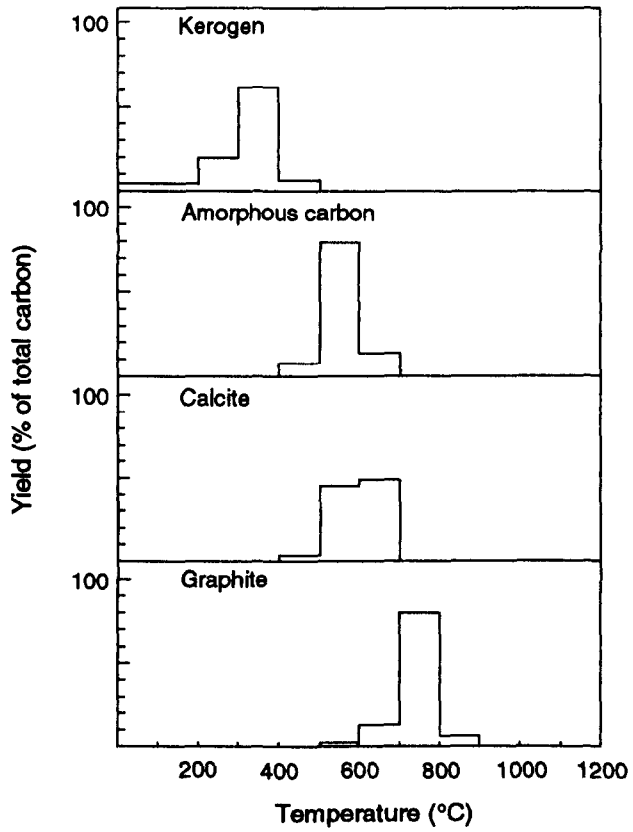
Bakken shale is an organic-rich component of the Bakken Formation (Mississippian-Devonian age), found in the Williston Basin of North Dakota and Montana, USA.

See *e.g.* Tissot and Welte (1984) and references therein.

Figure 3.3

Typical yield profiles of CO₂ obtained by stepped heating (100°C increments) of kerogen, amorphous carbon, calcite and graphite in excess of pure oxygen.

(After Wright and Pillinger, 1989)



The issue of whether progressive combustion of an isotopically homogeneous sample is accompanied by isotopic fractionation of the carbon was addressed by Swart *et al.* (1982) in the case of graphite and carbonate samples; no evidence for such fractionation was found. Terrestrial kerogen, however, does show a reproducible shift in $\delta^{13}\text{C}$ value; this is not attributed to kinetic isotope effects during combustion, but is either the result of ^{12}C -enrichment of side-chain components and aliphatic entities, which combust at lower temperature or, alternatively, the resolution of marine and non-marine components of differing carbon isotopic composition (Wright and Pillinger, 1989).

In the case of incremental heating in the absence of oxygen (referred to as 'pyrolysis' in much of the literature) to release fluid inclusion components, it might be anticipated that diffusion effects would be problematic, giving rise to attendant isotopic fractionation. Matthey *et al.* (1984) and Exley *et al.* (1986) used this technique to release gas trapped in vesicles during investigations of MORB glasses; no such effect was observed.

3.4.4.2 Static vacuum mass spectrometry: application to carbon stable isotope ratio analysis

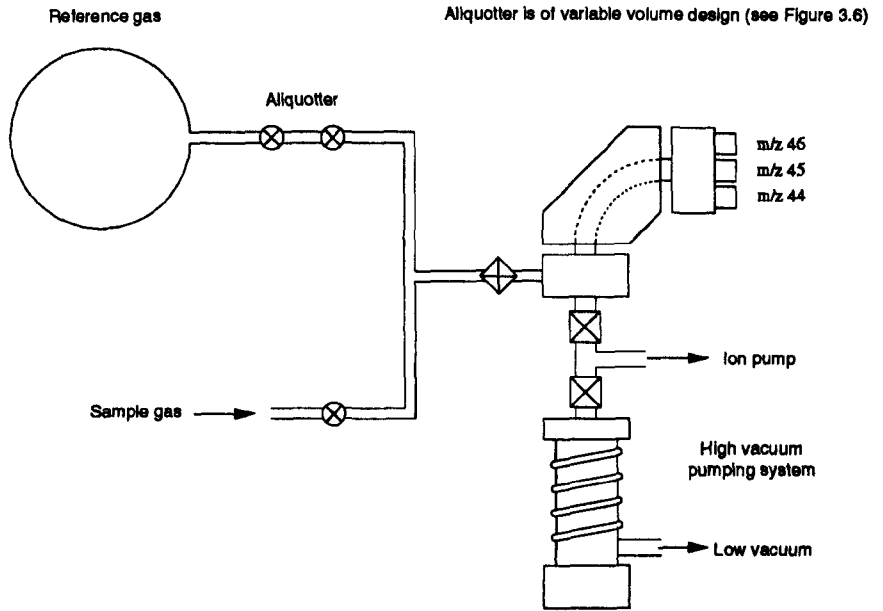
Comprehensive reviews of developments to improve the sensitivity of stable isotope ratio measurements since the late 1940s have been published by Pillinger (1984, 1992), with particular reference to the analysis of extraterrestrial samples. Until relatively recently, virtually all measurements of light element stable isotope ratios were undertaken using gas source mass spectrometers that were essentially based on the dynamic (continuously pumped) instrument originally described by Nier (1940, 1947), as improved by Murphey (1947) and McKinney *et al.* (1950). In these systems, the sample and reference gases, admitted *via* their respective capillaries to maintain viscous flow and hence minimise fractionation effects, are continuously pumped through the mass spectrometer. A changeover valve (Murphey, 1947) is used to switch either sample or reference gas to the ion source whilst the other gas is pumped to waste. The inherent inefficiency of this process results in only a very small proportion of the sample gas being ionised for subsequent isotopic analysis. In investigations where sample availability is not a major limitation, high precision isotopic analysis is possible with this arrangement (1σ error typically $\pm 0.005\%$ for $> \sim 1\ \mu\text{mol CO}_2$). Methods have been devised to improve the sensitivity of this arrangement (as reviewed by Wright and Pillinger, 1989), but these have not been widely used and are not considered further here. A significant recent advance, however, is the development of continuous-flow isotope-ratio monitoring mass spectrometry, as first proposed by Matthews and Hayes (1978). In this system, optimised for compatibility with gas chromatographic separation and on-line combustion of organic compounds, CO_2 entrained in a helium carrier gas stream is introduced directly into the mass spectrometer. Nanomole samples of CO_2 may be analysed rapidly, to a precision of $\pm 0.1\%$ according to Douthitt (1990).

Figure 3.4

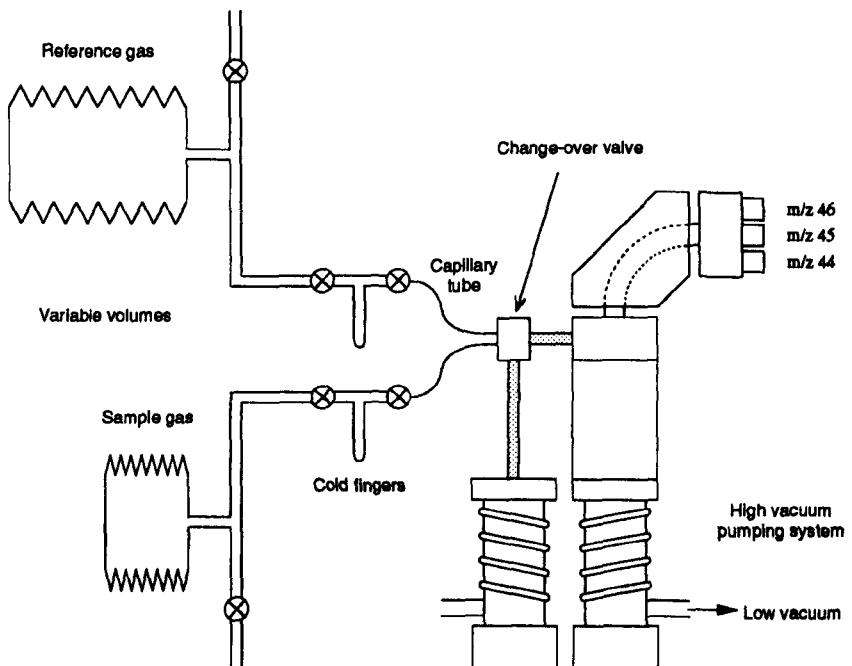
Schematic diagram illustrating the difference in principle between static vacuum and dynamically pumped mass spectrometer configurations, as used for carbon stable isotope ratio analysis.

(Adapted from Wright and Pillingier, 1989)

(a) Static vacuum system



(b) Dynamically pumped configuration



A radically different approach to stable isotope analysis was investigated in the 1970s, whereby the capillary inlet is dispensed with and the sample gas of interest admitted to the mass spectrometer after isolation of the latter from its associated pumping system, in the manner of noble gas isotopic analysis (Aldrich and Nier, 1948; Reynolds, 1956). Figure 3.4 illustrates the difference in operating principle between dynamic and 'static vacuum' mass spectrometers. The first successful application of static vacuum mass spectrometry to 'active' gases (which undergo thermal degradation and dissociation induced by electron impact) was for carbon, using methane and its fully-deuterated analogue, CD₄ (Gardiner *et al.*, 1978; Gardiner and Pillinger, 1979; Wright *et al.*, 1983). These species were found to be very stable, the half-life of CD₄ being ~10.5 hours in the mass spectrometer of Gardiner *et al.* (1978). Difficulties associated with converting sample carbon to CD₄, however, together with control of blank contributions and memory effects (McNaughton *et al.*, 1983; Carr, 1985) limited the usefulness of this approach.

In contrast to CD₄, carbon dioxide degrades rapidly in the ion source of a static vacuum mass spectrometer (Irako *et al.*, 1975; Gardiner and Pillinger, 1979), through dissociation on the hot ionising filament. Fallick *et al.* (1980), however, showed that there is no appreciable isotope fractionation effect associated with the degradation (similarly for methane and carbon monoxide). In view of the well-established and relatively uncomplicated procedures for preparing CO₂ from carbon sources (*e.g.* Sakai *et al.*, 1976; Swart *et al.*, 1983), a static vacuum mass spectrometer for the isotopic analysis of CO₂ was developed by Carr (1985); experimental details are also given by Carr *et al.* (1986). The resulting instrument ultimately attained a precision (1 σ) of about $\pm 1\%$ on 1×10^{-9} moles of CO₂. Under normal operation, the half-life of CO₂ in this instrument was approximately 28s (Ash, 1990), necessitating rapid data acquisition.

For carbon stable isotope ratio measurements, the sensitivity gain obtained by the instrument of Carr *et al.* (1986) over conventional systems was a factor of about $\times 1000$, for an attendant loss of precision of about $\times 100$. As dynamic vacuum mass spectrometers for stable isotope analysis generally operate to levels of analytical precision that greatly exceed the reproducibility of the extraction and purification methods used to prepare the sample gas, however, the sacrifice of this degree of analytical precision is not particularly critical for many applications in the geosciences.

The mass spectrometer described by Carr *et al.* (1986) was used, essentially unchanged, during the present investigation. Associated sample extraction and preparation methods, however, were substantially revised during the period of the present study, both as documented by Ash *et al.* (1990), and also by the present author with specific application to the analysis of traces of CO₂ and CH₄ trapped in quartz-hosted fluid inclusions. Details are given below.

Although originally conceived for the analysis of carbon stable isotopes in extraterrestrial samples, including meteorites (Carr *et al.*, 1983; Carr *et al.*, 1985; Grady *et al.*, 1985; Lewis *et al.*, 1983_{a,b}), and interplanetary dust particles (Wright *et al.*, 1988), a small number of terrestrial applications had also been investigated by the static vacuum mass spectrometer described by Carr *et al.* (1986) prior to the present work. These focused mainly on carbon sources in basaltic glasses and mantle xenoliths (Mattey *et al.*, 1984; Exley *et al.*, 1986).

3.4.4.3 Sample preparation for the measurement of carbon stable isotope ratios at the nanomole level by static vacuum mass spectrometry

3.4.4.3.1 The protocol of Carr *et al.* (1986)

Based on the stepped combustion technique of Swart *et al.* (1983), the extraction system developed by Carr *et al.* (1986) for the combustion/pyrolysis of the carbon-bearing sample, with subsequent purification, yield measurement, and transfer to the mass spectrometer of the resulting carbon dioxide, is illustrated schematically in Figures 3.5 and 3.6. Full details of the construction and operating protocol are described by Carr *et al.* (1986).

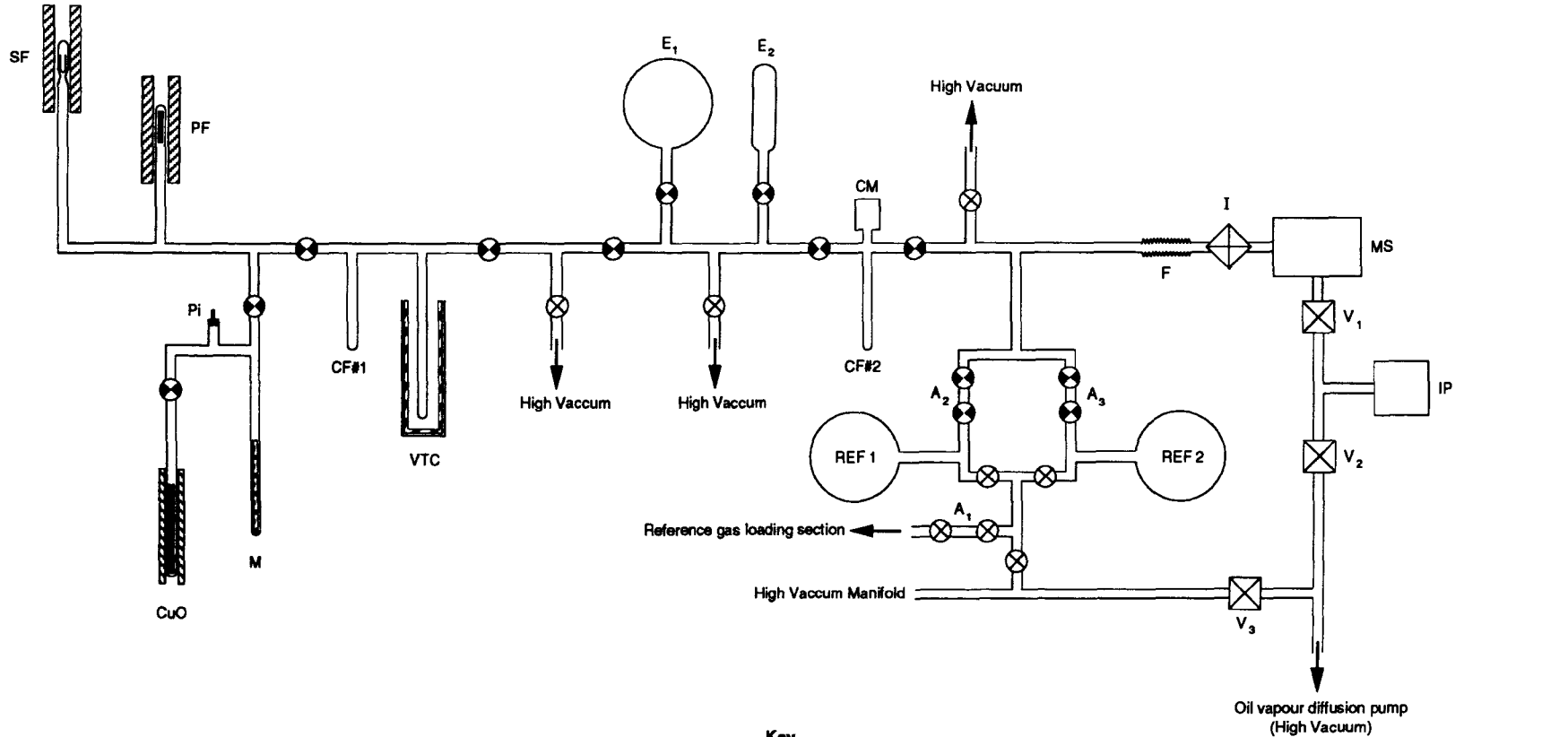
For stepped combustion, the oxygen supply was derived from heating CuO to 850°C. An important feature of the protocol was that the oxygen was then adsorbed onto a 5Å molecular sieve (M) at -196°C, after which the CuO was isolated (valved off) from the rest of the system. This served two purposes: firstly, the reduction of carbon blank levels, as any carbon dioxide present would be retained by the molecular sieve during the subsequent desorption of oxygen, at temperatures from about -50°C (Carr *et al.*, 1986) to 0°C (Ash *et al.*, 1990). Secondly, a large reservoir of oxygen could be generated by adsorbing gas onto the molecular sieve over a period of 15-20 minutes, with the CuO maintained at 850°C. An aliquot of oxygen for the combustion step was then obtained by warming the molecular sieve sufficiently to produce a pressure of ~500mbar of gas, as estimated by Pirani gauge (Pi).

A coil of platinum wire, maintained at 1050°C, formed an integral part (PF) of the combustion section. This was incorporated as a catalyst to promote the oxidation of low molecular weight hydrocarbons (particularly methane). The decomposition of nitrogen oxides, should these species be formed during the combustion process, is not effected by platinum at temperatures below ~1150°C (I P Wright, *pers. comm.*).

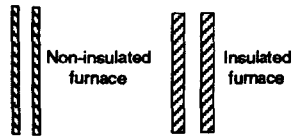
After a 30 minute combustion or pyrolysis step, gases in the extraction chamber were admitted to the purification section of the line, where CO₂ and various other components were condensed on the cold finger (CF#1) at liquid nitrogen temperature. In the case of a combustion step, excess oxygen was then re-adsorbed onto the molecular sieve at -196°C, for use in subsequent combustion steps. The extraction section was then isolated and any non-condensed gases present in the purification section pumped out.

Figure 3.5

Schematic diagram of the extraction line used for stepped combustion/pyrolysis in conjunction with carbon stable isotope ratio analysis by static vacuum mass spectrometry, as described by Carr *et al.*, 1986.



Key



- ⊗ J Young® type POR valve (not 'backed')
- ⊙ J Young® type PSU valve ('backed')
- I Inlet valve (Nupro®, compressed air actuated)
- V₁-V₃ VG® CR 38 valves

- SF Sample extraction furnace
- PF Silica tube containing Pt foil
- CuO Silica tube containing wire-form copper (II) oxide
- M 5Å molecular sieve

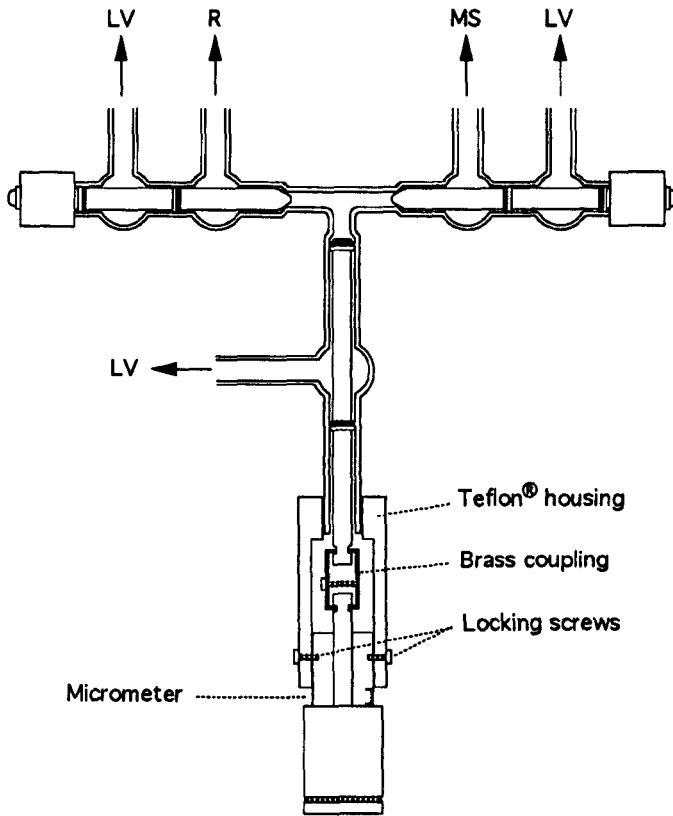
- CF# Cold finger
- VTC Variable temperature cryogenic trap
- CM Capacitance manometer (1 torr max.)
- E₁, E₂ Expansion volumes
- F Pyrex®-steel flexible coupling

- Pi Pirani gauge head
- A₁, A₂ Fixed volume aliquotters
- A₃ Variable volume aliquotter
- MS Mass spectrometer
- IP Ion pump

Figure 3.6

The variable volume aliquotter as described by Carr *et al.* (1986), illustrating also the construction of J Young® type 'PSU' valves (McNaughton *et al.*, 1983).

(After Carr *et al.*, 1986)

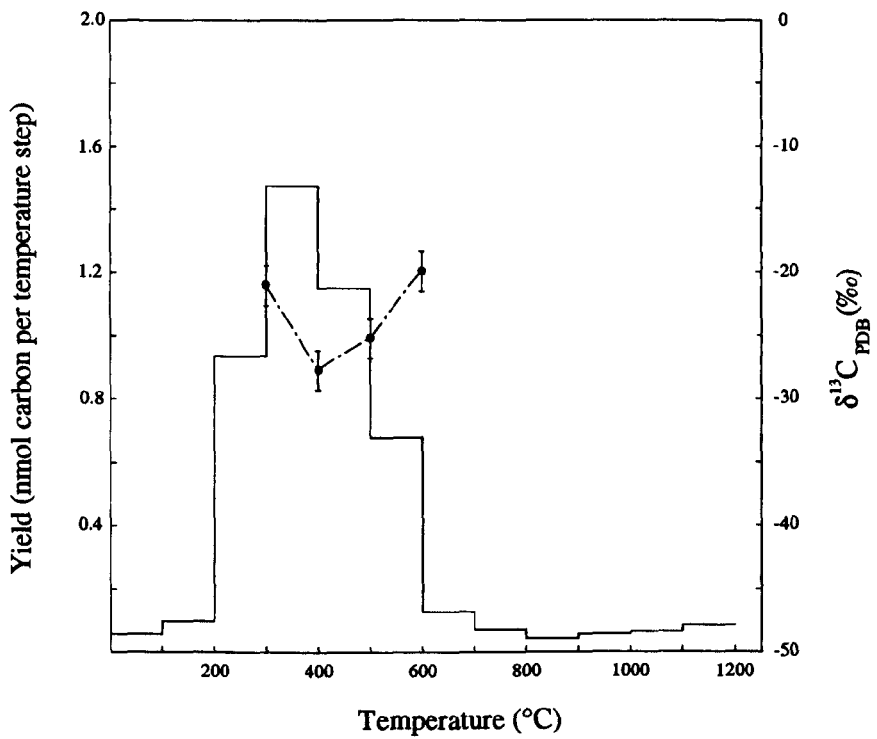


LV Low vacuum (backing)
MS Mass spectrometer
R Gas reservoir

Figure 3.7

Typical yield and isotopic composition of carbon blank released during a stepped combustion (100°C increments) using the gas preparation protocol of Carr *et al.*, 1986.

(Adapted from Carr *et al.*, 1986; Yates *et al.*, 1992)



Cryogenic separation (fractional distillation) was used to isolate the CO₂ sample gas from contaminants such as water and SO₂. This was achieved by transferring all the condensed gases from CF#1 into the variable temperature cryogenic trap VTC at -196°C, then raising the temperature of VTC to between -145 and -140°C.

The released CO₂ was then condensed in cold finger CF#2 at liquid nitrogen temperature, for subsequent yield measurement by calibrated capacitance manometer (CM). Isotopic analysis was then undertaken by admitting the gas directly into the mass spectrometer, *via* the inlet valve (I), after reducing the pressure where necessary by expanding the gas into an appropriate volume (E₁, E₂).

The yield and isotopic composition of the carbon blank released during a procedural stepped combustion using this system is shown in Figure 3.7. In this figure, the format of which is used extensively throughout the present Chapter, the yield of carbon obtained for each temperature step, normalised as a percentage of the total per °C, is indicated by the histogram, the scale of which is given in the left-hand ordinate axis. The isotopic value of the carbon released at each step is shown by the accompanying data points, complete with error bars ($\pm 1\sigma$), which refer to the right-hand ordinate axis ($\delta^{13}\text{C}$ value, per mil with respect to PDB). In Figure 3.7, the $\delta^{13}\text{C}$ values are typical of terrestrial organic matter.

3.4.4.3.2 The protocol of Ash *et al.* (1990)

The eventual discovery that the extraction and preparation system of Swart *et al.* (1983) as modified by Carr *et al.* (1986) did not give quantitative carbon yields was suggested by the findings of Tang, Lewis *et al.* (1988) and subsequently confirmed by experiments involving the combustion of diamonds (Ash, 1990), where a mean CO₂ yield of only 51.3% occurred. No isotopic fractionation was apparent, however, despite the low yields (Ash, 1990; Wright and Pillinger, 1989). Potential contributory causes of the low yield problem were identified by Ash (1990) as: (i) Loss of sample during initial evacuation from atmospheric pressure, particularly in the case of fine-grained samples; (ii) Oxygen deficiency during the combustion of large, carbon-rich samples; (iii) Trapping of CO₂ by the molecular sieve, at the beginning or end of the combustion step.

To overcome the shortcomings of the combustion procedure of Carr *et al.* (1986), modifications to the design and operating protocol were implemented by Ash (1990), as also detailed by Ash *et al.* (1990). The combustion section of the extraction line was modified to the configuration as shown in Figure 3.8, which is similar to that described by Boyd *et al.* (1988) for the preparation of nitrogen at the nanomole level. Oxygen for combustion steps was now supplied directly by a CuO furnace located within the volume of the combustion vessel.

Figure 3.8

The sample extraction and combustion section described by Ash *et al.* (1990), substituting for that of Carr *et al.* (1986) in the gas preparation system used in conjunction with carbon stable isotope ratio analysis at the nanomole level.

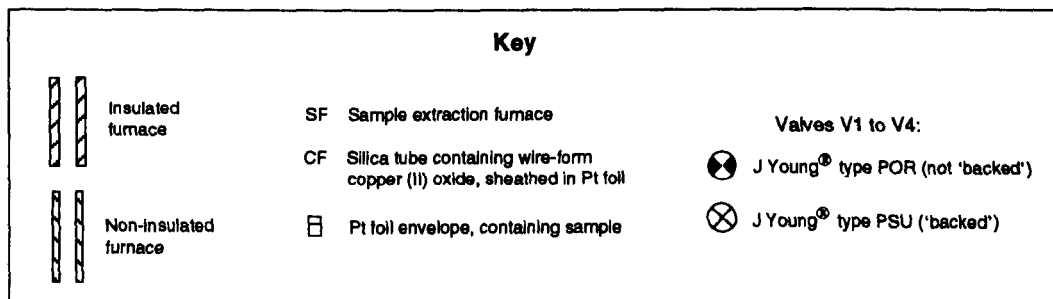
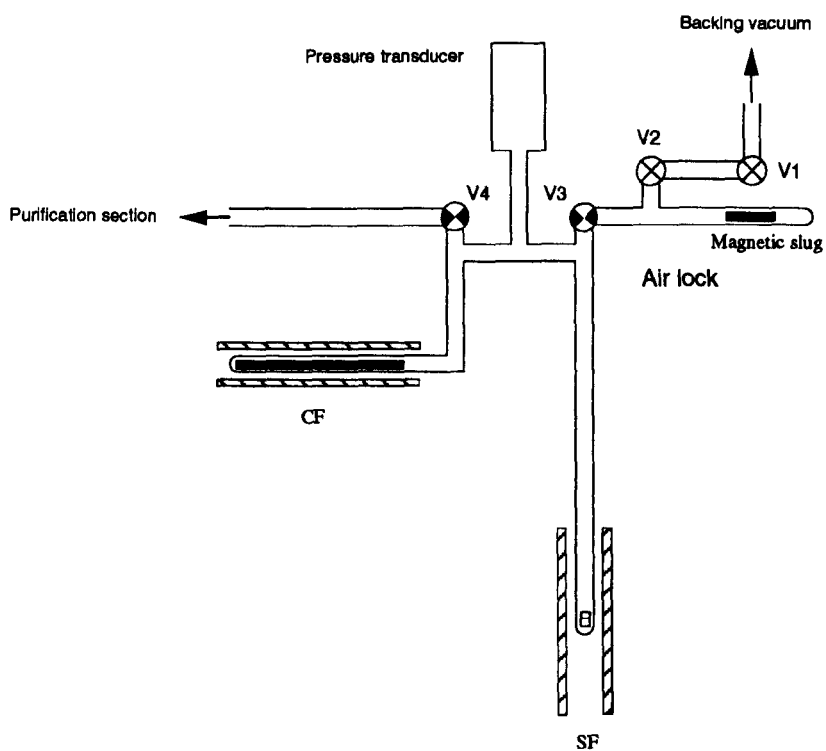
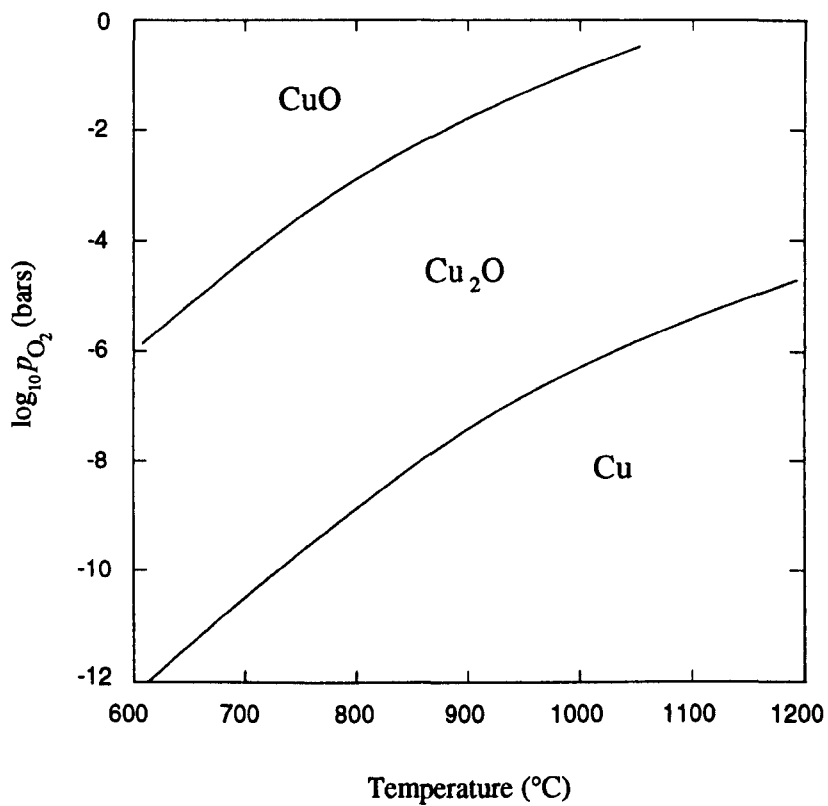


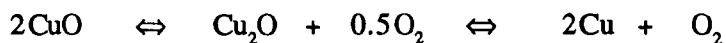
Figure 3.9

Stability fields of copper and copper oxides as a function of temperature and oxygen partial pressure.

(After Robinson and Kusakabe, 1975)



Deficiency of oxygen should not occur, as the partial pressure of this gas is maintained constant throughout the combustion process (if the CuO is maintained at constant temperature), *via* the equilibria:



For coexisting CuO and Cu₂O at 850°C, the corresponding equilibrium partial pressure of oxygen is ~10mbar, as shown in Figure 3.9. The CuO was sheathed in Pt foil to permit the furnace temperature to be raised to ~950°C without reaction occurring between CuO and the surrounding silica glass tubing. The molecular sieve was thus dispensed with, as was the requirement for a separate Pt finger maintained at 1050°C. The initially high carbon blank (~20ng per 30 minute combustion step) associated with the use of an on-line CuO furnace was overcome by successive recycling of the CuO through the temperature programme 950-600-450°C, with the removal of CO₂ at the end of each cycle by pumping.

A seldom-discussed advantage of using CuO as an oxygen source within the volume of the combustion vessel is that the total pressure during the post-combustion cryogenic separation stage is substantially reduced compared to the procedure advocated by Carr *et al.* (1986). In turn, this promotes the efficiency of cryogenic separation of carbon dioxide from the excess oxygen component. Using the protocol of Carr *et al.* (1986), any carbon dioxide not condensed during this process would be subsequently trapped by the molecular sieve during the oxygen re-adsorption stage and thus be excluded from the total CO₂ yield measurement.

Samples were introduced into an air-lock, which was subsequently evacuated to a pressure of $<5 \times 10^{-6}$ mbar before transferring the sample, by aid of a magnetic slug, into the combustion vessel. This avoided exposing both the combustion vessel and CuO to atmosphere during sample loading, with consequent advantages for minimising carbon blank levels. Samples were contained in a closed, pre-combusted Pt foil envelope (25µm thickness), to minimise the risk of loss during initial evacuation. Carbon blanks associated with this technique were only 10-20ng for a complete sample analysis; these could be reduced even further by using Pt foil of only ~5µm thickness and by treatment with dichloromethane (Yates *et al.*, 1989).

Using the revised sample combustion procedures, a mean yield value slightly in excess of 100% was obtained for the combustion of diamond powders (Ash, 1990), although the gas purification procedures remained unchanged. Sample run numbers T428 onwards refer to the use of the modified sample extraction protocol.

3.4.5 Dynamic vacuum mass spectrometry and associated sample preparation lines used in the present study

Two parallel investigations were initiated at the beginning of the present work. One involved the use of high sensitivity static vacuum mass spectrometry, to assess the application of this technique to the carbon stable isotope analysis of hydrothermal fluid inclusion components, where carbon may be present as coexisting CO₂ and CH₄ and at abundances of only a few ppm with respect to the host mineral. The second line of study was concerned with optimising the experimental protocol for fluid inclusion carbon stable isotope analysis by conventional mass spectrometry, including provision for the analysis of carbon dioxide and methane from the same sample.

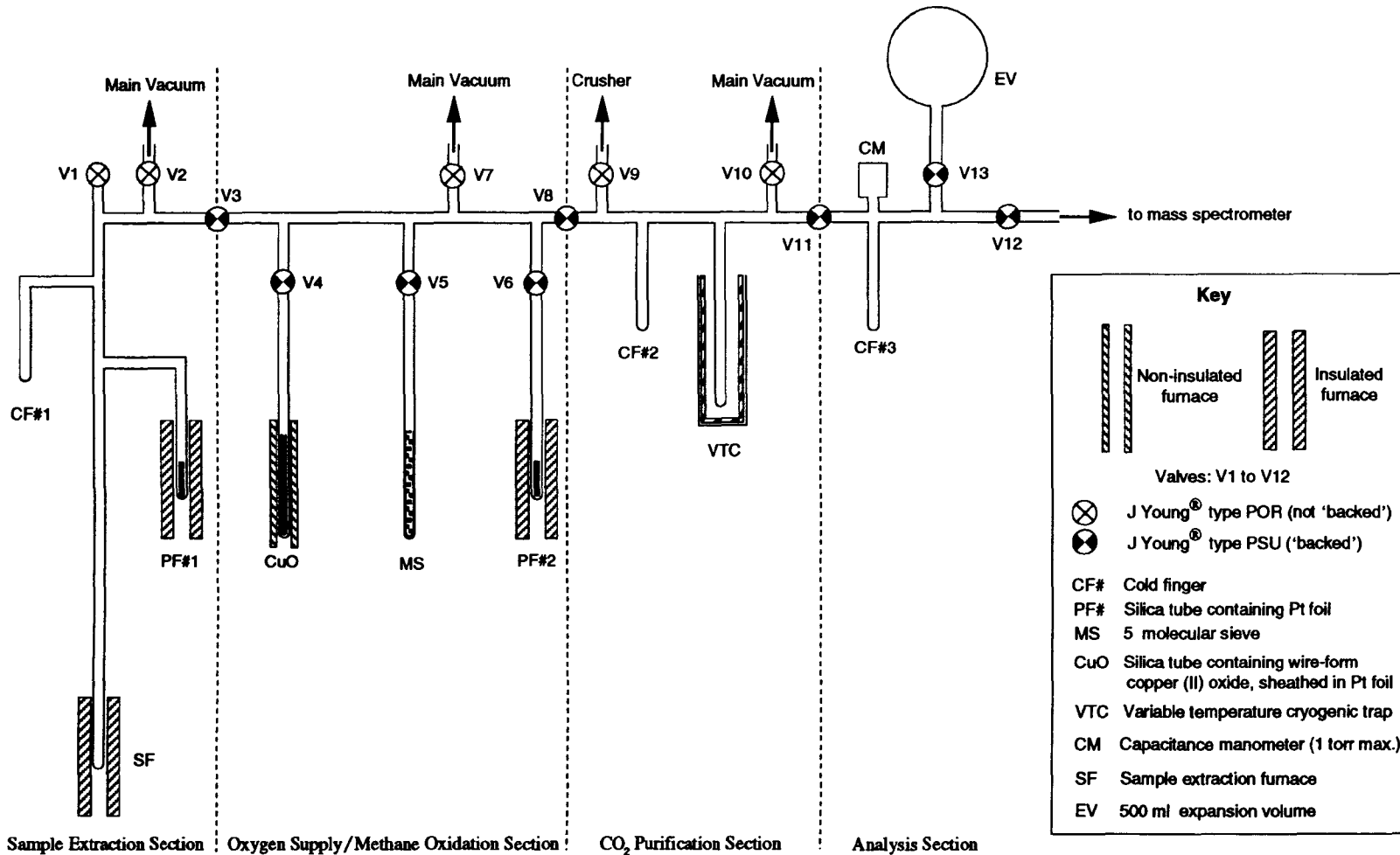
During the course of this second line of investigation, a parallel study by Jackson (Jackson *et al.* 1988a,b; Jackson, 1990) was in progress to optimise the stepped heating method for releasing carbon dioxide from fluid inclusions, for subsequent isotopic analysis by conventional mass spectrometry. The rock types used in that study, devised to address questions associated with charnockite formation in southern India, were of amphibolite and granulite facies. Although the same extraction line and coupled mass spectrometer (a VG[®]SIRA 24) were used as in the present author's work, the experimental procedures differed in detail, as discussed below.

The VG[®]SIRA 24 used in the protocol development work, and for many of the subsequent analytical measurements, is designed to give high precision measurements (ultimately to $\pm 0.005\%$, at the 1σ error level) for a major beam current of 5×10^{-9} A. As with all mass spectrometers, analytical precision (and accuracy) deteriorates as the amount of gas available for measurement decreases below the optimum value. For samples $> \sim 3\mu\text{gC}$ equivalent, the 1σ precision is better than $\pm 0.01\%$; the accuracy, however, deteriorates to about $\pm 0.5\%$ for a realistic minimum sample size of $0.5\mu\text{gC}$. Jackson (1990) found that samples as small as $0.2\mu\text{gC}$ could be analysed to an accuracy within $\pm 1\%$, although at these low operating pressures the measured $\delta^{13}\text{C}$ values were invariably less than the true values.

The gas extraction line used in conjunction with the SIRA 24 was based in principle on the system described by Swart *et al.* (1983), although different in detail; a schematic representation is shown in Figure 3.10. In a small number of cases, crushing was used to release the trapped inclusion volatiles, using a modified Nupro[®]SS6 stainless steel bellows valve (as described by Matthey *et al.*, 1989) sealed with a Cu gasket. Otherwise, sample loading was achieved after the removal of valve V1 stem; quartz grains were then admitted directly through a cleaned silica glass guide tube. No sample bucket was used (*cf.* Carr *et al.*, 1986). As with the extraction system of Carr *et al.* (1986), the reaction vessel (silica tube) was exposed to atmosphere each time a sample was loaded.

Figure 3.10

Schematic diagram of the extraction line used for stepped combustion/pyrolysis in conjunction with carbon stable isotope ratio analysis by VG[®]SIRA 24 mass spectrometer



The relatively low concentrations of CO₂ in the quartz samples used in the present study, together with the requirement to obtain stable carbon isotope ratios on the (generally much less abundant) coexisting CH₄, required that a quantity of sample grains totalling 500 to 1200mg was used per analysis.

After sample loading, the extraction vessel was evacuated to a pressure of <10⁻⁵mbar, a procedure which could generally be achieved in about 1 hour, although pumping overnight to achieve <10⁻⁶mbar was undertaken in most cases. Stepped heating, either in the presence or absence of pure oxygen (depending on the adopted protocol) was then used to release the fluid inclusion volatiles. In the case of a 'combustion' step, oxygen was concentrated and purified by the use of a 5Å molecular sieve, as discussed in Section 3.4.4.3.1 above. All heating steps were of 30 minutes duration.

Towards the end of the present study, the sample pyrolysis/combustion section of the extraction line was modified, for the requirements of other users, to that described by Ash *et al.* (1990). As this design is unsuitable for the admittance of relatively large quantities of mineral sample, the project work was completed at the NERC Isotope Geosciences Laboratory, using a new extraction line system designed by the present author (Figure 2.2), essentially based on the earlier (Figure 3.10) configuration. In this case, samples were collected in stopcock vessels (based on the same J Young® type POR valve as used in all of the extraction lines discussed in this chapter) fitted with greased B10 ground-glass sockets, for transfer to the inlet of a VG®SIRA Series II mass spectrometer in that laboratory.

3.4.6 The development of an experimental protocol appropriate to fluid inclusion extraction for small sample δ¹³C analysis

3.4.6.1 Initially-adopted procedures for the removal of 'contaminant' carbon

The starting point for the current investigation, irrespective of whether isotopic analyses were undertaken by static vacuum or conventional mass spectrometry, was to assume that the stepped combustion technique developed by Swart *et al.* (1983) for the removal of contaminant carbon from extraterrestrial samples was similarly applicable to the isolation of carbonaceous components in quartz-hosted terrestrial fluid inclusions. Two major differences, however, distinguish the nature of the sample material of the present study from that used in the work of Swart *et al.* (1983). Firstly, the carbon species of interest in the present investigation occur as components of an aqueous fluid phase, trapped in a chemically inert matrix, rather than as mineral or organic constituents of a solid matrix that requires chemical alteration (oxidation) to release the carbon. Secondly, major release of fluid from quartz samples used in the present study occurred below the combustion temperature (425±25°C) advocated by Swart *et al.* (1983) for the removal of organic contamination.

3.4.6.2 Preliminary $\delta^{13}\text{C}$ results using static vacuum mass spectrometry

During the development of the static vacuum mass spectrometer and associated sample preparation methods described by Carr *et al.* (1986) an initial 'feasibility study' was undertaken, at the present author's instigation, by Carr (1984, unpublished data), to assess the use of the instrument in analysing stable isotope ratios of fluid inclusion carbon compounds at the nanomole level. Results from this preliminary investigation are illustrated in Figure 3.11 (a - e). All heating steps were of 30 minutes duration.

Note that in Figure 3.11 (a) and (b), the samples were 'combusted' (heated in an atmosphere of ~500mbar of pure oxygen) to 425°C, before incremental heating *in vacuo*. 'Splits' of the same quartz sample were used to generate the data shown in Figure 3.11 (c), (d) and (e). Figure 3.11 (c) and (d) illustrates the effects of variation of 'combustion' temperature (450 and 425°C respectively), whereas Figure 3.11 (e) shows the results of stepped 'pyrolysis' without any pre-combustion stage.

The regime of 'combustion' at 425°C followed by 'pyrolysis' at higher temperatures was suggested by Carr (*pers. comm.*) as probably giving the best resolution between any organic contamination and the indigenous, trapped gas. Note that at this stage of development, the analytical precision of $\delta^{13}\text{C}$ measurement was about $\pm 5\%$ (1σ error). A further point of note (discussed below) is that the Pt finger, maintained at 1050°C throughout the stepped heating (see Section 3.4.4.3.1), was later found to retain significant quantities of adsorbed oxygen (Boyd, 1988; Boyd *et al.*, 1988) hence, in reality, traces of methane released during the 'pyrolysis' steps may have been oxidised to CO_2 on the surface of the platinum.

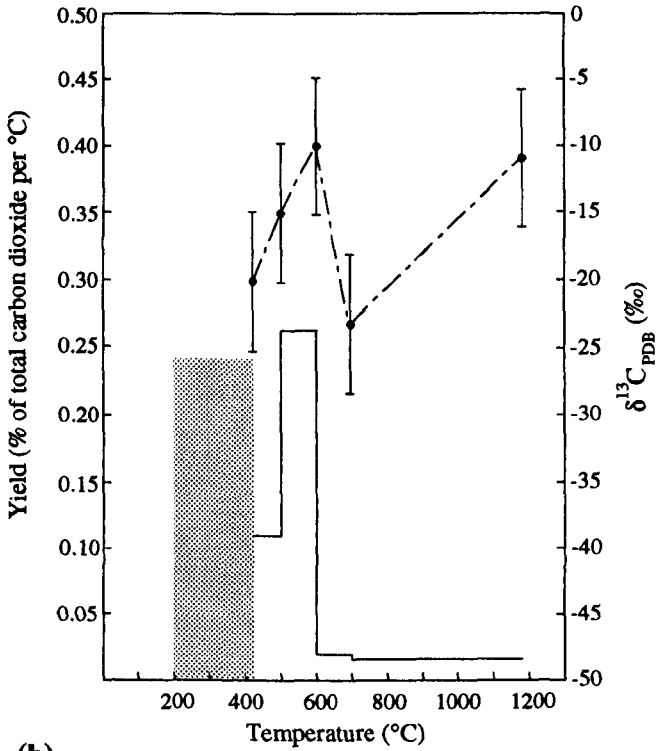
The carbon release profiles shown in Figure 3.11 are probably best interpreted as the result of mixing between different relative proportions of a carbon blank of $\delta^{13}\text{C}$ value *ca.* -25‰, and indigenous (fluid inclusion) carbon sources having a combined $\delta^{13}\text{C}$ value of *ca.* -10‰. The yield and isotopic composition of carbon released during a typical procedural (combustion) blank at this stage of development of the system was as shown in Figure 3.7. With reference to Figure 3.11, if the heating step at $\geq 550^\circ\text{C}$ is taken as the optimum discriminant between the carbon blank yield and carbon release from fluid inclusions, then the three $\delta^{13}\text{C}$ analyses of sample HEM-80-47 all lie within the range from -8 to -12‰. Furthermore, $\delta^{13}\text{C}$ results for the other two Hemerdon samples also fall in this range, within the limits of analytical precision. Wright and Pillinger (1989), referring to this preliminary investigation, concluded that the ratio of sample-to-blank carbon yield would have to be significantly improved for progress to be achieved.

Figure 3.11

Preliminary results obtained for stepped heating release and isolation of palaeofluid carbon $\Sigma(\text{CO}_2, \text{CH}_4)$ from hydrothermal fluid inclusions in quartz, with $^{13}\text{C}/^{12}\text{C}$ ratio determination at the nanomole level by static vacuum mass spectrometry. (R H Carr, 1984, unpublished data.)

Stepped heating up to 425°C in the presence of supplied oxygen; stepped heating *in vacuo* for all steps at higher temperature. 30 minutes per step. Pt foil at ~1050°C in contact with released gases during the extraction procedure.

(a)



Sample: **HEM-80-5** (T071)

Weight: 26.850 mg

ΣC (~20 to 425°C) = 265 ng (9.9 ppm)

$\Sigma \delta^{13}\text{C}$ (~20 to 425°C) = -20‰

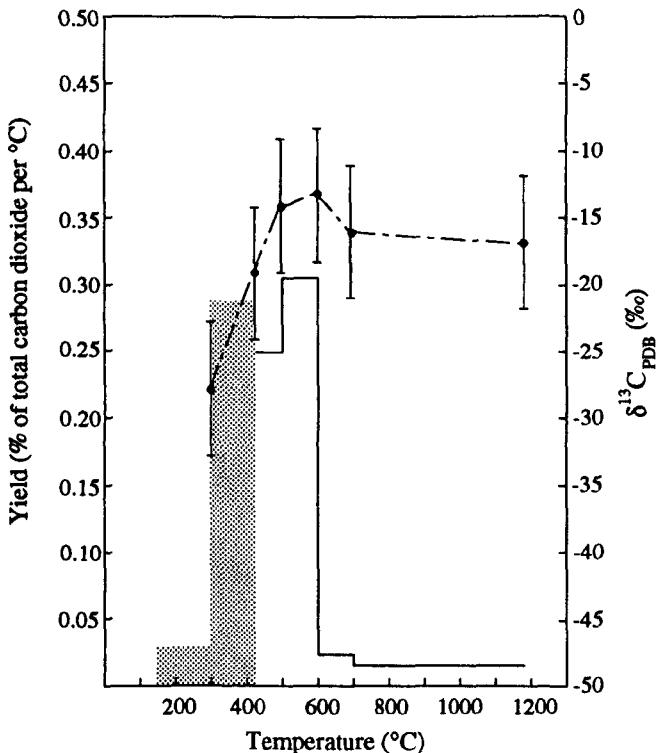
ΣC (425 to 600°C) = 168 ng (6.3 ppm)

$\Sigma \delta^{13}\text{C}$ (425 to 600°C) = -11.2‰

Temperature (°C)	Yield (ng C)	$\delta^{13}\text{C}_{\text{PDB}}$ (‰)
200	1	nm*
425	264	-20
500	40	-15
600	128	-10
700	11	-23
1180	42	-11

* not measured

(b)



Sample: **HEM-79-51** (T072)

Weight: 22.230 mg

ΣC (~20 to 425°C) = 171 ng (7.7 ppm)

$\Sigma \delta^{13}\text{C}$ (~20 to 425°C) = -19.9‰

ΣC (425 to 600°C) = 306 ng (13.8 ppm)

$\Sigma \delta^{13}\text{C}$ (425 to 600°C) = -13.4‰

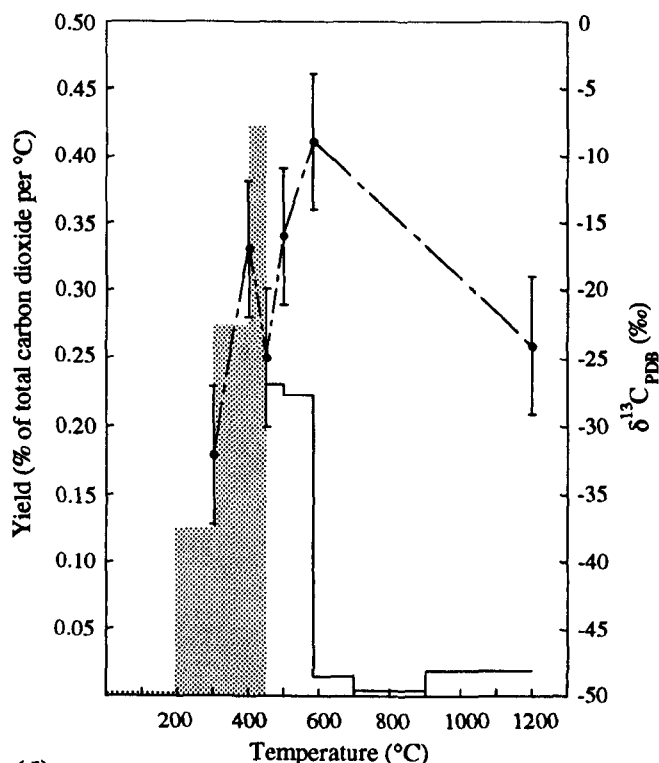
Temperature (°C)	Yield (ng C)	$\delta^{13}\text{C}_{\text{PDB}}$ (‰)
150	1	nm*
300	19	-28
425	151	-19
500	78	-14
600	128	-13
700	10	-16
1175	32	-17

* not measured

Figure 3.11 (continued)

Stepped heating up to 425/450°C in the presence of supplied oxygen; stepped heating *in vacuo* thereafter. 30 minutes per step. Pt foil at ~1050°C in contact with released gases during the extraction procedure.

(c)



Sample: **HEM-80-47** (T067)

Weight: 17.148 mg

ΣC (~20 to 450°C) = 170 ng (9.9 ppm)

$\Sigma \delta^{13}C$ (~20 to 450°C) = -22.7‰

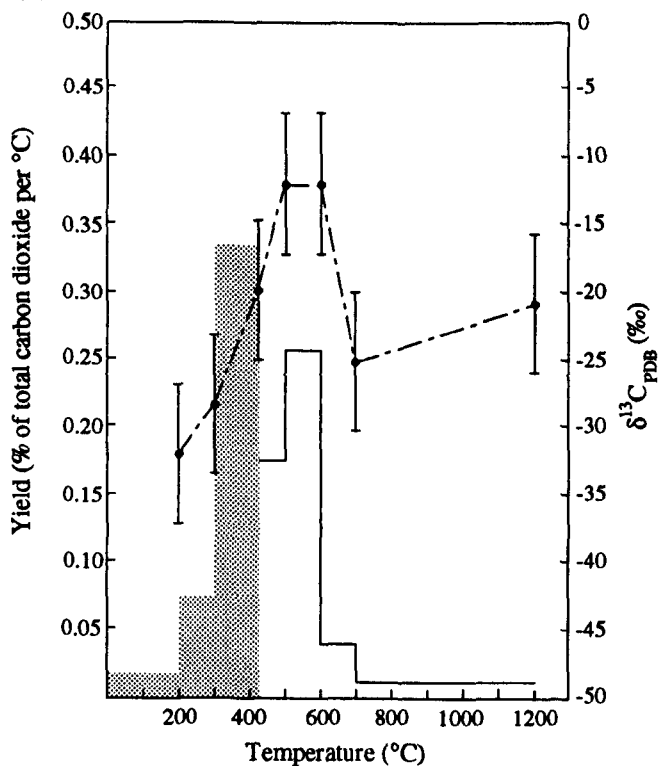
ΣC (450 to 585°C) = 85 ng (5.0 ppm)

$\Sigma \delta^{13}C$ (450 to 585°C) = -11.0‰

Temperature (°C)	Yield (ng C)	$\delta^{13}C_{PDB}$ (‰)
200	1	nm*
300	34	-32
400	76	-17
450	59	-25
500	32	-16
585	53	-8
700	5	nm*
900	2	nm*
1200	17	-24

* not measured

(d)



Sample: **HEM-80-47** (T073)

Weight: 20.600 mg

ΣC (~20 to 425°C) = 151 ng (7.3 ppm)

$\Sigma \delta^{13}C$ (~20 to 425°C) = -21.9‰

ΣC (425 to 600°C) = 112 ng (5.4 ppm)

$\Sigma \delta^{13}C$ (425 to 600°C) = -12.0‰

Temperature (°C)	Yield (ng C)	$\delta^{13}C_{PDB}$ (‰)
200	10	-32
300	21	-28
425	120	-20
500	38	-12
600	74	-12
700	11	-25
1150	24	-21

Figure 3.11 (continued)

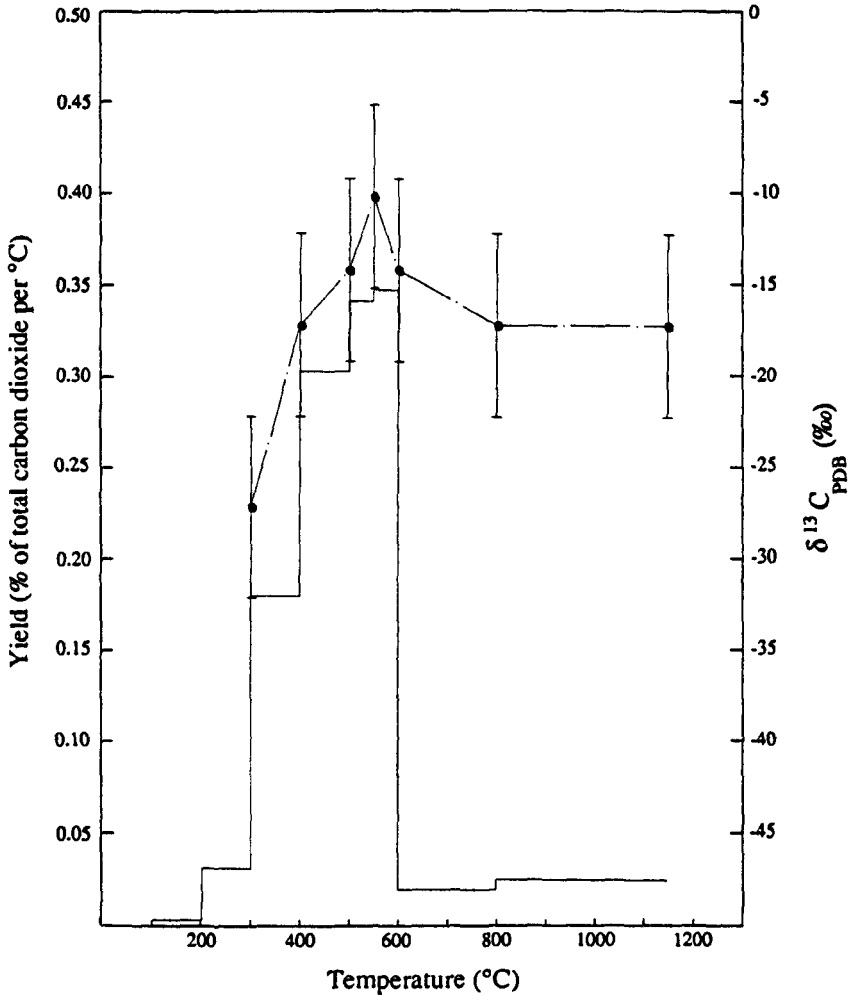
(e) Sample: **HEM-80-47** (T068)

Stepped heating in the absence of supplied oxygen.
Released gases exposed to Pt foil at $\sim 1050^\circ\text{C}$.

Sample weight: 24.370 mg

ΣC (~ 20 to 1150°C) = 315 ng (12.9 ppm)

$\Sigma \delta^{13}\text{C}$ (~ 20 to 1150°C) = -14.7‰



Temperature (°C)	Yield (ng C)	$\delta^{13}\text{C}_{\text{PDB}}$ (‰)
100	nm	nm
200	1	nm
300	10	-27
400	57	-17
500	96	-14
550	54	-10
600	55	-14
800	13	-17
1150	29	-17

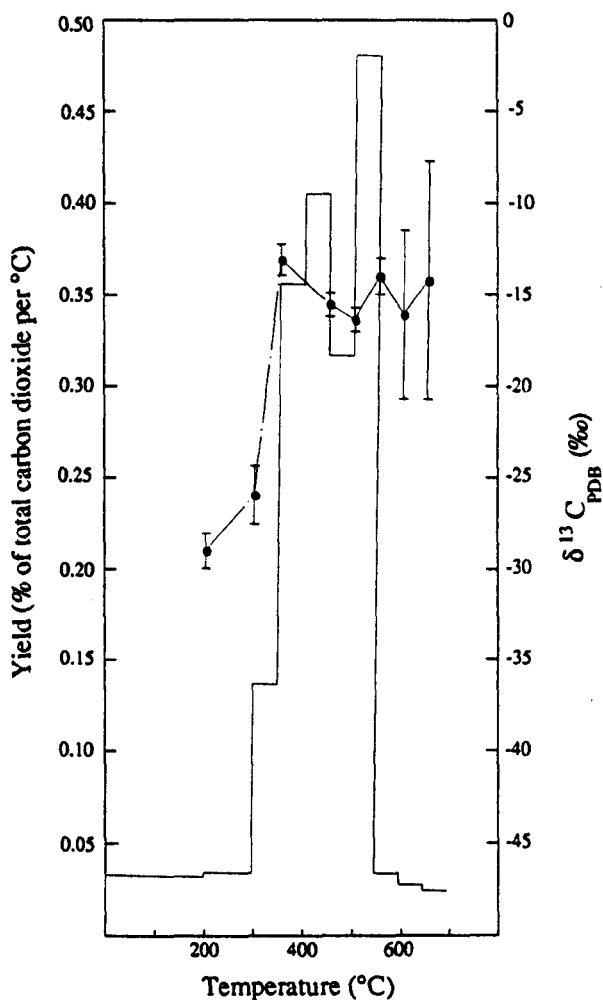
Figure 3.12

Stepped heating release of palaeofluid carbon $\Sigma(\text{CO}_2, \text{CH}_4)$ from hydrothermal fluid inclusions in quartz single grain (~20mg) replicates (sample HEM-80-1), with $^{13}\text{C}/^{12}\text{C}$ ratio determination by static vacuum mass spectrometry using the protocol of Carr *et al.* (1986). Pt catalyst at ~1050°C throughout.

(a) Run: T326 No supplied oxygen Sample weight: 21.287 mg

ΣC (~20 to 300°C) = 25.8 ng (1.21 ppm); $\Sigma \delta^{13}\text{C} = -27.8\text{‰}$

ΣC (300 to 600°C) = 223.0 ng (10.50 ppm); $\Sigma \delta^{13}\text{C} = -14.7\text{‰}$

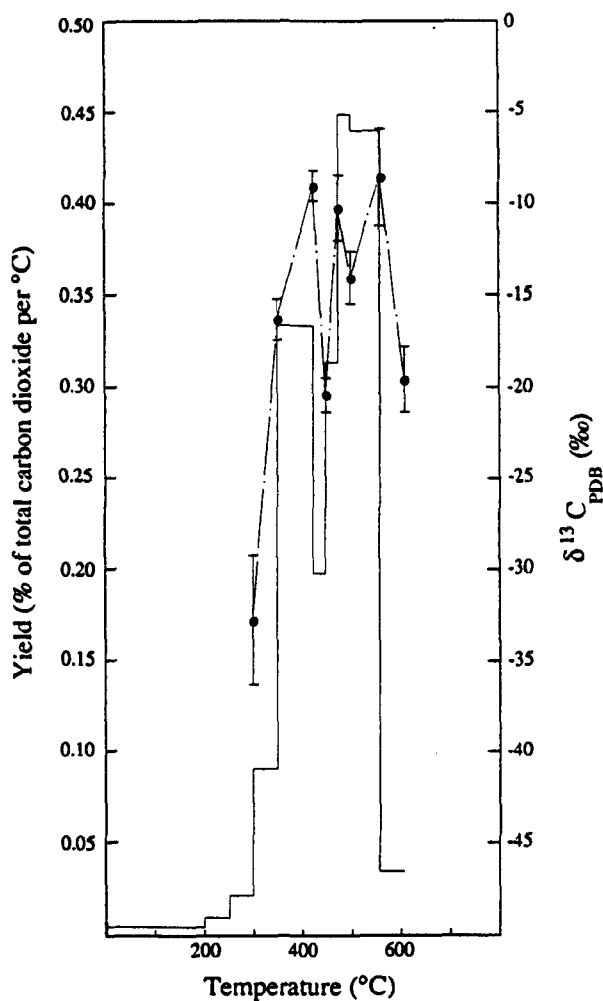


T (°C)	Yield (ng C)	Concentration (ppm C)	$\delta^{13}\text{C}$ (‰)	σ (‰)
200	16.8	0.79	-28.9	0.96
300	9.0	0.42	-25.8	1.60
350	17.8	0.83	-12.9	0.85
400	45.8	2.15	nm	
450	52.1	2.45	-15.3	0.65
500	40.9	1.92	-16.1	0.64
550	61.9	2.91	-13.7	1.00
600	4.6	0.22	-15.8	4.60
650	3.8	0.18	-13.9	6.50
700	3.4	0.16	nm	

Figure 3.12 (continued)

Stepped heating release of palaeofluid carbon $\Sigma(\text{CO}_2, \text{CH}_4)$ from hydrothermal fluid inclusions in quartz single grain (~20mg) replicates (sample HEM-80-1), with $^{13}\text{C}/^{12}\text{C}$ ratio determination by static vacuum mass spectrometry using the protocol of Carr *et al.* (1986). Pt catalyst at ~1050°C throughout.

(b) Run: T360 No supplied oxygen Sample weight: 24.122 mg
 ΣC (~20 to 300°C) = 8.4 ng (0.35 ppm); $\Sigma \delta^{13}\text{C} = -33\text{‰}$
 ΣC (300 to 610°C) = 353.9 ng (14.67 ppm); $\Sigma \delta^{13}\text{C} = -11.0\text{‰}$

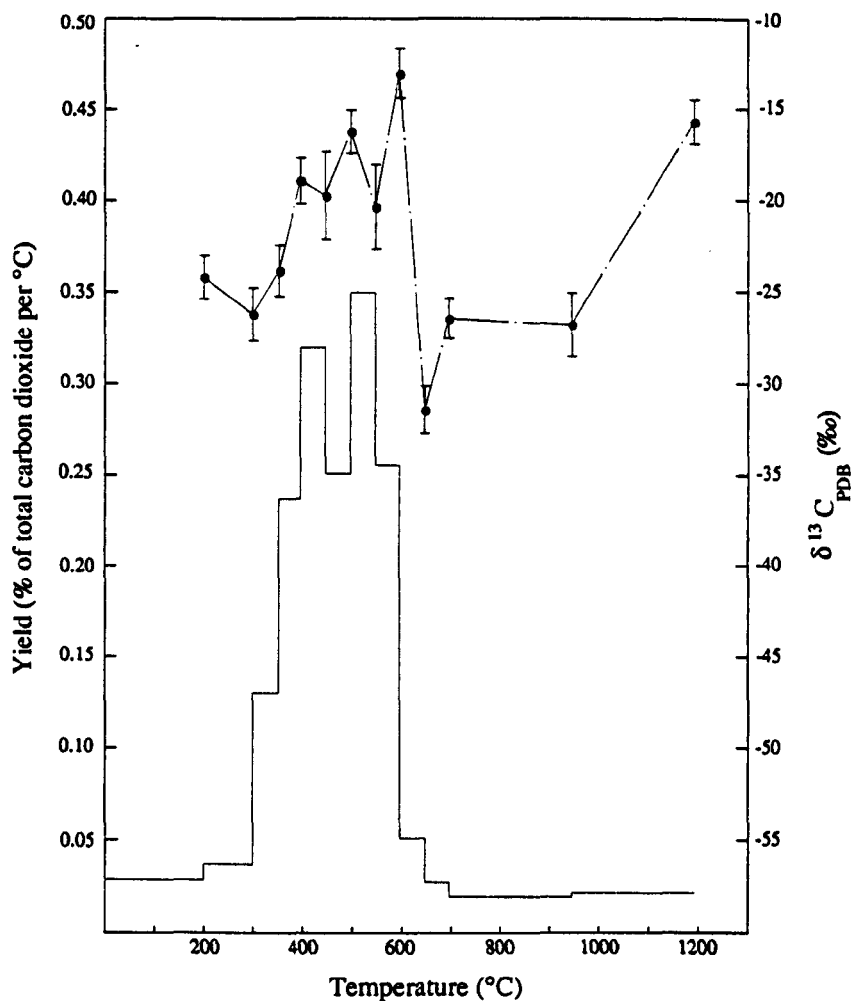


T (°C)	Yield (ng C)	Concentration (ppm C)	$\delta^{13}\text{C}$ (‰)	σ (‰)
200	2.3	0.10	nm	
250	1.7	0.07	nm	
300	4.4	0.18	-32.9	3.54
350	19.5	0.81	-16.4	1.12
425	108.5	4.50	-9.1	0.83
450	21.4	0.89	-20.5	0.94
475	34.0	1.41	-10.3	1.80
500	48.7	2.02	-14.1	1.42
560	114.6	4.75	-8.6	2.65
610	7.3	0.30	-19.6	1.80

Figure 3.12 (continued)

Stepped heating release of palaeofluid carbon $\Sigma(\text{CO}_2, \text{CH}_4)$ from hydrothermal fluid inclusions in quartz single grain (~20mg) replicates (sample HEM-80-1), with $^{13}\text{C}/^{12}\text{C}$ ratio determination by static vacuum mass spectrometry using the protocol of Carr *et al.* (1986). Pt catalyst at ~1050°C throughout.

(c) Run: T370 No supplied oxygen Sample weight: 23.734 mg
 ΣC (~20 to 302°C) = 66.8 ng (2.82 ppm); $\Sigma \delta^{13}\text{C} = -25\text{‰}$
 ΣC (302 to 600°C) = 548.0 ng (23.09 ppm); $\Sigma \delta^{13}\text{C} = -18.4\text{‰}$

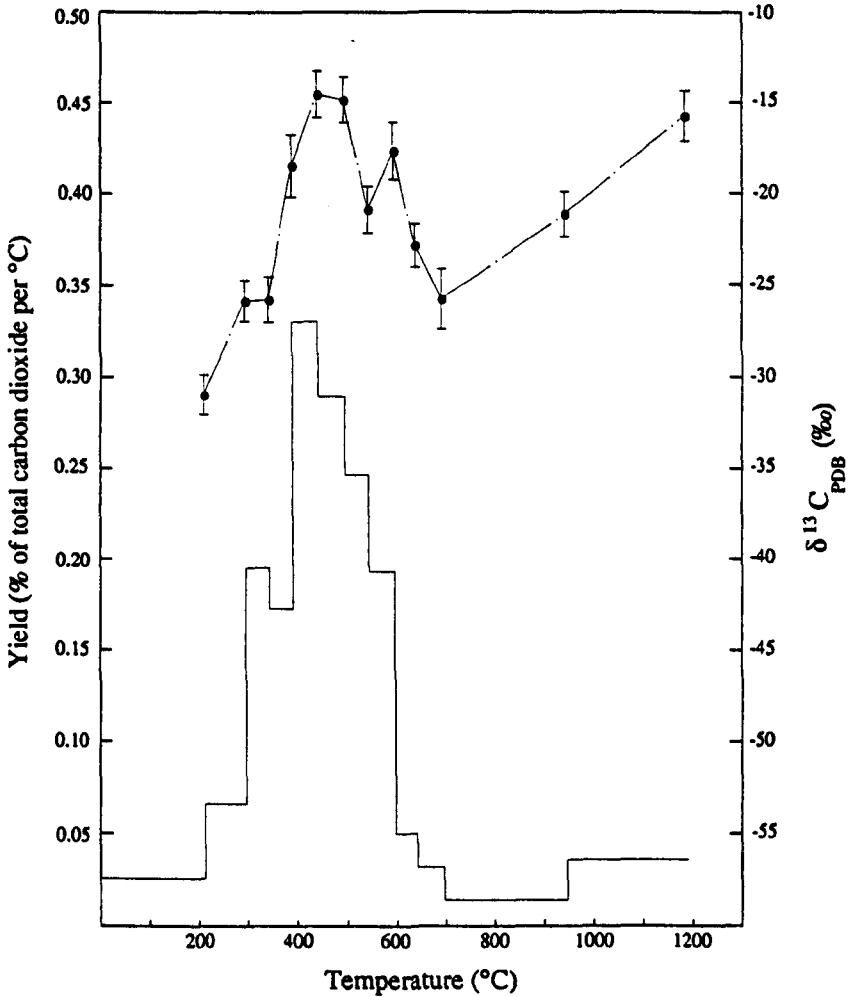


T (°C)	Yield (ng C)	Concentration (ppm C)	$\delta^{13}\text{C}$ (‰)	σ (‰)
200	40.1	1.69	-24.2	1.18
302	26.7	1.13	-26.2	1.46
355	49.7	2.09	-23.8	1.41
400	76.4	3.22	-18.9	1.26
450	114.6	4.83	-19.7	2.41
501	91.7	3.86	-16.2	1.19
552	127.9	5.39	-20.3	2.32
600	87.8	3.70	-13.0	1.37
652	19.1	0.81	-31.4	1.29
701	9.6	0.40	-26.4	1.09
951	34.4	1.45	-26.7	1.73
1200	38.2	1.61	-15.6	1.21

Figure 3.12 (continued)

Stepped heating release of palaeofluid carbon $\Sigma(\text{CO}_2, \text{CH}_4)$ from hydrothermal fluid inclusions in quartz single grain (~20mg) replicates (sample HEM-80-1), with $^{13}\text{C}/^{12}\text{C}$ ratio determination by static vacuum mass spectrometry using the protocol of Carr *et al.* (1986). Pt catalyst at ~1050°C throughout.

(d) Run: T372 Oxygen supplied Sample weight: 16.665 mg
 ΣC (~20 to 303°C) = 58.8 ng (3.53 ppm); $\Sigma \delta^{13}\text{C}$ = -28‰
 ΣC (303 to 605°C) = 377.7 ng (22.67 ppm); $\Sigma \delta^{13}\text{C}$ = -17.9‰



T (°C)	Yield (ng C)	Concentration (ppm C)	$\delta^{13}\text{C}$ (‰)	σ (‰)
216	28.6	1.72	-30.9	1.08
303	30.2	1.81	-25.8	1.13
351	49.1	2.95	-25.7	1.26
400	44.3	2.66	-18.4	1.70
452	89.8	5.39	-14.5	1.29
505	80.2	4.81	-14.8	1.27
553	61.9	3.71	-20.8	1.28
605	52.5	3.15	-17.6	1.56
650	11.8	0.71	-22.8	1.18
704	9.0	0.54	-25.7	1.65
955	18.1	1.09	-21.1	1.24
1201	46.2	2.77	-15.7	1.39

Further evidence for the critical influence of blank levels on the carbon isotopic analysis of fluid inclusion components is shown in Figure 3.12, which illustrates replicate stepped heating analyses, using the system of Carr *et al.* (1986), of sample HEM-80-1 (single grains of quartz). Results (a) and (b) were obtained by the present author, using incremental heating in the absence of supplied oxygen; (c) and (d) show the results of analyses undertaken on behalf of the author by Dr M M Grady. Note that the Pt catalyst adjacent to the sample extraction tube was maintained at 1050°C throughout, which possibly negated any distinction between 'combustion' and 'pyrolysis'. Note also the improved analytical precision associated with isotopic measurements. Salient features of these release profiles are as follows:

(i) In Figure 3.12(b), the carbon yield between ambient temperature and 300°C is comparable to the system blank recorded by Ash (1990) for the same line. Thus, the isotope values recorded for the 560 and 425°C steps (-8.6 and -9.1‰ respectively), where the sample-to-blank ratio is at a maximum (and probably in excess of 25:1), are likely to represent the closest approach to the true sample value. Note that the 'dip' at 450°C in the carbon yield profile is accompanied by a corresponding decrease in the associated $\delta^{13}\text{C}$ value, in accord with this explanation.

(ii) In Figure 3.12(a), $\delta^{13}\text{C}$ values obtained during the five heating increments from 350°C to 550°C, corresponding to the major fluid release, are relatively uniform at -12.9 to -16.1‰. However, the associated CO_2 yields ranged from 17.8 to 61.9 ngC, which is substantially lower than the yields (108.5, 114.6 ng) used to obtain the 'best estimate' of fluid inclusion $\delta^{13}\text{C}$ in example (b). Coupled with the higher blank value at low temperature (<300°C) in this instance, it is evident that the sample-to-blank ratio will be significantly worse than in case (b), thereby accounting for the 'lighter' $\delta^{13}\text{C}$ values. For fluid released between 400 and 550°C (three increments), the mean weighted $\delta^{13}\text{C}$ value is -14.9‰.

(iii) The effect of carbon blank masking the isotopic composition of the fluid inclusion release is further illustrated in examples (c) and (d), where the carbon yield values up to 300°C (prior to the onset of significant decrepitation of the quartz) are substantially higher than those recorded for examples (a) or (b). The mean weighted $\delta^{13}\text{C}$ values for gas released between ~350 and ~600°C (five steps) in the case of examples (c) and (d) are -17.9 and -16.8‰ respectively.

3.4.6.3 Investigation strategy: towards an 'optimised' stepped heating procedure

The experimental objectives at this stage of the study were twofold. Firstly, it was necessary to establish a methodology, with analysis by conventional mass spectrometry, whereby fluid inclusion stable carbon isotopic data obtained on small samples (~1 μgC equivalent), gave good agreement with results obtained using relatively large quantities of the same samples.

This, in turn, required a re-assessment of the suitability of the procedures of Swart *et al.* (1983), as adapted by Carr (1984, unpublished data) for minimising contamination in the case of fluid inclusion extraction from grains of quartz.

Secondly, after an appropriate (minimal blank) gas extraction procedure had been demonstrated, it was then possible to re-investigate the isotopic analysis of fluid inclusion carbon at the nanomole level, using static vacuum mass spectrometry, with the specific aims of: (i) achieving agreement between $\delta^{13}\text{C}$ analyses at the micromole and nanomole level, for the same sample, then (ii) using the high sensitivity of static vacuum mass spectrometry to investigate fluid inclusion carbon stable isotope ratios in quartz samples associated with high temperature hydrothermal mineralisation of the Dartmoor granite. In this latter case, although the abundance of carbon species was found to be at very low levels, other lines of evidence developed during the course of the present study suggested a common link with CO_2 -enriched fluids associated with other component plutons of the batholith.

A further experimental objective was to investigate procedures for obtaining $\delta^{13}\text{C}$ measurements of both fluid inclusion CO_2 and any coexisting CH_4 , where the latter may be present at sub-ppm levels with respect to the quartz host.

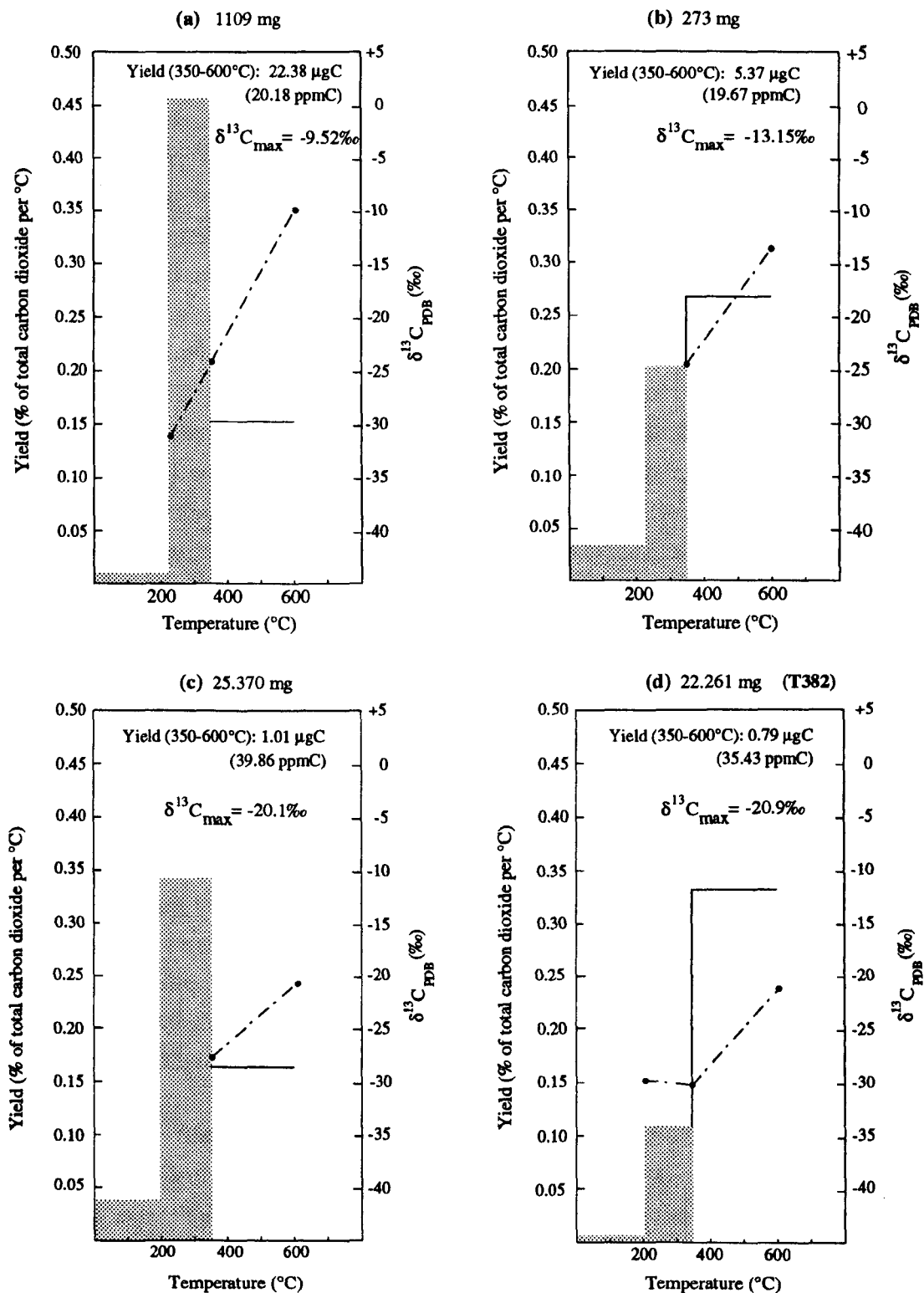
3.4.6.4 An assessment of procedures based on Swart *et al.* (1983) as applied to quartz grains used for fluid inclusion $\delta^{13}\text{C}$ analysis

A series of experiments was conducted, using a variety of quartz samples, to investigate in detail the effects of 'pre-combustion' followed by 'pyrolysis', as the optimum procedure for releasing fluid inclusion carbon components for subsequent analysis by conventional isotope ratio mass spectrometry. The analytical results are tabulated in full in Appendix B; only a summary of the findings, together with the respective conclusions, is presented here. The initial procedure was to adopt two 'combustion' steps up to 350°C , with a subsequent heating step in the absence of supplied oxygen, from 350 to 600°C (corresponding to the major fluid release), using an experimental protocol based on that of Carr *et al.* (1986). The procedural blank (empty vessel) for the extraction line system (Figure 3.10) was typically $\sim 50\text{ngC}$ for the high temperature step. Quartz samples (0.5-1mm grain size) were admitted into the extraction line directly, rather than being contained by silica buckets. The Pt catalyst was originally maintained at $\sim 1050^\circ\text{C}$ throughout both 'combustion' and 'pyrolysis' stages.

Figure 3.13 (a - d) illustrates the progressive ^{13}C depletion of the major fluid inclusion release (350 to 600°C) that occurred as the quartz sample size was reduced, in the case of sample HEM-80-1. If the carbon blank contribution (of $\delta^{13}\text{C}$ value in the range -25 to -30‰) was comprised essentially of two components, one resulting from airborne particulate contaminants (microbiological matter, dust, *etc.*) and the other from surficial organic material

Figure 3.13

Variation in measured yield and $\delta^{13}\text{C}$ of released carbon-bearing volatiles as a function of quartz sample size, using stepped heating in excess of pure oxygen ('combustion') to 350°C followed by stepped heating *in vacuo* ('pyrolysis') to 600°C. Released gases exposed to Pt foil catalyst at ~1050°C during extraction procedure. Sample: HEM-80-1.



Carbon stable isotope ratio analyses were undertaken using a dynamically-pumped instrument (VG[®]SIRA 24) except in case (d), where the static vacuum mass spectrometer described by Carr *et al.* (1986) was used.

adsorbed onto the sample grains, it might be expected that the magnitude of the airborne-derived contribution would be essentially independent of sample size, whereas that of the sample-derived contaminant would be linearly dependent on the number of quartz grains heated (assuming that all the grains were of identical surface area). The ratio of fluid inclusion carbon (present as CO₂ and CH₄) to that contained in contaminants adsorbed onto the quartz grains should, however, be independent of the number of grains (*i. e.* independent of the sample mass). The airborne-derived component probably comprised the majority of the system blank (~50 ng for the 350-600°C 'pyrolysis' step). These postulates, however, are not in accord with the experimental findings indicated in Figure 3.13.

With the Pt catalyst at room temperature, 'high resolution' stepped heating of a large quantity (1112.8 mg) of sample HEM-80-1 in the absence of supplied oxygen (CuO furnace valved off throughout) produced the results shown in Figure 3.14. Because of the quantity of sample used, in an extraction tube of only 5 mm internal diameter, temperature uniformity throughout the sample during stepped heating was unlikely to be maintained to great accuracy (as also for the case shown in Figure 3.13 a). The five heating increments representative of fluid inclusion release (300-600°C), however, exhibited a notably narrow δ¹³C range (1.5‰), with the observed profile being fully in accord with mixing between 'indigenous' CO₂ of homogeneous isotopic composition -9.5‰ and a relatively minor amount of a 'system blank' component characterised by δ¹³C ≈ -25‰. On the basis of these assumptions, the carbon blank during the analysis of this sample was at a minimum of ~23 ngC during the 400-450°C step and increased steadily thereafter to ~200 ng for the 650-700°C step.

When this extraction protocol (no supplied oxygen, Pt catalyst at room temperature) was applied to smaller quantities of the same quartz sample, necessarily using single-step heating (as the CO₂ yield was insufficient for multi-step isotopic analysis by conventional mass spectrometry), it was found that the δ¹³C value of the released CO₂ remained virtually unchanged as the quartz mass was reduced by a factor of ~6 from a starting point of 261 mg; the corresponding CO₂ yield decreased from 4.8 to 1 μgC equivalent (Appendix B, Table B2.1(b)). These results are evidently in marked contrast to the findings observed when using the 'pre-combustion' extraction technique. The relatively small differences between these data and the 'optimum' (indigenous) value of -9.5‰ was probably due to not isolating and discarding any CO₂ released below 300°C, prior to collecting the fluid inclusion release.

Crushing 3 chips (total mass 282.76 mg) of sample HEM-80-1 in a bakeable, stainless steel crusher, sealed with a Cu gasket and subsequently warmed to ~100°C, released CO₂ equivalent to 0.69 μgC. The released gas was not exposed to the Pt catalyst during the extraction procedure. The measured δ¹³C value was -9.6‰, in good agreement with the result obtained by stepped heating *in vacuo*.

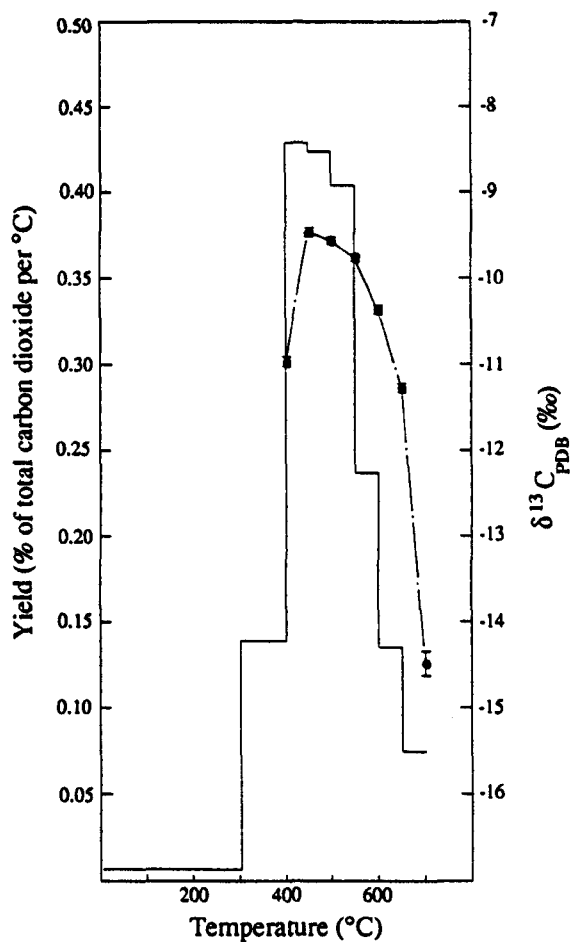
Figure 3.14

Carbon yield and $\delta^{13}\text{C}$ results of 'high resolution' stepped heating of quartz sample HEM-80-1, in the absence of supplied oxygen and with the on-line Pt foil catalyst at room temperature.

Sample weight: 1112.75 mg

$\Sigma \text{C} (-100 \text{ to } 700^\circ\text{C}) = 16.89 \mu\text{g} \text{ (15.18 ppm)}$ $\Sigma \delta^{13}\text{C} = -10.2\text{‰}$

$\Sigma \text{C} (300 \text{ to } 600^\circ\text{C}) = 14.89 \mu\text{g} \text{ (13.38 ppm)}$ $\delta^{13}\text{C}_{\text{max}} = -9.5\text{‰}$



Calculated carbon blank yields and sample-to-blank ratios, assuming simple two-component mixing of a homogenous fluid inclusion component characterised by $\delta^{13}\text{C} = -9.5\text{‰}$ and an isotopically homogenous blank of $\delta^{13}\text{C} = -25\text{‰}$.

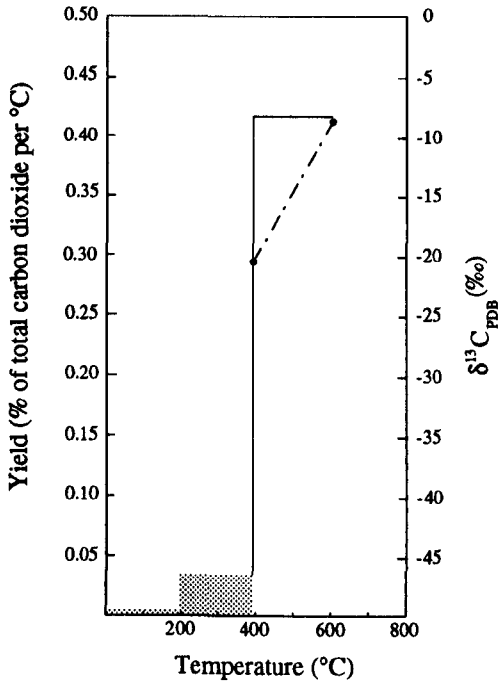
T (°C)	Yield (μg C)	Concentration (ppm C)	$\delta^{13}\text{C}$ (‰)
300	0.25	0.23	nm
400	2.34	2.10	-11.0
450	3.62	3.25	-9.5
500	3.57	3.21	-9.6
550	3.40	3.06	-9.8
600	2.00	1.76	-10.4
650	1.14	1.02	-11.3
700	0.62	0.56	-14.5

T (°C)	Blank (μg C)	Sample/blank
400	0.226	9.4
450	<0.012	>300
500	0.023	154.2
550	0.066	50.5
600	0.114	16.2
650	0.132	7.6
700	0.200	2.1

Figure 3.15

Carbonaceous volatiles released from fluid inclusion-bearing quartz: further examples of the $\delta^{13}\text{C}$ discrepancy between measurements using combined stepped 'combustion' and 'pyrolysis' in the presence of a Pt catalyst at $\sim 1050^\circ\text{C}$, versus data obtained by stepped heating *in vacuo* and with the Pt catalyst at room temperature.

(a) Sample HEM-80-39

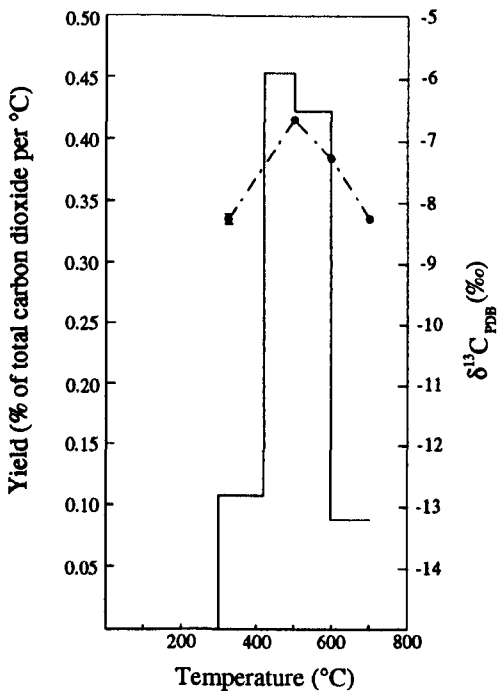


Stepped heating in the presence of oxygen for steps up to 390°C ; stepped heating *in vacuo* thereafter. Released gases exposed to Pt foil catalyst at $\sim 1050^\circ\text{C}$ during all extraction steps.

Quartz mass: 993.3 mg

Total CO_2 yield up to $600^\circ\text{C} \equiv 10.67 \mu\text{g C}$
(10.75 ppm)

$$\delta^{13}\text{C}_{\text{max}} = -8.59\text{‰}$$



Stepped heating *in vacuo*;
Pt foil catalyst at ambient temperature.

Quartz mass: 978.37 mg

Total CO_2 yield up to $600^\circ\text{C} \equiv 10.58 \mu\text{g C}$
(10.82 ppm)

$$\delta^{13}\text{C}_{\text{max}} = -6.72\text{‰}$$

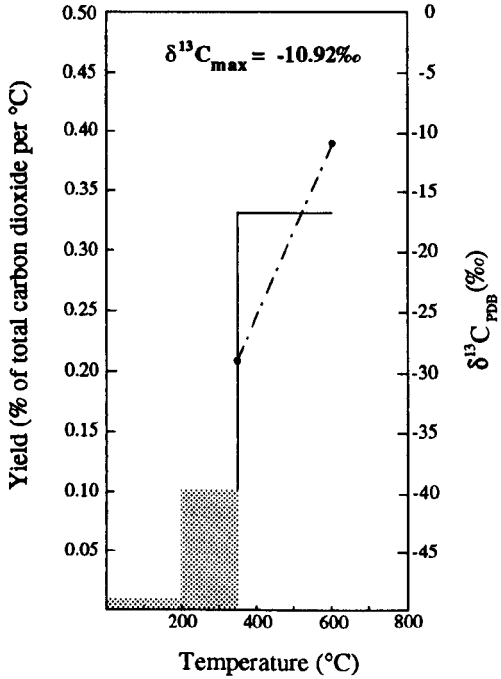
Figure 3.15 (continued)

(b) Sample HEM-80-44

Stepped heating in the presence of oxygen at low temperature (up to 352 and 364°C respectively); stepped heating *in vacuo* thereafter. Released gases exposed to Pt foil catalyst at ~1050°C during all extraction steps.

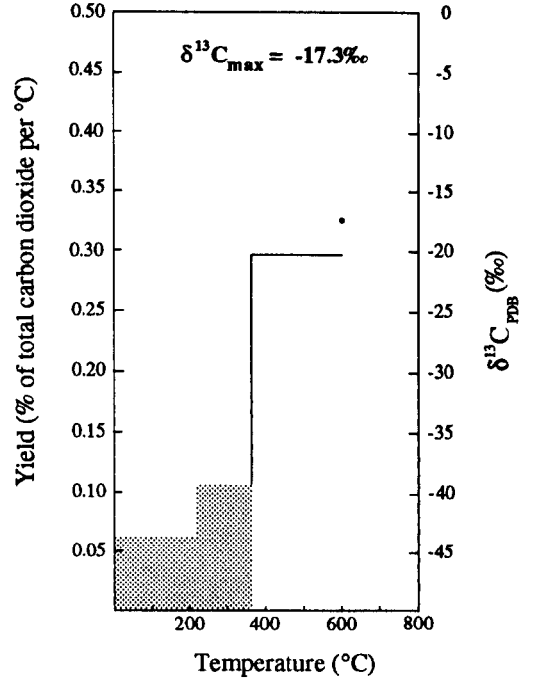
Quartz mass: 1005.2 mg

Total CO₂ yield (up to 602°C) ≅ 7.97 μg C
(7.93 ppm)

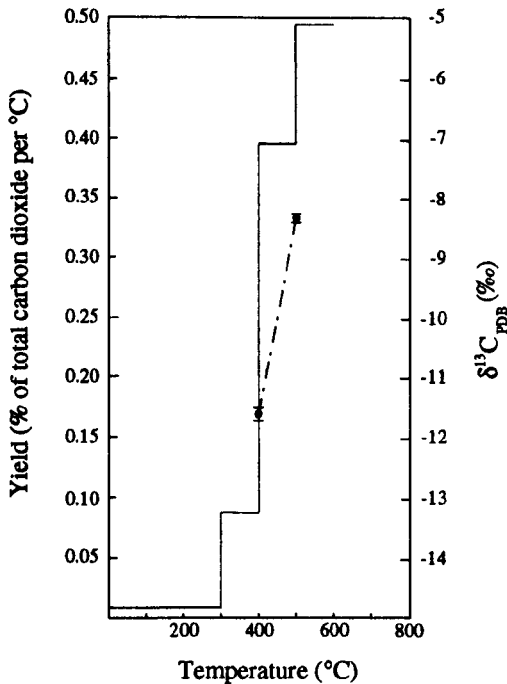


Quartz mass: 91.2 mg

Total CO₂ yield (up to 602°C) ≅ 1.29 μg C
(14.14 ppm)



Stepped heating *in vacuo* throughout; no 'combustion' steps. Pt foil catalyst at ambient temperature.



Quartz mass: 894.36 mg

Total CO₂ yield (up to 600°C) ≅ 6.97 μg C
(7.79 ppm)

$\delta^{13}\text{C}_{\text{max}} = -8.3\text{‰}$

Note: Isotopic composition of CO₂ released during 500-600°C step not recorded, as sample gas insufficiently purified (wet?)

Using other quartz samples that contained significant levels of palæofluid CO₂, similar findings were obtained regarding the dependence of the measured δ¹³C value on the extraction protocol adopted; the experimental data are reported in full in Appendix B. Examples are shown in Figure 3.15, for comparison with Figures 3.13 and 3.14.†

Further points arising from a consideration of the data presented in Appendix B are as follows:

(i) With the Pt catalyst at room temperature throughout, stepped heating in the presence of supplied oxygen, followed by stepped heating *in vacuo*, produced similar δ¹³C results as stepped heating *in vacuo* over the same temperature range (Table B2.2(b)).

(ii) Heating (single or multi-step) *in vacuo* from ambient temperature to ~600°C produced lower δ¹³C values and increased CO₂ yields when the Pt catalyst was at 1050°C than when the catalyst was at room temperature (Tables B2.2(c), B2.5(b), B2.7(b) and B2.7(c)).

Evidently, procedures based on the protocol of Swart *et al.* (1983) for the removal of organic contamination are not ideally applicable to the stepped heating of quartz grains for fluid inclusion δ¹³C analysis. The data reported in Appendix B, and as illustrated in Figures 3.13 to 3.15, may, however, be explained on the basis of:

(i) The 'oxygen storage' characteristics of Pt at high temperature

Boyd *et al.* (1988) suggested on the basis of empirical evidence that a layer of oxygen, adsorbed onto the surface of Pt foil (at 1150°C), causes methane oxidation (initially to carbon monoxide). Boyd (1988) showed that CuO at 300-500°C does not give rise to methane oxidation; this latter finding is in accord with experimental procedures used by Sakai *et al.* (1976), who used CuO at 450°C to separate methane (stable under such conditions) from carbon monoxide (oxidised to CO₂). As the platinum catalyst in the gas preparation line under consideration here is regularly exposed to oxygen, there is minimal possibility that the metal surface ever becomes depleted in this gas.

(ii) A consideration of the gaseous pyrolysis products of organic matter

Evans and Felbeck (1983a, 1983b) carried out a series of experimental studies of closed-system pyrolysis of organic matter from various sources. These authors showed that the gaseous pyrolysis products generated over the temperature range 300-500°C by Green River

† An additional, potential complication is that the palæofluid CO₂/CH₄ ratio varied significantly between the samples investigated, although methane was very much the minor carbon-bearing component. The relevant data are compiled in Table 3.4.

Table 3.2

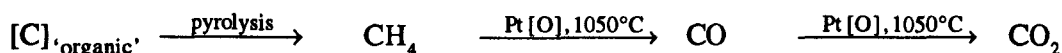
The distribution of carbon in gaseous pyrolysis products resulting from *in vacuo* heating to 440°C of various biological materials. (Adapted from Evans and Felbeck, 1983b)

	Cellulose	Lignin	Poplar Sawdust	Fucus
CO, % Yield	0.27	0.02	0.30	0.15
CO ₂ , % Yield	17.69	3.96	13.78	12.59
CH ₄ , % Yield	2.68	3.50	3.34	2.16
C ₂ H ₆ , % Yield	1.58	0.49	1.28	2.37
C ₃ H ₈ , % Yield	0.90	0.19	0.81	1.86
% Hydrocarbon Yield	5.70	4.25	5.96	8.70
C ₁ /(C ₂ +C ₃ +C ₄)	2.27	10.84	3.34	1.05
Alkanes/Alkenes	90.61	100.00	107.57	10.00

shale[†] were dominated by methane, which showed a steady increase in yield over the temperature range studied. Using biological materials as the source of carbon, and with a 440°C pyrolysis, the same authors compared the thermal degradation products obtained from a variety of samples including cellulose, lignin, sawdust of *Poplar*, and *Fucus* species (marine alga). The distribution of carbon in the resulting gaseous fractions is summarised in Table 3.2. A significant hydrocarbon component, with alkanes predominating, was found in the pyrolysis reaction mixture at 440°C; using lignin as the starting material, it is evident that the alkane yield exceeded that of carbon dioxide.

During *in vacuo* stepped heating of natural quartz samples up to 600°C, the release of low molecular weight alkanes (primarily methane), originating directly from fluid inclusions and also from the pyrolysis of airborne and surface-adsorbed organic matter, will only be problematic with regard to fluid inclusion $\delta^{13}\text{C}_{\text{CO}_2}$ analysis if the total oxidation of these components occurs in the reaction vessel chamber, prior to cryogenic separation and isolation of the CO_2 fraction.

Oxidation of CH_4 to CO by contact with platinum at 1150°C occurs rapidly (Boyd, 1988); whether significant oxidation to CO_2 takes place subsequently, during the 30 minute period of a standard heating increment, depends on the initial partial pressure of methane in the reaction vessel and also on the respective rate constants for the two consecutive first-order oxidation reactions:



If k_1 and k_2 are the respective rate constants for the oxidations of CH_4 and CO then the concentration of each component at time t is obtained as (see, *e. g.* Frost and Pearson, 1961):

$$[\text{CH}_4]_t = [\text{CH}_4]_0 e^{-k_1 t}$$

$$[\text{CO}]_t = [\text{CH}_4]_0 \frac{k_1}{k_2 - k_1} (e^{-k_1 t} - e^{-k_2 t})$$

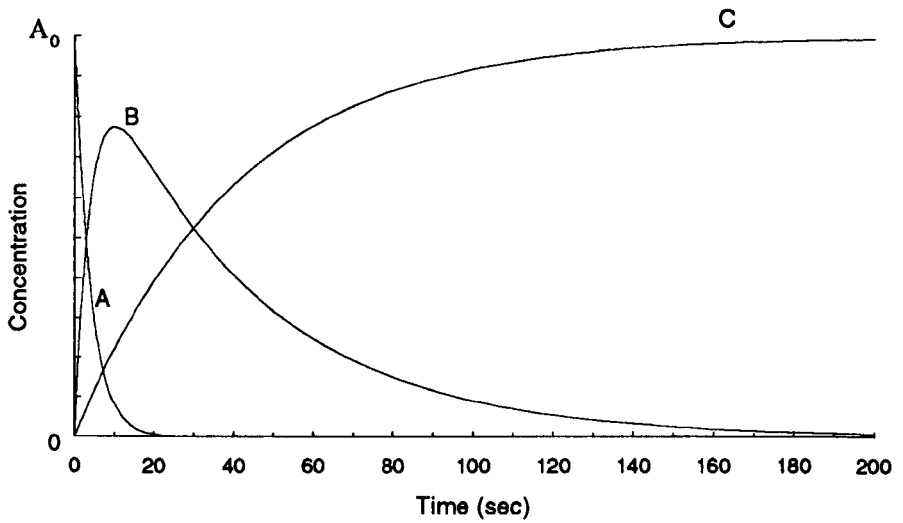
$$[\text{CO}_2]_t = [\text{CH}_4]_0 \left[1 + \frac{1}{k_1 - k_2} (k_2 e^{-k_1 t} - k_1 e^{-k_2 t}) \right]$$

where $[\text{CH}_4]_0$ refers to the initial concentration of methane. The concentration of three components A, B, C as a function of time in series first-order reactions is illustrated in Figure 3.16, for an example where $k_1 = 0.25 \text{ sec}^{-1}$ and $k_2 = 0.025 \text{ sec}^{-1}$.

[†] The Green River formation of Colorado, Wyoming and Utah, USA, is an organic-rich shale that contains a high abundance of both 'extractable' and 'insoluble' organic material.

Figure 3.16

The concentration of components A, B and C as a function of time in series first-order reactions, for a typical case where $k_1 = 0.25 \text{ sec}^{-1}$ and $k_2 = 0.025 \text{ sec}^{-1}$



The values chosen for the rate constants k_i approximate to those determined experimentally by Boyd (1988) for the sequential oxidation, in a reaction volume of 90 cm^3 , of methane to carbon monoxide and carbon dioxide in the presence of CuO at 440°C and Pt foil at 1150°C .

In the presence of both Pt at 1150°C and CuO at 440°C, Boyd (1988) showed that the ratio k_1/k_2 is ~9, but the CO oxidation step was probably effected primarily by the CuO under those circumstances; the same author did not investigate the oxidation rate of CO by the hot platinum alone. Jackson (1988), using the same extraction line as the present author, found that no detectable CO₂ formation occurred when a relatively large quantity (equivalent to >0.6torr pressure) of CH₄ was exposed to Pt at 1100°C for 30 minutes. However, the rapid subsequent formation of CO₂ on admitting the gas to CuO at 450°C was interpreted by Jackson (1988) as direct oxidation of CH₄ by the CuO. In the light of the work by Boyd (1988), an alternative explanation preferred by the present author is that, during the first stage of the experiment, Pt at 1100°C effected oxidation of CH₄ to CO; the latter was subsequently oxidised to CO₂ on exposure to CuO at 450°C.

The explanation offered for the experimental findings recorded in Appendix B and as illustrated in Figures 3.13 and 3.15 is therefore based on the premise that, for methane (derived from both indigenous, *i.e.* fluid inclusion, sources and from the pyrolysis of organic contaminant matter) at very low partial pressure in the extraction chamber, and in the absence of supplied oxygen, complete oxidation of this component to carbon dioxide will be effected by a chemisorbed oxygen layer on the Pt catalyst at ~1050°C, resulting in a shift of $\delta^{13}\text{C}_{\text{CO}_2}$ to lower values than would be otherwise observed. For relatively high partial pressures of methane in the system, carbon monoxide is the predominant oxidation product; this reservoir of ¹³C-depleted carbon does not then contribute to the measured $\delta^{13}\text{C}_{\text{CO}_2}$ result. For determination of the isotopic composition of fluid inclusion CO₂, the optimised procedure was therefore to perform stepwise heating *in vacuo*, without any pre-combustion step, and with the Pt foil catalyst at room temperature throughout the experiment.

Only in one instance during the present investigation did this stepped heating procedure give rise to anomalous results: Figure 3.17 shows the CO₂ yield and corresponding $\delta^{13}\text{C}$ data obtained in this case. A notably consistent isotopic profile for CO₂ extracted in the temperature range 400-600°C was recorded. However, the $\delta^{13}\text{C}$ value was 1.0‰ lower than that indicated for the fluid inclusion CO₂ by pyrolysis after pre-combustion and by single-step pyrolysis experiments (see Appendix B, Table B2.6). An anomalously high carbon blank level during the multi-step pyrolysis experiment is suggested as being the most probable explanation for these findings.

Because of the generally low absolute concentrations of carbon-bearing species in the samples used in the present study, 'high resolution' multi-step extraction was considered impractical in many instances. However, a two-step extraction, whereby gas released up to 300°C was discarded (because of a significant surficial/airborne contaminant component), whereas the 300-600°C yield was collected for analysis, was found to be generally satisfactory.

Figure 3.17

Carbon yield and $\delta^{13}\text{C}$ results of stepped heating of quartz sample SW-84-27 (Prince of Wales mine), in the absence of supplied oxygen and with the on-line Pt foil catalyst at room temperature.

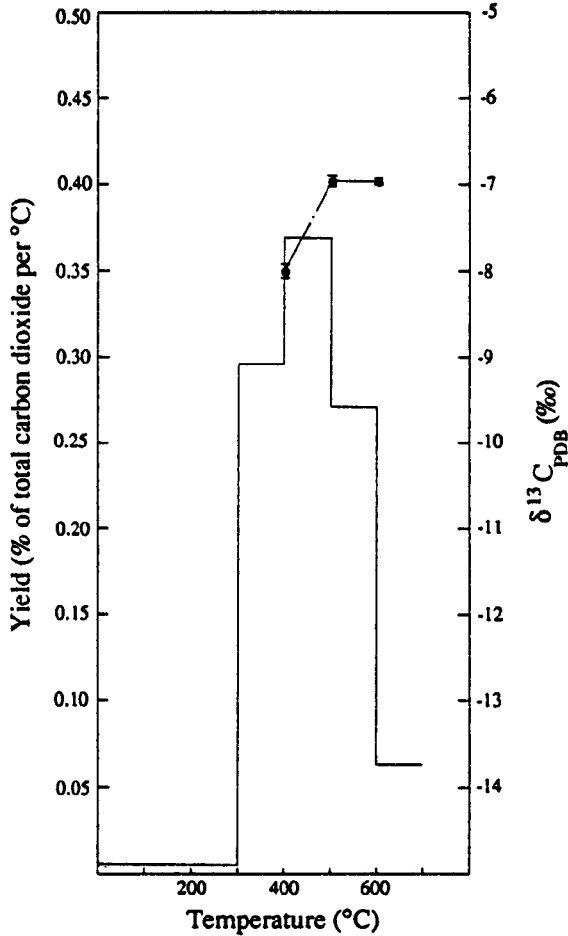
Sample weight: 1096.80 mg

ΣC (~100 to 700°C) = 6.02 μg (5.49 ppm)

For temperature range corresponding to the major release of fluid inclusions,

ΣC (300 to 600°C) = 5.11 μg (4.66 ppm) $\Sigma \delta^{13}\text{C}$ (300 to 600°C) = -7.3‰

$\delta^{13}\text{C}_{\text{max}} = -7.0\text{‰}$



T (°C)	Yield ($\mu\text{g C}$)	Concentration (ppm C)	$\delta^{13}\text{C}$ (‰)
300	0.05	0.04	nm
400	1.77	1.61	-8.1
500	2.21	2.02	-7.0
600	1.62	1.47	-7.0
700	0.37	0.34	nm

Occasional difficulties experienced with the revised stepped heating procedure were, firstly, evidence suggesting that the decomposition of carbonate grains was contributing to the peak CO₂ release, despite acid pre-treatment of the quartz sample grains. This was noted in the case of a small number of samples from Carrock Fell and could only be prevented by the use of crushing rather than heating as the fluid release procedure, if significant decarbonation occurred below 600°C. If the carbonates were derived from solid phases in the fluid inclusions, possibly nucleated since fluid entrapment, they should in any case be included in consideration of the total carbon reservoir of the fluid. The second problem was that hydrogen sulphide was occasionally found to be a contaminant species during stepped thermal extraction, identified by ion beam currents corresponding to m/z 32, 33 and 34 during mass spectrometric analysis. The presence of hydrogen sulphide was also manifest by unstable 45/44 and 46/44 ion beam ratios, together with measured δ¹³C values indicating anomalous enrichment in ¹³C.†

The persistence of H₂S in the extraction line derived from the elimination of any oxidation stage during stepped heating: CuO at 450°C converts H₂S to SO₂ (Mattey *et al.*, 1989), which may be subsequently removed by cryogenic isolation (using a slush bath of n-pentane/liquid nitrogen at -130°C). Any traces of CO would also be oxidised by CuO at 450°C, however, thereby contributing to the CO₂ blank value and consequently to the carbon isotope ratio measurements. In the case of stepped heating experiments where H₂S was detected as a trace contaminant (probably deriving primarily *via* the decomposition of finely-disseminated sulphide mineral phases, rather than as a significant component of the palæofluid), it was noted that the partial pressure of this species decreased markedly during carbon stable isotope ratio analysis by the VG[®]SIRA 24 instrument. The corresponding δ¹³C value simultaneously decreased, eventually stabilising as the H₂S concentration decreased to below the detection limit. It is suggested that this effect, an example of which is shown in Figure 3.18, may be attributed to reaction between the H₂S and metal components of the mass spectrometer inlet.

For samples analysed at the NERC Isotope Geosciences Laboratory, where no facility for direct coupling of the extraction line system to the mass spectrometer was available, the 300-600°C release was collected for isotope ratio analysis off-line. The relatively large amounts of CO₂ in such cases were cleaned of any H₂S contamination by reaction with lead formate, followed by further cryogenic (-130°C) purification.

† Wright and Pillinger (1989) noted that the formation of ¹²C³²S⁺ (m/z 44), ¹³C³²S⁺, ¹²C³³S⁺ (m/z 45) and ¹³C³³S⁺, ¹²C³⁴S⁺ (m/z 46) in the ion source would cause direct interference with the respective CO₂⁺ species having the same m/z values. However, in view of the natural abundances of ³³S and ³⁴S relative to ³²S (³²S/³⁴S=22.23 in the CDT international standard, as measured by Thode *et al.*, 1961; ³²S/³³S=123.46 in CDT according to Nielsen, 1978), it is suggested that the observed enhancement of δ⁴⁵ may possibly be due to a significant contribution from ¹²C³²S¹H⁺.

Figure 3.18

The effect of hydrogen sulphide as a contaminant species during stable isotope ratio analysis of carbon dioxide by VG[®]SIRA 24 mass spectrometer. (Sample: HEM-80-39)

Time (min.)	δ^{45} (1 σ)	δ^{46} (1 σ)	$\delta^{13}\text{C}_{\text{PDB}}$ (‰)
0	19.926 (0.114)	-16.127 (0.123)	-2.951
10	17.436 (0.107)	-17.664 (0.049)	-5.492
26	15.988 (0.033)	-18.837 (0.014)	-6.691
39	15.994 (0.034)	-18.508 (0.031)	-6.966

Sample size equivalent to 12 mgC. Major beam current (m/z 44) decreased from 1.07 to 0.88 nA during the experiment.

(a) Initial measurement (t = 0)

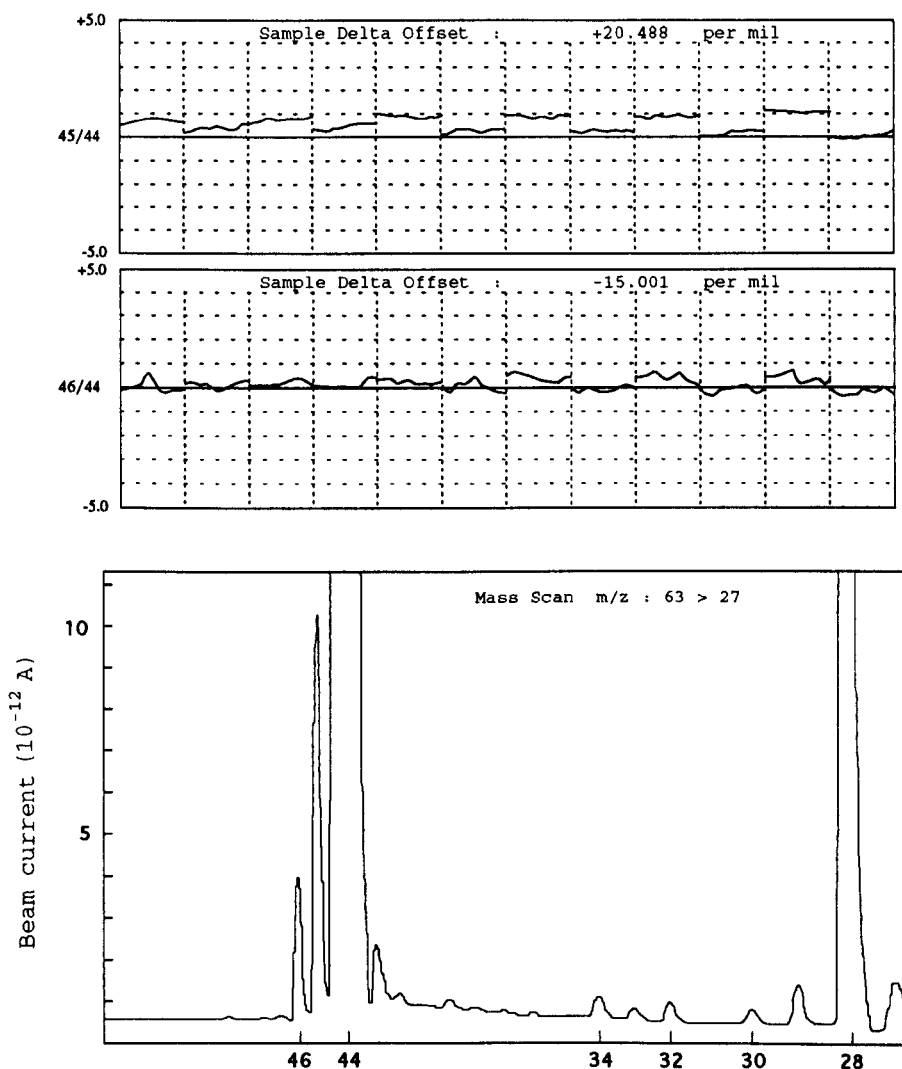
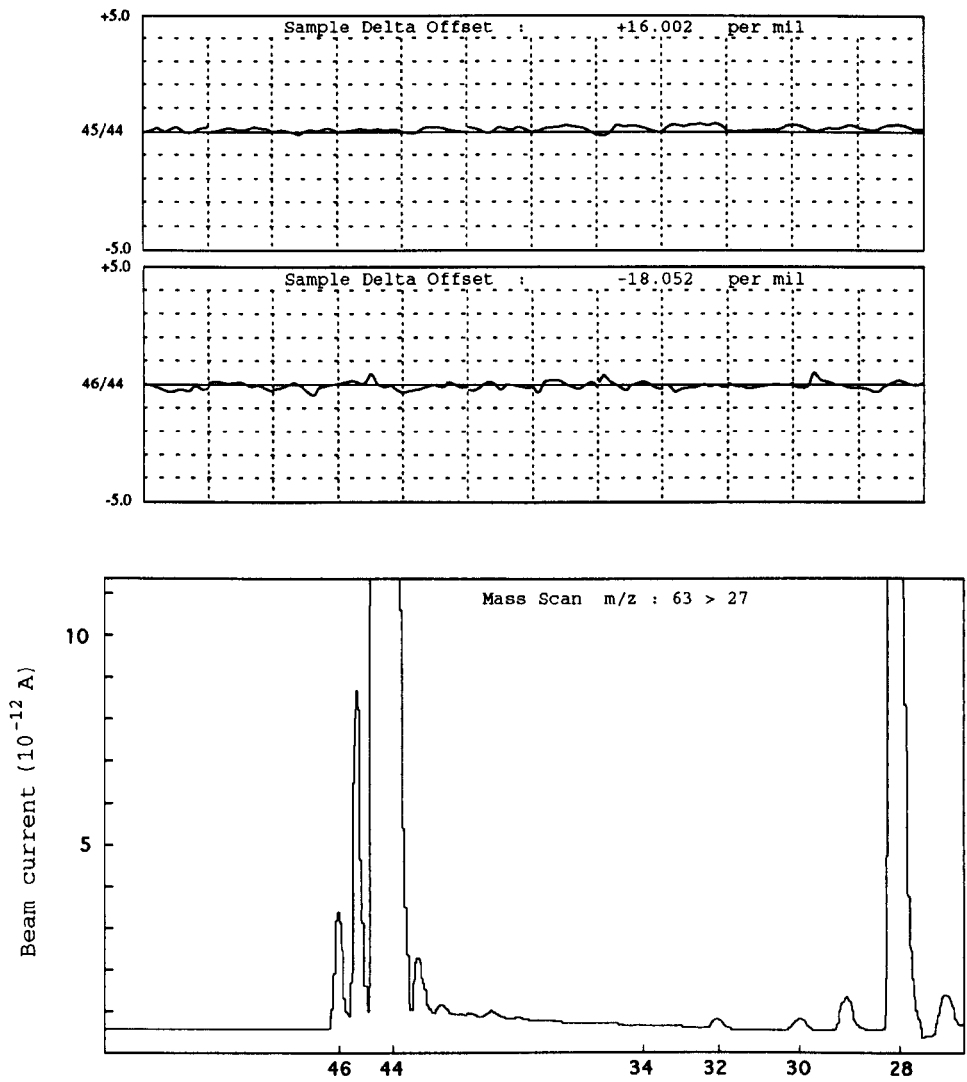


Figure 3.18 (continued)

(b) Measurement 26 minutes after initial admittance:



3.4.6.5 An assessment of the experimental protocol of Jackson *et al.* (1988b)

Jackson *et al.* (1988b) devised a stepped heating procedure whereby pre-combustion at 400°C in about 500 torr of pure oxygen was used in an attempt to remove surficial organic contamination, as recommended by Des Marais (1986) and Matthey *et al.* (1989). Stepped heating under pressures $<10^{-5}$ torr was then performed, as used by the present author. As recorded by Jackson (1990), however, all heating steps were performed with the released gas exposed to the on-line Pt catalyst at ~1100°C.

In view of the findings reported in Section 3.4.6.4, it seems probable that some CO₂ contribution from alkane oxidation would have occurred during the stepped heating of samples containing relatively low concentrations of carbon-bearing components, methane being derived from the pyrolysis (<600°C) of organic 'contaminants' and also being an acknowledged fluid inclusion constituent in several of the samples investigated (Jackson, 1990).

Figure 3.19 shows the carbon yield and $\delta^{13}\text{C}$ profile of a stepped heating experiment reported by Jackson *et al.* (1988a,b) and Jackson (1990), using quartz associated with an incipient charnockite from Kalanjur, southern India. In this experiment, oxygen was only supplied for the heating step up to 400°C, but the on-line Pt foil catalyst was at ~1100°C throughout. Also shown in Figure 3.19 is the corresponding carbon blank yield calculated by the present author from these results, assuming a simple two-component mixing between indigenous (fluid inclusion) carbon dioxide of isotopically homogeneous composition ($\delta^{13}\text{C}$ value -6.2‰) and a carbon blank of $\delta^{13}\text{C} = -25‰$. Note that the 'blank' in this case might include a contribution from the oxidation of traces of fluid inclusion methane, besides an 'adventitious' component. From these data it is apparent that, to explain the observed isotopic profile on the basis of this model, the total carbon blank per 100°C step never reduced below 119ngC equivalent (in contrast to the system blank quoted by Jackson *et al.*, 1988b, of typically <20ngC per step for temperatures up to 1200°C). Furthermore, the corresponding sample-to-blank ratio for the maximum fluid release step is 30.3 (*cf.* Figure 3.14, where the corresponding value is an order of magnitude greater).

In a follow-up study, using the same stepped heating procedure (Harris *et al.*, 1993), it was reported that the background blanks were typically 75-180ngCO₂ (*i.e.* 20-49ngC), with $\delta^{13}\text{C} \approx -25‰$, and that errors introduced by not background-correcting sample $\delta^{13}\text{C}$ results may be as high as $\pm 2‰$ for samples containing <30ppmCO₂.

Figure 3.19

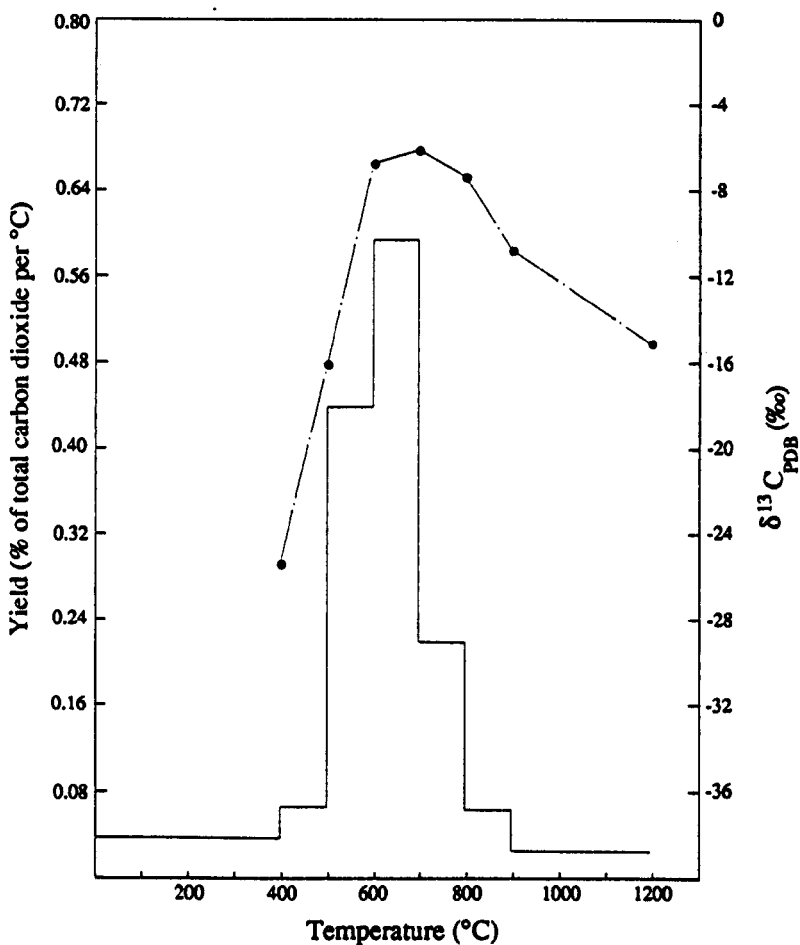
Carbon yield and $\delta^{13}\text{C}$ results of stepped heating of quartz sample TR10D associated with incipient charnockite formation, southern India, as reported by Jackson *et al.* (1988 a) and Jackson (1990).

Note that no oxygen was supplied during the extraction stage (for steps > 400°C), but that the released gases were exposed to Pt foil at ~1100°C.

Sample: TR10D (131.60 mg)

ΣC (400 to 1200°C) = 12.41 μg (94.30 ppm)

$\delta^{13}\text{C}_{\text{max}}$ = -6.2‰



Calculated carbon blank yields and sample-to-blank ratio, assuming simple two-component mixing of a homogenous fluid inclusion component, $\delta^{13}\text{C} = -6.2\text{‰}$, with an isotopically homogeneous blank, $\delta^{13}\text{C} = -25\text{‰}$.

T (°C)	Blank ($\mu\text{g C}$)	Sample/blank
400	1.24	~0
500	0.295	0.9
600	0.119	30.3
800	0.119	14.7
900	0.132	3.1
1200	0.303	1.1

One of the difficulties inherent in the stepwise heating approach for the isotopic analysis of fluid inclusions is to establish whether the sample-to-blank carbon yield ratio corresponding to the maximum in the isotopic profile is large enough to ensure that any blank contribution is less than the analytical precision of the isotopic measurement. In a single experiment using quartz from a massive charnockite from Kottaram, southern India, Jackson (1990) compared fluid inclusion $\delta^{13}\text{C}$ as determined by stepped heating with that obtained by crushing; the latter method yielded a value 2‰ greater, indicating that, in some instances at least, the influence of carbon blank yield during stepped heating above 400°C was not negligible.

3.4.7 Application of the optimised stepped heating procedure to $\delta^{13}\text{C}$ analysis of inclusion CO_2 by static vacuum mass spectrometry

3.4.7.1 Experimental details

The extraction line system described by Ash (1990) was used, with all heating steps performed in the absence of supplied oxygen. A single grain of quartz, weighing in the range 12–25 mg, was used for each analysis. The silica tube extraction vessel was maintained at -1200°C and pumped continuously under high vacuum ($<10^{-7}$ mbar) overnight, prior to transferring the loaded sample grain from the air-lock inlet (evacuated overnight to $<4 \times 10^{-6}$ mbar) at ambient temperature. Changes to the protocol of Ash (1990) were as follows:

(i) Quartz sample grains were not contained in a Pt foil envelope (as devised primarily to minimise loss of fine particulate matter during initial evacuation), but admitted directly into the air-lock. Samples were acid cleaned (6M HCl), then agitated ultrasonically with dichloromethane immediately prior to loading into the extraction line. The minimum exposure method of Matthey *et al.* (1989) was adopted; samples were transferred to the extraction line air-lock in a covered Petri dish containing dichloromethane.

(ii) The on-line CuO, used for stepped combustion experiments, was maintained at -80°C throughout, to minimise condensation of extracted fluid inclusion water without catalytic oxidation of any CO (if present) occurring.

(iii) A slush bath of n-pentane/liquid nitrogen (-130°C) was used to trap water in the extraction chamber during stepped heating, to prevent the subsequent transfer of water (the predominant component of the fluid inclusions) into the purification section of the line.

This experimental procedure, devised to minimise carbon blank yields, necessarily restricted analysis to the indigenous CO_2 component (*i.e.* excluded fluid inclusion methane). As CO_2 was by far the dominant carbon species in nearly all the samples investigated in the present study, consideration of how the procedures may be further modified to permit analysis of any coexisting methane component (at the sub-nanomole level) is deferred to the final section of this chapter.

Table 3.3

Comparison of carbon procedural blank yields (± 0.2 ngC) resulting from stepped heating in the presence/absence of supplied oxygen, using the extraction system described by Ash *et al.* (1990). The extraction (sample) tube was maintained at 1200°C overnight, with evacuation to $<10^{-7}$ mbar (and with the CuO furnace at 600°C) in all cases, prior to undertaking the reported measurements.

T (°C)	'Combustion' blank* (T716)	'Pyrolysis' blank* § (T715)	'Inclusion-free' quartz† 'pyrolysis' (T727)
200	7.6	0.8	<0.2
250	4.0	1.0	↓
300	5.9	0.6	<0.2
350	8.0	0.2	↓
400	8.8	0.8	↓
450	6.7	0.8	↓
500	3.8	1.0	↓
550	8.0		↓
600	5.2		3.3
800	3.3		3.6
1000			2.9
1200			4.2

Notes: * Empty extraction tube.

§ Air conditioning failure resulted in the laboratory temperature reaching 27°C during the course of this experiment, causing instability of the capacitance manometer used for the CO₂ yield measurements. Consequently, the experiment had to be abandoned after the 500°C step.

† Single grain of gem-quality quartz, mass 24.7305mg. System blank (30 minute step) with the empty extraction tube at 1200°C, measured immediately prior to transferring the sample from the air lock (see Figure 3.9) was below the detection limit (0.2ngC).

The CuO furnace was maintained at 80°C during incremental heating in the absence of supplied oxygen ('pyrolysis' runs T715 and T727).

'Combustion' blank (T716): ΣC (~20 to 800°C) = 61.3 ng.

The procedural carbon blank yield during stepped extraction, 50°C increments, in the absence of oxygen was generally <1ng per step. Table 3.3 gives the blanks obtained during stepped 'pyrolysis' (with/without an inclusion-free natural quartz sample); for comparison, the carbon yield resulting from stepped 'combustion' of the empty extraction tube is also shown.

3.4.7.2 Results: comparison with data obtained by 'conventional' mass spectrometry

Figure 3.20(a) shows the analytical results obtained for sample HEM-80-1 using the optimised stepped extraction procedure in conjunction with static vacuum mass spectrometry. For comparison with earlier results, refer to Figure 3.12(a - d). In the current example, it is seen that the temperature step (470-500°C) associated with the maximum (normalised) CO₂ yield also corresponds to the maximum value of the δ¹³C profile. Furthermore, this isotopic datum point corresponds, within the limits imposed by analytical precision, to the 'optimum' δ¹³C value of -9.5‰, as determined by both (i) 'high resolution' stepped heating in conjunction with dynamic vacuum mass spectrometry (Figure 3.14), using a sample of mass >50x larger than that adopted here, and (ii) 'conventional' analysis of the CO₂ released by crushing coarse grains of the quartz sample (Appendix B, Table B2.1(d)). Also noteworthy is that at no step where sufficient CO₂ was released to permit isotopic measurement with acceptable precision did the δ¹³C value decrease to below 4‰ of the 'optimum' result, thereby demonstrating improved sample-to-blank ratios compared to earlier extraction methods.

Similarly, the results obtained for sample CF-77-98 (from Carrock Fell) are illustrated in Figure 3.20(b). In this case, however, the peak release of fluid occurs at lower temperature, where mixing with any residual blank component would be expected to be more evident than for the previous example. The weighted mean δ¹³C value of CO₂ collected in the temperature range 200-575°C (corresponding to fluid inclusion release), however, was found to be -12.5‰; within the limits of analytical precision, this is indistinguishable from the value (-11.4‰) obtained by 'conventional' analysis of the CO₂ released by crushing coarse grains of the quartz sample (see Appendix B, Table B2.7).

Despite the adoption of procedures to minimise the carbon blank, the unpredictable nature of this component, with attendant consequences for the accuracy of measured isotope ratios, still occasionally gave rise to spurious results. This is illustrated in Figure 3.21, which shows duplicate analyses of sample CD-88-1 (Castle-an-Dinas mine, St Austell area). In both instances, the 1200°C 'pyrolysis' carbon blank (30 minute step), measured immediately prior to transferring the outgassed sample from the air-lock to the extraction tube, was below detection level (0.2ngC).

Figure 3.20

Yield profiles, together with $\delta^{13}\text{C}$ as measured by static vacuum mass spectrometry, of CO_2 released by stepped heating of quartz samples using the optimised extraction procedure: (a) HEM-80-1 (Hemerdon, S W England); (b) CF-77-98 (Carrock Fell, N W England).

(a) Sample: HEM-80-1 Run: T709

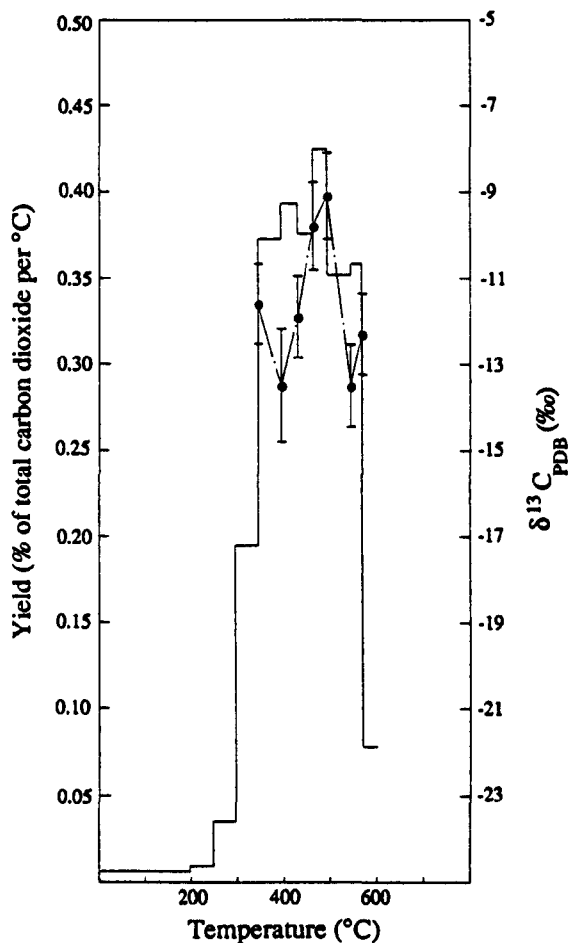
Sample weight: 20.3262 mg (single grain of quartz)

ΣC (~20 to 605°C) = 245.6 ng (12.08 ppm)

For the temperature range 300-575°C, corresponding to the major release of inclusion fluid,

ΣC (300 to 575°C) = 232.3 ng (11.43 ppm) $\Sigma \delta^{13}\text{C}$ (300 to 575°C) = -11.8‰

$\delta^{13}\text{C}_{\text{max}} = -9.1 \pm 1.0\text{‰}$ (1 σ error)



T (°C)	Yield (ng C)	Concentration (ppm C)	$\delta^{13}\text{C}$ (‰)	σ (‰)
200	2.5	0.12	nm	
250	1.0	0.05	nm	
300	4.2	0.21	nm	
350	23.9	1.18	-11.6	0.93
400	45.8	2.25	-13.5	1.32
435	33.8	1.66	-11.9	0.95
470	32.3	1.59	-9.8	1.02
500	31.3	1.54	-9.1	1.00
550	43.2	2.13	-13.5	0.96
575	22.0	1.08	-12.3	0.94
605	5.7	0.28	nm	

Figure 3.20 (continued)

(b) Sample: CF-77-98 Run: T706

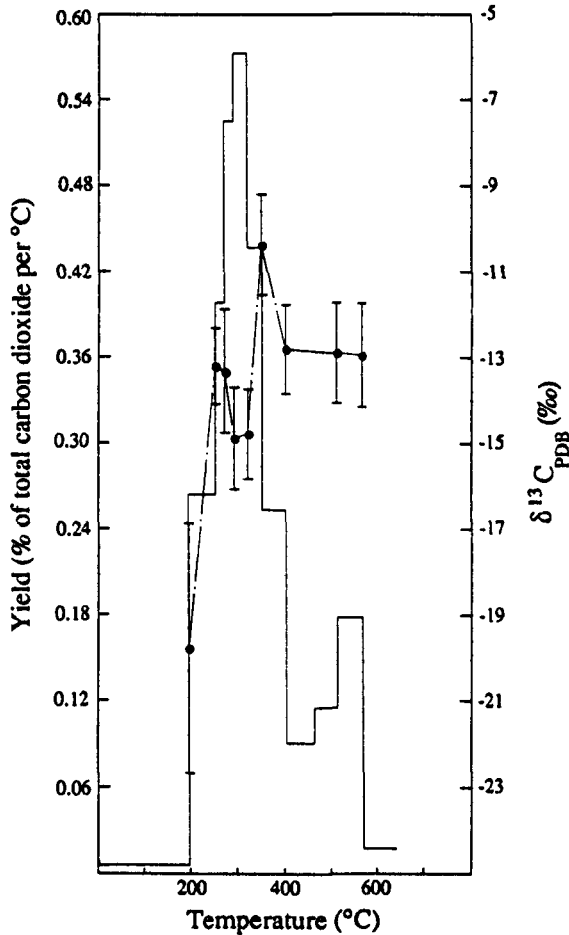
Sample weight: 18.7200 mg (single grain of quartz)

ΣC (~20 to 645°C) = 432.7 ng (23.11 ppm)

For the temperature range 200-575°C, corresponding to the major release of inclusion fluid,

ΣC (200 to 575°C) = 423.7 ng (22.63 ppm) $\Sigma \delta^{13}C$ (200 to 575°C) = -12.5‰

$\delta^{13}C_{\max} = -10.4 \pm 1.17\text{‰}$ (1 σ error)



T (°C)	Yield (ng C)	Concentration (ppm C)	$\delta^{13}C$ (‰)	σ (‰)
200	4.2	0.22	-19.8	2.91
260	68.4	3.65	-13.2	0.89
280	34.4	1.84	-13.3	1.44
300	45.3	2.42	-14.9	1.20
330	74.1	3.96	-14.8	1.06
360	56.5	3.02	-10.4	1.17
410	54.6	2.92	-12.8	1.03
470	23.3	1.24	nm	
520	24.8	1.32	-12.9	1.17
575	42.3	2.26	-13.0	1.21
645	4.8	0.26	nm	

Figure 3.21

Yield profile, together with $\delta^{13}\text{C}$ as measured by static vacuum mass spectrometry, of CO_2 released by optimised stepped heating of quartz sample CD-88-1 (from Castle-an-Dinas mine, St Austell region, S W England).

(a) Run: T725

Sample weight: 12.6249 mg (single grain of quartz)

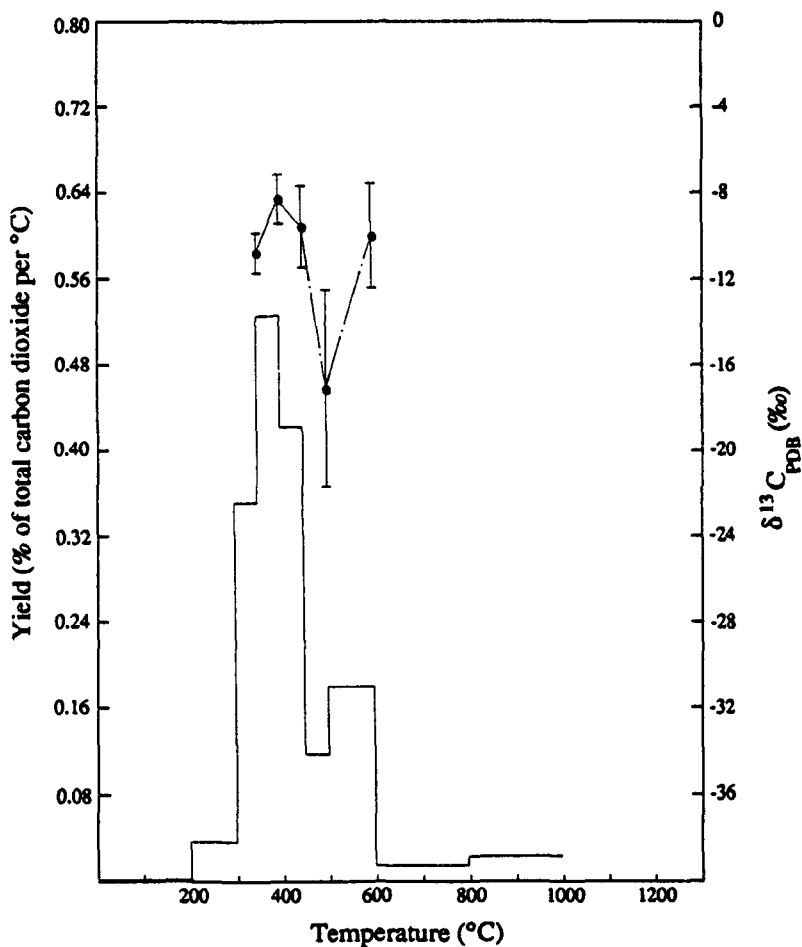
ΣC (~20 to 600°C) = 106.1 ng (8.40 ppm)

For the temperature range 300-600°C, corresponding to the major release of inclusion fluid,

ΣC (300 to 600°C) = 101.5 ng (8.04 ppm)

$\Sigma \delta^{13}\text{C}$ (300 to 600°C) = -10.0‰

$\delta^{13}\text{C}_{\text{max}} = -8.3 \pm 1.15\text{‰}$ (1 σ error)



T (°C)	Yield (ng C)	Concentration (ppm C)	$\delta^{13}\text{C}$ (‰)	σ (‰)
200	0.4	0.03	nm	
300	4.2	0.33	nm	
350	20.1	1.59	-10.8	0.94
400	30.0	2.37	-8.3	1.15
450	24.1	1.91	-9.6	1.90
500	6.7	0.53	-17.1	4.57
600	20.6	1.63	-10.0	2.42
800	3.1	0.24	nm	
1000	5.0	0.39	nm	

Figure 3.21 (continued)

(b) Run: T717

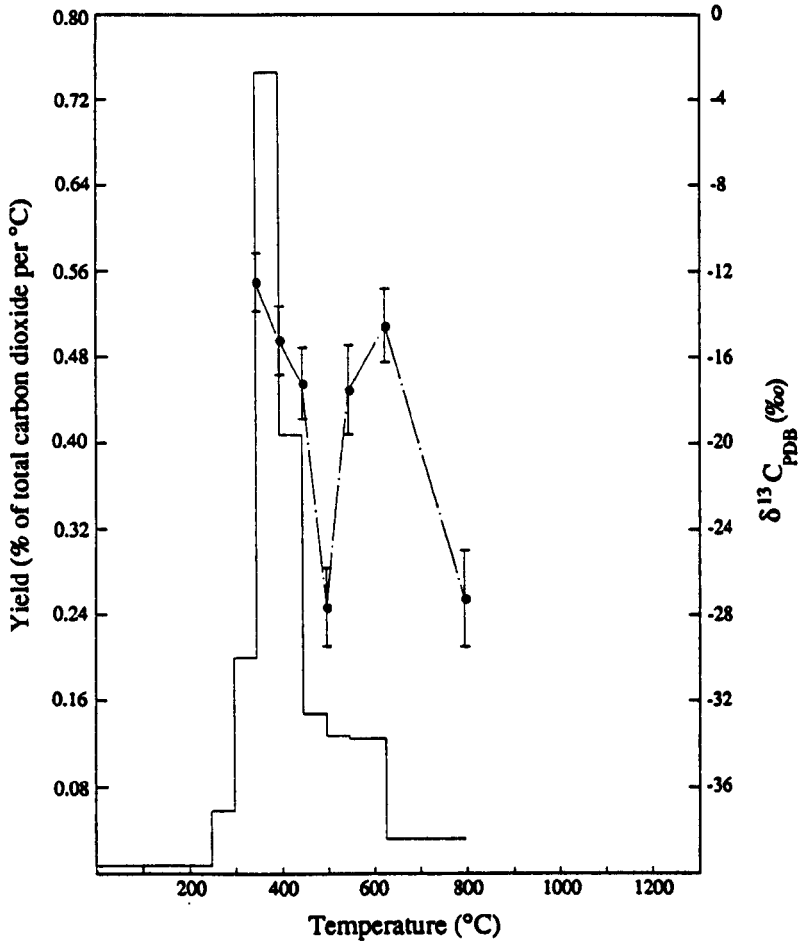
Sample weight: 18.5918 mg (single grain of quartz)

ΣC (~20 to 630°C) = 178.8 ng (9.62 ppm)

For the temperature range 300 - 630°C, corresponding to the major release of inclusion fluid,

ΣC (300 to 630°C) = 170.9 ng (9.19 ppm) $\Sigma \delta^{13}C$ (300 to 630°C) = -16.5‰

$\delta^{13}C_{\max} = -12.6 \pm 1.37\text{‰}$ (1 σ error)



T (°C)	Yield (ng C)	Concentration (ppm C)	$\delta^{13}C$ (‰)	σ (‰)
250	2.5	0.13	nm	
300	5.4	0.29	nm	
350	18.7	1.01	-12.6	1.37
400	69.9	3.76	-15.3	1.59
450	38.2	2.05	-17.3	1.67
500	13.8	0.74	-27.7	1.83
550	11.8	0.64	-17.6	2.09
630	18.5	1.00	-14.6	1.71
800	9.6	0.51	-27.3	2.24

In Figure 3.21 (a), the maximum value in the isotopic profile corresponds to the step (350-400°C) during which maximum yield of CO₂ was evolved. Furthermore, the associated δ¹³C value is the same, within analytical precision, as that determined by 'conventional' means (Table 3.4). Also, with the exception of one datum point corresponding to a well-defined minimum in the CO₂ yield profile (where the sample-to-blank ratio would be less favourable), the range of isotopic data is constrained to 2.5‰.

In contrast, although Figure 3.21 (b) shows a broadly similar isotopic profile (including the pronounced 'dip' corresponding to the 450-500°C temperature step), the δ¹³C results are shifted to more negative values. The explanation offered for this difference is that the contribution from carbon blank is notably greater in the case of Figure 3.21 (b). Evidence for this assertion is provided by comparison of the respective carbon yield data, notably in the temperature ranges 450-500°C and 600-800°C, where the contribution of palaeofluid carbon is very low (Figure 3.21 (a)). The correspondingly higher yields of carbon in Figure 3.21 (b) at these temperatures, together with an associated δ¹³C value of approximately -25‰, suggests that this carbon release is primarily of extraneous origin.

3.4.8 Carbon stable isotope analysis of fluid inclusion methane

3.4.8.1 Methane oxidation catalyst

Conventional procedures for the preparation of methane for carbon stable isotope ratio analysis generally involve quantitative oxidation of the methane to carbon dioxide, which may then be analysed directly by mass spectrometry. The catalytic combustion of methane was first observed by Davy (1817) over hot palladium and platinum wires; for total oxidation of methane, these two elements have been shown to be the most active catalysts (Anderson *et al.*, 1961). Carr *et al.* (1986) used a coil of Pt wire (>5cm) at ~1050°C to oxidise carbon-containing gases to carbon dioxide. Similarly, Schoell (1980) used a red-hot platinum wire to effect complete catalytic oxidation of standard methane in a closed reaction vessel. For the present work, platinum foil at ~1050°C was the catalyst used.

3.4.8.2 Experimental protocol adopted for δ¹³C analysis of fluid inclusion methane

An analytical protocol was devised to permit the δ¹³C analysis of fluid inclusion methane, generally present at considerably lower abundance levels than coexisting carbon dioxide in the palaeofluids. Methane was collected on a 5Å molecular sieve (at -196°C) during stepped heating of the quartz sample over the temperature range 300-600°C, either during a single step or the aggregate of several consecutive steps. The experimental procedure was as follows, with reference to Figure 3.10:

- (i) At the end of a heating step (with platinum foil PF#1 at ambient temperature throughout; trap CF#1 at liquid nitrogen temperature), residual gases (primarily methane and nitrogen) were transferred from the extraction section of the line to the 5Å molecular sieve (MS) at liquid nitrogen temperature, and subsequently isolated by valve V5.
- (ii) After measuring the yield and isotopic composition of the associated CO₂ component, the oxygen generation section of the line (evacuated to a pressure <10⁻⁵ torr) was isolated by closing valves V3 and V8. The CuO temperature was then raised to 850°C and valve V4 opened. After an equilibration period, valve V4 was closed again to isolate the CuO, the temperature of which was then reduced to 600°C, and the aliquot of oxygen contained between valves V3 and V8 adsorbed onto the molecular sieve (maintained at -196°C) by opening valve V5.
- (iii) The molecular sieve was then isolated again (valve V5 closed) and allowed to warm to room temperature. With all other valves closed in the oxygen generating section of the line, V5 was opened to allow expansion of the methane/oxygen mixture (together with nitrogen, *etc.*) into the section of the line bounded by valves V3 and V8. After an equilibration period, the molecular sieve was again isolated (valve V5 closed) and valve V6 opened to expand the 'chopped' reactant gas mixture into the silica finger PF#2 containing platinum foil at 1050°C.
- (iv) After allowing a twenty minute period for the methane oxidation to be effected by the hot Pt catalyst, the purification section of the line (maintained under high vacuum) was isolated from the pumping system (valve V10 closed) and trap CF#2 cooled to liquid nitrogen temperature. Valves V8 and V4 were then opened, to admit the reacted gases to CF#2 and to allow excess oxygen to be re-adsorbed by the CuO at 600°C.
- (v) After seven minutes, the CuO temperature was reduced to 450°C and a further ten minutes allowed for the re-adsorption of any remaining traces of oxygen. Any methane converted to CO rather than CO₂ by the Pt catalyst would be rapidly oxidised by the CuO, under these conditions.†
- (vi) Any residual gas (primarily nitrogen) was then pumped out, before transferring the oxidation product CO₂ to the variable-temperature cryotrap (VTC) for subsequent separation from the associated water component. The purified CO₂ was then transferred to the capacitance manometer finger (CF#3) for yield determination. Isotopic analysis was undertaken if the yield exceeded 400ngC equivalent.

† Subsequent to undertaking the methane δ¹³C analyses reported herein, a modified experimental procedure was adopted, whereby use of the molecular sieve as a storage reservoir for oxygen was avoided. The 'chopped' methane sample, not initially mixed with oxygen, was instead exposed to CuO at 850°C as well as PF#2 throughout the oxidation step. Excess oxygen was then re-adsorbed onto the CuO, initially at 600°C, then at 450°C, as before.

(vii) Yield values were corrected for the unreacted methane retained in the MS finger (step iii) immediately prior to the oxidation stage; the correction factor was determined as 1.30 for the relative volumes involved.

IAEA natural gas standard NGS-1 (81.4% methane) was used for testing the methane oxidation procedure. The results of replicate $\delta^{13}\text{C}$ analyses are given in Appendix B.

3.5 Results of the palaeofluid $\delta^{13}\text{C}$ analyses

3.5.1 Hydrothermal fluids characterised by W±Sn oxide association

Quartz vein samples representative of four of the principal wolframite occurrences (Beer and Ball, 1987) within the Cornubian batholith, namely Hemerdon mine, South Crofty mine, Cligga Head and Castle-an-Dinas mine, were used in the investigation, together with examples of lesser significance clustered around the minor granite intrusives between the Dartmoor and Bodmin Moor plutons. Sample locations are shown in Figure 3.22 (localities 1 to 8); further details and sample descriptions are recorded in Appendix A.

Table 3.4 gives the results of carbon yield and isotopic analysis of the total oxidised carbon component, ΣCO_2 , determined as CO_2 .[†] Also recorded are the measured ΣCO_2 -to-methane ratios. In a limited number of instances, carbon stable isotope ratio measurements were made on the coexisting methane. Figure 3.23 illustrates some of the salient features. Also shown on this figure are first-order estimates of the respective ΣCO_2 concentrations in the hydrothermal fluids, calculated on the basis of carbon dioxide and water yields as measured on different 'splits' of the same quartz samples.

Anomalously ^{13}C -enriched CO_2 ($\delta^{13}\text{C} > +4\text{‰}$) was discovered in an example from South Crofty mine; the corresponding stepped heating profile is shown in Figure 3.24. The $\delta^{13}\text{C}$ value of the coexisting methane was also notably more ^{13}C -enriched than methane measured elsewhere throughout the Cornubian region, suggesting a coupling of the isotope systematics. Furthermore, methane abundance in the palaeofluid exceeded that of CO_2 in this particular case (the only such example encountered during the study).

3.5.2 'Transitional' (pegmatitic-pneumatolytic) fluids

A small number of examples of quartz typifying granite-associated transitional rock types (preceding the earliest stages of hydrothermal mineralisation) were included for comparison.

[†] ΣCO_2 includes carbon dioxide derived from thermal decomposition of any bicarbonate or carbonate salts present, besides palaeofluid CO_2 .

Figure 3.22

Simplified map of S W England, indicating the location of samples included in the investigation of palaeofluid carbon species associated with early-stage granite-related hydrothermal processes

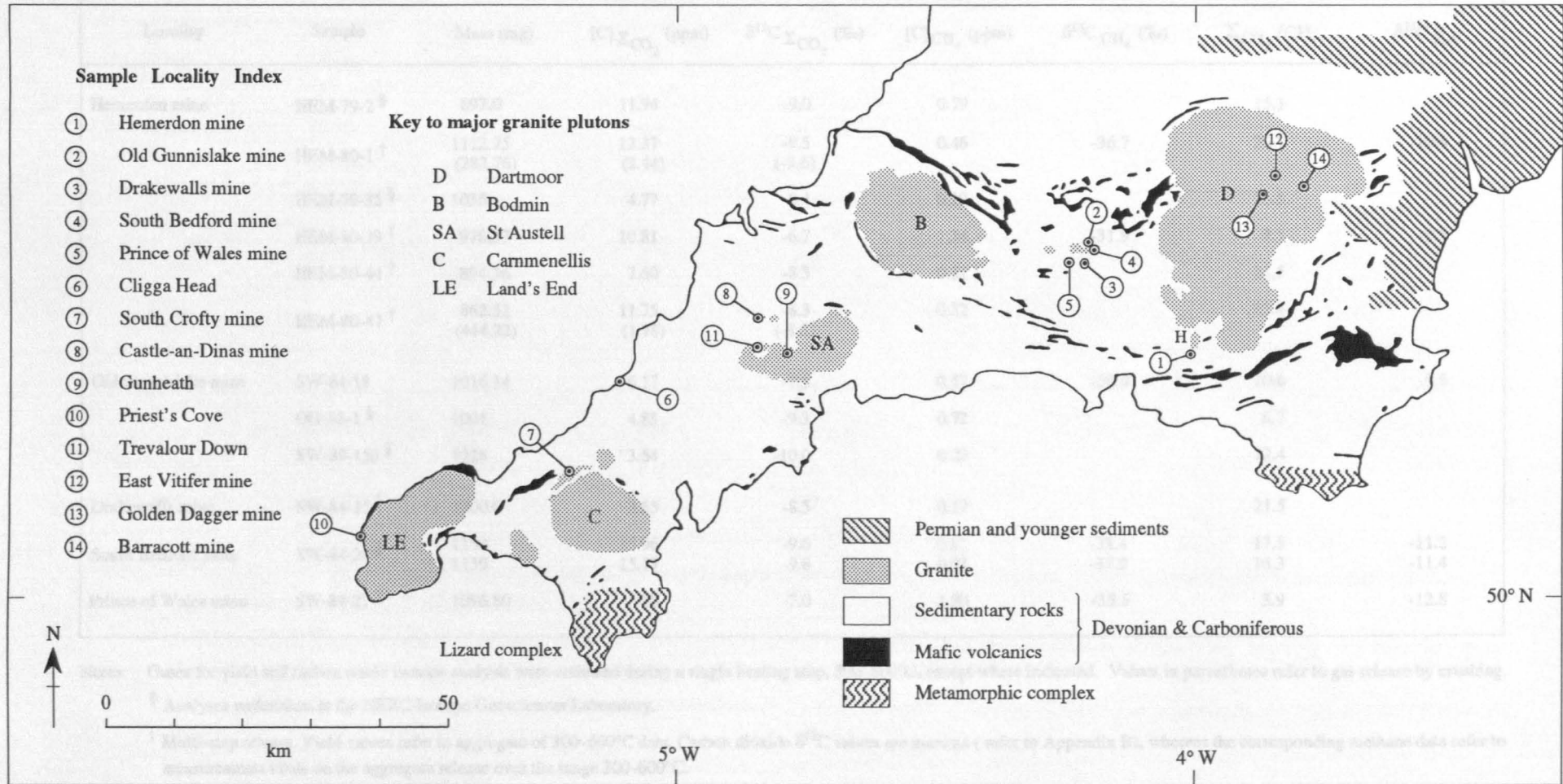


Table 3.4

The yield and $\delta^{13}\text{C}$ values of fluid inclusion carbon-bearing species extracted from quartz associated with early hydrothermal mineralisation and 'transitional' processes, SW England

Locality	Sample	Mass (mg)	[C] ΣCO_2 (ppm)	$\delta^{13}\text{C}_{\Sigma\text{CO}_2}$ (‰)	[C] CH_4 (ppm)	$\delta^{13}\text{C}_{\text{CH}_4}$ (‰)	$\Sigma\text{CO}_2/\text{CH}_4$	$\delta^{13}\text{C}_{\Sigma\text{C}}$
Hemerdon mine	HEM-79-2 §	897.0	11.94	-9.0	0.79		15.1	
	HEM-80-1 †	1112.75 (282.76)	13.37 (2.44)	-9.5 (-9.6)	0.46	-36.7	29.1	-10.4
	HEM-80-35 §	1035	4.77	-8.4	0.29		16.5	
	HEM-80-39 †	978.37	10.81	-6.7	1.34	-31.9	8.1	-9.5
	HEM-80-44 †	894.36	7.60	-8.3	0.31		24.5	
	HEM-80-47 †	862.52 (444.22)	11.75 (1.78)	-8.3 (-8.3)	0.32		35.4	
Old Gunnislake mine	SW-84-18	1016.14	6.17	-7.5	0.57	-30.8	10.6	-9.5
	OG-88-1 §	1001	4.83	-9.3	0.72		6.7	
	SW-89-150 §	1226	3.54	-10.0	0.29		12.4	
Drakewalls mine	SW-84-15 §	1200.0	3.65	-8.5	0.17		21.5	
South Bedford mine	SW-84-20 §	1150	15.96	-9.6	0.91	-38.4	17.5	-11.2
		1159	15.17	-9.8	0.93	-37.9	16.3	-11.4
Prince of Wales mine	SW-84-27 †	1096.80	5.10	-7.0	1.30	-35.5	3.9	-12.8

Notes: Gases for yield and carbon stable isotope analysis were collected during a single heating step, 300-600°C, except where indicated. Values in parentheses refer to gas release by crushing.

§ Analyses undertaken at the NERC Isotope Geosciences Laboratory.

† Multi-step release. Yield values refer to aggregate of 300-600°C data. Carbon dioxide $\delta^{13}\text{C}$ values are maxima (refer to Appendix B), whereas the corresponding methane data refer to measurements made on the aggregate release over the range 300-600°C.

Table 3.4 (continued)

Locality	Sample	Mass (mg)	[C] Σ CO ₂ (ppm)	$\delta^{13}\text{C}$ Σ CO ₂ (‰)	[C]CH ₄ (ppm)	$\delta^{13}\text{C}$ CH ₄ (‰)	Σ CO ₂ /CH ₄	$\delta^{13}\text{C}$ Σ C
Cligga Head	CH-88-1	863.8	5.22	-5.4	1.81	-33.6	2.9	-12.7
South Crofty mine	SC-88-2 [*]	996.8	-2.0	-6.3				
	SC-88-3 [†]	1045.5	3.89	+4.2	6.53	-27.4	0.6	-15.6
	SC-88-NIL ^a	1196.5	6.99	-9.1	0.32		22.0	
	SC-88-3ABC ^a	748.3	6.06	-7.3 ^{**}	3.09	-34.1	2.0	-16.4
701.0		6.23	-7.0	3.14	-35.2	2.0	-16.5	
Castle-an-Dinas mine	CD-88-1 ^a	892.7	3.70	-7.4	0.36		10.3	
Gunheath	LYGUN-15	764.9	5.54	-8.8				
	LYGUN-1	1289.2	3.38	-9.4				
Priest's Cove	LYPC-88	1011.2	3.66	-9.0				
Trelavour Downs	LYTD-88	824.6	2.93	-10.2				

Notes: Gases for yield and carbon stable isotope analysis collected during a single heating step, 300-600°C, except where indicated. Values in parentheses refer to gas release by crushing.

^a Analyses undertaken at the NERC Isotope Geosciences Laboratory.

[†] Multi-step release. Yield values refer to aggregate of 300-600°C data. Carbon dioxide $\delta^{13}\text{C}$ value is the maximum (with reference to Figure 3.24), whereas the corresponding methane result refers to measurements made on the aggregate release over the range 300-600°C.

^{*} Multi-step release. Severe contamination of the carbon dioxide fraction by hydrocarbons was noted for gas released above 480°C, despite cryogenic purification at -130°C. The isotopic datum point refers to the 300-480°C heating step.

^{**} Hydrogen sulphide present as a trace contaminant.

Figure 3.23

The yield and $\delta^{13}\text{C}$ of carbon dioxide extracted from quartz associated with early stage hydrothermal activity, S W England. Refer to Figure 3.22 for key to sampling localities

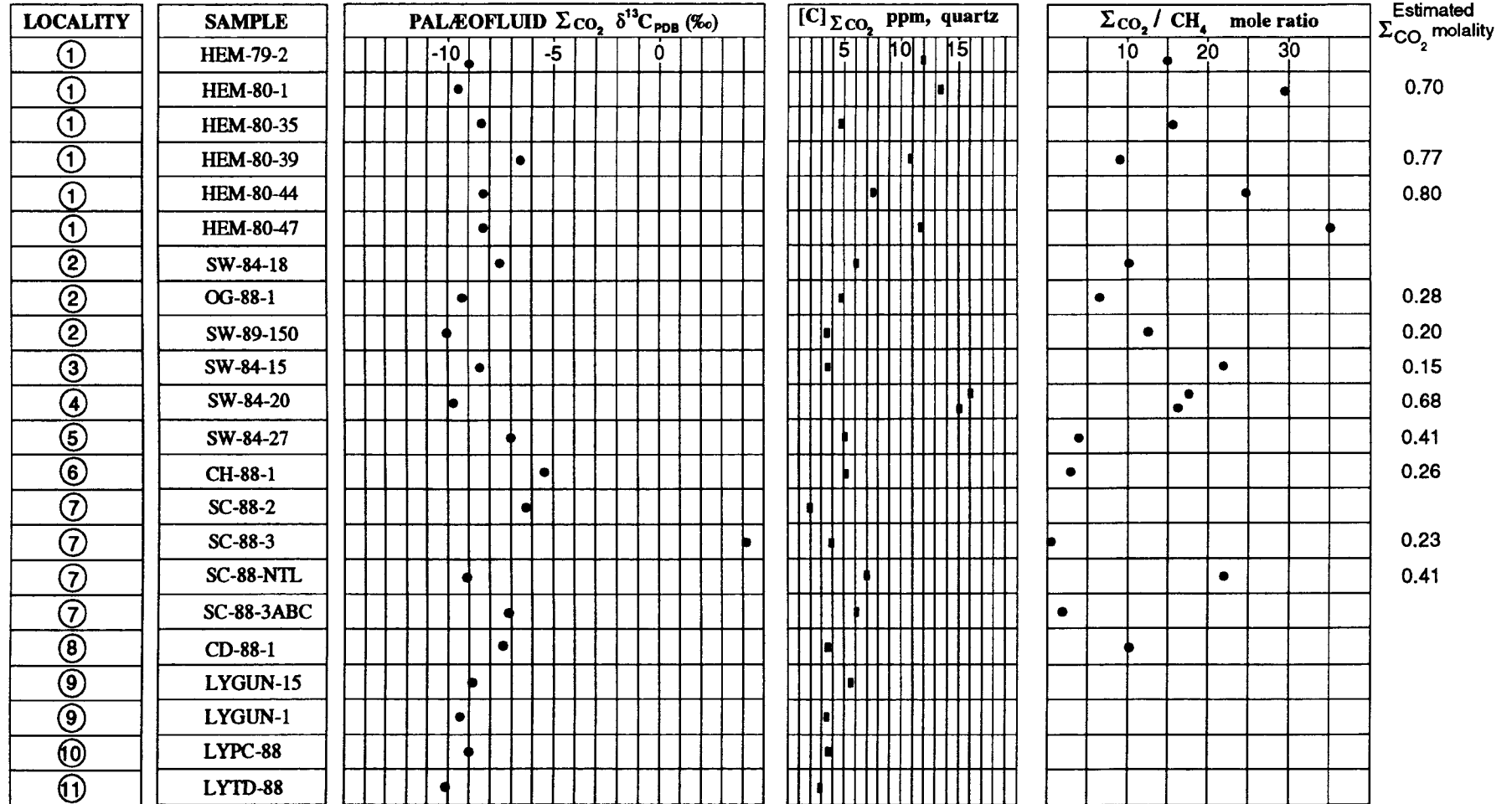


Figure 3.24

Carbon yield and $\delta^{13}\text{C}$ values of CO_2 released by stepped heating of quartz sample SW-88-3 (South Crofty mine), in the absence of supplied oxygen and with the on-line Pt foil catalyst at room temperature.

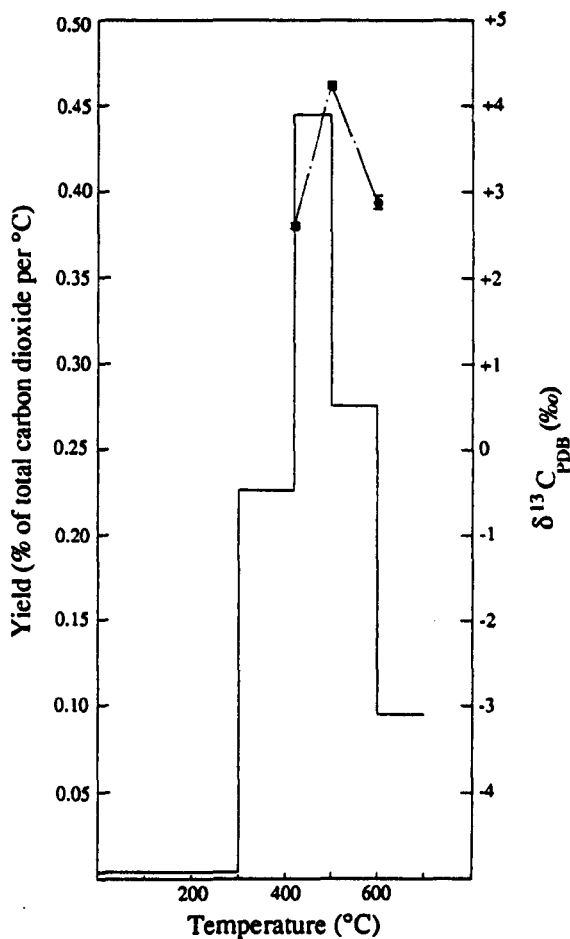
Sample weight: 1045.48 mg

ΣC (-100 to 700°C) = 4.52 μg (4.32 ppm)

For temperature range corresponding to the major release of fluid inclusions,

ΣC (300 to 600°C) = 4.06 μg (3.88 ppm) $\Sigma \delta^{13}\text{C}$ (300 to 600°C) = +3.3‰

$\delta^{13}\text{C}_{\text{max}} = +4.2‰$



T (°C)	Yield ($\mu\text{g C}$)	Concentration (ppm C)	$\delta^{13}\text{C}$ (‰)
300	0.03	0.03	nm
420	1.22	1.17	+2.6
500	1.60	1.53	+4.2
600	1.24	1.19	+2.9
700	0.43	0.41	nm

These were associated with the St Austell and Land's End granite outcrops and were supplied for palaeofluid carbon stable isotope analysis as part of a comprehensive study by Lin (1989) of pegmatitic and pneumatolytic evolution of Cornish granites. Preliminary analyses by the present author of the fluid inclusion volatile phase released by decrepitation of the quartz samples to 600°C indicated that CO₂ is the principal non-aqueous component; CO₂ yields were comparable to those reported here for fluids associated with the earliest oxide mineralisation.

Nitrogen and methane were also detected, but were present at much lower levels than the coexisting CO₂; the data were reported by Lin (1989). CO₂/CH₄ mole ratios ranged from ~10 for sample LYPC-88 (Priest's Cove, Land's End granite) to >20 for the other samples, all associated with the St Austell granite. The low absolute abundance of methane in these fluids precluded carbon stable isotope ratio determination of this component during the present investigation.

The palaeofluid carbon dioxide yield and associated δ¹³C results of these pegmatitic quartz and sheeted quartz-tourmaline veins are given in Table 3.4 and Figure 3.23, from which it is apparent that the values (-8.8 to -10.2‰) are similar to those characteristic of the fluids associated with W±Sn oxide mineralisation (-7.4 to -10.0‰). This provides a common link between the early pegmatitic fluids and subsequent hydrothermal stages; it also supports field observations (Lin, 1989) which illustrate the continuum of transitional processes relating the pegmatitic and pneumatolytic (including tourmalinisation and greisenisation, through to early oxide mineralisation) stages of hydrothermal evolution throughout the Cornubian batholith. On this basis, the CO₂ would seem to be a primary component of the magmatic-hydrothermal system, with local abundance possibly being related throughout the region to the degree of assimilation of predominantly pelitic, metasedimentary material into the granite protolith during anatexis and/or subsequent crustal contamination of magma during its ascent and emplacement.

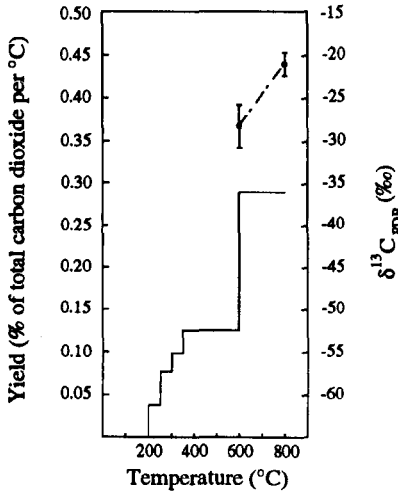
3.5.3 The Dartmoor hydrothermal system

An attempt was made to address the question of whether CO₂, present at very low abundances in hydrothermal fluids associated with the earliest quartz±tourmaline±cassiterite mineralisation of the Dartmoor granite, could be shown to be isotopically similar to (and therefore probably of similar origin as) that in CO₂-enriched early-stage fluids found associated with other plutons of the Cornubian batholith. The location and paragenesis of samples used are as reported in Appendix A. Stepped heating, using the 'optimised' extraction procedure in conjunction with static vacuum mass spectrometry, as described in Section 3.4.7, was applied to determine the carbon release profiles and associated δ¹³C isotopic composition. The results of the analyses are summarised in Figure 3.25.

Figure 3.25

Yield profiles, together with $\delta^{13}\text{C}$ as measured by static vacuum mass spectrometry, of CO_2 released during stepped heating of quartz associated with hydrothermal mineralisation of the Dartmoor granite.

(a) East Vitifer mine, tourmaline-cassiterite stage



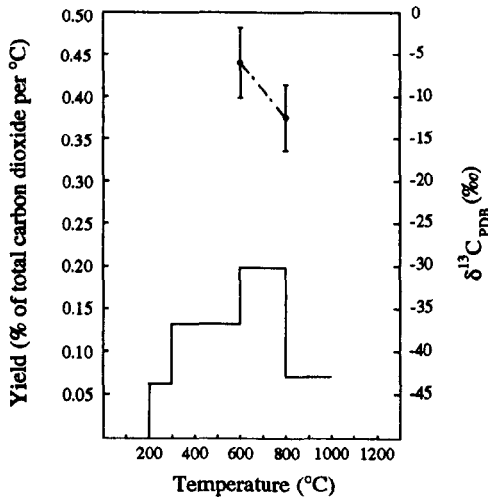
Sample: **SW-89-156 (T721)**

Sample weight: 16.7245 mg (single grain of quartz)

Total CO_2 yield in temperature range 300 to 600°C (corresponding to major release of fluid inclusions) = 18.4 ngC (1.10 ppmC)

T (°C)	Yield (ng C)	Concentration (ppm C)	$\delta^{13}\text{C}$ (‰)	σ (‰)
200	<0.2	<0.01	nm	
250	1.0	0.06	nm	
300	1.9	0.11	nm	
350	2.5	0.15	nm	
600	15.9	0.95	-28.2	2.68
800	29.4	1.76	-21.1	1.36

(b) Golden Dagger mine, earliest pegmatitic quartz



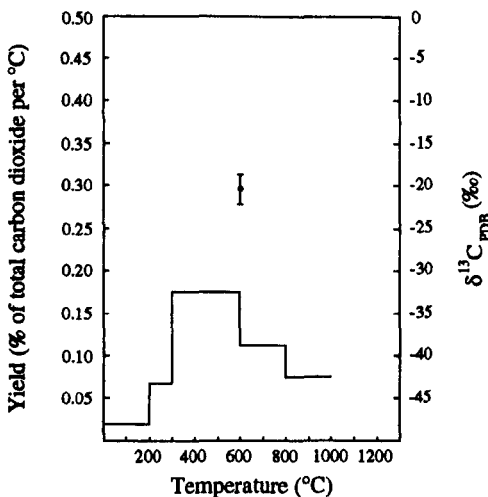
Sample: **SW-89-159 (T722)**

Sample weight: 13.6566 mg (single grain of quartz)

Total CO_2 yield in temperature range 300 to 600°C (corresponding to major release of fluid inclusions) = 8.6 ngC (0.63 ppmC)

T (°C)	Yield (ng C)	Concentration (ppm C)	$\delta^{13}\text{C}$ (‰)	σ (‰)
200	<0.2	<0.01	nm	
300	1.3	0.10	nm	
600	8.6	0.63	-6.0	4.13
800	8.6	0.63	-12.4	3.96
1000	3.1	0.22	nm	

(c) Golden Dagger mine, tourmaline-cassiterite stage



Sample: **SW-89-163 (T723)**

Sample weight: 16.9207 mg (single grain of quartz)

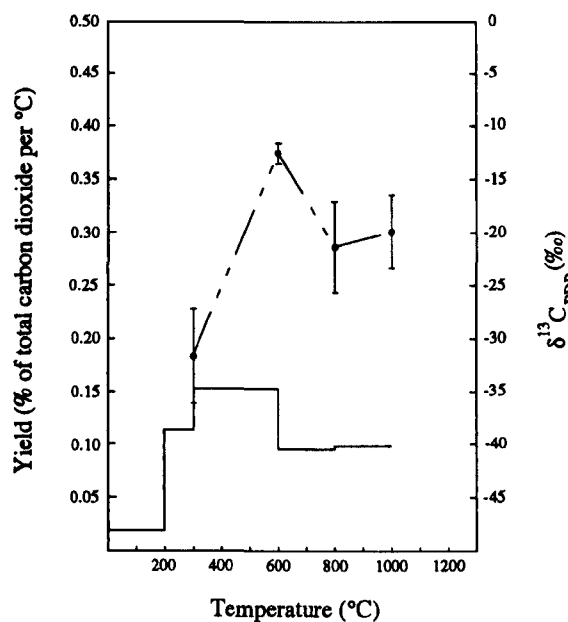
Total CO_2 yield in temperature range 300 to 600°C (corresponding to major release of fluid inclusions) = 13.4 ngC (0.79 ppmC)

T (°C)	Yield (ng C)	Concentration (ppm C)	$\delta^{13}\text{C}$ (‰)	σ (‰)
200	0.1	0.06	nm	
300	1.7	0.10	nm	
600	13.4	0.79	-20.3	1.73
800	5.7	0.34	nm	
1000	3.8	0.23	nm	

Note: 'nm' indicates 'not measured'

Figure 3.25 (continued)

(d) Barracott mine, tourmaline-cassiterite stage



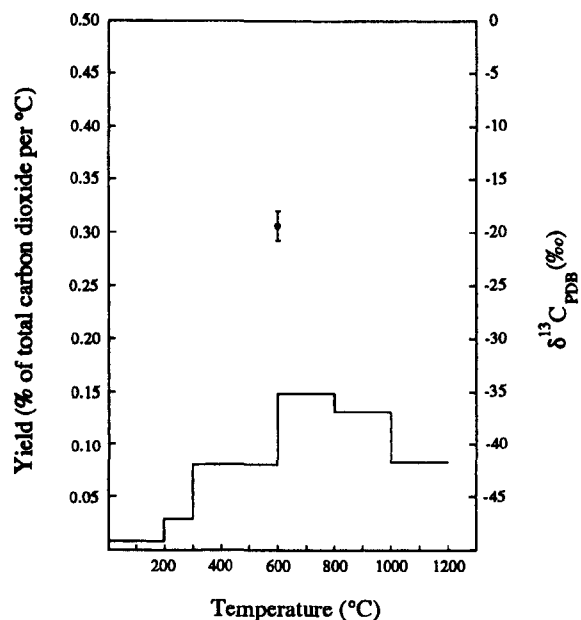
Sample: SW-89-164 (T724)

Sample weight: 18.6880 mg (single grain of quartz)

Total CO₂ yield in temperature range 300 to 600°C (corresponding to major release of fluid inclusions)

■ 22.9 ngC (1.23 ppmC)

T (°C)	Yield (ng C)	Concentration (ppm C)	$\delta^{13}\text{C}$ (‰)	σ (‰)
200	1.9	0.10	nm	
300	5.7	0.31	-31.7	4.46
600	22.9	1.23	-12.5	1.03
800	9.6	0.51	-21.3	4.30
1000	9.9	0.53	-19.8	3.41



Sample: SW-89-164 (T726)

Sample weight: 21.9134 mg (single grain of quartz)

Total CO₂ yield in temperature range 300 to 600°C (corresponding to major release of fluid inclusions)

■ 12.4 ngC (0.57 ppmC)

T (°C)	Yield (ng C)	Concentration (ppm C)	$\delta^{13}\text{C}$ (‰)	σ (‰)
200	0.8	0.03	nm	
300	1.5	0.07	nm	
600	12.4	0.57	-19.6	1.38
800	15.3	0.70	nm	
1000	13.4	0.61	nm	
1200	8.4	0.38	nm	

Note: Instability problems of the instrumentation prevented isotope ratio measurement of the CO₂ released above 600°C.

Interpretation of the salient features of Figure 3.25 is problematic, for several reasons:

- (i) It is apparent that only in two out of the five experiments did the 300-600°C CO₂ yield (expected to contain virtually all of any fluid inclusion component) exceed that recorded for the subsequent (600-800°C) step.
- (ii) Sample inhomogeneity is evident from the data presented in Figure 3.25(d), where duplicate analyses produced a significantly different CO₂ release profile.
- (iii) Despite precautions taken to minimise the system blank, the carbon blank yield associated with the quartz sample grains may be as high as 3-4ng for both the 300-600°C and 600-800°C heating steps (*cf.* Table 3.3). The source of the significant release of carbon at high temperature (>600°C) from the Dartmoor samples remains unknown, as does the extent to which this component contributes to the total carbon released at lower temperatures.

The stepped heating data produced during run T724 are perhaps the most instructive, as: (i) four isotopic measurements were recorded, whereas only two or even a single measurement was possible for the other samples; (ii) the CO₂ yield during the 300-600°C step significantly exceeded that for any other step during this run and, furthermore, was characterised by the most precise isotopic measurement (1σ error 1.03‰) of the series of experiments; (iii) the 300-600°C CO₂ yield also exceeded the values recorded over the same temperature interval for all of the other samples analysed and is therefore most likely to represent the closest approach to any fluid inclusion component. On this basis, it would appear that a lower δ¹³C limit of -12.5 ± 1‰ may be tentatively attributed to the fluid inclusion CO₂ component; this value probably includes a minor 'adventitious' component characterised by δ¹³C ≈ -27‰, as indicated by the result for the 200-300°C step. The carbon component released at higher temperatures appears to be characterised by a δ¹³C value of *ca.* -20‰; this is in close agreement with the result of the 600-800°C step during run T723, where the largest CO₂ yield for any individual step throughout the series of experiments was recorded. The same isotopic value was measured, however, for the 300-600°C CO₂ release in two instances (T723 and T726), which is perhaps best accounted for in terms of the mixing of a fluid inclusion component of δ¹³C value in the range -6 to -12‰ and an 'adventitious' carbon source characterised by δ¹³C ≈ -27‰.

It is noteworthy that the δ¹³C isotopic result (-6.0 ± 4.1‰) for the 300-600°C step of run T722 supports the case for a relatively ¹³C-enriched component associated with the fluid inclusion release. The sample used in this case is representative of the earliest stage of hydrothermal alteration of the Dartmoor granite; it is evident that the δ¹³C value of any associated palæofluid component is comparable to those measured by conventional mass spectrometry for CO₂-enriched 'transitional' fluids associated with the St Austell and Land's End granites (Section 3.5.2).

In summary, the stepped heating carbon yield profiles and associated isotopic data obtained during this study of the earliest hydrothermal alteration of the Dartmoor granite are inconclusive, although tentative evidence for a palæofluid CO₂ component of similar isotopic characteristics to the more abundant carbon found in transitional fluids elsewhere within the batholith was provided by isotopic data from two of the five samples analysed.

The substantial release at temperatures >600°C of carbon characterised by a δ¹³C value of *ca.* -20‰ is unlikely to include a significant fluid inclusion component; the isotopic data are, furthermore, not in accord with carbonate decomposition as the principal source. The origin of this carbon therefore remains enigmatic, although it would appear to be sample-derived rather than the manifestation of an enhanced procedural blank. Comparison with results obtained by identical procedures for samples where the palæofluid CO₂ yield was relatively substantial indicates that the CO₂ yield for the heating step subsequent to that during which the α-β transition of the quartz host occurred was typically in the range 3-6ngC (runs T706, T709 and T725; Figures 3.20 and 3.21 respectively), although a value of 9.6ngC was recorded during one experiment (run T717, Figure 3.21), with a corresponding δ¹³C value of -27.3±2.2‰ (1σ error).

3.5.4 Comparative data: examples from N W England and S China

3.5.4.1 Carrock Fell (N W England): wolframite-associated quartz veins

Compared to the examples of hydrothermal processes typified by association with W±Sn oxide assemblages in the Cornubian batholith region, the comparable system at Carrock Fell (associated with the Skiddaw granite) is distinguished by fluid inclusion evidence for a lesser degree of complexity, characterised by the predominance of simple, two-phase (liquid-vapour) inclusions, no post-entrapment nucleation of solid phases (daughter minerals)[†] and a salinity range restricted to between 6.8 and 9.6 equivalent wt% NaCl (Shepherd *et al.*, 1976). Fluid homogenisation temperatures recorded by these authors were also significantly lower (~235°C) than those reported elsewhere for the equivalent stage in S W England.

The present results, given in Table 3.5, indicate a significant abundance of palæofluid carbon, predominantly as CO₂ but also as coexisting CH₄, associated with the quartz. A notable feature of these data is that the methane is significantly depleted in ¹³C compared to the same component in the S W England fluids. The δ¹³C_{ΣC} values, however, occur within the range defined by the Cornubian data (Table 3.4).

[†] The absence of solid phases was reported by Shepherd *et al.* (1976), on the basis of an optical study of fluid inclusions in Carrock Fell vein quartz. During the present study, however, evidence for the presence of a carbonate phase was found in some examples; whether the carbonate was a component of the palæofluid, or derived from a microcrystalline phase intergrown with the quartz, could not be identified.

Table 3.5
Carbon yield and $\delta^{13}\text{C}$ isotopic composition of fluid inclusion components, Carrock Fell vein quartz

Sample	Mass (mg)	[C] $_{\Sigma\text{CO}_2}$ (ppm)	$\delta^{13}\text{C}_{\Sigma\text{CO}_2}$ (‰)	[C] $_{\text{CH}_4}$ (ppm)	$\delta^{13}\text{C}_{\text{CH}_4}$ (‰)	$\Sigma\text{CO}_2/\text{CH}_4$	$\delta^{13}\text{C}_{\Sigma\text{C}}$
CF-77-98 ‡	985.0	18.55	-10.89**	0.92	-49.2	20.1	-12.7
	1254.7	18.61	-10.93**	1.03	-47.7	18.1	-12.9
CF-77-79B ‡	1207.3	25.25	-11.35	0.58	-47.5	43.5	-12.2
	1238.9	25.57	-11.36	0.58	-47.0	44.0	-12.2
CF-77-39A †	989.81	14.43	-7.27	2.52	-54.5	5.8	-14.3
CF-76-25	1024.73	13.98	-11.84	0.66	-39.9	21.1	-13.1
	1139.79	13.58	-11.69	0.57	-42.0	23.7	-13.2

Notes: Gases for yield and carbon stable isotope analysis collected during a single heating step, 300 - 600°C, except where indicated.

‡ Analyses undertaken at the NERC Isotope Geosciences Laboratory.

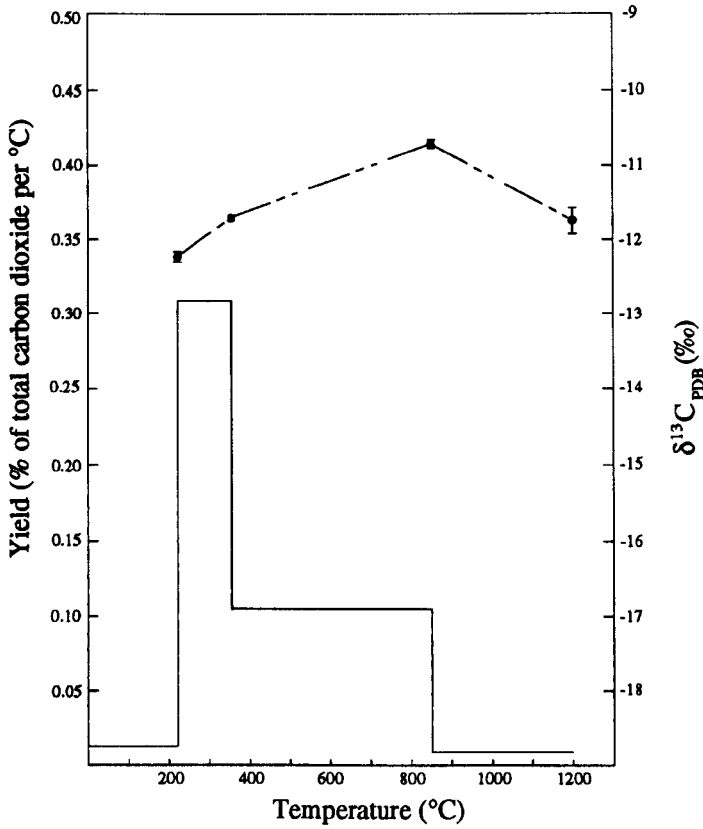
† Multi-step release. Yield values refer to aggregate of 300-600°C data. Carbon dioxide $\delta^{13}\text{C}$ value refers to 400-500°C step (minor contribution from carbonate decomposition noted in 500 - 600°C step - see Figure 26), whereas methane value is for total release in the temperature range 300 - 600°C.

** Possibly includes a minor contribution from carbonate decomposition (*cf.* Figure 3.26 and Appendix B: Table B2.7).

Figure 3.26

Yield profiles and corresponding $\delta^{13}\text{C}$ values of CO_2 released during stepped heating of hydrothermal vein quartz, Carrock Fell: evidence for the presence of an associated carbonate phase.

(a)

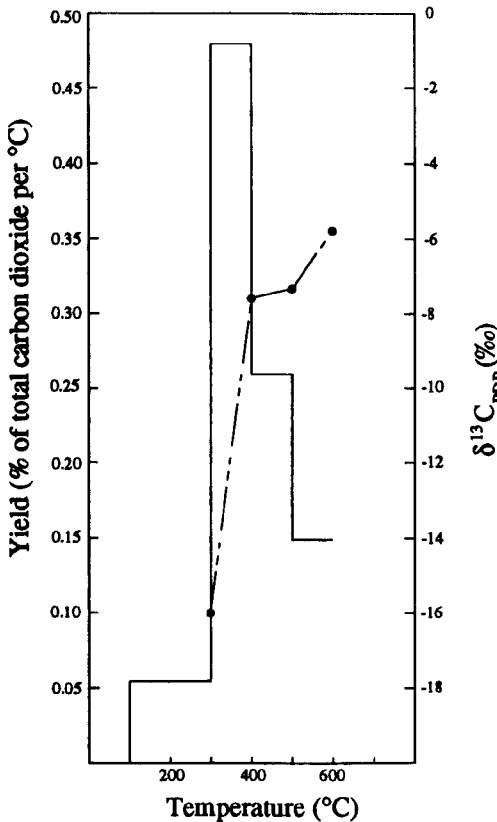


Sample: **CF-77-98**

Sample weight: 1060.6 mg

T (°C)	Yield (µg C)	Concentration (ppm C)	$\delta^{13}\text{C}$ (‰)
220	0.90	0.85	-12.2
356	14.52	13.69	-11.71
850	17.90	16.88	-10.71
1200	1.11	1.05	-11.7

(b)



Sample: **CF-77-39A**

Sample weight: 989.81 mg

T (°C)	Yield (ng C)	Concentration (ppm C)	$\delta^{13}\text{C}$ (‰)
300	1.77	1.78	-16.0
400	7.69	7.77	-7.54
500	4.17	4.22	-7.27
600	2.41	2.44	-5.7

The temperature at which maximum release of fluid occurred during stepped heating was significantly lower[†] than recorded for the S W England samples. Evidence for the decomposition of a carbonate component at temperatures >500°C was obtained in two examples (Figure 3.26).

3.5.4.2 S China: Transitional stages of hydrothermal evolution of the Yanshanian granites.

The transitional stages of hydrothermal evolution of granites of the Yanshanian cycle of south China are similar in many respect to those of S W England (Lin, 1989, and references therein). In particular, the Yanshanian granites are peraluminous 'S'-type biotite granites, which evolve to biotite-muscovite granites (and locally to muscovite and Li-mica granites); they are composite bodies, and are characterised by a chronology of intrusive and related hydrothermal activity spanning 10-25 Ma.

Preliminary analyses by the present author of a small number of examples of sheeted vein quartz associated with quartz+wolframite±molybdenite (±beryl) assemblages from Jiangxi and Hunan provinces of south China showed that CO₂ was the only significant non-aqueous volatile component in the palaeofluids, with estimated Σ_{CO_2} molalities ranging from 0.39 to 1.84. Nitrogen and methane were also detected, but were present at trace levels; the analytical data were reported by Lin (1989), together with relevant geological details.

Only in two examples (XHS-02 and YGX-05, from Xihuashan and Yaoguangxian respectively) was methane a significant component, with CO₂/CH₄ mole ratios of *ca.* 16 and 45 respectively. It is notable that, in these cases, the $\delta^{13}\text{C}$ values of the coexisting CO₂ were the most ¹³C-enriched of the group, indicating that the corresponding $\delta^{13}\text{C}_{\Sigma\text{C}}$ values were probably similar to those of the examples in which CO₂ represented the only significant carbon-bearing component. The results of carbon stable isotope ratio analysis of the palaeofluid CO₂ are reported in Table 3.6 and Figure 3.27.

The stepped heating release profile shown in Figure 3.27(a) is notable in several respects:

(i) The three isotopic data points corresponding to measurements of the fluid inclusion CO₂ are very consistent, with a range of less than 0.1‰. This is a testament to the potential effectiveness of the experimental procedure, under optimum conditions.

[†] An abundance of relatively large inclusions (consequently requiring lower internal pressures to fracture the host quartz), together with the observation that a discrete (liquid) CO₂ phase is not uncommon in the Carrock Fell quartz (T J Shepherd, *pers. comm.*), is in accord with lower decrepitation temperatures.

Table 3.6

Carbon yield and $\delta^{13}\text{C}$ values of fluid inclusion CO_2 extracted from quartz samples associated with wolframite-molybdenite vein mineralisation hosted by the Yanshanian granites of southern China.

Locality	Sample reference	Mass (mg)	Temperature ($^{\circ}\text{C}$)	Yield (μgC)	Concentration (ppm C)	$\delta^{13}\text{C}_{\text{PDB}}$ (‰)
Yaoguangxian	YGX-05	1105.24	-20-615	24.92	22.55	-4.12
Xihuashan	XHS-01	1093.29	-20-600	43.85	40.11	-5.39
Piaotang	PT-496 [†]	889.7	-20-308	2.77	3.11	-6.6
			300-408	6.00	6.74	-5.58

Note: [†] CO_2 released during temperature steps beyond 408 $^{\circ}\text{C}$ was contaminated by SO_2 despite cryogenic purification at -130 $^{\circ}\text{C}$, thus precluding isotopic analysis.

Figure 3.27

Yield profiles and $\delta^{13}\text{C}$ of CO_2 released by stepped heating of quartz associated with $\text{W}\pm\text{Mo}$ -bearing transitional vein systems in the Yanshanian granites of S China.

(Extractions undertaken in the absence of oxygen and with the on-line Pt catalyst at room temperature)

(a) Sample: XHS-02 (Locality: Xihuashan)

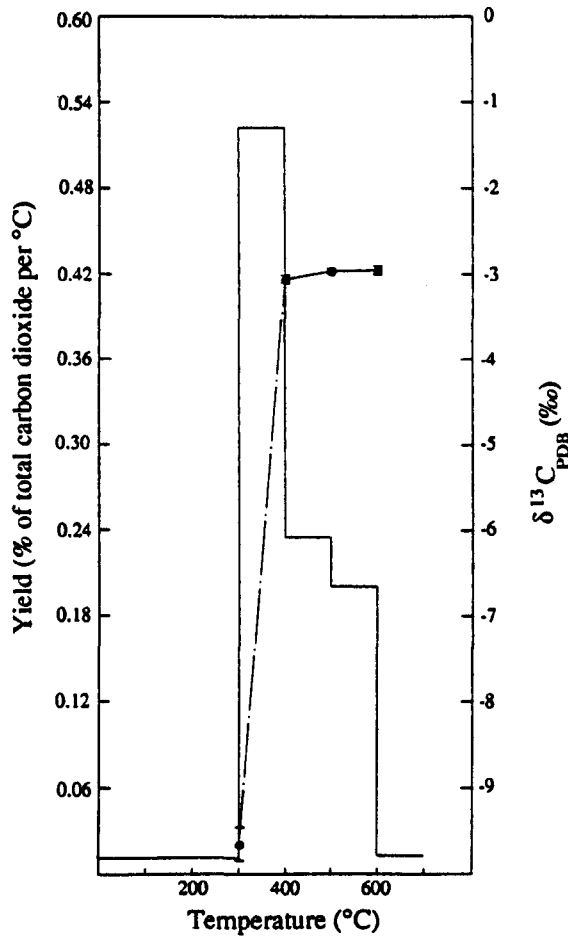
Sample weight: 1011.98 mg

ΣC (~100 to 700°C) = 14.95 μg (14.77 ppm)

For temperature range corresponding to the major release of fluid inclusions,

ΣC (300 to 600°C) = 14.30 μg (14.13 ppm) $\Sigma \delta^{13}\text{C}$ (300 to 600°C) = -3.0‰

$\delta^{13}\text{C}_{\text{max}} = -3.0\text{‰}$



T (°C)	Yield ($\mu\text{g C}$)	Concentration (ppm C)	$\delta^{13}\text{C}$ (‰)
300	0.47	0.46	-9.7
400	7.79	7.70	-3.07
500	3.51	3.47	-3.0
600	3.00	2.97	-3.0
700	0.18	0.18	nm

Figure 3.27 (continued)

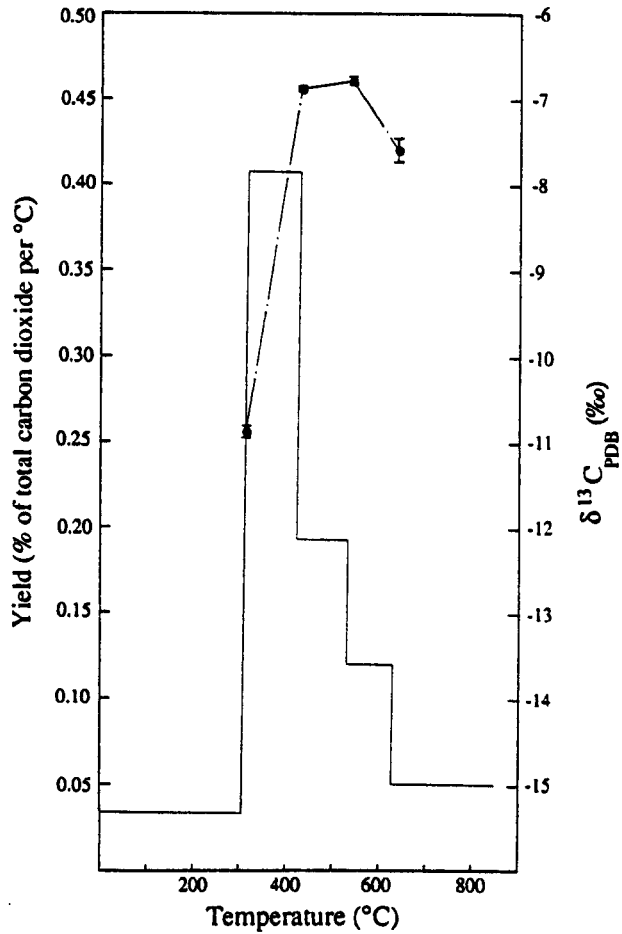
(b)

Sample: DP-560 (Locality: Dangping)

Sample weight: 1093.29 mg

ΣC (~100 to 850°C) = 6.74 μg (6.16 ppm)

$\delta^{13}\text{C}_{\text{max}} = -6.8\text{‰}$



T (°C)	Yield (μg C)	Concentration (ppm C)	δ ¹³ C (‰)
308	0.68	0.62	-10.9
420	3.07	2.81	-6.9
530	1.43	1.31	-6.8
630	0.81	0.74	-7.6
850	0.75	0.69	nm

(ii) On the basis of a simple model assuming mixing of a homogeneous fluid inclusion component ($\delta^{13}\text{C}$ value of -3.0‰) with an isotopically homogeneous CO_2 blank characterised by a $\delta^{13}\text{C}$ value of -25‰ , the experimental blank yield required to produce a shift of 0.1‰ (negative) in the fluid inclusion $\delta^{13}\text{C}$ measurement is $\sim 35\text{ ngC}$ (corresponding to a sample-to-blank ratio of ~ 220), for the $300\text{-}400^\circ\text{C}$ step. For the two subsequent heating increments, the corresponding blank yield values are approximately 16 ngC and 14 ngC respectively, with the sample-to-blank ratio remaining virtually unchanged. With regard to the lowest temperature step (ambient to 300°C) in Figure 3.27(a), the same model indicates that the blank contribution to the total CO_2 released during this step was *ca.* 143 ngC , with an equivalent sample-to-blank ratio of ~ 2.3 .

(iii) Incorporation of the data for the lowest temperature release (up to 300°C) results in a shift of 0.25‰ (negative) in the weighted mean $\delta^{13}\text{C}$ value. This indicates, for the present example, the magnitude of error in the fluid inclusion $\delta^{13}\text{C}$ measurement that would be incurred by the use of single-step heating (ambient to 600°C) to effect the release of CO_2 for isotope ratio analysis.

Table 3.6 includes the results of two single-step extractions (from ambient temperature), undertaken before the experimental procedure was optimised. In these cases, however, the substantial CO_2 yields indicate that any blank correction to the fluid inclusion isotopic data would have been very small.

On the basis of carbon isotope measurements of carbonate minerals, and application of the appropriate equilibrium fractionation factors, Zhang *et al.* (1984) estimated that the average $\delta^{13}\text{C}$ of the associated palæofluid carbon from Xihuashan and Piaotang (Jiangxi province) was -6.1‰ (11 samples). The associated $\delta^{13}\text{C}$ range, however, was not given. For examples from the same localities, and where the palæofluid carbon component consists essentially of CO_2 only, direct measurement of fluid inclusion CO_2 during the present work gave $\delta^{13}\text{C}$ values of -5.4‰ (sample XHS-01) and -5.6‰ (sample PT-496) respectively, as indicated in Table 3.6.

Zhang *et al.* (1984) suggested that the source of the palæofluid carbon was the granite magma; this was also in accord with the predominantly magmatic nature of the associated aqueous component, as shown on the basis of hydrogen and oxygen stable isotope data by the same authors.

3.6 Discussion

3.6.1 Salient features of the Cornubian palaeofluid carbon data

Examination of the yield and $\delta^{13}\text{C}$ data (Table 3.4) relating to quartz-hosted palaeofluid CO_2 and CH_4 associated with early hydrothermal mineralisation of the Cornubian batholith, together with information concerning the associated wall-rock lithology (Appendix A), reveals no discernible relationship between either the carbon speciation or ^{13}C distribution, on the one hand, and whether the quartz veins are granite-hosted or emplaced within metasedimentary rock, on the other. In the case of granite-hosted veins, no systematic variation was apparent between the carbon isotope data and extent of hydrothermal alteration (greisenisation) of the granite, either locally or on a regional basis.

A notable feature of the data set, on both a local and regional scale, is the large range of CO_2/CH_4 ratios (0.6 to >35 for the batholith as a whole), coupled with relatively small variation of the corresponding $\delta^{13}\text{C}_{\Sigma\text{C}}$ values (-9.5 to -16.5‰). Whereas CO_2 was the predominant carbon-bearing palaeofluid component in almost all cases investigated, relative ^{13}C -enrichment of this component, characterised by $\delta^{13}\text{C}$ values up to -5.4‰ (as at Cligga Head) was found to be associated, in general, with enhanced concentrations of coexisting CH_4 (relatively depleted in ^{13}C), which effectively 'buffered' variations in $\delta^{13}\text{C}_{\Sigma\text{C}}$. The most striking example relates to two samples (SW-88-3 and SW-88-3ABC, respectively) of methane-enriched palaeofluid from South Crofty mine, where the associated CO_2 components differed in isotopic composition by $>11\%$, yet the corresponding $\delta^{13}\text{C}_{\Sigma\text{C}}$ variation was $<1\%$.

Although the $\delta^{13}\text{C}$ values of the methane component are compatible with data from subaerial hydrothermal systems for which pyrolysis of organic matter (thermogenesis) has been proposed (Welhan, 1988), arguments advanced below suggest that this was probably not the primary mechanism in the case of the Cornubian system.

3.6.2 CO_2 in the Cornubian hydrothermal system: a primary magmatic component?

For magmas formed primarily by the partial melting of crustal rocks (rather than a mantle source), as is believed to be the case for the Cornubian batholith (see Chapter 1, Section 1.1.1), the $\delta^{13}\text{C}$ value of carbon in the magma might be expected to correspond to the average $\delta^{13}\text{C}$ value of crustal rocks assimilated in the melt. Calculations by Ohmoto and Rye (1979) suggest that, on a global scale, the crustal carbon reservoir in sedimentary and metasedimentary rocks should be predominantly derived from oxidised carbon (carbonates), with only ~22% from reduced (organic and graphitic) carbon sources, giving a mean $\delta^{13}\text{C}$ value of approximately -5.5‰, similar to that of the mantle. However, it seems reasonable to

infer that variations in crustal lithology will give rise to a wide range of $\delta^{13}\text{C}$ values in magmas derived from the anatexis of crustal rocks, depending on the local relative abundance of carbonate and organic carbon in the source rocks and, indeed, the isotopic compositions of these components.

In S W England, granite magmatism was protracted from about 293 to 275 Ma before present (Chesley *et al.*, 1993, and references therein), resulting in the emplacement of plutons (generally of a composite nature) into Palaeozoic metasediments and metavolcanic rocks. Furthermore, hydrothermal fluids responsible for the early, high temperature W±Sn oxide-bearing sheeted greisen bordered veins (and the cassiterite-bearing tourmaline veins and breccias) were broadly synchronous with the cooling of the individual granite magmas to ~320°C (Chapter 1, Section 1.1.2). Evidence presented in the present work (Chapters 2 and 5, respectively) supports suggestions that they are primarily fluids exsolved (at 700-800°C?) during crystallisation of the magmas at depth, and may be episodic due to the emplacement of younger magma within the same pluton (Chesley *et al.*, 1993). Carbon dissolved in the granitic melt (in oxidised form) is likely to be partitioned as CO_2 into the expelled, Cl-rich (Burnham, 1979) aqueous phase during cooling of the magma.

It is suggested, therefore, that CO_2 in the Cornubian palaeofluids is a primary, magmatic-hydrothermal component, derived directly from carbon assimilated in the granitic protoliths. On this basis, a correlation should obtain between the degree of 'S'-type character (as identified by *e.g.* $^{87}\text{Sr}/^{86}\text{Sr}$ initial ratios, initial ϵ_{Nd} values, $\delta^{18}\text{O}$ values and peraluminosity) of the component intrusives of the batholith, and carbon abundance in the associated early post-emplacement hydrothermal fluids. The Dartmoor granite intrusive, besides being the largest pluton of the batholith, was derived from a protolith of notably lower sedimentary content, on the basis of the indices referred to above; this is in agreement with the empirical finding of very low CO_2 abundance in the associated magmatic-hydrothermal fluids.

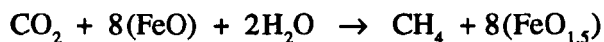
3.6.3 Controls on carbon speciation and ^{13}C distribution in the Cornubian palaeofluids

3.6.3.1 Carbon sources, fluxes and redox reactions

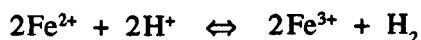
Any proposed hypothesis of the geochemical behaviour of palaeofluid carbon associated with the earliest stages of hydrothermal mineralisation of the Cornubian batholith requires an evaluation of the possible contributory carbon sources and also a consideration of potential redox mechanisms for controlling the carbon speciation. It has been postulated in Section 3.6.2 that the primary carbon-bearing component of the hydrothermal fluids was CO_2 , derived from the granite magma. The presence of coexisting CH_4 in the fluid inclusions suggests (i) partial reduction of the CO_2 , prior to fluid entrapment; alternatively, or additionally, (ii) an external carbon source, such as *via* the pyrolysis of metasedimentary rocks within the local metamorphic aureole.

The model of Giggenbach (1987) for redox processes governing the chemistry of fumarolic gas discharges from White Island, New Zealand, provides a useful analogy in many respects. For example, the outlet temperature of the fumaroles, over an area of only ~1 km², ranges from ~100°C to in excess of 700°C, thereby bridging the gap between 'geothermal' and 'magmatic' gases. The processes accompanying the rise of these high temperature fluids through the crust are therefore likely to be appropriate to a model of the magmatic-hydrothermal transition zone. Giggenbach (1987), in a detailed thermodynamic analysis, concluded that the overall redox process at White Island corresponds to the more or less successful conversion of initially oxidised, high-temperature magmatic gases (SO₂, CO₂) to their reduced counterparts (H₂S and CH₄) which are stable in the presence of lower temperature rock. According to Giggenbach (1987), CH₄ and NH₃ are formed at depth within the hydrothermal zones, where redox conditions are governed by the Fe(II)-Fe(III) buffer[†] of the rock system.

Giggenbach (1987) suggested that, under such conditions, prolonged interaction of a cooling, CO₂-rich gas with the rock matrix will cause gradual oxidation of the latter, with concomitant generation of methane:



In the Cornubian palæofluids, the wide range of CO₂/CH₄ ratios on a local scale, as seen from the Hemerdon and South Crofty data respectively (Table 3.4), together with the associated narrow range of δ¹³C_{ΣC} values, suggests that the fluid chemistry was primarily controlled by localised redox reactions, rather than through the operation of large scale buffering processes. As discussed in Chapter 5 of the present work, these fluids were generally high salinity brines and hence, at magmatic-hydrothermal temperatures, acidic. As noted by Giggenbach (1987), such fluids would be expected to promote wall-rock alteration through reactions such as:



The neutralisation of granite-derived, high-temperature acidic fluid by wall-rock interaction has been proposed by Bottrell and Yardley (1988) as the mechanism of oxide mineral formation and precipitation (*e. g.* cassiterite and specular hæmatite) in the St Austell district of

[†] It has been suggested that, for basaltic and andesitic magmas, a non-specific buffer simply involving Fe(II)-Fe(III) is possibly a more realistic approach, in the absence of detailed mineralogical information, than the commonly adopted magnetite-hæmatite system for evaluating redox buffering by the rock matrix; this issue is discussed in detail by Giggenbach (1987). (FeO) and (FeO_{1.5}) are used to represent, respectively, Fe²⁺ and Fe³⁺ incorporated into an unspecified oxide or aluminosilicate mineral.

S W England. Whether hydrogen generated under these conditions might react with CO₂ in the magmatic-hydrothermal fluid to give Fischer-Tropsch type synthesis of methane (catalysed by wall-rock constituents) is a matter for speculation, although equilibrium modelling suggests that the process is thermodynamically favourable (Ellis, 1957).

Hæmatite is commonly associated with W±Sn oxide mineralisation in S W England, particularly in the case of sheeted quartz greisen vein systems. In the absence of redox buffering, hæmatite will oxidise methane; the kinetics of this process have been investigated by Kiyosu and Krouse (1989), who also examined the associated carbon isotope fractionation (under flow conditions, to eliminate the possibility of carbon isotope exchange between the product CO₂ and reactant CH₄). Abiogenic oxidation of methane is possibly a significant mechanism for fractionating carbon isotopes in natural systems and has been postulated to explain the coexistence of light hydrocarbon gases enriched in ¹³C and CO₂ depleted in ¹³C (see Kiyosu and Krouse, 1989, and references therein). The temperature dependence of the oxidation rate of methane by hæmatite in the temperature range 450 to 650°C was given by Kiyosu and Krouse (1989) as:

$$\log_{10}k = (-1.75 \times 10^3/T) - 0.69 \quad (\text{min}^{-1})$$

The temperature dependence of the corresponding kinetic isotope fractionation, α , ($=k_{12}/k_{13}$) of the stable carbon isotopes was given by the same authors as:

$$10^3(\alpha - 1) = (7.44 \times 10^6/T^2) + 6.56$$

The oxidation of methane by hæmatite at lower temperatures, and the associated kinetic isotope effect, can thus be estimated by extrapolation from these empirical equations. For example, as noted by Kiyosu and Krouse (1989), the time required for 10% of a methane reservoir at 200°C to be oxidised by Fe₂O₃ is ~10⁻² years. Under such conditions (below ~320°C), carbon isotopic equilibration between CO₂ and CH₄ would be most unlikely (as discussed in Section 3.2.9), hence the kinetic model is appropriate. In view of geological models invoking successive pulses of magmatism and associated magmatic-hydrothermal mineralisation within individual plutons of the Cornubian batholith (Chesley *et al.*, 1993), oxidation of methane in high temperature hydrothermal fluids by reaction with earlier-formed hæmatite may be of some significance in the S W England system.

In contrast, a contributory mechanism to methane *formation* in the hydrothermal fluids is the oxidation by CO₂ of ammonia (or ammonium, in NH₄⁺-substituted micas). This reaction is a potential source of nitrogen in the palæofluids; a more detailed discussion is therefore deferred to Chapter 4 of the present work. Equilibrium thermodynamic modelling indicates that such a process is feasible under the temperature and pressure conditions appropriate to Cornubian magmatic-hydrothermal fluid evolution (Section 4.8.5).

3.6.3.2 Carbon stable isotope systematics

In Figure 3.28, the $\delta^{13}\text{C}$ data of methane from the Cornubian palaeofluids are plotted against the $\delta^{13}\text{C}$ values of the coexisting CO_2 component, together with isotherm contours corresponding to isotopic equilibrium at the stated temperatures. Also included, for comparative purposes, are the Carrock Fell data. It is apparent from these results that the CO_2 and CH_4 components are unlikely to be in isotopic equilibrium, as nearly all of the data points indicate temperatures significantly below the kinetic 'blocking' temperature of $\sim 320^\circ\text{C}$ proposed by Sheppard (1981).

The anomalous $\delta^{13}\text{C}_{\text{CO}_2}$ value of $+4.2\%$ recorded for sample SW-88-3 from South Crofty, together with the unusual predominance of methane as the major carbon-bearing species in the fluid, would be difficult to explain except on the basis of the postulate that the coexisting methane is derived from closed system reduction of a primary magmatic-hydrothermal CO_2 component. Furthermore, the concentration of coexisting N_2 is significantly higher (in terms of both absolute yield and estimated $\text{N}_{2(\text{aq})}$ molality) than recorded for any other sample in this study (see Figure 4.9), which is in accord with a common source for both the methane and nitrogen palaeofluid components. If it is assumed, for modelling purposes, that no secondary carbon source contributed to the fluid, the magmatic-hydrothermal CO_2 component would have been characterised initially by a $\delta^{13}\text{C}$ value equal to the weighted mean of the present-day $\delta^{13}\text{C}_{\text{CO}_2}$ and $\delta^{13}\text{C}_{\text{CH}_4}$ values, *i.e.* -15.6% (see Table 3.4). If the postulated CO_2 reduction is considered irreversible[†], and the reaction occurred at a temperature $>320^\circ\text{C}$ (*i.e.* above the suggested kinetic 'blocking' temperature for carbon isotope exchange and also prior to fluid entrapment by crystallisation of the host quartz), then the process may be approximated to that of fractional (Rayleigh) distillation. This is the situation whereby infinitesimal aliquots of isotopically-equilibrated product are successively removed from the reactant mixture, with no subsequent back reaction or isotopic exchange. The form of this well-established model (Rayleigh, 1896; see also Broucker and Oversby, 1971, and Hoefs, 1987) appropriate to the present case is:

$$R/R_0 = F^{(1/\alpha) - 1}$$

where R_0 is the initial $^{13}\text{C}/^{12}\text{C}$ ratio, R is the corresponding $^{13}\text{C}/^{12}\text{C}$ ratio in the residuum, F is the fraction of the initial component remaining and α is the equilibrium fractionation factor for carbon stable isotope exchange between CO_2 and CH_4 .

[†] Dubessy *et al.* (1989) reported values of $\sim 10^{27}$ to 10^{20} for the equilibrium constant for ammonia oxidation by carbon dioxide over the temperature range $300\text{-}900^\circ\text{C}$ (although their estimates appeared to be assume ideal gas behaviour and a total pressure of 1 atm.). If this mechanism was primarily responsible for CO_2 reduction in the present case, the assumption of irreversibility would seem to be reasonable.

Figure 3.28

Carbon stable isotope ratios in hydrothermal palaeofluid methane *versus* carbon dioxide, S W England (●) and Carrock Fell (○). Isotherms (°C) corresponding to isotopic equilibrium are calculated from the data of Richet *et al.* (1977).

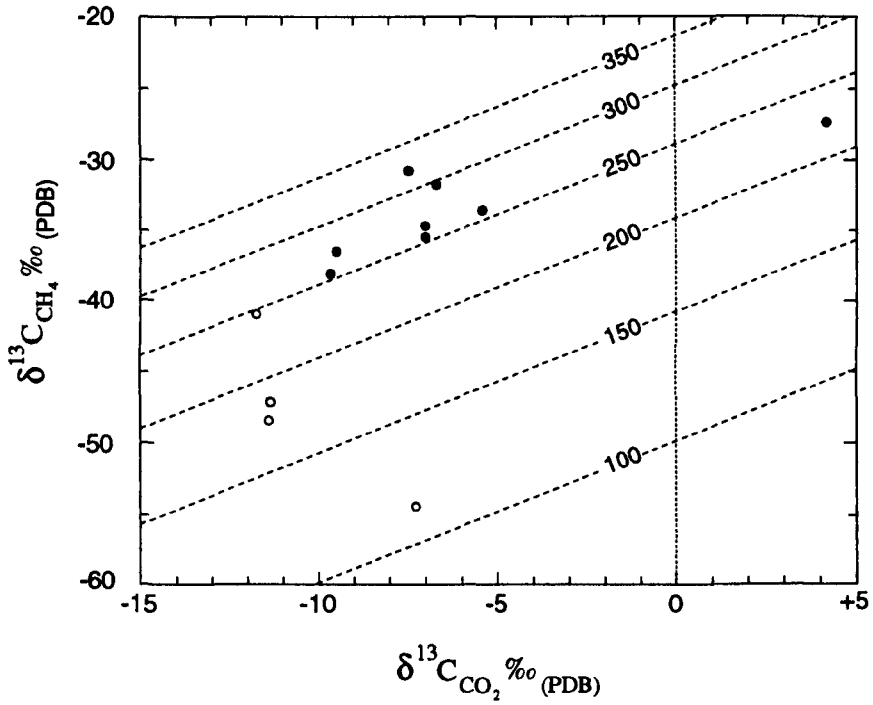


Table 3.7

Comparison of carbon isotope equilibrium fractionation factors $\alpha_{\text{CO}_2 - \text{CH}_4}$ compatible with Rayleigh distillation *versus* batch equilibration models for closed - system CO_2 reduction as the origin of fluid inclusion methane, measured CO_2/CH_4 ratios and associated ^{13}C distributions.

Locality (mine)	Sample	$\delta^{13}\text{C}_{\Sigma\text{C}}$	$\delta^{13}\text{C}_{\text{CO}_2}$	F	Rayleigh fractionation model			'Batch' equilibration	
					$\alpha_{\text{CO}_2 - \text{CH}_4}$	$1000 \log_e \alpha$	T (°C)	$1000 \log_e \alpha$	T (°C)
S W England									
Hemerdon	HEM-80-1	-10.4	-9.5	0.97	1.0276	27.2	270	27.1	271
	HEM-80-39	-9.5	-6.7	0.89	1.0248	24.5	304	25.4	291
Cligga Head	CH-88-1	-12.7	-5.4	0.74	1.0254	25.1	295	28.4	256
South Crofty	SC-88-3	-15.6	+4.2	0.37	1.0206	20.4	370	31.6	221
	SC-88-3ABC	-16.5	-7.0	0.66	1.0241	23.8	313	28.3	257
		-16.4	-7.3	0.66	1.0229	22.6	333	26.9	275
Old Gunnislake	SW-84-18	-9.5	-7.5	0.92	1.0234	23.1	325	23.6	317
South Bedford	SW-84-20	-11.4	-9.8	0.94	1.0279	27.6	265	27.7	265
		-11.2	-9.6	0.95	1.0300	29.6	243	29.7	241
Prince of Wales	SW-84-27	-12.8	-7.0	0.80	1.0265	26.1	282	28.6	254
N W England									
Carrock Fell	CF-77-98	-13.2	-11.4	0.95	1.0391	38.4	162	38.1	162
	CF-77-79B	-12.2	-11.35	0.98	1.0394	38.6	160	37.9	166
	CF-77-39A	-14.3	-7.27	0.85	1.0462	45.2	120	47.3	109
	CF-76-25	-13.1	-11.84	0.95	1.0284	28.0	260	27.9	261

Notes: See text (Section 3.6.4.2) for an explanation of terms used

F values were estimated from the measured CH_4 and CO_2 yields (Table 3.4)

Temperatures were obtained from the $\text{CO}_2 - \text{CH}_4$ fractionation curve of Friedman and O'Neil (1977)

From the definition of the δ value, it follows that:

$$R/R_0 = \left(1 + \frac{\delta_f}{1000}\right) / \left(1 + \frac{\delta_i}{1000}\right) = \frac{1000 + \delta_f}{1000 + \delta_i} = F^{(1/\alpha) - 1}$$

where δ_i and δ_f are the respective initial and final $\delta^{13}\text{C}$ values of the palaeofluid CO_2 .

Taking logarithms of both sides, with subsequent rearrangement, gives:

$$\alpha = \left[1 + \left\{\log_{10} \left(\frac{1000 + \delta_f}{1000 + \delta_i}\right) / \log_{10} F\right\}\right]^{-1}$$

from which the fractionation factor appropriate to this model may be determined. Substitution of the experimentally-determined values of δ_i , δ_f and F (Table 3.4) shows that the corresponding $\alpha_{\text{CO}_2 - \text{CH}_4} = 1.0206$, equivalent to a 20.6‰ difference between the $\delta^{13}\text{C}$ values of the product CH_4 (^{13}C -depleted) and reactant CO_2 . In turn, this corresponds to a temperature of $\sim 370^\circ\text{C}$, on the basis of the data compilation of Friedman and O'Neil (1977). Such a temperature value is realistic in the present example, indicating that this simple model is consistent with the experimental findings. An alternative model, in which equilibrium fractionation is maintained throughout ('batch' equilibration), may be represented (*e.g.* Matthey *et al.*, 1989) by:

$$\delta_f - \delta_i = (1-F) 10^3 \log_e \alpha$$

In this case, the corresponding value of $10^3 \log_e \alpha$ is 31.6, equivalent to an equilibration temperature of only $\sim 220^\circ\text{C}$, which is unrealistically low from an energetics viewpoint and also significantly less than the probable entrapment temperature of the fluid. This model corresponds to the situation depicted in Figure 3.28.

The Rayleigh fractionation model, however, is not generally compatible with the carbon speciation and isotopic data presented in this work. In Table 3.7, α values determined on the basis this model are listed, together with the corresponding equilibration temperatures, for all samples where yield and $\delta^{13}\text{C}$ data of coexisting CH_4 and CO_2 components are available. It is apparent that only for samples SC-88-3ABC and SW-84-18 is a realistic temperature predicted by the model; furthermore, in the latter example, the batch equilibration model predicts a broadly similar result. A surprising feature of Table 3.7 is that, for many examples, isotopic equilibration temperatures predicted on the basis of the two different models are in close agreement, although the actual values are outside the region where equilibrium effects are likely to control the ^{13}C distribution.

A further alternative for consideration is the hypothesis that only kinetic isotope effects are responsible for carbon isotope fractionation during the postulated CO_2 reduction. Certainly, this would be expected to give rise to ^{13}C enrichment of the residual CO_2 component but, in the absence of experimental data, a quantitative assessment is not possible.

Tentative support for the hypothesis of kinetic control of ^{13}C distribution in the palaeofluids is provided by a comparison of the Cornubian and Carrock Fell methane $\delta^{13}\text{C}$ results with data reported for low-temperature bacterial processes involving CO_2 reduction (as prevalent in older sediments), where isotopic fractionation is clearly mediated by kinetic effects and $\delta^{13}\text{C} < -60\text{‰}$ (Schoell, 1980, 1988). A progressive temperature reduction, from $\sim 350\text{--}450^\circ\text{C}$ for the Cornubian hydrothermal system, $\sim 250^\circ\text{C}$ for Carrock Fell, and $< 100^\circ\text{C}(?)$ for bacterially-produced methane, appears to be correlated with a systematic ^{13}C depletion. Whilst the possibility of a palaeofluid methane component derived from a separate carbon reservoir (metasediment pyrolysis?) rather than reduction of primary, magmatic-hydrothermal CO_2 cannot be entirely excluded, the relative insensitivity of $\delta^{13}\text{C}_{\Sigma\text{C}}$ values to local palaeofluid CO_2/CH_4 ratios, coupled with the evidence for isotopic disequilibrium, renders this improbable as the major source.

Occurrences of bituminous hydrocarbons at or near granite margins in SW England, particularly the northern margin of the Carnmenellis granite (*i.e.* in the vicinity of South Crofty mine) have been reported over many years (see Bath *et al.*, 1986; Parnell, 1988). At South Crofty mine, viscous hydrocarbon seeps from fracture zones in the granite are still periodically discovered; these occur within tens of metres of the contact with the local Devonian slates, at sites where mining activity has dilated the fractures. The source of these hydrocarbons is probably the Devonian slates (killas), which are particularly enriched in organic carbon at this locality (Parnell, 1988) despite episodes of regional and contact metamorphism.

It is reasonable to infer that any methane component resulting from the thermal degradation of local sediments or metasediments would be associated with water derived from metamorphic dehydration reactions. However, hydrothermal quartz veins hosted by the Dartmoor granite and located well away from the contact with regional metasedimentary rocks, are characterised by palaeofluid water δD values indistinguishable from those recorded for the nearby Hemerdon system, where hosting of some veins by the metasediments occurs. On this basis, therefore, there is little evidence to support the case for a significant pyrolytic methane component in the Hemerdon fluids. Early-stage palaeo-hydrothermal waters elsewhere in the Cornubian region, however, are distinguished by a relative enrichment in deuterium; this might be indicative of a local 'metamorphic water' component (Primmer, 1985), or may alternatively be attributed to other causes as discussed in Chapter 2 of the present work.

3.7 Summary and conclusions

The speciation and stable isotope characteristics of carbon in ancient hydrothermal fluids associated with the Cornubian batholith indicate that CO_2 was a primary component of

exsolved magmatic-hydrothermal fluids associated with pegmatites and the earliest stages of oxide mineralisation in the region. Palæofluid carbon abundance was thus controlled by (and is correlated with) the degree of incorporation of sedimentary material into the component granitic melts during anatexis, as measured by well-established indices of the 'S'-type character of the respective individual plutons. In accordance with this view, fluids associated with high-temperature hydrothermal alteration of the Dartmoor granite were found to contain very low abundances of carbon; the associated isotopic data tentatively suggest a common link with CO₂-enriched fluids associated with other component intrusives of the batholith.

The range of Cornubian palæofluid $\delta^{13}\text{C}_{\Sigma\text{C}}$ values is relatively narrow, despite significant variations in the associated CO₂/CH₄ ratios. Together with evidence for isotopic disequilibrium between the oxidised and reduced carbon species, this suggests that the primary CO₂ component was characterised by a $\delta^{13}\text{C}$ value closely approximating to the weighted mean of the measured fluid inclusion $\delta^{13}\text{C}_{\text{CO}_2}$ and $\delta^{13}\text{C}_{\text{CH}_4}$ data, and that any secondary sources of carbon, such as the pyrolysis of local low-grade metasediments at high crustal levels, were either absent or only of minor significance.

The present distribution of CO₂ and CH₄, as determined from fluid inclusion analysis by stepped heating methods, is probably the result of partial conversion of the initial, oxidised carbon component to methane, through fluid/wall-rock interaction. It is suggested that localised redox reactions involving Fe(II) ↔ Fe(III) and NH₄⁺ → N₂ probably controlled the carbon speciation. The associated ¹³C distribution in the fluids would seem to be best explained by kinetic fractionation of the carbon stable isotopes during such processes.

An investigation of stepped heating procedures for the extraction and isotopic characterisation of quartz-hosted fluid inclusion CO₂ at the micromole to nanomole level has shown that the associated procedural carbon blank yield may be reduced to the lowest levels by: (i) rigorous sample preparation procedures, including minimal exposure to atmosphere following ultrasonic agitation in dichloromethane immediately prior to loading into the extraction line (as recommended by Matthey *et al.*, 1989); (ii) *in vacuo* stepped heating, with carbonaceous release below 300°C being discarded.

Procedures involving the application of stepped combustion prior to incremental heating *in vacuo* and, in particular, the exposure of extracted sample gases to platinum at high temperature, were found to have a deleterious effect. Excellent agreement was generally obtained between $\delta^{13}\text{C}_{\text{CO}_2}$ values obtained by 'optimised' stepped heating, on the one hand, and direct analysis of CO₂ released by crushing of the host quartz, on the other.

Application of the stepped heating procedure to the extraction of fluid inclusion CO₂ from single quartz grains (~12-20mg), for carbon stable isotope analysis by high sensitivity, static vacuum mass spectrometry, using the instrument described by Carr *et al.* (1986), has shown

that under optimum conditions, and where the isotopic composition of the sample gas is enriched in ^{13}C by up to $\sim 20\%$ relative to the associated procedural blank component, 2-3 nanomoles of sample gas may be analysed with an attendant total extraneous contribution to the $\delta^{13}\text{C}$ value that is less than the analytical precision of the measurement (*i. e.* $< \pm 1\%$, at the 1σ level).

A procedure was devised to determine the $\delta^{13}\text{C}$ values of both fluid inclusion methane and coexisting carbon dioxide, in examples where the former may be present at sub-ppmC levels with respect to the quartz host. Using low blank, stepped heating (*in vacuo*) to extract the fluid components, optimum $\delta^{13}\text{C}$ reproducibility of $\pm 0.5\%$ was obtained on samples as small as 60 nanomoles of methane, with excellent replication of yield values. Isotopic analyses were undertaken using 'conventional' mass spectrometry in all cases.

3.8 Suggestions for further research

An ultra-high sensitivity carbon stable isotope ratio mass spectrometer to replace the instrument described by Carr *et al.* (1986) was under development during the period in which the experimental work for the present dissertation was undertaken. Referred to as 'MS86' and described by Prosser *et al.* (1990), thermal degradation effects have been reduced by the use of a closed ion source; incorporation of this type of source design was made feasible by the lower operating pressure associated with the reduction in sample gas aliquot size. The advantages conferred by the arrangement are that, firstly, the half-life of CO_2 in the ion source is extended to 450 seconds; secondly, increased ionisation efficiency. The resulting sensitivity enhancement minimises the attendant loss of precision associated with the analysis of smaller samples. Recent refinements to this instrument and the associated gas preparation and handling system have resulted in a level of performance whereby 10 pmol to 1 nmol CO_2 may be analysed to an accuracy within $\pm 0.5\%$, with attendant precision only becoming worse than $\sim \pm 1\%$ for < 80 pmol of gas (Yates *et al.*, 1992).

These developments, including the significant reduction of procedural carbon blanks during stepped combustion (Yates *et al.*, 1992) offer significant potential benefits to further research based on the present study. In particular, the isotopic characterisation of coexisting reduced and oxidised carbon in fluid inclusions may now be feasible for significantly lower abundances of these components than has hitherto been possible, subject to minor modifications to the gas handling system so as to permit the separation and isolation of extracted CO_2 and CH_4 .

From data given in Yates *et al.* (1992), a typical carbon procedural (combustion) blank yield over the temperature range 300-600°C (as used for palaeofluid release) is ~ 3 ngC. A significant proportion of this, however, presumably derives from the use of a Pt 'packet' for

containing the loaded sample; this would not be required in the case of quartz grain samples for fluid inclusion analysis. On this basis, it would appear that a lower limit of ~5 nmol of CH₄ is required to produce an acceptable minimum sample:blank ratio of ~20. However, this assessment neglects any contribution of extraneous, surficial carbon associated with the use of stepped heating. Vesicle opening by crushing would be the only way to virtually eliminate this adventitious component, with precautions taken to minimise metal-to-metal contact, which in itself may give rise to methane formation (Andrawes and Gibson, 1979). Further development work on sample extraction and preparation protocols therefore remains to be done to fully benefit from the enhanced mass spectrometer sensitivity.

In this context, it is noteworthy that a comprehensive investigation by Yates (1992) of carbon blanks associated with stepped combustion, using the ultra-high sensitivity MS86 mass spectrometer and associated sample preparation facility, showed that carbon contamination in any single experiment was highly variable in both $\delta^{13}\text{C}$ and absolute yield. Furthermore, the blank was not totally controlled by the sample preparation protocol utilised, but also by 'random' contamination events.

Improvements in the direct measurement of D/H ratios in methane by static vacuum mass spectrometry in recent years has resulted in the possibility of determining δD values to within $\pm 20\%$ on nanomole quantities of gas, provided that the associated $^{13}\text{C}/^{12}\text{C}$ ratio is known (Morse, 1991). With further refinements to improve the attendant precision, the possibility of hydrogen stable isotope analysis of fluid inclusion methane at the nanomole level may be realised, thereby providing an additional potential discriminant for elucidation of the source of reduced carbon in palæo-hydrothermal systems.

Further analyses of the Dartmoor quartz samples, using larger quantities of material (multiple grains), are needed to confirm or refute the tentative data which suggest the presence of a Dartmoor palæofluid carbon component of similar isotopic characteristics to that present, in greater abundance, in fluids associated with pegmatitic and early hydrothermal alteration of other granite intrusives in the Cornubian region.

Experimental data are needed on reaction rates and carbon isotope fractionation during CO₂ reduction by Fe(III) and NH₄⁺-bearing wall-rock components under hydrothermal conditions, to explore further the viability of such reactions as the primary source of methane in the ancient Cornubian fluids.

Chapter 4

Nitrogen stable isotope characterisation of palæo-hydrothermal fluids, SW England

4.1 Synopsis

The isotopic characterisation of traces of nitrogen species in ancient hydrothermal fluids provides a constraint on models relating to the source of the fluid. Reported here is the development and application of techniques, devised for the preparation and determination of nitrogen stable isotope ratios at the sub-nanomole level, to investigate the isotopic composition of trace levels of nitrogen in early mineralising fluids associated with granite cupolas of the Cornubian batholith, S W England.

Regional variations in the fluid inclusion nitrogen yield are compared with published values for the ammonium contents of the associated granite, pegmatites and hydrothermally-altered rocks. Comparisons are also made with ammonium abundances and nitrogen stable isotope distributions in Palæozoic metasediments from the thermal aureole of the Dartmoor granite.

Potential sources of the fluid phase nitrogen are assessed, with reference to the isotopic composition of nitrogen reservoirs in both the batholith and in the metasedimentary rocks. The speciation of nitrogen under hydrothermal conditions is discussed and equilibrium thermodynamic modelling used to investigate the reaction of reduced nitrogen with carbon dioxide, which is also present in the palæofluids, under a variety of conditions corresponding to crustal environments.

4.2 Introduction

4.2.1 Nitrogen stable isotope abundances in the terrestrial environment

The average natural abundance of ^{15}N in present-day atmosphere is 0.3663% (Junk and Svec, 1958). As this value is constant within analytical precision, atmospheric nitrogen is a reliable standard for natural ^{15}N abundance measurements (Mariotti, 1983). Results are usually presented in the delta notation, where:

$$\begin{aligned}\delta^{15}\text{N} &= 10^3 \times \left[\left[\left(\frac{^{15}\text{N}}{^{14}\text{N}} \right)_{\text{sample}} / \left(\frac{^{15}\text{N}}{^{14}\text{N}} \right)_{\text{AIR}} \right] - 1 \right] \text{‰} \\ &= 10^3 \times \left[\alpha_{\text{sample-AIR}} - 1 \right] \text{‰}\end{aligned}$$

Fractionation factors (α) for equilibria involving nitrogen exchange are summarised in Figure 4.1.

Figure 4.1

Temperature dependence of α -values for equilibria involving nitrogen exchange

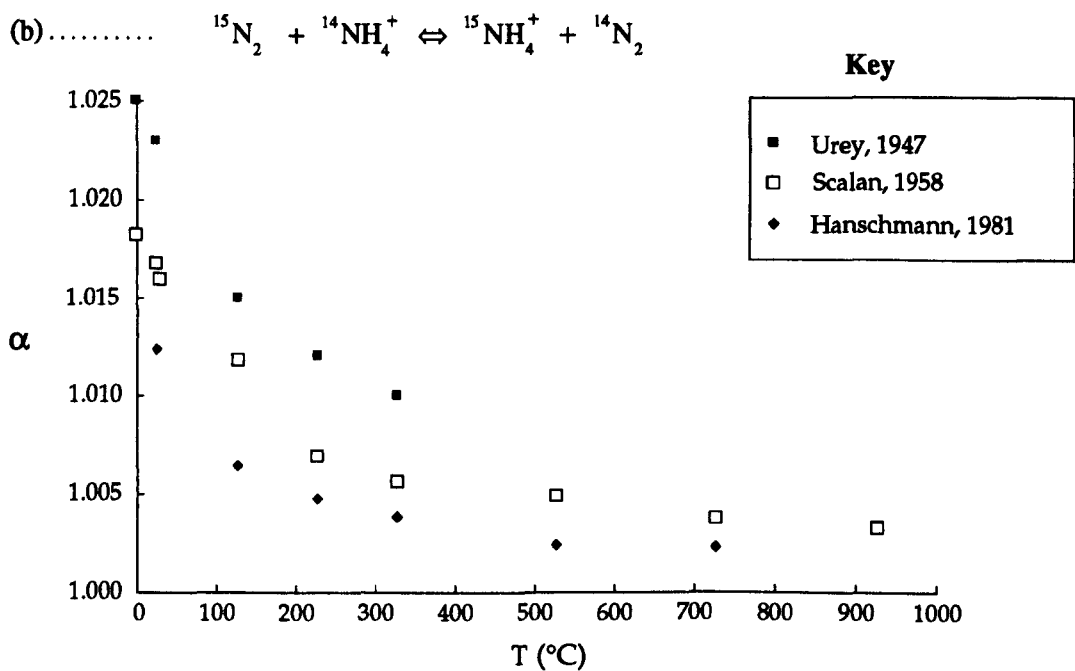
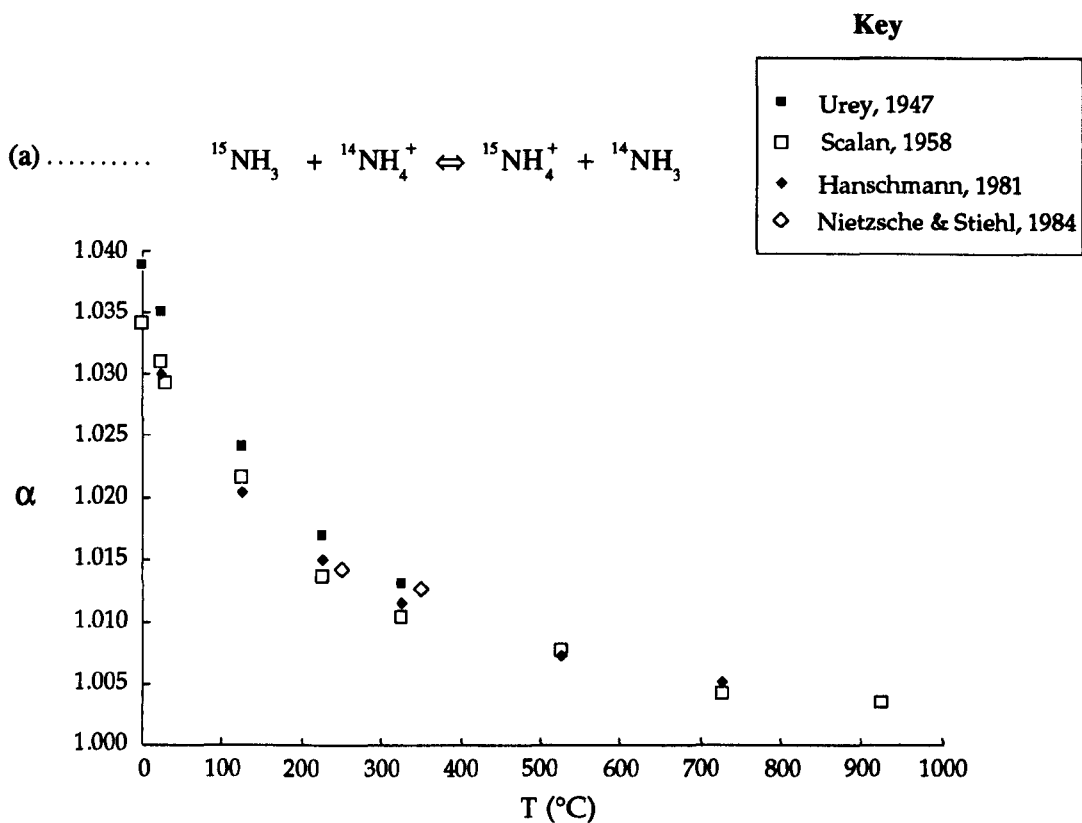
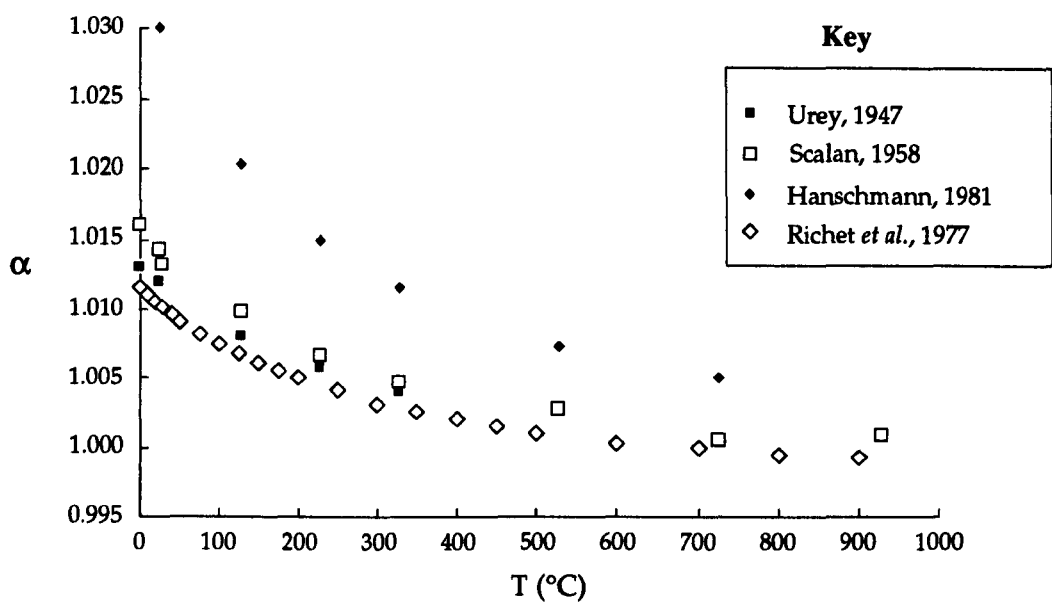
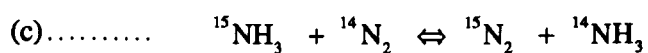


Figure 4.1 (continued)

Temperature dependence of α -values for equilibria involving nitrogen exchange



Note: The data of Nitzsche and Stiehl (1984) were subsequently reported by Haendel *et al.* (1986)

In contrast to the wide range of $\delta^{15}\text{N}$ values encountered in extraterrestrial samples[†], $\delta^{15}\text{N}$ values of terrestrial nitrogen and nitrogen compounds generally occur in the range from -20 to +20‰ relative to atmospheric nitrogen, with the notable exception of natural gas deposits, for which values from -20 to +45‰ have been recorded.

Compared to other light elements that occur as more than one stable isotope and are widespread in nature, relatively little has been published in the field of nitrogen isotope geochemistry. Part of the explanation for this may be that nitrogen abundance and isotopic composition in the upper lithosphere are essentially controlled by biological rather than inorganic processes (Létolle, 1980). Kinetic, rather than equilibrium, fractionation of nitrogen isotope distributions occurs under these circumstances.

The present investigation is concerned with the origin of molecular nitrogen that occurs as a trace component in early hydrothermal palaeofluids associated with the granite cupolas that collectively form the Cornubian batholith, S W England. A potential source of the nitrogen is the oxidation of NH_4^+ , which is an abundant species in both the regional low-grade Palaeozoic metasediments and locally within the batholith. Also to be considered is the evidence reported by Kelley *et al.* (1986) and Turner and Bannon (1992) for a palaeo-atmospheric component in these fluids, as suggested by noble gas isotopic studies.

The stratigraphic ages of the major Devonian and Carboniferous metasedimentary rock formations of the region are considered elsewhere in the present work (Section 6.3). From the Phanerozoic world maps of Smith *et al.* (1973), it is evident that the latitude of S W England during the deposition of the original pelagic sediments was $\sim 10^\circ\text{S}$. Sedimentation in the region during these periods is believed to have taken place in marine basins, some of which were deep (Selwood and Durrance, 1982; Thomas, 1982).

4.2.2 Biological processes affecting the distribution of nitrogen isotopes

The three primary processes involved in biological utilisation of nitrogen are: (i) fixation, whereby molecular nitrogen is reduced to ammonia; (ii) oxidation of ammonia to nitrite (nitrification) and subsequently to nitrate; (iii) denitrification *i. e.* the reduction of the nitrate ion to nitrogen gas. This latter process, involving bacterial degradation of organic matter in anoxic environments, is probably the only significant mechanism for generating molecular nitrogen from nitrogen compounds (Hutchinson, 1944; Hoefs, 1987). Vaccaro (1965) estimated that, without denitrification, the present rate of burial of organic nitrogen in marine sediments would deplete the atmospheric reservoir of nitrogen in about 100Ma. Indeed, it has been suggested (Lovelock, 1972) that if all biological activity were to cease, the

[†] Ion microprobe measurements have shown that, for nitrogen associated with SiC grains in carbonaceous meteorites, $\delta^{15}\text{N}$ values range from -850 to +4300‰ (Zinner *et al.*, 1987; Tang, Anders *et al.*, 1988).

concentration of atmospheric nitrogen would decrease over geological time from the present value of 78.084% (Pollack and Yung, 1980) to trace levels, as the most thermodynamically stable form of nitrogen is as nitrate ion (in solution in the oceans).

4.2.3 Kinetic isotope effects

Investigations of nitrogen kinetic isotope effects for the major biological processes occurring in nature have been reviewed by Létolle (1980) and Hoefs (1987). Essentially, isotope fractionations during the fixation of molecular nitrogen by autotrophic and heterotrophic bacteria are small. Hoering and Ford (1960) were unable to detect any fractionation between atmospheric nitrogen and biologically-synthesised matter; Delwiche and Steyn (1970) recorded ^{15}N depletion by about 5‰ in the organic material. As a result of the isotope fractionation effect associated with denitrification, the average $\delta^{15}\text{N}$ value of dissolved nitrate in the marine environment is about +6‰ (Cline and Kaplan, 1975; Sweeney *et al.*, 1978).

4.2.4 The oceanic environment

The contribution of the various sources and removal mechanisms of nitrogen compounds to/from the oceanic reservoir have been estimated by Holland (1973), Emery *et al.*, (1955) and Delwiche (1970). Most of the nitrogen in the oceans is present as $\text{N}_2(\text{aq})$ in secular equilibrium with atmospheric molecular nitrogen. NH_4^+ , NO_3^- and NO_2^- are also present; the concentrations being intimately linked to biological activity which in turn is dependant on locality, season and depth. Nitrogen input is primarily *via* atmospheric precipitation, river water (with organically-bound nitrogen present in detrital matter, besides ammonium and nitrate ions in solution), and also the biological fixation of molecular nitrogen by blue-green algæ (Cyanophyceæ) or bacteria (Cyanobacteria). Losses of nitrogen from the oceans occur through the processes of denitrification, as discussed above, and sediment burial (Cline and Kaplan, 1975; Sweeney *et al.*, 1978). Nitrogen isotopic compositions of some common components of the oceanic reservoir are summarised in Table 4.1.

4.2.5 Diagenesis of nitrogen in sediments

The fate of organic nitrogen, from early diagenesis to amphibolite facies, has been summarised by Dubessy and Ramboz (1986). A two-stage release of nitrogen was described, after Tissot and Welte (1984). During early diagenesis, NH_4^+ is released through microbial processes at near surface temperatures, *via* the degradation of proteins (mainly from algæ, bacteria and plankton). Humins and ultimately kerogen are also formed during this stage. At higher temperatures (150-250°C), however, thermal maturation of kerogen (metagenesis) releases N_2 , by the breakdown of heterocyclic structures containing C=N-C bonds. During diagenesis, the mobilised ammonium may be incorporated into clay minerals (Mortland, 1958).

Table 4.1

Nitrogen stable isotope ratios in some common components of the oceanic reservoir
(after Cline and Kaplan, 1975).

	Range in $\delta^{15}\text{N}$ (‰ _{AIR})	Mean $\delta^{15}\text{N}$ (‰ _{AIR})
Organisms:		
Phytoplankton	+5.2 to +9.7	+7.5
Zooplankton	+12.8	+12.8
Fish	+9.9 to +20.5	+15.9
Dissolved inorganic nitrogen:		
N_2	- 0.2 to +0.7	+0.4
NO_3^-	+4.8 to +7.5	+6.2
Ammonia	+6.5 to +7.5	+7.0
Sediments:		
Ammonia	+2.9 to +5.3	+4.1
Organic nitrogen	+4.7 to +6.0	+5.4
Total nitrogen	+5.3 to +13.4	+5.7
Precipitation (rain):		
NO_3^-	-7.2 to +3.4	- 1.7
Ammonia	-0.1 to +9.0	+4.6

- Notes:**
1. The precipitation data were recorded at a continental station and therefore may not be applicable to oceanic input.
 2. Rau *et al.* (1987) give a more recent, though not as comprehensive, compilation of $\delta^{15}\text{N}$ ranges for selected oceanic nitrogen reservoirs.

4.2.6 Nitrogen stable isotope distributions in igneous rocks

In general, more attention has been focused on natural variations in the nitrogen isotope abundance ratio in meteorites, lunar rocks and planetary atmospheres than on terrestrial samples. Geiss and Bochsler (1982) summarised the data available at the time. With regard to terrestrial igneous rocks, Wlowska (1972) and Sakai *et al.* (1984) reviewed the distribution of nitrogen isotopes in igneous systems, as indicated by data available at the respective times. A more recent study was undertaken by Zhang (1988).

Mayne (1957), in a study of thirteen samples of various rock types, ranging from Pre-Cambrian dunite to a 1942-erupted olivine basalt, found a substantial variation (by a factor of about 25) in the yield of nitrogen extracted and also reported an inverse correlation between $\delta^{15}\text{N}$ value and nitrogen concentration. Negative $\delta^{15}\text{N}$ values were reported for five of the thirteen samples. Apart from one sample of obsidian of recent age, which gave $\delta^{15}\text{N}$ of +30.9‰, nitrogen isotope data ranged from -15.6 to +9.9‰.

Scalan (1958), in a much more comprehensive survey (134 analyses), measured $\delta^{15}\text{N}$ values of -4 to +16‰, with +2 to +4‰ as the most common range and an average value for all determinations of +4.9‰. Only five samples exhibited negative $\delta^{15}\text{N}$ values; it was suggested that, in these cases, the preparation or handling was probably responsible for fractionation of the sample. Thus, the finding by Mayne (1957) that isotopic variation varied from $\delta^{15}\text{N} < 0$ in rocks with high nitrogen concentrations to $\delta^{15}\text{N} > 0$ in rocks with little nitrogen was not supported. Scalan (1958) also reported that most of the nitrogen contained in the igneous samples investigated was in the form of the ammonium ion. The same author also noted that if the molecular nitrogen of the Earth's atmosphere was derived from this source, only equilibria involving the ammonium ion would give rise to significant fractionation of nitrogen isotopes, at temperatures in excess of 800K.

Becker and Clayton (1977) reported that $\delta^{15}\text{N}$ values of ocean island basalts (OIB) and ultramafic rocks were close to +17‰. Since then, several investigations of the nitrogen isotope geochemistry of oceanic basalts have been reported, generally focusing on the implications for the concentration and isotopic composition of nitrogen in the Earth's mantle (Sakai *et al.*, 1984; Exley *et al.*, 1986/87; Javoy *et al.*, 1986; Javoy and Pineau, 1986; Zhang, 1988). Considerable variation exists between the oceanic basalt data sets, both in terms of nitrogen concentration and $\delta^{15}\text{N}$ values. A wide range of nitrogen concentrations and $\delta^{15}\text{N}$ values has similarly been reported for nitrogen within natural diamonds† (Hirsch *et al.*, 1986; Wand, 1980; Becker, 1982; Javoy *et al.*, 1984).

† About 98% of natural diamonds (type I) contain between 0.003 and 0.3 wt% of nitrogen as impurity, largely as 'voidites'.

Boyd *et al.* (1987) and Boyd (1988), reported isotopic uniformity of diamond phenocryst coats on a regional scale, suggesting a uniform nitrogen reservoir underlying the continental lithosphere, and having a $\delta^{15}\text{N}$ value close to -5‰ (and similar to the results presented by Javoy *et al.*, 1986, for volcanic gases). Furthermore, the isotopic uniformity of this mantle reservoir appeared unchanged since at least the mid-Archean, on the basis of the age of samples included in that study. If this postulate is correct, degassing of magma during ascent may explain why the nitrogen isotope distribution in both MORB and OIB glasses does not reflect the value of a uniform nitrogen reservoir at depth.

4.2.7 Atmospheric nitrogen

As noted by Pollack and Yung (1980) and Holland (1984), the relationship between atmospheric nitrogen and that stored in the crust and mantle, both as molecular and in combined form, is complex. It relates to factors such as the relative importance of early catastrophic degassing (Fanale, 1971; Sarda, 1985) compared to continuous degassing of the Earth, the mechanism of planetary accretion and core formation, and the potential transfer of nitrogen to the mantle *via* subduction. Eugster and Munoz (1966) suggested that decomposition of ammonium-bearing silicates is a possible source of atmospheric nitrogen.

Little is known about the isotopic composition of nitrogen in the Earth's early atmosphere. For the purpose of the present investigation, the report by Gibson *et al.* (1985) that cherts of age 3.5 Ga from Baberton (South Africa), that have remained closed to argon loss and not been subjected to thermal metamorphism (De Wit *et al.*, 1982), contained nitrogen of similar isotopic composition to present-day atmosphere (within experimental error), suggests the possibility that the distribution of nitrogen isotopes in the atmosphere has remained constant since at least Archean times.

4.2.8 Nitrogen stable isotope distributions in metamorphic rocks

It appears that little has been published in this field. Papers by Haendel *et al.* (1986) and Junge *et al.* (1990), together with references contained therein, are the only reports known to the present author[†]. The most comprehensive investigation is by Haendel *et al.* (1986), who

[†] Since this chapter was prepared, Bebout and Fogel (1992) have published a comprehensive study of nitrogen isotope variations in progressively metamorphosed sedimentary rocks of the Catalina Schist, a subduction-related metamorphic terrane in southern California. These authors discussed the nitrogen data in the context of progressive devolatilisation, together with mechanisms of nitrogen release into the fluid phase during metamorphism. The nitrogen systematics appeared to be in accord with N_2 - NH_4^+ exchange (using the nitrogen isotope fractionation factors of Hanschmann, 1981) and a devolatilisation process intermediate between batch volatilisation (non-incremental release, with all of the released fluid equilibrated with the rock) and Rayleigh distillation (sequential removal of infinitesimal aliquots of fluid, each equilibrated with the rock system). It was noted that the measured depletion in nitrogen concentration, and associated $\delta^{15}\text{N}$ shifts, were incompatible with NH_3 - NH_4^+ equilibrium exchange at 350-600°C, the temperature range over which most of the devolatilisation occurred.

investigated the content and isotopic composition of 'fixed' nitrogen (ammonium) in metasedimentary rocks from prograde metamorphic zones in the Erzgebirge, eastern Germany. It was found that the nitrogen content decreased and $\delta^{15}\text{N}$ correspondingly increased with increasing metamorphic grade. In all samples (43), regardless of rock type, the 'fixed' nitrogen was enriched in ^{15}N with respect to atmosphere. Furthermore, it was found that the geochemical and isotopic effects of regional and contact metamorphism are very similar, with changes being mainly controlled by temperature. Various model experiments were reported, including the effect on nitrogen content and $\delta^{15}\text{N}$ of heating and leaching of metasedimentary rocks, together with an investigation of the relevant isotopic fractionation factors and equilibration times. Haendel *et al.* (1986) concluded that, during contact metamorphism, nitrogen isotope exchange between NH_4^+ and N_2 was the dominant mechanism, assuming equilibrium conditions. This is in contrast to Hoefs (1987), who postulated that, as the main source of nitrogen in igneous (and metamorphic) rocks is present as ammonium, the $\text{NH}_4^+ - \text{NH}_3$ isotope exchange reaction should be of great importance.

Junge *et al.* (1990) reported nitrogen isotope data for 40 whole-rock samples from the eastern Erzgebirge. Their study encompassed the various granite types and country rocks, together with metasomatically altered rocks and also breccias. A wide range of $\delta^{15}\text{N}$ values was reported, including -4.1 to +12.3 ‰ for the granites. The corresponding nitrogen contents for the granites varied from 8 to 50 ppm.

4.2.9 Ammonium in igneous and sedimentary rocks

Investigations by Stevenson (1959, 1962), Wlotzka (1961) and Vinogradov (1963) established that a significant part of the nitrogen stored in both igneous and sedimentary rocks is in the form of ammonium ions contained within the lattice structures of silicates. In igneous rocks, this ammonium is associated mainly with the K-bearing primary minerals, whereas phyllosilicates host the major reservoir of NH_4^+ in the case of sedimentary rocks. Vedder (1965), in a study of the infra-red absorption spectra of muscovites, concluded that NH_4^+ substitutes for K^+ in the interlayer sites of these micas. This finding was subsequently confirmed by other investigators (Karyakin *et al.*, 1973, and Higashi, 1978, in the case of micas; Yamamoto and Nakahira, 1966, for sericites). Karyakin *et al.* (1973) also noted that ammonium in micas is more thermally stable than the water, with maximum liberation of nitrogen occurring in the range 800-900°C; in muscovite, nitrogen release was incomplete even at the melting point of the mineral. Erd *et al.* (1964) showed that the ammonium analogue of monoclinic potassium feldspar (buddingtonite) occurred in rocks that had undergone hydrothermal alteration by ammonia-bearing groundwaters. Urano (1971) reported that metasediments derived from a pelitic source often contained several hundred ppm of ammonium and, furthermore, inferred that the melting of such metasediments was the source of ammonium in granitic magmas.

Itihara and Honma (1979), in an investigation of the ammonium content of biotites from metamorphic and granitic rocks of Japan, noted a positive correlation with the biotite $^{18}\text{O}/^{16}\text{O}$ ratios in the case of granitic rocks, as well as a marked difference in the average ammonium content between granitic rocks from non-metamorphic terranes (22 ppm), metamorphosed granitic rocks (67 ppm) and metasediments (279 ppm). These authors concluded that, in the case of granitic rocks, enrichment of ammonium in biotite resulted from interaction between the granite magma and the surrounding sedimentary rocks. The relatively high levels of NH_4^+ in biotites in metasedimentary rocks, on the other hand, were diagnosed as being due to the direct inheritance of organic nitrogen from the sediments. In support of this assertion, the authors noted that the total nitrogen content of Recent and Palaeozoic sediments is similar; only the ratio of NH_4^+ to total nitrogen varies. Itihara and Honma (1979) also found that biotites in migmatites contained an even higher ammonium concentration than those from the local metasedimentary rocks, thus indicating the involvement of a metamorphic fluid or anatectic magma enriched in NH_4^+ .

The same authors, in a sequel paper, (Honma and Itihara, 1981) extended their investigations by determining the partition coefficients of ammonium between the various component minerals of metamorphic and granitic rocks. It was found that the ammonium distribution is quite systematic, indicating that NH_4^+ is a stable geochemical component, participating in high temperature geological processes. It was suggested that the ammonium distribution (as well as those of Rb and Cs) could be explained on the basis of its ionic radius and the shortest cation-O distances in the crystal lattice. Respective ionic radii of six co-ordinate K^+ , Rb^+ and NH_4^+ are given by Shannon (1976) as 1.52, 1.66 and 1.61 Å; these values are more recent than the data used by Honma and Itihara (1981), but the conclusions remain unchanged.

Ammonium concentrations were found by Honma and Itihara (1981) to be in the order: biotite > muscovite > K-feldspar > plagioclase. This sequence differs from that reported by Hall (1988) for both unaltered and greisenised granite from Cligga Head, S W England, which is of particular relevance to the present investigation. In this latter case, the sequence of decreasing NH_4^+ content was found to be: biotite > orthoclase (K-feldspar) > muscovite. Hall's results were, however, in accord with findings reported by Wlotzka (1972) for a pegmatite from western Germany.

In general, ammonium present in rocks may be classified (see *e.g.* Hall, 1989) as either 'fixed' or 'exchangeable', according to whether the ion is an integral component of the mineral lattice structure, substituting isomorphously for potassium (as in the case of K-feldspars and micas) or, alternatively, is able to undergo cationic exchange (as in the case of zeolites and montmorillonite). For unaltered granites, and other potassium-rich igneous rocks, most if not all of the ammonium is 'fixed', whereas a substantial proportion of the

ammonium present in hydrothermally-altered rocks, or those lacking potassium-bearing minerals in which ammonium may substitute isomorphously, is 'exchangeable'.

In a study of the ammonium content of spilitised volcanic rocks (greenstones) from S W England, Hall (1989) showed that spilitic alteration caused a major enrichment in ammonium of these igneous rocks; furthermore, most of the ammonium was 'fixed' and correlated approximately with the K_2O content of the rock. Although it cannot be ascertained at what stage the spilitic alteration occurred, *i.e.* whether it was contemporaneous with volcanic eruption on the sea floor, or resulted from subsequent interaction with marine sediments, it is most probable that the source of the ammonium was the sedimentary succession into which the volcanics were erupted. This is in accord with the findings of Von Damm *et al.* (1985), who reported that enhanced levels of ammonium were present in submarine hydrothermal solutions of Holocene ($<10^4$ a) age in the Gulf of California; the enrichment in ammonium was attributed to the presence of organic-rich sediments overlying the local oceanic crust.

An alternative source of ammonium, however, might be *via* reaction between seawater and volcanic rocks equilibrated with metallic iron and magnetite at temperatures of 100-200°C, as suggested by Holland (1984) as a mechanism for generating NH_4^+ in the Earth's earliest oceans:



As noted by Hall (1989) and references therein, hydrothermal alteration of ocean floor basaltic rocks is very common and often produces spilitic mineral assemblages. The same author also suggested that subduction of these ammonium-enriched basic igneous rocks may provide a mechanism by which atmospheric nitrogen is returned to the mantle, possibly to re-appear eventually at the surface as a result of subduction-related magmatism.

4.2.10 Nitrogen in crustal fluids - the fluid inclusion evidence

The occurrence of nitrogen in fluid inclusions has been documented in the case of evaporites (*e.g.* Roedder, 1972; Guilhaumou *et al.*, 1981) and in metamorphic and palæo-geothermal environments (*e.g.* Swanenberg, 1980; Kreulen and Schuiling, 1982; Bussink, 1984; Bottrell, 1988; Darimont *et al.*, 1988). Surprisingly, perhaps, the geochemistry of nitrogen in palæofluids has received relatively little attention and reports of nitrogen in fluid inclusions are still comparatively scarce in the scientific literature. In a study of the phase behaviour of the system CO_2 - CH_4 - N_2 in fluid inclusions, van den Kerkhof (1988) concluded that non-aqueous fluids in metamorphic and magmatic rocks are mainly restricted to binary mixtures between two end-members of this system.

Investigations documenting the presence of nitrogen in fluid inclusions generally rely on a combination of microthermometric observations of the phase behaviour of individual inclusions as a function of temperature, in conjunction with either micro-Raman spectrometric analysis of the non-aqueous phase of individual inclusions (for a review, see Dubessy *et al.*, 1989) or, alternatively, bulk crushing of the sample under vacuum and subsequent analysis of the released gases by chromatography (*e.g.* Kreulen and Schuiling, 1982). Microthermometric examination of the phase behaviour of fluid inclusions is generally regarded as the starting point for any subsequent investigation. However, unambiguous detection of nitrogen in fluid inclusions is not possible from microthermometric analysis alone, even in the case of N₂-rich inclusions (*e.g.* Swanenberg, 1980). Identification of the presence of nitrogen in individual inclusions is possible by micro-Raman spectrometric analysis, but the technique is restricted to the non-aqueous fluid phase. Molecular nitrogen, like CO₂, has a low relative Raman scattering cross-section compared to methane, for which the detection limit is almost an order of magnitude lower. The absolute detection limit in terms of molecules of nitrogen per unit volume of fluid cannot be quantified, as it depends on instrumental factors, inclusion geometry and on the other components present in the inclusion (Burke and Lustenhouwer, 1987). However, estimates by these authors give detection limits of ~0.1 to 0.2 mole% for molecular nitrogen in a CO₂ vapour bubble of ~30µm diameter at 20°C. Wopenka and Pasteris (1986) have considered in detail the precision and accuracy of this type of analysis.

For the present investigation of nitrogen in palæofluids from SW England, microthermometric studies of most of the relevant hydrothermal systems have been documented: Jackson *et al.* (1977), Charoy (1979 and 1981), Bull (1982), Scrivener (1982), Shepherd *et al.* (1985), Scrivener *et al.* (1986), Bannon (1989). With one single exception (Bannon, 1989), also reported in Turner and Bannon (1992), no evidence for a liquid CO₂ (and thus non-aqueous) phase at ambient temperature was found during any of these studies. The presence of CO₂ in the aqueous phase was detected, however, through CO₂-hydrate (clathrate) formation at sub-ambient temperatures by Bull (1982), Shepherd *et al.* (1985), Scrivener *et al.* (1986) and Bannon (1989) in a limited number of cases. It is therefore evident that Raman spectral analysis is inapplicable to the detection of a trace nitrogen component in the palæofluids investigated in the present study.

The presence of nitrogen as a minor component in fluids associated with specific episodes of hydrothermal activity after batholith emplacement in SW England was first identified during studies involving the present author (Shepherd *et al.*, 1985; Shepherd and Miller, 1988); the investigations focused on fluids associated with early W±Sn oxide mineralisation. The experimental procedure involved thermal extraction of inclusion fluid from quartz under high vacuum, with a combination of cryogenic separation (fractional distillation), manometry and quadrupole mass spectrometry to estimate the chemical composition of the fluid volatiles.

Details are given in Shepherd and Miller (1988). It was found that nitrogen was generally the second most abundant non-aqueous volatile component in the palæofluids, after carbon dioxide. Distinct regional variation of nitrogen abundance was noted. For example, this component was found to be virtually absent in hydrothermal fluids associated with early mineralisation (quartz+tourmaline±cassiterite) of the Dartmoor granite, but was a significant feature of localities characterised by the occurrence of W±Sn oxides.

It is quite probable that the presence of nitrogen at low levels in aqueous crustal fluids is much more common than the paucity of the current literature would suggest. The practical difficulties associated with the reliable detection and quantification of this component in such a system, together with limited understanding of the sources and significance of nitrogen in crustal fluids, have probably precluded its wider investigation.

4.2.11 Nitrogen stable isotope ratio analysis of crustal fluids

The few reported fluid inclusion $\delta^{15}\text{N}$ analyses known to the present author have almost all originated from the University of Utrecht, Holland, and appear to be confined to an investigation of the Dôme de l'Agout, in the southern part of the Massif Central, France (Kreulen, 1981 and 1983; Kreulen *et al.*, 1982) and of Panasqueira, Portugal (Bussink, 1981, 1984; Bussink *et al.* 1984). Apart from the last two references, these are conference abstracts. The only details concerning experimental procedures are given by Bussink (1984) and Bussink *et al.* (1984), who referred to releasing N_2 from the fluid inclusions by decrepitation at about 900°C in the presence of CuO to oxidise any coexisting methane. Excess oxygen was then removed by slowly cooling to about 700°C; nitrogen was subsequently collected by freezing onto an adsorbent at liquid nitrogen temperature. The $\delta^{15}\text{N}$ results for sixteen samples, including early-stage quartz and wolframite, were generally between +3 and +5‰.

For fluid inclusions in syn-metamorphic quartz segregations from the Dôme de l'Agout, $\delta^{15}\text{N}$ values ranged from -3 to +5‰; negative values typically occurred in the chlorite-sericite schists, whereas positive values were found for inclusion nitrogen in the higher grade rocks. Isotopic analyses of fluid inclusion nitrogen from low grade metamorphic quartz veins from the Llanbedr formation, north Wales, have been reported by Bottrell *et al.* (1988); the data were obtained using a static vacuum mass spectrometry system similar to that described in the present work, albeit at an earlier stage of development.

4.2.12 The speciation of nitrogen in hydrothermal fluids

It is pertinent to enquire whether molecular nitrogen is likely to be the only nitrogen species in the fluid inclusions, as this will have important consequences for the design of a suitable experimental protocol and for the interpretation of $^{15}\text{N}/^{14}\text{N}$ ratios.

Consideration of nitrogen speciation in natural waters at 25°C indicates that $\text{N}_{2(\text{aq})}$ is stable relative to all other aqueous species over a wide range of pH and redox conditions. For kinetic reasons, however, molecular nitrogen is probably a redox inert component under these conditions; if the other species under consideration are regarded as metastable with regard to $\text{N}_{2(\text{aq})}$, then NH_4^+ becomes the dominant component. This is illustrated in Figure 4.2, from which it is seen that $\text{NH}_{3(\text{aq})}$ is dominant over NH_4^+ only under conditions of $\text{pH} \geq 9$. Bottrell (Bottrell and Miller, 1990) produced similar calculations for the various stability fields at 325°C, which is more appropriate to metamorphic and hydrothermal environments (except that the data again relate to 1 atm. pressure); the conclusions are largely unchanged. Although at 25°C, $\text{NH}_{3(\text{aq})}$ is dominant over NH_4^+ only under conditions of $\text{pH} \geq 9$, Duit *et al.* (1986) and Bos *et al.* (1988) noted that the situation changes under hydrothermal conditions (data are available only up to 300°C): above ~220°C and in the presence of chloride, $\text{NH}_{3(\text{aq})}$ becomes dominant even in acidic solutions; there is little tendency to form NH_4Cl .

Experimental evidence for NH_4^+ in hydrothermal fluids is scant. Klyakhin and Levitskiy (1968) reported the presence of ammonium in gas-liquid inclusions in fluorites from the USSR. More recently, Dubessy *et al.* (1989) reported that ammonia or ammonium ions have never been detected in natural fluid inclusions by Raman analysis. In this latter paper, as well as in earlier works (Dubessy, 1985; Dubessy and Ramboz, 1986), it was stated that N_2 is predominant over NH_3 in a fluid if:

$$\Sigma (\text{N}_2 + \text{NH}_3) \text{ mole fractions} \geq 10^{-4}, \quad \text{and/or} \quad f_{\text{O}_2} > \text{Q-F-M}$$

Holland (1984) had previously derived a similar result when considering the oxidation state of nitrogen dissolved in basaltic melts. These equilibrium calculations are based on the control of the respective nitrogen and ammonia mole fractions by the reaction



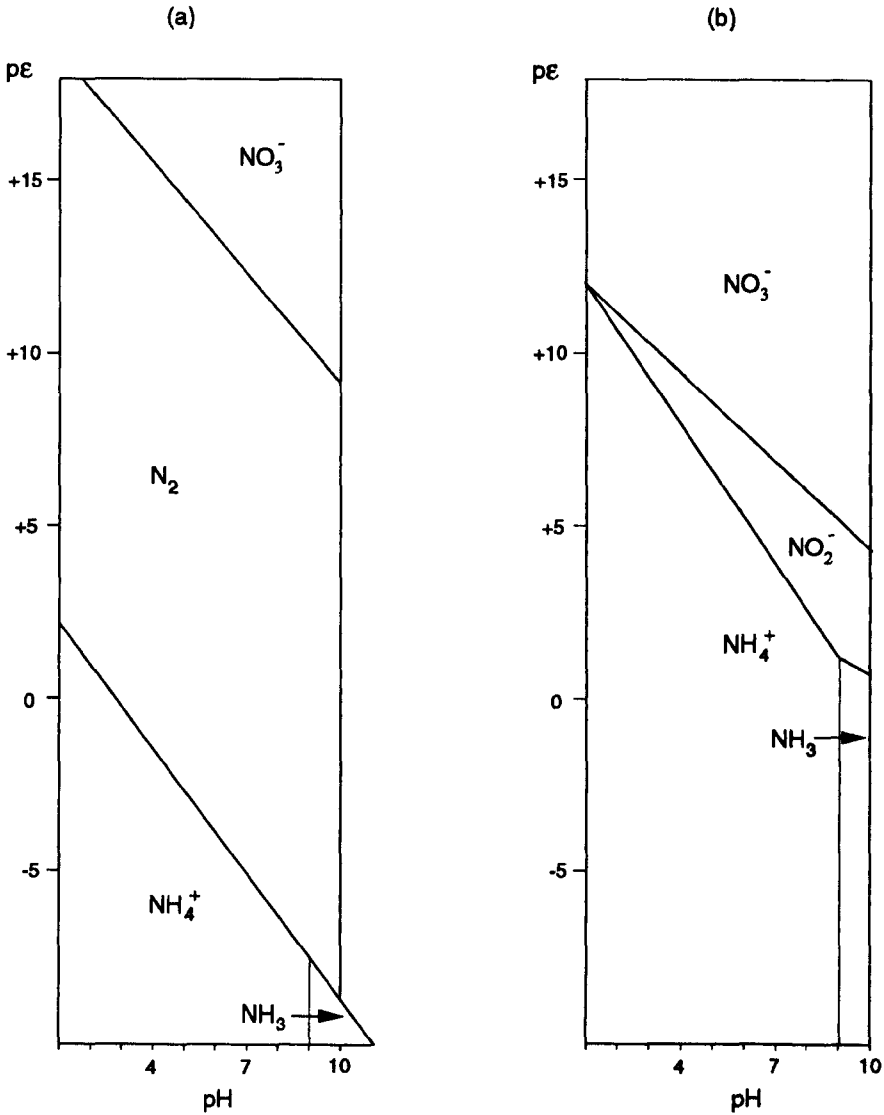
for which $\log_{10} K$ values vary from -57.22 at 25°C to -18.33 at 777°C, 1 atm. (Holland, 1984). Bos *et al.* (1988) also used f_{O_2} to fix the $(f_{\text{NH}_3})^2/f_{\text{N}_2}$ ratio; their calculations, which assumed non-ideal gas behaviour but ideal mixing, indicated that, at 550°C and 2 kbar, and with f_{O_2} fixed by the Ni-NiO buffer, a partial $(\text{N}_2 + \text{NH}_3)$ pressure greater than 10^{-3} bar

Figure 4.2

Aqueous redox equilibria involving stable nitrogen species at 25°C, 1atm. (after Stumm and Morgan, 1981).

(a). N_2 considered chemically reactive;

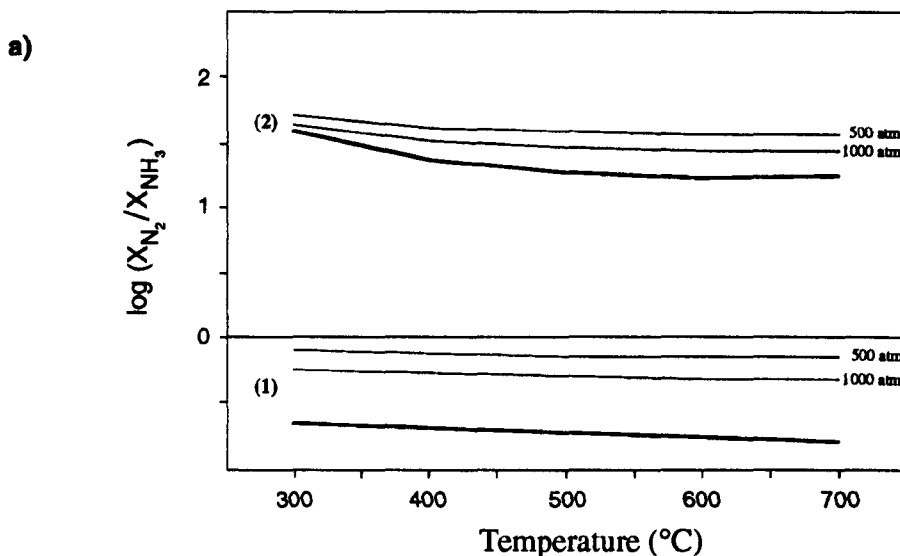
(b). N_2 considered redox inert, *i.e.* the other species shown are regarded as metastable with respect to N_2 .



pE is the (hypothetical) electron activity at equilibrium. It is related to the equilibrium redox potential E_H (volts, hydrogen scale) by: $pE = -\log_{10}[\epsilon^-] = E_H / 2.303 RTF^{-1}$, with the usual notation, $= 16.90 E_H$ at 25°C

Figure 4.3

The predicted equilibrium speciation of nitrogen in hydrothermal fluids.

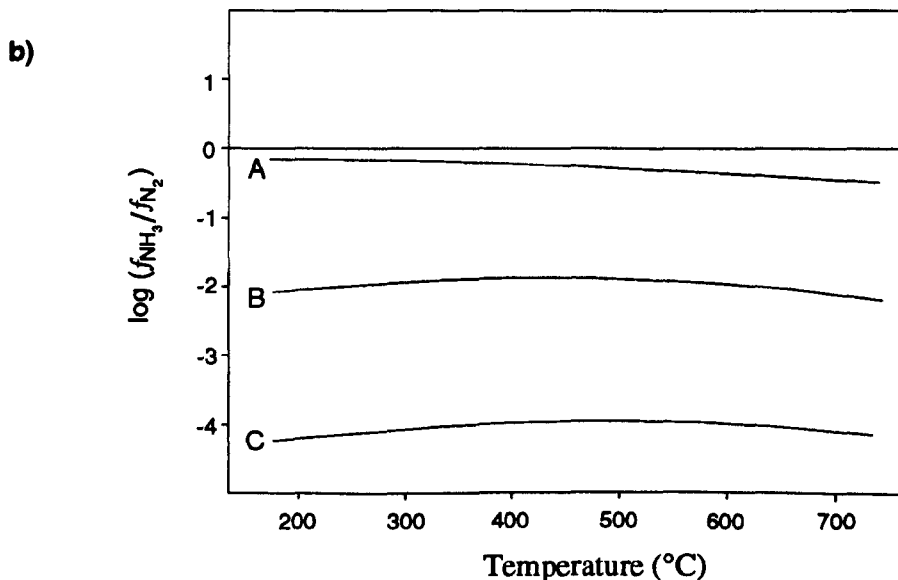


Relative mole fractions of nitrogen and ammonia, as a function of temperature, in the case of the following reactant mixtures under equilibrium conditions:

$$(1) \quad X_{CH_4} = X_{H_2O} = 0.5; \quad X_{N_2} + X_{NH_3} = 2 \times 10^{-4}$$

$$(2) \quad X_{CH_4} = X_{H_2O} = 0.4; \quad X_{N_2} + X_{NH_3} = 0.2$$

Bold curves are estimated from Dubessy and Ramboz (1986); total pressure and details of the assumed model not specified by those authors. Other data calculated using the method of Gordon and McBride (1971), assuming ideal mixing of ideal components.



Relative fugacities of ammonia and nitrogen, as a function of temperature and $(NH_3 + N_2)$ partial pressure, calculated by Bos *et al.* (1988) for a total pressure of 2 kbar. Ideal mixing assumed; redox state fixed by Ni-NiO. A, B and C refer to $(NH_3 + N_2)$ partial pressures of 0.001, 1 and 1000 bar respectively.

fixes nitrogen as the dominant species. Furthermore, it was shown that, under these conditions and for a given value of $p_{(N_2 + NH_3)}$, the f_{N_2}/f_{NH_3} ratio appeared to be relatively unchanged over a large range of temperatures. These results are summarised in Figure 4.3, together with comparable data generated by the present author using the equilibrium thermodynamic modelling procedure of Gordon and McBride (1971).

From the well-established observation that nitrogen in the form of NH_4^+ commonly substitutes for K^+ in natural potassium silicates, it is evident that some transport of NH_4^+ must occur in hydrothermal systems. The above arguments suggest that if equilibrium thermodynamic control is maintained, such transport is limited to ammonium concentrations corresponding to mole fractions of less than *ca.* 0.5×10^{-5} for a fluid of redox state defined by the Q-F-M oxygen buffer. Dubessy *et al.* (1987) showed that theoretical f_{O_2} values defining the redox state of early post-emplacement palaeofluids at Cligga Head, Cornwall - typical of samples included in the present investigation - lie within the limits defined by the Q-F-M (lower limit) and Ni-NiO oxygen buffers.

Until techniques such the modified crush-leach procedures of Bottrell *et al.* (1988), in conjunction with *e.g.* ion exchange chromatography, are applied to investigate NH_4^+ concentrations in fluid inclusions, the levels of any such component must remain a subject for speculation.

4.3 Objectives of the research

The principle objective was to investigate the concentration and isotopic composition of nitrogen in fluids associated with early mineralisation of the granites of the Cornubian batholith, S W England, in localities where previous investigations had indicated that nitrogen was a significant (although trace) component of the fluid. The findings could then be related to local nitrogen reservoirs and thus potential sources of the hydrothermal fluid nitrogen assessed. For comparison, it was also necessary to determine the nitrogen content and $\delta^{15}N$ isotopic composition of local metasedimentary rocks: two transects across the thermal aureole of the Dartmoor granite were sampled for this purpose (Chapter 6). Specific questions that could then be addressed were:

1. What is the source of the molecular nitrogen in the fluids? The ammonium ion is an abundant species in both the metasedimentary envelope and locally within the batholith, where it substitutes isomorphously for potassium in micas and feldspars (Honma and Itihara, 1981). In the metasedimentary rocks, nitrogen may additionally be present in 'organic' form. Is oxidation of ammonium from one or more of these reservoirs the primary process? Release of NH_4^+ from ammonium-bearing micas to a fluid phase may occur *via* metasomatism involving H^+ or K^+ ; also by the breakdown of micas during metamorphism. Degassing of

deep-seated nitrogen has been suggested as a possible nitrogen source in the case of N₂-rich metamorphic palaeofluids elsewhere (Kreulen and Schuiling, 1982); local tectonic conditions render this an unlikely source in the present study. (Note: Duit *et al.*, 1986, argued that the palaeofluid nitrogen investigated by Kreulen and Schuiling, 1982, was probably of sedimentary rather than deep-seated origin.)

2. Is there any relationship between the nitrogen content of the fluid inclusions and NH₄⁺ concentrations in the associated granite pluton, pegmatites and hydrothermally altered rocks? The distribution of ammonium within the granites of S W England has been investigated by Hall (1988), who also established that a good correlation exists between NH₄⁺ content of the intrusions and initial ⁸⁷Sr/⁸⁷Sr ratios and peraluminosity.

3. Can a palaeo-atmospheric nitrogen component be identified? ⁴⁰Ar-³⁹Ar investigations (Kelley *et al.*, 1986; Bannon, 1989; Turner and Bannon, 1992) of fluid inclusions from some of the localities used in the present investigation have indicated that argon of atmospheric derivation may be present in the fluids.

4. Does significant variation exist between the isotopic composition of fluid inclusion nitrogen associated with the different granite plutons of the Cornubian batholith, indicative of isotopic heterogeneity in the source and/or localised fractionation effects?

5. If evidence suggests that the palaeofluid nitrogen may be derived from the granites, as a primary component of an evolving, exsolved magmatic fluid phase, can the nitrogen be used as a conservative tracer of magmatically-derived fluids, from early pegmatitic to later hydrothermal stages?

6. Is there any systematic relationship between the concentration and isotopic composition of nitrogen and other components of the palaeofluids; in particular, carbon species?

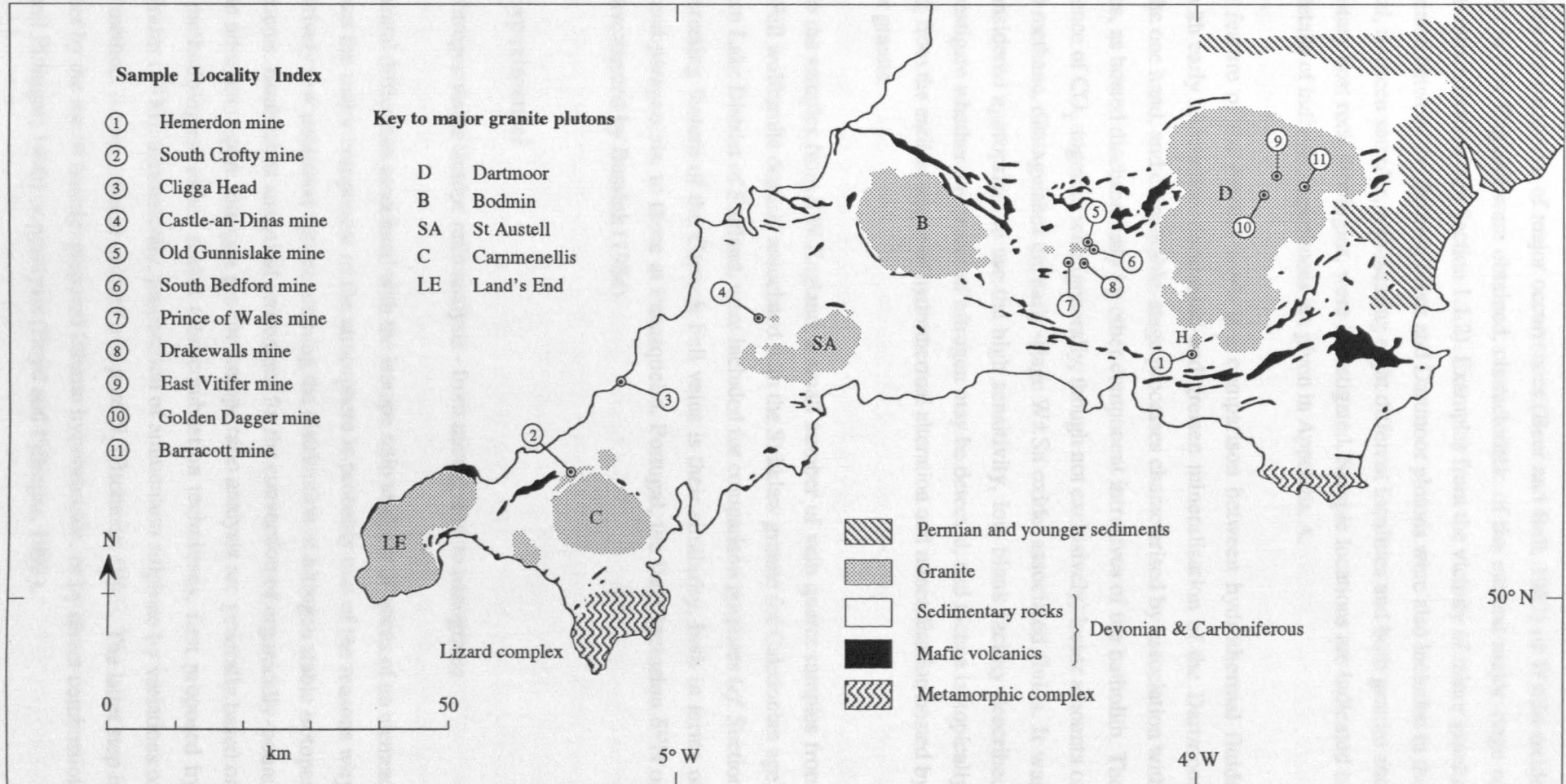
To address these questions, it was necessary to investigate the application of experimental techniques devised for the preparation and determination of nitrogen quantities and isotope ratios at the sub-nanomole level, to the measurement of traces of nitrogen in hydrothermal fluid inclusions.

4.4 Location of samples

The empirically-established local enrichment of CO₂ and N₂ in quartz-hosted fluid inclusions associated with the occurrence of wolframite in S W England (Shepherd *et al.*, 1985; Shepherd and Miller, 1988), was taken as a starting point for the present investigation.

Figure 4.4

Simplified map of S W England, indicating the location of samples included in the investigation of palaeofluid nitrogen associated with early-stage hydrothermal mineralisation in the region



Quartz samples representative of major occurrences (Beer and Ball, 1987) of $W\pm Sn$ oxide mineralisation in S W England were obtained, characteristic of the earliest major stage of hydrothermal mineralisation (see Section 1.1.2). Examples from the vicinity of minor granite intrusives located between the Bodmin Moor and Dartmoor plutons were also included in the study. In total, fourteen samples, representing eight different localities and both granite and metasedimentary host rock lithologies, were investigated. Sample locations are indicated in Figure 4.4; details of individual specimens are given in Appendix A.

A recurring feature of the present work is a comparison between hydrothermal fluids associated with early tourmaline-dominated and greisen mineralisation of the Dartmoor granite, on the one hand, and comparable-stage processes characterised by association with $W\pm Sn$ oxides, as hosted diachronously by other component intrusives of the batholith. The notable presence of CO_2 , together with (generally, though not exclusively) lesser amounts of nitrogen and methane, distinguishes the early-stage $W\pm Sn$ oxide-associated fluids. It was therefore considered appropriate to use the high sensitivity, low blank facility described below to investigate whether any traces of nitrogen may be detected, and thence isotopically characterised, from the earliest stages of hydrothermal alteration and mineralisation hosted by the Dartmoor granite.

In addition to the samples from S W England, a small number of vein quartz samples from the Carrock Fell wolframite deposit, associated with the Skiddaw granite (of Caledonian age) in the northern Lake District of England, were included for comparison purposes (*cf.* Section 3.3). An interesting feature of the Carrock Fell veins is their similarity, both in terms of mineralogy and paragenesis, to those at Panasqueira, Portugal, the fluid inclusion $\delta^{15}N$ of which was investigated by Bussink (1984).

4.5 Experimental

4.5.1 Nitrogen stable isotope ratio analysis - from micrograms to nanograms

The experimental difficulties associated with the isotope ratio analysis of traces of an element that constitutes the major component of the atmosphere is probably one of the reasons why there are relatively few published data concerning the distribution of nitrogen stable isotopes in natural systems. Established analytical procedures for the conversion of organically-bound and inorganic nitrogen to pure nitrogen gas for isotope ratio analysis are generally based on one of two methodologies: either sealed tube combustion techniques, first proposed by Stump and Frazer (1973); alternatively, preparation of ammonium sulphate by variations of the Kjeldahl method, for subsequent oxidation to pure N_2 (Bremner, 1965). The latter step is achieved either by the use of freshly-prepared lithium hypobromide, or by direct combustion (*e.g.* Boyd and Pillinger, 1990) or pyrolysis (Boyd and Pillinger, 1991).

Interest in developing appropriate analytical procedures for the investigation of nitrogen isotope distributions in extra-terrestrial material, with the availability of lunar samples in the early 1970s, resulted in a procedure involving the release of nitrogen *via* incremental ('stepped') heating (e.g. Chang *et al.*, 1974; Becker and Clayton, 1975), which presented a means of discriminating between indigenous nitrogen-bearing phases and terrestrially-derived contamination, of both atmospheric and 'organic' derivation. The principle of stepped heating was also used by Becker and Clayton (1975) to resolve different indigenous nitrogen components within the same sample.

A major practical limitation associated with measuring the stable isotope ratio of nitrogen gas is that this component is not readily concentrated, by virtue of its low boiling point (-196°C at 1 atm. external pressure), into a small volume reservoir near the inlet of a conventional gas-source mass spectrometer. This necessarily imposes constraints on the minimum quantity of nitrogen required, a problem not encountered in the case of carbon dioxide as used in carbon and oxygen isotopic studies. Transfer of nitrogen to a low-volume inlet system may be achieved through Toepler pumping, freezing at liquid helium temperature, or trapping on an appropriate adsorbent at low temperature. Nevins *et al.* (1985), and references therein, reviewed some of these issues. Generally, to meet the inlet pressure requirements of a typical mass spectrometric analyser, a minimum of $\sim 1 \mu\text{mol}$ of N_2 is required to produce an isotopic analysis of acceptable precision.

As a radical alternative to the conventional McKinney *et al.* (1950) type of analyser arrangement, whereby reference and sample gas, admitted *via* their respective capillaries to maintain viscous flow, are continually pumped to waste during the measurement procedure, thereby resulting in very low efficiency (but high precision), the feasibility of using a noble gas type of arrangement (after Reynolds, 1956) for the isotopic measurement of active gases was investigated in the 1970s (Irako *et al.*, 1975; Gardiner and Pillinger, 1979). The first practical applications of this method, as applied to nitrogen, were published by Brown and Pillinger (1981) and by Frick and Pepin (1981). As the gas of interest is introduced into the mass spectrometer after the isolation of the latter from the pumping system (hence the term 'static vacuum' mass spectrometry), the efficiency is greatly enhanced, resulting in an increase in sensitivity of some three orders of magnitude compared to a conventional, dynamic instrument. There is an attendant loss of precision, but this is only by one order of magnitude. This increased analytical uncertainty, however, is still generally smaller than errors introduced during sample preparation and purification procedures.

Developments in the application of static vacuum mass spectrometry and associated sample preparation techniques during the past decade have resulted in the capability of routine, high precision determinations of nitrogen stable isotope ratios at the sub-nanomole level (Wright *et al.*, 1988; Boyd, 1988; Pillinger, 1992; also Hashizume and Sugiura 1990), which has

been applied to investigations of both extra-terrestrial and terrestrial samples. A development of the mass spectrometer system described by Wright *et al.* (1988) was used in the present investigation. This instrument was capable of obtaining comparative nitrogen isotopic compositions ($\delta^{15}\text{N}$ values) to a precision of $\pm 0.24\%$ from samples of 0.4 nmol (Wright *et al.*, 1988). The absolute accuracy, as obtained by the analysis of samples of known isotopic compositions, is quoted by the same authors as being about $\pm 0.5\%$.

To utilise the advantages inherent in the high sensitivity offered by static vacuum mass spectrometry, it is essential that the levels of blank associated with sample preparation techniques be minimised accordingly. A detailed description and evaluation of the sample preparation and purification techniques, devised for use with the above-mentioned mass spectrometer, have been given by Boyd (1988) and Boyd *et al.* (1988). These procedures formed the basis for the present investigation, although with appropriate modification of details.

Preliminary measurements by the present author (Shepherd and Miller, 1988) indicated that the maximum levels of nitrogen in quartz-hosted fluid inclusions associated with W±Sn oxide mineralisation in S W England corresponded to only about 0.1 to 0.3 mole% of the hydrothermal fluid, the water component of which generally comprised less than 1500 ppm of the quartz host mass. Nitrogen concentrations of ~5 ppm or less, with respect to the quartz, were therefore anticipated in the present investigation. Isotopic analysis of this component would not be feasible without the high sensitivity available through the use of static vacuum mass spectrometry. Furthermore, the high sensitivity permitted incremental thermal extraction experiments, with isotopic analysis of released nitrogen at each step, to be performed on samples consisting of only two or three individual quartz grains weighing ~12 to 20 mg each. This has obvious advantages for sample selection and preparation procedures.

4.5.2 The development of an appropriate experimental protocol

The sample preparation procedures described by Boyd (1988) were primarily devised for the isotopic analysis of nitrogen extracted from inclusions in diamonds. As the nitrogen in these samples was already present as the diatomic, molecular species, combustion of the host matrix was appropriate to release the nitrogen, whilst at the same time enabling information to be obtained on the carbon isotopic composition of the diamond. In a similar fashion, stepped pyrolysis or combustion experiments on extraterrestrial materials are performed to obtain information about the nature of the indigenous nitrogen carrier phases, through melting/thermal decomposition/oxidation of the latter.

For the present investigation, however, the situation is quite different. The nitrogen is already in molecular form, dissolved in a saline, aqueous phase which is, in turn, trapped as fluid

inclusions within a refractory, crystalline matrix. Quartz samples were used exclusively throughout this investigation, on account of the thermal stability and degree of purity of this mineral. Thermal extraction in the absence of oxygen (no combustion) was the procedure used to release the fluid from the quartz, followed by isolation and purification of the nitrogen component.

Individual quartz grains were selected using a binocular optical microscope, then cleaned in boiling 6M HCl and doubly-distilled water, dried in air at $\sim 100^{\circ}\text{C}$ and weighed. Just prior to loading into the extraction line for stepped heating, the quartz grains were treated with CH_2Cl_2 in an ultrasonic bath for 10 minutes. After ultrasonic agitation, the grains were stored under clean CH_2Cl_2 , taken to the stepped heating extraction line and loaded directly from the CH_2Cl_2 . This procedure is based on that advocated by Matthey *et al.* (1989) for minimising surficial organic contamination. Reagents used were of Analar[®] grade. Tweezers used for sample handling were pre-cleaned by ultrasonic agitation with CH_2Cl_2 .

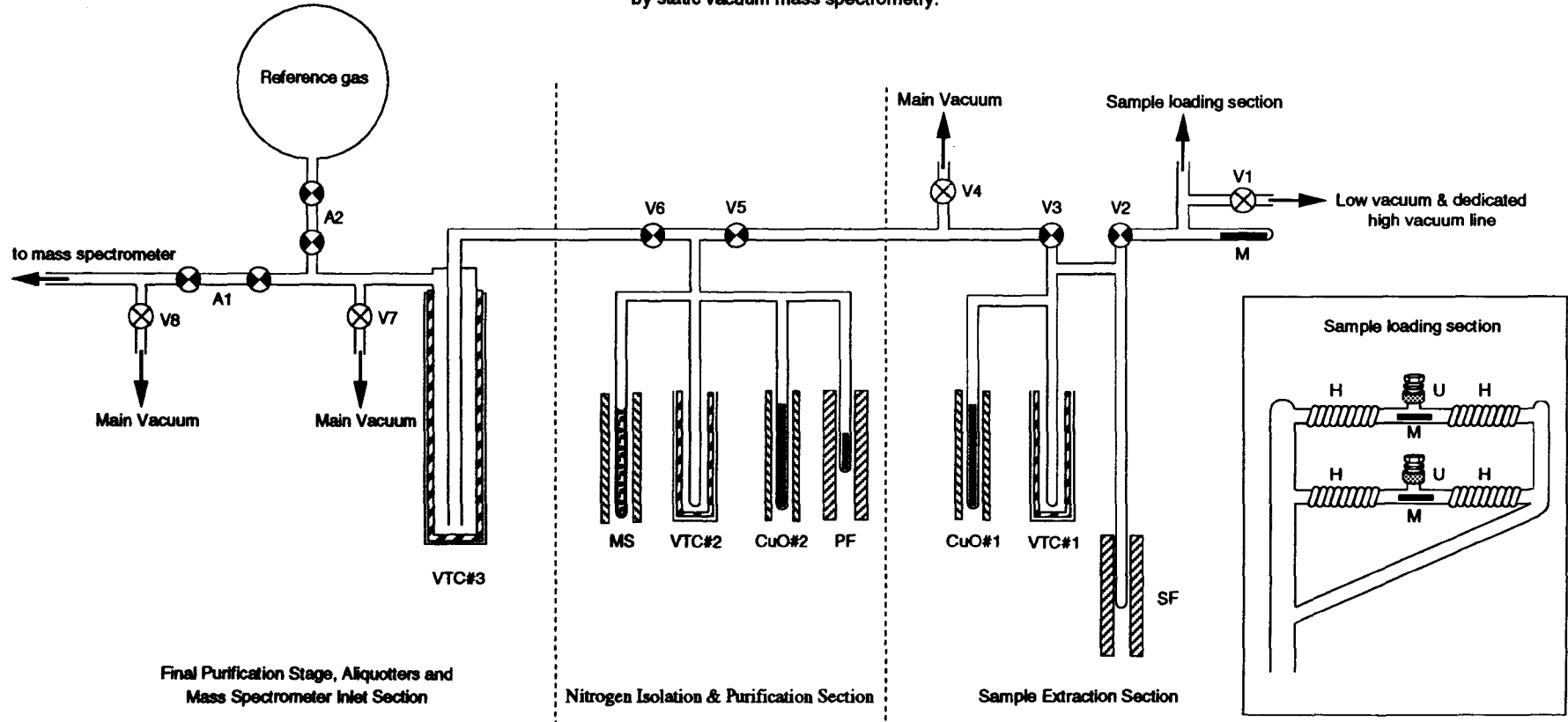
The extraction line is shown schematically in Figure 4.5. Samples (up to four at a time) were loaded directly into an air-lock section, which was isolated from the rest of the vacuum system. Samples were admitted by removing the modified Cajon[®] 'Ultratorr' unions (U) which served as blanking caps. Magnetic manipulation of glass-encased iron slugs (M) allowed each sample to be positioned under one of the four heating coils (H), which were subsequently maintained at $\sim 250^{\circ}\text{C}$ to aid desorption of atmospheric nitrogen and volatile organic matter. The air-lock was then sealed and evacuated to a base pressure of $\sim 10^{-3}$ torr; evacuation to higher vacuum was undertaken using an oil vapour diffusion pump which was dedicated to pumping this section of the line only.

Samples were loaded the night before they were analysed, and pumped under high vacuum (to reach $<10^{-5}$ torr) for at least twelve hours, with the heating coils in use. Meanwhile, the silica tube (reaction vessel) used for thermally extracting nitrogen from the samples was maintained under high vacuum ($<10^{-6}$ torr) and at a temperature of 1200°C , to desorb any atmospheric nitrogen and to minimise contamination by organic material or pump oil.

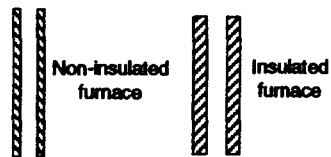
Before analysis of a sample commenced, the reaction vessel, still at 1200°C , was isolated from the associated high vacuum pumping system and the nitrogen background yield accumulated during 39 minutes 'pyrolysis' was determined from the value of the m/z 28 ion beam current, after the gas had been subjected to the full purification procedures as described by Boyd *et al.* (1988) and admitted to the mass spectrometer. During stepwise pyrolysis, with full purification of the released nitrogen, the duration of each heating increment was 39 minutes, using a protocol devised by Boyd (*pers. comm.*) and detailed in Appendix C. This included the time taken to heat the sample to the target temperature and to subsequently transfer the nitrogen to a molecular sieve at -196°C .

Figure 4.5



Schematic diagram of the vacuum line used for thermal extraction (incremental heating) and subsequent purification of fluid inclusion nitrogen for stable isotope ratio analysis by static vacuum mass spectrometry.



Key



Valves V1 to V8:

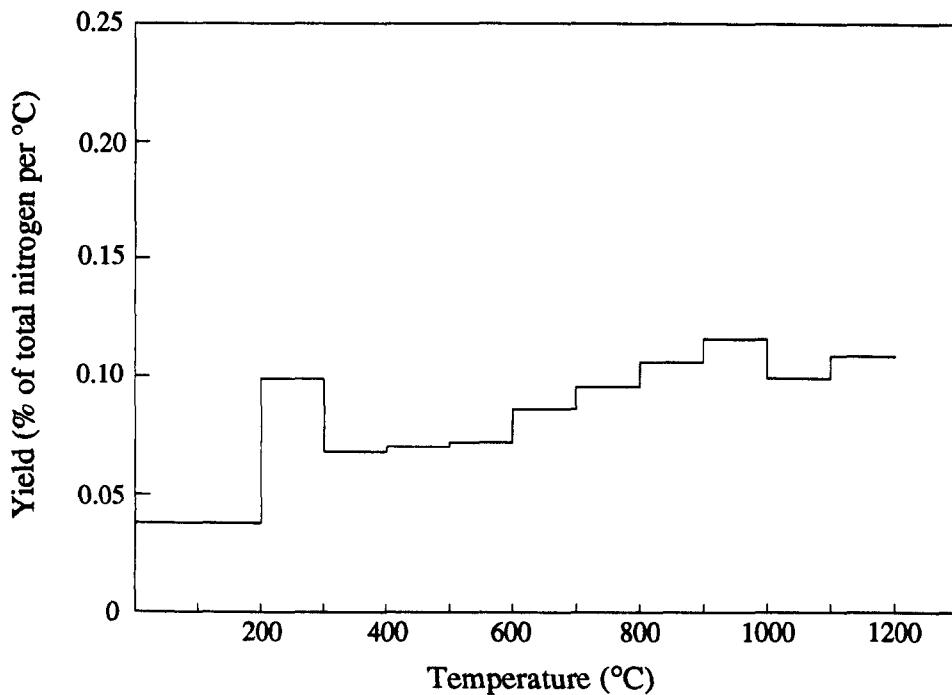
-  J Young® type POR (not 'backed')
-  J Young® type PSU ('backed')
- A1, A2 Gas aliquotters

- SF Sample extraction furnace
- VTC# Variable temperature cryogenic trap
- CuO# Silica tube containing wire-form copper (II) oxide, sheathed in Pt foil
- MS 5Å molecular sieve

- PF Silica tube containing Pt foil
- M Magnetic slug, in Pyrex® capsule
- U Modified Cajon® union
- H Heating tape

Figure 4.6

Procedural nitrogen blank during stepped thermal extraction for nitrogen stable isotope ratio analysis by static vacuum mass spectrometry



Stepped heating in the absence of supplied oxygen.

System blank 1.6 ng N, measured with reaction tube at 1100°C before briefly opening valve that isolates evacuated sample loading section from reaction tube (thereby simulating admittance of sample).

ΣN (~100 to 1200°C) = 10.29 ng

Insufficient nitrogen yield per step for stable isotope ratio analysis.

Temperature (°C)	Yield (ng N)
200	0.79
300	1.02
400	0.71
500	0.73
600	0.75
700	0.89
800	0.98
900	1.09
1000	1.19
1100	1.02
1200	1.12

Although a pre-extraction nitrogen blank yield of <1ng was usual, with the reaction tube at 1200°C, values up to ~2ng could be tolerated if the nitrogen yield from the sample was substantial. If the nitrogen blank was significantly higher than 2ng, it was usually attributable to contamination in the reaction vessel and found to be best cured by replacing the reaction tube with a new, pre-combusted (1200°C) section of silica. This necessarily entailed a subsequent 'down' time of several days, whilst the glassware outgassed to give an acceptably low background pressure. High nitrogen blanks were generally found to cause sample data to be strongly biased towards enrichment in ^{15}N with respect to AIR (thus indicating that atmospheric nitrogen was not the contaminant, as all samples investigated were characterised by $\delta^{15}\text{N}>0$). Prior to transferring the quartz sample grains to the reaction vessel from the evacuated air-lock, the reaction vessel was allowed to cool to ~250°C, corresponding to the temperature of the heating coils used for the initial outgassing.

An on-line (*i. e.* adjacent to the silica tube reaction vessel, with no intervening valve) copper oxide furnace, consisting of a silica tube containing oxygen-depleted CuO in wirewound form, and used as an oxygen supply in the case of stepped combustion experiments (see Figure 4.5), was maintained at a temperature of about 80°C throughout the extraction procedure, to minimise condensation of extracted fluid inclusion water.

A stepwise extraction profile for the measurement of total system nitrogen blank yield is shown in Figure 4.6. For this experiment, the loading air-lock was momentarily opened to atmosphere and the above-described sequence of procedures followed, to simulate the loading of a sample into the reaction vessel on the following day.

Initial experiments to establish an appropriate extraction procedure for the analysis of fluid inclusion nitrogen were concerned with addressing the following:

- (i) Is an adsorbed atmospheric nitrogen component detectable at low extraction temperature? If so, what is the minimum temperature at which this may be reduced to inconsequential levels and hence above which any nitrogen component may be considered indigenous to the sample?
- (ii) Is there any evidence of 'organic' contamination in the low temperature releases?
- (iii) Although theory suggests that no significant contribution to the total fluid phase nitrogen will be derived from species other than N_2 , the possible effects of an ammonium component in the fluid should be considered.
- (iv) In the case of 'high resolution' incremental release of fluid inclusion nitrogen over the temperature range shown to correspond to the release of fluid inclusion water, it might be expected that there should be no significant variation of nitrogen isotopic composition, within the limits of experimental error, if it is assumed that:

- (a) N_2 is the only nitrogen component of significance in the fluid; (b) the fluid was homogeneous at the time of entrapment; (c) any nitrogen contribution from overprinting by later hydrothermal events is insignificant.
- (v) Any ammonium-bearing authigenic micas within the sample would be expected to contribute to the total nitrogen, but would probably not break down below 600°C. A significant contribution of nitrogen derived from this source would represent something of a paradox, in view of the very low levels of ammonium predicted for the parent fluid. Kelley *et al.* (1986) postulated that radiogenic argon released from samples included in the present investigation might be located in small authigenic micas trapped in the fluid inclusions; this argon was not released in significant quantities below 800°C, however.

Procedures adopted for purification of the released nitrogen were as reported in detail by Boyd *et al.* (1988) for stepped pyrolysis. A principal feature involves exposure of the released gases to Pt foil at 1150°C, in the presence of CuO maintained at 850°C to provide an oxygen source. Under these conditions, any carbon monoxide, methane or higher hydrocarbons present would be quantitatively converted to CO_2 . Similarly, hydrogen would be oxidised to water, whilst sulphur species converted to SO_2 . In the present investigation, by far the most abundant component released during thermal extraction of fluid inclusion volatiles was water, the mass yield of which was generally some two to three orders of magnitude greater than that of the coexisting nitrogen.

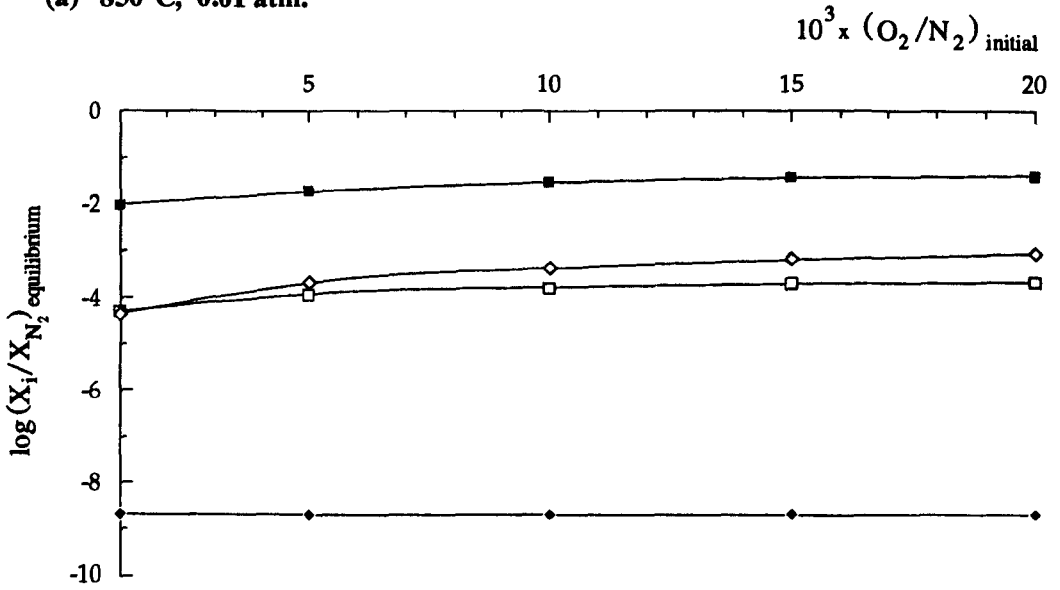
To avoid transferring relatively large amounts of water to the purification section of the line, it was decided to incorporate additional cryogenic trapping during the sample extraction stage. Experiments were therefore conducted to assess the effects of maintaining variable temperature cryogenic trap VTC#1 at (nominally) -170°C throughout the duration of a stepwise heating run, thereby minimising the amount of water (and CO_2) transferred to the nitrogen purification section. This modification would only be problematic if not all the nitrogen in the sample extraction section of the line was in the form of molecular N_2 , or alternatively if any N_2 became trapped in ice formed in VTC#1. Any N_2O or NO_2 present would also be condensed, whilst the vapour pressure of NO (melting point -163.6°C at 1 atm. external pressure) would be low. However, as the thermal extraction was conducted in the absence of oxygen, the formation of nitrogen oxides at this stage was regarded as being extremely unlikely and not considered further.† Of greater concern was the possibility of ammonia being released with the nitrogen gas, as a primary component of the hydrothermal fluid (existing as NH_4^+ at room temperature or $NH_3(aq)$ at temperatures greater than ~220°C).

† Boyd *et al.* (1988) did not detect nitrogen oxide formation in this system during incremental combustion.

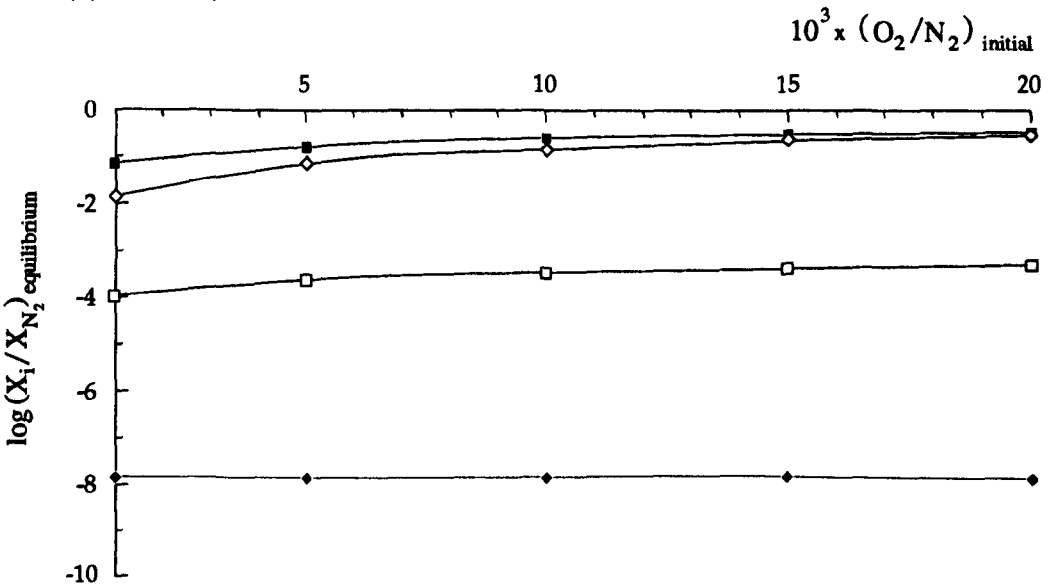
Figure 4.7

Equilibrium compositions, as a function of reactant stoichiometry, predicted by thermodynamic modelling using the computational procedures of Gordon and McBride (1971), for initial reactants N_2 and O_2 under isothermal, isobaric conditions.

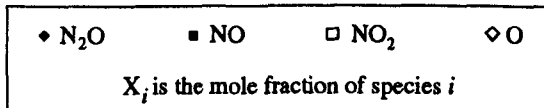
(a) 850°C, 0.01 atm.



(b) 1150°C, 0.01 atm.



Key



If no cryogenic trapping at -170°C is employed during thermal extraction, any ammonia present should in any case be completely converted to molecular nitrogen by CuO at 850°C in the purification section of the line. There is, however, the complication that platinum catalyses the oxidation of ammonia directly to nitric oxide at $700\text{-}900^{\circ}\text{C}$ at relatively low pressures (see *e.g.* Cotton and Wilkinson, 1988). Further oxidation to NO_2 would also occur to some extent, although this species would subsequently be removed during cryogenic trapping of any oxidation products during the purification routine.

Even if detectable quantities of ammonia had been produced in the first place during stepped heating experiments, it is difficult to assess whether its oxidation to NO/NO_2 rather than N_2 during nitrogen purification is likely to have been of significant importance in the present system. NO is known to have a very short half life (~ 0.5 seconds) in the mass spectrometer used (Boyd, 1988), but secondary effects lasting for several weeks were noted by the same author.

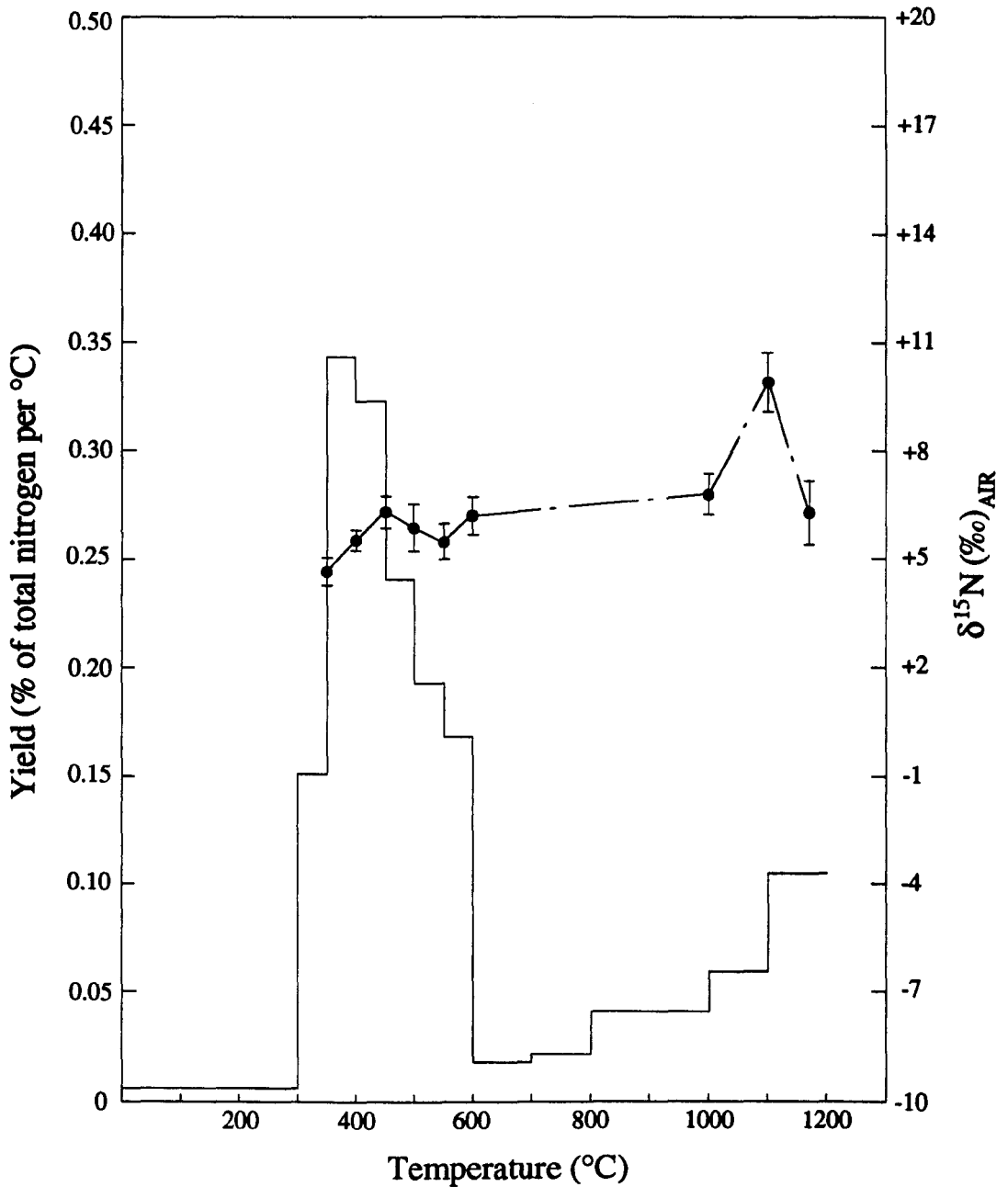
In the absence of any ammonia in the initial reactant mixture, thermodynamic modelling predicts equilibrium compositions as indicated in Figure 4.7 for the reaction between molecular nitrogen and oxygen as a function of initial molar ratio and for temperatures of 850°C (that of the CuO oxygen reservoir during gas purification) and 1150°C (simulating reaction on the Pt finger). The 0.01 atm. total pressure closely approximates the partial pressure of O_2 in equilibrium with $\text{CuO}/\text{Cu}_2\text{O}$ at 850°C (see Figure 3.9). An oxygen-to-nitrogen initial molar ratio of 1,000:1 corresponds to ~ 6.7 nanomoles of N_2 , equivalent to a partial pressure of $\sim 1.0 \times 10^{-5}$ atm. in the purification section (volume 15 cm^3 according to Boyd, 1988). The presence of traces of methane in the reactant mixture, as was the case for samples included in the present investigation, does not significantly affect the results presented.

With regard to whether cryogenic trapping at *ca.* -170°C during the thermal extraction of fluid inclusion volatiles affects the isotopic data subsequently obtained for the nitrogen component, through the removal of ammonia from the total nitrogen-bearing fraction, no such effect was detected, suggesting that ammonia was either absent or present at sufficiently low levels as to be insignificant.

The results of 'high resolution' incremental heating of quartz sample HEM-80-1 with the variable temperature cryogenic trap VTC#1 maintained at -170°C (nominal) throughout the duration of the experiment are shown in Figure 4.8, from which the following salient conclusions may be drawn:

Figure 4.8

Stepwise thermal release of nitrogen *in vacuo* from quartz sample HEM-80-1



NITROGEN analysis:

Stepped heating in the absence of supplied oxygen

Sample: HEM-80-1 Weight: 58.711 mg

ΣN (~100 to 1200°C) = 285.32 ng (4.86 ppm)

$\Sigma \delta^{15}N$ (~100 to 1200°C) = 6.06 ‰

ΣN (300 to 600°C) = 200.48 ng (3.42 ppm)

$\Sigma \delta^{15}N$ (300 to 600°C) = 5.65 ‰

Temperature (°C)	Yield (ng N)	[N] (ppm)	$\delta^{15}N$ (‰) _{AIR}	σ (‰)
300	4.11	0.07	nm	
350	21.27	0.36	4.6	0.39
400	48.59	0.83	5.4	0.30
450	45.67	0.78	6.2	0.43
500	34.05	0.58	5.8	0.65
550	27.20	0.46	5.4	0.50
600	23.70	0.40	6.1	0.52
700	4.87	0.08	nm	
800	5.97	0.10	nm	
1000	22.98	0.39	6.7	0.56
1100	16.78	0.29	9.9	0.83
1200	30.13	0.51	6.3	0.89

- (i) Yield of nitrogen below 300°C is minimal and insufficient for isotopic analysis with an acceptable degree of precision. This indicates that the sample preparation procedures advocated are effective at minimising contamination and, furthermore, that loss of indigenous nitrogen incurred by outgassing the quartz sample at 300°C would be negligible. Fluid inclusion homogenisation temperatures reported for early W±Sn oxide-associated hydrothermal fluids at the other S W England localities included in this investigation are generally >300°C; it is therefore reasonable to infer that outgassing at 300°C should not adversely affect the recorded yield of indigenous nitrogen in these cases.
- (ii) An abrupt reduction in nitrogen release to very low levels is noted for the temperature step 600-700°C. Mass decrepitation of fluid inclusions during the α - β quartz inversion would be consistent with the observed nitrogen release profile and is also consistent with findings reported elsewhere (see Bodnar *et al.*, 1989).
- (iii) The isotopic composition of nitrogen released during the six heating increments between 300 and 600°C is notably uniform, within the limits of experimental error. A minor contribution from adsorbed atmosphere is probably present in the gas yielded during the lowest temperature step (300-350°C); this is confirmed by the associated ⁴⁰Ar peak being larger than for any subsequent heating step. It is also consistent with the corresponding $\delta^{15}\text{N}$ value being slightly enriched in the lighter isotope compared with the results for the subsequent five steps. If the sample had been outgassed at 350°C, however, a significant amount of indigenous nitrogen would have been lost. For the 350-600°C temperature range, the weighted mean of the five consecutive $\delta^{15}\text{N}$ results is 5.8‰, with all the measurements falling within $\pm 0.4\%$ of this value.
- (iv) Although nitrogen release at temperatures immediately above the α - β quartz transition is minimal, the progressive release of nitrogen at higher temperatures is a notable feature of the stepwise heating profile. Kelley *et al.* (1986) investigated argon release from similar samples and found that the proportion of argon released below 600°C was never more than 40% of the total up to 1600°C; releases above 600°C featured maxima at between ~700 and 1000°C and also between 1100 and 1500°C. The high temperature release of nitrogen in the present case is equally difficult to explain. Possible sources include sub-micron inclusions or lattice defects or, alternatively, captive micas. In the present case, the isotopic composition of nitrogen released between 800-1000°C and from 1100-1200°C is similar to that released during the 300-600°C increments, suggesting that micro-inclusions are probably the source. A further enrichment in ¹⁵N of >3‰ is seen, however, in the case of nitrogen released between 1000 and 1100°C; this would be compatible with the decomposition of an ammonium-bearing solid phase, although the possibility that this single result is spurious cannot be discounted.

In the light of these findings, it was decided to outgas the quartz samples at 300°C, to minimise the contribution from any adsorbed atmospheric component without significantly affecting the yield of nitrogen indigenous to the sample. Nitrogen was then collected over the temperature interval 300-600°C, corresponding to the major release from fluid inclusions, for the determination of yield and isotopic composition. By collecting the fluid inclusion nitrogen in a single heating step, it was possible to reduce the quantity of quartz required, compared to a multi-step analysis, whilst at the same time ensuring that the amount of nitrogen released was generally two orders of magnitude greater than the nitrogen blank of the analytical system. Samples generally consisted of three quartz grains, total weight 30-50mg; the maximum grain size was restricted by the internal diameter of the quartz reaction tube (4 mm). In the case of samples found to contain very low levels of nitrogen (sub-ppm), the number of grains was increased accordingly.

At higher temperatures, the decomposition of trapped micas and/or feldspars may be a significant source of nitrogen; this release would be superimposed on that derived from nitrogen dissolved in the quartz lattice and/or derived from the opening of sub-micron inclusions. To compare the isotopic composition of nitrogen released at high temperature (>600°C) with that representative of the fluid inclusions, a 600-1100°C heating step was also undertaken in many cases.

4.6 Results of the palaeofluid $\delta^{15}\text{N}$ analyses

The results of nitrogen yield and isotope ratio analysis for the SW England samples are given in Table 4.2. Considerably more analyses (duplicates) were undertaken than is shown in this table, but a reproducible shift of $\delta^{15}\text{N}$ to 'heavier' values was noted when the nitrogen blank was greater than ~2ng. This effect was less severe for the 300-600°C temperature step, but still detectable. Rather than attempt to correct for bias introduced by the blank, all data thus affected are excluded from further consideration here.

The data for major fluid inclusion nitrogen release (300-600°C) are illustrated in Figure 4.9, which also gives estimates of corresponding $\text{N}_{2(\text{aq})}$ molality values, derived using water yields from 'splits' of the same samples and assuming a homogeneous fluid phase. As secondary inclusions unrelated to the primary crystallisation event will inevitably be present to some extent, the $\text{N}_{2(\text{aq})}$ molality estimates probably represent lower limit values, if it is assumed that the secondary inclusions contained fluid of predominantly meteoric origin.

It is apparent from the experimental results that, whereas the $\delta^{15}\text{N}$ range for the 300-600°C nitrogen release is from 5.0 to 13.0‰_(AIR), data from fifteen of the eighteen samples investigated fall within the range $6.5 \pm 1.5\%$.

Table 4.2

Nitrogen yield and $\delta^{15}\text{N}$ data from S W England quartz samples associated with early hydrothermal mineralisation of the Cornubian granites

Location	Sample reference	Nitrogen release 300-600°C			Nitrogen release 600-1100°C		
		Yield (ppm N)	$\delta^{15}\text{N}$ ‰ _{AIR}	($\pm\sigma$)	Yield (ppm N)	$\delta^{15}\text{N}$ ‰ _{AIR}	($\pm\sigma$)
Hemerdon	(1) HEM-79-2	5.2	6.3	(0.34)			
	(1) HEM-80-1	6.4	6.5	(0.49)			
	(1) HEM-80-39	4.3	5.1	(0.53)			
	(1) HEM-80-44	2.2	5.7	(0.62)	0.23	7.2	(1.02)
	(1) HEM-80-47	2.2	6.7	(0.45)	0.42	6.5	(0.92)
South Crofty	(2) SC-88-3	13.8	5.0	(0.43)	0.99	4.2	(0.78)
	(2) SC-88-3 ABC	13.3	5.0	(0.29)			
Cligga Head	(3) CH-88-1	3.2	5.1	(0.59)	0.48	5.3	(0.70)
Castle-an-Dinas	(4) CD-88-1	6.6	7.0	(0.57)	0.29	6.7	(0.43)
		6.2	6.7	(0.25)			
Old Gunnislake	(5) OG-88-1	2.9	10.0	(0.55)	1.5	9.6	(0.35)
	(5) SW-89-150	2.6	8.2	(0.29)			
South Bedford	(6) SW-84-20	3.6	6.6	(0.47)	0.18	nm	
Prince of Wales	(7) SW-84-27	6.3	6.2	(0.27)			
		7.1	7.1	(0.31)	0.37	4.4	(0.47)
Drakewalls	(8) SW-84-15	3.5	7.0	(0.63)			
		2.0	6.8	(0.56)	0.22	8.8	(0.93)
East Vitifer	(9) SW-89-156	0.48	6.0	(0.30)			
		1.0	8.8	(0.39)	0.29	12.7	(0.30)
Golden Dagger	(10) SW-89-159	0.37	6.7	(0.33)			
	(10) SW-89-163	0.28	7.3	(0.30)			
Barracott	(11) SW-89-164	1.4	13.0	(0.30)	0.42	8.4	(0.54)
		*0.07	*9.9	(0.75)	†0.12	†9.6	(0.56)
		0.14	5.2	(0.69)	0.15	7.7	(0.40)

Notes:

- (1) ‡Locations generally refer to mine identifiers.
Associated number in parentheses refers to locality as indicated on Figure 4.4.
- (2) * 500-600°C step datum point. Stepped heating was performed, using a combination of 50 and 100°C temperature increments, from 300 to 600°C: only the 500-600°C step yielded sufficient nitrogen for isotopic analysis of acceptable precision. Total nitrogen yield for the 300-600°C release was approximately 0.2ppm.
- (3) † 600-1000°C step datum point.
- (4) 'nm' indicates *not measured*.

Figure 4.9

Nitrogen yield and $\delta^{15}\text{N}$ data for S W England palaeo-hydrothermal fluids extracted from quartz. Refer to Figure 4.4 for key to sampling localities.

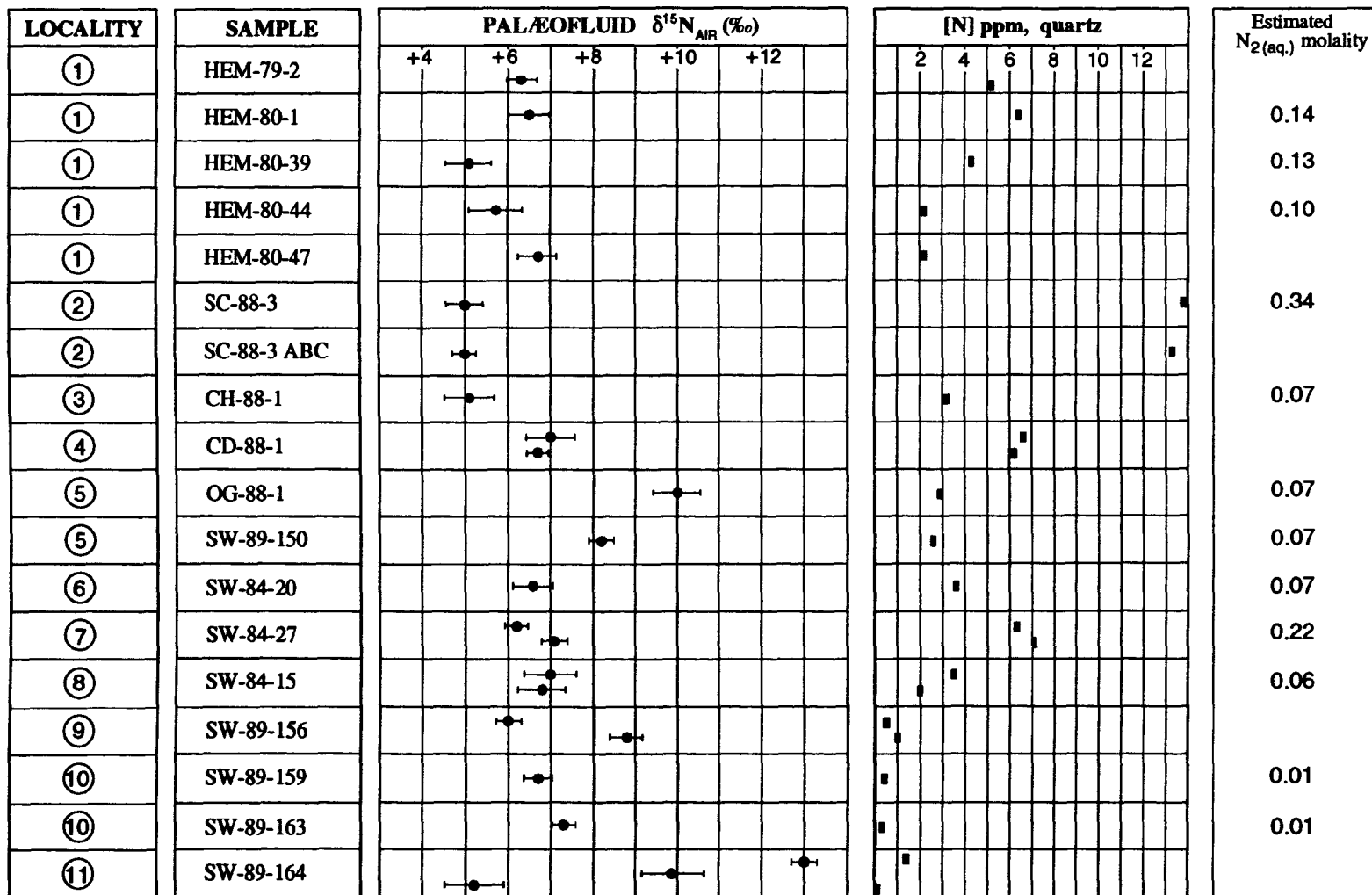


Table 4.3Nitrogen yield and $\delta^{15}\text{N}$ data for Carrock Fell quartz samples.

Sample reference	Temperature ($^{\circ}\text{C}$)	Yield (ppm N)	$\delta^{15}\text{N}\text{‰}_{(\text{AIR})}$	σ (‰)
CF-76-7	300-600	12.8	5.1	0.24
CF-76-25	300-600	10.3	5.3	0.34
CF-77-39A	300-600	13.0	4.3	0.31
CF-77-77A	300-600	7.5	4.3	0.30
CF-77-77B	300-600	12.1	4.5	0.22
CF-77-98	300-600	12.0	3.7	0.38
CF-77-98	600-1100	0.30	4.0	2.31

Of the three that do not lie within these limits, the two samples from Old Gunnislake mine gave a mean $\delta^{15}\text{N}$ value of $9.1 \pm 0.9\text{‰}$, which is also in good agreement with the measured high temperature $\delta^{15}\text{N}$ value. It is also notable that the high temperature release comprised approximately 33% of the total nitrogen yield, a considerably higher proportion than was found in any other sample. Triplicate analyses of SW-89-164 (hosted by the Dartmoor granite), the only other sample which did not fit the $6.5 \pm 1.5\text{‰}$ range, indicated heterogeneous distribution of nitrogen, with variable nitrogen yield and no systematic relationship between $\delta^{15}\text{N}$ and nitrogen yield. (Similarly poor reproducibility was also obtained during quartz $\delta^{18}\text{O}$ analysis of sample SW-89-164.) Although it may be argued that the $\delta^{15}\text{N}$ result of 9.9‰ is probably the most reliable, since the nitrogen released at high temperature was characterised by a similar $\delta^{15}\text{N}$ value, it would be unwise to base any hypothesis about nitrogen sources on such data.

With regard to the high temperature ($600\text{--}1100^\circ\text{C}$) nitrogen releases, where data are available (Table 4.2), it is seen that a majority (six) of the eleven analyses produced $\delta^{15}\text{N}$ results indistinguishable from those of the corresponding low temperature releases, within the limits of analytical precision. Nitrogen released at $>600^\circ\text{C}$, and characterised by $\delta^{15}\text{N}$ values $1\text{--}4\text{‰}$ 'heavier' than the corresponding release at $<600^\circ\text{C}$ (as noted for three samples), might be attributable to thermal breakdown of ammonium-bearing solids. Only in two cases was the nitrogen found to be depleted in ^{15}N with respect to the corresponding low temperature release: one of these was non-reproducible (sample SW-89-164), whereas the datum for SW-84-27 (Prince of Wales mine), showing a shift of -2.7‰ , is difficult to explain.

Table 4.3 gives the comparable data for the five samples analysed from Carrock Fell. Because of nitrogen blank problems, only in the case of one sample was reliable $\delta^{15}\text{N}$ measurement possible of nitrogen released at $>600^\circ\text{C}$. All the $\delta^{15}\text{N}$ values fall within the range $4.5 \pm 0.8\text{‰}_{(\text{AIR})}$.

4.7 $\delta^{15}\text{N}$ of the Cornubian granites and metasedimentary rocks

4.7.1 The granites

The present investigation coincided with a study by Boyd *et al.* (1993) of the distribution and isotopic characterisation of nitrogen associated with the granites of the Cornubian batholith. Stepped combustion procedures were used to release the nitrogen from both whole-rock and mineral separates; after purification, the nitrogen was analysed for isotopic composition by static vacuum mass spectrometry. Rather than attempt to duplicate that work in the present study, attention was instead focused on the nitrogen isotopic composition of the associated metasedimentary rocks.

4.7.2 The Palaeozoic metasediments

Determination of the yield and isotopic composition of nitrogen in metasedimentary rocks is complicated by the nitrogen being present in combined form, either as the ammonium ion (which, in turn, may be either 'fixed' or 'exchangeable') in ammonium-bearing clay minerals; additionally, nitrogen may be present in organic components at various stages of thermal maturation. Some of the organically-fixed nitrogen may be in a form readily hydrolysed to yield ammonia, whereas nitrogen bound in kerogen, that organic constituent of sedimentary rock that is neither soluble in aqueous alkaline solutions nor extractable using the common organic solvents (Tissot and Welte, 1984), remains intractable. As referred to above, the extraction of organically-bound and inorganic nitrogen for isotope ratio analysis is generally based on either sealed tube combustion techniques, or on variations of the Kjeldahl method. Minagawa *et al.* (1984) compared the two methods and recommended combustion to 850°C, using a double-walled tube, to prepare nitrogen for isotope ratio analysis in the case of biogeochemical samples. These authors analysed kerogen from Tanner Basin sediments, off the coast of southern California, by both methods: the Kjeldahl method was found to give only 88% of the nitrogen yield as obtained by the combustion method and, furthermore, the nitrogen was slightly depleted in ¹⁵N (by 0.21‰) compared to that obtained by combustion. Further adaptations of the sealed combustion tube method have been reported recently (Kendall and Grim, 1990), and a procedure appropriate to static vacuum mass spectrometry devised (Boyd and Pillinger, 1990).

Experimental details of the procedures used to determine the yield and isotopic composition of nitrogen in metasedimentary rocks during the present investigation are presented in Chapter 6, together with the corresponding results. The nitrogen isotopic composition of ammonium-rich samples was found to range from +0.7 to +3.0‰_(AIR), except at the Dartmoor granite contact, where a value of +7.4‰ was noted.

4.8 Discussion

4.8.1 Fluid inclusion nitrogen stable isotope data

The most notable feature of the palaeofluid nitrogen isotope data for S W England is the relatively narrow range of values (see Figure 4.9), considering that the data set includes both endo- and exo-granitic quartz veins. In the case of the samples from Hemerdon, for example, both granite and killas host rock lithologies are represented, as are greisen-bordered veins and veins not exhibiting hydrothermal alteration, yet the variation in $\delta^{15}\text{N}$ among the five samples investigated is only 1.6‰. This indicates that the source of the molecular nitrogen was a reservoir of uniform isotopic composition and, furthermore, that

any local isotopic fractionation effects involving nitrogen were minor compared to processes operating on a larger scale throughout the batholith.

Additional support for a domination of the nitrogen isotopic characteristics by processes presumed to occur within the batholith, or possibly at the contact zone, is provided by the lack of correlation between $\delta^{15}\text{N}$ values and nitrogen yield. For example, the palaeofluid nitrogen from South Crofty has identical isotopic composition (5.0‰_{AIR}) within experimental error, to that from Cligga Head, even though there is an approximately four-fold difference in nitrogen yield (both with respect to the quartz and as nitrogen molality in the fluid).

Of particular interest is the observation that quartz samples associated with early mineralisation of the central Dartmoor region, well away from contact with Palaeozoic metasediments, contain measurable traces of nitrogen, albeit at the sub-ppm level with respect to the quartz. Furthermore, this component has a $\delta^{15}\text{N}$ signature similar to that found for nitrogen-enriched samples from the other localities included in this study. In conjunction with the reported distribution of ammonium throughout the granites of S W England (Section 4.8.2), this finding provides the strongest evidence for palaeofluid nitrogen being derived from ammonium-bearing minerals located within the granite.

Although there is some overlap between the Carrock Fell fluid inclusion $\delta^{15}\text{N}$ data and those obtained for the S W England samples, it is seen that the fluids at Carrock Fell are in general comparatively less enriched in ^{15}N . The Carrock Fell data are similar to those obtained by Bussink (1984) for the majority of quartz-wolframite samples investigated from Panasqueira, Portugal. Interestingly, wall-rock alteration at Carrock Fell is minimal (Shepherd *et al.*, 1976), being evident only in the granite where the rock is converted to a quartz-muscovite greisen; this is similar to the situation at Cligga Head, where similar palaeofluid $\delta^{15}\text{N}$ values were obtained.

4.8.2 Ammonium contents and the 'S'-type characteristics of the S W England granites

Evidence of a substantial sedimentary (pelitic) contribution to the parent magmas of the S W England granites is provided by high initial $^{87}\text{Sr}/^{86}\text{Sr}$ ratios of the individual plutons (Darbyshire and Shepherd, 1985, 1987), ϵ_{Nd} data (Darbyshire and Shepherd, 1987, 1994), together with high K_2O contents and enrichment of trace elements most abundant in pelitic sediments: B, As, Li, Sn (Hall, 1990).

In a survey of the ammonium contents of S W England granites, Hall (1988) found that ammonium levels differed markedly between intrusions, in contrast to the uniformity of major element compositions. Also reported was that pegmatite formation and greisenisation were both associated with an enrichment of ammonium, compared to the parent granite.

Enhanced ammonium in the greisenised granites was attributed to high NH_4^+ concentrations in the metasomatising fluid. It was noted that minor granite intrusions which contained high levels of NH_4^+ were also the foci of intense post-emplacement hydrothermal activity. One of the most significant observations of Hall (1988) was the correlation between the average ammonium content of the S W England granites and their initial $^{87}\text{Sr}/^{86}\text{Sr}$ ratios and peraluminosity. This supported the assertion that ammonium in the granites is derived from a sedimentary source, incorporated during anatexis either in the magma source region or as the result of magma contamination at a higher level prior to emplacement.

For the present investigation, it is notable that the very low levels of fluid inclusion nitrogen associated with syn/post-emplacement hydrothermal activity in central Dartmoor correlate well with the finding by Hall (1988) that the mean NH_4^+ content of the Dartmoor intrusion (11 ppm) is the lowest of all those investigated from the Cornubian batholith. Conversely, the highest levels of NH_4^+ reported by Hall (1988) for both unaltered and greisenised granites in the region were from Cligga Head; this correlates with the present finding of significant quantities (which may be arbitrarily defined for this purpose as 2ppmN or greater, with respect to the quartz host) of nitrogen in the associated early post-emplacement fluids at this locality.

Unfortunately, data for the NH_4^+ contents of the other relevant minor intrusives (Carn Brea, Gunnislake, Hemerdon Ball) were not available. However, other lines of evidence suggest a significant sedimentary component to the granites. For example, initial ϵ_{Nd} values for the Hemerdon Ball and Dartmoor granites (Darbyshire and Shepherd, 1987) indicate a greater contribution of crustal material to the magma in the case of Hemerdon Ball (initial ϵ_{Nd} ca. -7.0) compared to the adjacent Dartmoor pluton (initial ϵ_{Nd} -4.7). Also, initial ϵ_{Nd} values of -6.9 to -7.3 for the Carnmenellis granite (Darbyshire and Shepherd, 1990) indicate similarity to Hemerdon Ball.† Major element oxide analyses of the Hemerdon Ball granite (Darbyshire and Shepherd, 1987), confirm the peraluminous nature of this intrusive. For the Gunnislake granite, Bull (1982) reported similar findings.

As published nitrogen isotope data for the Skiddaw granite (N W England) are not available, it is difficult to extend the discussion of the origin of palæofluid nitrogen at S W England to the Carrock Fell locality. Furthermore, as noted by O'Brien *et al.* (1985), the Lake District granites are not readily classified as typically 'I'-type or 'S'-type. Hall (1987) noted that there is no apparent correlation between the ammonium content and initial $^{87}\text{Sr}/^{86}\text{Sr}$ ratios of Caledonian-age granites of the British Isles, although significant correlation between

† More recent results (Darbyshire and Shepherd, 1994) include ϵ_{Nd} values for the following plutons: Gunnislake (-6.9), Castle-an-Dinas, East (-7.6), St Austell (-6.2 to -7.7), Bodmin (-7.2), Land's End (-6.1 to -6.2), and coarse-grained Carn Marth granite (-7.0). These data support the assertion that the Dartmoor granite protolith assimilated a lesser degree of sedimentary material than others of the batholith.

ammonium content and peraluminosity was obtained. In that study, however, only the Shap granite was included from the Lake District. Cooper and Bradley (1990) analysed the ammonium content of granitic rocks sampled from exposed components of the Lake District batholith, in an attempt to identify evidence for an ammonium-rich sedimentary protolith. The unaltered Skiddaw granite was reported to have a low ammonium content (24 ppm), whereas highly altered specimens of the same granite, containing appreciable secondary muscovite, sericite and clay, contained ammonium contents up to 251 ppm. Granites sampled from all parts of the batholith were found to contain low levels (<30 ppm) of ammonium, in cases where alteration was observed to be minimal. It was concluded by Cooper and Bradley (1990) that, as discussed by Hall (1987), the low primary ammonium content of the Lake District granites was not, *per se*, evidence to either support or refute the hypothesis of a sedimentary protolith.

4.8.3 Palæo-atmospheric nitrogen in the fluid inclusions? Argon isotope evidence

It has been suggested (Kelley *et al.*, 1986; Shepherd and Miller, 1988; Turner and Bannon, 1992) that a substantial proportion of the argon component in fluid inclusions associated with W±Sn oxide mineralisation in S W England may be of palæo-atmospheric origin, implying a meteoric source of the associated waters. Kelley *et al.* (1986) reported ⁴⁰Ar-³⁹Ar analyses of three samples of vein quartz from Hemerdon, including one (HEM-79-2) which was used in the present investigation of nitrogen isotopes. Similarly, Turner and Bannon (1992) included sample SW-84-15 (Drakewalls mine) from the present study, together with early wolframite-associated quartz from Old Gunnislake mine.

A meteoric origin of the palæowaters in early-stage hydrothermal fluids of the Cornubian region is not in accord with the principal findings of the present work. Substantial excess of ³⁶Ar in hydrothermal quartz from the north Pennines, accompanied by unfractionated atmospheric noble gas abundances (Stuart and Turner, 1992), indicates that present-day air, trapped in re-sealed microfractures, is a possible alternative explanation for the findings of Kelley *et al.* (1986) and the other studies referred to above. The stripping of noble gases of atmospheric origin from sedimentary rocks during hydrothermal circulation has also been proposed (Turner and Bannon, 1992).

For samples from Hemerdon, Kelley *et al.* (1986) estimated atmospherically-derived ⁴⁰Ar concentrations of 506±80µl/l in the palæofluids and noted that this value is similar to that for (non-saline) air-equilibrated water at STP. Saline fluids would be argon-saturated at lower concentrations, although the present salinity of the fluid inclusions is not of direct relevance if high salinity values resulted from fluid-rock interaction after the fluids were isolated from equilibration with the atmosphere.

On the basis of the hypothesis by Kelley *et al.* (1986) that their experimentally-determined atmospheric ^{40}Ar concentrations of $506 \pm 80 \mu\text{l/l}$ in the Hemerdon fluid inclusions were derived from air-equilibrated groundwaters which subsequently retained their full argon budget despite burial and heating to $>400^\circ\text{C}$, the corresponding nitrogen concentration in the fluids should be $\sim 1.8 \times 10^4 \mu\text{l/l}$, on the basis of the solubility data of Weiss (1970). This corresponds to a nitrogen molality of only $\sim 8 \times 10^{-4}$. The molality of nitrogen in the Hemerdon palaeofluids, as estimated during the present study, is *ca.* 0.10-0.14 (see Figure 4.9). It is evident, therefore, that the contribution of any atmospheric component to the nitrogen yield and $\delta^{15}\text{N}$ data obtained during the present work will be insignificant.

4.8.4 Sources of the palaeofluid nitrogen - isotopic considerations

The two major reservoirs of nitrogen in crustal rocks of S W England are, firstly, the metasediments, where values in excess of 1000 ppm of NH_4^+ have been recorded; secondly, the granites, where average NH_4^+ values for the unaltered whole rocks range from 11 ppm at Dartmoor to 179 ppm at Cligga Head (Hall, 1988) and where hydrothermal alteration is associated with a substantial enrichment in NH_4^+ content. Pegmatites, although not a major rock type in the region, are substantially enriched in NH_4^+ compared to the associated granites; pegmatite from Megilligar Rocks in Cornwall contains the highest ammonium content (332 ppm) yet recorded from an igneous rock (Hall, 1988). This enrichment of ammonium in pegmatites suggests that aqueous fluids exsolved from crystallising magma may have initially contained substantial amounts of NH_4^+ .

Considering first the hypothesis that palaeofluid nitrogen was primarily derived from interaction between the metasediments and hydrothermal fluids, $\delta^{15}\text{N}$ values for the former were found to be *ca.* 3 to 4‰ lower than those of the fluids, except when the metasediment was very close to the granite contact (Chapter 6, this work). To obtain a $\delta^{15}\text{N}$ value in the range of $6.5 \pm 1.5\text{‰}_{(\text{AIR})}$ for molecular nitrogen (as is the case for the majority of palaeofluids analysed from S W England) by the oxidation of ammonium-bearing phases in the local metasediments would therefore require either:

- (i) Release of nitrogen only at the granite contact zone and involving quantitative oxidation of ammonium that was retained after contact metamorphism. It is difficult to envisage a mechanism for such a scheme.
- (ii) Leaching by hydrothermal fluids of soluble ^{15}N -enriched ammonium or ammonia from metasediments located away from the granite contact zone, with subsequent quantitative oxidation of this component.

With regard to (ii), experiments by Haendel *et al.* (1986) on metasedimentary rocks demonstrated that ammonium with a $\delta^{15}\text{N}$ value at least 10‰ greater than that of the whole-

rock may be extracted by leaching with either water or 2M KCl solution (at room temperature and atmospheric pressure). The same authors also noted that the measured fractionation factors were in accord with equilibrium isotopic exchange between NH_4^+ and NH_3 at 200-300°C.

No comparable experiments have been performed on metasediments from S W England, as far as the author is aware. It should also be noted that Haendel *et al.* (1986) did not investigate the leaching of ammonium under pressure and temperature conditions more appropriate to crustal fluids. If the S W England metasediments contained a soluble ammonium fraction enriched in ^{15}N by 10-15‰ compared to the whole-rock, and assuming that this fraction was the major source of nitrogen to the fluid phase, nitrogen isotope equilibration between NH_4^+ and N_2 would require a temperature of ~100 to 200°C, depending on whether the fractionation data of Scalan (1958) or Hanschmann (1981) are used (see Figure 4.1) to account for the observed palæofluid $\delta^{15}\text{N}$ values. This temperature range is substantially lower than that associated with the hydrothermal activity considered here. Alternatively, if it is considered that the speciation of nitrogen released by leaching is as NH_3 (which is probable in this case, as discussed above), then consideration of isotopic equilibration between NH_3 and N_2 indicates that, at realistic hydrothermal temperatures, the diatomic molecular species would be *enriched* in ^{15}N , relative to the ammonia, giving rise to substantially greater palæofluid $\delta^{15}\text{N}$ values than actually measured.

The alternative hypothesis to that of direct mobilisation of nitrogen from the metasediments is to consider the granites and associated hydrothermally altered rocks as the dominant source of palæofluid nitrogen. In one sense, the sedimentary rocks must ultimately be the source of all the crustal nitrogen, if the fixed nitrogen in the granites was assimilated by magma during anatexis. The data of Boyd *et al.* (1993) show that 8 out of 10 whole-rock granite samples analysed for $\delta^{15}\text{N}$ were in the range 8.4 to 10.2‰_(AIR). These analyses included samples from the Cligga Head, Hingston Down, Bodmin Moor, Carnmenellis and Land's End intrusives. Two samples that did not lie within this range ($\delta^{15}\text{N}$ values 5.1 and 7.0‰, from the St. Austell and Dartmoor intrusives respectively) had low Sr contents (<20ppm) and also contained the lowest NH_4^+ concentrations (15 and 8ppm, respectively). Nitrogen isotope analyses of muscovite and orthoclase from Cligga Head were also reported, for both the unaltered and greisenised granite. These data showed that there was no difference, within the limits of analytical precision, between the $\delta^{15}\text{N}$ of the muscovite from the unaltered granite, and that from the greisenised granite, even though the concentration (as ammonium) was substantially higher in the altered granite. This makes an interesting comparison with the findings of the present study with regard to Hemerdon, *i.e.* that the fluid inclusion $\delta^{15}\text{N}$ is independent of whether the host quartz vein is greisen-bordered or not. With reference to orthoclase, Boyd *et al.* (1993) found that samples from the hydrothermally-altered granite were relatively enriched in ^{15}N by approximately 1‰.

It is apparent from comparing the fluid inclusion $\delta^{15}\text{N}$ data (generally $6.5 \pm 1.5\text{‰}_{(\text{AIR})}$) with those from the granite whole-rock samples (mostly $9.3 \pm 0.9\text{‰}$, according to Boyd *et al.*, 1993), that the difference of approximately 3‰ is in accord with isotopic equilibration between ammonium and molecular nitrogen:



at temperatures between ~350 to 500°C, using the fractionation factors of Hanschmann (1981). This corresponds well with the temperature range for the hydrothermal deposition of quartz samples used in the present study. Note, however, that the data cannot distinguish the case of initial equilibration at hydrothermal temperatures from that of initial isotopic equilibration at magmatic temperatures followed by equilibrated exchange during cooling down to a 'blocking temperature', where kinetic factors effectively prevent further isotopic exchange. Sheppard (1981) reported that, for carbon exchange between CO_2 and CH_4 in geothermal fluids, isotopic equilibrium is maintained down to around 320°C; comparable data for nitrogen exchange between NH_4^+ and N_2 are unknown to the present author.

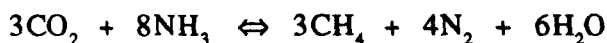
Note that if Scalan's (1958) data for the fractionation of nitrogen between N_2 and NH_4^+ are used instead of Hanschmann's, the temperatures obtained are substantially higher (~950°C mean), indicating isotopic equilibration under magmatic conditions but no subsequent equilibration during post-magmatic cooling. This, in turn, would imply physical separation of the diatomic and ammonium components during cooling from magmatic temperatures.

4.8.5 The oxidation of ammonia by C^0 and C^{IV} components: potential mechanisms for the release of nitrogen to the fluid phase

Apart from thermal decomposition and dehydration (Hallam and Eugster, 1976), the release of ammonium ions from NH_4^+ -substituted Al-silicates to a fluid phase may occur by cation exchange with species such as H^+ ('proton metasomatism') and K^+ ; also NH_4Cl and NH_4OH (Duit *et al.*, 1986). Hydrogen ion exchange is probably the dominant mechanism (Bottrell, *pers. comm.*), the extent of this metasomatism being controlled by the pH. As discussed above, the current consensus of opinion based on equilibrium thermodynamic models suggests that N_2 predominates over NH_4^+ and NH_3 in crustal fluids, although Hallam and Eugster (1976) used similar considerations to conclude that $f_{\text{NH}_3} > f_{\text{N}_2}$ in the Earth's crust. What needs to be identified, however, is the chemical pathway for the oxidation of ammonium ions and/or ammonia (depending on pH, salinity and temperature) released from ammonium-bearing micas.

Haendel *et al.* (1986) noted that, during stepwise heating of a (200°C dried) phyllite *in vacuo*, both nitrogen and ammonia were released in the temperature interval between 400 and 700°C, whereas only molecular nitrogen was formed above 700°C. This latter finding was attributed to a rapid and quantitative oxidation by the rock.

In the case of ammonia in hydrothermal solutions, Kreulen and Schuiling (1982) first postulated the following reaction for post-entrapment generation of nitrogen in fluid inclusions:



Duit *et al.* (1986) proposed a similar reaction for the oxidation of ammonium ions liberated from biotite:



These latter authors also suggested that the water and hydrogen ions produced during this reaction may subsequently be used in retrograde hydrolysis reactions, such as the conversion of biotite to chlorite and the transformation of potassium feldspar to muscovite. In evidence, Duit *et al.* (1986) noted that $\text{CH}_4\text{-N}_2$ inclusions are particularly abundant in the vicinity of chloritised biotites and also in retrograde, recrystallised quartz at the Dôme de l'Agout, indicating that the inclusions are probably related to the liberation of nitrogen during retrograde metamorphism.

Dubessy *et al.* (1989) calculated the equilibrium constant of the above reaction between CO_2 and NH_3 as a function of temperature for the range 300-900°C. Although not explicitly stated, it would appear that their data relate to ideal gas conditions at 1 atm. pressure. The resulting values were found to lie within the limits of $\sim 10^{27}$ to 10^{20} . What this analysis does not illustrate, however, is the effect of competing reactions in the equilibrium mixture. For the present study, the computational procedures of Gordon and McBride (1971), adapted by the present author to incorporate the modified Redlich-Kwong equation of state of Holloway (1981), were used to evaluate the reaction between ammonia and carbon dioxide at temperatures of 300-900°C and for pressures of 1, 250, 500 and 1000 atm. For these calculations, ideal gas conditions were assumed to apply for the case of 1 atm. pressure, whereas ideal mixing of 'real' gases was considered for the calculations as applied to higher pressures.

The equation of state used to calculate the respective fugacity coefficients, although devised for gas mixtures of the C-H-O-N system, does not include provision for the non-ideality of ammonia. Hence the fugacity coefficient of this component was taken to be unity throughout the calculations. Equilibrium compositions were determined by the procedure of Gordon and McBride (1971), based on the minimisation of free energy. As ammonia is shown to be a trace component in the product mixture under a wide range of (T, P) conditions, however, its contribution to the total free energy of the system will be very small and consequently the effects of this approximation should not significantly affect the results obtained.

Figure 4.10

Predicted equilibrium compositions (mole fractions) resulting from the reaction between $8\text{NH}_3 + 3\text{CO}_2$ under a range of temperatures and pressures corresponding to crustal environments. Gordon and McBride (1971) procedure used for modelling, adapted to incorporate fugacity coefficients calculated using the equation of state of Holloway (1981) for total pressures $>1\text{atm}$, except for ammonia, which was assumed to behave ideally under all conditions.

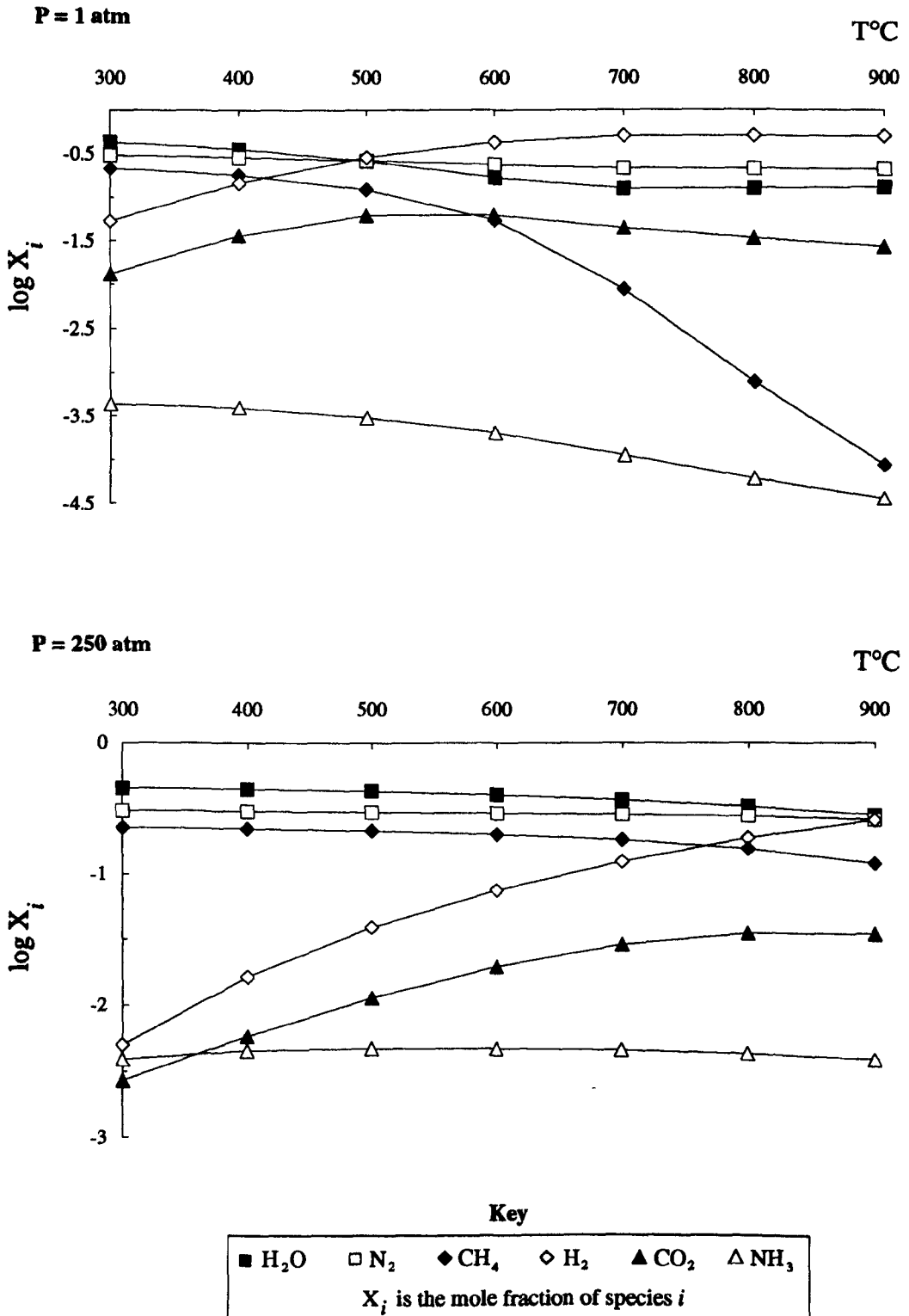
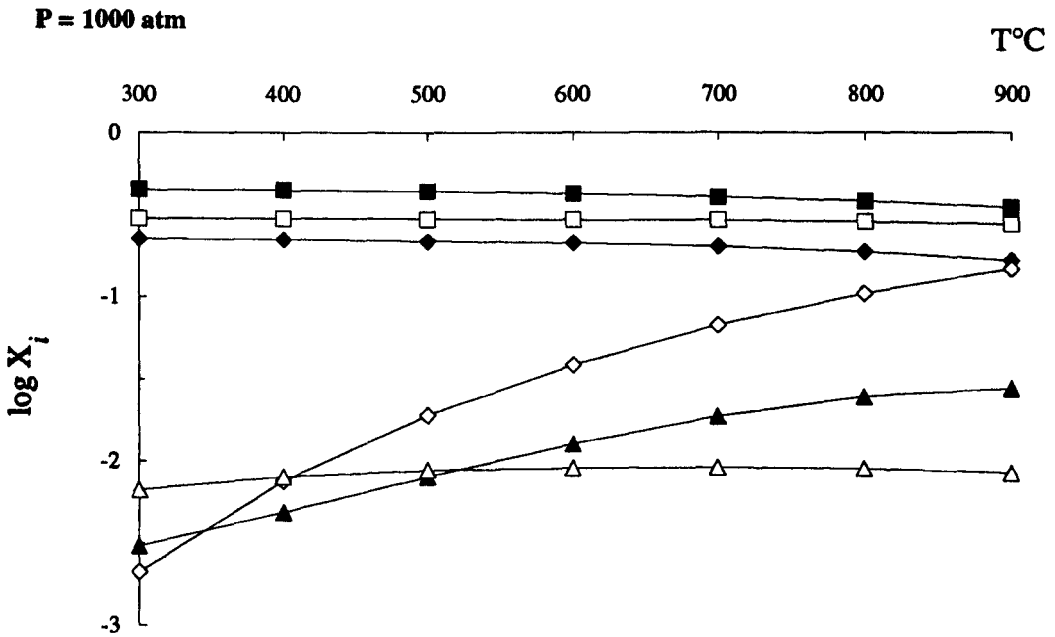
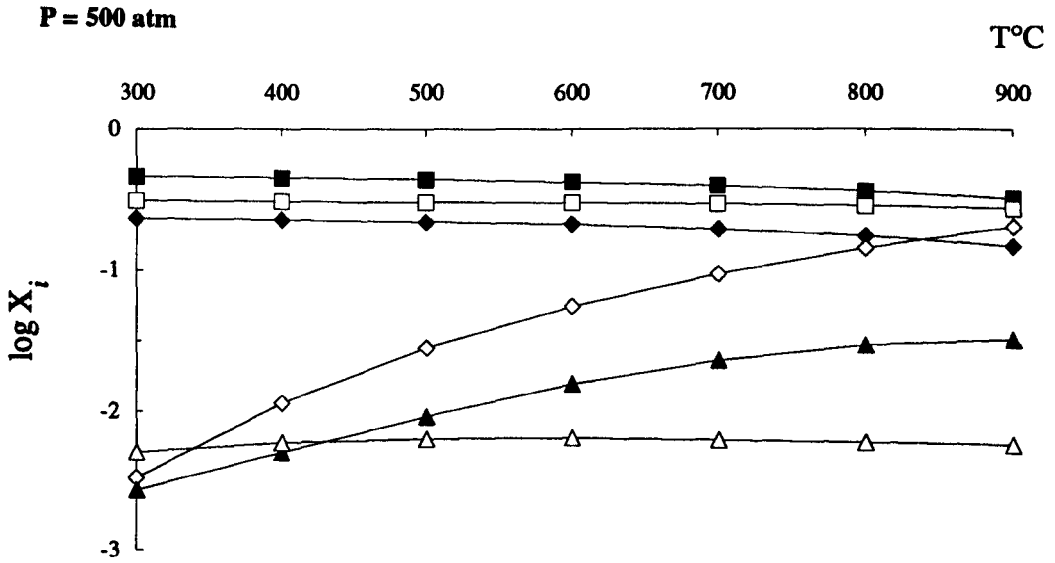


Figure 4.10 (continued)



Key

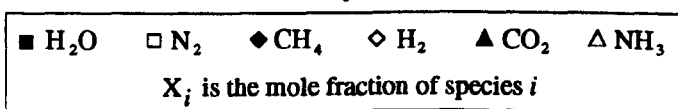


Figure 4.10 shows the predicted equilibrium compositions resulting from the reaction between ammonia and carbon dioxide under a range of temperatures and pressures corresponding to crustal environments, using the reactant stoichiometry as given by Kreulen and Schuiling (1982). The formation of molecular nitrogen, methane and water is shown to be favoured under the specified conditions, indicating that this postulated reaction is a viable mechanism for the source of molecular nitrogen in the palaeofluids. With regard to the equilibrium composition calculations, it should be noted that the thermodynamic database did not include NH_4^+ , which has therefore been excluded from the computations.

The oxidation of ammonia by graphite, as an alternative to carbon dioxide, has also been shown to be theoretically feasible on thermodynamic grounds (Bottrell and Miller, 1990). Calculations by Bottrell (*ibidem*) for the reaction



at 327°C, 1.8kbar, and assuming ideal mixing of real components, produced an estimate for the equilibrium constant of $10^{10.0}$. It should be noted, however, that the effects of competing reactions such as ammonia decomposition are not considered by this analysis. Furthermore, under hydrous conditions, oxidation-reduction reactions of graphite with water will be of significance. Although reaction between graphite and ammonia may be a feasible source of molecular nitrogen input to a hydrothermal fluid phase in certain lithologies, it is considered that this mechanism was unlikely to have been of significance in the Cornubian system.

4.9 Summary and Conclusions

Experimental techniques devised for the preparation and determination of nitrogen yields and stable isotope ratios at the sub-nanomole level have been assessed and applied to the study of traces of nitrogen in palaeo-hydrothermal fluids, trapped as fluid inclusions in vein quartz. Early post-emplacement palaeofluids associated with granite intrusives of the Cornubian batholith, S W England, and characterised by association with W±Sn oxide mineralisation, have been shown to contain nitrogen at concentrations ranging from about 10^{-2} to 0.34 molal, and corresponding to <1 to 13.8 ppm with regard to the respective quartz host. An empirical association between palaeofluid nitrogen concentrations and published ammonium contents of the associated granite pluton is evident.

The concentration and $\delta^{15}\text{N}$ values of nitrogen in the fluids do not appear to be significantly influenced by the host rock lithology. This is particularly evident at Hemerdon, where examples of veins hosted by unaltered granite, greisenised granite, and killas were investigated. These results suggest that little interaction occurred between the fluid and nitrogen sources in the host rock at high crustal levels in the evolving hydrothermal systems.

The $\delta^{15}\text{N}$ isotopic data for the fluids range from +5 to +10‰_(AIR), which is indicative of an organic precursor. Most of the $\delta^{15}\text{N}$ results are grouped within the range $6.5 \pm 1.5\%$. A notable finding of the investigation is that nitrogen at sub-ppm levels may be isolated and isotopically characterised from quartz representative of the earliest pegmatitic and cassiterite stage fluids hosted by the Dartmoor granite; furthermore, the isotopic characteristics are the same as found for fluids which are richer in nitrogen and associated with Cornubian granites of a more pronounced 'S'-type character. The source of nitrogen to the fluid phase is probably the oxidation of NH_4^+ , which is an abundant species in both the regional metasedimentary rocks and locally within the batholith. By way of comparison with the fluid inclusion data for S W England, $\delta^{15}\text{N}$ values of palæofluid nitrogen from five samples of early vein quartz (hosted by granite or gabbro) from the Carrock Fell wolframite deposit, Cumbria, all fall within the range $4.5 \pm 0.8\%$ _(AIR).

The incorporation of a substantial pelitic component to the parent magmas of the Cornubian granites during anatexis is generally accepted, on the basis of initial $^{87}\text{Sr}/^{86}\text{Sr}$ ratios and ϵ_{Nd} values, generally peraluminous major element chemistry, high K_2O contents and high concentrations of elements (such as B, As, Li) abundant in pelitic sediments. Published work has shown that there is a good correlation between the average ammonium content of the individual intrusions and the corresponding initial $^{87}\text{Sr}/^{86}\text{Sr}$ ratios and peraluminosity, indicating that the ammonium in the granites is probably derived from a sedimentary source, although at what stage is uncertain. The apparent correlation between the nitrogen content of the fluids and the ammonium content of the associated granite, as identified in the present work, supports the hypothesis that the granites are the most probable source of nitrogen in the fluids.

Using the most recently-published fractionation factors (Hanschmann 1981) for nitrogen isotopic equilibration between N_2 and NH_4^+ , together with whole-rock $\delta^{15}\text{N}$ data for the granites (Boyd *et al.*, 1993), it is evident that most of the isotopic data are in accord with equilibrated nitrogen exchange between N_2 in the palæofluid and NH_4^+ in the granites, at temperatures corresponding to hydrothermal activity (about 350-500°C) in the region. Initial equilibration temperatures cannot be determined from the isotopic data; consequently it is not possible to identify at what level in the system the oxidation of ammonium occurred. The more ^{15}N -enriched palæofluid at Old Gunnislake mine (measured $\delta^{15}\text{N}$ values of $8.2 \pm 0.29\%$ and $10.0 \pm 0.55\%$) may be explained by quantitative oxidation of granitic ammonium, if it is assumed that the $\delta^{15}\text{N}$ value of the Gunnislake granite falls within the range of 8.4-10.2‰ published for Cornubian granite whole-rock samples containing $> \sim 32$ ppm NH_4^+ . The same mechanism is also proposed for the Dartmoor system, where mean $\delta^{15}\text{N}$ values of early-stage hydrothermal fluids from three of the four samples analysed were within the range 6.7-7.3‰; identical, within experimental error, to the published $\delta^{15}\text{N}$ value of the host granite.

Equilibrium thermodynamic modelling suggests that the oxidation of ammonia by carbon dioxide, which invariably occurs with the nitrogen component in the palaeofluids investigated, is a viable mechanism for nitrogen formation under a wide range of (P,T) conditions.

It is considered that the most feasible mechanism by which nitrogen of isotopic composition +5 to +10‰_(AIR) in the fluids may be derived directly from the oxidation of ammonium in the metasedimentary rocks would be *via* selective metasomatic release to the fluid phase of a labile ammonium component relatively enriched in ¹⁵N.

4.10 Suggestions for further work

Apart from the exploratory investigation of hydrothermal fluids associated with early mineralisation of the Dartmoor granite, the present study has focused on localities where nitrogen is a readily identifiable component, albeit at trace levels, of the ancient hydrothermal systems. In the light of the findings reported above, the use of nitrogen stable isotopes as tracers of magmatic-hydrothermal fluids derived from 'S'-type granites would appear to be feasible. Further work would be required to test how widely this idea may be applicable.

In view of the proposed mechanism for the oxidation of ammonium in the granite by carbon dioxide, model experiments in which granite whole-rock samples are exposed to a CO₂-rich aqueous fluid under simulated hydrothermal conditions are needed to confirm the viability of this hypothesised source of molecular nitrogen.

Leaching experiments on SW England metasedimentary rocks under hydrothermal conditions, with subsequent nitrogen isotopic analysis of any soluble NH₄⁺ fraction released, would help to establish whether several ammonium components of differing nitrogen isotopic composition may be present and also their relative propensities to partition into the solution phase.

Chapter 5

The chemical composition of early mineralising fluids of the Cornubian batholith

5.1 Synopsis

Recent improvements in crush-leach procedures for the extraction and chemical analysis of quartz-hosted fluid inclusions have been applied to an investigation of the solute chemistry of ancient fluids that characterised the earliest stages of high-temperature hydrothermal mineralisation associated with the granites of SW England. In particular, a comparative regional study has been undertaken of electrolyte concentrations in quartz-hosted aqueous inclusions characteristic of early, high-temperature (300-450°C) fluids associated with the presence of W±Sn oxide assemblages in the region. The results, particularly when assessed in conjunction with complementary δD and $\delta^{18}O$ stable isotope data obtained on the associated palæo-water components (Chapter 2 of the present work), constrain hypotheses concerning the origin of these fluids in terms of the extent of contributions from 'magmatic' and other sources.

W±Sn oxide assemblages are virtually absent from hydrothermal veins hosted by the Dartmoor granite, which is anomalous in many respects amongst the intrusives that collectively form the Cornubian batholith. Hydrothermal mineralisation of the Dartmoor granite typically comprises assemblages of tourmaline, cassiterite, hæmatite and quartz, with individual deposits being distributed in a pattern indicative of large scale zoning within the pluton. In the present study, a detailed investigation of the chemical composition of palæofluids associated with various stages of mineralisation of the Dartmoor granite was undertaken, using representative examples from localities in the central and north-eastern regions of the pluton. Comparisons of the fluid electrolyte compositions associated with the different parageneses, in conjunction with complementary stable isotope data (δD , $\delta^{18}O$), were used to assess the extent to which the primary fluids may have been diluted by local groundwaters during the progressive stages of protracted hydrothermal activity. The data also permit contrasts to be made between the nature of the early, high-temperature hydrothermal fluids hosted by the Dartmoor granite, on the one hand, and comparable stage fluids as characterised by W±Sn oxide mineralisation elsewhere within the batholith. Such information contributes to a better understanding of the hydrothermal phenomena associated with mineralisation of the Cornubian granites and establishes a framework for interpretation of the associated geochemical processes that operated diachronously on a regional scale throughout the batholith.

5.2 Introduction

5.2.1 Procedures for the extraction and electrolyte analysis of aqueous fluid inclusions

Fluid inclusions trapped during mineral formation often provide the only direct access to information about the chemical composition of ancient (formerly high-temperature) crustal fluids at depth. Furthermore, knowledge of the electrolyte compositions of such fluids is of importance in the formulation and testing of geochemical models of fluid-rock interaction. Since the earliest investigations of fluid inclusion compositions by Davy (1822), a wide range of techniques has been applied to this field, as reviewed recently by Roedder (1990).

Significant progress has been made during recent years with the application of modern microbeam techniques to analyses of aqueous fluid inclusion electrolytes. For example, Diamond *et al.* (1991) used secondary ion mass spectrometry (SIMS) to determine cation ratios in individual inclusions in quartz and obtained good agreement with results obtained by bulk crush-leach analysis; Böhlke and Irwin (1992, and references therein) applied laser ablation to individual inclusions in neutron-irradiated hydrothermal minerals, in conjunction with noble gas isotope ratio analysis, to measure the relative concentrations of palæofluid Cl, Br, I and K.

Most published analyses of fluid inclusion electrolyte compositions, however, have been largely based on variations of the established crush-leach method as pioneered by Roedder (1958) and Roedder *et al.* (1963). In its original form, this involved the crushing under vacuum, in a copper tube, of sufficient quantity of mineral sample to enable a few mg of fluid to be extracted. The crushed sample was leached with high-purity demineralised water, with subsequent analysis of the filtrate by colourimetric and flame photometric methods. All samples were carefully selected and electrolytically cleaned before use. Quartz is generally the preferred host mineral for this type of analysis, on account of its chemical purity and minimal contamination of the leach solution[†], although results have been reported for inclusions in *e.g.* halite (Lazar and Holland, 1988) and calcite (Christie *et al.*, 1989).

As noted by Roedder (1984), it is probable that many of the numerous analyses of fluid inclusion leachate composition that have subsequently appeared in the scientific literature are of questionable or unverifiable accuracy, because of insufficiently rigorous experimental procedures and/or a lack of detailed information about the techniques adopted.

[†] Christie *et al.* (1989) showed that contamination from trace impurities in the host quartz may be a problem in crush-leach analyses of low-salinity, inclusion-poor material. In particular, Ca, Mg, Li and Zn, occasionally in balance with chloride, were found to be largely derived from the quartz, using water leaches; high levels of Al were also associated with the same problem. In the present study, these difficulties do not arise, due to the abundance of inclusions of high salinity.

Banks and Yardley (1992) and Channer and Spooner (1992) have recently reviewed the principal difficulties with crush-leach methods for the analysis of fluid inclusion electrolytes. These include:

(i) Problems associated with the presence of mineral impurities. The presence of even trace quantities of extraneous solid phases can drastically affect the chemical composition of the leachate, as manifest by anomalous enhancement of the abundances of elements such as Ca, Mg, Al and Fe (depending on the nature of the impurity) and contribute to charge imbalance (generally manifest as an excess of cations).

(ii) General lack of validation of procedures by recognised standards (usually synthetic inclusions of independently-verified composition); also few inter-laboratory (and inter-procedural) comparisons.

(iii) The extraction of multiple generations of inclusions, each with a distinct chemical composition. This problem is sample dependent to a large extent. It can be significantly reduced in some cases by developing procedures which require a smaller quantity of material, thereby permitting a greater degree of control over sample characterisation. Ultimately, it can only be resolved by single inclusion analysis.

(iv) Adsorption of polyvalent cations during crushing. Bottrell *et al.* (1988) showed that this was a serious problem; even with 1.28M HNO₃ as the leach solution, recovery of Ca and Mg was <80%, for solutions of initial respective concentration 1.00 and 0.100 µg/ml. A leaching solution of composition 0.13M HNO₃ + 200µg/ml La³⁺ (as LaCl₃) was found to be the most effective adsorption inhibitor. These findings indicated that most previous published analyses for divalent cations in fluid inclusions were likely to be significantly in error.

Bottrell *et al.* (1988) utilised multiple crushes of ~2g quartz in stainless steel or copper tubes, followed by leaching with doubly-distilled water or acidified LaCl₃, according to the elements to be analysed. Leachate solutions were analysed for Na (and K) by flame emission spectrophotometry (FES); other elements were determined by a variety of analytical procedures, in order to optimise sensitivity in each case. Element abundances were recorded as ratios to Na, following established practice.

Further refinements to the procedures of Bottrell *et al.* (1988) were subsequently reported by Banks and Yardley (1992), who developed a miniaturised adaptation of the crush-leach method. In particular, these latter authors showed that reproducible and accurate multi-element (Na, K, Mg, Fe, Mn, Zn) leachate analyses could be obtained on as little as 70mg of quartz sample, using a clean agate pestle and mortar to crush the quartz and using acidified

LaCl₃ as the leaching solution.[†] Furthermore, Banks and Yardley (1992) validated their procedures by analysis of a synthetic fluid inclusion sample. Additional developments by the same authors, such as the use of ion chromatography for the analysis of fluid inclusion anions (halogens and sulphate) were incorporated in the procedures used to investigate the fluid inclusion electrolyte chemistry of samples used in the present study.

5.2.2 The chemical composition of granite-hosted thermal groundwaters in S W England: evidence for (low-temperature) hydrothermal alteration of the granite?

The presence of thermal (up to 55°C) and saline groundwaters as inflows in Cornish tin mines has been documented since the second half of the last century (Miller, 1865; Phillips, 1873). These are the only saline groundwaters recorded from igneous rocks in the UK and contain up to 19,300 mg l⁻¹ total dissolved solids (11,890 mg l⁻¹ Cl⁻), with notably high concentrations of lithium, together with enhanced levels of other minor elements. The origin and evolution of saline and thermal groundwaters in the Carnmenellis granite has been investigated by Edmunds and co-workers (Edmunds *et al.*, 1984; Edmunds *et al.*, 1985; Edmunds *et al.*, 1987; Edmunds and Savage, 1991); these studies have shown that the thermal groundwaters are probably of meteoric origin, being almost identical to shallow, non-thermal waters in terms of $\delta^{18}\text{O}$ ($-5.5 \pm 0.5\%$) and δD ($-34 \pm 5\%$), and have circulated to a depth of ~1200m. The temperature of these waters is higher than would be expected purely on the basis of the average regional geothermal gradient (29.0°C km⁻¹ in the granite; up to 50°C km⁻¹ in the aureole) and implies the operation of upward convection processes. An 'end-member' high-salinity^{††} fluid component of approximate age ~10⁴ to 10⁶a was identified, containing possibly up to 30,000 mg l⁻¹ total dissolved solids.

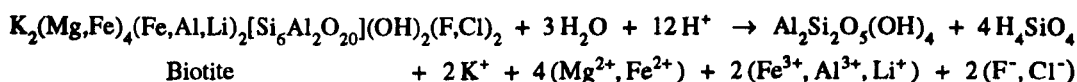
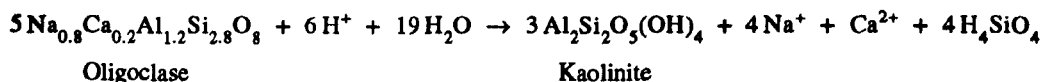
Edmunds *et al.* (1987) proposed that acid hydrolysis of plagioclase[‡] and biotite in the granite were the principal origins of the groundwater salinity and distinctive chemical compositions.

[†] The samples were of high temperature, hydrothermal quartz associated with the St Austell granite, S W England, and contained an abundance of inclusions with an approximate salinity of 15 wt % NaCl equivalent. That analyses for only six elements were reported was due to the small volume of acidified lanthanum chloride leaching solution used (1-2 ml), which precluded analysis by *e.g.* inductively-coupled plasma atomic emission spectrometry. Na and K concentrations were determined using FES; other elements were analysed by graphite furnace atomic absorption spectrometry.

^{††} 'Salinity' is defined as the amount of dissolved salts, with Br and I represented by the equivalent quantity of Cl and all bicarbonate and carbonate converted to oxide. It is expressed in g/kg (‰). 'Chlorinity', by contrast, refers to the chloride content of the water, including the chloride equivalent of other halides, in g/kg (‰). 'Standard' modern sea water has a chlorinity of 19.4‰ and corresponding salinity of 35.5‰.

[‡] Na- and Ca- feldspars form a continuous series of solid solutions, termed the plagioclase feldspars. These are triclinic Na-Ca aluminosilicates, ranging in composition from 100% albite (NaAlSi₃O₈) to 100% anorthite (CaAl₂Si₂O₈). Oligoclase is characterised by 70-90% albite, 10-30% anorthite.

As noted by Edmunds *et al.* (1987), plagioclase and biotite (amongst other rock-forming minerals) derive their compositions under conditions of high-temperature fluid-rock interaction and are generally thermodynamically unstable under hydrous conditions at lower temperature. The following reaction schemes were considered probable:



The formation of alternative reaction products of the acid hydrolysis of plagioclase, particularly laumontite ($\text{CaAl}_2\text{Si}_4\text{O}_{12}\cdot 4\text{H}_2\text{O}$) and possibly other clay minerals, was also suggested in accord with this scheme and would be consistent with field observations.[†]

A significant feature of the thermal groundwaters was the relative depletion of Na/Ca ratios (1.3 to 4.0, on a molar basis) compared with bulk feldspar compositions. This was attributed to preferential reaction of Ca-rich centres of zoned plagioclase. The high Li⁺ concentration (up to 125 mg l⁻¹) was related by Edmunds *et al.* (1987) to stoichiometric biotite hydrolysis. Cl⁻, like Li⁺, is probably conservative in that its release into thermal groundwaters is unlikely to lead to subsequent assimilation into a secondary mineral lattice. The Cl⁻ component of the groundwaters, however, whilst also postulated to originate from biotite, was considered to be derived by hydroxyl exchange without structural breakdown of the mineral. Concentrations in the thermal groundwaters of several minor and trace elements, including Sr, Ba, F, B, Br and Rb, were attributed to hydrolysis reactions of aluminosilicate minerals.

5.2.3 Hydrothermal alteration of the granite at higher temperature: evidence from model experiments

In an experimental investigation of the interaction of meteoric groundwater (simulated by a dilute Na-Ca-Cl-HCO₃ fluid of total dissolved salts <120 mg l⁻¹) with the Carnmenellis granite at 250°C and 50 MPa (500 bar), Savage *et al.* (1985) showed that the dissolution of plagioclase and K-feldspar was the dominant feature, with the concomitant precipitation of a Ca-aluminosilicate (probably laumontite), smectite, calcite and anhydrite. Interestingly, the nature of the hydrothermal alteration was similar to that reported by Giggenbach (1981) for geothermal systems of New Zealand. Savage *et al.* (1987) extended the results of the earlier

[†] It has been suggested that the biotite → kaolinite reaction rarely occurs in practice; the intermediate muscovite is generally formed, with the subsequent muscovite → kaolinite step being relatively unusual (Scrivener, 1982). Alternatively, the biotite may be altered to chlorite.

study by Savage *et al.* (1985) to show that the final reacted fluids were saturated with respect to quartz and fluorite and that concentrations of 15 of the 17 analysed chemical components showed net increases in the fluid phase, the exceptions being Ca (at 250°C) and Mg (at 250°C and at lower temperatures). It was also found that, under the experimental conditions used, certain trace elements (Li, B and Sr) did not behave conservatively in the fluid phase but were either incorporated into solids or adsorbed onto mineral surfaces.

The significance of these results is that they bridge the transition in temperature between the thermal groundwater studies of Edmunds *et al.* (1987, and references therein) and the (ancient) magmatic-hydrothermal regimes which provide the focus of interest of the present investigation.

5.2.4 The Dartmoor granite: magmatic activity and early hydrothermal alteration

5.2.4.1 Chronology of magmatic activity

Darbyshire and Shepherd (1985), in an investigation of the Rb-Sr geochronology of granite magmatism and associated mineralisation in S W England, reported an emplacement age of 280 ± 1 Ma for the Dartmoor granite, with an associated $^{87}\text{Sr}/^{86}\text{Sr}$ initial ratio of 0.7101 ± 0.0004 . The age relationship between the Dartmoor granite and associated mineralisation was not investigated by these authors, however. More recently, a thermochronological study of the Cornubian batholith by Chesley *et al.* (1993), whilst reporting U-Pb and $^{40}\text{Ar}/^{39}\text{Ar}$ ages for the Dartmoor granite statistically indistinguishable from the Rb-Sr age given by Darbyshire and Shepherd (1985), showed that the cooling rate of this pluton (~ 60 to 85°C Ma^{-1}) was significantly slower than any other in the batholith, implying that the Dartmoor granite may be exposed at a deeper level.[†] On the basis of $^{40}\text{Ar}/^{39}\text{Ar}$ age spectra of muscovite samples, Chesley *et al.* (1993) concluded that the Dartmoor pluton is a composite body, having resulted from multiple episodes of magmatism, as suggested on the basis of field observations (*e.g.* Brammall and Harwood, 1932). According to Schneider (1990), the earliest stage of magma emplacement was characterised by initial crystallisation at ~ 5 kbar pressure, $\sim 800^\circ\text{C}$ and a water content of 4.5%

[†] This finding concerning the cooling rate, however, is disputed by the results of a parallel investigation by Clark and co-workers (Clark *et al.*, 1993; Chen *et al.*, 1993), using similar techniques. On the basis of their data, these authors suggested that there was no distinction between the cooling rates of component plutons of the batholith. Willis-Richards and Jackson (1989), on the other hand, proposed accelerated cooling of the Dartmoor granite, supposedly the result of rapid unroofing.

5.2.4.2 Paragenetic stages of hydrothermal mineralisation

The Dartmoor granite is unusual in several respects, among the plutons that collectively form the Cornubian batholith of SW England. High-temperature tourmaline-quartz veins are widely distributed in the marginal and roof zones of the pluton, locally hosting cassiterite and hæmatite which occur separately or together in very variable proportions. The intra-granitic hydrothermal veins are sulphide-deficient, in contrast to those hosted by the surrounding metasedimentary country rocks, and are characterised by a relatively restricted mineralogy. Comprehensive accounts of the geology are to be found in Hawkes (1982) and Scrivener (1982); summaries incorporating more recent data have been given by Darbyshire and Shepherd (1985) and Chesley *et al.* (1993). According to Scrivener (1982), four distinct paragenetic stages of hydrothermal mineralisation of the Dartmoor granite may be recognised; the classification proposed by Scrivener (1982) is adopted throughout the present work.

The initial stage (Stage I) involved fracture-filling deposition of tourmaline throughout the pluton, probably as the consequence of rapid decompression of highly saline, boron-rich fluids exsolved from late-stage magma. Deposition of quartz+tourmaline±cassiterite assemblages (Stage II) followed; widespread evidence for fluid boiling, both before and during the deposition of cassiterite, was reported on the basis of fluid inclusion evidence (Scrivener, 1982; Shepherd *et al.*, 1985). Hæmatite±quartz deposition (particularly well-developed in central Dartmoor and in the north-eastern part of the pluton) marked the post-cassiterite stage of mineralisation and characterises Stage III. The presence of a large area of the granite in which hæmatite (both specular and micaceous) occurs is a feature unique to Dartmoor, among the plutons of the Cornubian batholith. Scrivener (1982) noted that coarse, specular hæmatite is prevalent in the Birch Tor & Vitifer district of central Dartmoor, whereas micaceous hæmatite predominates in cassiterite-deficient veins located in the north-east of the pluton, close to the contact zone; it was postulated that this may reflect the level in the hydrothermal system at which the mineralisation is exposed. Low temperature deposition of chalcedonic quartz characterised the final stage of the paragenetic sequence (Stage IV). The partial or complete alteration of plagioclase to clay minerals (primarily kaolinite) in both coarse-grained and fine-grained granite is evident in several areas on Dartmoor, mostly in the southern parts of the pluton; the initial alteration may also be the product of hydrothermal activity (Hawkes, 1982).

Wall-rock alteration associated with hydrothermal mineralisation in the central region of the Dartmoor granite is complex. Albite, orthoclase, chlorite, sericite and kaolin are all present†;

† Orthoclase is the common rock-forming alkali feldspar KAlSi_3O_8 . Chlorite is a hydroxy Mg-Fe aluminosilicate mineral of stoichiometric composition $(\text{Mg,Fe})_3(\text{Si,Al})_4\text{O}_{10}(\text{OH})_2(\text{Mg,Fe})_3(\text{OH})_6$. Sericite is the term used to describe a fine-grained white mica.

sericitic alteration of the granite is particularly pervasive (Scrivener, 1982). The same author reported that, whilst it is difficult to establish the chronology of alteration phenomena, because of overlap in the sequence (and multiple episodes of hydrothermal activity), the formation of albite occurred early and was contemporaneous with the major deposition of tourmaline (Stage I), whereas the growth of orthoclase was recognised to be associated with later tourmaline and cassiterite deposition (Stage II).

5.2.5 Sampling localities

Two sets of (quartz) samples were used for the present investigation. The first consisted of examples representative of various stages of hydrothermal alteration of the Dartmoor granite, from the earliest, high-temperature pegmatitic stage, through quartz+tourmaline±cassiterite assemblages, to later (and lower temperature) hæmatite±quartz mineralisation. Appendix A details the sample descriptions and documents the sampling localities included in this work, from which it is apparent that most of the Dartmoor material derived from East Vitifer and Golden Dagger mines, in the central region of the pluton exposure and well away from the metasedimentary contact zone. A notable exception is the sample (SW-89-157) collected from the north lode of Great Rock mine (north-eastern Dartmoor), in close proximity to the contact and distinguished by the presence of pyrite as well as hæmatite, which contrasts strongly with the sulphur-deficient environment characteristic of the intra-granitic hydrothermal veins.

The second set of samples was selected as representative of quartz associated with the earliest post-pegmatitic stage hydrothermal fluids, characterised by the deposition of W±Sn oxide assemblages throughout S W England. Examples were included from four of the principal wolframite occurrences associated with the Cornubian batholith, viz. Hemerdon mine, Cligga Head, South Crofty mine and Castle-an-Dinas mine (St Austell district), together with examples associated with minor granite intrusives (Gunnislake and Hingston Down) located between the Dartmoor and Bodmin Moor plutons. W±Sn oxide assemblages occur as fissure veins in the granites (sometimes in the form of stockworks and vein swarms, such as at Cligga Head and Hemerdon) and killas country rock. Intra-granitic vein swarms in the region are usually associated with greisening (the development of micaceous borders, through pneumatolytic alteration) and the presence of potassium feldspar.

Samples from Hemerdon included examples of both endo-granitic and killas-hosted veins, both of which are, in general, greisen bordered, with variable amounts of K-feldspar. Sulphides are present in only minor quantities at Hemerdon, occurring as irregular patches of pyrite in the host rocks (Beer and Ball, 1987). The W±Sn oxide assemblages occur primarily in the granite, in association with both quartz-feldspar and greisen-bordered veins; the latter are distributed as swarms, similar to those found at Cligga Head. As noted by Beer and

Scrivener (1982), the granite within the mineralised stockwork has undergone extensive hydrothermal alteration, with hæmatitic staining and variable near-surface kaolinisation. Minor occurrences of arsenopyrite are present at depth.

5.3 Research objectives

There were two principal objectives to the present investigation. One was to characterise chemically, on a regional basis, palæo-hydrothermal fluids associated with early W±Sn oxide mineralisation in S W England. 'Splits' of the quartz samples used in this study were also investigated with respect to fluid inclusion δD and $\delta^{18}O$ isotopic composition (Chapter 2) and stable isotopic characterisation of trace carbon species and molecular nitrogen in the fluids (Chapters 3 and 4 respectively). Analysis of the associated electrolyte compositions therefore provides additional constraints on the nature and origin of these fluids, which represent the transition from pegmatites to hydrothermal oxide mineralisation in the region. Such information also indicates the extent of fluid-rock interaction between the granites (and/or metasedimentary country rocks) and the evolving hydrothermal system, ultimately leading to a better understanding of the high-temperature hydrothermal alteration of component plutons of the Cornubian batholith.

The second objective involved a comparative assessment of fluids responsible for the various paragenetic stages of early hydrothermal mineralisation of the Dartmoor granite. Such information, in conjunction with δD and $\delta^{18}O$ measurements of the associated waters (Chapter 2), provides a basis for assessing the extent to which magmatically-equilibrated fluids were involved in the hydrothermal system, from the earliest pegmatitic quartz, through quartz+tourmaline±cassiterite (Stage II) assemblages, to low-temperature quartz+hæmatite deposition (Stage III). In turn, this provides a basis for assessing whether external fluids entered vein fractures of the Dartmoor granite at an early stage after emplacement. The comparison might also be expected to lend support to (or refute) arguments for the degree of 'S'-type character of the host pluton influencing the chemical composition of the associated magmatic-hydrothermal system.

5.4 Experimental

Fluid inclusion crush-leach analyses were undertaken using procedures largely based on the work of Bottrell *et al.* (1988); further information is provided in Banks *et al.* (1991), although procedures have since been modified in detail to incorporate more recent developments. As noted by Banks *et al.* (1991), sample preparation is of critical importance; all extraneous grains must be removed and stringent cleaning procedures subsequently applied, prior to extraction of the inclusion fluids. In the present work, quartz samples were prepared in

accordance with the recommendations of Bottrell *et al.* (1988), except that a coarser grain size (0.5-1.0mm) was used. The inclusions were opened by grinding, using an agate mortar and pestle; approximately 2g of quartz grains were used for each leaching experiment. Acidified LaCl₃ solution (200ppm La³⁺ in 0.13M HNO₃) was used for leaching in the case of cation (and boron) analyses; separate 'splits' of the quartz were crushed and subsequently leached using doubly-distilled water for anion analyses.[†] Inclusion-free quartz samples were prepared using the same procedures, to determine blank levels.

Each leachate solution was analysed by inductively-coupled plasma atomic emission spectrometry (ICP-AES) for the following cations: Na, K, Ca, Mg, Al, Ba, Li, Sr, Fe, Mn, Cu and Zn, together with B (as borate). ICP-AES has the advantage of simultaneous multi-element analysis on relatively small volumes of solution and is also particularly suitable for certain elements, such as boron. As noted by Bottrell *et al.* (1988), however, these advantages are generally at the expense of poorer detection limits and sensitivity compared to other methods. Na and K abundances were additionally determined by flame emission spectrometry (FES) and the concentrations of Cu, Pb, As, Be and Bi measured by graphite furnace atomic absorption spectrometry (GFAAS). Rb and U concentrations were determined by isotope dilution mass spectrometry. Anion analyses (F, Cl, Br, I and sulphate) were undertaken using ion chromatography. All analytical data were initially converted to element concentrations ratios (by mass) relative to Na, for comparison purposes. Following chemical analysis of the Dartmoor fluid inclusion leachates, 'splits' of the same quartz samples were used to supply Dr D M Wayne (University of Leeds) with replicate leachate solutions for determinations of the isotopic composition of fluid inclusion Sr and Pb.

5.5 Results - fluid inclusion leachate analyses

For both the investigation of quartz-hosted palæo-hydrothermal fluid electrolyte compositions associated with the different stages of early mineralisation of the Dartmoor granite, and for the comparative assessment of fluids characterised by W±Sn oxide association, the fluid inclusion leachate data are presented in a similar manner.

5.5.1 Dartmoor hydrothermal quartz

Element relative abundances in the fluid inclusion leachate solutions normalised by mass to Na=10,000 are shown in Table 5.1(a). Duplicate crush-leach cation (and borate) analyses were undertaken in two cases, with generally very good reproducibility of the resulting data.

[†] Apart from the obvious problem of chloride interference from use of LaCl₃ in 0.13M HNO₃ as the leaching solution for anion analysis, nitrate ion interferes with the analysis of bromide.

In Table 5.1(b), the same results are reported in terms of element mole ratios relative to Na, from which the degree of ionic charge imbalance (as characterised by the $\Sigma Q^+ - \Sigma |Q^-|$ charge difference and by the corresponding $\Sigma Q^+ / \Sigma |Q^-|$ ratio) has been determined in all cases.[†] For the seven samples representative of Stages I and II of the paragenetic sequence, it is seen that the charge balances are excellent. Moreover, the example representative of Stage III fluids from East Vitifer mine exhibits reasonably good charge balance. Only in the case of quartz associated with hæmatite deposition at Great Rock mine is the charge balance relatively poor. However, the anomalously high Al concentration noted for this example indicates probable contamination of the leachate by feldspar; also, the excessive abundance of Fe may be attributed to the presence of residual hæmatite, intergrown with the quartz.

To reconstruct the original inclusion fluid electrolyte concentrations (absolute values) from the corresponding leachate data, recourse is made to estimates of the inclusion fluid salinities as determined during microthermometric studies. Microthermometric analysis allows only first-order estimates of palæofluid salinities to be derived in many of the examples included in the present investigation, however, because of the presence, in variable proportions, of distinct inclusion types (monophase or multi-phase; predominantly vapour-rich or otherwise; with or without one or more solid phases), generally characterised by different salinity ranges.[‡]

Furthermore, salinity data based on *e.g.* halite dissolution temperatures or final ice melting temperatures (or $\text{CO}_2 \cdot 5\frac{3}{4} \text{H}_2\text{O}$ clathrate melting temperature, in the case of CO_2 -bearing inclusions), are usually expressed in terms of wt% NaCl equivalent; this simplification may lead to chloride concentration estimates that are significantly in error in the case of complex, multi-element chloride solutions (as considered here, on the basis of the present evidence). For these reasons, estimates of bulk palæofluid salinities are presented in terms of probable lower and upper limit values in the present work, as derived from an assessment of microthermometric data reported in the literature. It must be emphasised that the reconstructed palæofluid electrolyte compositions (absolute concentrations) based on these salinity estimates are therefore subject to the significant uncertainties inherent in the interpretation of the microthermometric measurements.

[†] For the charge balance calculations, it has been assumed that all Fe in solution is divalent, as indicated by several experimental studies of iron-chloride complexing in (sulphur-free) hydrothermal fluids (Fein *et al.*, 1992, and references therein). Also, all B is assumed to be present as BO_3^{3-} .

[‡] A wide range of salinity may in some cases be attributed to boiling of the fluid. In such cases, however, most constituent solutes should be strongly partitioned into the liquid phase, thus not significantly affecting the respective ratios to sodium.

Table 5.1(a)

Dartmoor hydrothermal quartz: fluid inclusion leachate data. Element relative abundances (by mass), normalised to Na = 10,000

Locality (mine): Paragenesis: Sample reference:	Golden Dagger		Barracott	East Vitifer		Golden Dagger	East Vitifer	Great Rock			
	Stage I	Stage I	Stage II	Stage II	Stage II	Stage II (III)	Stage II (III)	Stage III			
	SW-89-159	SW-89-160	SW-89-164	SW-89-155	SW-89-156	SW-89-162	SW-89-163	SW-89-154	SW-89-157		
Na	10,000	10,000	10,000	10,000	10,000	10,000	10,000	10,000	10,000		
K	2,239	2,401	1,888	1,934	1,870	2,322	1,557	1,568	2,113	1,944	2,112
Ca	4,386	4,415	3,928	4,067	4,115	3,962	4,030	4,004	5,582	4,099	6,450
Mg	23	28	41	34	26	20	36	35	98	58	74
Al	194	202	155	151	124	108	259	271	346	338	11,183
Ba	22	23	27	28	21	27	12	14	21	21	57
Be	0.24	na	0.34	0.23	0.16	0.15	1.39	1.31	0.75	0.55	na
Li	40	25	35	35	40	33	83	83	35	68	46
Sr	80	81	73	74	72	72	67	67	91	68	51
Rb	40	na	na	33	22	39	32	29	32	24	na
Fe	1,021	1,033	458	471	848	1,030	497	465	968	922	2,226
Mn	580	202	606	631	496	501	445	427	667	468	1,267
Pb	35	22	29	30	27	22	20	21	54	24	26
Zn	116	119	127	125	98	93	88	87	142	93	194
Cu	5	6	3	5	5	8	12	12	19	28	11
As	25	na	16	12	14	14	27	25	26	25	na
Bi	0.5	na	nd	nd	0.4	0.5	nd	nd	1	1.3	na
U	3.77	na	0.45	0.25	0.46	2.3	na	2.35	2.0	1.0	0.03
B	179	200	132	114	138	140	254	255	363	180	63
SO ₄	80	236	134	na	125	51	43	na	106	66	na
F	130	na	374	na	132	74	1,304	na	467	73	na
Cl	25,738	25,082	24,923	na	24,600	25,218	21,976	na	27,453	23,763	24,950
Br	46	40	45	na	47	45	32	na	53	44	45
I	3.2	2.8	1.3	na	3.1	1.7	1.5	na	1.5	0.8	0.9

Notes: (1) na indicates *not analysed*; nd indicates *not detected*.

(2) Samples SW-89-157 and SW-89-160 were treated with fluorosilicic acid, H₂SiF₆, in an attempt to remove traces of feldspar.

The use of H₂SiF₆ to selectively remove feldspar from quartz was recommended by Syers *et al.* (1968), although the feldspar grain size in their experiments was <50µm.

(3) Residual intergrown feldspar in sample SW-89-157 is probably responsible for the anomalously high Al, Ca and Mg values.

(4) Sample SW-89-161 (Golden Dagger mine, stage III) gave very low ion yield, as shown in Appendix G (Tables G3, G4 and G5), hence analytical results not considered here.

Table 5.1(b)

Dartmoor hydrothermal quartz: fluid inclusion leachate data. Element mole ratios, normalised to Na = 1

Locality (mine): Paragenesis: Sample reference:	Golden Dagger		Barracott	East Vitifer		Golden Dagger		East Vitifer	Great Rock
	Stage I	Stage I	Stage II	Stage II	Stage II	Stage II (III)	Stage II (III)	Stage III (II)	Stage III
	SW-89-159	SW-89-160	SW-89-164	SW-89-155	SW-89-156	SW-89-162	SW-89-163	SW-89-154	SW-89-157
Na	1	1	1	1	1	1	1	1	1
K	0.1317	0.1412	0.1124	0.1100	0.1365	0.0919	0.1242	0.1143	0.1242
Ca	0.2516	0.2532	0.2293	0.2360	0.2273	0.2304	0.3202	0.2351	0.3700
Mg	0.0022	0.0026	0.0035	0.0025	0.0019	0.0034	0.0093	0.0055	0.0070
Al	0.0165	0.0172	0.0130	0.0106	0.0092	0.0226	0.0295	0.0288	0.9529
Ba	0.00037	0.00039	0.00046	0.00035	0.00045	0.00022	0.00035	0.00035	0.00095
Be	0.00006	na	0.00007	0.00004	0.00004	0.00034	0.00019	0.00014	na
Li	0.0132	0.0083	0.0116	0.0132	0.0109	0.0275	0.0116	0.0225	0.0152
Sr	0.00210	0.00213	0.00193	0.00189	0.00189	0.00176	0.00239	0.00178	0.00134
Rb	0.00108	na	na	0.00059	0.00105	0.00082	0.00086	0.00065	na
Fe	0.0420	0.0425	0.0191	0.0349	0.0424	0.0198	0.0398	0.0380	0.0916
Mn	0.0243	0.0085	0.0259	0.0208	0.0210	0.0182	0.0279	0.0196	0.0530
Pb	0.00039	0.00024	0.00033	0.00030	0.00024	0.00023	0.00060	0.00027	0.00029
Zn	0.00408	0.00418	0.00443	0.00345	0.00327	0.00308	0.00499	0.00327	0.00682
Cu	0.00018	0.00022	0.00014	0.00018	0.00029	0.00043	0.00069	0.00101	0.00040
As	0.00077	na	0.00043	0.00043	0.00043	0.00080	0.00080	0.00077	na
Bi	0.000006	na	nd	0.000004	0.000006	nd	0.000011	0.000014	na
U	0.000036	na	0.000003	0.000004	0.000022	0.000023	0.000019	0.000010	<0.000001
B	0.0381	0.0425	0.0262	0.0293	0.0298	0.0541	0.0772	0.0383	0.0134
SO ₄	0.00191	0.00565	0.00321	0.00299	0.00122	0.00103	0.00254	0.00158	na
F	0.0157	na	0.0453	0.0160	0.0090	0.1578	0.0565	0.0088	na
Cl	1.6690	1.6265	1.6162	1.5952	1.6353	1.4251	1.7802	1.5409	1.6179
Br	0.00132	0.00115	0.00129	0.00135	0.00129	0.00092	0.00152	0.00127	0.00129
I	0.00006	0.00005	0.00002	0.00006	0.00003	0.00003	0.00003	0.00001	0.00002
Total cationic charge, ΣQ^+	1.8526	1.8291	1.7348	1.7576	1.7750	1.7462	2.0405	1.8362	5.0608
Total anionic charge, ΣQ^-	-1.8041	-1.7666	-1.7476	-1.7066	-1.7373	-1.7482	-2.0749	-1.6690	-1.6594
Charge difference, $\Sigma Q^+ - \Sigma Q^- $	0.0484	0.0626	-0.0128	0.0509	0.0376	-0.0020	-0.0344	0.1672	3.4014
Charge ratio, $\Sigma Q^+ / \Sigma Q^- $	1.027	1.035	0.993	1.030	1.022	0.999	0.983	1.100	3.050

Notes: (1) na indicates not analysed; nd indicates not detected.

(2) For charge balance calculations, the following formal oxidation states were assumed: Fe = +2, Mn = +2, As = +3, Bi = +3, U = +6, B = -3.

(3) SW-89-162 and SW-89-164 data are mean values of duplicate analyses.

(4) SW-89-157 and SW-89-160 were treated with fluorosilicic acid, H₂SiF₆. Residual intergrown feldspar in SW-89-157 probably responsible for anomalous Al, Ca and Mg values.

Fluid inclusion microthermometric analysis by Shepherd *et al.* (1985) of quartz-hosted inclusions associated with Stages II and III (respectively) of hydrothermal mineralisation of the Dartmoor granite in the Birch Tor & Vitifer region indicated that four basic types of (intimately associated) inclusion may be described, exhibiting a wide range of salinities. For the present study, the salinity data of Shepherd *et al.* (1985) were used and the assumption made that bulk salinity is predominantly controlled by the halite-bearing, multi-phase inclusions. Shepherd *et al.* (1985) reported that inclusions containing 20-25 wt% NaCl contained significant amounts of CaCl₂, as inferred from the associated very low eutectic temperatures (<-50°C); otherwise (excepting the notable absence of any detectable CO₂) the fluids were apparently similar in many respects to those associated with early oxide mineralisation at nearby Hemerdon.

Shepherd *et al.* (1985) reported that Stage III quartz at Birch Tor was poor in inclusions and that those present were invariably devoid of solid phases at room temperature; the corresponding salinity values were <20 wt% NaCl equivalent. Unpublished microthermometric measurements by Scrivener (*pers. comm.*) indicated that fluids associated with late-stage hæmatite deposition at Great Rock mine were cooler (~180°C) and of lower salinity than those characteristic of the comparable stage at Birch Tor. This could not be verified in the present study because the quartz (sample SW-89-157) from Great Rock mine was disseminated as small, irregular grains in a predominantly hæmatite matrix; it was consequently not feasible to have polished thin sections prepared from such material.

Scrivener (1982) reported that fluid inclusions are virtually absent from Stage I quartz (and associated tourmaline) from Dartmoor. In contrast, optical examination by the present author of polished thin sections of early pegmatitic quartz examples included in the current investigation (samples SW-89-159 and SW-89-160, from Golden Dagger mine) indicated the presence of relatively large inclusions, sparsely distributed, together with an abundance of trails of much smaller inclusions, probably of secondary origin. Multiple daughter salts were also observed. For the purposes of the present investigation, it was assumed that, to a first approximation, the salinity range of the Stage I fluids is similar to that derived from published data relating to Stage II examples.

Estimates of palæofluid electrolyte concentration limits associated with the various paragenetic stages of hydrothermal mineralisation of the Dartmoor granite, as determined on the basis of the present fluid inclusion leachate results in conjunction with salinities derived from microthermometric data, are reported in Tables 5.2(a) and 5.2(b), in terms of µg/cm³H₂O and as element molal concentrations, respectively.

Table 5.2(a)

Reconstructed palaeofluid electrolyte concentrations (ppm) corresponding to estimated salinity limits of quartz-hosted aqueous inclusion fluids associated with hydrothermal mineralisation of the Dartmoor granite

Locality (mine) :	Golden Dagger				Baracott		East Vitifer			
Paragenesis :	Stage I		Stage I		Stage II		Stage II		Stage II	
Sample reference :	SW-89-159		SW-89-160		SW-89-164		SW-89-155		SW-89-156	
Wt % NaCl equivalent:	25	35	25	35	25	35	25	35	25	35
Na	55,572	77,801	56,666	79,333	57,970	81,159	58,378	81,730	57,099	79,939
K	12,443	17,420	13,606	19,048	11,078	15,509	10,917	15,283	13,258	18,562
Ca	24,374	34,123	25,018	35,026	23,174	32,443	24,023	33,632	22,623	31,672
Mg	128	179	159	222	217	304	152	212	114	160
Al	1,078	1,509	1,145	1,603	887	1242	724	1,013	617	863
Ba	122	171	130	182	159	223	123	172	154	216
Be	1.3	1.9	na	na	1.7	2.3	0.9	1.3	0.9	1.2
Li	222	311	142	198	203	284	234	327	188	264
Sr	445	622	459	643	426	597	420	588	411	576
Rb	222	311	na	na	191	268	128	180	223	312
Fe	5,674	7,943	5,854	8,195	2,693	3,770	4,950	6,931	5,881	8,234
Mn	3,223	4,512	1,145	1,603	3,585	5,020	2,896	4054	2,861	4,005
Pb	195	272	125	175	171	239	158	221	126	176
Zn	645	902	674	944	730	1,023	572	801	531	743
Cu	28	39	34	48	23	32	29	41	46	64
As	139	195	na	na	81	114	82	114	80	112
Bi	3	4	na	na	nd	nd	2	3	3	4
U	21	29	na	na	2	3	3	4	13	18
B	995	1,393	1,133	1,587	713	998	806	1,128	799	1,119
SO ₄	445	622	1,337	1,872	777	1,088	730	1,022	291	408
F	722	1,011	na	na	2,168	3,035	771	1,079	423	592
Cl	143,031	200,244	142,131	198,983	144,480	202,272	143,611	201,055	143,992	201,589
Br	256	358	227	317	261	365	274	384	257	360
I	18	25	16	22	8	11	18	25	10	14

Notes: (1) The salinity limit values were chosen on the basis of microthermometric data reported by Shepherd *et al.* (1985).

(2) na indicates *not analysed*. nd indicates that the component was *not detected* in the fluid inclusion leachate solution.

(3) For a wt % NaCl equivalent value of *x*, the total mass of dissolved salts, in units of μg per g of fluid, = $10,000x$. For each sample, therefore, the element relative abundances (by mass), as determined by fluid inclusion leachate analyses, were normalised to sum to this value to generate the data shown.

Table 5.2(a) continued

Reconstructed palaeofluid electrolyte concentrations (ppm) corresponding to estimated salinity limits of quartz-hosted aqueous inclusion fluids associated with hydrothermal mineralisation of the Dartmoor granite

Locality (mine) :	Golden Dagger				East Vitifer		Great Rock	
Paragenesis :	Stage II (III)		Stage II (III)		Stage III (II)		Stage III	
Sample reference :	SW-89-162		SW-89-163		SW-89-154		SW-89-157	
Wt% NaCl equivalent:	25	35	25	35	15	25	5	15
Na	61,348	85,887	51,397	71,955	35,453	59,088	8,510	25,529
K	9,586	13,420	10,860	15,204	6,892	11,487	1,797	5,392
Ca	24,643	34,501	28,690	40,165	14,532	24,220	?	?
Mg	218	305	504	705	206	343	?	?
Al	1,626	2,276	1,778	2,490	1,198	1,997	?	?
Ba	80	112	108	151	74	124	49	146
Bc	8.3	12	4	5.4	1.9	3.2	na	na
Li	509	713	180	252	241	402	39	117
Sr	411	575	468	655	241	402	43	130
Rb	187	262	164	230	85	142	na	na
Fe	2,951	4,131	4,975	6,965	3,269	5,448	1,894	5,683
Mn	2,675	3,745	3,428	4,799	1,659	2,765	1,078	3,235
Pb	126	176	278	389	85	142	22	66
Zn	537	752	730	1,022	330	550	165	495
Cu	74	103	98	137	99	165	9	28
As	160	223	134	187	89	148	na	na
Bi	nd	nd	5	7	5	8	na	na
U	14	20	10	14	4	6	0.03	0.08
B	1,561	2,186	1,866	2,612	638	1064	54	161
SO ₄	264	369	545	763	234	390	na	na
F	8,000	11,200	2,400	3,360	259	431	na	na
Cl	134,818	188,745	141,099	197,539	84,247	140,411	21,232	63,696
Br	196	275	272	381	156	260	38	115
I	9	13	8	11	3	5	1	2

- Notes: (1) Estimates of Ca, Mg, Al and Fe concentrations were not feasible for SW-89-157 because of probable contamination of leachate solution by feldspar.
(2) na indicates *not analysed*. nd indicates that the component was *not detected* in the fluid inclusion leachate solution.
(3) Because of overprinting by later stage fluids, selection of samples that contain purely Stage II or Stage III fluids is probably not feasible.
Where a paragenetic stage is shown in parentheses, this indicates that minor veining by the associated fluids may be of significance.

Table 5.2(b)

Reconstructed palaeofluid electrolyte concentrations (molal) corresponding to estimated salinity limits of quartz-hosted aqueous inclusion fluids associated with hydrothermal mineralisation of the Dartmoor granite

Locality (mine) :	Golden Dagger				Barracott		East Vitifer			
Paragenesis :	Stage I		Stage I		Stage II		Stage II		Stage II	
Sample reference :	SW-89-159		SW-89-160		SW-89-164		SW-89-155		SW-89-156	
Wt % NaCl equivalent:	25	35	25	35	25	35	25	35	25	35
Na	3.223	5.206	3.286	5.309	3.362	5.431	3.386	5.469	3.312	5.349
K	0.424	0.685	0.464	0.750	0.378	0.610	0.372	0.601	0.452	0.730
Ca	0.811	1.310	0.832	1.344	0.771	1.245	0.799	1.291	0.753	1.216
Mg	0.007	0.011	0.009	0.014	0.012	0.019	0.008	0.013	0.006	0.010
Al	0.053	0.086	0.057	0.091	0.044	0.071	0.036	0.058	0.030	0.049
Ba	0.0012	0.0019	0.0013	0.0020	0.0015	0.0025	0.0012	0.0019	0.0015	0.0024
Be	0.0002	0.0003	na	na	0.0002	0.0004	0.0001	0.0002	0.0001	0.0002
Li	0.043	0.069	0.027	0.044	0.039	0.063	0.045	0.072	0.036	0.058
Sr	0.0068	0.0109	0.0070	0.0113	0.0065	0.0105	0.0064	0.0103	0.0063	0.0101
Rb	0.0034	0.0055	na	na	0.0029	0.0047	0.0020	0.0032	0.0034	0.0055
Fe	0.135	0.219	0.140	0.226	0.064	0.104	0.118	0.191	0.140	0.227
Mn	0.078	0.126	0.028	0.045	0.087	0.141	0.070	0.114	0.069	0.112
Pb	0.0013	0.0020	0.0008	0.0013	0.0011	0.0018	0.0010	0.0016	0.0008	0.0013
Zn	0.013	0.021	0.014	0.022	0.015	0.024	0.012	0.019	0.011	0.017
Cu	0.0006	0.0009	0.0007	0.0012	0.0005	0.0008	0.0006	0.0010	0.0010	0.0015
As	0.0025	0.0040	na	na	0.0014	0.0023	0.0015	0.0023	0.0014	0.0023
Bi	0.00002	0.00003	na	na	nd	nd	0.00001	0.00002	0.00002	0.00003
U	0.00012	0.00019	na	na	0.00001	0.00002	0.00002	0.00002	0.00007	0.00012
B	0.123	0.198	0.140	0.226	0.088	0.142	0.099	0.161	0.099	0.159
SO ₄	0.006	0.010	0.019	0.030	0.011	0.017	0.010	0.016	0.004	0.007
F	0.051	0.082	na	na	0.152	0.246	0.054	0.087	0.030	0.048
Cl	5.379	8.689	5.345	8.635	5.434	8.777	5.401	8.725	5.415	8.748
Br	0.0043	0.0069	0.0038	0.0061	0.0044	0.0070	0.0046	0.0074	0.0043	0.0069
I	0.00019	0.00030	0.00017	0.00027	0.00008	0.00013	0.00019	0.00031	0.00010	0.00016

- Notes: (1) The salinity limit values were chosen on the basis of microthermometric data reported by Shepherd *et al.* (1985).
(2) na indicates *not analysed*. nd indicates that the component was *not detected* in the fluid inclusion leachate solution.
(3) For a wt % NaCl equivalent value of x , the total mass (g) of dissolved salts per kg of water = $1000x/(100 - x)$. For each sample, the element relative abundances (by mass), as determined from the fluid inclusion leachate analyses, were therefore normalised to sum to this value, then converted to number of moles, to generate the results shown.

Table 5.2(b) continued

Reconstructed palaeofluid electrolyte concentrations (molal) corresponding to estimated salinity limits of quartz-hosted aqueous inclusion fluids associated with hydrothermal mineralisation of the Dartmoor granite

Locality (mine) :	Golden Dagger				East Vitifer		Great Rock	
Paragenesis :	Stage II (III)		Stage II (III)		Stage III (II)		Stage III	
Sample reference :	SW-89-162		SW-89-163		SW-89-154		SW-89-157	
Wt% NaCl equivalent:	25	35	25	35	15	25	5	15
Na	3.558	5.748	2.981	4.815	1.814	3.427	0.390	1.306
K	0.327	0.528	0.370	0.598	0.207	0.392	0.048	0.162
Ca	0.820	1.324	0.954	1.542	0.427	0.806	?	?
Mg	0.012	0.019	0.028	0.045	0.010	0.019	?	?
Al	0.080	0.130	0.088	0.142	0.052	0.099	?	?
Ba	0.0008	0.0013	0.0010	0.0017	0.0006	0.0012	0.0004	0.0012
Be	0.0012	0.0020	0.0006	0.0009	0.0003	0.0005	na	na
Li	0.098	0.158	0.035	0.056	0.041	0.077	0.006	0.020
Sr	0.0063	0.0101	0.0071	0.0115	0.0032	0.0061	0.0005	0.0017
Rb	0.0028	0.0046	0.0025	0.0040	0.0011	0.0022	na	na
Fe	0.070	0.114	0.119	0.192	0.069	0.130	?	?
Mn	0.065	0.105	0.083	0.134	0.036	0.067	0.021	0.069
Pb	0.0008	0.0013	0.0018	0.0029	0.0005	0.0009	0.0001	0.0004
Zn	0.011	0.018	0.015	0.024	0.006	0.011	0.003	0.009
Cu	0.0015	0.0025	0.0020	0.0033	0.0018	0.0035	0.0002	0.0005
As	0.0028	0.0046	0.0024	0.0038	0.0014	0.0026	na	na
Bi	nd	nd	0.00003	0.00005	0.00003	0.00005	na	na
U	0.00008	0.00013	0.00006	0.00009	0.00002	0.00003	0.0000001	0.0000004
B	0.193	0.311	0.230	0.372	0.069	0.131	0.005	0.018
SO ₄	0.004	0.006	0.008	0.012	0.003	0.005	na	na
F	0.561	0.907	0.168	0.272	0.016	0.030	na	na
Cl	5.070	8.190	5.307	8.572	2.796	5.281	0.630	2.114
Br	0.0033	0.0053	0.0045	0.0073	0.0023	0.0043	0.0005	0.0017
I	0.00010	0.00016	0.00008	0.00013	0.00003	0.00005	0.00001	0.00002

Notes: (1) Estimates of Ca, Mg, Al and Fe concentrations were not feasible for SW-89-157 because of probable contamination of leachate solution by feldspar.

(2) Because of overprinting by later stage fluids, selection of samples that contain purely Stage II or Stage III fluids is probably not feasible.

Where a paragenetic stage is shown in parentheses, this indicates that minor veining by the associated fluids may be of significance.

5.5.2 Hydrothermal quartz associated with W±Sn oxide mineralisation

Table 5.3(a) shows the results of the fluid inclusion leachate analyses for constituent anion and cation concentrations, normalised by mass to Na=10,000. In contrast to the Dartmoor samples, Rb and U concentrations were not determined, nor were fluid inclusion Sr and Pb isotopic analyses undertaken. Table 5.3(b) presents the data in terms of element mole ratios relative to Na. On defining the percentage charge imbalance as $100 \times |1 - \{\Sigma Q^+ / \Sigma |Q^-|\}|$, it is evident that the ionic charge balances are excellent for both Hemerdon sample HEM-80-1 (1.4%) and the sole example from Cligga Head (4.7%). Two further samples from Hemerdon (HEM-79-2 and HEM-79-50) exhibited ionic charge imbalances of <10%, whereas the corresponding data for the ten other leachates included in the investigation indicate a significant excess of cations, with values ranging from 14.3 to 93.9%.† Possible explanations for these findings are discussed in Section 5.6.2.1.

Estimates of absolute concentrations of electrolytes in the Hemerdon palæofluids are presented in Table 5.4(a), which gives element concentrations by mass ($\mu\text{g}/\text{cm}^3\text{H}_2\text{O}$); the corresponding molal values are given in Table 5.4(b). Comparable data for samples from Cligga Head, South Crofty mine, and quartz associated with minor occurrences of W±Sn oxides in the Gunnislake-Hingston Down area, are presented in Tables 5.5(a) and 5.5(b). Microthermometrically-derived salinity data from the following sources were used to estimate the respective molality limits of individual elements as present in the inclusion fluids:

(a) *Hemerdon:*

The salinity of the Hemerdon palæofluids was reported by Kelley *et al.* (1986) to be 30 ± 5 wt% NaCl equivalent. Salinity limits of 25 and 35 wt% NaCl equivalent were therefore used here.

(b) *Cligga Head:*

Salinity limits of the Cligga Head fluids were estimated from the data of Jackson *et al.* (1977) and Charoy (1981). The former reported salinities ranging from 2-12 wt% NaCl equivalent, although most of their values clustered between 6 and 12%. Charoy (1981) noted that the characteristics of the early fluids at Cligga were very similar in both veins and wall-rock greisen, with salinities of 8-10 wt% NaCl equivalent.

† The lack of information on the fluoride content of many of the leachate solutions will serve to enhance the calculated ionic charge imbalance in those cases, possibly to a significant degree. The magnitude of this error may be estimated by comparing the total cationic-to-anionic charge ratios of all samples for which fluoride analyses were undertaken, with the corresponding ratios calculated on the basis of excluding the fluoride contribution to the total anionic charge. The resulting increase in percentage charge imbalances are: 5.4, 5.6, 11.2 and 14.5%, for samples HEM-80-1, HEM-80-35, HEM-80-50 and CH-88-1, respectively.

For the present interpretation, a range of 8 to 12 wt% NaCl equivalent was therefore considered to be representative. It is worth noting, however, that Campbell and Panter (1990) measured the salinities of 69 primary inclusions in vein quartz from Cligga Head and reported a range of 3.7-12.3 wt% NaCl equivalent.

(c) *South Crofty mine:*

Scrivener *et al.* (1986) reported a wide range of salinities for fluids inferred to be responsible for W±Sn oxide mineralisation at South Crofty mine, as associated with extensive early tourmalinisation and pegmatite development. These authors noted that microthermometric measurements were difficult, owing to the scarcity of suitable primary and pseudo-secondary inclusions. Measurements were undertaken on quartz sampled from the Complex and 3ABC lodes; quartz from the latter location was subsequently forwarded by Dr Scrivener for inclusion in the present investigation (sample SC-88-3ABC). Salinity values were reported to be comparable with those of a 'typical' quartz+tourmaline±cassiterite vein from Birch Tor, Dartmoor. Examination of the salinity data presented by Scrivener *et al.* (1986) suggests, however, that the salinity ranges of three-phase (liquid-vapour-halite) and CaCl₂-rich inclusions from South Crofty (predominantly influencing the bulk salinity) are shifted to slightly lower values compared to data from corresponding inclusion types at Birch Tor. Limits of 20 and 30 wt% NaCl equivalent were therefore assigned for the present study.

(d) *Gunnislake-Hingston Down area:*

In a comprehensive investigation of the geology and mineralisation of an area around Tavistock, SW England, Bull (1982) included microthermometric examination of quartz associated with early-stage W±Sn oxide occurrences in the Gunnislake-Hingston Down area. Analysis of an example from Old Gunnislake mine gave salinity values of 5.1-6.3 wt% NaCl equivalent, for primary inclusions in which the formation of the clathrate CO₂-hydrate was not detected during low temperature observations. Where CO₂-hydrate formation was observed, the corresponding salinities were <3 wt% NaCl equivalent. Turner and Bannon (1992) subsequently published microthermometric data for the same sample[†]; their results also appeared in Bannon (1989). Inclusions containing a discrete CO₂ phase were found; the salinity of the associated aqueous phase was 3.0 wt% NaCl equivalent. The salinity of coexisting inclusions devoid of CO₂ was reported as 15 wt% NaCl equivalent, substantially higher than as reported by Bull (1982) and used as an upper limit in the present case.

[†] Supplied to these authors from the sample collection used for the present dissertation (sample reference SW-84-18; see Appendix A). Fluid electrolyte analysis was not undertaken on this particular sample.

Microthermometric analysis by Bull (1982) of quartz-hosted inclusions associated with cassiterite from Drakewalls mine indicated that the salinity range was very similar to that noted for early-stage fluids from Old Gunnislake mine. In contrast, Bannon (1989), as reported also by Turner and Bannon (1992), found a salinity range of 8.8-11.4 wt% NaCl equivalent, on the basis of measurements taken on a sample supplied from the collection prepared for the present investigation (sample SW-84-15). Limits of 8 to 12 wt% NaCl equivalent were assigned for the present study.

Thermometric data for inclusions representative of early hydrothermal fluids at South Bedford mine were reported by Bull (1982), who undertook measurements on a quartz sample subsequently included in the present investigation (SW-84-20). CO₂-hydrate formation at low temperature was reported to occur in most of the (primary) inclusions investigated. Salinities ranged from 5.2 to 10.9 wt% NaCl equivalent. Although comparable data for similar stage fluids at the Prince of Wales mine are not available, it is considered unlikely that the salinity values will lie outside the relatively narrow range defined by the collective results for the other samples from the Gunnislake-Hingston Down area included in the present study. Salinity limits were therefore estimated as for the Old Gunnislake sample, *i. e.* 5 to 15 wt% NaCl equivalent.

Highly anomalous fluid inclusion leachate results were obtained during the present study from wolframite-associated quartz originating from the Castle-an-Dinas mine (St Austell district). These data are shown in Table 5.6, which indicates the very low ionic strength of the parent fluid[†] and also the unusually low relative abundance of Na. The finding that Al was the predominant solute species, together with the gross imbalance of ionic charges as calculated from the element concentration data, indicates that the results of the leachate analysis were probably dominated by a contribution from solid phases (feldspars?).

[†] The very low abundance of solutes in the leachate cannot be simply attributed to a correspondingly low fluid inclusion content in the host quartz, as inclusion water yield was sufficient for D/H isotopic ratio analysis at the usual precision (Chapter 2).

Table 5.3(a)

S W England quartz samples associated with W±Sn oxide mineralisation: fluid inclusion leachate data. Element relative abundances (by mass), normalised to Na = 10,000

Locality :	Hemerdon mine	Hemerdon mine	Hemerdon mine	Hemerdon mine	Hemerdon mine	Hemerdon mine	Hemerdon mine	Cligga Head	South Crofty mine	South Crofty mine	Old Gunnislake mine	Drakewalls mine	South Bedford mine	Prince of Wales mine
Sample reference :	HEM-79-2	HEM-80-1	HEM-80-35	HEM-80-39	HEM-80-44	HEM-80-47	HEM-80-50	CH-88-1	SC-88-2	SC-88-3	SW-89-150	SW-84-15	SW-84-20	SW-84-27
Na	10,000	10,000	10,000	10,000	10,000	10,000	10,000	10,000	10,000	10,000	10,000	10,000	10,000	10,000
K	3,128	2,458	3,363	2,615	3,199	2,395	2,577	2,211	1,660	2,332	1,595	2,255	1,437	2,018
Ca	2,603	3,452	3,928	3,148	5,557	3,316	3,715	1,009	3,262	9,619	2,943	2,009	2,374	850
Mg	20	32	40	41	192	84	84	86	25	112	69	63	106	67
Al	176	141	159	264	486	231	301	497	375	304	359	391	128	340
Ba	15	28	47	18	97	19	33	35	15	nd	18	16	22	10
Be	na	0.52	0.63	na	1.06	na	0.66	1.05	0.32	0.31	0.38	0.43	na	na
Li	64	117	43	77	45	73	47	93	39	33	75	125	60	62
Sr	37	58	80	49	107	65	51	47	53	58	67	78	55	72
Fe	1,867	1,479	1,718	1,278	2,998	1,316	1,226	408	174	665	398	246	593	1,241
Mn	788	1,008	643	714	1,194	593	982	773	232	254	250	211	191	453
Pb	na	43	27	45	43	25	27	75	7	26	12	4	9	10
Zn	315	223	250	241	234	165	268	278	33	1,293	182	16	57	700
Cu	2	24	29	8	33	52	66	84	5	40	10	nd	5	10
As	na	66	9	na	121	na	16	9	3	7	4	12	na	na
Bi	na	1,142	11	na	126	na	7	2	4	7	6	4	na	na
B	416	471	287	428	336	318	368	495	174	488	388	602	204	664
SO ₄	90	497	132	97	570	458	189	291	28	94	128	97	54	87
F	na	1,216	634	na	na	na	1,406	1,488	na	na	na	na	na	na
Cl	21,097	22,320	21,439	19,798	20,944	20,270	20,839	14,971	18,653	15,254	14,749	14,556	16,837	14,076
Br	40	36	32	30	30	26	39	19	17	17	9	22	19	25
I	2.4	0.18	1.6	1.0	0.19	2.8	2.2	1.8	1.8	2.5	1.3	3.0	2.2	1.3

Note: na indicates not analysed ; nd indicates not detected .

Table 5.3(b)

S W England quartz samples associated with W±Sn oxide mineralisation: fluid inclusion leachate data. Element mole ratios, normalised to Na = 1

Locality :	Hemerdon mine	Hemerdon mine	Hemerdon mine	Hemerdon mine	Hemerdon mine	Hemerdon mine	Hemerdon mine	Cligga Head	South Crofty mine	South Crofty mine	Old Gunnislake mine	Drakewalls mine	South Bedford mine	Prince of Wales mine
Sample reference :	HEM-79-2	HEM-80-1	HEM-80-35	HEM-80-39	HEM-80-44	HEM-80-47	HEM-80-50	CH-88-1	SC-88-2	SC-88-3	SW-89-150	SW-84-15	SW-84-20	SW-84-27
Na	1	1	1	1	1	1	1	1	1	1	1	1	1	1
K	0.1839	0.1445	0.1977	0.1538	0.1881	0.1408	0.1515	0.1300	0.0976	0.1371	0.0938	0.1326	0.0845	0.1187
Ca	0.1493	0.1980	0.2253	0.1806	0.3187	0.1902	0.2131	0.0579	0.1871	0.5517	0.1688	0.1152	0.1362	0.0488
Mg	0.0019	0.0030	0.0038	0.0039	0.0182	0.0079	0.0079	0.0081	0.0024	0.0106	0.0065	0.0060	0.0100	0.0063
Al	0.0150	0.0120	0.0135	0.0225	0.0414	0.0197	0.0256	0.0423	0.0320	0.0259	0.0306	0.0333	0.0109	0.0290
Ba	0.00025	0.00047	0.00079	0.00030	0.00162	0.00032	0.00055	0.00059	0.00025	nd	0.00030	0.00027	0.00037	0.00017
Be	na	0.00013	0.00016	na	0.00027	na	0.00017	0.00027	na	0.00008	0.00010	0.00011	na	na
Li	0.0212	0.0388	0.0142	0.0255	0.0149	0.0242	0.0156	0.0308	0.0129	0.0109	0.0248	0.0414	0.0199	0.0205
Sr	0.00097	0.00152	0.00210	0.00129	0.00281	0.00171	0.00134	0.00123	0.00139	0.00152	0.00176	0.00205	0.00144	0.00189
Fe	0.0769	0.0609	0.0707	0.0526	0.1234	0.0542	0.0505	0.0168	0.0072	0.0274	0.0164	0.0101	0.0244	0.0511
Mn	0.0330	0.0422	0.0269	0.0299	0.0500	0.0248	0.0411	0.0323	0.0097	0.0106	0.0105	0.0088	0.0080	0.0190
Pb	na	0.00048	0.00030	0.00050	0.00048	0.00028	0.00030	0.00083	0.00008	0.00029	0.00013	0.00004	0.00010	0.00011
Zn	0.01107	0.00784	0.00879	0.00847	0.00823	0.00580	0.00942	0.00977	0.00116	0.04546	0.00640	0.00056	0.00200	0.02461
Cu	0.00007	0.00087	0.00105	0.00029	0.00119	0.00188	0.00239	0.00304	0.00018	0.00145	0.00036	nd	0.00018	0.00036
As	na	0.00203	0.00028	na	0.00371	na	0.00049	0.00028	0.00009	0.00021	0.00037	0.00037	na	na
Bi	na	0.01256	0.00012	na	0.00139	na	0.00008	0.00002	0.00004	0.00008	0.00007	0.00004	na	na
B	0.0885	0.1002	0.0610	0.0910	0.0715	0.0676	0.0783	0.1053	0.0370	0.1038	0.0825	0.1280	0.0434	0.1412
SO ₄	0.0022	0.0119	0.0032	0.0023	0.0136	0.0110	0.0045	0.0070	0.0007	0.0023	0.0031	0.0023	0.0013	0.0021
F	na	0.1471	0.0767	na	na	na	0.1701	0.1801	na	na	na	na	na	na
Cl	1.3681	1.4474	1.3902	1.2838	1.3581	1.3144	1.3513	0.9708	1.2096	0.9892	0.9564	0.9439	1.0918	0.9128
Br	0.00115	0.00104	0.00092	0.00086	0.00086	0.00075	0.00112	0.00055	0.00049	0.00049	0.00026	0.00063	0.00055	0.00072
I	0.00004	<0.00001	0.00003	0.00002	<0.00001	0.00005	0.00004	0.00003	0.00003	0.00005	0.00002	0.00005	0.00004	0.00002
Total cationic charge, ΣQ ⁺	1.7969	1.8939	1.9336	1.8023	2.3923	1.7983	1.8993	1.5505	1.6258	2.5249	1.6342	1.5615	1.5025	1.5307
Total anionic charge, ΣQ ⁻	-1.6390	-1.9198	-1.6573	-1.5624	-1.6007	-1.5400	-1.7847	-1.4812	-1.3350	-1.3024	-1.2089	-1.3332	-1.2287	-1.3397
Charge difference, ΣQ ⁺ - Σ Q ⁻	0.1579	-0.0259	0.2763	0.2399	0.7917	0.2583	0.1146	0.0693	0.2907	1.2225	0.4253	0.2284	0.2738	0.1909
Charge ratio, ΣQ ⁺ / Σ Q ⁻	1.096	0.986	1.167	1.154	1.495	1.168	1.064	1.047	1.218	1.939	1.352	1.171	1.223	1.143

Notes: (1) na indicates *not analysed*; nd indicates *not detected*.

(2) For charge balance calculations, the following formal oxidation states were assumed: Fe = +2, Mn = +2, As = +3, Bi = +3, B = -3

(3) The exclusion of fluorine from the charge balance calculations in many cases, due to the lack of data, may contribute significantly to the calculated degree of ionic charge imbalance (excess of cations) in those examples.

Table 5.4(a)

Reconstructed palaeofluid electrolyte concentrations (ppm) corresponding to estimated salinity limits of quartz-hosted aqueous inclusion fluids associated with hydrothermal W±Sn oxide mineralisation, Hemerdon

Sample reference :	HEM-79-2		HEM-80-39		HEM-80-1		HEM-80-35		HEM-80-44		HEM-80-47		HEM-80-50	
Host rock :	Granite (greisen-bordered vein)		Granite (greisen-bordered vein)		Killas		Killas		Killas		Killas		Killas/greenstones (?) (tourmaline also present)	
Wt% NaCl equivalent:	25	35	25	35	25	35	25	35	25	35	25	35	25	35
Na	61,485	86,079	64,347	90,085	55,789	78,105	58,311	81,636	53,980	75,572	63,438	88,813	59,180	82,852
K	19,232	26,925	16,827	23,557	13,713	19,198	19,610	27,454	17,268	24,176	15,193	21,271	15,251	21,351
Ca	16,005	22,406	20,256	28,359	19,258	26,962	22,905	32,067	29,997	41,996	21,036	29,450	21,985	30,780
Mg	123	172	264	369	179	250	233	327	1,036	1,451	533	746	497	696
Al	1,082	1,515	1,699	2,378	787	1,101	927	1,298	2,623	3,673	1,465	2,052	1,781	2,494
Ba	92	129	116	162	156	219	274	384	524	733	121	169	195	273
Be	na	na	na	na	3	4	4	5	6	8	NA	NA	4	5
Li	394	551	495	694	653	914	251	351	243	340	463	648	278	389
Sr	227	318	315	441	324	453	466	653	578	809	412	577	302	423
Fe	11,479	16,071	8,224	11,513	8,251	11,552	10,018	14,025	16,183	22,657	8,348	11,688	7,255	10,158
Mn	4,845	6,783	4,594	6,432	5,624	7,873	3,749	5,249	6,445	9,023	3,762	5,267	5,811	8,136
Pb	na	na	290	405	240	336	157	220	232	325	159	222	160	224
Zn	1,937	2,711	1,551	2,171	1,244	1,742	1,458	2,041	1,263	1,768	1,047	1,465	1,586	2,220
Cu	12	17	51	72	134	187	169	237	178	249	330	462	391	547
As	na	na	na	na	368	515	52	73	653	914	na	na	95	133
Bi	na	na	na	na	6,371	8,920	64	90	680	952	na	na	41	58
B	2,558	3,581	2,754	3,856	2,628	3,679	1,674	2,343	1,814	2,539	2,017	2,824	2,178	3,049
SO ₄	553	775	624	874	2,773	3,882	770	1,078	3,077	4,308	2,905	4,068	1,119	1,566
F	na	na	na	na	6,784	9,498	3,697	5,176	na	na	na	na	8,321	11,649
Cl	129,715	181,601	127,394	178,351	124,521	174,329	125,014	175,019	113,056	158,279	128,588	180,023	123,326	172,656
Br	246	344	193	270	201	281	187	261	162	227	165	231	231	323
I	15	21	6	9	1.0	1.4	9	13	1.0	1.4	18	25	13	18

- Notes: (1) The salinity of quartz-hosted fluid inclusions associated with W±Sn oxide mineralisation, Hemerdon, was reported by Kelley *et al.* (1986) as 30±5 wt % NaCl equivalent, on the basis of microthermometric analysis.
(2) na indicates *not analysed*. nd indicates that the component was *not detected* in the fluid inclusion leachate solution.
(3) For a wt % NaCl equivalent value of x, the total mass of dissolved salts, in units of µg per g of fluid, = 10,000x. For each sample, therefore, the element relative abundances (by mass), as determined by fluid inclusion leachate analyses, were normalised to sum to this value to generate the data shown.

Table 5.4(b)

Reconstructed palaeofluid electrolyte concentrations (molal) corresponding to estimated salinity limits of quartz-hosted aqueous inclusion fluids associated with hydrothermal W±Sn oxide mineralisation, Hemerdon

Sample reference :	HEM-79-2		HEM-80-39		HEM-80-1		HEM-80-35		HEM-80-44		HEM-80-47		HEM-80-50	
Host rock :	Granite (greisen - bordered vein)		Granite (greisen - bordered vein)		Killas		Killas		Killas		Killas		Killas/ greenstones (?) (tourmaline also present)	
Wt% NaCl equivalent:	25	35	25	35	25	35	25	35	25	35	25	35	25	35
Na	3.566	5.760	3.732	6.028	3.236	5.227	3.382	5.463	3.131	5.057	3.679	5.943	3.432	5.544
K	0.656	1.059	0.574	0.927	0.468	0.755	0.669	1.080	0.589	0.951	0.518	0.837	0.520	0.840
Ca	0.532	0.860	0.674	1.089	0.641	1.035	0.762	1.231	0.998	1.612	0.700	1.130	0.731	1.181
Mg	0.007	0.011	0.014	0.023	0.010	0.016	0.013	0.021	0.057	0.092	0.029	0.047	0.027	0.044
Al	0.053	0.086	0.084	0.136	0.039	0.063	0.046	0.074	0.130	0.209	0.072	0.117	0.088	0.142
Ba	0.0009	0.0014	0.0011	0.0018	0.0015	0.0024	0.0027	0.0043	0.0051	0.0082	0.0012	0.0019	0.0019	0.0031
Be	na	na	na	na	0.0004	0.0007	0.0005	0.0009	0.0008	0.0014	na	na	0.0006	0.0009
Li	0.076	0.122	0.095	0.154	0.125	0.203	0.048	0.078	0.047	0.075	0.089	0.144	0.053	0.086
Sr	0.003	0.006	0.005	0.008	0.005	0.008	0.007	0.011	0.009	0.014	0.006	0.010	0.005	0.007
Fe	0.274	0.443	0.196	0.317	0.197	0.318	0.239	0.386	0.386	0.624	0.199	0.322	0.173	0.280
Mn	0.118	0.190	0.112	0.180	0.136	0.220	0.091	0.147	0.156	0.253	0.091	0.147	0.141	0.228
Pb	na	na	0.0019	0.0030	0.0015	0.0025	0.0010	0.0016	0.0015	0.0024	0.0010	0.0016	0.0010	0.0017
Zn	0.039	0.064	0.032	0.051	0.025	0.041	0.030	0.048	0.026	0.042	0.021	0.034	0.032	0.052
Cu	0.0003	0.0004	0.001	0.002	0.003	0.005	0.004	0.006	0.004	0.006	0.007	0.011	0.008	0.013
As	na	na	na	na	0.007	0.011	0.001	0.002	0.012	0.019	na	na	0.002	0.003
Bi	na	na	na	na	0.041	0.066	0.000	0.001	0.004	0.007	na	na	0.0003	0.0004
B	0.315	0.510	0.340	0.549	0.324	0.524	0.206	0.333	0.224	0.361	0.249	0.402	0.269	0.434
SO ₄	0.008	0.012	0.009	0.014	0.038	0.062	0.011	0.017	0.043	0.069	0.040	0.065	0.016	0.025
F	na	na	na	na	0.476	0.769	0.259	0.419	na	na	na	na	0.584	0.943
Cl	4.878	7.880	4.791	7.739	4.683	7.565	4.702	7.595	4.252	6.868	4.836	7.812	4.638	7.492
Br	0.004	0.007	0.003	0.005	0.003	0.005	0.003	0.005	0.003	0.004	0.003	0.004	0.004	0.006
I	0.00016	0.00025	0.00007	0.00011	0.00001	0.00002	0.00010	0.00016	0.00001	0.00002	0.00019	0.00030	0.00014	0.00022

Notes: (1) The salinity of quartz-hosted fluid inclusions associated with W±Sn oxide mineralisation, Hemerdon, was reported by Kelley *et al.* (1986) as 30±5 wt % NaCl equivalent, on the basis of microthermometric analysis.

(2) na indicates *not analysed*. nd indicates that the component was *not detected* in the fluid inclusion leachate solution.

(3) For a wt % NaCl equivalent value of *x*, the total mass (g) of dissolved salts per kg of water = 1000*x*/(100 - *x*). For each sample, the element relative abundances (by mass), as determined from the fluid inclusion leachate analyses, were therefore normalised to sum to this value, then converted to number of moles, to generate the results shown.

Table 5.5(a)

Reconstructed palaeofluid electrolyte concentrations (ppm) corresponding to estimated salinity limits of quartz-hosted aqueous inclusion fluids associated with hydrothermal W±Sn oxide mineralisation: Cligga Head, South Crofty and minor occurrences in the Gunnislake-Hingston Down area

Locality :	Cligga Head		South Crofty mine		South Crofty mine	Old Gunnislake mine		Drakewalls mine		South Bedford mine		Prince of Wales mine		
Sample reference :	CH-88-1		SC-88-2		SC-88-3	SW-89-150		SW-84-15		SW-84-20		SW-84-27		
Wt % NaCl equivalent:	8	12	20	30	20	30	5	15	8	12	5	15	5	15
Na	24,335	36,503	57,536	86,303	49,254	73,881	15,989	47,967	26,050	39,075	15,551	46,652	16,294	48,882
K	5,381	8,071	9,551	14,326	11,486	17,229	2,550	7,651	5,874	8,811	2,235	6,704	3,288	9,864
Ca	2,455	3,683	18,768	28,152	47,377	71,066	4,706	14,117	5,233	7,850	3,692	11,075	1,385	4,155
Mg	209	314	144	216	552	827	110	331	164	246	165	495	109	328
Al	1,209	1,814	2,158	3,236	1,497	2,246	574	1,722	1,019	1,528	199	597	554	1,662
Ba	85	128	86	129	nd	nd	29	86	42	63	34	103	16	49
Be	2.6	3.8	1.8	2.8	1.5	2.3	0.6	1.8	1.1	1.7	na	na	na	na
Li	226	339	224	337	163	244	120	360	326	488	93	280	101	303
Sr	114	172	305	457	286	429	107	321	203	305	86	257	117	352
Fe	993	1,489	1,001	1,502	3,275	4,913	636	1,909	641	961	922	2,766	2,022	6,066
Mn	1,881	2,822	1,335	2,002	1,251	1,877	400	1,199	550	824	297	891	738	2,214
Pb	183	274	40	60	128	192	19	58	10	16	14	42	16	49
Zn	677	1,015	190	285	6,369	9,553	291	873	42	63	89	266	1,141	3,422
Cu	204	307	29	43	197	296	16	48	nd	nd	8	23	16	49
As	22	33	17	26	34	52	19	58	31	47	na	na	na	na
Bi	5	7	23	35	34	52	10	29	10	16	na	na	na	na
B	1,205	1,807	1,001	1,502	2,404	3,605	620	1,861	1,568	2,352	317	952	1,082	3,246
SO ₄	708	1,062	161	242	463	694	205	614	253	379	84	252	142	425
F	3,621	5,432	na	na	na	na	na	na	na	na	na	na	na	na
Cl	36,433	54,649	107,321	160,982	75,132	112,698	23,582	70,746	37,918	56,877	26,182	78,547	22,935	68,806
Br	46	69	98	147	84	126	14	43	57	86	30	89	41	122
I	4	7	10	16	12	18	2	6	8	12	3	10	2	6

Notes: (1) The salinity limits were chosen on the basis of microthermometric data published by Jackson *et al.* (1977), Charoy (1981) and Campbell and Panter (1990) for Cligga Head; Scrivener *et al.* (1986) for South Crofty; Bull (1982) and Turner and Baunton (1992) for the various localities in the Gunnislake-Hingston Down area.

(2) na indicates *not analysed*. nd indicates that the component was *not detected* in the fluid inclusion leachate solution.

(3) For a wt % NaCl equivalent value of *x*, the total mass of dissolved salts, in units of µg per g of fluid, = 10,000*x*. For each sample, therefore, the element relative abundances (by mass), as determined by fluid inclusion leachate analyses, were normalised to sum to this value to generate the data shown.

Table 5.5(b)

Reconstructed palaeofluid electrolyte concentrations (molal) corresponding to estimated salinity limits of quartz-hosted aqueous inclusion fluids associated with hydrothermal W±Sn oxide mineralisation: Cligga Head, South Crofty and minor occurrences in the Gunnislake-Hingston Down area.

Locality :	Cligga Head		South Crofty mine		South Crofty mine		Old Gunnislake mine		Drakewalls mine		South Bedford mine		Prince of Wales mine	
Sample reference :	CH-88-1		SC-88-2		SC-88-3		SW-89-150		SW-84-15		SW-84-20		SW-84-27	
Wt % NaCl equivalent:	8	12	20	30	20	30	5	15	8	12	5	15	5	15
Na	1.151	1.804	3.128	5.363	2.678	4.591	0.732	2.455	1.232	1.931	0.712	2.387	0.746	2.501
K	0.150	0.235	0.305	0.523	0.367	0.630	0.069	0.230	0.163	0.256	0.060	0.202	0.089	0.297
Ca	0.067	0.104	0.585	1.003	1.478	2.533	0.124	0.414	0.142	0.223	0.097	0.325	0.036	0.122
Mg	0.009	0.015	0.007	0.013	0.028	0.049	0.005	0.016	0.007	0.012	0.007	0.024	0.005	0.016
Al	0.049	0.076	0.100	0.171	0.069	0.119	0.022	0.075	0.041	0.064	0.008	0.026	0.022	0.072
Ba	0.0007	0.0011	0.0008	0.0013	nd	nd	0.0002	0.0007	0.0003	0.0005	0.0003	0.0009	0.0001	0.0004
Be	0.0003	0.0005	0.0003	0.0004	0.0002	0.0004	0.0001	0.0002	0.0001	0.0002	na	na	na	na
Li	0.035	0.056	0.040	0.069	0.029	0.050	0.018	0.061	0.051	0.080	0.014	0.047	0.015	0.051
Sr	0.001	0.002	0.004	0.007	0.004	0.007	0.001	0.004	0.003	0.004	0.001	0.003	0.001	0.005
Fe	0.019	0.030	0.022	0.038	0.073	0.126	0.012	0.040	0.012	0.020	0.017	0.058	0.038	0.128
Mn	0.037	0.058	0.030	0.052	0.028	0.049	0.008	0.026	0.011	0.017	0.006	0.019	0.014	0.047
Pb	0.0010	0.0015	0.0002	0.0004	0.0008	0.0013	0.0001	0.0003	0.00005	0.00009	0.0001	0.0002	0.0001	0.0003
Zn	0.011	0.018	0.004	0.006	0.122	0.209	0.005	0.016	0.007	0.0011	0.001	0.005	0.018	0.062
Cu	0.003	0.005	0.0006	0.0010	0.004	0.007	0.0003	0.0009	nd	nd	0.0001	0.0004	0.0003	0.0009
As	0.0003	0.0005	0.0003	0.0005	0.0006	0.0010	0.0003	0.0009	0.0005	0.0007	na	na	na	na
Bi	0.00003	0.00004	0.0001	0.0002	0.0002	0.0004	0.00005	0.00016	0.00005	0.00008	na	na	na	na
B	0.121	0.190	0.116	0.198	0.278	0.476	0.060	0.203	0.158	0.247	0.031	0.104	0.105	0.353
SO ₄	0.008	0.013	0.002	0.004	0.006	0.010	0.002	0.008	0.003	0.004	0.001	0.003	0.002	0.005
F	0.207	0.325	na	na	na	na	na	na	na	na	na	na	na	na
Cl	1.117	1.752	3.784	6.487	2.649	4.541	0.700	2.348	1.163	1.823	0.777	2.607	0.681	2.283
Br	0.0006	0.0010	0.0015	0.0026	0.0013	0.0022	0.0002	0.0006	0.0008	0.0012	0.0004	0.0013	0.0005	0.0018
I	0.00004	0.00006	0.0001	0.0002	0.0001	0.0002	0.00002	0.00006	0.00007	0.00010	0.00003	0.00010	0.00002	0.00006

- Notes: (1) The salinity limits were chosen on the basis of microthermometric data published by Jackson *et al.* (1977), Charoy (1981) and Campbell and Panter (1990) for Cligga Head; Scrivener *et al.* (1986) for South Crofty; Bull (1982) and Turner and Bannon (1992) for the various localities in the Gunnislake-Hingston Down area.
- (2) na indicates *not analysed*. nd indicates that the component was *not detected* in the fluid inclusion leachate solution.
- (3) For a wt % NaCl equivalent value of x , the total mass (g) of dissolved salts per kg of water = $1000x/(100 - x)$. For each sample, the element relative abundances (by mass), as determined from the fluid inclusion leachate analyses, were therefore normalised to sum to this value, then converted to number of moles, to generate the results shown.

Table 5.6

Leachate analysis of quartz associated with W±Sn oxide, Castle-an Dinas mine (St. Austell district): an anomalous example of very low ion yield, with gross imbalance of charge probably caused by the presence of residual feldspar

Element	Concentration in leachate (ppb)	Abundance by mass, relative to Na ≡ 10,000	Molar ratio to Na
Na	65	10000	1.000
K	90	13846	0.814
Ca	242	37231	2.136
Mg	33	5077	0.480
Al	262	40308	3.434
Ba	3	462	0.008
Li	33	5077	1.682
Sr	8	1231	0.032
Fe	115	17692	0.728
Mn	5	769	0.032
Pb	nd	-	-
Zn	10	1538	0.054
Cu	1	154	0.006
As	4	615	0.019
Bi	2	308	0.003
Be	0.54	83	0.021
Cl	(146.6)	22553	1.462
B	1	153	0.033
F	(22.1)	3400	0.411
Br	(0.61)	94	0.003
I	(0.008)	1.2	0.00002
Total cationic charge, ΣQ^+			20.860
Total anionic charge, ΣQ^-			-1.974

- Notes: (i) Raw data corrected for procedural blanks. nd indicates *not detected*.
- (ii) Halogen concentrations measured using ion chromatography; Cu, As, Bi and Be data obtained by GFAAS; other cations (except alkali metals) and boron (as borate) analysed by ICP-AES.
- (iii) Na concentration in the leachate is anomalously low, both in absolute and relative terms.
- (iv) Halogen data in parentheses were derived from normalising raw data on pre-concentrated leachate solutions (containing 850ppb Na). Br/Cl and I/Cl ratios are consistent with the respective data from S W England quartz samples associated with W±Sn oxides, as reported in the present study.

5.6 Discussion

5.6.1 Hydrothermal fluids associated with early mineralisation of the Dartmoor granite

5.6.1.1 Chemical characteristics: salient features

Data presented in Tables 5.1(a) and 5.1(b) show that palæo-hydrothermal fluids hosted by the Dartmoor granite consist primarily of Na-Ca-K chloride brines, containing relatively high concentrations of B, F, Li, Al, Fe and Mn. The most notable feature of the present findings is the relative invariance of chemical composition to both paragenetic stage and locality. This uniformity of electrolyte composition parallels the finding, as reported in Chapter 2 of the present work, that the δD values of the corresponding water components are characterised by a relatively narrow range and appear not to depend on the associated mineral assemblage or proximity to the metasedimentary contact.

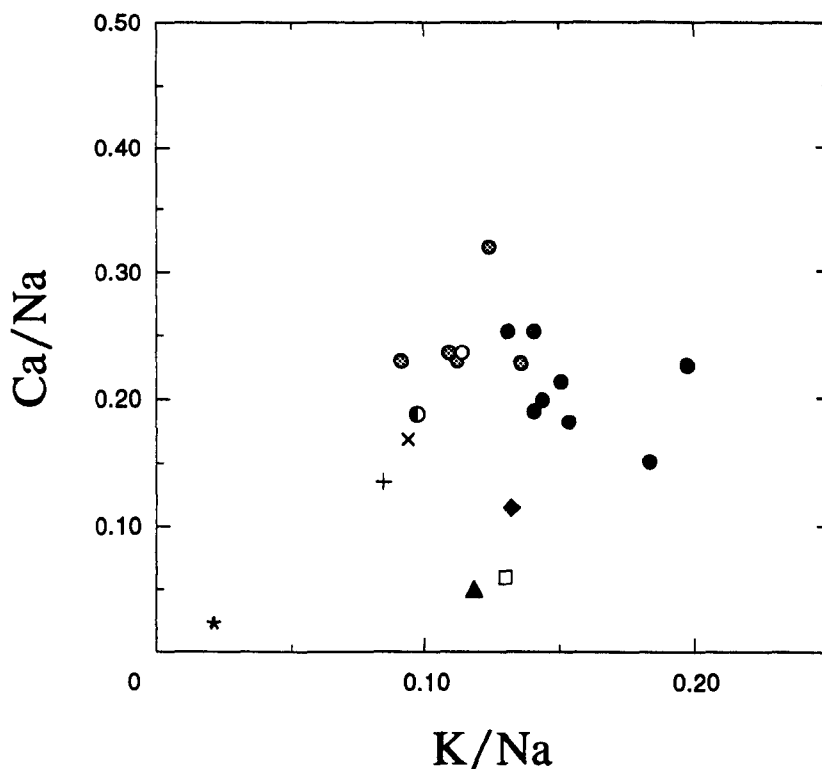
A notable feature of the data is that, whereas Na is the predominant cation, the abundance of Ca exceeds that of K in all samples investigated. Furthermore, the K/Na and Ca/Na mole ratios show relatively little variation, as illustrated in Figure 5.1. A mechanism to explain the relative enrichment of Ca in the Dartmoor hydrothermal fluids (which are characterised by larger Ca/Na ratios than are any of the Cornubian palæo-hydrothermal systems associated with W±Sn oxide mineral assemblages, as shown in Figure 5.1) is Ca-Na exchange during high-temperature albitisation of plagioclase feldspars in the granite. Such fluid-rock interaction would be consistent with field observations (*e.g.* Scrivener, 1982; Shepherd *et al.*, 1985) that albite formation was associated with the earliest phase of hydrothermal activity. To explain the present finding that palæofluid Ca/Na values are independent of both locality and associated mineral assemblage (as a proxy for temperature), it is necessary to postulate that the measured Ca contents of the Stage II and III palæofluids reflect an initial, high-temperature interaction with the anorthite component of plagioclase, with no subsequent gain (or loss) of Ca during cooling, prior to fluid entrapment.

In view of the ubiquitous presence of early, high-temperature tourmaline mineralisation in the region, the levels of B and F in the present examples of Stage I fluids might be expected to be significantly greater than those actually found, unless tourmaline deposition occurred prior to entrapment of these fluids. Evidence that such precipitation occurred is provided by the finding of higher B, and substantially higher F, concentrations (normalised to Na) in Stage II fluids from the same locality (Golden Dagger mine).

Although present at lower abundances (0.01-0.03 molal), Zn is also a significant component of all the fluids investigated, as seen from Table 5.2(b). The ubiquitous presence of high concentrations of Fe (and also Zn) in the hydrothermal fluids is consistent with the assertion that the fluids have not encountered sulphur-bearing wall-rocks.

Figure 5.1

Ca/Na and K/Na molar ratios: comparison between palaeofluids of the Dartmoor hydrothermal system and fluids characterised by association with early W±Sn oxide mineralisation in SW England



Key

Dartmoor : ● Stage I ⊗ Stage II ○ Stage III

● Hemerdon mine ◆ Drakewalls mine
● South Crofty mine + South Bedford mine
□ Cligga Head ▲ Prince of Wales mine
× Old Gunnislake mine

* Sea water (present day)

Note: Samples for which fluid inclusion leachate analysis gave anomalously high levels of Al and/or relatively poor ionic charge balance (excess of cations) are excluded from consideration here, as implied solid phase impurities may contribute significantly to the measured Ca levels. Thus, with reference to Tables 6.1(b) and 6.3(b), data from samples SW-89-157 (Great Rock mine, Dartmoor), HEM-80-44 (Hemerdon mine) and SC-88-3 (South Crofty mine) are not included.

5.6.1.2 Cation ratio geothermometry and fluid-rock interaction

The application of empirical geothermometers based on cation ratios (*e.g.* Fournier and Truesdell, 1973; Lagache and Weisbrod, 1977; Giggenbach, 1988) to high-salinity fluids has been discussed recently by Pauwels *et al.* (1993). One of the most commonly-used cation geothermometer is that based on Na/K ratios. Lagache and Weisbrod (1977) showed empirically that the Na/K ratio in hydrothermal solutions in equilibrium with 2-alkali (Na, K) feldspars is effectively independent of pressure and chloride molality, in the case of a homogeneous fluid[†], and that a linear relationship with temperature exists. No corresponding geothermometer for hydrothermal fluids in equilibrium with Na- K- and Ca-feldspars is known to the present author, although such a system would be more appropriate to the present discussion.

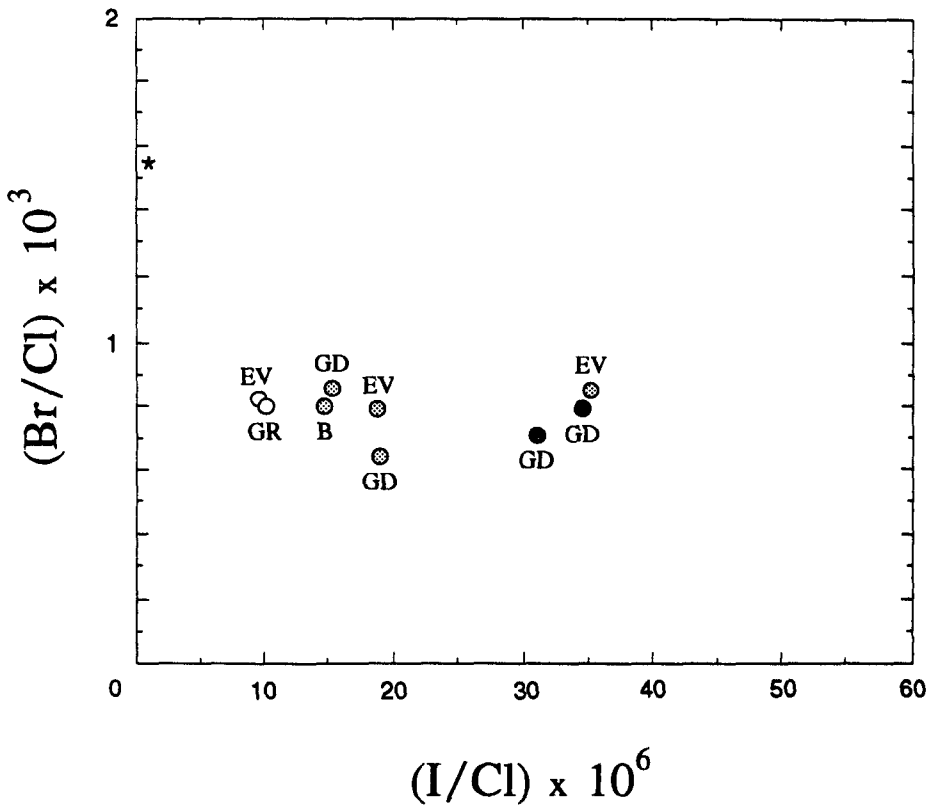
Bottrell and Yardley (1988) noted that K/Na ratios in the earliest granite-associated hydrothermal fluids of the Cornubian region are unlikely to be of value for geothermometry because tourmaline and muscovite precipitation at relatively high temperature would have modified this parameter since the fluid separated from its parent 2-feldspar granite. Similarly, Charoy (1981) noted that temperatures derived from fluid inclusion K/Na ratios in samples from Cligga Head formed a sequence opposite to that expected on the basis of the associated mineral paragenesis and microthermometric analyses. Charoy (1981) suggested that a constant state of disequilibrium existed between the hydrothermal fluids and the granite.

In the present study, Dartmoor hydrothermal fluid inclusion K/Na ratios ranged from 0.092 to 0.141, as shown in Table 5.1(b) and Figure 5.1. Assuming that the fluids achieved chemical equilibrium with the host granite up to the time of entrapment, the corresponding temperature range is *ca.* 310-390°C, on the basis of the data of Lagache and Weisbrod (1977). This is in reasonably good agreement with values for Stage II fluids as deduced from microthermometry (Shepherd *et al.*, 1985), especially as the measured K/Na ratios represent a composite analysis of more than one fluid inclusion population in a given sample and therefore relate to the predominant inclusion type. Furthermore, on the basis of the K/Na geothermometer, the Stage I fluid examples group at the high end of the temperature range. Stage III examples, however, have K/Na ratios corresponding to unrealistically high temperatures; the actual values are 350°C and 365°C for samples SW-89-154 (East Vitifer mine) and SW-89-157 (Great Rock mine) respectively. A possible explanation for this is preferential, low-temperature hydrolysis of plagioclase, as suggested by Charoy (1981) to account for similarly anomalous palæofluid K/Na geothermometry results associated with kaolinite formation at Cligga Head.

[†] If liquid/vapour phase separation - 'unmixing' - has occurred, the invariance of the K/Na molar ratio to total pressure is true in the case of the liquid phase.

Figure 5.2

Br/Cl and I/Cl molar ratios: Dartmoor pegmatitic and mineralising palæofluids



Key

Locality (mine)

B Barracott
EV East Vitifer
GD Golden Dagger
GR Great Rock

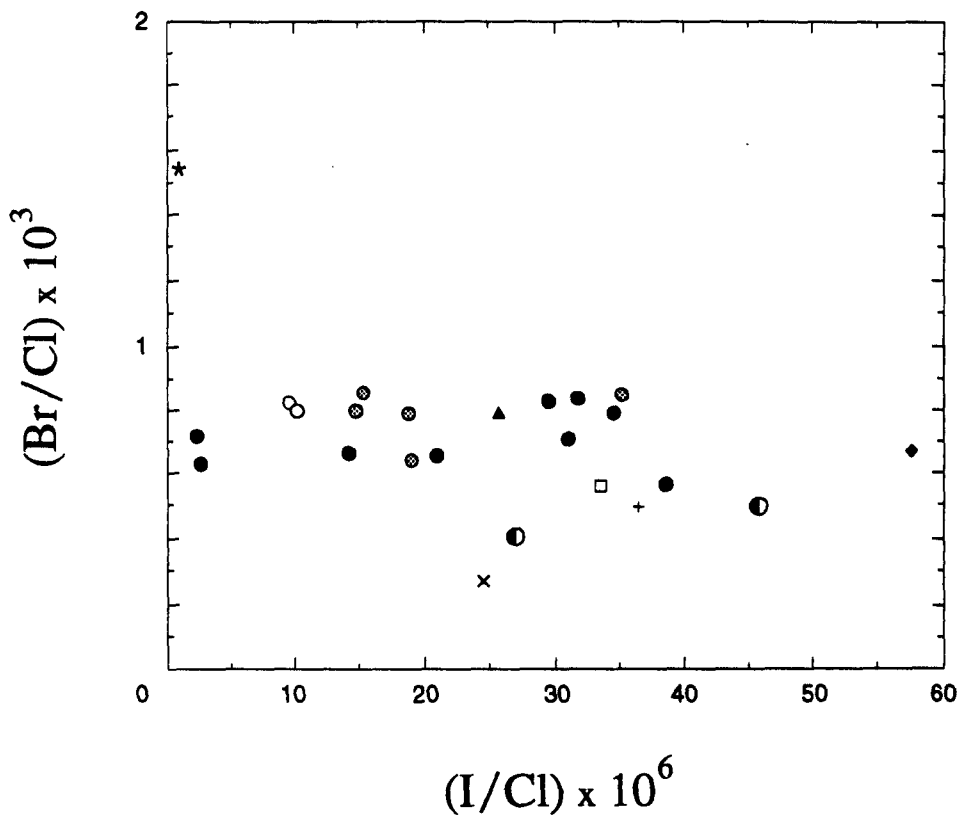
Paragenesis

● Stage I
⊗ Stage II
○ Stage III

* Sea water (present day)

Figure 5.3

Br/Cl and I/Cl molar ratios: comparison between palaeofluids of the Dartmoor hydrothermal system and fluids characterised by association with early W±Sn oxide mineralisation in SW England



Key

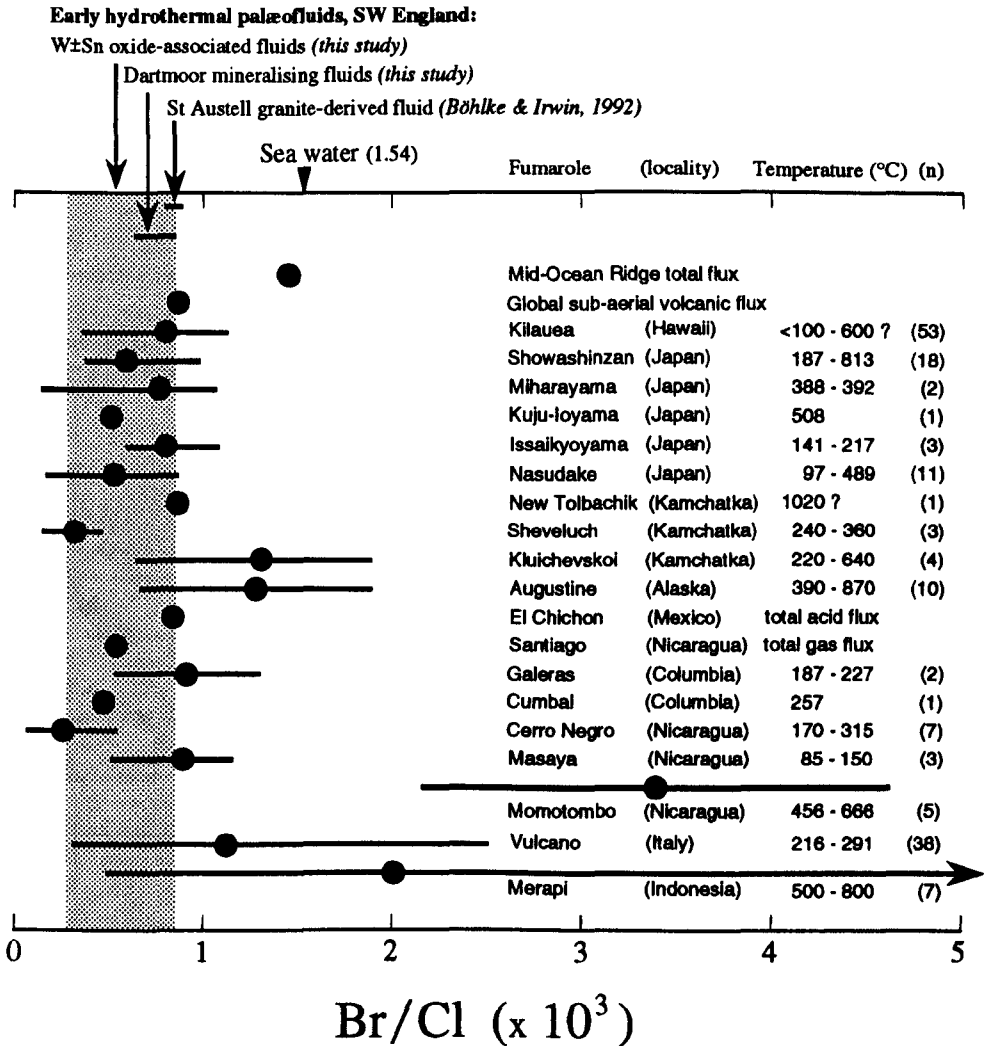
Dartmoor : ● Stage I ⊗ Stage II ○ Stage III

- Hemerdon mine
- ◆ Drakewalls mine
- South Crofty mine
- +
- South Bedford mine
- Cligga Head
- ▲ Prince of Wales mine
- × Old Gunnislake mine
- * Sea water (present day)

Figure 5.4

(a). Br/Cl molar ratios in volcanic fumarole condensates: comparison with early hydrothermal palaeofluids, S W England.

(Adapted from Böhlke and Irwin, 1992)



Notes: (1) Bars indicate the ranges of values; filled circles indicate the respective means. (n) refers to the number of analyses. Refer to Böhlke and Irwin (1992) for sources of original data.

(2) The St Austell palaeofluid result reported by Böhlke and Irwin (1992) refers to fluid inclusions from a quartz-tourmaline-topaz rock (greisen) from St Mewan's Beacon, St Austell, a split of the same sample analysed for fluid inclusion electrolyte composition by Bottrell and Yardley (1988). Subsequent analysis by Banks (unpublished data) of a further split of this sample for fluid inclusion Br/Cl ratio gave a result of 6.1×10^{-4} , which is not dissimilar to the value given by Böhlke and Irwin (1992) of $(8.5 \pm 0.4) \times 10^{-4}$.

Subsequent analysis by Dr D A Banks at the University of Leeds (unpublished data, *pers. comm.*) of fluid inclusion halogen ratios in a further split of the same sample, using procedures adopted for the present work, gave a Br/Cl mole ratio of 6.1×10^{-4} , which is not very different from the $(8.5 \pm 0.4) \times 10^{-4}$ obtained by Böhlke and Irwin (1992). With regard to the corresponding I/Cl ratio, however, Banks obtained a significantly lower value of 6.0×10^{-6} , compared to the $(81 \pm 3) \times 10^{-6}$ reported by Böhlke and Irwin (1992).†

The Br/Cl and I/Cl ratios obtained during the present study are shown in Figures 5.2 and 5.3. With regard to the Dartmoor hydrothermal system, it is apparent from Figure 5.2 that the Br/Cl values are invariant of paragenetic stage and are uniformly about half that of present-day seawater, being very similar to that reported for the St Austell granite-hosted palaeofluid trapped at 500-600°C. The Dartmoor hydrothermal I/Cl ratios, however, range from ~11 to ~41x that of present-day seawater and also exhibit a systematic relative enrichment in iodine in the earlier (higher temperature) stages of paragenesis. These I/Cl data thus contrast with the finding (obtained in the same laboratory, using identical procedures) that the high-temperature 'magmatic' fluid associated with the St Austell granite is characterised by a corresponding value of ~7x that of present-day seawater.

Böhlke and Irwin (1992) compared their halogen data for St Austell granite-associated fluid inclusions with published analyses of halogen compositions of volcanic fumarole gas condensates and estimates of oceanic and total global volcanic fluxes. As noted by Böhlke and Irwin (1992) and references therein, fluctuation of halogen abundances through cycles of condensation and sublimation in fumarole conduits may serve to limit the interpretation of such measurements. However, early (1960s) data from fumaroles in Japan led to the observation that 'magmatic' fluids are characterised by Br/Cl ratios less than that of present-day seawater, whereas the corresponding I/Cl ratios are significantly greater than that of present-day seawater. In Figure 5.4, the halogen ratio data obtained during the present study are compared with those of volcanic gases from several modern evolved magmatic arcs, as compiled by Böhlke and Irwin (1992). On the basis of these data it is apparent that the Dartmoor fluid inclusion Br/Cl and I/Cl results correspond closely to those associated with (modern) volcanic gases at many localities on a global scale. It should be noted, however, that similar halogen ratios have been reported to occur in fluids associated with very different environments, including some sedimentary basin brines, so that a halogen ratio 'signature' characteristic of high-temperature aqueous fluids in continental magmatic systems is not unique (Böhlke and Irwin, 1992).

† Two samples of synthetic fluid inclusions of known composition, supplied by the Centre pour Recherche sur la Géologie de l'Uranium (CREGU) at Nancy, France, were used as calibration standards at the Leeds laboratory. Good agreement was obtained between the experimentally-determined and actual halogen ratio values (D A Banks, *pers. comm.*).

5.6.1.4 Sr and Pb isotopes in the hydrothermal fluids hosted by the Dartmoor granite

Sr and Pb are both transported in hydrothermal fluids; their respective isotopic characteristics may be used to derive information about the sources of these elements and also as tracers of fluid-rock interaction. Pb, in particular, has been shown to be highly mobile (and probably transported as PbCl^+) in high-level crustal fluid systems operating over distances of up to $\sim 10^3$ km (McCulloch and Woodhead, 1993, and references therein). Detailed consideration of the fluid inclusion U-Pb and Rb-Sr results and isotope systematics is not within the scope of the present dissertation and will be presented elsewhere (Wayne *et al.*, in preparation). For the purpose of the present work, a comparison of the fluid inclusion Rb-Sr data with those of the host granite and regional metasedimentary rocks is given in Section 6.4.3.1.3.

5.6.2 Chemical characteristics of fluids associated with W±Sn oxide mineralisation of the Cornubian batholith

5.6.2.1 Ionic charge imbalance of leachates: possible explanations

As noted in Section 5.5.2, and shown in Table 5.3(b), many of the fluid inclusion leachates obtained from quartz associated with occurrences of W±Sn oxide mineralisation exhibited >10% imbalance of ionic charge, with $\Sigma Q^+ / \Sigma |Q^-| > 1$ in all of these cases. Even so, the charge balances compare favourably with other recent studies: Channer and Spooner (1992) reported $\Sigma Q^+ / \Sigma |Q^-|$ values of 1.50-2.17 for leachate analyses of quartz-hosted fluid inclusions from a granitic pegmatite (Tanco, south-east Manitoba, Canada). The main fluid inclusion populations in the samples investigated by Channer and Spooner (1992) contained a discrete CO_2 phase; the coexisting aqueous phase was therefore saturated with respect to dissolved inorganic carbon species. Channer and Spooner (1992) estimated from published solubility data the total dissolved inorganic carbon concentrations in the aqueous inclusions at room temperature, for the empirical mean salinity value; the ionic charge balances of the leachate solutions were then recalculated assuming that the total dissolved inorganic carbon was present either entirely as HCO_3^- , or entirely as CO_3^{2-} . As discussed in Section 3.2.7 of the present work, the latter case is quite unrealistic, requiring an improbably high pH value. For the same reason, it is also doubtful that HCO_3^- would be of significance in pegmatite-associated fluids. Although the revised charge balances were closer to unity, the values still ranged from 1.24 to 1.69 on the assumption of total dissolved inorganic carbon being present exclusively as HCO_3^- . Channer and Spooner (1992) suggested that partial dissolution of microscopic Mg- and Ca-bearing mineral inclusions were possibly responsible for the residual charge imbalances. Some authors (*e.g.* Kazahaya, 1986) have (unwisely!) assumed that ionic charge imbalance of fluid inclusion leachates is attributable exclusively to the presence of HCO_3^- and have consequently used the $\Sigma Q^+ / \Sigma |Q^-|$ values to derive the

concentration of HCO_3^- in the leachate solutions, whilst neglecting the possibility that cation excess may result from the presence of solid phase impurities in the host lattice.

In the present study, the fact that leachate charge balances were very close to unity for some, but not all, of the samples associated with $\text{W}\pm\text{Sn}$ oxide assemblages, despite the presence of significant quantities of dissolved inorganic carbon in the aqueous fluid inclusions of all these samples (as discussed in Chapter 3), demonstrates that the postulate of HCO_3^- being responsible for charge imbalances cannot be substantiated, at least for the samples investigated herein. Furthermore, if the sulphate concentrations measured in the leachate solutions (Tables 3(a) and 3(b)) accurately reflect the total palaeofluid sulphur abundances[†], reduced sulphur species are not responsible for the deficiency of anionic charge, either. The finding that significant quantities of nitrogen were released from separate 'splits' of these quartz samples during heating from 600 to 1100°C (Chapter 4 of the present work - see Figure 4.8 and Table 4.2) is consistent with the idea that microscopic inclusions of ammonium-bearing minerals were present; such material, whether authigenic or trapped during crystal growth, is a potential source of the recorded charge imbalances.

5.6.2.2 Comparative overview: constraints on the origins of component elements

If it is postulated that the chemical compositions of the hydrothermal fluids reflect equilibration with the respective associated 2-feldspar granite, with no subsequent modification prior to fluid entrapment (which, in turn, implies the absence of fluid-rock interaction with the local killas, besides the lack of precipitation of Na- and K-bearing minerals), model temperatures for the separation of the fluids from granite may be derived on the basis of the K/Na cation ratio geothermometer of Lagache and Weisbrod (1977). The fluids at Hemerdon are characterised by consistently higher K/Na ratios than encountered for similar stage ($\text{W}\pm\text{Sn}$ oxide-associated) fluids elsewhere in the region (see Figure 5.1) and correspond to a temperature range of *ca.* 400-490°C; there is no systematic variation with vein host lithology. The upper temperature limit indicated by this model is higher than fluid trapping temperatures estimated by Shepherd *et al.* (1985) on the basis of microthermometric data, although not substantially so. Application of the same cation geothermometry model to comparable stage fluids at the other localities investigated gives temperatures of *ca.* 310-395°C. It may be noted that these lower temperature values coincide with microthermometric evidence for the fluids being of lower salinity than at Hemerdon (Section 5.5.2) and also deuterium-enrichment of the water, consistent with a meteoric component (Chapter 2).

[†] Reduced sulphur species would be gradually oxidised by exposure to air during the time interval between the crush-leach extraction and anion analysis. Diamond *et al.* (1990), using similar procedures, assumed that the oxidation process was complete and hence that measured sulphate values reflect elemental sulphur concentration, not speciation.

Examination of the Hemerdon fluid inclusion leachate composition data (Tables 5.3 and 5.4) reveals a clear distinction between the granite-hosted veins and those hosted by killas, in terms of Cu and S abundances (as ratios with respect to Na); the two granite-hosted examples (HEM-79-2 and HEM-80-39 respectively) are both relatively depleted in these elements. Stage I and II hydrothermal fluids hosted by the Dartmoor granite (Table 5.1) contain similarly low levels of Cu. The pattern observed for Cu does not apply, however, to other chalcophile elements such as Fe or Zn; the presence of high levels of both of these elements in all the Hemerdon examples suggests that the fluids have not interacted to any great extent with sulphide-bearing wall-rocks, although evidence for a limited degree of interaction is provided by the finding of higher Cu concentrations in killas-hosted veins.

Cu and S concentrations are low in the Cornubian granites, relative to the regional shales and volcanic rocks (Hall, 1990). This is in accord with the postulate that, in the hydrothermal fluids, these elements were primarily derived from an aqueous phase exsolved during the crystallising of granite magma, rather than arising from subsequent leaching of wall-rocks. The data reported by Hall (1990) also show, however, that Zn is depleted in the granites, relative to the regional shales and volcanic rocks, whereas fluid inclusion leachate analysis by Bottrell and Yardley (1988) demonstrated that very high levels of Zn (~0.02m) are associated with a primary granite-derived, high temperature (500-600°C) hydrothermal fluid from the St Austell district (the associated Cu content was not measured). Indeed, Zn/Cu ratios in the granite-hosted vein fluids at Hemerdon and Dartmoor, as reported in the present work, greatly exceed those typical of the regional granites, shales and volcanic rocks.†

The contrasting behaviour of Cu and Zn during magma crystallisation may provide a clue to this anomaly: Lowenstern *et al.* (1991) showed that Cu, unlike Zn, is preferentially partitioned into a magmatic vapour phase rather than the associated melt. These authors suggested that, in silicate melts with a high water content, or containing low-solubility gases such as CO₂, vapour saturation may occur at relatively low pressure (shallow depth), thereby providing a low-density volatile phase into which Cu could partition (probably as a chloride complex). Nevertheless, it is difficult to envisage a plausible mechanism that explains the palæofluid Zn/Cu ratios, without recourse to the idea that Zn is preferentially concentrated, relative to Cu, in the saline fluids exsolved from crystallising magma.

Salient features of the early hydrothermal fluids from Cligga Head, South Crofty mine, and localities in the Gunnislake-Hingston Down area, include:

† Typical Zn/Cu ratio values in the granites, shales and volcanic rocks are: 4, 3 and 2.4 respectively (by weight), as derived from the results of Hall (1990).

- (a) Consistently lower Ca/Na ratios than are characteristic of the hydrothermal system hosted by the Dartmoor granite; the values are also generally lower than those of the Hemerdon system. K/Na ratios are, without exception, lower than those recorded in the Hemerdon fluids; the range of values is similar to that which characterises the Dartmoor hydrothermal system. These points are illustrated in Figure 5.1.
- (b) Generally lower levels of Fe and Mn (relative to Na), compared to the fluids at Hemerdon. Furthermore, the Fe/Mn mole ratio is less than unity (0.52) in the example from Cligga Head and also in one of the South Crofty specimens (0.74), whereas the corresponding range at Hemerdon (1.2 to 2.6) is not dissimilar to that of the fluids characteristic of early hydrothermal mineralisation in the Gunnislake-Hingston Down area (1.1 to 3.0). For comparison, corresponding values of the Dartmoor granite-hosted samples investigated in the present work ranged from 0.74 to 5.0, with no apparent correlation with paragenetic stage.
- (c) In the Cligga Head example, the reduced level of Fe was not coupled with a reduction in Zn concentration; furthermore, palæofluid Cu and Pb abundances (relative to Na) were notably higher than in any other specimen investigated in the present study. In other respects (with the notable exception of the low Ca/Na ratio), the early-stage fluid at Cligga Head was not dissimilar, in terms of electrolyte composition, to fluids associated with the corresponding paragenetic assemblage at Hemerdon. It is interesting to note that Hall (1971) reported that the unaltered Cligga granite is unusually rich in Cu and suggested that this element was leached out of the granite by hydrothermal fluids responsible for greisenization. Hall (1971) also reported that the unaltered granite is enriched in Pb and Zn, relative to the corresponding values for average granitic rocks.
- (d) It is difficult to make substantive inferences from the South Crofty data because of the degree of contamination of one of the samples (SC-88-3) by mineral impurities, as shown by the relatively high degree of ionic charge imbalance in the corresponding leachate data, coupled with the observation that the other sample from this locality (SC-88-2) was found (during *in vacuo* stepped heating extraction for palæofluid carbon stable isotope analysis - Chapter 3) to contain significant quantities of hydrocarbons. Apart from Fe/Na and Mn/Na ratios being substantially lower than the corresponding values in the Hemerdon fluids, the most notable finding is probably the low values of total sulphur abundance (relative to Na), which are comparable to those characteristic of the granite-hosted vein samples from Hemerdon.
- (e) Low abundances of sulphur are also characteristic of early-stage hydrothermal fluids associated with minor granite intrusions in the Gunnislake-Hingston Down area. At the Prince of Wales mine, this is coupled with anomalously high levels of Zn, significantly higher Fe and Mn abundances (relative to Na) than encountered elsewhere in the area, together with the lowest palæofluid Ca/Na ratio recorded in the present study.

Figure 5.3 shows that the range of Br/Cl ratios in the early hydrothermal fluids at Hemerdon is similar to that of the mineralising palaeofluids hosted by the Dartmoor granite, whereas quartz-hosted fluids associated with W±Sn oxide assemblages at Cligga Head, South Crofty mine, and several localities in the Gunnislake-Hingston Down area, are generally typified by lower Br/Cl values. Comparison with Br/Cl ratios of modern volcanic gases, as discussed in Section 5.6.1.3 and illustrated in Figure 5.4(a), lends support to the idea (but does not unequivocally prove) that these halogen components of the hydrothermal palaeofluids are primarily of magmatic origin.†

With regard to the corresponding I/Cl data, two examples of killas-hosted quartz veins from Hemerdon (samples HEM-80-1 and HEM-80-44 respectively) contained fluids characterised by I/Cl mole ratios (2.25×10^{-6} and 2.53×10^{-6} respectively) fairly close to that of modern seawater (0.84×10^{-6}); the majority of the Hemerdon palaeofluids analysed, however, had I/Cl ratios within the range defined by the corresponding data for the Dartmoor mineralising fluids, as shown in Figure 5.3. This Figure also indicates that, with the exception of examples from Drakewalls and South Crofty mines, which exhibit relative enrichment of I, the I/Cl data relating to quartz-hosted palaeofluids characterised by association with early W±Sn oxide mineralisation at other localities in the Cornubian province are within the range defined by the Hemerdon fluids.

Figure 5.4(b) compares the total data set with I/Cl ratios in (modern) volcanic fumarole condensates and illustrates that, whereas the range of I/Cl values in modern magmatic systems is very large, the results of the present study, in conjunction with the corresponding Br/Cl data, are not incompatible with a magmatic origin for the iodine component of the palaeofluids responsible for early hydrothermal oxide-associated mineralisation in S W England.

Levels of boron (normalised to Na) in the fluids associated with early W±Sn oxide assemblages are notably higher than in the fluids associated with early mineralisation of the Dartmoor granite. This may be explained on the basis of the extensive tourmaline precipitation associated with the earliest phase of hydrothermal activity hosted by the Dartmoor granite. In general terms, boron abundances are greatly enhanced in argillaceous sediments (*ca.* 100ppm) compared to igneous rocks (*ca.* 10ppm), whereas the boron content of modern seawater is, at 4.5ppm, lower than either of these lithological types (Spivack *et al.*, 1987, and references therein). This is explained on the basis of the major flux to the oceans being by direct injection from igneous degassing, rather than by fluvial transport

† Available data on metamorphic fluids are inadequate for comparison, as noted by Yardley *et al.* (1993). These authors also indicated, however, that oilfield brines are characterised by halogen ratios which plot in fields quite distinct from the present S W England results (see their Figure 5).

following chemical weathering; the incorporation of boron from seawater by weathered clay minerals is then probably responsible for the reported enrichments. On this basis, it may be possible to distinguish between a fluid which has interacted with sediments from one which has interacted with igneous rocks. In the case of hydrothermal systems, Spivack *et al.* (1987) showed that interaction between seawater and argillaceous sediments in seafloor hydrothermal systems in the Guaymas Basin, Gulf of California, resulted in elevation of the dissolved boron content by a factor of 3 to 4.

Hall (1990) showed that the granites of S W England are universally enriched in boron to an extreme degree, with concentrations of 20 to 30 times that typifying an 'average' granite outside this region. In a water-saturated granitic melt, the addition of 5 wt% or more of B_2O_3 lowers the solidus temperature at 1 kbar by 125°C (Chorlton and Martin, 1978), reflecting the substitution of tetrahedrally co-ordinated boron for aluminium in the melt and the resulting effect on the thermal stability of feldspars. The liquidus temperature was reported to be similarly affected. Hall (1990) also showed that the average boron concentration in the Cornubian granites is, on a weight basis, typically 3.8 times that in the adjacent shales and ~24 times that in the regional volcanic rocks. Furthermore, elements which have anomalously high concentrations in the Cornubian granites (B, Li and Sn) are moderately enriched in the shales; conversely, elements such as Ba and Sr, which have very low abundances in the granites, are moderately depleted in the shales. Hall (1990) was therefore able to show that the Cornubian geochemical anomaly predates the formation of the granite batholith, even though it is in the batholith that the most extreme trace element enrichments are found.

Fluorine was not included in the study by Hall (1990) of the geochemistry of the Cornubian province. In the present work, the limited availability of fluid inclusion leachate analyses for fluorine concentration precludes a comprehensive assessment of palaeofluid fluorine variations with vein host rock lithology or locality. The generally low levels of fluorine in the hydrothermal fluids hosted by the Dartmoor granite probably reflects the widespread occurrence of early tourmaline deposition[†], although the lack of correlation with boron abundance (see Table 5.1) suggests that other factors were also important, such as the incorporation of fluorine into mica group minerals. Conversely, the generally higher levels of fluorine in the hydrothermal fluids at Hemerdon probably represent the relatively restricted availability of mineral 'sinks' for this element at Hemerdon, rather than reflecting a greater enrichment of fluorine in the granite 'source'.[‡]

† According to Scrivener (1982), Table 8, fluorine constitutes approximately 0.4 to 0.8 weight percentage of tourmaline from Dartmoor.

‡ Geochemical modelling at 300°C of a fluid of comparable composition (Yardley *et al.*, 1993) indicates that Al may be primarily present as AlF_3 , whereas Ca occurs mainly as a bicarbonate complex. This accounts for both the relatively high levels of Al and also the lack of high-temperature fluorite deposition, despite significant abundances of both Ca and F in the fluid.

5.6.2.3 Palæofluid Pb concentrations at Hemerdon: comparison with an earlier study

An exploratory voltammetric investigation of Pb abundances in quartz-hosted hydrothermal fluid inclusions, undertaken earlier by the present author, included samples from the Hemerdon Sn-W deposit (Miller and Shepherd, 1984). The results of this study, undertaken as a prelude to the potential investigation of fluid inclusion Pb isotopic composition, indicated that the early mineralising fluids at Hemerdon may contain Pb concentrations in excess of $1000\mu\text{g}/\text{cm}^3\text{H}_2\text{O}$. These values were, however, derived on the basis of fluid inclusion water yields (obtained on 'splits' of the same samples) that were subsequently found to be in error (too low); the corresponding palæofluid Pb abundance values will consequently be lower than those published, although the revised values still indicate significant levels of Pb, in absolute terms.

One quartz sample from Hemerdon (HEM-80-1) included in the study by Miller and Shepherd (1984) was also investigated for fluid inclusion electrolyte composition in the present work. A direct comparison may therefore be made of estimates of the fluid inclusion Pb abundance data for this sample, as determined independently by the two different procedures:

- (i) Using the revised water yield value (with respect to the quartz host) of 1337 ppm for sample HEM-80-1 (Shepherd and Miller, 1988), in conjunction with the bulk Pb content of $0.73\mu\text{g}$ per gram of quartz as reported in Miller and Shepherd (1984), the average (bulk) concentration of Pb in the inclusion fluids of this sample, as determined by voltammetric analysis following total dissolution of the quartz, in conjunction with independent determination of the palæo-water content of the quartz, is $0.73/(10^6/1337) = 546\mu\text{gPb}$ per $\text{cm}^3\text{H}_2\text{O}$, equivalent to $(546 \times 10^{-6})/(207.2 \times 10^3) = 2.6 \times 10^{-3}$ molal Pb.
- (ii) As seen from Table 5.4(b), the fluid inclusion Pb concentration (molal) in sample HEM-80-1 as determined from leachate analysis in conjunction with the estimated salinity value of 30 ± 5 wt% NaCl equivalent (Kelley *et al.*, 1986) is $(2.0 \pm 0.5) \times 10^{-3}$ molal.

The results of fluid inclusion Pb analysis by the two different methods are thus remarkably close, considering the inherent assumptions and uncertainties. It should be noted, however, that procedures based on the total dissolution of quartz for the analysis of fluid inclusion components (as used by Miller and Shepherd, 1984; also by Darbyshire and Shepherd, 1985) necessarily neglects partitioning of the species of interest between the fluid phase and the quartz under hydrothermal conditions. Although the partition coefficients for most electrolytes are likely to be strongly in favour of the solution phase, it is preferable, in the

absence of supporting experimental data[†], to undertake the relevant measurements on the fluid phase directly (*i. e.* on leachates).

5.7 Summary and conclusions

The application of recent developments in fluid inclusion crush-leach analytical procedures to an investigation of early mineralising fluids hosted by the Dartmoor granite has revealed a surprising uniformity of palæofluid electrolyte composition, from the earliest pegmatitic quartz stage, through quartz+tourmaline±cassiterite association, to the stage characterised by quartz±hæmatite deposition. The excellent charge balances obtained for most of the analysed leachates support the assertion that the reported compositions are representative of the dominant generation of fluid in each case. Early mineralising fluids hosted by the central region of the Dartmoor granite exposure, isolated from contact with regional metasedimentary and volcanic rocks, provide a useful reference point for evaluating the origins of salinity and chemical composition of early fluids associated with other granites of the Cornubian region, where the comparable stage is characterised by W±Sn oxide assemblages and the vein host lithology is not exclusively granitic.

It is proposed that the electrolyte compositions of the Dartmoor-hosted fluids are compatible with the postulate of magmatic-hydrothermal origin, with little evidence for mixing with external fluids. Whereas published microthermometric studies have drawn attention to the high salinity of fluids associated with quartz±tourmaline±cassiterite veins of central Dartmoor and remarked on the presence of Ca in these Na-K chloride brines, Ca/K molar ratios exceeded unity in all fluids investigated in the present study, from earliest pegmatite-associated examples to those associated with quartz±hæmatite deposition. Furthermore, the enrichment of these fluids in B, F, Li, Al, Fe Mn and Zn shows an affinity with higher temperature (500-600°C) granite-derived fluids elsewhere in the batholith (St Austell area). For comparison, the results of Bottrell and Yardley (1988) are shown in Table 5.7.

The ubiquitous presence of high concentrations of Fe and Zn in the fluids is in accord with the isolation of these fluids from contact with sulphur-bearing wall-rocks, such as the regional Palæozoic metasediments. Sulphur concentrations in the fluids were not negligible, however: reconstructed compositions of the original fluids indicate that values were typically $(11 \pm 8) \times 10^{-3}$ molal, which places constraints on estimates of granite-derived sulphur input to hydrothermal systems elsewhere in S W England. Copper concentrations were notably low in the fluids, which is in accord with the relative depletion of this element in the granite.

[†] Rossman *et al.* (1987) reported Rb, Sr, Nd and Sm concentrations in naturally-occurring quartz; comparable data for Pb would appear to be lacking. According to Peucker-Ehrenbrink and Behr (1993), solid phase micro-impurities (such as feldspar or mica), rather than fluid inclusions or elements fixed in the quartz lattice, are the predominant hosts for most elements even in "carefully-cleaned" quartz.

Table 5.7

Fluid inclusion leachate analysis, as reported by Bottrell and Yardley (1988), of a granite-hosted topaz-quartz-tourmaline rock from St. Mewan's Beacon, St. Austell district: an example of a primary, granite-derived fluid.

(After Bottrell and Yardley, 1988)

Element	Molar ratio to Na ($\pm 1\sigma$) in leachate	Inferred composition of original fluid (molar)
Na	1.00 (by definition)	1.719
K	0.208 \pm 0.007	0.357
Ca	0.140 \pm 0.005	0.240
Fe	0.125 \pm 0.003	0.214
B	0.051 \pm 0.00007	0.087
Al	0.045 \pm 0.0008	0.077
Mn	0.034 \pm 0.002	0.059
Li	0.018 \pm 0.001	0.031
Zn	0.014 \pm 0.0007	0.024
Mg	0.003 \pm 0.00007	0.005
Rb	0.003 \pm 0.001	0.005
Sr	0.0009	0.002
Ba	0.0006	0.001
Cl	1.746 \pm 0.042	3.000
F	0.025 \pm 0.006	0.043
Total cationic charge, ΣQ^+		3.431
Total anionic charge, ΣQ^-		-3.305

Br/Cl and I/Cl molar ratios in the Dartmoor hydrothermal system, $(7.5 \pm 1) \times 10^{-4}$ and $(22 \pm 13) \times 10^{-6}$ respectively, are compatible with a magmatic origin for these elements, on the basis of a comparison with the corresponding values for volcanic fumarole condensates. The data are also similar to results, obtained in the same laboratory, of halogen ratio determinations on the high-temperature, granite-derived fluid from the St Austell area referred to above, supporting further the link between such high-temperature fluids and those responsible for early hydrothermal mineralisation of the central and north-eastern regions of the Dartmoor granite.

Application of the same crush-leach analytical procedures to investigate the compositions of early hydrothermal fluids characterised by association with $W \pm Sn$ oxide assemblages in the Cornubian region resulted in a greater degree of leachate charge imbalance in many cases, although the charge balances compare favourably with those published in other recent studies. The presence of significant levels of dissolved inorganic carbon compounds, which distinguishes these fluids from those of the hydrothermal system hosted by the Dartmoor granite, was shown to be not the cause of leachate charge imbalances. The presence of microscopic mineral inclusions was considered to be the most probable source.

The early hydrothermal fluids at Hemerdon are broadly similar, in terms of electrolyte composition, to those hosted by the Dartmoor granite. The principal differences, in general terms, are the greater enrichment of potassium and relative depletion of calcium at Hemerdon, together with even greater absolute abundances of F, B, Fe, Mn, Li, Al and Zn, as inferred from the reconstructed palæofluid compositions. The latter, in particular, demonstrate the very high capacity of these high-chlorinity fluids to transport metals. Pb concentrations in the Hemerdon fluids, as determined in the present investigation, are in good agreement with the result of an earlier study based on different analytical procedures.

At other localities in SW England, early hydrothermal fluids characterised by association with $W \pm Sn$ oxide assemblages were found to have consistently lower K/Na ratios than at Hemerdon; the values were similar to those of the quartz \pm tourmaline \pm cassiterite \pm hæmatite associated hydrothermal fluids hosted by the Dartmoor granite, although the corresponding Ca/Na ratios were lower than those of the Dartmoor system. Evidence for a magmatic-hydrothermal component in the $W \pm Sn$ oxide-associated fluids at Cligga Head, South Crofty mine and localities in the Gunnislake-Hingston Down area is provided by the strong enrichment of boron (the abundance of which exceeds that of calcium at Cligga Head, Drakewalls mine and the Prince of Wales mine), distinctive minor element distributions and halogen ratios. The lower absolute abundances reflect the lower salinity values of many of these fluids, compared to the Hemerdon examples, which is consistent with the postulate of mixing with (dilution by) a low salinity, meteoric component.

The relative concentration of sulphur species (with respect to other components) in the fluids at South Crofty and the Gunnislake-Hingston Down localities was surprisingly low, in view of the proximity of (or even hosting of the quartz veins by) Palaeozoic metasedimentary rocks, and indicates that leaching of the killas by the hydrothermal fluid systems did not occur to any significant extent in these examples.

5.8 Suggestions for further research

In view of the findings by Hall (1990) that the Cornubian granites are anomalously enriched in tin (as well as boron and lithium), together with the fact that many of the samples investigated in the present study were associated with cassiterite deposits, it would be instructive to investigate the concentrations of tin in the fluid inclusion leachates. Lockett (1987) attempted to apply isotope dilution analysis to determine the abundance of tin in fluid inclusions, following crush-leach extraction procedures; what emerged from that study was the finding that procedural blank levels were surprisingly high and derived from a variety of sources. Whereas the detection sensitivity of ICP-AES for tin (~100ppb or less) is probably sufficient for the analysis of fluid inclusion leachates in the present case (but necessitating the use of HCl as the leaching agent, rather than HNO₃), it is likely that a high and variable blank would be found (S H Bottrell, *pers. comm.*), reflecting significant background levels of this element in the laboratory environment. Further work remains to be done to overcome these problems.

The analysis, possibly by ion chromatography, of ammonium levels in the fluid inclusion leachates (if ammonium is present at all - see the discussion in Chapter 4, Section 4.2.12) would be of value to a consideration of nitrogen speciation in the fluids. Channer and Spooner (1992) reported minimum detection limits of 0.6ppb for NH₄⁺, using a Dionex® 2000i-SP ion chromatograph. Similarly, analysis of reduced sulphur levels in the fluid inclusions is feasible, using the technique developed by Bottrell and Miller (1989). This has a detection limit corresponding to ~20ppm of sulphur in the inclusion fluids.

To lend further support to the hypothesis that hydrothermal fluids associated with early oxide mineralisation in the Cornubian province were primarily of magmatic origin, it would be advantageous to apply the fluid inclusion leachate procedures referred to in this work to determine the electrolyte compositions of fluids hosted by the unaltered granites, for direct comparison.

North-south trending 'cross-course' quartz-fluorite veins in the Tamar valley, located south-east of the Gunnislake-Kit Hill area and hosting Pb-Zn mineralisation, are known to be derived from fluids of high salinity, relatively enriched in Ca and deposited at 110-170°C (Shepherd and Scrivener, 1987, and references therein). The age of these structures has been

established as ~235Ma (Darbyshire and Shepherd, 1990). The fluids responsible for the cross-course veins were possibly mobilised in response to changes in the regional tectonic stress field (Shepherd and Scrivener, 1987). To date, however, these fluids have generally been considered to be evolved basinal brines, by analogy with systems elsewhere (Shepherd and Scrivener, 1987; Shepherd *et al.*, 1985), or Mesozoic seawater (Durrance *et al.*, 1982). The suggestion was offered in Chapter 2 of the present work that these fluids might be derived from inclusions in the unaltered granites, fractured by a changing tectonic stress regime. The salinity and calcium enrichment of these fluids (Shepherd and Scrivener, 1987) is not incompatible with such an explanation, on the basis of the present findings. Investigation of the electrolyte compositions of these fluids, using the procedures described in the present work, would help to test this hypothesis.

Appropriately-designed experimental studies of fluid-rock interaction under hydrothermal conditions, involving leaching experiments on both granites and killas and with subsequent analysis of the reacted fluids for electrolyte composition, are needed to investigate further the hypothesis that the chemical compositions of high-salinity magmatic-hydrothermal fluids at 300-450°C do not undergo substantial modification during contact with the killas.

The high levels of boron in early hydrothermal mineralising fluids of the Cornubian region, as established in the present work, are in accord with a magmatic origin for the fluids. This has been argued herein on the basis of the substantial enrichment of boron in the granites of S W England (Hall, 1990), relative to both 'average' granite compositions and also to the local country rocks; also the central rôle of this element in the earliest mineralisation of the Dartmoor granite (Scrivener, 1982), and the abundance of boron in higher-temperature (500-600°C) granite-derived fluids in the Cornubian region (Bottrell and Yardley, 1988). In view of these findings, it is suggested that the application of boron isotope studies may shed further light on the source and transfer mechanisms of boron in the hydrothermal solutions. With regard to the Cornubian shales, Hall (1990) found that the associated boron contents varied from about 50 to 150ppm, with no examples in which boron concentrations were low.

There are two naturally-occurring stable isotopes of boron, ^{10}B and ^{11}B , the relative abundances of which are approximately 1:4. Because of the large relative mass difference, exceeded only by $^2\text{H}/^1\text{H}$ and $^{18}\text{O}/^{16}\text{O}$, large natural variations of $^{11}\text{B}/^{10}\text{B}$ occur, with $\delta^{11}\text{B}$ values† ranging from -31‰ in terrestrial rocks to +39‰ in modern seawater. The average continental crustal is characterised by values of -8 to +2‰.

† Boron stable isotopic variations are generally reported using the conventional delta notation, with reference to the standard NBS SRM 951, a boric acid powder:

$$\delta^{11}\text{B} = 10^3 \times \left[\left[\frac{(^{11}\text{B}/^{10}\text{B})_{\text{sample}}}{(^{11}\text{B}/^{10}\text{B})_{\text{standard}}} \right] - 1 \right] \text{‰}$$

Aqueous speciation of boron is dominated by the tetrahedral $\text{B}(\text{OH})_4^-$ anion and the trigonal $\text{B}(\text{OH})_{3(\text{aq})}$ entity; the equilibrium between these two species is dependent on both pH and temperature. $\text{B}(\text{OH})_4^-$ is relatively enriched in ^{10}B and is preferentially adsorbed onto clay minerals from aqueous solutions. Boron isotopic fractionation between tourmaline and coexisting fluid/vapour is $\sim 2\%$ at 750°C and $6.5\text{-}8\%$ at 350°C (Slack, 1989), with preferential enrichment of ^{10}B in the fluid.

Determination of boron stable isotope ratios is usually undertaken by thermal ionisation mass spectrometry of $\text{Cs}_2\text{B}_4\text{O}_7$, (prepared by the addition of Cs_2CO_3 to aqueous samples), giving a $\delta^{11}\text{B}$ precision of 0.24% at the 2σ level (see Spivack *et al.*, 1987, and references therein). A relatively recent variation of the usual procedure is to undertake the isotopic analysis by negative thermal ion mass spectrometry; this utilises the ease of conversion of boron to BO_2^- ions and permits untreated solutions to be loaded directly onto the filaments of a reverse polarity mass spectrometer. This has obvious advantages for the minimisation of contamination. Using such a procedure, boron concentrations as low as 0.06ppm may be detected and $\delta^{11}\text{B}$ measured with a 2σ precision of 1.9% (Vengosh *et al.*, 1989). With reference to the fluid inclusion leachates of hydrothermal quartz hosted by, for example, the Dartmoor granite, as prepared during the present work, absolute concentrations of boron in the leachate solutions ranged (with the exceptions of samples SW-89-157 and SW-89-161) from 169 to 660ppb (as borate), which should be sufficient to enable fluid inclusion $\delta^{11}\text{B}$ analysis to be performed.

Chapter 6

Palaeozoic metasediments of SW England: geochemical and isotopic constraints on the effects of granite emplacement. An exploratory study, with reference to the Dartmoor granite

6.1 Synopsis

An exploratory investigation was made of the effects of the intrusion of the Dartmoor granite into local Palaeozoic host rocks, in terms of the alteration of both geochemical composition, and of the isotopic composition of selected trace elements, in the metasedimentary rocks. For this purpose, two traverses were sampled across the metamorphic aureole - one of Upper Famennian (Kate Brook) Slate, to the south-west of the pluton; the other comprised of Namurian (Crackington Formation) mudstones located north-east of the granite. In addition, a small number of borehole drillcore samples of Devonian sedimentary rock from localities west of the St Austell granite were included, for comparison purposes.

Geochemical compositions of the metasedimentary rocks are compared with published data for the Cornubian region as a whole and indications for chemical alteration in the vicinity of the Dartmoor granite contact zone examined, to assess whether any localised effects resulting from the influx of an exsolved aqueous magmatic fluid may be detected.

The Rb-Sr isotope systematics of the metasedimentary rocks of the Dartmoor granite aureole are compared with corresponding published data for the granite and also with fluid inclusion leachates of quartz associated with early hydrothermal mineralisation hosted by the granite. Resulting constraints on the chronology of mineralisation are discussed, together with the evidence for magmatic fluid infiltration *versus* closed system thermal resetting of the isotope systematics in the metasedimentary rocks during contact metamorphism.

Carbon and nitrogen abundances (the former as both carbonate and 'organic' carbon, the latter as ammonium), together with the respective stable isotopic compositions, were determined in the metasediment samples to investigate the influence of granite emplacement on these trace elements, which have been shown elsewhere in the present work to be of significance in early hydrothermal fluid systems associated with W±Sn oxide mineralisation in the Cornubian region and also to be probably of magmatic origin. The findings are discussed in terms of the feasibility of carbon and nitrogen assimilation into the granitic magma at a high crustal level, as an alternative (or an addition) to the anatexis mechanism proposed in earlier chapters of this work.

The present chapter attempts to assess the extent to which carbon and nitrogen were assimilated into the granite from the surrounding low-grade (high anchizone/low greenschist facies) metasedimentary rocks at a high crustal level during granite emplacement. Two traverses across the thermal aureole of the Dartmoor granite were sampled: one representative of Upper Devonian metasediments, the other of Carboniferous mudstones. The former was of a stratigraphic type - Kate Brook Slate - which is also the predominant country rock at nearby Hemerdon and in the Gunnislake-Kit Hill area, where both granite and killas-hosted early hydrothermal quartz veins are characterised by relative enrichment of carbon compounds and molecular nitrogen in the palæofluids. Namurian shales of the Crackington Formation, representative of the youngest rocks intruded by the Dartmoor granite, were sampled for the second traverse.

All samples were analysed for chemical composition, to provide a comparison with the granite. Rb-Sr isotopic determinations of whole-rock samples were made in order to examine whether any systematic variation with distance from the granite contact was apparent of $^{87}\text{Sr}/^{86}\text{Sr}$ back-corrected (on the assumption of closed-system behaviour) to the time of granite emplacement. The carbon (carbonate and 'organic' carbon) and nitrogen (as ammonium) contents of the metasediment samples, together with the respective stable isotopic compositions, were analysed to assess the effects of contact metamorphism on these components of the mudstones and to examine the possibility of their incorporation into the granitic magma during its emplacement.

6.3 Salient features of the regional metasedimentary rocks, with reference to the thermal aureole of the Dartmoor granite

6.3.1 General observations

A detailed consideration of the lithology of the mainly sedimentary rock sequences that comprise and surround the metamorphic aureole of the Dartmoor granite is outside the scope of the present work. Detailed accounts of specific aspects are to be found in *e.g.* Hawkes (1982), Selwood and Durrance (1982), Thomas (1982), Bull (1982) and Whiteley (1983) and references therein. All the rocks were regionally metamorphosed (at low grade) before emplacement of the granite. The southern part of the Dartmoor pluton penetrated folded sequences of mainly argillaceous and silty Devonian rocks containing scattered calcareous horizons and sporadic tuff, lava and intrusions of mafic igneous origin. In contrast, the northern part of the granite intruded rocks of Carboniferous age; lithostratigraphically these consist of Culm Measures (Ugbrooke and Crackington Formation) and earlier formations (Transition Group and Lower Culm).

According to Hawkes (1982), mineralogical evidence (assemblages characteristic of hornblende-hornfels facies metamorphism) suggests that the temperature and water vapour pressure in the inner regions of the Dartmoor aureole were probably of the order of 500-600°C and 1-2 kbar respectively. The extent of the aureole (approximately 0.75 to 3.25 km horizontal distance from the contact, depending on the general inclination of the latter) indicates that such pressures were maintained for a considerable length of time. This, in turn, implies confining pressures equivalent to a cover of at least 1-3 km. Hawkes (1982) also attributed the effects of the contact metamorphism primarily to the increase in temperature and to the circulation of hydrous fluids from the intruded granite. In the outer parts of the aureole, thermal spotting of slates is recognised, whereas closer to the contact, conversion to quartz-biotite-andalusite assemblages occurred. Within the thermal aureole, sedimentary rocks were converted to fine-grained calc-silicate hornfelses, containing a variety of accessory minerals. Mafic igneous rocks developed hornblende assemblages towards the inner parts of the aureole.

6.3.2 Kate Brook Slate

The Kate Brook Slate formation is a major sequence in the study area. It consists of a thick, monotonous sequence of hard, greenish-grey slates with sporadic thin sandstones, is now allochthonous and is everywhere fault-bounded (Selwood and Durrance, 1982). The remarkable lithological uniformity, even allowing for repetition of beds by folding, appears to have persisted through a very considerable thickness of strata. The mineralogy is dominated by chlorite with accessory micaceous minerals, all generally characterised by a grain size of <0.01 mm (Whiteley, 1983). The age of the formation is late Devonian, probably late Famennian (Whiteley, 1983; Molyneux and Owens, 1990), on the basis of palynomorphic evidence, which equates to an age of 364 ± 2 Ma on the time scale of Harland *et al.* (1990). West of Dartmoor, slates identical to the Kate Brook Slate occur in an extensive east-west tract of country intruded by the Kit Hill and Gunnislake granites; in total, the outcrop extends from Tintagel to Chudleigh. The depth of the formation is unknown, although it is estimated to be at least 480 m, on the basis of borehole evidence from the vicinity of Devon Great Consols mine, near Gunnislake (Whiteley, 1983). The Kate Brook Slate is quite barren of fossils throughout a considerable thickness of the succession (Selwood and Durrance, 1982). Rare fossil-bearing horizons indicate that the substrate was not inimical to life, and as there is no evidence to support the possibility of very rapid sedimentation, it seems that the depth of water may have been a limiting factor. The development of anoxic conditions is an alternative possibility. Basinal deposition is suggested by the lithology, in which the thin sandstones were introduced as distal turbidites (Selwood and Durrance, 1982); the indication is that accumulation took place in the axial part of a basin.

6.3.3 Crackington Formation shales

The pattern of Carboniferous sedimentation (Culm Measures) in S W England is consistent with the development of a deep water marine trough which accumulated a thick succession of shales and sandstones (Thomas, 1982). At the end of the Devonian, increased subsidence, coupled with a reduced supply of sediment, is believed to have resulted in overall deepening of the trough and consequently greater uniformity of the deep-water conditions. The Crackington Formation is a sequence of Upper Culm shales with thin turbidite sandstones and is a succession widespread throughout north and central Devon. The samples investigated in the present study are of Namurian age, H-R zones (R C Scrivener, *pers. comm.*), which corresponds to 324.5 ± 4 Ma on the time scale of Harland *et al.* (1990).

6.4 An investigation of selected characteristics of metasedimentary rocks sampled across the thermal aureole of the Dartmoor granite

6.4.1 Samples used in the present study

Kate Brook Slate samples (twelve) were collected along a traverse (~3 km length) across the metamorphic aureole of the Dartmoor granite, to the south-west of the pluton, providing a suite of material representative of various stages of metamorphic alteration. A further sample was subsequently collected, at greater distance from the contact, to provide an example undisturbed by the thermal effects of the granite intrusion. The suite of Crackington Formation mudstones was collected from an area to the north-east of the pluton; the relatively poor exposure in this case prevented such a systematic approach to the sampling. Six examples were taken; although not strictly representing a traverse across the aureole, the samples were collected at various distances from the granite contact and the set was therefore deemed to be equally valuable. Road or railway cuttings were chosen where possible for collection of the sample suites, as such sites usually provide the best source of unweathered material. All weathered surfaces were, in any case, removed prior to subsequent preparation for analysis. Details of the respective sample localities are given in Appendix A.

In addition to the above, drillcore material of Devonian age was made available to the author from three borehole sites to the west of the St Austell granite. The site localities are documented in Appendix A. Metasediments from these drillcores were included in the present study, for comparison with the rock samples from the Dartmoor granite thermal aureole.

Initial preparation of whole-rock powders for geochemical and isotopic analysis consisted of sawing off all exposed surfaces, followed by use of a hydraulic rock-splitter to reduce the size of individual samples, where necessary, prior to jaw-crushing. This produced aggregate-sized material, which was subsequently reduced to a fine powder (-200 mesh) using an agate Tema[®] mill.

6.4.2 Chemical compositions of the metasedimentary rocks

Results of X-ray fluorescence analyses of the Kate Brook Slate for major and minor elements (as oxides), together with trace elements, are presented in Tables 6.1(a) and 6.1(b) respectively. The analyses were carried out at the University of Keele on the author's behalf, using fused beads for major and minor elements, and pressed powder pellets for trace elements. The corresponding data sets for the Crackington Formation samples and for the Devonian sub-surface (drillcore) samples obtained from an area to the west of the St Austell granite (and beyond the associated metamorphic aureole) are shown in the companion Tables 6.1(c) and 6.1(d). Additionally, measurements of carbon, nitrogen and sulphur concentrations were undertaken using an elemental analyser; all the resulting data were near or below the respective detection limits of the instrumentation, as shown in Table 6.2. The carbon and nitrogen results were used as a guide, prior to undertaking higher precision yield measurements during the course of $\delta^{13}\text{C}$ and $\delta^{15}\text{N}$ analyses.

No systematic trend of element depletion or enrichment with increasing distance from the Dartmoor granite contact is discerned from the data obtained in the present study. If the thermal metamorphic effects on the mudstones due to granite emplacement were accompanied by pervasive infiltration of a (high salinity) hydrous phase from the granite, as suggested by *e.g.* Hawkes (1982), it might be expected that the geochemical expression of such an event would be retained in the rocks of the metamorphic aureole. Indeed, the general uniformity of elemental composition of the rocks examined in the present investigation raises the question of what, if any, chemical changes to the Palaeozoic sedimentary rocks of the region accompanied the emplacement of the granites.

Since these data were obtained, Hall (1990) reported the results of a systematic investigation of the geochemical composition of the major rock types of the Cornubian region. The results of that study demonstrated that elements which are present in abnormally high abundances in the Cornubian granites (in particular, boron, lithium and tin) are moderately abundant in the shales; conversely, those elements which are present in very low concentrations in the granites (barium and strontium) are present in moderately low concentrations in the shales. Those findings indicated that the geochemically anomalous features of the region predate the formation of the granite batholith, even though it is in the batholith that the most extreme trace element enrichments are found.

The results of the present study largely confirm the findings of Hall (1990) regarding element distribution in the shales, although it is unfortunate that B, Sn and Ba concentration data (not readily obtained by X-ray fluorescence analysis) were not available in the present study, for comparison.

Table 6.1(a)

X-ray fluorescence analyses of Kate Brook Slate from an area south - west of the Dartmoor granite:
Major and minor element compositions (weight percentages, as oxides)

	S13	S7	S8	S9	S10	S11	S12	S6	S5	S4	S3	S2	S1	AGV-1
SiO ₂	58.79	54.02	55.24	56.98	52.37	51.88	55.65	55.82	53.28	59.34	59.08	59.55	64.25	59.67
TiO ₂	0.91	0.98	0.94	0.94	0.98	1.00	0.91	0.90	0.96	0.98	1.09	0.99	0.96	1.04
Al ₂ O ₃	20.45	23.77	23.45	21.66	25.11	24.95	22.55	22.33	23.84	19.60	21.66	20.44	16.96	17.14
Fe ₂ O ₃ (T)	8.34	9.27	8.45	9.06	9.08	9.09	8.78	8.77	8.99	6.75	2.52	7.11	4.25	6.89
MnO	0.08	0.09	0.16	0.15	0.17	0.16	0.08	0.15	0.09	0.05	0.01	0.09	0.01	0.09
CaO	0.06	0.10	0.10	0.29	0.19	0.19	0.06	0.26	0.19	0.25	1.19	0.12	0.99	4.88
MgO	2.14	2.16	2.14	2.35	2.38	2.36	2.27	2.31	2.35	2.55	2.45	1.78	4.45	1.62
Na ₂ O	0.10	0.56	0.41	0.85	0.30	0.28	0.21	0.79	0.28	1.22	4.49	0.18	0.83	4.13
K ₂ O	4.79	4.39	4.25	3.74	4.69	4.81	4.45	3.97	4.91	4.10	2.91	3.69	0.05	2.88
P ₂ O ₅	0.13	0.12	0.13	0.18	0.13	0.13	0.06	0.13	0.12	0.12	0.08	0.08	0.03	0.50
LOI	3.72	4.70	4.62	4.02	4.73	4.73	4.48	4.10	4.49	4.93	3.75	5.73	1.73	1.07
Total	99.50	100.16	99.86	100.22	100.13	99.57	99.50	99.52	99.50	99.89	99.22	99.76	94.51	99.92

- Notes:
- (1) The data were supplied by the University of Keele department of geology and were determined using an ARL 8420 spectrometer.
 - (2) All sample references are prefixed by SW-87-
 - (3) Sample localities are listed in Appendix A.
 - (4) AGV-1 is a USGS standard. LOI refers to loss on ignition. Fe₂O₃ (T) refers to total iron.
 - (5) Samples are listed in order of increasing distance from the granite contact.
 - (6) The analysis of sample S1 was repeated three times, in view of the very low total. An XRD trace showed that the sample consisted largely of tourmaline and quartz; the low total was therefore attributed to the non-determination of boron and fluorine (both of which would be present in the tourmaline).

Table 6.1(b)

X-ray fluorescence analyses of Kate Brook Slate from an area south-west of the Dartmoor granite:
Trace element compositions (ppm)

	S13	S7	S8	S9	S10	S11	S12	S6	S5	S4	S3	S2	S1	AGV-1
Cr	105	120	115	109	126	119	121	109	121	117	114	130	111	10
Cu	43	27	31	26	31	32	37	26	26	51	31	40	4	63
Ga	25	31	34	34	31	37	36	30	35	27	26	27	52	21
Nb	18	18	18	17	19	19	17	18	18	19	19	18	14	14
Ni	46	66	57	55	63	64	56	57	66	63	39	32	11	16
Pb	56	26	30	6	34	30	31	36	5	22	30	33	43	32
Rb	354	213	216	203	235	235	268	211	253	206	188	171	8	67
Sr	39	115	107	76	102	104	60	109	66	46	201	59	130	673
Th	21	20	19	16	20	18	20	20	17	18	15	16	13	5
V	141	184	198	155	199	188	165	192	193	179	177	213	226	106
Y	31	29	35	28	32	33	33	26	29	32	40	28	10	19
Zn	80	113	122	130	124	123	87	102	130	74	52	130	23	88
Zr	162	157	157	140	156	156	145	146	146	184	198	179	163	231
(TiO ₂)	(1.03)	(1.12)	(1.10)	(1.08)	(1.13)	(1.10)	(1.01)	(1.09)	(1.14)	(1.04)	(1.17)	(1.13)	(1.10)	(1.08)

- Notes:
- (1) The data were supplied by the University of Keele department of geology and were determined using an ARL 8420 spectrometer.
 - (2) All sample references are prefixed by SW-87-
 - (3) Sample localities are listed in Appendix A.
 - (4) Samples are listed in order of increasing distance from the granite contact.
 - (5) AGV-1 is a USGS standard. TiO₂ values are in weight percent.

Table 6.1 (c)

X-ray fluorescence analyses of Crackington Formation metasediments from an area north - east of the Dartmoor granite

a) Major and minor element compositions (weight percentages as oxides)

	S14	S17	S18	S16	S15	S19	AGV-1
SiO ₂	60.53	54.83	59.73	54.01	50.40	62.43	59.67
TiO ₂	0.82	0.99	1.00	0.93	1.08	0.92	1.04
Al ₂ O ₃	20.61	23.14	20.55	23.75	25.46	17.97	17.14
Fe ₂ O ₃ (T)	7.07	9.05	4.14	9.52	9.57	7.05	6.89
MnO	0.06	0.16	0.01	0.16	0.17	0.10	0.09
CaO	0.06	0.13	2.52	0.14	0.25	0.23	4.88
MgO	1.95	2.35	2.49	2.48	2.43	2.24	1.62
Na ₂ O	0.10	0.28	4.50	0.45	0.32	0.95	4.13
K ₂ O	4.73	4.40	1.87	4.51	5.09	3.09	2.88
P ₂ O ₅	0.11	0.13	0.12	0.11	0.17	0.11	0.50
LOI	3.90	4.22	3.08	4.36	4.70	4.73	1.07
Total	99.93	99.68	100.01	100.43	99.63	99.83	99.92

b) Trace element compositions (ppm)

	S14	S17	S18	S16	S15	S19	AGV-1
Cr	99	122	126	120	140	120	10
Cu	152	34	51	23	74	41	63
Ga	24	30	23	28	37	25	21
Nb	17	19	18	18	20	15	14
Ni	42	58	64	66	68	92	16
Pb	55	64	23	20	27	17	32
Rb	343	273	114	250	289	145	67
Sr	50	53	266	89	81	58	673
Th	13	14	13	18	19	15	5
V	169	181	195	170	199	189	106
Y	32	34	22	19	38	30	19
Zn	74	108	14	89	121	168	88
Zr	143	158	185	152	165	169	231
(TiO ₂)	(0.93)	(1.11)	(1.05)	(1.10)	(1.20)	(1.03)	(1.08)

Notes: (1) The data were supplied by the University of Keele department of geology and were determined using an ARL 8420 spectrometer.

(2) All sample references are prefixed by SW-87-

(3) Sample localities are listed in Appendix A.

(3) Samples are listed in order of increasing distance from the granite contact.

(4) LOI refers to loss on ignition. Fe₂O₃ (T) refers to total iron.

(5) AGV-1 is a USGS standard. TiO₂ values in (b) are in weight percent.

Table 6.1 (d)

X-ray fluorescence analyses of Devonian metasediments (borehole drillcores)
from an area west of the St Austell granite

a) Major and minor element compositions (weight percentages as oxides)

	HF1	HF2	HF3	AGV-1
SiO ₂	56.09	48.68	45.60	59.67
TiO ₂	1.05	1.98	1.12	1.04
Al ₂ O ₃	21.47	19.80	29.62	17.14
Fe ₂ O ₃ (T)	9.19	11.73	8.97	6.89
MnO	0.12	0.14	0.05	0.09
CaO	0.23	2.42	0.30	4.88
MgO	2.69	4.66	2.06	1.62
Na ₂ O	1.17	1.81	1.02	4.13
K ₂ O	3.77	2.40	5.31	2.88
P ₂ O ₅	0.12	0.33	0.11	0.50
LOI	4.54	6.20	5.52	1.07
Total	100.44	100.14	99.67	99.92

b) Trace element compositions (ppm)

	HF1	HF2	HF3	AGV-1
Cr	124	183	143	10
Cu	32	48	30	63
Ga	26	27	43	21
Nb	21	25	21	14
Ni	76	94	58	16
Pb	27	40	33	32
Rb	214	120	237	67
Sr	74	200	235	673
Th	22	13	21	5
V	206	283	215	106
Y	36	41	36	19
Zn	121	325	119	88
Zr	189	217	158	231
(TiO ₂)	(1.18)	(2.15)	(1.33)	(1.08)

Notes: (1) The data were supplied by the University of Keele department of geology and were determined using an ARL 8420 spectrometer.

(2) Sample descriptions and localities are listed in Appendix A.

(3) LOI refers to loss on ignition. Fe₂O₃ (T) refers to total iron.

(4) AGV-1 is a USGS standard. TiO₂ values in (b) are in weight percent.

Table 6.2**C, N and S analyses of SW England metasedimentary rock samples**

(All data were supplied by Dr S H Bottrell; analyses were undertaken at the University of Leeds department of Earth sciences, using a Carlo Erba® model 1106 elemental analyser)

- a) Upper Devonian rocks from an area south-west of the Dartmoor granite
(Samples are listed in order of increasing distance from the granite contact - see Appendix A)

Sample reference	Wt% C _(total)	Wt% N	Wt% S
SW-87-S13	nd	nd	0.04
SW-87-S7	nd	nd	nd
SW-87-S8	nd	0.03	0.04
SW-87-S9	nd	nd	0.04
SW-87-S10	nd	0.05	nd
SW-87-S11	nd	nd	0.03
SW-87-S12	nd	nd	0.06
SW-87-S6	nd	0.01	0.06
SW-87-S5	nd	0.07	0.11
SW-87-S4	0.32	nd	2.24
SW-87-S3	0.28	nd	0.63
SW-87-S2	0.65	0.05	0.13
SW-87-S1	nd	nd	nd

- b) Carboniferous rocks from an area north-east of the Dartmoor granite
(Samples are listed in order of increasing distance from the granite contact - see Appendix A)

Sample reference	Wt% C _(total)	Wt% N	Wt% S
SW-87-S14	nd	nd	nd
SW-87-S17	nd	nd	0.10
SW-87-S18	0.41	nd	1.34
SW-87-S16	nd	0.01	0.05
SW-87-S15	nd	0.07	0.05
SW-87-S19	0.54	0.03	0.11

- c) Devonian rocks (borehole cores) from an area west of the St Austell granite
(Sample localities are given in Appendix A)

Sample reference	Wt% C _(total)	Wt% N	Wt% S
HF1	nd	nd	nd
HF2	nd	0.07	0.05
HF3	0.54	0.03	0.11

- Notes: (1) nd indicates 'not detected'. The detection limits of the carbon and sulphur analyses were $\approx 0.025\%$ (250 ppm); the corresponding value for the nitrogen analyses was $\approx 0.01\%$ (100 ppm).
 (2) Analyses were undertaken on untreated, powdered samples. Although the background values (including nitrogen) were acceptably low, reproducibility close to the detection limits is poor.
 (3) Samples (1-3 mg) for N and C analysis were combusted in tin cups at 1400°C in a He/O₂ atmosphere. Sulphur determinations were undertaken separately.

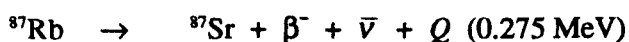
What is of significance in the present data set, however, is that the calcium contents are in general considerably lower than the average value for shales (0.74% as CaO) given by Hall (1990). The few exceptions to this observation are substantially enriched in calcium, by comparison, indicating the presence of a significant amount of carbonate in those examples.

6.4.3 Strontium, carbon and nitrogen isotopic behaviour during contact metamorphism of metasediments by the Dartmoor granite

6.4.3.1 Strontium isotope studies

6.4.3.1.1 Introduction: Sr isotope systematics

The relative natural abundances (as percent values) in common terrestrial matter of the four naturally-occurring, long-lived isotopes of strontium (^{84}Sr , ^{86}Sr , ^{87}Sr and ^{88}Sr) and the two of rubidium (^{85}Rb and ^{87}Rb) are approximately 0.56:9.87:7.04:82.53 and 72.17: 27.83 respectively. ^{87}Sr is a radiogenic isotope, produced by emission of a beta particle and anti-neutrino from ^{87}Rb :



The associated decay constant (λ) is $1.42 \times 10^{-11} \text{ a}^{-1}$ (Steiger and Jäger, 1977), corresponding to a half-life of 48.8 Ga. On this time scale, the abundances of ^{84}Sr , ^{86}Sr and ^{88}Sr are invariant; any increase in the $^{87}\text{Sr}/^{86}\text{Sr}$ ratio in a (closed) rock system, for example, may be attributed solely to the decay of ^{87}Rb . For this reason, it is usual to present the abundances of ^{87}Sr and ^{87}Rb as normalised values with respect to the corresponding abundance of ^{86}Sr ; the amount of ^{87}Sr produced by the decay of ^{87}Rb over time t is then given by:

$$(^{87}\text{Sr}/^{86}\text{Sr}) = (^{87}\text{Sr}/^{86}\text{Sr})_0 + (^{87}\text{Rb}/^{86}\text{Sr}) (e^{\lambda t} - 1)$$

where $(^{87}\text{Sr}/^{86}\text{Sr})_0$ refers to the initial ratio ($t = 0$). Modern instrumentation permits high precision determination of $^{87}\text{Sr}/^{86}\text{Sr}$ ratios, ultimately to ± 10 ppm or better.

Isotopic evolution of Sr into distinct reservoirs over geological time, from a primordial $^{87}\text{Sr}/^{86}\text{Sr}$ value of ~ 0.699 , reflects the corresponding Rb/Sr ratios. In general terms, differentiation of the Earth has occurred via a process of fractional crystallisation, which concentrates Sr, and even more so Rb, into the melt, resulting in high Rb/Sr ratios in the continental crust and, correspondingly, a progressive reduction in the Rb/Sr ratio of the residual mantle. Consequently, present-day mantle (and oceanic crust) is characterised by a relatively depleted $^{87}\text{Sr}/^{86}\text{Sr}$ ratio of $\sim 0.703 \pm 0.001$, whereas continental crust is enriched in radiogenic ^{87}Sr , with $^{87}\text{Sr}/^{86}\text{Sr}$ values of > 0.710 and with the greatest enrichment occurring in the older continental blocks.

The process of mineral formation fractionates Rb with respect to Sr, but does not fractionate ^{87}Sr with respect to ^{86}Sr . In all but very young igneous and metamorphic rocks, the minerals that concentrate Rb with respect to Sr, such as micas and potassium feldspars, will be characterised by higher $^{87}\text{Sr}/^{86}\text{Sr}$ ratios than those that do not concentrate Rb. In contrast to sedimentary rocks such as shales and sandstones, which mainly consist of minerals derived from older rocks and hence of a range of Rb/Sr ratios (and consequently exhibit $^{87}\text{Sr}/^{86}\text{Sr}$ ratios that vary on a relatively small scale), sedimentary rocks that consist of minerals precipitated from solution, such as limestones and dolomites, are generally more homogeneous, have low Rb/Sr ratios, and are predominantly comprised of calcium and magnesium carbonates that formed in isotopic equilibrium with seawater. The $^{87}\text{Sr}/^{86}\text{Sr}$ ratio in marine carbonates is an excellent indicator of the $^{87}\text{Sr}/^{86}\text{Sr}$ ratio in seawater at the time of mineral deposition and has varied significantly over geological time (*e.g.* Holland, 1984; Veizer, 1989). Use of the $^{87}\text{Sr}/^{86}\text{Sr}$ isotope ratio to characterise the origin of groundwaters in crystalline rocks and to evaluate the degree of interaction of these waters with the host rocks and/or fracture minerals is well established (*e.g.* Fritz *et al.*, 1987; McNutt, 1987).

The strontium isotope systematics of sedimentary rocks that have been subjected to very low grade metamorphism are generally complex. Consequently, application of the Rb-Sr dating technique to shales is potentially fraught with difficulties, as summarised by Harland *et al.* (1990). One of the major problems is the uncertainty in initial $^{87}\text{Sr}/^{86}\text{Sr}$ ratio and the uniformity of this ratio from sample to sample. Shales generally consist of a mixture of detrital and diagenetic components and consequently the initial $^{87}\text{Sr}/^{86}\text{Sr}$ isotopic ratio is not homogeneous. Furthermore, Dasch (1969) demonstrated that, during the deposition of deep-sea sediments, detrital influences dominate; even prolonged contact between seawater and the detrital silicate fraction does not result in complete strontium isotopic equilibration. Other factors are the variable durations of diagenesis and the susceptibility to resetting, even at sub-greenschist to greenschist metamorphic grade.

In spite of these drawbacks, Rb-Sr dating of low metamorphic grade mudrocks has been successfully applied to a variety of geological problems (*e.g.* Evans, 1990), including even diagenetic zone shales (J A Evans, unpublished data). Mudrock regression lines that satisfy the criterion for an isochron are unlikely to result from the mixing of two or more detrital components with different Rb/Sr ratios, ages and/or initial $^{87}\text{Sr}/^{86}\text{Sr}$ ratios, as such a process would generally produce a mixing array with significant scatter (O'Nions *et al.*, 1973). What is not always clear, however, is what the isochron age represents.

6.4.3.1.2 Experimental

$^{87}\text{Sr}/^{86}\text{Sr}$ ratios in the Cornubian metasedimentary rock samples were determined to six decimal places, with a precision of better than 50ppm (1σ), using a VG[®] 354 thermal ionisation mass spectrometer. The corresponding $^{87}\text{Rb}/^{86}\text{Sr}$ values were determined to approximately 0.5% (1σ) from these data in conjunction with Rb/Sr atomic ratios as determined by X-ray fluorescence spectrometry.

6.4.3.1.3 Results and discussion

The measured Rb and Sr concentrations, with corresponding isotope ratios, are presented in Table 6.3. In Table 6.4 are shown the $^{87}\text{Sr}/^{86}\text{Sr}$ values back-corrected (assuming closed system behaviour) to an age of 280Ma, the age of emplacement of the Dartmoor granite (Darbyshire and Shepherd, 1985; Chesley *et al.*, 1993).

It is apparent from Table 6.4(a) that four of the five Kate Brook Slate samples obtained from well within the boundary of the thermal aureole give remarkably similar $^{87}\text{Sr}/^{86}\text{Sr}$ values ($0.71962 \pm 0.00031 - 0.00049$) when back-corrected to 280Ma. In contrast, those sampled outside or on the border of the aureole display a wide range of values, with no apparent systematic variation. This latter finding probably reflects the initial heterogeneity of the detrital grains. Regression of the complete data set (Kate Brook Slate) yields an 'errorchron', as shown in Figure 6.1(a). However, if the (five) samples from within the boundary of the aureole are considered in isolation, the regression diagram produces a linear array (MSWD 5.7) as shown in Figure 6.1(b), corresponding to an age statistically indistinguishable from that of the emplacement of the Dartmoor granite. The slope of this regression line is controlled by a single sample (SW-87S-13) that is considerably more enriched in ^{87}Rb than the others. Removal of this sample from the data set improves the fit of the regression to give an isochron (MSWD value 2.0) corresponding to an age of 262 ± 11 Ma and initial $^{87}\text{Sr}/^{86}\text{Sr}$ ratio of 0.72139 ± 0.00107 . Nitrogen stable isotope data (see below) indicate that sample SW-87S-13 was subjected to a higher temperature during granite emplacement than other samples collected from the aureole. The enrichment of ^{87}Sr in this sample, with respect to the other Kate Brook Slate examples from the thermal aureole, was not due to the incorporation of a granite-derived component, however, as the granite (280Ma ago) was considerably depleted in ^{87}Sr relative to all the shales (back-corrected to 280Ma ago) investigated in this study. If, however, the four-point isochron obtained by excluding sample SW-87-S13 from the group of Upper Devonian shales located within the aureole is considered to be representative of a metamorphic event, it is difficult to explain why the corresponding age should be younger than that of granite emplacement. Also problematic is the marked enrichment in radiogenic strontium of sample SW-87-S11, relative to the other Kate Brook Slate samples investigated.

Table 6.3

Rubidium and strontium concentrations, together with $^{87}\text{Sr}/^{86}\text{Sr}$ and $^{87}\text{Rb}/^{86}\text{Rb}$ isotopic ratios, in metasedimentary rocks from S W England. Sample localities are given in Appendix A.

- a) Upper Devonian rocks (metamorphosed Kate Brook Slate) from a traverse across the thermal aureole (south - west) of the Dartmoor granite
(Samples are listed in probable order of increasing distance from the granite contact)

Sample	Rb (ppm)	Sr (ppm)	$^{87}\text{Rb}/^{86}\text{Sr}$	$^{87}\text{Sr}/^{86}\text{Sr}$
SW-87-S13	352	35.4	29.15	0.837190
SW-87-S7	211	108	5.665	0.742495
SW-87-S8	213	99.6	6.199	0.744333
SW-87-S9	200	71.3	8.154	0.751609
SW-87-S10	235	96.6	7.052	0.747873
SW-87-S11	233	95.9	7.061	0.766982
SW-87-S12	264	55.6	13.83	0.778321
SW-87-S6	208	102	5.939	0.742870
SW-87-S5	252	62.3	11.77	0.763412
SW-87-S4	203	40.6	14.51	0.769154
SW-87-S3	184	188	2.848	0.724444
SW-87-S2	169	53.8	9.150	0.753407
SW-87-S1	4.8	121	0.1146	0.713410

- b) Carboniferous rocks (Crackington Formation) sampled across the thermal aureole (north - east) of the Dartmoor granite
(Samples are listed in order of increasing distance from the granite contact, except that SW-87-S18 and SW-87-S16 were approximately equidistant from the granite)

Sample	Rb (ppm)	Sr (ppm)	$^{87}\text{Rb}/^{86}\text{Sr}$	$^{87}\text{Sr}/^{86}\text{Sr}$
SW-87-S14	342	46.4	21.53	0.804588
SW-87-S17	273	49.0	16.25	0.781785
SW-87-S18	112	255	1.274	0.716092
SW-87-S16	247	82.5	8.712	0.753494
SW-87-S15	287	76.1	10.98	0.759673
SW-87-S19	143	53.3	7.767	0.753152

- c) Devonian rocks (borehole drillcores) from an area west of the St Austell granite

Sample	Rb (ppm)	Sr (ppm)	$^{87}\text{Rb}/^{86}\text{Sr}$	$^{87}\text{Sr}/^{86}\text{Sr}$
HF1	209	68.3	8.906	0.757030
HF2	118	189	1.814	0.722595
HF3	235	224	3.037	0.727162

Note: Analytical errors associated with these data are of the order of 5% on the Rb and Sr concentrations, 0.5% on the $^{87}\text{Rb}/^{86}\text{Sr}$ values and less than 0.005% on the $^{87}\text{Sr}/^{86}\text{Sr}$ ratio measurements, respectively, at the 1 σ level

Table 6.4

S W England metasedimentary rocks: $^{87}\text{Sr}/^{86}\text{Sr}$ isotopic ratios back - corrected to an age of 280 Ma, assuming closed - system behaviour

- a) Upper Devonian rocks (metamorphosed Kate Brook Slate) from an area south - west of the Dartmoor granite.
(Samples are listed in probable order of increasing distance from the granite contact)

Sample	$^{87}\text{Sr}/^{86}\text{Sr}$ @ 280Ma	Notes
SW-87-S13	0.72107	Very close to the granite contact
SW-87-S7	0.71993	"
SW-87-S8	0.71964	"
SW-87-S9	0.71913	Within the metamorphic aureole
SW-87-S10	0.71978	"
SW-87-S11	0.73885	On the border of the aureole (close to biotite isograd)
SW-87-S12	0.72323	Outside the aureole
SW-87-S6	0.71921	"
SW-87-S5	0.71652	"
SW-87-S4	0.71135	"
SW-87-S3	0.71310	"
SW-87-S2	0.71696	"
SW-87-S1	0.71295	" (near to greenstones)

- b) Carboniferous rocks (Crackington Formation) from north - east of the Dartmoor granite

Sample	$^{87}\text{Sr}/^{86}\text{Sr}$ @ 280Ma	Approximate distance from the granite contact
SW-87-S14	0.71883	350m N of granite boundary
SW-87-S17	0.71706	400m N of granite boundary
SW-87-S18	0.71102	600m N of granite boundary
SW-87-S16	0.71879	600m NE of granite boundary
SW-87-S15	0.71591	1500m NE of granite boundary (outside aureole)
SW-87-S19	0.72221	2100m NNE of granite boundary (outside aureole)

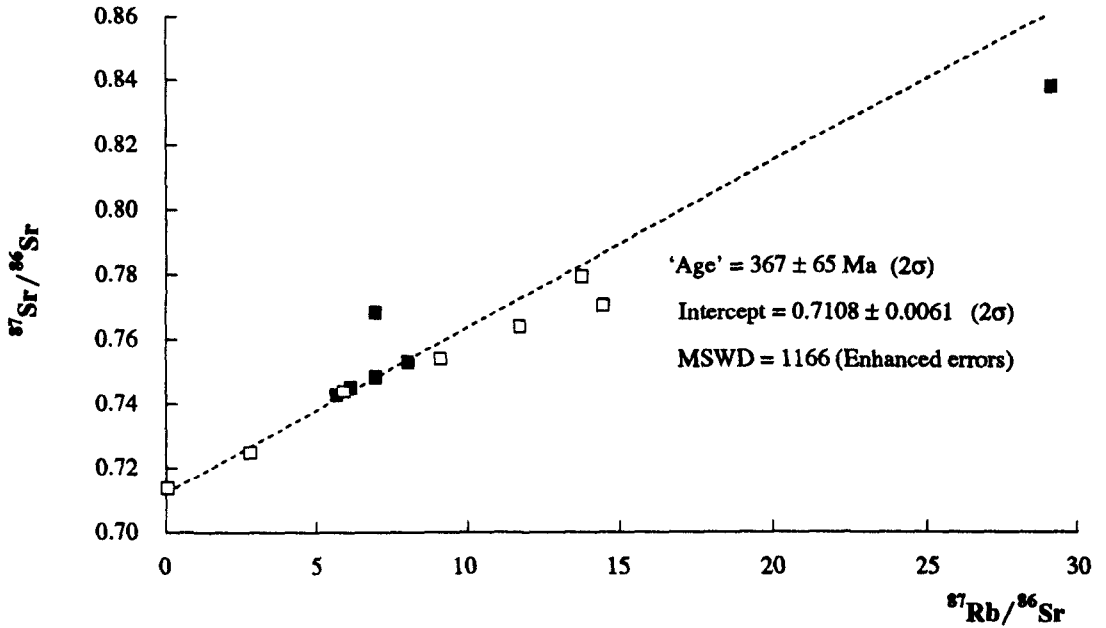
- c) Devonian rocks from west of the St Austell granite (outside the thermal aureole)

Sample	$^{87}\text{Sr}/^{86}\text{Sr}$ @ 280Ma
HF1	0.72155
HF2	0.71537
HF3	0.71506

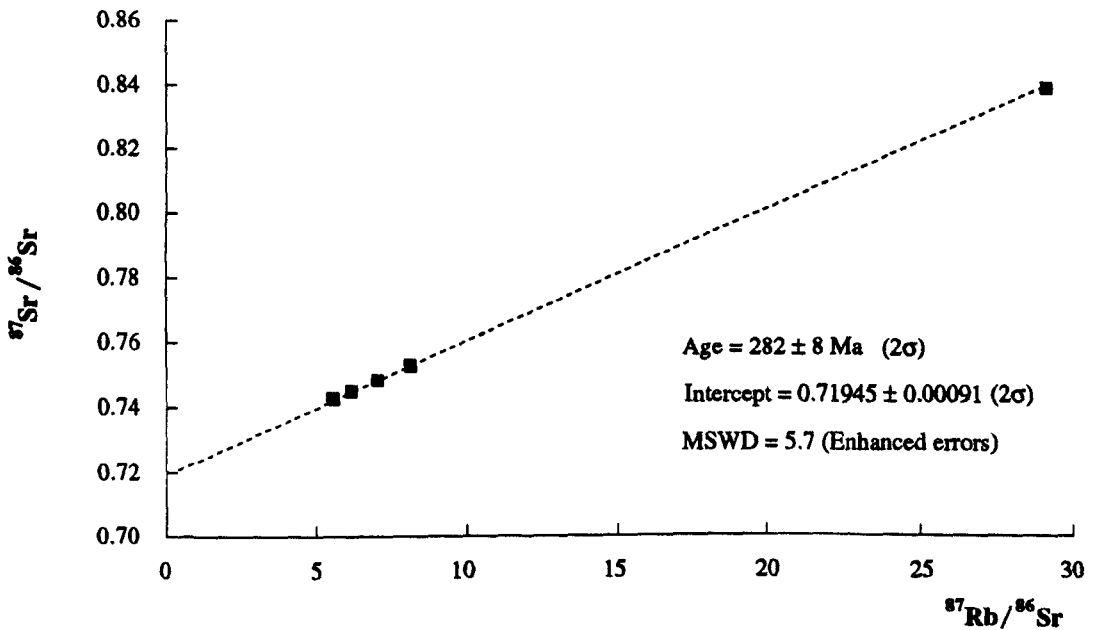
Figure 6.1

$^{87}\text{Sr}/^{86}\text{Sr}$ and $^{87}\text{Rb}/^{86}\text{Sr}$ ratios in Kate Brook Slate sampled across the thermal aureole (south-west) of the Dartmoor granite

(a) Complete data set: present-day whole-rock $^{87}\text{Sr}/^{86}\text{Sr}$ ratios, presented as a regression line 'errorchron' against the corresponding $^{87}\text{Rb}/^{86}\text{Sr}$ values



(b) Samples located within the thermal aureole of the granite



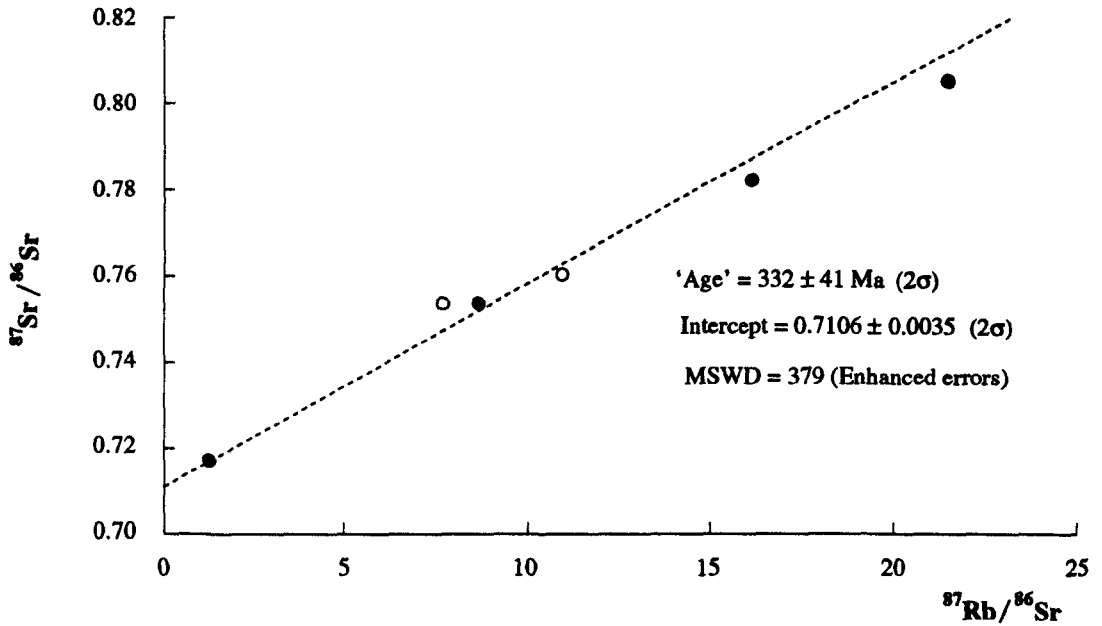
Key to sample locations

- Within the aureole
- Outside the aureole
- On the aureole border (close to biotite isograd)

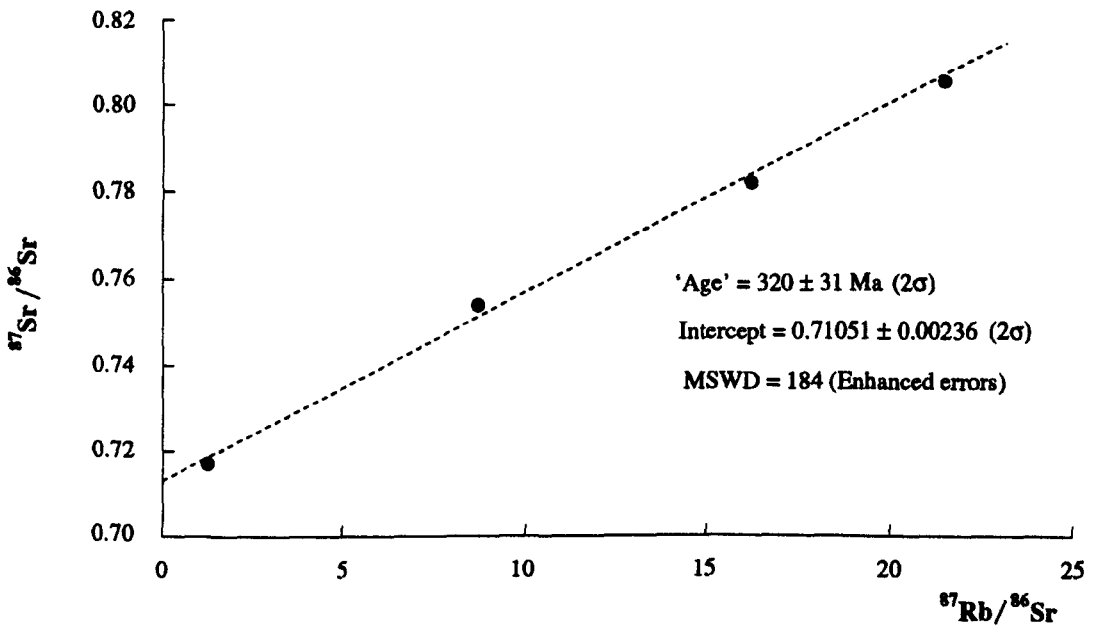
Figure 6.2

$^{87}\text{Sr}/^{86}\text{Sr}$ and $^{87}\text{Rb}/^{86}\text{Sr}$ ratios in Crackington Formation rocks sampled across the thermal aureole (north-east) of the Dartmoor granite

(a) Complete data set: present-day whole-rock $^{87}\text{Sr}/^{86}\text{Sr}$ ratios, presented as a regression line 'errorchron' against the corresponding $^{87}\text{Rb}/^{86}\text{Sr}$ values



(b) Samples located within the thermal aureole of the granite

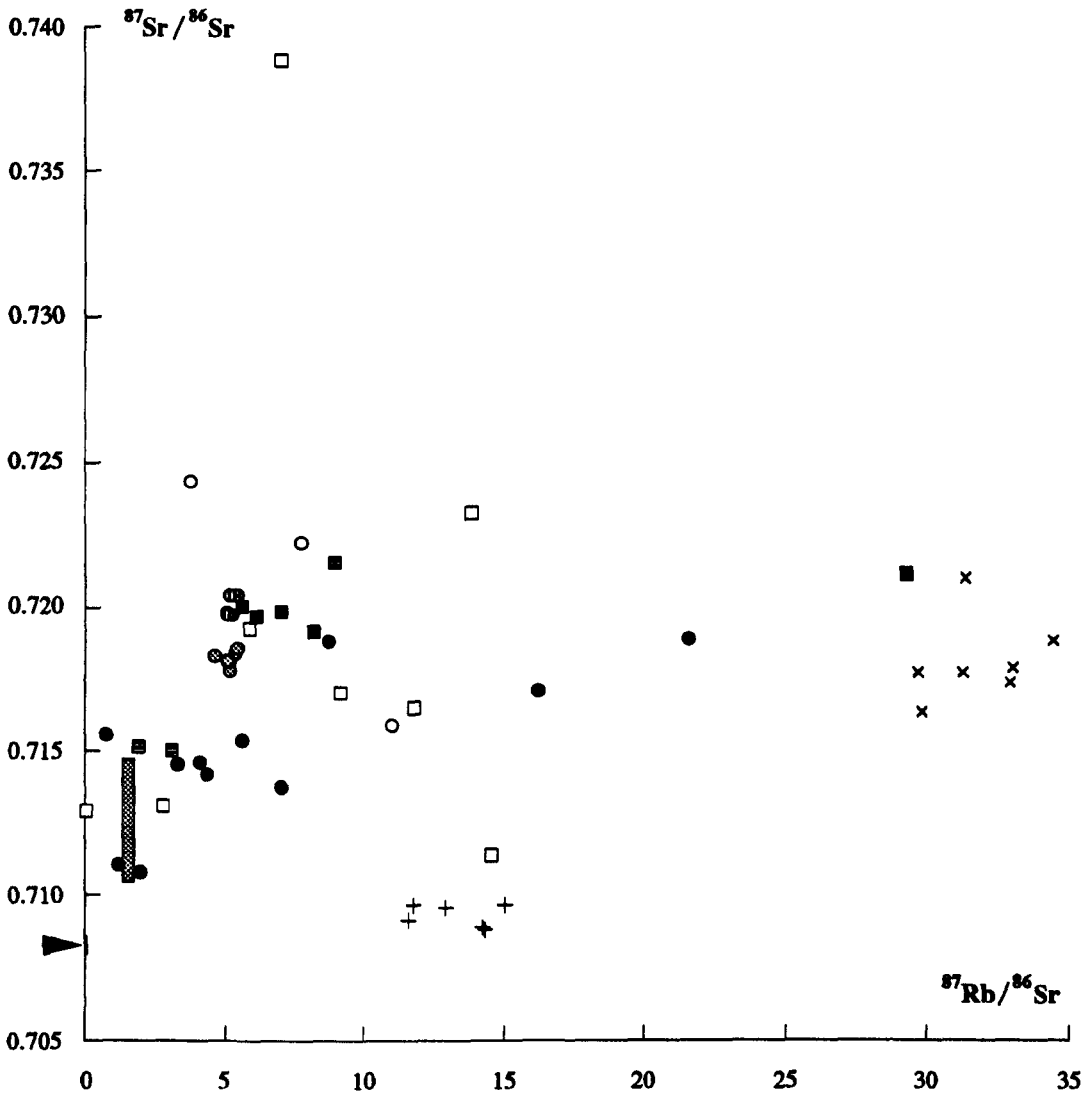


Key to sample locations

- Within the aureole
- Outside the aureole

Figure 6.3

$^{87}\text{Sr}/^{86}\text{Sr}$ and $^{87}\text{Rb}/^{86}\text{Sr}$ ratios from Figures 6.1 and 6.2, back-corrected to an age of 280Ma on the basis of closed-system behaviour. Also shown, for comparison, are the corresponding values for the Dartmoor and Hemerdon Ball granites, together with data from other Cornubian metasediments, early hydrothermal fluids hosted by the Dartmoor granite, and contemporaneous seawater



Key

- } Kate Brook Slates from a traverse across the thermal aureole (south-west) of the Dartmoor granite.
- } (Filled squares indicate samples within the thermal aureole)
- } Crackington Formation (Namurian) metasediments sampled across the thermal aureole (to the north
- } and east) of the Dartmoor granite. (Filled circles indicate samples within the thermal aureole)
- Borehole drill-core samples (Devonian age) from west of the St Austell granite
- + Dartmoor granite (Darbyshire and Shepherd, 1985)
- × Hemerdon Ball granite (Darbyshire and Shepherd, 1987)
- ▨ Range of early hydrothermal fluids hosted by the Dartmoor granite (Wayne *et al.*, *in prep.*)
- ▶ Seawater at 280Ma before present, estimated from the data of Burke *et al.* (1982)
- Diagenetic zone shales (Crackington Formation), Wanson Mouth, near Bude
- Anchizone metasediments (Crackington Formation), Crackington Haven
- Epizone shales (Upper Devonian), Boscastle

} Bishop (1990)

Notes: (i) All metasediment and granite data refer to whole-rock samples

(ii) Data points as shown are considerably larger than the associated analytical uncertainties

In contrast, the strontium isotope results obtained from the admittedly limited data set for the Namurian rocks show no evidence of a resetting event around the time of granite emplacement. Linear regression of the complete data set (six samples) gives a considerable degree of scatter about the regression line, as shown in Figure 6.2(a). A plot of the data from the four samples located within the aureole gives an errorchron 'age' of 320 ± 30 Ma, as indicated in Figure 6.2(b). The data fit may be considerably improved by rejecting one of these sample points (SW-87S-16), to produce an isochron (MSWD = 0.3) corresponding to an 'age' of 308 ± 2 Ma (2σ) and initial ratio of 0.71052 ± 0.00017 (2σ). There is, however, no obvious justification for such a procedure.

Figure 6.3 illustrates the present data set of $^{87}\text{Sr}/^{86}\text{Sr}$ and Rb/Sr ratios back-corrected to the time of emplacement of the Dartmoor granite, for comparison with the corresponding values for other Cornubian metasediments, the Dartmoor and adjacent Hemerdon Ball granites, early hydrothermal fluids hosted by the Dartmoor granite, and contemporaneous seawater. Several notable features are apparent from this Figure:

(i) The Kate Brook Slate samples from within the thermal aureole of the Dartmoor granite, although substantially more enriched in ^{87}Sr than the granite, have $^{87}\text{Sr}/^{86}\text{Sr}$ ratios within the range recorded for the nearby Hemerdon Ball granite, on the basis of the whole-rock data of Darbyshire and Shepherd (1987). Back-correction of the latter shows that the average $^{87}\text{Sr}/^{86}\text{Sr}$ ratio of the Hemerdon Ball granite at 300 Ma before present equates to the $^{87}\text{Sr}/^{86}\text{Sr}$ ratio (0.7094) of the Dartmoor granite (Darbyshire and Shepherd, 1985) at the time of its emplacement. To explain the difference in $^{87}\text{Sr}/^{86}\text{Sr}$ characteristics of these two plutons, it may therefore be postulated that either the initial $^{87}\text{Sr}/^{86}\text{Sr}$ ratios were similar at the respective times of emplacement and that the Hemerdon Ball granite is 20 Ma older than the adjacent Dartmoor intrusive; alternatively, the two granites are of a similar age but the incorporation of a greater component of sedimentary matter in the initial melt at Hemerdon resulted in the relative enrichment of ^{87}Sr . A combination of these 'end member' standpoints may alternatively be postulated. The case for a greater component of sedimentary matter in the Hemerdon Ball granite is supported by the Nd isotope data of Darbyshire and Shepherd (1987, 1994), besides the indirect evidence presented elsewhere in the present work.

(ii) $^{87}\text{Sr}/^{86}\text{Sr}$ ratios measured in fluid inclusion leachates of quartz associated with quartz±tourmaline±cassiterite±haematite assemblages hosted by the Dartmoor granite (Wayne *et al.*, *in prep.*; see also this work, Chapter 5) are consistently more ^{87}Sr -enriched than the Dartmoor granite, when all data are back-corrected to 280 Ma. By assuming that the granite was the sole source of the strontium in these fluids, the age of the fluids may be estimated on the basis of calculating at what age, after emplacement, the $^{87}\text{Sr}/^{86}\text{Sr}$ ratio of the granite equated to the contemporaneous limiting values of the fluid inclusion $^{87}\text{Sr}/^{86}\text{Sr}$

results.† By approximating the palæofluid $^{87}\text{Sr}/^{86}\text{Sr}$ initial ratios to be the present-day values back-corrected to age 280Ma, the lower limit (0.7123_{280}) corresponds to that of the granite at $271 \pm 14\text{Ma}$ (2σ), on the basis of the Dartmoor granite data (fourteen whole-rock samples) of Darbyshire and Shepherd (1985), whereas the upper limit of the palæofluid $^{87}\text{Sr}/^{86}\text{Sr}$ range (0.7141_{280}) corresponds to that of the granite at $266 \pm 22\text{Ma}$ (2σ) before present.

(iii) The resetting of the whole-rock Rb-Sr systematics of the Upper Devonian metasediment samples from within the thermal aureole of the Dartmoor granite, to coincide with the emplacement age of the pluton but with a corresponding initial $^{87}\text{Sr}/^{86}\text{Sr}$ ratio ~ 0.01 greater than that of the granite (0.71945 ± 0.0009 compared to 0.7094 ± 0.0003 , 2σ errors) suggests that the thermal effect of the intrusion ('closed system' resetting) is predominant over any superimposition of a strontium isotopic signature derived from fluids exsolved from the granite during its emplacement ('open system' resetting).

6.4.3.2 Carbon stable isotope compositions of the metasediments

6.4.3.2.1 Scope of the investigation

Black shales generally contain relatively high concentrations of organic matter and are not common in S W England. To investigate the variation of carbon stable isotopic composition in sedimentary sequences in the region, in terms of distance from the local granite contact, it was recognised that the two sample suites collected across the Dartmoor granite thermal aureole during the present study may not be sufficient to give a representative picture. It was also acknowledged that slates in the vicinity of the Carnmenellis granite were more likely to be enriched in carbonaceous matter, in view of evidence for the presence of bitumens in that locality (Parnell, 1988) and also the distinctive fluid inclusion compositions in early hydrothermal quartz from South Crofty mine, as reported in the present work (Section 3.5.1). Areas of sedimentary cover where gravity data give an indication to the depth of buried granite, such as the shallow northern extension of the Carnmenellis granite, together with the Kit Hill pluton, would be appropriate (P M Allen, *pers. comm.*) for similar studies.

The Kate Brook Slate samples collected across the Dartmoor granite thermal aureole were considered particularly appropriate for the present investigation, however, on the basis of the following criteria:

- (i) Good exposure of relatively unweathered material, across the aureole.
- (ii) Close proximity to the Hemerdon Ball granite, located within the metamorphic aureole of the Dartmoor pluton but associated with an early palæo-hydrothermal fluid regime

† Only quartz samples leached using 0.13M HNO_3 spiked with 200ppm La^{3+} (as LaCl_3) are considered here; those leached with La-free acid invariably gave lower Sr yields.

exhibiting relative enrichment in carbonaceous components, in contrast to the Dartmoor granite-hosted hydrothermal system (see Sections 3.5.1 and 3.5.3 of the present work).

(iii) The Kate Brook Slate is representative of the sedimentary country rocks into which were emplaced the minor granite intrusives of the Gunnislake-Kit Hill area. These plutons are associated with early hydrothermal fluids containing similar levels of carbon-bearing species as the comparable stage fluids at Hemerdon.

The methodology was to determine the carbon abundance in the metasedimentary rocks, in terms of both carbonate and 'organic' carbon components, together with the respective stable isotopic compositions, and hence to undertake an exploratory assessment of the effects of the emplacement of the Dartmoor granite as recorded by the carbon systematics of these rocks.

6.4.3.2.2 Experimental

6.4.3.2.2.1 Carbonate analysis

Weighed quantities (~500mg) of the powdered whole-rock samples were reacted *in vacuo* overnight with 100% phosphoric acid under temperature-controlled conditions (25.18°C), following a method similar to that of McCrea (1950). Carbon dioxide yields were recorded manometrically and the gas samples analysed for stable isotopic composition using a VG® SIRA Series II mass spectrometer. Raw data were corrected for instrumental and isobaric interference effects (Craig, 1957; Deines, 1970). Calcite $\delta^{18}\text{O}$ data were recorded from those whole-rock samples that yielded sufficient CO_2 for isotopic analysis at acceptable levels of precision. The calcite $\delta^{18}\text{O}$ value relates to that of the liberated CO_2 by:

$$\delta^{18}\text{O}_{\text{calcite}} = [(\delta^{18}\text{O}_{\text{CO}_2} + 1000)/\alpha_{\text{CO}_2\text{-calcite}}] - 1000$$

where, for the temperature of equilibration, $\alpha_{\text{CO}_2\text{-calcite}} = 1.0125$. The $\delta^{18}\text{O}_{\text{calcite}}$ results were converted to the corresponding values referred to SMOW, rather than PDB (as used for the raw data), by use of the relationship (Friedman and O'Neil, 1977):

$$\delta^{18}\text{O}_{\text{sample-SMOW}} = 1.03086 \delta^{18}\text{O}_{\text{sample-PDB}} + 30.86 \text{ (‰)}$$

6.4.3.2.2.2 'Organic' carbon analysis

Powdered whole-rock samples were treated with 6M HCl at 60°C, to remove carbonates and sulphides, prior to oven drying at 110°C. Weighed quantities (~350mg) of sample were intimately mixed in an agate mortar with powdered CuO, pre-fired to 950°C, to give a weight

ratio of approximately 2:1 rock:CuO.[†] In each case, the mixture was loaded into a pre-fired (1100°C) silica tube (9mm external diameter, ~16cm length) which had been sealed at one end and incorporated a constriction ~11.5cm from the sealed end. The samples were then evacuated and subsequently sealed at the constriction by means of a glassblowing torch. Each resulting ampoule was then sheathed with a steel tube, to give protection to other samples in the event of an ampoule exploding in the furnace used to contain all samples during the course of the oxidation. A temperature of 900°C, maintained for ~3 hours, was used to promote the oxidation, after which the furnace was allowed to cool slowly to room temperature. During this period, unreacted molecular oxygen, released from the CuO at temperatures greater than ~600°C, was resorbed.

CO₂ was extracted by 'cracking' the ampoules *in vacuo*, followed by standard cryogenic separation procedures utilising liquid nitrogen (-196°C) and n-pentane/liquid nitrogen slush (-130°C) traps to separate the CO₂ from the water component (and SO₂) also produced during the oxidation process. Carbon dioxide yields were recorded and isotopic analyses performed as for the carbonate-derived components.

6.4.3.2.3 Results and discussion

The CO₂ yields obtained from phosphoric acid treatment of the whole-rock powders indicated that the inorganic carbon content of all the metasedimentary rock samples collected from the vicinity of the Dartmoor granite was very low; the results were all within 2.3±1.1 ppmC (at the 1σ level). Furthermore, mass spectral scans showed that the CO₂ was significantly contaminated in most cases, predominantly with hydrocarbons but also with sulphur species in some cases. For this reason, the data were considered to be of little value. As an approximate indication of typical δ¹³C values, duplicates of sample SW-87-S10, which gave relatively 'clean' CO₂ traces, were characterised by δ¹³C_(PDB) values of -16.0 and -15.7‰ respectively. Another comparably 'clean' sample (SW-87-S14) gave -16.8‰.

In contrast, the three drillcore samples (Devonian rocks) from west of the St Austell granite were relatively enriched in inorganic carbon; the yield in one example exceeded 3800ppmC. No contamination of the released CO₂ was apparent. These results are reported in Table 6.5(b).

The 'organic' carbon yield and corresponding δ¹³C results for the samples from the Dartmoor granite aureole are reported in Table 6.5(a). On the basis of the very low

[†] It is important that the whole-rock powder is intimately mixed with the ground CuO prior to the oxidation process, to effect complete conversion. Decreased CO₂ yields otherwise result (S. H. Bottrell, unpublished data), with concomitant scope for isotopic fractionation.

Table 6.5

(a) 'Organic' carbon content and corresponding stable isotopic composition of metasedimentary rocks from two traverses across the thermal aureole of the Dartmoor granite

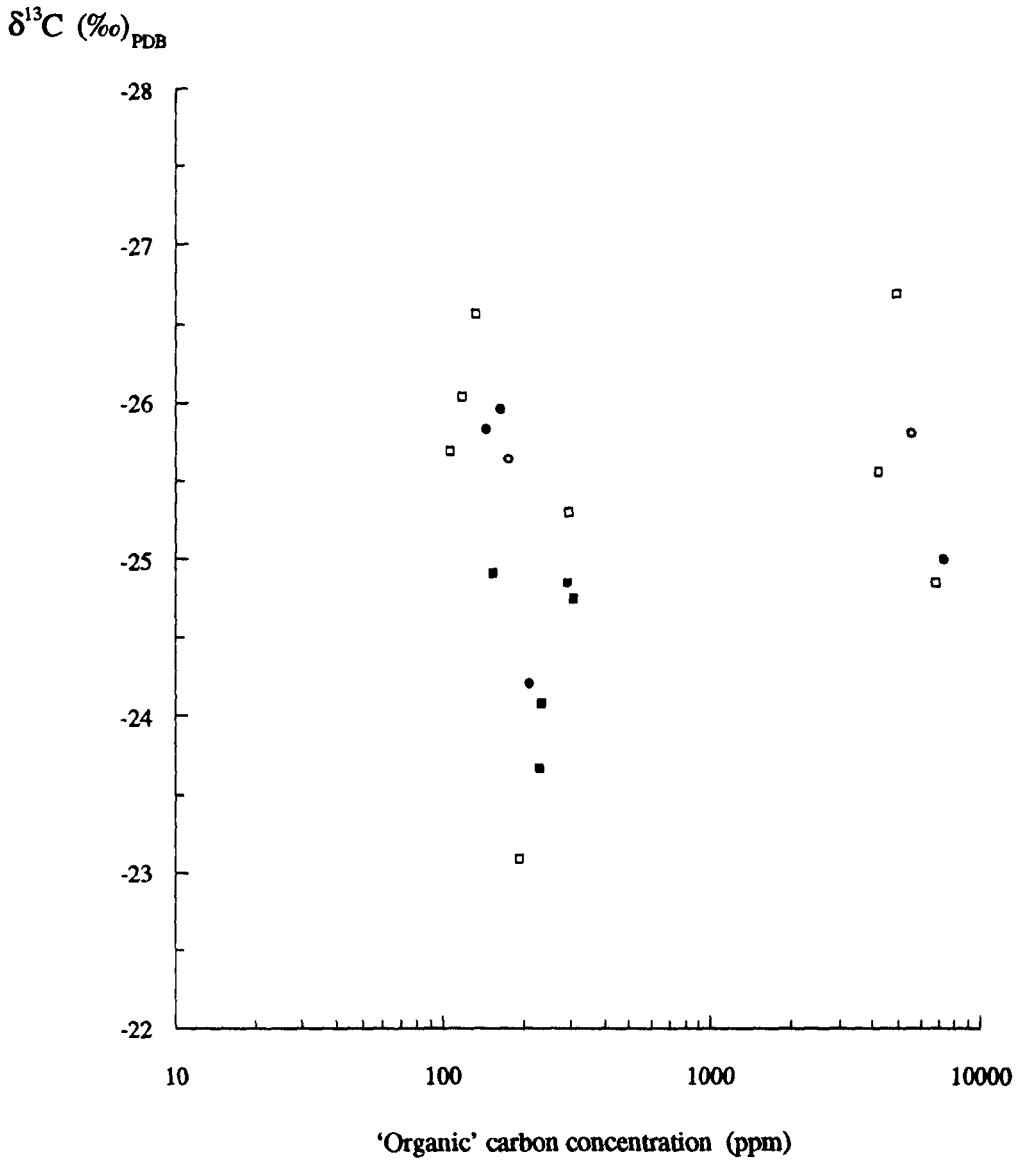
	Sample reference	ppm C	$\delta^{13}\text{C}$ (‰) _{PDB}	
	<i>Upper Devonian examples</i>			
Notes: (1) The isotopic data were reproducible to within 0.05‰, except for those samples containing only ~100ppm carbon, in which case the precision was marginally worse. (2) All yield and isotopic data were corrected for the procedural blank contribution. The blank (which was probably derived almost exclusively from the CuO used to perform the oxidation) was <6µgC, and had an isotopic composition of -27.68‰. (3) The inorganic carbon content of all these samples was very low: 2.3±1.1 ppm (1σ), hence the isotopic values quoted are also representative of the total carbon reservoirs. (4) NBS-22 standard oil gave a $\delta^{13}\text{C}$ value of -29.86‰, which is significantly less than the accepted value of -29.63‰. Coleman and Cox (1981), however, using similar procedures in the same laboratory, reported a value of -29.84±0.04 (1σ) on the basis of 12 determinations. The data presented here were therefore not adjusted on the basis of the NBS-22 measurement.	SW-87-S13	140	-24.88	
	SW-87-S7	302	-24.73	
	<i>duplicate</i>	293	-24.73	
	SW-87-S8	281	-24.84	
	SW-87-S9	221	-24.07	
	SW-87-S10	214	-23.66	
	SW-87-S11	100	-25.97	
	<i>duplicate</i>	106	-26.03	
	SW-87-S12	92	-25.64	
	SW-87-S6	285	-25.29	
	SW-87-S5	179	-23.06	
	SW-87-S4	5000	-26.68	
	SW-87-S3	4229	-25.54	
	SW-87-S2	6957	-24.85	
	<i>duplicate</i>	6974	-24.80	
	SW-87-S1	120	-26.55	
		<i>Carboniferous examples</i>		
		SW-87-S14	131	-25.81
		SW-87-S17	152	-25.95
	SW-87-S18	5594	-25.79	
	SW-87-S16	198	-24.20	
	SW-87-S15	163	-25.62	
	SW-87-S19	7397	-24.99	

(b) 'Organic' and carbonate carbon contents and corresponding stable isotopic compositions of metasedimentary rocks of Devonian age (borehole drillcore material) from an area to the west of the St Austell granite. Sample locations are documented in Appendix A.

Sample reference	'Organic' carbon		Carbonate (assumed to be calcite)			Total carbon	
	ppm C	$\delta^{13}\text{C}$ (‰) _{PDB}	ppm C	$\delta^{13}\text{C}$ (‰) _{PDB}	$\delta^{18}\text{O}$ (‰) _{SMOW}	ppm C	$\delta^{13}\text{C}$ (‰) _{PDB}
HF1	3190	-27.19	92	-10.83	18.03	3284	-26.72
HF2	1645	-26.19	3821	-10.19	15.36	5466	-15.01
HF3	2856	-30.63	198	-13.83	15.68	3054	-29.54

Figure 6.4

Carbon content and corresponding stable isotope variations of the 'organic' component of metasedimentary rocks from the vicinity of the Dartmoor granite



Key

- Upper Devonian examples from a traverse across the south-western region of the thermal aureole of the Dartmoor granite
 -
 - Carboniferous examples from across the north-eastern region of the thermal aureole of the Dartmoor granite
 -
- Samples from within the aureole are indicated by the filled symbols

corresponding inorganic carbon yields, the 'organic' carbon data may be taken to be representative of the respective total carbon contents. Figure 6.4 illustrates the same data set diagrammatically. Comparable data for the borehole samples are presented in Table 6.5(b), which also shows the relative contributions of carbonate and 'organic' carbon fractions to the respective total carbon contents of these samples.

With regard to the effect of intrusion of the Dartmoor granite into the local Upper Devonian shales, as recorded by the carbon content and associated stable isotope data of the latter, the following salient features are apparent from Table 6.5(a) and Figure 6.4:

(i) The carbon concentration data are strongly bimodal, with no samples containing between 300 and 4229 ppmC. Examples of both carbon-enriched and carbon-depleted rocks occur in Kate Brook Slate outside the thermal aureole, with an associated large range of stable isotopic compositions (-23.06 to -26.68‰). No systematic pattern is evident.

(ii) With the sole exception of sample SW-87-S1, which was shown by XRF analysis to consist largely of tourmaline and quartz and is therefore atypical, it is notable that the samples located furthest from the granite contact were also those relatively enriched in carbon. The abrupt transition from carbon-depleted to carbon-enriched rock occurs outside the limit of the aureole, however.

(iii) No systematic shift in the isotopic data with increasing distance from the granite boundary is discerned. This parallels the established finding that $^{13}\text{C}/^{12}\text{C}$ ratios in sedimentary organic matter is not drastically changed during diagenesis or higher-grade metamorphic processes (Deines, 1980).

(iv) Although the data were corrected for the procedural blank contribution, it is difficult to assess to what extent adsorbed atmospheric carbon-bearing contaminants (dust and microbiological matter) may have contributed to the reported results, bearing in mind the finely powdered nature of the sample (*cf.* Section 3.2.4). This is of particular relevance to the data obtained from the carbon-depleted samples. Evidence that any such contribution was relatively uniform is provided by the duplicate analyses of samples SW-87-S7 and SW-87-S11 (Table 6.5), where consistent yield and isotopic results were obtained even though the absolute carbon yield was only $\approx 103(\text{ppmC}) \times 0.350(\text{g of sample}) = 36\mu\text{gC}$ in the case of sample SW-87-S11. This latter value may therefore be considered to represent the upper limit (in terms of yield) of the carbon blank component derived from adsorption of airborne contaminants. The fact that the associated $\delta^{13}\text{C}$ result was $-26.00 \pm 0.03\text{‰}$ rather than the value of *ca.* -27.5‰ as generally associated with such 'adventitious' carbon (*e.g.* Nadeau *et al.*, 1990) implies that the actual yield of this component was probably significantly lower than the potential upper limit value.

With reference to the Carboniferous (Namurian) rocks analysed, it is notable that, in contrast to the Kate Brook Slate, one sample located within the thermal aureole (~600m north of the granite boundary) was enriched in carbon (5594ppmC). The associated isotopic composition, however, was indistinguishable (within the limits of the analytical precision) from that of the most carbon-depleted example of the group (131 ppmC), located closest to the granite contact.

From the results in Table 6.5, it is clear that the only samples in this investigation that contained significant quantities of carbonate were from the borehole drillcores (Devonian age rocks) from west of the St Austell granite and located well outside the associated metamorphic aureole. The carbon and oxygen isotopic compositions of these carbonates indicate that they are not directly of marine origin.[†] It is noteworthy that the carbon results are similar to total palaeofluid carbon (weighted mean $\delta^{13}\text{C}_{\text{CO}_2} + \delta^{13}\text{C}_{\text{CH}_4}$) values encountered in early, high temperature hydrothermal fluids associated with W±Sn oxide assemblages in the Cornubian region (see Chapter 3 of the present work). This lends support to the idea that CO₂ derived from the thermal breakdown of such carbonates (under conditions such as anatexis and assimilation into granitic protoliths?) is the carbon source for these palaeofluid components.

6.4.3.3 Nitrogen stable isotope compositions of the metasediments

6.4.3.3.1 Scope of the investigation

Chapter 4 of the present work contains a detailed discussion of nitrogen stable isotope geochemistry, with reference to the trace molecular nitrogen component present in early palaeo-hydrothermal fluids characterised by association with W±Sn oxide occurrences in the Cornubian region. The purpose of the present investigation was to obtain information on the nitrogen stable isotopic composition of 'extractable' ammonium in the local Palaeozoic metasedimentary rocks, for comparison with the palaeofluid data. In particular, to assess what effects granite intrusion imposed on the nitrogen systematics of these rocks.

6.4.3.3.2 Experimental

A preliminary discussion of the alternative techniques available for measurement of the yield and isotopic composition of nitrogen in sedimentary rocks has been presented in Section 4.7.2. For the present investigation, it was not considered practicable to attempt to resolve the relative abundances and isotopic compositions of nitrogen from organically-bound,

[†] Marine carbonates have $\delta^{18}\text{O}$ values ranging from +20 to +30‰, relative to SMOW, with corresponding $\delta^{13}\text{C}$ values of generally ~0‰ relative to PDB (see *e.g.* Faure, 1986, and references therein).

fixed-inorganic and exchangeable sites.[†] Sealed-tube combustion of the metasediment samples at 550 and 1100°C respectively was initially considered as a possible means of discriminating between organic and other sources of nitrogen. Kydd and Levinson (1986) recommended firing samples in air at 550°C for four minutes to remove any organic fraction from ammonium silicates; a modification of this procedure was also adopted by Bottrell and Miller (1990), prior to nitrogen yield determinations by combustion at 1100°C. A major difficulty with sealed-tube combustion techniques as applied to sedimentary rocks, however, is that copious amounts of water are liberated during heating. Consequently, steam pressures sufficient to cause explosion of the sealed tube are easily encountered unless adequate precautions are taken. Furthermore, a detailed investigation by Boyd *et al.* (1993) of the oxidation characteristics of ammonium in micas and feldspars separated from S W England granites, including Cligga Head and Hingston Down, demonstrated that not all the ammonium is released from feldspars by combustion below 1300°C. Boyd *et al.* (1993) also reported that substantial kinetic fractionation of the nitrogen isotopes occurred during high-temperature stepped combustion experiments on these mineral separates.

It is worthy of mention that, more than thirty-five years ago, Scalan (1958) investigated a variety of methods for extracting nitrogen from rocks and minerals, for subsequent isotopic analysis; only vacuum fusion in molten NaOH was considered to be effective in releasing the total nitrogen content. More recently, work by Zhang (1988) supports the use of fusion methods as providing the highest efficiency of nitrogen extraction. An alternative based on laser microprobe techniques, in conjunction with nitrogen isotope analysis by static vacuum mass spectrometry, shows great potential (Franchi *et al.*, 1989).

Hall (1988) used a variation of the Kjeldahl method (essentially based on the procedure reported by Urano, 1971) to estimate the amount of ammonium present in S W England country rocks. The same author noted, however, that any acid-resistant kerogen component would not contribute to the values obtained. For the present study, a similar approach was used to determine the yield of 'extractable' ammonium from the metasediments associated with the thermal aureole of the Dartmoor granite. For the acid extraction procedure, 1g of powdered whole-rock was reacted with a mixture of 2ml of 1:1 H₂SO₄ and 10ml HF; details of the method are given by Bradley *et al.* (1990).

For nitrogen stable isotope analysis of the metasediments, a similar experimental procedure was used to extract nitrogen from the samples, except that ammonia was collected as ammonium sulphate in H₂SO₄, for sealed (double) silica tube combustion at 850°C using the procedure recommended by Minagawa (1984). 500mg of pre-fired (850°C) wire-form CuO

[†] Classification of the different sites of nitrogen in igneous and sedimentary rocks is given in Section 4.2.9.

was used to effect the oxidation in all cases. Isotopic analyses were undertaken using a VG® SIRA Series II mass spectrometer.

To obtain sufficient molecular nitrogen for isotopic analysis with acceptable precision in each case, it was necessary to scale up the quantity of powdered rock reacted with HF/H₂SO₄, from 1 to 3 g (with a proportional increase in the quantities of acid used). After evaporating the resulting slurry down at ~100°C to a minimum volume, a second 30 ml aliquot of HF was added; this procedure was repeated once more in due course. However, the efficiency of the acid extraction procedure was found to be significantly reduced by scaling up the quantities of reactants used, as indicated by the resulting ammonium yields.

Before commencing the HF/H₂SO₄ extraction procedure, an estimate of the maximum contribution of 'organic' (including kerogen-derived) nitrogen to the total nitrogen content of the metasedimentary rock samples was made by performing a 550°C sealed-tube combustion (30 minutes) of sample SW-87-S19. This thinly-bedded sandy mudstone of Carboniferous age, darkened by organic matter, contained the highest 'extractable' ammonium yield, as reported below. Pre-fired (850°C) CuO was ground and intimately mixed with the powdered rock sample (1:3 weight ratio), prior to heating *in vacuo* at 550°C.

Sample SW-87-S19 was located outside the thermal aureole of the Dartmoor granite. For comparison, similar analyses were made of both Carboniferous and Devonian metasediments collected close to the granite contact (samples SW-87-S14 and SW-87-S7 respectively). The results obtained for these latter samples indicated that only 3.6 and 2.6% respectively of the total ammonium yield was in the form of organically-bound nitrogen, a proportion of which might be in the form of kerogen. In the case of sample SW-87-S19, this value increased to 6.6%, which was still not considered sufficient to invalidate the use of acid extraction for the preparation of ammonia and thence nitrogen for stable isotope ratio analysis.

6.4.3.3.3 Results and discussion

The results of the analyses for 'extractable' ammonium content are presented in Table 6.6. In Table 6.7 are shown the δ¹⁵N isotopic data obtained from the metasedimentary rocks; all samples were extracted and analysed in duplicate. Also shown in this Table are the corresponding ammonium yield values, which may be compared with the data given in Table 6.6. It is apparent from Table 6.7 that the ammonium yields obtained by scaling up the quantities of sample and reagents used were substantially lower than those obtained using the standard procedure for ammonium yield determination; this latter procedure has been verified by international laboratory comparison (Bradley *et al.*, 1990). The reproducibility of the nitrogen stable isotope data, however, was apparently not related to the ammonium yield reproducibility.

Table 6.6

'Extractable' ammonium contents of metasedimentary rocks from the vicinity of the Dartmoor granite, determined using the procedures of Bradley *et al.* (1990). Analyses were undertaken on behalf of the author by D A Bradley. Samples are listed in order of increasing distance from the granite contact; the respective localities are given in Appendix A. Results of duplicate analyses are given in parentheses. The detection limit was ~10ppm.

Upper Devonian		Carboniferous	
Sample reference	[NH ₄ ⁺] (ppm)	Sample reference	[NH ₄ ⁺] (ppm)
SW-87-S13	602	SW-87-S14	706
SW-87-S7	1000	SW-87-S17	469
SW-87-S8	982	SW-87-S18	88
SW-87-S9	942	SW-87-S16	1050
SW-87-S10	1160	SW-87-S15	942
SW-87-S11	(212, 220)	SW-87-S19	(1020, 1100)
SW-87-S12	422		
SW-87-S6	1010		
SW-87-S5	1060		
SW-87-S4	(77, 71)		
SW-87-S3	70		
SW-87-S2	855		
SW-87-S1	(<10, 17)		

Table 6.7

Nitrogen stable isotopic composition of 'extractable' ammonium in metasedimentary rocks sampled across the thermal aureole of the Dartmoor granite. Results are tabulated in order of increasing distance from the granite contact. The respective sample localities are given in Appendix A.

(a) Upper Devonian metasediments

Sample reference	$\delta^{15}\text{N} \text{‰}_{(\text{AIR})}$ (mean)		NH_4^+ yield (ppm)	NH_4^+ yield data from Table 7.6 (ppm)
SW-87-S13	7.1	7.4	384	602
	7.7		390	
SW-87-S7	3.5	3.0	795	1000
	2.5		601	
SW-87-S10	3.0	3.1	nm	1160
	3.2		806	
SW-87-S5	1.1	0.7	701	1060
	0.2		677	

(b) Carboniferous metasediments

Sample reference	$\delta^{15}\text{N} \text{‰}_{(\text{AIR})}$ (mean)		NH_4^+ yield (ppm)	NH_4^+ yield data from Table 7.6 (ppm)
SW-87-S16	2.8	2.0	728	1050
	1.2		747	
SW-87-S15	2.7	2.4	792	942
	2.1		824	
SW-87-S19	2.3	2.3	626	1020, 1100
	2.3		935	

Note: nm indicates 'not measured'

For example, the best $\delta^{15}\text{N}$ replication ($<0.1\%$) was obtained on the sample (SW-87-19) for which the greatest variation of ammonium yield was found between duplicates. In contrast, where reproducibility of ammonium yield was to within 1% (sample SW-87-S7), the maximum variation of $\delta^{15}\text{N}$ was noted (1%).

It is notable that the Kate Brook Slate sample collected closest to the Dartmoor granite boundary (SW-87S-13) was characterised by a $\delta^{15}\text{N}$ value of *ca.* +7.4‰ and contained a lower ammonium content than samples SW-87S-7 and SW-87S-8, next nearest to the contact. This is in accord with the findings of Haendel et al. (1986), who noted substantial increases in the $\delta^{15}\text{N}$ values of mica schist sampled within one metre of the Ehrenfriedersdorf granite contact. It is also in agreement with the results of Bebout and Fogel (1992), who reported a similar phenomenon in connection with the Catalina schist, a subduction-related metamorphic terrane in southern California. These latter authors discussed the nitrogen data in the context of progressive devolatilisation, together with mechanisms of nitrogen release into the fluid phase during metamorphism (see Section 4.2.8 of the present work). Bebout and Fogel (1992) postulated that the high $\delta^{15}\text{N}$ values in the sedimentary rocks at the granite contact indicated that nitrogen released into the associated fluids would have been correspondingly depleted in ^{15}N . Their model, however, would appear to be inappropriate to an explanation of the source of molecular nitrogen in early hydrothermal fluids associated with the Cornubian batholith, where palæofluid $\delta^{15}\text{N}$ measurements (Section 4.6) indicate *enrichment* of ^{15}N in the fluids, relative to the metasediments. Together with the $\delta^{15}\text{N}$ measurements of Boyd *et al.* (1993) on the granites, recycling of the sedimentary nitrogen (ammonium) through the granites would appear to be a more probable scenario, prior to incorporation in the hydrothermal regime.

For comparison with the S W England metasediments, duplicate $\delta^{15}\text{N}$ analyses of a sample of Ordovician shale from Carrock Fell, included in the same batch, gave a value of $+0.53 \pm 0.1\%$ _(AIR). Although it would be unwise to formulate a hypothesis to explain the origin of molecular nitrogen in the early stage hydrothermal fluid system at Carrock Fell on the basis of duplicate analyses of a single example of local shale, in conjunction with the palæofluid $\delta^{15}\text{N}$ results reported in Table 4.4, it is notable that there appears to be a similar isotopic relationship between the nitrogen in the fluids and that in the sedimentary rocks (*i. e.* relative enrichment of ^{15}N in the fluids, generally by $\sim 4\%$) at both Carrock Fell and the various S W England localities studied in the present work.

6.5 Summary and conclusions

Any conclusions inferred from geochemical or isotopic data associated with metasedimentary rock samples from traverses across the thermal aureole of a granite must be tempered with the realisation that, in the absence of *e. g.* detailed gravity measurements to indicate the depth of

burial of the granite at the respective sampling sites, estimates of distance to the granite boundary must be viewed as provisional. What is easier to establish, for present purposes, is whether a given sample was within the boundary of the thermal aureole of the pluton. On this basis, the following conclusions were drawn:

No systematic variation of elemental composition with increasing distance from the Dartmoor granite boundary was apparent in the mudrock examples studied in the present investigation. Any pervasive infiltration of an exsolved hydrous phase from the granitic magma during emplacement therefore occurred on a sufficiently large scale, and beyond the boundary of the metamorphic aureole, to overprint any pre-existing geochemical 'signature'. Alternatively, confinement of the hydrous phase may be postulated to explain the lack of significant geochemical inhomogeneity across the thermal aureole.

The $^{87}\text{Sr}/^{86}\text{Sr}$ isotopic ratio in Kate Brook Slate from south-west of the Dartmoor granite and within the contact aureole shows a high degree of uniformity when back-corrected to the time of emplacement of the granite (280Ma before present); the data indicate that the Rb-Sr isotope systematics of the mudrocks were reset by emplacement of the granite, with a corresponding initial $^{87}\text{Sr}/^{86}\text{Sr}$ value ~ 0.010 greater than that of the granite. This resetting does not extend to samples outside the thermal aureole, nor to examples of the youngest (Namurian) metasediments intruded by the granite, either within or outside the aureole. The results obtained on the Kate Brook Slate indicate that the isotopic system was not overprinted by external (exsolved magmatic) fluids during granite emplacement.

Fluid inclusion strontium isotope data indicate that the age of the earliest hydrothermal fluids hosted by the central region of the Dartmoor granite, at 271 ± 7.4 Ma, overlaps statistically with the published age for the granite emplacement, although the associated errors permit a hiatus of up to ~ 18 Ma between granite emplacement and hydrothermal activity.

Ammonium contents of the metasedimentary rocks of (and beyond) the Dartmoor granite aureole collectively ranged from <10 to >1000 ppm and showed no systematic variation with distance from the granite boundary. The nitrogen isotopic composition of several ammonium-rich samples was determined; mean values ranging from $+0.7$ to $+3.0\text{‰}_{(\text{AIR})}$ were obtained, except at the granite contact, where a value of $+7.4\text{‰}$ was noted. Problems with low yields were encountered, however, in 'scaling up' ammonium extraction procedures based on whole-rock dissolution in conjunction with Kjeldahl distillation, as developed to determine the ammonium contents of geological samples. The experimental data indicate that no substantial fractionation of the nitrogen stable isotope ratio was associated with low recovery yields of ammonium during extraction, although reproducibility of the isotopic data was erratic. For future studies, development work on the experimental technique is clearly warranted.

The preliminary data obtained during the present study do not support the idea of substantial nitrogen loss from the metasediments during emplacement of the Dartmoor granite and consequently any incorporation of sedimentary nitrogen into the cooling granitic melt at a high crustal level would probably have been minimal.

Stable isotope ratio analysis of nitrogen in aureole metasediments of low ammonium content, and located away from the immediate vicinity of the granite boundary, would be of value in determining whether any systematic relationship exists between ammonium content and associated $\delta^{15}\text{N}$ value (*cf.* Bebout and Fogel, 1992). This would help to identify whether the high $\delta^{15}\text{N}$ value and relatively low ammonium abundance at the granite boundary are thermal devolatilisation effects, caused by granite emplacement.

The inorganic carbon contents of all metasedimentary rock samples investigated from the vicinity of the Dartmoor granite (within and outside the aureole) were very low (2.3 ± 1.1 ppmC, 1σ error). The 'organic' carbon abundance data were strongly bimodal; samples enriched in organic matter contained several thousand ppm of carbon. No systematic variation was discernible in the associated stable isotope characteristics, with either carbon abundance or proximity to the granite boundary.

Significant quantities of inorganic carbon were found in borehole drillcore samples of Devonian age, obtained from localities west of (and outside the thermal aureole of) the St Austell granite. Isotopic data indicated that these carbonates were not directly of marine origin. Furthermore, the $\delta^{13}\text{C}$ values were similar to those obtained for the total carbon content of early hydrothermal fluids characterised by W±Sn oxide association in the Cornubian region. This latter finding suggests that the palæofluid carbon may have been derived from the thermal breakdown of such a source, although the mechanism by which it was incorporated into the fluids is not unambiguously identified.

Chapter 7

Synthesis and concluding remarks

7.1 Overview

As each chapter has a separate conclusions section, the objectives here are to summarise the salient findings of the present work, including advances in experimental techniques; secondly, to consider the overall implications of the geochemical and isotopic data with respect to a self-consistent description of hydrothermal processes associated with early mineralisation of the Cornubian batholith. The ultimate objective of such an assessment is to delineate the relation between episodes of granite magmatism and spatially-associated high-temperature hydrothermal phenomena in the region, particularly with respect to the source of the fluids.

7.2 Experimental procedures

There are two principal achievements resulting from the present work:

(i) A detailed appraisal of existing methods has led to the development of a low-blank, stepped-heating protocol for the extraction and subsequent isotopic analysis of CO_2 from fluid inclusions in quartz, allowing reliable data to be obtained from much smaller samples than possible hitherto. The technique was validated, using both dual inlet (dynamically pumped) and static vacuum gas source mass spectrometry, by demonstrating consistency of $\delta^{13}\text{C}$ results from quartz sample replicates over an approximately 50-fold mass range down to ~20mg, besides giving consistency with $\delta^{13}\text{C}$ of CO_2 released by crushing the quartz. Ultimately, the level of blank during stepped heating was sufficiently low to enable $\delta^{13}\text{C}$ measurements to be made on 2-3 nanomoles of gas, with an attendant accuracy within the analytical precision of measurement ($<\pm 1\%$ at the 1σ level). A procedure for abundance and $\delta^{13}\text{C}$ measurements on coexisting fluid inclusion CH_4 and CO_2 was also devised; optimum $\delta^{13}\text{C}$ reproducibility of $\pm 0.5\%$ was obtained on replicate extractions of fluid inclusion CH_4 as small as 60 nanomoles, using 'conventional' (dual inlet) gas source mass spectrometry.

(ii) Experimental procedures for the preparation and isotopic characterisation of nitrogen at the sub-nanomole level have been adapted to $\delta^{15}\text{N}$ measurements of fluid inclusion nitrogen, extracted by stepped heating. The analytical precision was usually $<\pm 0.5\%$ at the 1σ level, on sample aliquots of ~0.8 nanomoles of N_2 admitted to the mass spectrometer. Nitrogen blank yield during fluid inclusion extraction and purification was generally two orders of magnitude less than the sample yield, when the latter exceeded ~2.7 nanomoles.

7.3 Principal findings of the research

(i) A comparison of hydrothermal fluids (represented by quartz-hosted fluid inclusions) associated with early-stage W±Sn oxide mineralisation throughout the Cornubian region revealed that carbon-bearing species (carbon dioxide and methane, in varying proportions) and molecular nitrogen were present as trace components (generally 2-15ppm C or N, with respect to the quartz host) in all cases. In contrast, abundances of these species in comparable-stage fluids hosted by the Dartmoor granite (associated with quartz+tourmaline±cassiterite assemblages) were considerably lower.

(ii) Extension of the comparison to fluids hosted by early pegmatitic quartz of the Land's End and St Austell granites showed that the presence of nitrogen and carbon-bearing volatiles in the earliest (high temperature) phase of hydrothermal activity was not restricted to W±Sn oxide association.

(iii) Isotopic analysis showed that the range of palæofluid $\delta^{13}\text{C}_{\Sigma\text{C}}$ values was relatively narrow, from -9.5 to -16.5‰_(PDB), despite variation in the associated CO_2/CH_4 ratios of almost 50-fold. The data indicated isotopic disequilibrium between coexisting methane and carbon dioxide. An unusual example from the vicinity of the Carnmenellis granite contained an excess of methane over carbon dioxide, anomalous ^{13}C -enrichment of both carbon species ($\delta^{13}\text{C}_{\text{CO}_2}$ of +4.2‰; $\delta^{13}\text{C}_{\text{CH}_4}$ of -27.4‰), yet with palæofluid $\delta^{13}\text{C}_{\Sigma\text{C}}$ of -15.6‰.

(iii) Modelling of the carbon isotope data suggests that the results are best explained in terms of partial reduction of a primary reservoir of carbon dioxide (by wallrock reaction), with kinetic effects controlling the ^{13}C distribution. The apparent independence of palæofluid CO_2/CH_4 ratios to whether the host quartz is located in granite or metasedimentary rock, together with the 'buffering' of $\delta^{13}\text{C}_{\Sigma\text{C}}$ values, mitigates against a local thermogenic methane source.

(iv) Although the data are inconclusive, preliminary application of high sensitivity, static vacuum mass spectrometry indicated that carbon dioxide characterised by $\delta^{13}\text{C}$ values in the region of -6 to -12‰ may be present at ultra-trace levels in fluids associated with early mineralisation of the Dartmoor granite.

(v) The inorganic carbon content of Devonian and Carboniferous metasedimentary rocks sampled from within and adjacent to the metamorphic aureole of the Dartmoor granite was uniformly low (2.3 ± 1.1 ppm, 1σ). The corresponding 'organic' carbon abundances were strongly bimodal; samples most enriched in organic matter contained several thousand ppm of carbon. No systematic variation between the abundance of 'organic' carbon and either the corresponding $\delta^{13}\text{C}$ value or proximity from the granite contact was apparent.

(vi) Examples of Devonian metasediments relatively enriched in inorganic carbon (92-3821 ppmC) were discovered in borehole drillcores from an area to the west of the St Austell granite. Isotopic analysis of the carbonates showed that the $\delta^{13}\text{C}$ values were within the $\delta^{13}\text{C}_{\Sigma\text{C}}$ range characteristic of palaeofluids associated with early-stage hydrothermal processes hosted by the Cornubian batholith. This supports the view that the palaeofluid carbon may have been derived from such a source, although the transfer mechanism (such as *via* assimilation of the carbonate into granite protoliths during anatexis, or by direct thermal degradation of the metasedimentary rock during magma ascent) is not uniquely identified.

(vii) $\delta^{15}\text{N}$ measurements, by static vacuum mass spectrometry, of palaeofluid molecular nitrogen associated with early-stage W±Sn oxide mineralisation at seven localities in the Cornubian province gave mean values ranging from 5.0 to 6.9‰_(AIR). Two samples collected from Old Gunnislake mine gave corresponding values of $8.2 \pm 0.29\%$ and $10.0 \pm 0.55\%$ (1 σ error), respectively.

(viii) Neither the concentration of nitrogen in the fluids, nor the associated $\delta^{15}\text{N}$ value, appeared to depend on whether the quartz host was located in unaltered granite, greisenised granite or metasedimentary rock. The highest concentration of nitrogen, however, both with respect to the quartz host (up to 13.8 ppm) and as nitrogen molality (~ 0.34) in the fluid, was found in samples from South Crofty mine, in the vicinity of the Carnmenellis granite. Published work has recently shown that this pluton contains the highest concentrations of ammonium (93-109 ppm, with $\delta^{15}\text{N} \approx 8.8\%$), compared to the other major Cornubian granite intrusives, whereas the Dartmoor pluton contains the lowest (8 ppm, with $\delta^{15}\text{N} \approx 7.0\%$). Extraction and isotopic analysis, during the present work, of nitrogen from hydrothermal fluids associated with early-stage mineralisation of the Dartmoor granite, indicated that sub-ppm abundances (with respect to the quartz) were present, corresponding to nitrogen molality in the fluid of $\sim 10^{-2}$. Furthermore, mean $\delta^{15}\text{N}$ values of three of the four samples investigated were in the range 6.7-7.3%. The apparent correlation between the nitrogen content of the fluids and the ammonium content of the associated granite supports the hypothesis that the granites are the most probable source of nitrogen in the fluids.

(ix) The 'extractable' NH_4^+ content of regional Devonian and Carboniferous metasedimentary country rocks from and beyond the thermal aureole of the Dartmoor granite ranged from <10 ppm to >1000 ppm. No systematic variation with distance from the contact zone was evident. Preliminary data from samples containing >600 ppm indicated that this NH_4^+ was characterised by $\delta^{15}\text{N}$ values in the range of $1.9 \pm 1.2\%$, except at the granite contact, where a value of $7.4 \pm 0.3\%$ was recorded. The data do not support the idea of substantial nitrogen loss from the metasediments during emplacement of the Dartmoor granite; incorporation of sedimentary nitrogen into the cooling magma at a high crustal level was thus probably minimal.

(x) On the basis of published $\delta^{15}\text{N}$ data for the Cornubian granites, together with the most recently-reported relevant isotopic fraction factors, palaeofluid $\delta^{15}\text{N}$ values of 5.0 to 6.9‰ are in accord with equilibrated nitrogen isotope exchange with ammonium in the granite, at the hydrothermal (300-500°C) stage, or at magmatic temperatures if $\text{N}_2\text{-NH}_4^+$ equilibration was subsequently maintained during cooling. The more ^{15}N -enriched palaeofluid at the Old Gunnislake mine locality may be explained by quantitative oxidation of granitic ammonium, if it is assumed that the $\delta^{15}\text{N}$ value of the Gunnislake granite falls within the range of 8.4-10.2‰ recorded for Cornubian granite whole-rock samples containing greater than ~32ppm NH_4^+ . The same mechanism is proposed for the Dartmoor system, where palaeofluid nitrogen isotope compositions are also similar to those of the host granite. Nitrogen isotope data indicate that regional ammonium-rich metasedimentary rocks are not likely to have been the direct source of the palaeofluid nitrogen.

(xi) Carbon dioxide was invariably released with the nitrogen component from all quartz samples investigated herein. Equilibrium modelling indicates that oxidation of ammonia by carbon dioxide under magmatic or hydrothermal conditions is a thermodynamically viable mechanism for the formation of molecular nitrogen. This reaction may also have been one of the principal redox routes by which methane was generated in magmatic-hydrothermal regimes associated with the batholith. Indeed, the greatest abundances of methane were associated with anomalously high levels of nitrogen. Control of carbon speciation, however, is also likely to have been effected by wallrock $\text{Fe(II)} \leftrightarrow \text{Fe(III)}$ redox reactions on a local scale, prior to fluid entrapment.

(xii) Fluids associated with oxide mineralisation of the Dartmoor granite, from the earliest pegmatitic quartz, through quartz+tourmaline±cassiterite, to cooler (~180°C) fluids associated with quartz+hæmatite, were characterised by a surprising uniformity of chemical composition. Excellent charge balances were obtained for most of the leachate analyses. Ca/K molar ratios exceeded unity in all cases. Furthermore, the enrichment in B, F, Li, Al, Fe, Mn and Zn indicated similarity to published values for higher temperature (500-600°C) fluids from the St Austell region and implied to be of granitic derivation. Br/Cl and I/Cl molar ratios in the Dartmoor granite-hosted fluids, $(7.5 \pm 1) \times 10^{-4}$ and $(22 \pm 13) \times 10^{-6}$ respectively, are compatible with a magmatic origin for these elements.

(xiii) The palaeowater isotopic characteristics (δD , $\delta^{18}\text{O}$) of early mineralising fluids hosted by the Dartmoor granite are generally characterised by a narrow range (δD -24 to -33‰; $\delta^{18}\text{O}$ values 7.1 to 8.1‰), and exhibit no systematic variation with associated paragenetic stage. The hydrogen isotope data, in particular, are in accord with a magmatic origin of the fluids, if isotopic exchange occurred under equilibrium conditions between the fluids and hydrous silicates of the granite at sub-solidus temperatures. The relative invariance of isotopic and chemical composition to paragenetic association thus supports the idea of protracted (and

episodic) magmatic-hydrothermal activity hosted by the Dartmoor granite, with no significant influx of external fluids into the fracture systems.

(xiv) Palæowater δD values of early W±Sn oxide-stage hydrothermal fluids associated with the Hemerdon Ball granite are indistinguishable from those of fluids associated with early tourmaline and greisen mineralisation of the Dartmoor granite. Despite extension of the hydrothermal system at Hemerdon into the metasedimentary country rock, the palæowater δD and $\delta^{18}O$ values appear to be invariant to whether the associated quartz host is located in granite or metasediments. Furthermore, in terms of solute electrolyte composition, early hydrothermal fluids at Hemerdon were broadly similar to those hosted by the Dartmoor granite. The principal difference was greater enrichment of potassium and depletion of calcium (relative to sodium) at Hemerdon.

(xv) Early hydrothermal fluids characterised by W±Sn oxide association at many other localities in S W England were characterised by relative enrichment in deuterium (δD values of the palæowaters being up to *ca.* -10‰). Published work has reported that such fluids were of relatively low salinity, compatible with a predominantly meteoric origin of the water. The present work, however, shows that such fluids were anomalously enriched in boron and contained distinctive minor element distributions and halogen ratios that support the case for a magmatic component. Furthermore, K/Na ratios were generally similar to those of early mineralising fluids hosted by the Dartmoor granite (although the corresponding Ca/Na values were lower).

(xvi) Few data were obtained on the isotopic composition of palæowaters associated with 'main stage' (sulphide) mineralisation, during the present work. Preliminary assessment indicated a range of δD values (-14 to -32‰) broadly coinciding with that obtained overall for early W±Sn oxide-associated fluids of the Cornubian region.

(xvii) Analyses of palæowater δD and $\delta^{18}O$ values of late-stage (age ~230Ma), cross-course fluids from the Tamar valley region (located some distance from the present-day granite outcrops and associated with lower temperature hydrothermal activity) do not support either of the two alternatives proposed in the literature for their origin, *viz.* Mesozoic seawater or sedimentary basin brines. The δD values (-35 to -55‰) indicate that a fluid origin based on the release (through changes in the regional tectonic stress field) of primary magmatic fluid from inclusions in a sub-surface component of the batholith is a potential explanation. The relatively ^{18}O -depleted nature of the fluids, however, ($\delta^{18}O$ values of *ca.* 1.5-4.7‰) would require that any initial 'magmatic' value was substantially shifted by equilibrated oxygen isotope exchange at low temperatures between the fluid and wall rocks (as proposed in the literature in the case of Canadian Shield brines and pore waters in oceanic sediments).

(xviii) An apparent lack of systematic variation in elemental composition of metasedimentary rocks sampled across and beyond the thermal aureole of the Dartmoor granite was noted. This suggests that emplacement of the Dartmoor granite was not accompanied by chemical overprinting of the country rocks, such as might be expected from pervasive infiltration of an exsolved aqueous phase from the cooling magma. This view is supported by $^{87}\text{Sr}/^{86}\text{Sr}$ measurements on Devonian metasediments (Kate Brook Slate) from the aureole, indicating that the Rb-Sr isotope systematics were reset by the emplacement of the granite, but with a corresponding initial $^{87}\text{S}/^{86}\text{Sr}$ ratio ~ 0.010 greater than that of the granite.

7.4 Concluding remarks

The exposed granite intrusives of the Cornubian batholith and associated mineralisation provide an excellent setting for a geochemical and isotopic investigation of the relation between hydrothermal activity and plutonism. Despite several recent studies of hydrothermal phenomena associated with the earliest stages of alteration and mineralisation of the batholith, the source of the fluids and the extent to which fluid compositions reflect high-level crustal processes involving the metasedimentary and metavolcanic country rocks is still a matter of debate. Opinion is divided on whether the granites served primarily as a heat source, driving hydrothermal systems which consisted essentially of meteoric water (with salinity subsequently deriving from water-rock interaction), or were themselves the source of at least the earliest fluids, through exsolution of an aqueous phase during the cooling of emplaced magma.

The distinctive contrast between early-stage mineralisation of the Dartmoor granite, on the one hand, and that associated with Hemerdon Ball, a minor pluton located within the metamorphic aureole of the Dartmoor intrusive, provided a focal point in the present work for testing hypotheses concerning the origin of fluids which characterised early stages of hydrothermal activity hosted diachronously throughout the batholith. Several lines of evidence throughout the present work support the assertion that the granites were primarily or exclusively the source of palæofluid constituents in the high-temperature pegmatitic stage and earliest mineralising fluids. One of the principal findings is that the abundance of traces of nitrogen and carbon-bearing species in the fluids may be directly linked to the degree of 'S'-type character of the associated granite intrusive. Published work has demonstrated (by initial $^{87}\text{Sr}/^{86}\text{Sr}$ and ϵ_{Nd} values, together with normative corundum data) that the extent of incorporation of sedimentary material by the parent magmas varies considerably between component intrusives of the batholith; also, that ammonium concentrations in the granites (and associated $\delta^{15}\text{N}$ values) reflect the proportion of pelitic constituents in the metasedimentary material assimilated *via* the anatexis of crustal rocks.

A corollary of the present experimental work is that carbon-bearing species and nitrogen in palæo-hydrothermal systems are probably much more widespread than recognised hitherto, albeit at trace or ultra-trace levels. Limitations imposed by the lack of appropriate analytical techniques have probably precluded wider recognition of the value of these components (particularly the isotopic compositions thereof) as tracers of fluid origin.

The results presented herein support the idea of a general, genetic link between granite magmatism and the earliest hydrothermal fluids of the Cornubian region. Such fluids are likely to have been derived by exsolution of a hydrosaline phase during the cooling of granitic magma. This explanation is also in accord with field evidence for a continuum linking the pegmatitic and 'pneumatolytic' stages of hydrothermal fluid evolution.

Geochemical and isotopic data from Palæozoic metasedimentary rocks of (and immediately beyond) the metamorphic aureole of the Dartmoor granite indicate that major depletion or overprinting of metasediment constituents, at a crustal level equivalent to present-day exposure, did not occur during granite emplacement. Comparable data from a traverse across the aureole of the Hemerdon Ball granite (or of the Carnmenellis pluton) would be appropriate to confirm whether this finding was also true at localities where early-stage hydrothermal fluids contain significant abundances of carbon-bearing species and nitrogen. Although anatectic incorporation of pelitic material appears to be the most probable route by which carbon and nitrogen was incorporated into the granitic protoliths, and thence into an exsolved aqueous phase after granite emplacement, assimilation of such material during magma ascent, at levels deeper than present exposure, cannot be categorically excluded.

With regard to whether the role of the granites was primarily as a heat source, with the associated hydrothermal fluids being essentially of meteoric derivation, the present work indicates that this was not the case, at least for high-temperature fluids associated with W±Sn oxide mineralisation at Hemerdon, early tourmaline and oxide mineralisation of the Dartmoor granite, and comparable-stage phenomena associated with the St Austell and Land's End granites. However, published work by other authors has shown that elsewhere in the Cornubian region, such as South Crofty mine, Cligga Head, and at various localities in the vicinity of the Gunnislake granite, the earliest hydrothermal stage was apparently characterised by fluids of relatively low salinity. Furthermore, the present work has shown that such fluids were also relatively enriched in deuterium, compared to the more saline examples (as at Dartmoor, Hemerdon, *etc.*). Explanations proposed elsewhere to account for these findings envisage either the progressive dilution of an initial magmatic (high salinity) fluid by low salinity groundwaters of meteoric origin, or indeed that the waters were entirely meteoric in derivation, with constituent solutes resulting from leaching of wallrocks. The hydrogen isotope data reported in the present work are consistent with the former of these two explanation.

In many respects, the findings of the present work broadly concur with the 'emanative centres' theory of Dines (1956), in the sense that the granites are considered to be the source of high-temperature hydrothermal fluids which, whilst not temporally related on a batholith-wide scale, are associated both spatially and temporally with particular episodes of magmatic intrusion that occurred diachronously throughout the batholith. 'Main-stage' hydrothermal activity, as characterised by quartz-sulphide assemblages, has not been the focus of attention of the present work. To extend the 'emanative centres' comparison to these fluids requires an assessment of whether the constituents were also primarily of magmatic origin. Application of the techniques reported in the present work may contribute to such an appraisal.

Appendix A

Sample inventory

(1) Samples used for palaeofluid inclusion analysis (quartz unless specified otherwise)

S W England

'Pegmatitic' (transitional) rock types preceding earliest hydrothermal oxides:

Examples associated with the St Austell and Land's End granites, respectively.

Supplied by Dr C Halls and Lin Yucheng, Imperial College, University of London.

Sample Reference	Description	Grid reference
<i>Gunheath</i> (<i>St Austell granite</i>) LYGUN-1 LYGUN-15	Sheeted quartz-tourmaline vein, greisen lode. Miarolytic pegmatite pods and cavities: Quartz, coexisting with feldspar, muscovite / gilbertite, tourmaline.	SW 200 568
<i>Priest's Cove</i> , (<i>Land's End granite</i>) LYPC-88	Pegmatitic quartz pod with aplite, fluorite, topaz and wolframite.	SW 352 316
<i>Trelavour Downs</i> (<i>St Austell granite</i>) LYTD-88	Pegmatitic quartz (unidirectional solidification textures) with protolithionite.	SW 960 575

Quartz ± tourmaline ± cassiterite ± hæmatite assemblages hosted by the Dartmoor granite:

Stages of mineral paragenesis referred to below are as defined by Scrivener (1982). Samples were collected under the guidance of, or supplied by, Dr R C Scrivener of the British Geological Survey.

Sample Reference	Description	Grid reference
<i>East Vitifer mine</i> SW-89-154 SW-89-155 SW-89-156	Stage III mineralisation (with some Stage II present also). Collected <i>in situ</i> by the author. Stage II mineralisation Collected <i>in situ</i> , as above. Stage II mineralisation. Quartz and tourmaline, with little cassiterite.	SX 705 825
<i>Great Rock mine</i> SW-89-157	N lode. Hæmatite, pyrite and minor quantities of quartz. Stage III mineralisation. Collected <i>in situ</i> by the author.	SX 827 815
<i>Golden Dagger mine</i> SW-89-159 SW-89-160 SW-89-161 SW-89-162 SW-89-163	Early quartz from pegmatitic pod within body of aplite. Collected <i>in situ</i> from adit roof by the author. Earliest pegmatitic quartz (Stage I), as above, with feldspar and tourmaline. Dump material. Predominantly Stage III, although some Stage II also present. Quartz, tourmaline, hæmatite. Dump material. Mainly Stage II (with Stage III veining). Dump material Predominantly Stage II mineralisation, although some Stage III veining. Quartz, tourmaline, cassiterite & a little hæmatite. Adit level.	SX 679 803
<i>Barracott mine</i> SW-89-164	Quartz, tourmaline, cassiterite (Stage II). Supplied from Torquay museum collection.	SX 738 819

Sn-W oxide-stage assemblages associated with the Cornubian batholith:

Sample Reference	Description	Grid reference
<i>Hemerdon mine</i>	Quartz vein samples, supplied by Dr T J Shepherd of the British Geological Survey, from drill cores made available by Amax Exploration (UK) Inc.	SX 570 585
HEM-79-2	Borehole DDH36, 229.5m depth. Granite hosted, greisen-bordered quartz vein.	
HEM-80-1	Borehole DDH68, 150.8m depth. Killas hosted. Mica, greisen borders and feldspar apparently absent. Wolframite present.	
HEM-80-35	Borehole DDH72, 118.2m depth. Killas hosted. Mica, greisen borders and feldspar apparently absent.	
HEM-80-39	Borehole DDH74, 33.9m depth. Granite hosted, greisen-bordered quartz vein. Wolframite present.	
HEM-80-44	DDH H74, 94.9m depth. Killas hosted. Wolframite present.	
HEM-80-47	Borehole DDH H74, 137.5m depth. Killas hosted. Mica, greisen borders and feldspar apparently absent.	
HEM-80-50	Borehole DDH H74, ~193m depth. Hosted by greenstones (?) and killas. Quartz vein and tourmaline.	
<i>South Crofty mine</i>	(Carn Brea granite)	SW 675 411
SC-88-2	North Pool A zone. Sub-level below 335 fathom level. Quartz, wolframite, feldspar. Collected <i>in situ</i> by the author, with Dr R C Scrivener.	
SC-88-3	North Pool quartz lode, 380 fathom level. Quartz, wolframite. Collected <i>in situ</i> by the author, as above.	
SC-88-3ABC	3ABC lode, 360 fathom level. Early cassiterite with quartz and feldspar. (Same generation as W-bearing fluid.) Sample supplied by Dr R C Scrivener.	
SC-88-NTL	North Tincroft lode (N branch from Robinson's shaft), 360 fathom level. Quartz, arsenopyrite & wolframite. Sample supplied by Dr R C Scrivener.	
<i>Cligga Head</i>	(Cligga granite)	SW 737 538
CH-88-1	Quartz with wolframite. Supplied by Dr R C Scrivener.	
<i>Castle-an-Dinas mine</i>		SW 945 624
CD-88-1	Quartz with wolframite, adit level. Supplied by Dr R C Scrivener.	
<i>Drakewalls mine</i>	Country rocks: killas overlying granite.	SX 425 707
SW-84-15	Veinlets of quartz/cassiterite/wolframite stockwork. Collected by Bull (1982): sample ref. D2. Representative of cassiterite mineralisation.	
SW-84-16	As above (Bull, 1982: sample ref. D2). Representative of wolframite mineralisation.	
<i>Old Gunnislake mine</i>	Mostly granite hosted, but some workings in killas.	SX 435 725
SW-84-18	Quartz, wolframite. Collected by Bull (1982): ref. M149.	
OG-88-1	Quartz, wolframite; lode in adit. Supplied by Dr R C Scrivener.	
SW-89-150	Early quartz, with some wolframite. Collected <i>in situ</i> by the author, in conjunction with J T Chesley.	
<i>South Bedford mine</i>	Granite on west, overlain by metamorphosed killas with elvan dykes to East; junction outcrops beneath R Tamar.	SX 433 721
SW-84-20	Quartz, wolframite. Collected by Bull (1982): ref. M77.	
<i>Prince of Wales mine</i>	Killas hosted.	SX 407 708
SW-84-25	Quartz, wolframite. Collected by Bull (1982): ref. M47.	
SW-84-27	Quartz, wolframite. Collected by Bull (1982): ref. M50.	

Sulphide-stage assemblages:

(All samples supplied by Dr R C Scrivener)

Sample Reference	Description	Grid reference
<i>South Caradon mine</i> SW-84-1	Host: granite (Bodmin Moor) overlain by killas in SE. Main stage sulphide mineralisation. All vein material: chalcopyrite, pyrite, chlorite, quartz.	SX 272 700
<i>West Caradon mine</i> SW-84-2	Intra-granitic (Bodmin Moor). All vein material; main stage mineralisation. Same paragenesis as sample SW-84-1.	SX 263 702
<i>Devon Great Consols</i> SW-84-14	(Includes Wheal Emma mine, amongst others.) Borehole sample (depth 1189' 08") from the collection of Bull (1982): sample ref. D3. Small vein of quartz & chalcopyrite, in vicinity of Devon Great Consols.	SX 4275 7320
<i>Wheal Emma mine</i> SW-84-17	Hosted by metamorphosed killas. Quartz, arsenopyrite vein sample. Supplied from the collection of Bull (1982).	SX 441 738
<i>Wheal Arthur mine</i> SW-84-19	Country rock: killas. Quartz, chalcopyrite. Supplied from the collection of Bull (1982): sample M86.	SX 430 700
<i>Cotehele Consols</i> SW-84-22	Country rock: killas. Arsenopyrite strings in quartz/chlorite. Supplied from the collection of Bull (1982): sample M98.	SX 421 694
<i>Okeltor mine</i> SW-84-23	Country rock: killas. Arsenopyrite strings in vuggy quartz. Supplied from the collection of Bull (1982): sample M92.	SX 454 690

N-S cross-course veins: Galena and sphalerite, with minor silver minerals in quartz/fluorite gangue.
All samples supplied by Dr R C Scrivener and collected from mine dumps.

Sample Reference	Description	Grid reference
<i>Wheal Wrey mine</i> SW-84-9 SW-84-10	Country rock: killas. Quartz Quartz	SX 297 659
<i>Wheal Mary Ann</i> SW-84-12	Country rocks: killas with contemporaneous volcanics. Late quartz	SX 288 639
<i>Lockridge mine</i> SW-88-4	Country rock: killas. Quartz	SX 439 665
<i>North Hooe mine</i> SW-88-5	Country rock: killas. Quartz	SX 427 661
<i>Buttspill mine</i> SW-88-6	Country rock: killas. Quartz	SX 437 678
<i>South Tamar Consols</i> SW-88-8 SW-88-9	Country rock: killas. Quartz Quartz associated with sphalerite	SX 437 645

Note: Samples originally collected by Bull (1982) were supplied to the present author by
Dr R C Scrivener, from collections held at the Exeter office of the British Geological Survey.

Sample Reference	Description	Grid reference
<i>Birch Tor & Vitifer mine</i> SW-81-14	Host: Dartmoor granite Quartz+cassiterite ('Stage II' mineralisation)	SX 681 812

Carrock Fell mine, Cumbria (N W England)

Grid reference: NY 322 329

W oxide-stage assemblages:

Vein quartz samples, made available by Dr T J Shepherd of the British Geological Survey, who collected the material *in situ* from the Harding vein.

Sample Reference	Description
CF-76-7	Lower level; gabbro host rocks; quartz-wolframite-scheelite
CF-76-25	Lower level; granite host rocks; quartz, carbonates
CF-77-39A	1A level; gabbro host rocks; quartz-wolframite
CF-77-39B	1A level; gabbro host rocks; quartz (post-dating wolframite)
CF-77-77A	Main level (North); granite host rocks; quartz (post-dating wolframite)
CF-77-77B	Main level (North); granite host rocks; quartz-wolframite
CF-77-98	1A level; gabbro host rocks; quartz (post-dating wolframite)

S China

'Transitional' rock types associated with Yanshanian granites:

Quartz-wolframite vein samples from Jiangxi and Hunan provinces.

Supplied by Dr C Halls and Lin Yucheng, Imperial College, University of London.

Sample Reference	Location	Description
<i>Hunan province</i>		
YGX-05	Yaoguangxian	Quartz-wolframite-molybdenite. Massive wolframite; vein located entirely within granite and greisen bordered.
<i>Jiangxi province</i>		
XHS-01	Xihuashan	Quartz-wolframite-molybdenite. Massive wolframite and molybdenite; vein located entirely within granite and greisen bordered.
XHS-02	Xihuashan	Quartz-wolframite-molybdenite. Endogranitic.
PT-496	Piaotang	Quartz-wolframite-topaz-mica-sulphide. 496 m level, No.3 vein. Hosted by country rock.
DP-560	Dangping	560m level at Banbianshan; quartz vein with beryl. Endogranitic.

(2) Metasedimentary rocks from the vicinity of the Dartmoor granite, S W England

Samples are listed in order of decreasing distance from the granite contact.

Upper Devonian metasediments from an area south-west of the Dartmoor granite:

Sample Reference	Location	Grid reference
SW-87-S1	Plym bridge	SX 525587
SW-87-S2	300m SSW of Bickleigh viaduct.	SX 521613
SW-87-S3	50m SSW of Bickleigh viaduct.	SX 522614
SW-87-S4	100m NNW of Bickleigh viaduct.	SX 523616
SW-87-S5	50m SSW of road bridge, Bickleigh.	SX 525619
SW-87-S6	100m NNE of Bickleigh road bridge.	SX 526620
SW-87-S12	50m S of Ham Green viaduct.	SX 525626
SW-87-S11	Heleball Wood.	SX 527631
SW-87-S10	Heleball Wood.	SX 527634
SW-87-S9	Heleball Wood, 40m S of road bridge.	SX 527636
SW-87-S8	10m S of tunnel near Leighbeer farm.	SX 530640
SW-87-S7	20m N of tunnel near Leighbeer farm.	SX 530643
SW-87-S13	Collected between Shaugh bridge and Shaugh Mill.	SX 533635

Carboniferous (Crackington Formation) metasediments from an area north-east of the Dartmoor granite:

Sample Reference	Location	Grid reference
SW-87-S14	Track beneath Willingstone Rock.	SX 761893
SW-87-S17	Quarry above Steps bridge.	SX 798882
SW-87-S18	50m S of Steps bridge.	SX 805882
SW-87-S16	Small quarry, B3212.	SX 794883
SW-87-S15	Crossroads NE of Clifford bridge.	SX 782898
SW-87-S19	B3193, 150m S of Dunsford Cross.	SX 821888

Notes: Samples SW-87-S7 and SW-87-S8 were located virtually equidistant from the granite contact. Sample SW-87-S13 was probably closer, although this was difficult to assess with certainty.

The Upper Devonian samples were collected under the guidance of Mr A J J Goode, of the British Geological Survey Exeter office, whereas Dr R C Scrivener advised on the selection of the Carboniferous metasediment examples.

(3) Devonian metasedimentary rocks sampled to the west of the St Austell granite, S W England

Heat flow borehole drillcore material, supplied by Dr B Smith of the British Geological Survey. In total, five boreholes were drilled from surface to 300m at various locations across Cornwall, in order to measure heat flow within the killas as part of a Hot Dry Rock Geothermal Energy Project initiative. The sites ranged from near Newquay in the north to Veryan in the south. 10-20cm length sections of drillcore (80mm diameter) were available from three of these boreholes for use in the present study. The following details relating to these samples were obtained from an unpublished, internal technical note of the Camborne School of Mines ('Heat flow boreholes field report', document reference RB/AG/SER/406/05/01: TN03/23, dated 20 January 1988):

General notes:

The heat flow boreholes were all located in regionally metamorphosed Devonian sediments, known locally as killas. HF1 and HF2 locations were in the Meadfoot Beds, Lower Devonian, which consists of slates, shales and siltstones, with some volcanic tuffs and greenstones. HF3, by contrast, was obtained from part of the Gramscatho Beds (Middle Devonian), which consist of slightly coarser sediments, silts and sandstones. Graded sandstones become dominant with depth in all cases. Volcanic tuffs occur in HF3, with greenstones. Very little mineralisation is present in the drillcore samples, except in the case of HF2. Shallow dipping quartz veins are present in all of the boreholes. All drillcores contain fairly similar gently dipping sediments, including slates, shales, sandstones and volcanic ash.

Sample reference: HF1

Location: Treago Farm, Crantock. Grid reference: SW 782602. Depth: 150.99 - 151.19m.

The relevant section of the core log indicates that the rock type of this particular sample was shale (slate), with gentle folding, especially around quartz veins.

Sample reference: HF2

Location: Gwinear Farm. Grid reference: SW 804575. Depth: 297.07 - 297.17m.

On the boundary of tuff (above) and shale (slate) containing thin tuff beds.

Sample reference: HF3

Location: Trevispian Vean, Trispen. Grid reference: SW 852503. Depth: 150.60 - 150.75m.

Shales and tuff.

Appendix B

Stepped heating data: carbon yields and $\delta^{13}\text{C}$ results as a function of the analytical protocol

B.1

Procedural combustion/pyrolysis carbon blanks of the extraction line used in conjunction with the VG[®]SIRA 24 mass spectrometer. Sample: gem quality (inclusion-free) quartz. Released gases exposed to Pt foil catalyst at ~1050°C during extraction stage in all cases.

Weight (mg)	Release	T (°C)	Yield ($\mu\text{g C}$)	Yield (ppm C)	$\delta^{13}\text{C}$ (‰)
200	Combustion	220	0.04	0.22	nm
	Combustion	350	0.27	1.36	nm
	Pyrolysis	600	0.38	1.90	nm
Empty vessel	Pyrolysis (no pre-combustion)	350-600	0.07	-	nm

B.2

The measured variation of carbon yield (as CO_2) and corresponding $\delta^{13}\text{C}$ isotopic composition, as a function of the quartz sample mass and analytical protocol, during stepped thermal release of fluid inclusion components from hydrothermal vein quartz.

Table B2.1 Sample: HEM-80-1

(a) Stepped 'combustion' to 350°C followed by 'pyrolysis' to 600°C (in the presence of a Pt foil catalyst at ~1050°C during the extraction stage in all cases).

Weight (mg)	Release	T (°C)	Yield ($\mu\text{g C}$)	Yield (ppm C)	$\delta^{13}\text{C}$ (‰)
1109	Combustion	220	1.16	1.05	-30.8
	Combustion	350	34.57	31.17	-23.91
	Pyrolysis	600	22.38	20.18	-9.52
273	Combustion	220	0.57	2.09	nm
	Combustion	350	2.09	7.66	-24.6
	Pyrolysis	600	5.37	19.67	-13.15
53.61	Combustion	205	0.05	0.86	nm
	Combustion	350	0.55	10.20	nm
	Pyrolysis	620	2.44	45.58	-22.9
25.37	Combustion	200	0.18	7.25	nm
	Combustion	350	1.25	49.30	-27.3
	Pyrolysis	600	1.01	39.86	-20.1
† 22.26	Combustion	200	0.13	0.60	-29.3
	Combustion	350	1.55	6.95	-29.6
	Pyrolysis	600	0.79	35.43	-20.9

Note: † Isotopic analysis by static vacuum mass spectrometry.

- (b) Single-step 'pyrolysis', in the absence of supplied oxygen; Pt catalyst at room temperature.

Weight (mg)	T (°C)	Yield (µg C)	Yield (ppm C)	δ ¹³ C (‰)
261.00	630	4.78	18.33	-10.22
125.34	630	2.60	20.71	-10.7
44.07	630	0.99	22.40	-10.0

- (c) 'High resolution' stepped heating, in the absence of supplied oxygen; Pt catalyst at room temperature.

Weight (mg)	T (°C)	Yield (µg C)	Yield (ppm C)	δ ¹³ C (‰)
1112.75	300	0.25	0.23	nm
	400	2.34	2.10	-11.0
	450	3.62	3.25	-9.5
	500	3.57	3.21	-9.6
	550	3.40	3.06	-9.8
	600	2.00	1.76	-10.4
	650	1.14	1.02	-11.3
	700	0.62	0.56	-14.5

- (d) Crushing of 3 quartz chips, using low volume, stainless steel screw action crusher, sealed with copper gasket. Bakeout tape at ~100°C applied. Released gases not exposed to Pt catalyst.

Sample weight: 282.76mg Yield: 0.69 µgC (2.44ppmC) δ¹³C: -9.6‰

Table B2.2 Sample: HEM-80-39

- (a) Stepped 'combustion' followed by 'pyrolysis'. Released gases exposed to a Pt foil catalyst at ~1050°C during all extraction steps.

Weight (mg)	Release	T (°C)	Yield (µg C)	Yield (ppm C)	δ ¹³ C (‰)
993.3	Combustion	200	0.08	0.08	nm
	Combustion	390	0.72	0.73	-20.5
	Pyrolysis	612	9.87	9.94	-8.59

- (b) Stepped 'combustion' followed by 'pyrolysis'. Released gases exposed to a Pt foil catalyst at room temperature during all extraction steps.

Weight (mg)	Release	T (°C)	Yield (µg C)	Yield (ppm C)	δ ¹³ C (‰)
100.4	Combustion	205	0.03	0.27	nm
	Combustion	362	0.08	0.75	nm
	Pyrolysis	600	1.36	13.59	-6.6

- (c) Single-step 'pyrolysis', in the absence of supplied oxygen.

Weight (mg)	Pt catalyst	T (°C)	Yield (µg C)	Yield (ppm C)	δ ¹³ C (‰)
1123.64	~25°C	600	11.95	10.64	-6.96
106.24	~25°C	620	1.27	11.91	-7.0
130.80	~1050°C	610	1.37	10.51	-7.7

- (d) Stepped heating, in the absence of supplied oxygen and with the Pt catalyst at room temperature.

Weight (mg)	T (°C)	Yield (µg C)	Yield (ppm C)	δ ¹³ C (‰)
978.37	300	0.01	0.01	nm
	420	1.49	1.52	-8.3
	500	4.19	4.29	-6.72
	600	4.89	5.00	-7.34
	700	1.01	1.03	-8.3

Table B2.3 Sample: HEM-80-44

- (a) Stepped 'combustion' followed by 'pyrolysis'. Released gases exposed to Pt foil at ~1050°C during all extraction steps.

Weight (mg)	Release	T (°C)	Yield (µg C)	Yield (ppm C)	δ ¹³ C (‰)
1005.2	Combustion	204	0.15	0.14	nm
	Combustion	352	1.19	1.19	-29.1
	Pyrolysis	602	6.63	6.60	-10.92
91.2	Combustion	220	0.18	1.99	nm
	Combustion	364	0.20	2.15	nm
	Pyrolysis	602	0.91	10.00	-17.3

- (b) Single-step 'pyrolysis', in the absence of supplied oxygen; Pt catalyst at room temperature.

Weight (mg)	T (°C)	Yield (µg C)	Yield (ppm C)	δ ¹³ C (‰)
107.81	625	0.85	7.85	-9.6

- (c) Stepped heating, in the absence of supplied oxygen and with the Pt catalyst at room temperature.

Weight (mg)	T (°C)	Yield (µg C)	Yield (ppm C)	δ ¹³ C (‰)
894.36	300	0.17	0.19	nm
	400	0.61	0.68	-11.6
	500	2.76	3.08	-8.3
	600	3.43	3.84	nm*

Note: * Sample contaminated (wet?)

- (d) Crushing of several quartz chips, using low volume, stainless steel screw action crusher, sealed with copper gasket. Bakeout tape at ~77°C applied. Released gases not exposed to Pt catalyst.

Sample weight: 256.69mg Yield: 0.35 µgC (1.38ppmC) δ¹³C: -8.7‰

Because of the very low yield, the accuracy of the isotopic measurement was probably ~0.5%.

Table B2.4 Sample: HEM-80-47

- (a) Stepped heating, in the absence of supplied oxygen and with the Pt catalyst at room temperature (sample outgassed at 300°C).

Weight (mg)	T (°C)	Yield (µg C)	Yield (ppm C)	δ ¹³ C (‰)
862.52	300-400	1.61	1.87	-10.5
	500	4.11	4.77	-8.32
	600	4.41	5.11	nm*

Note: * CO₂ from this step was contaminated by hydrogen sulphide.

- (b) Crushing of several quartz chips, using low volume, stainless steel screw action crusher, sealed with copper gasket. Bakeout tape at ~70°C applied. Released gases not exposed to Pt catalyst.

Sample weight: 444.22mg Yield: 0.79 µgC (1.78ppmC) δ¹³C: -8.3‰

Table B2.5 Sample: SW-84-18

- (a) Stepped 'combustion' followed by 'pyrolysis'. Released gases exposed to Pt foil at ~1050°C during all extraction steps.

Weight (mg)	Release	T (°C)	Yield (µg C)	Yield (ppm C)	δ ¹³ C (‰)
1004.0	Combustion	390	2.33	2.31	-11.5
	Pyrolysis	620	3.36	3.35	-9.1

- (b) Single-step 'pyrolysis', in the absence of supplied oxygen.

Weight (mg)	Pt catalyst	T (°C)	Yield (µg C)	Yield (ppm C)	δ ¹³ C (‰)
1016.14	~25°C	300-600	6.27	6.17	-7.48
603.26	~25°C	630	3.77	6.24	-8.7
100.17	~25°C	635	0.69	6.86	-11.0
101.0	~1050°C	613	0.81	7.98	-17.4

Table B2.6 Sample: SW-84-27

- (a) Stepped 'combustion' followed by 'pyrolysis'. Released gases exposed to Pt foil at ~1050°C during all extraction steps.

Weight (mg)	Release	T (°C)	Yield (µg C)	Yield (ppm C)	δ ¹³ C (‰)
1121.0	Combustion	350	1.00	0.90	-11.3
	Pyrolysis	610	4.87	4.34	-6.01

(b) Single-step 'pyrolysis', in the absence of supplied oxygen; Pt catalyst at room temperature.

Weight (mg)	T (°C)	Yield (µg C)	Yield (ppm C)	δ ¹³ C (‰)
1049.0	600	5.71	5.44	-6.66
252.3	625	1.46	5.80	-6.4

(c) Stepped heating, in the absence of supplied oxygen and with the Pt catalyst at room temperature.

Weight (mg)	T (°C)	Yield (µg C)	Yield (ppm C)	δ ¹³ C (‰)
1096.8	300	0.05	0.04	nm
	400	1.77	1.61	-8.1
	500	2.21	2.02	-7.0
	600	1.62	1.47	-7.0
	700	0.37	0.34	nm

Table B2.7 Sample: CF-77-98

(a) Stepped 'combustion' to ~350°C followed by stepped 'pyrolysis' to higher temperatures. Released gases exposed to Pt foil at ~1050°C during all extraction steps.

Weight (mg)	Release	T (°C)	Yield (µg C)	Yield (ppm C)	δ ¹³ C (‰)
1010.1	Combustion	220	0.64	0.64	-19.6
	Combustion	362	13.60	13.46	-13.92
	Pyrolysis	625	16.06	15.91	-11.63
	Pyrolysis	850	1.69	1.68	-11.9
	Pyrolysis	1200	1.46	1.45	-15.5
51.12	Combustion	220	1.81	35.31	-27.1
	Combustion	370	1.26	24.70	-16.4
	Pyrolysis	600	0.57	11.17	-12.0

(b) Single-step heating, in the absence of supplied oxygen.

Weight (mg)	Pt catalyst	T (°C)	Yield (µg C)	Yield (ppm C)	δ ¹³ C (‰)
480	~25°C	600	16.77	34.93	-11.03
45.24	~25°C	600	1.54	33.96	-11.2
28.99	~25°C	600	0.92	31.72	-11.4
21.6	~25°C	600	0.95	44.13	-11.5
22.65	~1050°C	600	0.98	35.44	-15.4

(c) Stepped heating, in the absence of supplied oxygen.

Weight (mg)	Pt catalyst	T (°C)	Yield (µg C)	Yield (ppm C)	δ ¹³ C (‰)
1060.6	~25°C	220	0.90	0.85	-12.2
		356	14.52	13.69	-11.71
		850	17.90	16.88	-10.71
		1200	1.11	1.05	-11.7
159.04	~25°C	220	0.17	1.03	nm
		350	2.73	17.18	-12.2
		600	2.43	15.27	-11.1
137.88	~1050°C	225	0.31	2.25	
		350	2.73	17.07	-13.6
		620	2.44	17.69	-14.4

(d) Crushing of quartz chips, using low-volume, stainless steel screw action crusher, sealed with copper gasket. Bakeout tape at ~77°C applied. Released gases not exposed to Pt catalyst.

Sample weight: 271.01 mg Yield: 2.89 µgC (10.67 ppmC) δ¹³C: -11.4‰

B.3

Results of carbon stable isotope replicate analyses of IAEA natural gas standard NGS-1 (A8), using the preparation procedures described in Section 3.4.5.6.2. This material was collected (and supplied to the author) by G Hut, University of Groningen, The Netherlands. The gas is coal related and consists of 81.4% CH₄ (δ¹³C value of -28.95±0.21‰, 1σ error), with the remainder being primarily nitrogen (14.2%), together with CO₂ (1.1%), C₂H₆ (2.8%, δ¹³C value of -26.03±0.35‰) and C₃H₈ (0.4%, δ¹³C value of -20.79‰). Higher alkanes are present at trace levels.

Aliquot (µgC)	δ ¹³ C _(PDB) ‰
146	-29.29
146	-29.15
151	-28.94
80	-29.45

Appendix C

Details of the gas purification protocol (after S R Boyd, unpublished) adopted during the investigation of $^{15}\text{N}/^{14}\text{N}$ stable isotope ratios in nanomole quantities of fluid inclusion nitrogen. Analyses were undertaken using the mass spectrometer and associated preparation line described by Wright *et al.* (1988) and Boyd (1988). Refer to Figure 4.5 of the present work for details of the preparation line.

Timer setting [†]
(min. sec.)

First step only

63.00	Commence first extraction step.
53.30	Reference gas aliquot into final purification stage (VTC#3)*.
52.00	Reference gas aliquot admitted into mass spectrometer.
40.30	Reference gas aliquot (#2) into final purification stage (VTC#3).
39.00	Reference gas aliquot admitted into mass spectrometer.
28.30	Molecular sieve (MS) cooled to -196°C.
27.30	Reference gas aliquot into final purification stage (VTC#3).
26.30	Reference gas aliquot admitted into mass spectrometer.
26.00	Sample gas transferred from extraction section to MS at -196°C.
24.00	Sample gas completely transferred to MS; purification section isolated. MS temperature raised to -200°C; temperature of CuO in purification section (CuO#2) raised to 850°C. Next heating step commenced.
18.00	CuO#2 temperature reduced from 850 to 600°C. Liquid nitrogen trap placed around VTC#2; temperature of VTC#2 maintained at -185°C.
14.30	Reference gas aliquot into final purification stage (VTC#3).
13.00	Reference gas aliquot admitted into mass spectrometer.
11.30	CuO#2 temperature reduced from 600 to 450°C.
1.30	Sample gas aliquot into final purification stage (VTC#3)
0.00	Sample gas aliquot admitted into mass spectrometer.
-6.00	Timer set to 33.00 minutes on commencement of pump-out of sample gas from mass spectrometer. (This allows provision for the analysis of two aliquots of reference gas between each sample gas aliquot).

Notes:

[†] Time before admitting sample gas to mass spectrometer inlet.

* Variable temperature cold trap VTC#3 maintained at -185°C throughout.

References

- Abrajano T. A., Sturchio N. C., Böhlke J. K., Lyon G. L., Poreda R. J. and Stevens C. M. (1988) Methane-hydrogen gas seeps, Zambales Ophiolite, Philippines: deep or shallow origin? In: M. Schoell (Guest-Editor), *Origins of methane in the Earth*. Chem. Geol. **71**, 211-222.
- Abrajano T. A., Sturchio N. C., Kennedy B. M., Lyon G. L., Muehlenbachs K. and Böhlke J. K. (1990) Geochemistry of reduced gas related to serpentinization of the Zambales ophiolite, Philippines. Appl. Geochem. **5**, 625-630.
- Alderton D. H. M. (1978) Fluid inclusion data for lead-zinc ores from southwest England. Trans. Instit. Mining and Metallurgy **87**, B132-135.
- Alderton D. H. M. and Harmon R. S. (1991) Fluid inclusion and stable isotope evidence for the origin of mineralizing fluids in south-west England. Min. Mag. **55**, 605-611.
- Aldrich T. and Nier A. O. (1948) Argon 40 in potassium minerals. Phys. Rev. **74**, 876-877.
- Althaus E. and Herold G. (1987) Hydrothermal reactions between rock forming minerals, Falkenberg granite and heat exchange fluids in hot dry rock systems. Geol. Jahrb. **E39**, 177-192.
- Amari S., Anders E., Virag A. and Zinner E. (1990) Interstellar graphite in meteorites. Nature **345**, 238-240.
- Andrawes F. F. and Gibson E. K., Jr. (1979) Release and analysis of gases from geological samples. Amer. Mineral. **64**, 453-463.
- Arnorsson S. and Gunnlaugsson E. (1985) New gas geothermal exploration - calibration and application. Geochim. Cosmochim. Acta **49**, 1307-1325.
- Arthur M. A., Dean W. E. and Claypool G. E. (1985) Anomalous ^{13}C enrichment in modern marine organic carbon. Nature **315**, 216-218.
- Ash R. D. (1990) Interstellar dust from primitive meteorites: a carbon and nitrogen isotope study. Unpublished PhD thesis, The Open University, UK. 220 pp.
- Ash R. D., Arden J. W. and Pillinger C. T. (1989) Light nitrogen associated with silicon carbide in Cold Bokkeveld. Meteoritics **24**, 248-249.
- Ash R. D., Arden J. W., Grady M. M., Wright I. P. and Pillinger C. T. (1990) Recondite interstellar carbon components in the Allende meteorite revealed by preparative precombustion. Geochim. Cosmochim. Acta **54**, 455-468.
- Ash R. D., Arden J. W., Wright I. P., Grady M. M. and Pillinger C. T. (1988) An interstellar dust component rich in ^{12}C . Nature **336**, 228-230.
- Baertschi P. (1976) Absolute ^{18}O content of standard mean ocean water. Earth Planet. Sci. Lett. **31**, 341-344.

- Bakker R. J. and Jansen J. B. H. (1990) Preferential water leakage from fluid inclusions by means of mobile dislocations. *Nature* **345**, 58-60.
- Banks D. A. and Yardley B. W. D. (1992) Crush-leach analysis of fluid inclusions in small natural and synthetic samples. *Geochim. Cosmochim. Acta* **56**, 245-248.
- Bannon M. P. (1989) Argon isotope studies of fluid inclusions in quartz and fluorite from areas of mineralization. Unpublished PhD thesis, University of Sheffield, UK. 110 pp. (& appendices)
- Barker C. and Torkelson B. E. (1975) Gas adsorption on crushed quartz and basalt. *Geochim. Cosmochim. Acta* **39**, 212-218.
- Bath A. H., Brassell S. C., Eglinton G., Hill R. I., Hooker P. J., O'Nions R. K., Oxburgh E. R., Parnell J., Robinson N. and Spiro B. (1986) Deep source gases and hydrocarbons in the UK. crust. Rep. Fluid Processes Res. Group, Br. Geol. Surv., FLP 86-2. (ISBN 0 85272 126 9)
- Bebout G. E. and Fogel M. L. (1992) Nitrogen-isotope compositions of metasedimentary rocks in the Catalina Schist, California: Implications for metamorphic devolatilization history. *Geochim. Cosmochim. Acta* **56**, 2839-2849.
- Becker R. H. (1982) Nitrogen isotopic ratios of individual diamond samples. Abstracts, Fifth International Conference on Geochronology, Cosmochronology and Isotope Geology, 1982.
- Becker R. H. and Clayton R. N. (1975) Nitrogen abundances and isotopic compositions in lunar samples. *Proc. Lunar Planet. Sci. Conf. VI*, Pergamon, New York. pp. 2131-2149.
- Becker R. H. and Clayton R. N. (1977) Nitrogen isotopes in igneous rocks. *Eos, Trans. Amer. Geophys. Union* **58**, 536.
- Becker R. H. and Epstein S. (1981) Carbon isotope ratios in some low- $\delta^{15}\text{N}$ lunar breccias. *Proc. Lunar Planet. Sci. Conf. XII*, 289-293.
- Beer K. E. and Ball T. K. (1987) Tungsten mineralisation and magmatism in SW England. *Chron. rech. min.* **487**, 53-62.
- Beer K. E. and Scrivener R. C. (1982) Metalliferous mineralisation. In: E. M. Durrance and D. J. Laming (Editors), *The Geology of Devon*. University of Exeter Press. Chapter 6 (pp. 117-145).
- Bergman S. C. and Dubessy J. (1984) CO_2 -CO fluid inclusions in a composite peridotite xenolith: implications for upper mantle oxygen fugacity. *Contrib. Mineral. Petrol.* **85**, 1-13.
- Bigeleisen J., Perlman M. L. and Prosser H. C. (1952) Conversion of hydrogenic materials to hydrogen for isotopic analysis. *Anal. Chem.* **24**, 1356-1357.
- Bishop P. M. E. (1990) Isotope systematics and microstructures of slates from south-west England and north Wales. Unpublished PhD thesis, University of Leeds, UK. 235 pp.
- Blank J. G., Stolper E. M. and Carroll M. R. (1993) Solubilities of carbon dioxide and water in rhyolitic melt at 850°C and 750 bars. *Earth Planet. Sci. Lett.* **119**, 27-36.

- Bodnar R. J., Binns P. R. and Hall D. L. (1989) Synthetic fluid inclusions - VI. Quantitative evaluation of the decrepitation behaviour of fluid inclusions in quartz at one atmosphere confining pressure. *J. Metamorphic Geol.* **7**, 229-242.
- Böhlke J. K. and Irwin J. J. (1992) Laser microprobe analyses of Cl, Br, I and K in fluid inclusions: implications for sources of salinity in some ancient hydrothermal fluids. *Geochim. Cosmochim. Acta* **56**, 203-255.
- Bos A., Duit W., van der Eerden Ad M. J. and Jansen J. B. H. (1988) Nitrogen storage in biotite: an experimental study of the ammonium and potassium partitioning between 1M-phlogopite and vapour at 2kb. *Geochim. Cosmochim. Acta* **52**, 1275-1283.
- Bott M. H. P., Day A. A. and Masson-Smith D. (1958) The geological interpretation of gravity and magnetic surveys in Devon and Cornwall. *Phil. Trans. R. Soc.* **251A**, 161-191.
- Bottinga Y. (1969) Calculated fractionation factors for carbon and hydrogen isotope exchange in the system calcite-CO₂-graphite-methane-hydrogen and water vapor. *Geochim. Cosmochim. Acta* **33**, 49-64.
- Bottrell S. H. (1986) The origin of the gold mineralization of the Dolgellau district, North Wales: the chemistry and role of the fluids. Unpublished PhD thesis, University of East Anglia, UK. 452 pp.
- Bottrell S. H., Carr L. P. and Dubessy J. (1988) A nitrogen-rich metamorphic fluid and coexisting minerals in slates from North Wales. *Min. Mag.* **52**, 451-457.
- Bottrell S. H. and Miller M. F. (1989) Analysis of reduced sulfur species in inclusion fluids. *Econ. Geol.* **84**, 940-945.
- Bottrell S. H. and Miller M. F. (1990) The geochemical behaviour of nitrogen compounds during the formation of black shale hosted quartz-vein gold deposits, north Wales. *Appl. Geochem.* **5**, 289-296.
- Bottrell S. H. and Yardley B. W. D. (1988) The composition of a primary granite-derived ore fluid from S W England, determined by fluid inclusion analysis. *Geochim. Cosmochim. Acta* **52**, 585-588.
- Bottrell S. H., Yardley B. W. D. and Buckley F. (1988) A modified crush-leach method for the analysis of fluid inclusion electrolytes. *Bull. Minéral.* **111**, 279-290.
- Boyd S. R. (1988) A study of carbon and nitrogen isotopes from the Earth's mantle. Unpublished PhD thesis, The Open University, UK. 213 pp.
- Boyd S. R., Hall, A. and Pillinger C. T. (1993) The measurement of $\delta^{15}\text{N}$ in crustal rocks by static vacuum mass spectrometry: application to the origin of the ammonium in the Cornubian batholith, southwest England. *Geochim. Cosmochim. Acta* **57**, 1339-1347.
- Boyd S. R., Matthey D. P., Pillinger C. T., Milledge H. J., Mendelsohn M. and Seal M. (1987) Multiple growth events during diamond genesis: an integrated study of carbon and nitrogen isotopes and nitrogen aggregation state in coated stones. *Earth Planet. Sci. Lett.* **86**, 341-353.
- Boyd S. R. and Pillinger C. T. (1990) Determination of the abundance and isotopic composition of nitrogen within organic compounds: a sealed tube technique for use with static vacuum mass spectrometers. *Meas. Sci. Technol.* **1**, 1176-1183.

- Boyd S. R. and Pillinger C. T. (1991) Rubidium sulphate - ammonium sulphate solid solution: a standard for use during the determination of nitrogen abundance and isotopic composition at the ppm level by static-vacuum mass spectrometry. *Anal. Chem.* **63**, 1332-1335.
- Boyd S. R., Wright I. P., Franchi I. A. and Pillinger C. T. (1988) Preparation of sub-nanomole quantities of nitrogen gas for stable isotopic analysis. *J. Phys. E: Sci. Instrum.* **21**, 876-885.
- Bradley A. D., Vickers B. P., Peachey D. and Levinson A. A. (1990) The geochemical significance of two different chemical attacks used in ammonium litho geochemistry. *Appl. Geochem.* **5**, 471-473.
- Brammell A. and Harwood H. F. (1932) The Dartmoor granites: genetic relationships. *Quart. J. Geol. Soc.* **88**, 171-237.
- Briden J. C., Drewry G. E. and Smith A. G. (1974) Phanerozoic equal-area world maps. *J. Geol.* **82**, 555-574.
- Brigham R. H. and O'Neil J. R. (1985) Genesis and evolution of water in a two-mica pluton: a hydrogen isotope study. *Chem. Geol.* **49**, 159-177.
- Brooks M., Doody J. J. and Al-Rawi F. R. J. (1984) Major crustal reflectors beneath S W England. *J. Geol. Soc. London* **141**, 97-103.
- Broucker W. S. and Oversby V. M. (1971) *Chemical equilibrium in the Earth*. McGraw-Hill, 318 pp.
- Brown P. W. and Pillinger C. T. (1981) Nitrogen concentrations and isotopic ratios from separated lunar soils. *Meteoritics* **16**, 298.
- Bull B. W. (1982) *Geology and mineralisation of an area around Tavistock, south west England*. Unpublished PhD thesis, University of Exeter, UK. 338 pp.
- Burke E. A. J. and Lustenhouwer W. J. (1987) The application of a multichannel laser Raman microprobe (Microdil-28) to the analysis of fluid inclusions. *Chem. Geol.* **61**, 11-17.
- Burke W. H., Denison R. E., Hetherington E. A., Koepnick R. B., Nelson H. F. and Otto J. B. (1982) Variation of seawater $^{87}\text{Sr}/^{86}\text{Sr}$ throughout Phanerozoic time. *Geology* **10**, 516-519.
- Burnham C. W. (1979) Magmas and hydrothermal fluids. In: H. L. Barnes (Editor), *Geochemistry of hydrothermal ore deposits*, pp. 71-136. John Wiley & Sons.
- Burnham C. W. and Ohmoto H. (1980) Late-stage processes of felsic magmatism. *Min. Soc. Japan Special Issue* **8**, 1-11.
- Bussink R. W. (1981) Fluid inclusion studies of the W-Sn ore deposits of Panasqueira, Portugal. Abstracts, sixth European Conference on Research in Fluid Inclusions, Utrecht.
- Bussink R. W. (1984) Geochemistry of the Panasqueira tungsten-tin deposit, Portugal. *Geologica Ultraiectina* **33**, 1-170.
- Bussink R. W., Kreulen R. and de Jong A. F. M. (1984) Gas analyses, fluid inclusions and stable isotopes of the Panasqueira W-Sn deposits, Portugal. *Bull. Minéral.* **107**, 703-713.

- Campbell A. R. and Panter K. S. (1990) Comparison of fluid inclusions in coexisting (cogenetic?) wolframite, cassiterite, and quartz from St. Michael's Mount and Cligga Head, Cornwall, England. *Geochim. Cosmochim. Acta* **54**, 673-681.
- Carr R. H. (1985) High sensitivity stable carbon isotope ratio mass spectrometry: instrument development and applications. Unpublished PhD thesis, University of Cambridge, UK. 252 pp.
- Carr R. H., Wright I. P., Joines A. T. and Pillinger C. T. (1986) Measurement of carbon stable isotopes at the nanomole level: a static mass spectrometer and sample preparation technique. *J. Phys. E: Sci. Instrum.* **19**, 798-808.
- Carr R. H., Wright I. P., Pillinger C. T., Lewis R. S. and Anders E. (1983) Interstellar carbon in meteorites: isotopic analysis using static mass spectrometry. *Meteoritics* **18**, 277.
- Channer D. M. DeR. and Spooner E. T. C. (1992) Analysis of fluid inclusion leachates from quartz by ion chromatography. *Geochim. Cosmochim. Acta* **56**, 249-259.
- Chappell B. W. and White A. J. R. (1974) Two contrasting granite types. *Pacific Geol.* **8**, 173-174.
- Charoy B. (1979) Definition et importance des phénomènes deutériques et des fluides associés dans les granites. Conséquences métallogéniques. *Sci. Terre, Nancy, Mem.* **37**, 364 pp.
- Charoy B. (1981) Post-magmatic processes in south-west England and Brittany. *Ussher Proc. Soc.* **5**, 101-115.
- Chen Y., Clark A. H., Farrar E., Wasteneys H. A. H. P., Hodgson M. J. and Bromley A. V. (1993) Diachronous and independent histories of plutonism and mineralization in the Cornubian batholith, southwest England. *J. Geol. Soc. London* **150**, 1183-1191.
- Chesley J. T., Halliday A. N., Snee L. W., Mezger K., Shepherd T. J. and Scrivener R. C. (1993) Thermochronology of the Cornubian batholith: implications for pluton emplacement and protracted hydrothermal mineralization. *Geochim. et Cosmochim. Acta* **57**, 1817-1835.
- Chorlton L. B. and Martin R. F. (1978) The effect of boron on the granite solidus. *Canadian Mineralogist* **16**, 239-244.
- Christie A. B. (1989) Problems of crush-leach analyses of low-salinity inclusion-poor material. *Chem. Geol.* **78**, 35-51.
- Clark A. H., Chen Y., Farrar E., Wasteneys H. A. H. P., Stimac J. A., Hodgson M. J., Willis-Richards J. and Bromley A. V. (1993) The Cornubian Sn-Cu (-As, W) metallogenetic province: product of a 30 m.y. history of discrete and concomitant anatexis, intrusive and hydrothermal events. *Proc. Ussher Soc.* **8**, 112-116.
- Clark I. D. and Lauriol B. (1992) Kinetic enrichment of stable isotopes in cryogenic calcites. *Chem. Geol. (Isotope Geosciences Section)* **102**, 217-228.
- Clayton R. N. and Mayeda T. K. (1963) The use of bromine pentafluoride in the extraction of oxygen from oxides and silicates for isotopic analysis. *Geochim. Cosmochim. Acta* **27**, 43-52.

- Cline J. D. and Kaplan I. R. (1975) Isotopic fractionation of dissolved nitrate during denitrification in the Eastern tropical North Pacific ocean. *Marine Chemistry* **3**, 271-299.
- Coleman M. L. and Cox M. A. (1981) Inter-laboratory calibration of carbon isotope value for NBS-22 lubricating oil. Institute of Geological Sciences, Isotope Geology Unit Stable Isotope Report No. 63, 10 pp.
- Coleman M. L., Shepherd T. J., Durham J. J., Rouse J. E. and Moore G. R. (1982) Reduction of water with zinc for hydrogen isotope analysis. *Anal. Chem.* **54**, 993-995.
- Cooper D. C. and Bradley A. D. (1990) The ammonium contents of granites in the English Lake District. *Geol. Mag.* **127**, 579-586.
- Coplen T. B. (1988) Normalization of oxygen and hydrogen isotope data. *Chem. Geol. (Isotope Geosciences Section)* **72**, 293-297.
- Coplen T. B., Wildman J. D. and Chen J. (1991) Improvements in the gaseous hydrogen-water equilibration technique for hydrogen isotope ratio analysis. *Anal. Chem.* **63**, 910-912.
- Cornwell J. D. (1967) Palæomagnetism of the Exeter lavas, Devonshire. *Geophys. J. R. astr. Soc.* **12**, 181-196.
- Cotton F. A. and Wilkinson G. (1988) *Advanced inorganic chemistry*. John Wiley & Sons, 1455 pp.
- Craig H. (1953) The geochemistry of the stable carbon isotopes. *Geochim. Cosmochim. Acta* **3**, 53-92.
- Craig H. (1957) Isotopic standards for carbon and oxygen and correction factors for mass spectrometric analysis of CO₂. *Geochim. Cosmochim. Acta* **12**, 133-149.
- Craig H. (1961a) Isotopic variations in meteoric waters. *Science* **133**, 1702-1703.
- Craig H. (1961b) Standard for reporting concentrations of deuterium and oxygen-18 in natural waters. *Science* **133**, 1833-1834.
- Criss R. E. (1991) Temperature dependence of isotopic fractionation factors. In: H. P. Taylor, Jr., J. R. O'Neil and I. R. Kaplan (Editors), *Stable Isotope Geochemistry: A tribute to Samuel Epstein*. Special Publication No. 3 of the Geochemical Society, pp. 11-16.
- Criss R. E. and Taylor H. P., Jr. (1986) Meteoric-hydrothermal systems. In: J. W. Valley, H. P. Taylor, Jr., and J. R. O'Neil (Editors), *Stable isotopes in high temperature geological processes*. *Reviews in mineralogy* **16**, Mineralogical Society of America, pp. 425-444.
- Dangerfield J. and Hawkes J. R. (1969) Unroofing of the Dartmoor granite and possible consequences with regard to mineralization. *Proc. Ussher Soc.* **2**, 122-131.
- Dansgaard W. (1964) Stable isotopes in precipitation. *Tellus* **16**, 436-468.
- Darbyshire D. P. F. and Shepherd T. J. (1985) Chronology of granite magmatism and associated mineralization, S W England. *J. Geol. Soc. London* **142**, 1159-1177.

- Darbyshire D. P. F. and Shepherd T. J. (1987) Chronology of magmatism in south-west England: the minor intrusions. *Proc. Ussher Soc.* **6**, 431-438.
- Darbyshire D. P. F. and Shepherd T. J. (1990) Rb-Sr and Sm-Nd constraints on the age of mineralisation and the origin of hydrothermal fluids in S W England. *Geological Society of Australia, Abstracts 27: Seventh International Conference on Geochronology, Cosmochronology and Isotope Geology*, p. 24. Note: ϵ_{Nd} values do not appear in the published abstract, but were presented on the related conference poster.
- Darbyshire D. P. F. and Shepherd T. J. (1994) Nd and Sr isotope constraints on the origin of the Cornubian batholith, Southwest England. *In press*, *J. Geol. Soc. London*.
- Darimont A., Burke E. and Touret J. (1988) Nitrogen-rich metamorphic fluids in Devonian metasediments, Bastogne, Belgium. *Bull. Minéral.* **111**, 179-182.
- Dasch E. J. (1969) Strontium isotopes in weathering profiles, deep-sea sediments, and sedimentary rocks. *Geochim. Cosmochim. Acta* **33**, 1521-1552.
- Davy H. (1817) Some new experiments and observations on the combustion of gaseous mixtures, with an account of a method of preserving a continued light in mixtures of inflammable gases and air without flame. *Philos. Trans. R. Soc. London* **107**, 77-85.
- Davy H. (1822) On the state of water and aeriform matter in cavities found in certain crystals. *Royal Soc. London Philos. Trans.* **2**, 367-376.
- Deines P. (1970) Mass spectrometer correction factors for the determination of small isotopic variations of carbon and oxygen. *Int. J. Mass Spectr. Ion Phys.* **4**, 283-295.
- Deines P. (1979) A note on hydrogen isotope fractionation involving acidic and basic solutions. *Geochim. Cosmochim. Acta* **43**, 1575-1577.
- Deines P. (1980) The isotopic composition of reduced carbon. In: P. Fritz and J. Ch. Fontes (Editors), *Handbook of environmental isotope geochemistry, 1. The terrestrial environment A*. Elsevier, pp. 329-405.
- Deines P., Harris J. W. and Gurney J. J. (1987) Carbon isotopic composition, nitrogen content and inclusion composition of diamonds from the Roberts Victor kimberlite, South Africa: evidence for ^{13}C depletion in the mantle. *Geochim. Cosmochim. Acta* **51**, 1227-1243.
- De Wit M. J., Hart R., Martin A. and Abbot P. (1982) Archaen abiogenic and probable biogenic structures associated with mineralized hydrothermal vent systems and regional metasomatism, with implications for greenstone belt studies. *Econ. Geol.* **77**, 1783-1801.
- Delwiche C. C. (1970) The nitrogen cycle. *Sci. Amer.* **223**, 136-147.
- Delwiche C. C. and Steyn P. L. (1970) Nitrogen fractionation in soils and microbial reactions. *Environ. Sci. Technol.* **4**, 929-935.
- Des Marais D. J. (1978) Carbon, nitrogen and sulphur in Apollo 15, 16 and 17 rocks. *Proc. Lunar Planet. Sci. Conf.* **IX**, 2451-2467.

- Des Marais D. J. (1983) Light element geochemistry and spallogensis in lunar rocks. *Geochim. Cosmochim. Acta* **47**, 1769-1781.
- Des Marais D. J. (1986) Carbon abundance measurements in oceanic basalts: the need for consensus. *Earth Planet. Sci. Lett.* **79**, 21-26.
- Des Marais D. J., Donchin J. H., Nehrig N. L. and Truesdell A. H. (1981) Molecular evidence for the origin of geothermal hydrocarbons. *Nature* **292**, 826-828.
- Des Marais D. J. and Moore J. G. (1984) Carbon and its isotopes in mid-oceanic basaltic glasses. *Earth Planet. Sci. Lett.* **69**, 43-57.
- Des Marais D. J., Stallard M. L., Nehring N. L. and Truesdell A. H. (1988) Carbon isotope geochemistry of hydrocarbons in the Cerro Prieto geothermal field, Baja California Norte, Mexico. In: M. Schoell (Guest-Editor), *Origins of methane in the Earth*. *Chem. Geol.* **71**, 159-167.
- Deuser W. G. (1970) Extreme $^{13}\text{C}/^{12}\text{C}$ variations in Quaternary dolomites from the continental shelf. *Earth Planet. Sci. Lett.* **69**, 43-57.
- Diamond L. W., Jackman J. A. and Charoy B. (1991) Cation ratios of fluid inclusions in a gold-quartz vein at Brusson, Val d' Ayas, northwestern Italian Alps; comparison of bulk crush-leach results with SIMS analyses of individual inclusions. *Chem. Geol.* **90**, 71-78.
- Dines H. G. (1956) The metalliferous mining region of south-west England. *Memoir Geol. Surv. Gt. Brit.* London: HMSO (1988 reprint), 795 pp.
- Douthitt C. B. (1990) Isotope ratio monitoring mass spectrometry: a possible approach to a stable isotope microprobe. Geological Society of Australia, Abstracts **27**: Seventh International Conference on Geochronology, Cosmochronology and Isotope Geology, p. 28.
- Dubessy J. (1984) Simulation des équilibres chimiques dans le système C-O-H. Conséquences méthodologiques pour les inclusions fluides. *Bull. Minéral.* **107**, 155-168.
- Dubessy J. (1985) Contribution à l'étude des interactions entre paléo-fluides et minéraux à partir de l'étude des inclusion fluides par microspectrométrie Raman. Conséquences métallogéniques. Unpublished PhD thesis, Inst. National Polytechnique de Lorraine, Nancy, France. 198 pp.
- Dubessy J., Poty B. and Ramboz C. (1989) Advances in C-O-H-N-S fluid geochemistry based on micro-Raman spectrometric analysis of fluid inclusions. *Eur. J. Mineral.* **1**, 517-534.
- Dubessy J. and Ramboz C. (1986) The history of organic nitrogen from early diagenesis to amphibolite facies: mineralogical, chemical, mechanical and isotopic implications. 5th international symposium on water-rock interaction. Reykjavik, Iceland. Extended abstracts, 171-174.
- Dubessy J., Ramboz C., Nguyen-Trung C., Cathelineau M., Charoy B., Cuney M., Leroy J., Poty B. and Weisbrod A. (1987) Physical and chemical controls (f_{O_2} , T, pH) of the opposite behaviour of U and Sn-W as exemplified by hydrothermal deposits in France and Great Britain, and solubility data. *Bull. Minéral.* **110**, 261-281.

Dugan

- Dugan J. P., Jr., Borthwick J., Harmon R. S., Gagnier M. A., Glahn J. E., Kinsel E. P., MacLeod S. and Viglino J. A. (1985) Guanidine hydrochloride method for determination of water oxygen isotope ratios and the oxygen-18 fractionation between carbon dioxide and water at 25°C. *Anal. Chem.* **57**, 1734-1736.
- Duit W., Jansen B. H., Breemen A. Van and Bos A. (1986) Ammonium micas in metamorphic rocks as exemplified by Dôme de l'Agout (France). *Amer. J. Sci.* **286**, 702-732.
- Durrance E. M., Bromley A. V., Bristow C. M., Heath M. J. and Penman J. M. (1982) Hydrothermal circulation and post-magmatic changes in granites of south-west England. *Proc. Ussher Soc.* **5**, 304-320.
- Edmunds W. M., Andrews J. N., Burgess W. G., Kay R. L. F. and Lee D. J. (1984) The evolution of saline and thermal groundwaters in the Carnmenellis granite. *Min. Mag.* **48**, 407-424.
- Edmunds W. M., Kay R. L. F. and McCartney (1985) Origin of saline groundwaters in the Carnmenellis granite: natural processes and reaction during Hot Dry Rock reservoir circulation. *Chem. Geol.* **49**, 287-301.
- Edmunds W. M., Kay R. L. F., Miles D. L. and Cook J. M. (1987) The origin of saline groundwaters in the Carnmenellis granite, Cornwall (UK.): further evidence from minor and trace elements. In: P. Fritz and S. K. Frape (Editors), *Saline waters and gases in crystalline rocks*. Geological Association of Canada Special Paper 33, pp. 127-143.
- Edmunds W. M. and Savage D. (1991) Geochemical characteristics of groundwater in granites and related crystalline rocks. In: R. A. Downing and W. B. Wilkinson (Editors), *Applied groundwater hydrology: a British perspective*, pp. 266-282. Clarendon Press.
- Eggler D. H. and Kadik A. A. (1993) The system $\text{NaAl}_3\text{O}_8\text{-H}_2\text{O-CO}_2$ to 20kbars pressure: 1. Compositional and thermodynamic relations of liquids and vapors coexisting with albite. *Amer. Mineral.* **64**, 1036-1048.
- Ellis A. J. (1957) Chemical equilibrium in magmatic gases. *Amer. J. Sci.* **255**, 416-431.
- Emery K. O., Orr W. L. and Rittenberg S. C. (1955) Nutrient budgets in the ocean. In: *Essays in natural sciences in honor of Captain Allan Hancock*. University Press, California USA, pp. 299-310.
- Erd R. C., White D. E., Fahey J. J. and Lee D. E. (1964) Buddingtonite, an ammonium feldspar with zeolitic water. *Amer. Mineral.* **49**, 831-850.
- Eugster H. P. (1957) Heterogeneous reactions involving oxidation and reduction at high pressures and temperatures. *J. Chem. Phys.* **26**, 1760-1761.
- Eugster H. P. (1985) Granites and hydrothermal ore deposits: a geochemical framework. *Min. Mag.* **49**, 7-24.
- Eugster H. P. (1981) Metamorphic solutions and reactions. In: D. T. Rickard and F. E. Wickham (Editors), *Chemistry and geochemistry of solutions at high temperatures and pressures*. Physics and Chemistry of the Earth **13 & 14**, 461-503.
- Eugster H. P. and Munoz J. (1966) Ammonium micas: possible sources of atmospheric ammonia and nitrogen. *Science* **151**, 683-686.

- Evans J. A. (1990) Resetting of Rb-Sr whole-rock isotope systems during low-grade metamorphism, north Wales. Unpublished PhD thesis, University of London, UK. 211 pp.
- Evans R. J. and Felbeck G. T., Jr., (1983a) High temperature simulation of petroleum formation - I. The pyrolysis of Green River Shale. *Org. Geochem.* **4**, 135-144.
- Evans R. J. and Felbeck G. T. Jr., (1983b) High temperature simulation of petroleum formation - III. Effect of organic starting material structure on hydrocarbon formation. *Org. Geochem.* **4**, 153-160.
- Exley R. A., Boyd S. R., Matthey D. P. and Pillinger C. T. (1986/87) Nitrogen isotope geochemistry of basaltic glasses: implications for mantle degassing and structure? *Earth Planet. Sci. Lett.* **81**, 163-174.
- Exley R. A., Matthey D. P., Clague D. A. and Pillinger C. T. (1986) Carbon isotope systematics of a mantle "hotspot": a comparison of Loihi Seamount and MORB glasses. *Earth Planet. Sci. Lett.* **78**, 189-199.
- Exley R. A., Matthey D. P. and Pillinger C. T. (1987) Low temperature carbon components in basaltic glasses - reply to comment by H. Craig. *Earth Planet. Sci. Lett.* **82**, 387-390.
- Fallick A. E., Gardiner L. R., Jull A. J. T. and Pillinger C. T. (1980) Instrumental effects in the application of static mass spectrometry to high sensitivity carbon isotope measurements. *Adv. Mass Spectrometry* **8A**, 309-317.
- Fanale F. P. (1971) A case for catastrophic early degassing of the Earth. *Chem. Geol.* **8**, 79-105.
- Farquhar J. and Chacko T. (1991) Isotopic evidence for involvement of CO₂-bearing magmas in granulite formation. *Nature* **354**, 60-63.
- Faure G. (1986) Principles of isotope geology. John Wiley & Sons, 589 pp.
- Fein J. B., Hemley J. J., D'Angelo W. M., Komninou A. and Sverjensky D. A. (1992) Experimental study of iron-chloride complexing in hydrothermal fluids. *Geochim. Cosmochim. Acta* **56** 3179-3190.
- Fein J. B. and Walther J. V. (1987) Calcite solubility in supercritical CO₂-H₂O fluids. *Geochim. Cosmochim. Acta* **51**, 1665-1673.
- Fine G. and Stolper E. (1986) Dissolved carbon dioxide in basaltic glasses: concentrations and speciation. *Earth Planet. Sci. Lett.* **76**, 263-278.
- Fisher C. R., Kennicutt M. C (II) and Brooks J. M. (1990) Stable carbon isotopic evidence for carbon limitation in hydrothermal vent vestimentiferans. *Science* **247**, 1094-1096.
- Fournier R. O. and Truesdell A. H. (1973) An empirical Na-K-Ca geothermometer for natural waters. *Geochim. Cosmochim. Acta* **37**, 1255-1275.
- Franchi I. A., Boyd S. R., Wright I. P., and Pillinger C. T. (1989) Applications of lasers in small-sample stable isotopic analysis. In: W. C. Shanks III and R. E. Criss (Editors), *New frontiers in stable isotope research: Laser probes, ion probes, and small-sample analysis*. US Geol. Survey Bull. 1890, 51-59.

- French B. M. (1966) Some geological implications of equilibrium between graphite and a C-H-O gas phase at high temperatures and pressures. *Rev. Geophys.* **4**, 223-253.
- Freund F. (1986) Solute carbon and carbon segregation in magnesium oxide single crystals - a secondary ion mass spectrometry study. *Phys. Chem. Miner.* **13**, 262-276.
- Freund F., Kathrein H., Wengeler H. and Knobel R. (1980) Carbon in solid solution in forsterite - a key to the untractable nature of reduced carbon in terrestrial and cosmogenic rocks. *Geochim. Cosmochim. Acta* **44**, 1319-1333.
- Frick U. and Pepin R. O. (1981 a) On the distribution of noble gases in Allende: a differential oxidation study. *Earth Planet. Sci. Lett.* **56**, 45-63.
- Frick U. and Pepin R. O. (1981 b) Microanalysis of nitrogen isotope abundances: association of nitrogen with noble gas carriers in Allende. *Earth Planet. Sci. Lett.* **56**, 64-81.
- Friedman I. (1953) Deuterium content of natural waters and other substances. *Geochim. Cosmochim. Acta* **4**, 89-103.
- Friedman I. and O'Neil J. R. (1977) Compilation of stable isotope fractionation factors of geochemical interest. In: M. Fleischer (Editor), *Data of Geochemistry*, Chapter KK; US Geol. Survey Prof. Paper 440-KK.
- Fritz B., Clauer N., Kam M. (1987) Strontium isotope data and geochemical calculations as indicators for the origin of saline waters in crystalline rocks. In: P. Fritz and S. K. Frape (Editors), *Saline waters in crystalline rocks*. Geol. Assoc. Canada Special Paper **33**, 121-126.
- Frost A. A. and Pearson R. G. (1961) *Kinetics and mechanism*. John Wiley & Sons, 403 pp.
- Fuex A. N. and Baker D. R. (1973) Stable carbon isotopes in selected granitic, mafic and ultramafic rocks. *Geochim. Cosmochim. Acta* **37**, 2509-2521.
- Galimov E. M. (1988) Sources and mechanisms of gaseous hydrocarbons in sedimentary rocks. In: M. Schoell (Guest-Editor), *Origins of methane in the Earth*. *Chem. Geol.* **71**, 77-95.
- Galimov E. M. (1991) Isotope fractionation related to kimberlite magmatism and diamond formation. *Geochim. Cosmochim. Acta* **55**, 1697-1708.
- Gardiner L. R., Jull A. J. T. and Pillinger C. T. (1978) Progress towards a direct measurement of $^{13}\text{C}/^{12}\text{C}$ ratios for hydrolysable carbon in lunar soil by static mass spectrometry. *Proc. Lunar Planet. Sci. Conf. IX*, 2167-2193.
- Gardiner L. R. and Pillinger C. T. (1979) Static mass spectrometry for the determination of active gases. *Anal. Chem.* **51**, 1230-1236.
- Garlick G. D. (1969) The stable isotopes of oxygen. In: K. H. Wedepohl (Editor), *Handbook of Geochemistry*, 8B. Springer-Verlag.
- Geiss J. and Bochsler P. (1982) Nitrogen isotopes in the solar system. *Geochim. Cosmochim. Acta* **46**, 529-548.

- Gibson E. K., Jr., Carr L. P. and Pillinger C. T. (1985) Nitrogen isotopic composition of Archaean samples: evidence of the Earth's early atmosphere? *Proc. Lunar Planet. Sci. Conf. XVI*, 270-271.
- Giggenbach W. F. (1980) Geothermal gas equilibria. *Geochim. Cosmochim. Acta* **44**, 2021-2032.
- Giggenbach W. F. (1981) Geothermal mineral equilibria. *Geochim. Cosmochim. Acta* **45**, 393-410.
- Giggenbach W. F. (1982) Carbon-13 exchange between CO₂ and CH₄ under geothermal conditions. *Geochim. Cosmochim. Acta* **46**, 159-165.
- Giggenbach (1984) Mass transfer in hydrothermal systems - a conceptual approach. *Geochim. Cosmochim. Acta* **48**, 2693-2711.
- Giggenbach W. F. (1987) Redox processes governing the chemistry of fumarolic discharges from White Island, New Zealand. *Appl. Geochem.* **2**, 143-161.
- Giggenbach W. F. (1988) Geothermal solute equilibria. Derivation of Na-K-Mg-Ca geoindicators. *Geochim. Cosmochim. Acta* **52**, 2749-2765.
- Gilmour I. (1986) The distribution of carbon stable isotopes within sedimentary organic matter. Unpublished PhD thesis, University of Cambridge, UK. 240 pp.
- Gilmour I. and Pillinger C. T. (1985) Stable carbon isotopic analysis of sedimentary organic matter by stepped combustion of sedimentary samples. *Organic Geochem.* **8**, 421-426.
- Gold T. (1979) Terrestrial sources of carbon and earthquake out-gassing. *J. Petrol. Geol.* **1**, 3-19.
- Gold T. and Soter S. (1982) Abiogenic methane and the origin of petroleum. *Energy Explor. Exploit.* **1**, 89-104.
- Gonfiantini R. (1981) The δ -notation and the mass-spectrometric measurement techniques. In: J. R. Gat and R. Gonfiantini (Editors), *Stable isotope hydrology, deuterium and oxygen-18 in the water cycle*. International Atomic Energy Agency, Vienna, Technical Report Series No. 210, Chapter 4 (pp. 35-84).
- Gonfiantini R. (1978) Standards for stable isotope measurements in natural compounds. *Nature* **271**, 534-536.
- Gordon S. and McBride B. J. (1971) Computer program for calculation of complex chemical equilibrium compositions, rocket performance, incident and reflected shocks, and Chapman-Jouguet detonations. NASA Special Publication SP-273, National Aeronautical and Space Administration, Washington DC, USA.
- Grady M. M. (1982) The content and isotopic composition of carbon in stony meteorites. Unpublished PhD thesis, University of Cambridge, UK. 216 pp.
- Grady M. M. and Pillinger C. T. (1990) ALH 85085: nitrogen isotope analysis of a highly unusual primitive chondrite. *Earth Planet. Sci. Lett.* **97**, 29-40.
- Grady M. M., Wright I. P., Swart P. K. and Pillinger C. T. (1985) The carbon and nitrogen isotopic composition of ureilites: implications for their genesis. *Geochim. Cosmochim. Acta* **49**, 903-916.

- Graff J. and Rittenberg D. (1952) Microdetermination of deuterium in organic compounds. *Anal. Chem.* **24**, 878-881.
- Graham C. M. and Sheppard S. M. F. (1980) Experimental hydrogen isotope studies, II. Fractionations in the systems epidote-NaCl-H₂O, epidote-seawater, and the hydrogen isotopic composition of natural epidotes. *Earth Planet. Sci. Lett.* **49**, 237-251.
- Green D. H., Eggins S. M. and Yaxley G. (1993) The other carbon cycle. *Nature* **365**, 210-211.
- Guilhaumou N, Dhamelincourt P., Touray J. C. and Touret J. (1981) Etude des inclusion fluides du système N₂-CO₂ de dolomites et de quartz de Tunisie septentrionale. Données de la microcryoscopie et de l'analyse à effet Raman. *Geochim. Cosmochim. Acta* **45**, 657-673.
- Haendel D., Mühle K., Nitzsche H.-M., Stiehl G. and Wand U. (1986) Isotopic variations of the fixed nitrogen in metamorphic rocks. *Geochim. Cosmochim. Acta* **50**, 749-758.
- Hagemann R., Nief G. and Roth E. (1970) Absolute isotopic scale for deuterium analysis of natural waters. Absolute D/H ratio for SMOW. *Tellus* **22**, 712-715.
- Hall A. (1971) Greisenisation in the granite of Cligga Head, Cornwall. *Proc. Geol. Ass.* **82**, 209-230.
- Hall A. (1987) The ammonium content of Caledonian granites. *J. Geol. Soc. London* **144**, 671-674.
- Hall A. (1988) The distribution of ammonium in granites from South-West England. *J. Geol. Soc. London* **145**, 37-41.
- Hall A. (1989) Ammonium in spilitized basalts of southwest England and its implications for the recycling of nitrogen. *Geochem. J.* **23**, 19-23.
- Hall A. (1990) Geochemistry of the Cornubian tin province. *Mineral. Deposita* **25**, 1-6.
- Hall D. L. and Bodnar R. J. (1990) Methane in fluid inclusions from granulites: A product of hydrogen diffusion? *Geochim. Cosmochim. Acta* **54**, 641-651.
- Hall W. and Friedman I. (1963) Composition of fluid inclusions, Cave-in-Rock fluorite district, Illinois and Upper Mississippi Valley zinc-lead district. *Econ. Geol.* **58**, 886-911.
- Hallam M. and Eugster H. P. (1976) Ammonium silicate stability relations. *Contrib. Mineral. Petrol.* **57**, 227-244.
- Halls C., Exley C. S. and Brunton E. (1985) A bibliography of magmatism and mineralization in S W England. Institution of Mining and Metallurgy, 80 pp.
- Hampton C. M. and Taylor P. N. (1983) The age and nature of the basement of southern Britain: evidence from Sr and Pb isotopes in granites. *J. Geol. Soc. London* **140**, 499-509.
- Hanschmann G. (1981) Berechnung von Isotopieeffekten auf quantenchemischer Grundlage am Beispiel stickstoffhaltiger Moleküle. *Zfi-Mitt.* **41**, 19-39.
- Harland W. B., Armstrong R. L., Cox A. V., Craig L. E., Smith A. G. and Smith D. G. (1990) A geologic time scale 1989. Cambridge University Press, 263 pp.

- Harris N. B. W., Jackson D. H., Matthey D. P., Santosh M. and Bartlett J. (1993) Carbon-isotope constraints on fluid advection during contrasting examples of incipient charnockite formation. *J. Metamorphic Geol.* **11**, 833-843.
- Harting P. and Maass I. (1980) Neue Ergebnisse zum Kohlenstoff-Isotopenaustausch im System $\text{CH}_4\text{-CO}_2$. In: Mitteilungen zur 2. Arbeitstagung 'Isotope in der Natur' November 1979, Vol. 2b, Leipzig, pp. 13-24.
- Hashizume K. and Sugiura N. (1990) Precise measurement of nitrogen isotopic composition using a quadrupole mass spectrometer. *Mass. Spectrosc.* **38**, 269-286.
- Hawkes J. R. (1982) The Dartmoor granite and later volcanic rocks. In: E. M. Durrance and D. J. Laming (Editors), *The Geology of Devon*. University of Exeter Press. Chapter 5 (pp. 85-116).
- Heggie M. I. (1992) A molecular pump in quartz dislocations. *Nature* **355**, 337-339.
- Heinrich C. A. (1990) The chemistry of hydrothermal tin(-tungsten) ore deposition. *Econ. Geol.* **85**, 457-481.
- Hemley J. J. (1959) Some mineralogical equilibria in the system $\text{K}_2\text{O-Al}_2\text{O}_3\text{-SiO}_2\text{-H}_2\text{O}$. *Amer. J. Sci.* **257**, 241-270.
- Higashi S. (1978) Dioctahedral mica minerals with ammonium ions. *Mineral. J.* **9**, 16-27.
- Hirsch P. B., Hutchinson J. L. and Titchmarsh J. (1986) Voidites in diamond. Evidence for a crystalline phase containing nitrogen. *Phil. Mag. A* **54**, L49-L54.
- Hoefs J. (1987) Stable isotope geochemistry. Springer-Verlag, 241 pp.
- Hoering T. C. and Ford H. T. (1960) Isotope effect in the fixation of nitrogen by *Azotobacter*. *J. Amer. Chem. Soc.* **82**, 376-378.
- Holland H. D. (1973) Ocean water, nutrients and atmospheric oxygen. In: E. Ingerson (Editor), *Proc. Symp. Hydrogeochem. Biogeochem.* The Clarke Co., Washington DC, USA, **2**, 68-81.
- Holland H. D. (1978) The chemistry of the atmosphere and oceans. John Wiley & Sons, 351 pp.
- Holland H. D. (1984) The chemical evolution of the atmosphere and oceans. Princeton University Press, USA, 582 pp.
- Hollister L. S. (1990) Enrichment of CO_2 in fluid inclusions by removal of H_2O during crystal-plastic deformation. *J. Struct. Geol.* **12**, 895-901.
- Holloway J. R. (1987) Igneous fluids. In: I. S. E. Carmichael and H. P. Eugster (Editors), *Thermodynamic modelling of geological materials: minerals, fluids and melts*. Reviews in mineralogy **17**, Mineralogical Society of America, pp. 211-233.
- Holloway J. R. (1981) Compositions and fluid volumes of supercritical fluids in the Earth's crust. In: L. S. Hollister and M. L. Crawford (Editors), *Fluid inclusions: applications to petrology*. Mineralogical Association of Canada, short course handbook **6**.

- Holloway J. R. and Reese R. L. (1974) The generation of N_2 - CO_2 - H_2O fluids for use in hydrothermal experimentation. I. Experimental method and equilibrium calculations in the C-O-H-N system. *Amer. Mineral.* **59**, 587-597.
- Holub R. and Voňka P. (1976) The chemical equilibrium of gaseous systems. D. Reidel Publishing Company, 279 pp.
- Honma H. and Ithihara Y. (1981) Distribution of ammonium in minerals of metamorphic and granitic rocks. *Geochim. Cosmochim. Acta* **45**, 983-988.
- Holser W. T., Schidlowski M., Mackenzie F. T. and Maynard J. B. (1988) Biogeochemical cycles of carbon and sulfur. In: C. B. Gregor, R. M. Garrels, F. T. Mackenzie and J. B. Maynard (Editors), *Chemical cycles in the evolution of the Earth*. John Wiley & Sons, pp. 105-173.
- Horita J. (1988) Hydrogen isotope analysis of natural waters using an H_2 -water equilibration method: a special implication to brines. *Chem. Geol. (Isotope Geosciences Section)* **72**, 89-94.
- Horita J. (1989) Analytical aspects of stable isotopes in brines. *Chem. Geol. (Isotope Geosciences Section)* **79**, 147-158.
- Horita J., Cole D. R. and Wesolowski D. J. (1993) The activity-composition relationship of oxygen and hydrogen isotopes in aqueous salt solutions: II. Vapor-liquid water equilibration of mixed salt solutions from 50 to 100°C and geochemical implications. *Geochim. Cosmochim. Acta* **57**, 4703-4711.
- Hulston J. R. (1986) Further isotopic evidence on the origin of methane in geothermal systems. 5th Int. Symp. on Water-Rock Interaction, Reykjavik, Aug. 1986. Extended Abstracts, pp. 270-273.
- Hulston J. R. and McCabe W. J. (1962) Mass spectrometer measurements in the thermal areas of New Zealand. *Geochim. Cosmochim. Acta* **26**, 399-410.
- Hutchinson G. E. (1944) Nitrogen in the biogeochemistry of the atmosphere. *Amer. Sci.* **32**, 178-195.
- Irako M., Oguri T. and Kanomata I (1975) The static operation mass spectrometer. *Japan J. Appl. Phys.* **14**, 523-543.
- Ithihara Y. and Honma H. (1979) Ammonium in biotite from metamorphic and granitic rocks of Japan. *Geochim. Cosmochim. Acta* **43**, 503-509.
- Jackson D. H. (1990) Charnockite formation in southern India. Unpublished PhD thesis, The Open University, UK. 223 pp.
- Jackson D. H., Matthey D. P. and Harris N. W. B. (1988a) Carbon isotope compositions of fluid inclusions in charnockites from southern India. *Nature* **333**, 167-170.
- Jackson D. H., Matthey D. P., Santosh M. and Harris N. W. B. (1988b) Carbon stable isotope analysis of fluid inclusions by stepped heating. *Mem. Geol. Soc. India* **11**, 149-158.
- Jackson N. J., Halliday A. N. and Sheppard S. M. F. (1982) Hydrothermal activity in the St Just mining district, Cornwall, England. In: A. M. Evans (Editor), *Metallization associated with acid magmatism*. John Wiley & Sons, pp. 137-179.

- Jackson N. J., Moore J. McM. and Rankin A. H. (1977) Fluid inclusions and mineralisation at Cligga Head, Cornwall, England. *J. Geol. Soc. London* **134**, 343-349.
- Jackson N. J., Willis-Richards J., Manning D. A. C. and Sams M. S. (1989) Evolution of the Cornubian ore field, southwest England: Part II. Mineral deposits and ore-forming processes. *Econ. Geol.* **84**, 1101-1133.
- Javoy M. and Pineau F. (1986) The volatile record of a 'popping' rock from the mid-Atlantic ridge at 15°N: concentrations and isotopic compositions. *Terra Cognita* **6**, 2, 191.
- Javoy M., Pineau F. and Delorme H. (1986) Carbon and nitrogen isotopes in the mantle. *Chem. Geol.* **57**, 41-62.
- Javoy M., Pineau F. and Demaiffe D. (1984) Nitrogen and carbon isotopic composition in the diamonds of Mbuji Mayi (Zaire). *Earth Planet. Sci. Lett.* **68**, 399-412.
- Javoy M., Pineau F. and Iiyama I. (1978) Experimental determination of the isotopic fractionation between gaseous CO₂ and carbon dissolved in tholeiitic magma: a preliminary study. *Contrib. Mineral. Petrol.* **67**, 35-39.
- Junge C., Schidlowski M., Eichmann R. and Pietrek H. (1975) Model calculations for the terrestrial carbon cycle: carbon isotope geochemistry and evolution of photosynthetic oxygen. *J. Geophys. Res.* **80**, 4542-4552.
- Junge F., Seltmann R. and Stiehl G. (1990) Nitrogen isotope characteristics of breccias, granitoids and greisens from Eastern Erzgebirge tin ore deposits (Sadisdorf; Altenberg), GDR. In: U. Wand and G. Strauch (Editors), *Proceedings of the 5th working meeting 'Isotopes in Nature'*. Central Institute of Isotope and Radiation Research, Leipzig, Germany, 1990. pp. 321-322.
- Junk G. and Svec H. J. (1958) The absolute abundance of the nitrogen isotopes in the atmosphere and compressed gas from various sources. *Geochim. Cosmochim. Acta* **14**, 234-243.
- Karyakin A. V., Volynets V. F. and Kriventsova G. A. (1973) Investigation of nitrogen compounds in micas by infrared spectroscopy. *Geokhimiya* **3**, 439-442.
- Kazahaya K. (1986) Isotopic and chemical studies on hydrothermal solutions. Unpublished PhD thesis, Tokyo Institute of Technology, Tokyo, Japan. 185 pp.
- Kazahaya K. and Matsuo S. (1985) A new ball-milling method for extraction of fluid inclusions from minerals. *Geochem. J.* **19**, 45-54.
- Kelley S. P., Turner G., Butterfield A. W. and Shepherd T. J. (1986) The source and significance of argon isotopes in fluid inclusions from areas of mineralization. *Earth Planet. Sci. Lett.* **79**, 303-318.
- Kelly W. C. and Rye R. O. (1979) Geologic, fluid inclusion and stable isotope studies of the tungsten deposits of Panasqueira, Portugal. *Econ. Geol.* **74**, 1721-1819.
- Kendall C. and Coplen T. B. (1985) Multisample conversion of water to hydrogen by zinc for stable isotope determination. *Anal. Chem.* **57**, 1437-1440.

- Kendall C. and Grim E. (1990) Combustion tube method for measurement of nitrogen isotope ratios using calcium oxide for total removal of carbon dioxide and water. *Anal. Chem.* **62**, 526-529.
- Kishima N. and Sakai H. (1980) Oxygen-18 and deuterium determination on a single water sample of a few milligrams. *Anal. Chem.* **52**, 356-358.
- Kiyosu Y. and Krouse H. R. (1989) Carbon isotope effect during abiogenic oxidation of methane. *Earth Planet. Sci. Lett.* **95**, 302-306.
- Klyakhin V. A. and Levitskiy N. F. (1968) Possible role of NH_4^+ in the hydrothermal process. *Akademiya Nauk SSSR, Sibirskoe Otdelenie, Geologiya i Geofizika* **9**, 10-15.
- Knauth L. P. and Beeunas M. A. (1986) Isotope geochemistry of fluid inclusions in Permian halite, with implications for the isotopic history of ocean water and the origin of saline formation waters. *Geochim. Cosmochim. Acta* **50**, 419-433.
- Kokubu N., Mayeda T. and Urey H. C. (1961) Deuterium content of minerals, rocks and liquid inclusions from rocks. *Geochim. Cosmochim. Acta* **21**, 247-256.
- Koster van Groos A. F. and Ter Heege J. P. (1973) The high-low quartz transition up to 10 kilobars pressure. *J. Geol.* **81**, 717-723.
- Kreulen R. (1980) CO_2 -rich fluids during regional metamorphism on Naxos (Greece): carbon isotopes and fluid inclusions. *Amer. J. Sci.* **280**, 745-771.
- Kreulen R. (1981) Nitrogen and carbon isotopes in fluid inclusions from the Dôme de l'Agout, France. Abstract, 7th European colloquium of Geochronology, Cosmochronology and Isotope Geology; Israel Acad. Sci. and Humanities, Jerusalem.
- Kreulen R. (1983) Nitrogen and carbon isotopes of metamorphic fluids in the Dôme de l'Agout; origin and fluid-rock interaction. Abstracts, 7th symposium European Current Research on Fluid Inclusions, Orléans, France. p.38.
- Kreulen R. (1987) Thermodynamic calculations of the C-O-H system applied to fluid inclusions: are fluid inclusions unbiased samples of ancient fluids? *Chem. Geol.* **61**, 59-64.
- Kreulen R. and Schuiling R. D. (1982) N_2 - CH_4 - CO_2 fluids during the formation of the Dôme de l'Agout, France. *Geochim. Cosmochim. Acta* **46**, 193-203.
- Kreulen R., van Breemen A. and Duit W. (1982) Nitrogen and carbon isotopes in metamorphic fluids from the Dôme de l'Agout, France. Abstracts, fifth International Conference on Geochronology, Cosmochronology and Isotope Geology, Japan. p.191.
- Kydd R. A. and Levinson A. A. (1986) Ammonium halos in lithochemical exploration for gold at the Horse Canyon carbonate-hosted deposit, Nevada, USA. *Appl. Geochem.* **1**, 407-417.
- Lagache M. and Weisbrod A. (1977) The system: two alkali feldspars - $\text{KCl-NaCl-H}_2\text{O}$ at moderate to high temperatures and low pressures. *Contrib. Mineral. Petrol.* **62**, 77-101.
- Laming D. J. C. (1982) The New Red Sandstone. In: E. M. Durrance and D. J. Laming (Editors), *The Geology of Devon*. University of Exeter Press. Chapter 7 (pp. 148-178).

- Landis G. P. and Rye R. O. (1974) Geologic, fluid inclusion and stable isotope studies of the Pasto Buena tungsten-base metal ore deposit, northern Peru. *Econ. Geol.* **69**, 1025-1059.
- Lazar B. and Holland H. D. (1988) The analysis of fluid inclusions in halite. *Geochim. Cosmochim. Acta* **52**, 485-490.
- Leat P. T., Thompson R. N., Morrison M. A., Hendry G. L. and Trayhorn S. C. (1987) Geodynamic significance of post-Variscan intrusive and extrusive potassic magmatism in S W England. *Trans. Roy. Soc. Edinburgh: Earth Sciences* **77** (for 1986), 349-360.
- Leroy J. (1979) Contribution à l'étalonnage de la pression interne des inclusions fluides lors de leur décrépitation. *Bull. Soc. française Minéral. Cristall.* **102**, 584-593.
- Létolle R. (1980) Nitrogen-15 in the natural environment. In: P. Fritz and J. Ch. Fontes (Editors), *Handbook of Environmental Isotope Geochemistry, Vol. 1, The Terrestrial Environment (A)*. Elsevier. Chapter 10, pp. 407-433.
- Lewis R. S., Anders E., Swart P. K., Grady M. M. and Pillinger C. T. (1983a) Isotopically anomalous carbon in the Murchison meteorite and its association with noble gas components. *Proc. Lunar Planet. Sci. Conf. XIV*, 438-439.
- Lewis R. S., Grady M. M., Wright I. P., Pillinger C. T. and Fallick A. E. (1983b) Isotopic composition of C and N in noble gas host phases in CI carbonaceous and Type 3 ordinary chondrites. *Proc. Lunar Planet. Sci. Conf. XIV*, 438-439.
- Lin Y. (1989) Comparative aspects of pegmatitic and pneumatolytic evolution in Cornish granites. Unpublished PhD thesis, University of London, UK. 247 pp.
- Lockett A. E. (1987) A technique for the determination of tin by isotope dilution and its application to fluid inclusions. Unpublished MSc dissertation, University of Leeds, UK. 54 pp.
- Longstaffe F. J. (1987) Stable isotope studies of diagenetic processes. In: T. K. Tyser (Editor), *Stable isotope geochemistry of low temperature processes*. Mineralogical Association of Canada short course handbook, Volume 13, pp. 187-257.
- Lovelock J. E. (1972) Gaia as seen through the atmosphere. *Atmos. Environ.* **6**, 570-580.
- Lowenstern J. B., Mahood G. A., Rivers M. L. and Sutton S. R. (1991) Evidence for extreme partitioning of copper into a magmatic vapour phase. *Science* **252**, 1405-1409.
- Lyon G. L. and Hulston J. R. (1984) Carbon and hydrogen isotopic compositions of New Zealand geothermal gases. *Geochim. Cosmochim. Acta* **48**, 1161-1171.
- Magaritz M. and Gat J. R. (1981) Review of the natural abundance of hydrogen and oxygen isotopes. In: J. R. Gat and R. Gonfiantini (Editors), *Stable isotope hydrology, deuterium and oxygen-18 in the water cycle*. International Atomic Energy Agency, Vienna, Technical Report Series No. 210, Chapter 5 (pp. 85-102).
- Mango F. D., Hightower J. W. and James A. T. (1994) Role of transition-metal catalysis in the formation of natural gas. *Nature* **368**, 536-538.

- Mariotti A. (1983) Atmospheric nitrogen is a reliable standard for natural ^{15}N abundance measurements. *Nature* **303**, 685-687.
- Mathez E. A. (1987) Carbonaceous matter in mantle xenoliths: composition and relevance to the isotopes. *Geochim. Cosmochim. Acta* **51**, 2339-2347.
- Mathez E. A., Blacic J. D., Beery J., Hollander M. and Maggiore C. (1987) The geochemistry of carbon in mantle peridotites. *Geochim. Cosmochim. Acta* **48**, 1849-1859.
- Mathez E. A., Blacic J. D., Beery J., Maggiore C. and Hollander M. (1986) Carbon in olivine by nuclear reaction analysis. 4th. Int. Kimberlite Conf. Extended Abstr. Geol. Soc. Australia. Abstract No. 16, pp.273-275.
- Mathez E. A. and Delaney J. R. (1981) The nature and distribution of carbon in submarine basalts and peridotite nodules. *Earth Planet. Sci. Lett.* **56**, 217-232.
- Mathez E. A., Dietrich V. J., Holloway J. R. and Boudreau A. E. (1989) Carbon distribution in the Stillwater Complex and evolution of vapor during crystallization of Stillwater and Bushveld magmas. *J. Petrol.* **30**, 153-173.
- Matsuhisa Y., Goldsmith J. R. and Clayton R. N. (1979) Oxygen isotope fractionation in the systems quartz-albite-anorthite-water. *Geochim. Cosmochim. Acta* **43**, 1131-1140.
- Mattey D. P. (1987) Carbon isotopes in the mantle. *Terra Cognita* **7**, 31-37.
- Mattey D. P. (1990) Carbon isotopes in basalt glass: significance of 'light carbon', vapour-melt fractionation effects and mantle source variations. *Eos*, April 24, p645.
- Mattey D. P., Carr R. H., Wright I. P. and Pillinger C. T. (1984) Carbon isotopes in submarine basalts. *Earth Planet. Sci. Lett.* **70**, 196-206.
- Mattey D. P., Exley R. A. and Pillinger C. T. (1989) Isotopic composition of CO_2 and dissolved carbon species in basalt glass. *Geochim. Cosmochim. Acta* **53**, 2377-2386.
- Mattey D. P. and Macpherson C. (1993) High-precision oxygen isotope microanalysis of ferromagnesian minerals by laser-fluorination. *Chem. Geol. (Isotope Geosciences Section)* **105**, 305-318.
- Mattey D. P., Taylor W. R., Green D. H. and Pillinger C. T. (1990) Carbon isotopic fractionation between CO_2 vapour, silicate and carbonate melts: an experimental study to 30 kbar. *Contrib. Mineral. Petrol.* **104**, 492-505.
- Matthews D. E. and Hayes J. M. (1978) Isotope-ratio-monitoring gas chromatography-mass spectrometry. *Anal. Chem.* **50**, 1465-1473.
- Mavrogenes J. A. and Bodnar R. J. (1994) Hydrogen movement into and out of fluid inclusions in quartz: Experimental evidence and geologic implications. *Geochim. Cosmochim. Acta* **58**, 141-148.
- Mayne K. I. (1957) Natural variations in the nitrogen isotope abundance ratio in igneous rocks. *Geochim. Cosmochim. Acta* **12**, 185-189.

- McCrea J. M. (1950) On the isotope chemistry of carbonates and a palæotemperature scale. *J. Chem. Phys.* **18**, 849-857.
- McCulloch M. T. and Woodhead J. D. (1993) Lead isotope evidence for deep crustal-scale fluid transport during granite petrogenesis. *Geochim. Cosmochim. Acta* **57**, 659-674.
- McKinney C. R., McCrea J. M., Epstein S., Allen H. A. and Urey H. C. (1950) Improvements in mass spectrometers for the measurement of small differences in isotope abundance ratios. *Rev. Sci. Instrum.* **21**, 724-730.
- McNaughton N. J., Abell P. I., Wright I. P., Fallick A. E. and Pillinger C. T. (1983) Preparation of nanogram quantities of deuteromethane for stable carbon isotope analysis. *J. Phys. E: Sci. Instrum.* **16**, 505-511.
- McNutt R. H. (1987) $^{87}\text{Sr}/^{86}\text{Sr}$ ratios as indicators of water/rock interactions: Application to brines found in Precambrian age rocks from Canada. In: P. Fritz and S. K. Frape (Editors), *Saline waters in crystalline rocks*. Geol. Assoc. Canada Special Paper **33**, 121-126.
- Metcalfe R., Banks D. A. and Bottrell S. H. (1992) An association between organic matter and localised, prehnite-pumpellyite alteration, at Builth Wells, Wales, UK. *Chem. Geol.* **102**, 1-22.
- Miller M. F. and Shepherd T. J. (1984) The determination of lead in fluid inclusions using voltammetric trace analysis: an exploratory investigation. *Chem. Geol.* **42**, 249-259.
- Miller, W. A. (1865) Chemical examination of a hot spring containing caesium and lithium in Wheal Clifford, Cornwall. Report of the British Association, 34th Meeting, pp. 36-36.
- Milodowski A. E. and Morgan D. J. (1980) Identification and estimation of carbonate minerals at low levels by evolved gas analysis. *Nature* **286**, 248-249.
- Minagawa M., Winter D. A. and Kaplan I. R. (1984) Comparison of Kjeldahl and combustion methods for measurement of nitrogen isotope ratios in organic matter. *Anal. Chem.* **56**, 1859-1861.
- Molyneux S. G. and Owens B. (1990) Spores and acritarchs from samples of the Kate Brook Slates, Devon. Brit. Geol. Survey Tech. Report WH/90/343R.
- Moore W. J. (1972) Physical chemistry. Longman, 977 pp.
- Morgan G. B. VI, Chou I.-M. and Pasteris J. D. (1992) Speciation in experimental C-O-H fluids produced by the thermal dissociation of oxalic acid dihydrate. *Geochim. Cosmochim. Acta* **56**, 281-294.
- Morse A. D. (1991) Attempts to analyse D/H ratios of sub-micromole quantities of hydrogen: applications in the study of ordinary chondrites. Unpublished PhD thesis, The Open University, UK. 237 pp.
- Morse A. D., Wright I. P. and Pillinger C. T. (1993) An investigation into the cause of memory effects associated with the conversion of H_2O to H_2 for D/H measurement. *Chem. Geol. (Isotope Geosciences Section)* **107**, 147-158.
- Mortland M. M. (1958) Reactions of ammonia in soils. *Adv. Agron.* **10**, 325-348.

- Muehlenbachs K. (1986) Alteration of the oceanic crust and the ^{18}O history of seawater. In: J. W. Valley, H. P. Taylor, Jr., and J. R. O'Neil (Editors), *Stable isotopes in high temperature geological processes*. Reviews in mineralogy **16**, Mineralogical Society of America, pp. 425-444.
- Muehlenbachs K. and Clayton R. N. (1976) Oxygen isotope composition of the oceanic crust and its bearing on seawater. *J. Geophys. Res.* **81**, 4365-4369.
- Murata K. J., Friedman I. and Madsen B. M. (1967) Carbon-13-rich diagenetic carbonates in Miocene formations of California and Oregon. *Science* **156**, 1484-1486.
- Murphey B. F. (1947) The high temperature variation of the thermal diffusion factors for binary mixtures of H, D and He. *Phys. Rev.* **72**, 834-837.
- Nadeau S., Pineau F., Javoy M. and Francis D. (1990) Carbon concentrations and isotopic ratios in fluid-inclusion-bearing upper-mantle xenoliths along the northwestern margin of North America. *Chem. Geol.* **81**, 271-297.
- Nevins J. L., Altabet M. A. and McCarthy J. J. (1985) Nitrogen isotope ratio analysis of small samples: sample preparation and calibration. *Anal. Chem.* **57**, 2143-2145.
- Nielsen H. (1978) Sulphur isotopes in nature. In: K. H. Wederphol (Editor), *Handbook of Geochemistry*, Chapter 16-B. Springer-Verlag.
- Nier A. O. (1940) A mass spectrometer for routine abundance measurements. *Rev. Sci. Instrum.* **11**, 212-216.
- Nier A. O. (1947) A mass spectrometer for isotope and gas analysis. *Rev. Sci. Instrum.* **18**, 398-411.
- Niggli P. (1929) Ore deposits of magmatic origin: their genesis and natural classification. Thomas Murby and Co., London. 93 pp.
- Nitzsche H. M. and Stiehl G (1984) Untersuchungen zur Isotopenfraktionierung des Stickstoffs in den Systemen Ammonium/Ammoniak and Nitrid/Stickstoff. *ZfI Mitt.* **84**, 283-291.
- O'Brien C., Plant J. A., Simpson P. R. and Tarney J. (1985) The geochemistry and petrogenesis of the granites of the English Lake District. *J. Geol. Soc. London* **142**, 1139-1157.
- Oberhauser G., Kathrein H., Demortier G., Gonska H. and Freund F. (1983) Carbon in olivine single crystals analysed by the $^{12}\text{C}(\text{D},\text{p})^{13}\text{C}$ method and by photoelectron spectroscopy. *Geochim. Cosmochim. Acta* **47**, 1117-1129.
- Ohba T. (1987) $^{18}\text{O}/^{16}\text{O}$ and D/H ratio determinations for small amounts of water. *Geochem. J.* **21**, 183-186.
- Ohmoto H. (1986) Stable isotope geochemistry of ore deposits. In: J. W. Valley, H. P. Taylor, Jr., and J. R. O'Neil (Editors), *Stable isotopes in high temperature geological processes*. Reviews in mineralogy **16**, Mineralogical Society of America, pp. 491-559.
- Ohmoto H. and Kerrick D. (1977) Devolatilization equilibria in graphitic systems. *Amer. J. Sci.* **277**, 1013-1044.

- Ohmoto H. and Rye R. O. (1979) Isotopes of sulfur and carbon. In: H. L. Barnes (Editor), *Geochemistry of hydrothermal ore deposits*, pp. 509-567. John Wiley & Sons.
- O'Neil J. R. and Epstein S. (1966) A method for oxygen isotope analysis of milligram quantities of water and some of its applications. *J. Geophys. Res.* 71, 4955-4961.
- O'Neil J. R. (1986) Theoretical and experimental aspects of isotopic fractionation In: J. W. Valley, H. P. Taylor, Jr., and J. R. O'Neil (Editors), *Stable isotopes in high temperature geological processes*. Reviews in mineralogy 16, Mineralogical Society of America, pp. 1-40.
- O'Nions R. K., Oxburgh E. R., Hawkesworth C. J. and Macintyre R. M. (1973) New isotopic and stratigraphical evidence on the age of the Ingletonian: probable Cambrian of northern England. *J. Geol. Soc. London* 129, 445-452.
- Parnell J. (1988) Migration of biogenic hydrocarbons into granites: a review of hydrocarbons in British plutons. *Marine and Petroleum Geol.* 5, 385-396.
- Pauwels H., Fouillac C. and Fouillac A. M. (1993) Chemistry and isotopes of deep geothermal saline fluids in the Upper Rhine Graben: Origin of compounds and water-rock interactions. *Geochim. Cosmochim. Acta* 57, 2737-2749.
- Pearce J. A., Harris N. B. W. and Tindle A. G. (1984) Trace element discrimination diagrams for the tectonic interpretation of granitic rocks. *J. Petrol.* 25, 956-983.
- Peucker-Ehrenbrink B. and Behr H.-J. (1993) Chemistry of hydrothermal quartz in the post-Variscan "Bavarian Pfahl" system, F.R. Germany. *Chem. Geol.* 103, 85-102.
- Phillips J. A. (1873) The rocks of the mining districts of Cornwall and their relation to metalliferous deposits. *Quarterly J. Geol. Soc. London* 31, 319-345.
- Pillinger C. T. (1984) Light element stable isotopes in meteorites - from grams to picograms. *Geochim. Cosmochim. Acta* 48, 2739-2766.
- Pillinger C. T. (1992) New technologies for small sample stable isotope measurement: static vacuum gas source mass spectrometry, laser probes and gas chromatography-isotope ratio mass spectrometry. *Int. J. Mass Spectrometry and Ion Processes* 118/119, 477-501.
- Pineau F. and Javoy M. (1983) Carbon isotopes and concentrations in mid-ocean ridge basalts. *Earth Planet. Sci. Lett.* 62, 239-257.
- Piperov N. B. and Penchev N. P. (1973) A study on gas inclusions in minerals. Analysis of the gases from micro-inclusions in allanite. *Geochim. Cosmochim. Acta* 37, 2075-2097.
- Pollack J. B. and Yung Y. L. (1980) Origin and evolution of planetary atmospheres. *Ann. Rev. Earth Planet. Sciences* 8, 425-487.
- Primmer T. J. (1985) Discussion on the possible contribution of metamorphic water to the mineralizing fluid of south-west England: preliminary stable isotope evidence. *Proc. Ussher Soc.* 6, 224-228.

- Prosser S. J., Wright I. P. and Pillinger C. T. (1990) A preliminary investigation into isotopic measurement of carbon at the picomole level using static vacuum mass spectrometry. *Chem. Geol.* **83**, 71-88.
- Ramboz C., Schnapper D. and Dubessy J. (1985) The P-V-T-X-fO₂ evolution of H₂O-CO₂-CH₄-bearing fluid in a wolframite vein: reconstruction from fluid inclusion studies. *Geochim. Cosmochim. Acta* **49**, 205-219.
- Rankin A. H. and Alderton D. H. M. (1985) Chemistry and evolution of hydrothermal fluids associated with the granites of southwest England. In: *High heat production (HHP) granites, hydrothermal circulation and ore genesis*. Institution of Mining and Metallurgy, pp.345-364.
- Rau G. H., Arthur M. A. and Dean W. E. (1987) ¹⁵N/¹⁴N variations in Cretaceous Atlantic sedimentary sequences: implication for past changes in marine nitrogen biogeochemistry. *Earth Planet. Sci. Lett.* **82**, 269-279.
- Rayleigh J. W. S. (1896) Theoretical considerations respecting the separation of gases by diffusion and similar processes. *Philos. Mag.* **42**, 493.
- Reynolds J. H. (1956) High sensitivity mass spectrometer for noble gas analysis. *Rev. Sci. Instrum* **27**, 928-934.
- Richet P., Bottinga Y. and Javoy M. (1977) A review of hydrogen, carbon, nitrogen, oxygen, sulphur, and chlorine stable isotope fractionation among gaseous molecules. *Ann. Rev. Planet. Sci.* **5**, 65-110
- Robinson B. W. and Kusakabe M. (1975) Quantitative preparation of sulfur dioxide, for ³⁴S/³²S analyses, from sulfides by combustion with cuprous oxide. *Anal. Chem.* **47**, 1179-1181.
- Roedder E. (1958) Technique for the extraction and partial analysis of fluid-filled inclusions from minerals. *Econ. Geol.* **53**, 235-269.
- Roedder E. (1972) Composition of fluid inclusions. In: M. Fleischer (Editor), *Data of Geochemistry*, US Geol. Surv. Professional Paper 440-JJ, 164 pp.
- Roedder E. (1984) Fluid inclusions. *Reviews in Mineralogy* **12**, Mineralogical Society of America; 644 pp.
- Roedder E. (1990) Fluid inclusion analysis - Prologue and epilogue. *Geochim. Cosmochim. Acta* **54**, 495-507.
- Roedder E., Ingram B. and Hall W. E. (1963) Studies of fluid inclusions III: Extraction and quantitative analysis of inclusions in the milligram range. *Econ. Geol.* **58**, 353-374.
- Rosasco G. J. and Roedder E. (1979) Application of a new Raman microprobe spectrometer to nondestructive analysis of sulfate and other ions in individual phases in fluid inclusions in minerals. *Geochim. Cosmochim. Acta* **43**, 1907-1915.
- Rossmann G. R., Weis D. and Wasserburg G. J. (1987) Rb, Sr, Nd and Sm concentrations in quartz. *Geochim. Cosmochim. Acta* **51**, 2325-2329.

- Rumble D., III, Duke E. F. and Hoering T. L. (1986) Hydrothermal graphite mobility in New Hampshire: evidence of carbon mobility during regional metamorphism. *Geology* **14**, 452-455.
- Rumble D., III, and Hoering T. L. (1986) Carbon isotope geochemistry of graphite vein deposits from New Hampshire, USA. *Geochim. Cosmochim. Acta* **50**, 1239-1247.
- Rye R. O. and O'Neil J. R. (1968) The ^{18}O -content of water in primary fluid inclusions from Providencia, north central Mexico. *Econ. Geol.* **63**, 232-238.
- Sackett W. M. and Chung H. M. (1979) Experimental confirmation of the lack of carbon isotope exchange between methane and carbon oxides at high temperatures. *Geochim. Cosmochim. Acta* **43**, 273-276.
- Sakai H., Des Marais D. J., Ueda A. and Moore J. G. (1984) Concentrations and isotope ratios of carbon, nitrogen and sulphur in ocean-floor basalts. *Geochim. Cosmochim. Acta* **48**, 2433-2441.
- Sakai H., Smith J. W., Kaplan I. R. and Petrowski C. (1976) *Geochem. J.* (1976) Micro-determinations of C, N, S, H, He, metallic Fe, $\delta^{13}\text{C}$, $\delta^{15}\text{N}$ and $\delta^{34}\text{S}$ in geological samples. *Geochem. J.* **10**, 85-96.
- Sarda P., Staudacher T. and Allègre C. J. (1985) $^{40}\text{Ar}/^{36}\text{Ar}$ in MORB glasses: constraints on atmosphere and mantle evolution. *Earth Planet. Sci. Lett.* **72**, 357-375.
- Savage D., Cave M. R. and Milodowski A. E. (1985) Interaction of meteoric groundwater with Carnmenellis granite at 250°C and 50 MPa: an experimental study. In: *High heat production (HHP) granites, hydrothermal circulation and ore genesis*. Institution of Mining and Metallurgy, pp. 315-327.
- Savage D., Cave M. R., Milodowski A. E. and George I. (1987) Hydrothermal alteration of granite by meteoric fluid: an example from the Carnmenellis granite, United Kingdom. *Contrib. Mineral. Petrol.* **96**, 391-405.
- Savin S. M. and Epstein S. (1970) The oxygen and hydrogen isotope geochemistry of clay minerals. *Geochim. Cosmochim. Acta* **34**, 25-42.
- Saxena S. K. (1989) Oxidation state of the mantle. *Geochim. Cosmochim. Acta* **53**, 89-97.
- Scalan R. S. (1958) The isotopic composition, concentration, and chemical state of the nitrogen in igneous rocks. Unpublished PhD thesis, University of Arkansas, USA. 79 pp.
- Schidlowski M., Hayes J. M. and Kaplan I. R. (1983) Isotopic inferences of ancient biochemistries: carbon, sulfur, hydrogen and nitrogen. In: J. W. Schopf (Editor), *Earth's earliest biosphere: its origin and evolution*. Princeton University Press, pp. 149-186.
- Schneider F. (1990) Pétrographie, pétrologie et géochimie des granites du massif de Dartmoor (Devon, GB) et des minéralisations associées (W, Sn). Modélisation des processus. Ecole des Mines de Paris Mémoires des Sciences de la Terre, No. 11, 223 pp.
- Schoell M. (1980) The hydrogen and carbon isotopic composition of methane from natural gases of various origins. *Geochim. Cosmochim. Acta* **44**, 649-661.
- Schoell M. (1988) Multiple origins of methane in the Earth. In: M. Schoell (Guest-Editor), *Origins of methane in the Earth*. *Chem. Geol.* **71**, 1-10.

- Schopf J. W. and Klein C. (Editors) (1992) *The Proterozoic biosphere: a multidisciplinary study*. Cambridge University Press, 1348 pp.
- Scrivener R. C. (1982) Tin and related mineralisation of the Dartmoor granite. Unpublished PhD thesis, University of Exeter, UK. 229 pp.
- Scrivener R. C., Shepherd T. J. and Garrioch N. (1986) Ore genesis at Wheal Pendarves and South Crofty mine, Cornwall - a preliminary fluid inclusion study. *Proc. Ussher Soc.* **6**, 412-416.
- Selwood E. B. and Durrance E. M. (1982) The Devonian rocks. In: E. M. Durrance and D. J. Laming (Editors), *The Geology of Devon*. University of Exeter Press. Chapter 2 (pp. 15-41).
- Shackleton R. M., Ries A. C. and Coward M. P. (1982) An interpretation of the Variscan structures in S W England. *J. Geol. Soc.* **139**, 533-541.
- Shannon R. D. (1976) Revised effective ionic radii and systematic studies of interatomic distances in halides and chalcogenides. *Acta Cryst.* **A32**, 751-767.
- Shepherd T. J., Beckinsale R. D., Rundle C. C. and Durham J. (1976) Genesis of Carrock Fell tungsten deposits, Cumbria: fluid inclusion and isotopic study. *Trans. Inst. Mine. Metall. (Sect. B: Appl. Earth Sci.)* **85**, B63-B73.
- Shepherd T. J. and Miller M. F. (1988) Fluid inclusion volatiles as a guide to tungsten deposits, southwest England: applications to other Sn-W provinces in western Europe. In: J. Boissonnas and P. Omenetto (Editors), *Mineral deposits within the European Community*. Springer-Verlag, pp. 29-52.
- Shepherd T. J., Miller M. F., Scrivener R. C. and Darbyshire D. P. F. (1985) Hydrothermal fluid evolution in relation to mineralization in southwest England, with special reference to the Dartmoor-Bodmin area. In: *High heat production (HHP) granites, hydrothermal circulation and ore genesis*. Institution of Mining and Metallurgy, pp. 345-364.
- Shepherd T. J. and Scrivener R. C. (1987) Role of basinal brines in the genesis of polymetallic vein deposits, Kit Hill-Gunnislake area, S W England. *Proc. Ussher Soc.* **6**, 491-497.
- Sheppard S. M. F. (1977) The Cornubian batholith, SW England: D/H and $^{18}\text{O}/^{16}\text{O}$ studies of kaolinite and other alteration minerals. *J. Geol. Soc. London* **133**, 573-591.
- Sheppard S. M. F. (1981) Stable isotope chemistry of fluids. In: D. T. Rickard and F. E. Wickham (Editors), *Chemistry and geochemistry of solutions at high temperatures and pressures*. *Physics and Chemistry of the Earth* **13 & 14**, 419-433.
- Sheppard S. M. F. (1986) Characterization and isotopic variations in natural waters. In: J. W. Valley, H. P. Taylor, Jr., and J. R. O'Neil (Editors), *Stable isotopes in high temperature geological processes*. *Reviews in mineralogy* **16**, Mineralogical Society of America, pp. 165-183.
- Sherwood B., Fritz P., Frapé S. K., Macko S. A., Weise S. M. and Welhan J. A. (1988) Methane occurrences in the crystalline rocks of the Canadian Shield. In: M. Schoell (Guest-Editor), *Origins of methane in the Earth*. *Chem. Geol.* **71**, 223-236.
- Slack J., Palmer M. R. and Stevens B. P. J. (1989) Boron isotope evidence for the involvement of non-marine evaporites in the origin of the Broken Hill ore deposits. *Nature* **342**, 3189-3195.

- Smith A. G., Briden J. C. and Drewry G. E. (1973) Phanerozoic world maps. In: N. F. Hughes (Editor), *Organisms and continents through time*. Special Papers in Palaeontology No. 12, pp. 1-42.
- Spivack A. J., Palmer M. R. and Edmond J. M. (1987) The sedimentary cycle of the boron isotopes. *Geochim. Cosmochim. Acta* **51**, 1939-1949.
- Steiger R. H. and Jäger E. (1977) Sub-commission on geochronology: Convention on the use of decay constants in geo- and cosmochronology. *Earth Planet. Sci. Lett.* **36**, 359-362.
- Stevenson F. J. (1959) On the presence of fixed ammonium in rocks. *Science* **130**, 221-222.
- Stevenson F. J. (1962) Chemical state of the nitrogen in rocks. *Geochim. Cosmochim. Acta* **26**, 797-809.
- Stolper E. and Holloway J. R. (1988) Experimental determination of the solubility of carbon dioxide in molten basalt at low pressure. *Earth Planet. Sci. Lett.* **87**, 397-408.
- Stone J., Hutcheon I. D., Epstein S. and Wasserburg G. J. (1991) Correlated Si isotope anomalies and large ^{13}C enrichments in a family of exotic SiC grains. *Earth Planet. Sci. Lett.* **107**, 570-581.
- Stone M. and Exley C. S. (1985) High heat production granites of southwest England and their associated mineralization: a review. In: *High heat production (HHP) granites, hydrothermal circulation and ore genesis*. Institution of Mining and Metallurgy, pp. 571-593.
- Stuart F. M. and Turner G. (1992) The abundance and isotopic composition of the noble gases in ancient fluids. *Chem. Geol. (Isotope Geosciences Section)* **101**, 97-109.
- Stumm W. and Morgan J. J. (1981) *Aquatic chemistry*. John Wiley & Sons, 780 pp.
- Sudzuki N. (1987) A water conversion method for D/H ratio analyses and its accuracy. *Geochem. J.* **21**, 29-33.
- Suzuoki T. and Epstein S. (1977) Hydrogen isotope fractionation between OH-bearing minerals and water. *Geochim. et Cosmochim. Acta* **40**, 1229-1240.
- Sverjensky D. A. (1992) Linear free energy relations for predicting dissolution rates of solids. *Nature* **358**, 310-313.
- Sverjensky D. A. and Molling P. A. (1992) A linear free energy relationship for crystalline solids and aqueous ions. *Nature* **356**, 231-234.
- Swanenberg H. E. C. (1980) Fluid inclusions in high-grade metamorphic rocks from SW Norway. PhD thesis, University of Utrecht, Holland. 147 pp.
- Swart P. K., Grady M. M. and Pillinger C. T. (1982) Isotopically distinguishable carbon phases in the Allende meteorite. *Nature* **297**, 381-383.
- Swart P. K., Grady M. M. and Pillinger C. T. (1983) A method for the identification and elimination of contamination during carbon isotopic analyses of extraterrestrial samples. *Meteoritics* **18**, 137-154.

- Sweeney R. E., Liu K. K. and Kaplan I. R. (1978) Oceanic nitrogen isotopes and their uses in determining the source of sedimentary nitrogen. In: B. W. Robinson (Editor), *Stable Isotopes in the Earth Sciences*, DSIR New Zealand, Bull. 220, pp. 9-26.
- Tang M., Anders E. and Zinner E. (1988) Noble gases, C, N and Si isotopes in interstellar SiC from the Murchison carbonaceous. In: Lunar Planet. Sci. XIX: Houston, Lunar and Planetary Institute, pp. 1177-1178.
- Tang M., Lewis R. S., Anders E., Grady M. M., Wright I. P. and Pillinger C. T. (1988) Isotopic anomalies of Ne, Xe, and C in meteorites. I. Separation of carriers by density and chemical resistance. *Geochim. Cosmochim. Acta* **52**, 1221-1234.
- Taylor B. E. (1986) Magmatic volatiles: isotopic variation of C, H, and S. In: J. W. Valley, H. P. Taylor, Jr., and J. R. O'Neil (Editors), *Stable isotopes in high temperature geological processes*. Reviews in mineralogy **16**, Mineralogical Society of America, pp. 185-225.
- Taylor B. E. (1987) Stable isotope geochemistry of ore-forming fluids. In: T. K. Tyser (Editor), *Stable isotope geochemistry of low temperature processes*. Mineralogical Association of Canada short course handbook, Volume **13**, pp. 337-445.
- Taylor H. P., Jr. (1974) The application of oxygen and hydrogen isotope studies to problems of hydrothermal alteration and ore deposition. *Econ. Geol.* **69**, 843-883.
- Taylor H. P., Jr. (1977) Water/rock interactions and the origin of H₂O in granitic batholiths. *J. Geol. Soc. London* **133**, 509-558.
- Taylor H. P., Jr. (1979) Oxygen and hydrogen isotope relationships in hydrothermal mineral deposits. In: H. L. Barnes (Editor), *Geochemistry of hydrothermal ore deposits*. John Wiley & Sons, pp. 236-277.
- Taylor H. P. and Sheppard S. M. F. (1986) Igneous rocks: I. Processes of isotopic fractionation and isotope systematics. In: J. W. Valley, H. P. Taylor, Jr., and J. R. O'Neil (Editors), *Stable isotopes in high temperature geological processes*. Reviews in mineralogy **16**, Mineralogical Society of America, pp. 227-271.
- Taylor S. R. and McLennan S. M. (1985) The continental crust: its composition and evolution. Blackwell Scientific Publications, 312 pp.
- Thode H. G., Monster J. and Dunford H. B. (1961) Sulphur isotope geochemistry. *Geochim. Cosmochim. Acta* **25**, 150-174.
- Thomas J. M. (1982) The Carboniferous rocks. In: E. M. Durrance and D. J. Laming (Editors), *The Geology of Devon*. University of Exeter Press. Chapter 3 (pp. 42-65).
- Thompson A. B. (1992) Water in the Earth's upper mantle. *Nature* **358**, 295-302.
- Tingle T. N., Green H. W. and Finnerty A. A. (1988) Experiments bearing on the solubility and diffusivity of carbon in olivine. *J. Geophys. Res.* **93**, 15289-15304.
- Tingle T. N., Hochella M. F., Becker C. H. and Malhotra R. (1990) Organic compounds on crack surfaces in olivine from San Carlos, Arizona, and Hualalai Volcano, Hawaii. *Geochim. Cosmochim. Acta* **54**, 477-485.

- Tingle T. N., Mathez E. A. and Hochella M. F. (1991) Carbonaceous matter in peridotites and basalts studied by XPS, SALI and LEED. *Geochim. Cosmochim. Acta* **55**, 1345-1352.
- Tissot B. P. and Welte D. H. (1984) *Petroleum formation and occurrence*. Springer-Verlag, 699 pp.
- Tse R. S., Wong S. C. and Yen C. P. (1980) Determination of deuterium/hydrogen ratios in natural waters by Fourier transform nuclear magnetic resonance spectrometry. *Anal. Chem.* **52**, 2445-2448.
- Tsong L. S. T. and Knipping U. (1986) Comment on "Solute carbon and carbon segregation in magnesium oxide single crystals - a secondary ion mass spectrometer study", by F. Freund. *Phys. Chem. Miner.* **13**, 277-279.
- Tsong L. S. T., Knipping U., Loxton Magee C. and Arnold C. (1985) Carbon on surfaces of magnesium oxide and olivine single crystals: Diffusion from bulk or surface contamination? *Phys. Chem. Mineral.* **12**, 261-270.
- Turner G. and Bannon M. P. (1992) Argon isotope geochemistry of inclusion fluids from granite-associated mineral veins in southwest and northeast England. *Geochim. Cosmochim. Acta* **56**, 227-243.
- Urano H. (1971) Geochemical and petrological study on the origins of metamorphic rocks and granitic rocks by determination of fixed ammoniacal nitrogen. *J. Earth Sciences, Nagoya University, Japan* **19**, 1-24.
- Urey H. C. (1932) An isotope of hydrogen of mass 2 and its concentration. (Abstr.) *Phys. Rev.* **39**, 864.
- Urey H. C. (1947) The thermodynamic properties of isotopic substances. *J. Chem. Soc.*, 562-581.
- Urey H. C. (1948) Oxygen isotopes in Nature and the laboratory. *Science* **108**, 489-497.
- Vaccaro R. F. (1965) Inorganic nitrogen in sea water. In: J. P. Riley and G. Skirrow (Editors), *Chemical Oceanography*. Academic Press. **1**, 365-404.
- Van den Kerkhof A. M. (1988) The system CO₂-CH₄-N₂ in fluid inclusions: theoretical modelling and geological applications. PhD thesis, Free University of Amsterdam, Holland, 206 pp.
- Van Zeggeren F. and Storey S. H. (1970) *The computation of chemical equilibria*. Cambridge University Press, 176 pp.
- Vedder W. (1965) Ammonium in muscovite. *Geochim. Cosmochim. Acta* **29**, 221-228.
- Veizer J. (1989) Strontium isotopes in seawater through time. *Ann. Rev. Earth Planet. Sci.* **17**, 141-167.
- Vengosh A., Chivas A. R. and McCulloch M. T. (1989) Direct determination of boron and chlorine isotopic compositions in geological materials by negative thermal-ionization mass spectrometry. *Chem. Geol.* **79**, 333-343.
- Vennemann T. W. and O'Neil J. R. (1993) A simple and inexpensive method of hydrogen isotope and water analyses of minerals and rocks based on zinc reagent. *Chem. Geol. (Isotope Geosciences Section)* **103**, 227-234.

- Vinogradov A. P., Florenskii K. P. and Volynets V. F. (1963) Ammonia in meteorites and igneous rocks. *Geochemistry* **10**, 905-916.
- Vityk M. O., Krouse H. R. and Demihov Y. N. (1993) Preservation of $\delta^{18}\text{O}$ values of fluid inclusion water in quartz over geological time in an epithermal environment: Beregov deposit, Transcarpathia, Ukraine. *Earth Planet. Sci. Lett.* **119**, 561-568.
- Von Damm K. L., Edmond J. M., Measures C. I. and Grant B. (1985) Chemistry of submarine hydrothermal solutions at Guaymas Basin, Gulf of California. *Geochim. Cosmochim. Acta* **49**, 2221-2237.
- Wahlen M., Tanaka N., Henry R., Yoshimari T., Fairbanks R. G., Sheruesh A. and Broecker W. S. (1987). ^{13}C , D and ^{14}C in methane. *Eos (Trans. Amer. Geophys. Union)* **68**, 1220.
- Wahler W. (1956) Über die in Kristallen eingeschlossenen Flüssigkeiten und Gase. *Geochim. Cosmochim. Acta* **9**, 105-135.
- Wand U., Nitzsche H.-M., Mühle K. and Wetzel K. (1980) Nitrogen isotope composition in natural diamonds - First results. *Chem. Erde* **39**, 85-87.
- Watson J. V., Fowler M. B., Plant J. A. and Simpson P. R. (1984) Variscan-Caledonian comparisons: late orogenic granites. *Proc. Ussher Soc.* **6**, 2-12.
- Weiss R. F. (1970) The solubility of nitrogen, oxygen and argon in water and seawater. *Deep Sea Res.* **17**, 721-735.
- Welhan J. A. (1981) Carbon and hydrogen gases in hydrothermal systems: the search for a mantle source. Unpublished PhD thesis, University of California, San Diego, California, USA. 194 pp.
- Welhan J. A. (1987a) Characteristics of abiogenic methane in rocks. In: P. Fritz and S. K. Frape (Editors), *Saline water and gases in crystalline rocks*. Geological Association of Canada Special Paper **33**, pp. 225-233.
- Welhan J. A. (1987b) Stable isotope hydrology. In: T. K. Tyser (Editor), *Stable isotope geochemistry of low temperature processes*. Mineralogical Association of Canada short course handbook, Volume **13**, pp. 129-161.
- Welhan J. A. (1988) Origins of methane in hydrothermal systems. In: M. Schoell (Guest-Editor), *Origins of methane in the Earth*. *Chem. Geol.* **71**, 183-198.
- Whiteley M. J. (1983) The geology of the St Mellion outlier, Cornwall, and its regional setting. Unpublished PhD thesis, University of Exeter, UK. 264 pp. (& maps)
- Wickman F. E. (1956) The cycle of carbon and the stable carbon isotopes. *Geochim. Cosmochim. Acta* **9**, 136-153.
- Willis-Richards J. and Jackson N. J. (1989) Evolution of the Cornubian ore field: Part I. Batholith modelling and ore distribution. *Econ. Geol.* **84**, 1078-1100.

- Wilson G. A. and Eugster H. P. (1990) Cassiterite solubility and tin speciation in supercritical chloride solutions. In: R. J. Spencer and I-Ming Chou (Editors), *Fluid-mineral interactions: A tribute to H. P. Eugster*. Special Publication No. 2 of the Geochemical Society, pp. 179-195.
- Wlowska F. (1961) Untersuchungen zur Geochemie des Stickstoffs. *Geochim. Cosmochim. Acta* **24**, 106-154.
- Wlowska F. (1972) Nitrogen. In: K. H. Wedepohl (Editor), *Handbook of Geochemistry*, sections 7-B to 7-O. Springer-Verlag.
- Wood B. J. (1993) Carbon in the core. *Earth Planet. Sci. Lett.* **117**, 593-607.
- Wopenka B. and Pasteris J. D. (1986) Limitations to quantitative analysis of fluid inclusions in geological samples by laser Raman microprobe spectroscopy. *Appl. Spectroscopy* **40**, 144-151.
- Worth R. Hansford (1953) The physical geography of Dartmoor. In: G. M. Spooner and F. S. Russell (Editors), *Worth's Dartmoor*, pp. 3-46. (Latest edition published in 1968 by David and Charles.) Article compiled posthumously from unpublished manuscript (No. 2) 'On the structure of Dartmoor'.
- Wright I. P., Boyd S. R., Franchi I. A. and Pillinger C. T. (1988) High-precision determination of nitrogen stable isotope ratios at the sub-nanomole level. *J. Phys. E: Sci. Instrum.* **21**, 865-875.
- Wright I. P., Carr R. H. and Pillinger C. T. (1988) Carbon stable isotope analysis of individual deep-sea spherules. *Meteoritics* **23**, 339-348.
- Wright I. P., McNaughton N. J., Fallick A. E., Gardiner L. R. and Pillinger C. T. (1983) A high precision mass spectrometer for stable carbon isotope analysis at the nanogram level. *J. Phys. E: Sci. Instrum.* **16**, 497-504.
- Wright I. P. and Pillinger C. T. (1989) Carbon isotopic analysis of small samples by use of stepped-heating extraction and static mass spectrometry. In: W. C. Shanks III and R. E. Criss (Editors), *New frontiers in stable isotope research: Laser probes, ion probes, and small-sample analysis*. US Geol. Survey Bull. **1890**, 9-34.
- Yamamoto T. and Nakahira M. (1966) Ammonium ions in sericites. *Amer. Mineral.* **51**, 1775-1778.
- Yardley B. W. D., Banks D. A., Bottrell S. H. and Diamond L. W. (1993) Post-metamorphic gold-quartz veins from NW Italy: the composition and origin of the ore fluid. *Min. Mag.* **57**, 407-422.
- Yates P. D. (1992) The content and stable isotopic composition of carbon in spherical micrometeorites. Unpublished PhD thesis, The Open University, UK. 274 pp.
- Yates P. D., Wright I. P. and Pillinger C. T. (1992) Application of high-sensitivity carbon isotope techniques - a question of blanks. *Chem. Geol. (Isotope Geoscience Section)* **101**, 81-91.
- Yates P. D., Wright I. P., Pillinger C. T. and Hutchison R. (1989) Carbon isotopic measurements of deep sea spherules. *Proc. Lunar Planet. Sci. Conf.* **XX**, 1227-1228.
- Zhang D. (1988) Nitrogen concentrations and isotopic compositions of some terrestrial rocks. Unpublished PhD dissertation, University of Chicago, USA. 156 pp.

- Zhang D., Huang F. and Zheng S. (1984) The oxygen, hydrogen and carbon isotope studies of tungsten-bearing granitoids. In: Xu K. and Tu G. (Editors), *Geology of granites and their metallogenetic relations* (Proceedings of the International Symposium held at Nanjing, China, October 1982). Science Press, Beijing, China, pp. 875-890.
- Zhang L., Liu J., Zhou H. and Chen Z. (1989) Oxygen isotope fractionations in the quartz-water-salt system. *Econ. Geol.* **84**, 1643-1650.
- Zhang Y. and Zindler A. (1993) Distribution and evolution of carbon and nitrogen in Earth. *Earth Planet. Sci. Lett.* **117**, 331-345.
- Ziegenbein D. and Johannes N. J. (1980) Graphite in C-H-O fluids: an unsuitable compound to buffer fluid composition at temperatures up to 700°C. *N. Jb. Miner. Abh.* **7**, 289-305.
- Zijderveld J. D. A. (1967) The natural remanent magnetizations of the Exeter volcanic traps (Permian, Europe). *Tectonophysics* **4**, 121-153.
- Zinner E. and Epstein S. (1987) Heavy carbon in individual oxide grains from the Murchison meteorite. *Earth Planet. Sci. Lett.* **84**, 359-368.
- Zinner E., Tang M. and Anders E. (1987) Large isotopic anomalies of Si, C, N and noble gases in interstellar silicon carbide from the Murray meteorite. *Nature* **330**, 730-732.

Addenda

The following section contains a compilation of material that was excluded from the examined thesis in order to keep the total length of the submitted work to within prescribed limits. Inclusion of these addenda herein is by permission of the Research Degrees Committee of the Open University. Addenda I and II refer to the reproducibility of data presented in Chapter 2; Addenda III-VI are compilations of data from which various Figures presented in Chapter 4 were constructed. Addenda VII and IX document laboratory procedures (not devised by the author) as used to obtain experimental data reported in Chapters 5 and 6 respectively. Addenda VIII and XII report analytical data obtained by Dr D M Wayne on samples supplied by the author; these data are reported herein with the permission of Dr Wayne. Addendum IX reports the author's interpretation of data obtained by Dr Wayne. Addendum X was prepared for the author by Dr N J Fortey.

Table of contents

I	Reproducibility of δD analyses, S W England palæo-hydrothermal waters thermally extracted <i>in vacuo</i> from quartz	334
II	Reproducibility of $\delta^{18}O$ analyses, S W England hydrothermal quartz	335
III	Nitrogen equilibrium isotope effects: ^{15}N - ^{14}N fractionation factors	336
IV	The equilibrium speciation of nitrogen in hydrothermal fluids	338
V	Reaction between N_2 and O_2 at 850 and 1150°C: predicted reaction products at thermodynamic equilibrium, 0.01 atm total pressure	339
VI	Reaction between CO_2 and NH_3 : predicted reaction products at thermodynamic equilibrium, for a variety of P,T conditions	340
VII	Experimental procedures adopted for the extraction and chemical analysis of fluid inclusion leachates	342
VIII	Sr and Pb isotopic compositions of fluid inclusion leachates associated with early hydrothermal mineralisation of the Dartmoor granite	351
IX	The time-dependant variation of $^{87}Sr/^{86}Sr$ in Rb-bearing systems: application to the age determination of early hydrothermal fluids hosted by the Dartmoor granite	353
X	Petrographic descriptions of metasedimentary rock samples collected in the vicinity of the Dartmoor granite	355
XI	Analytical procedures used for Rb-Sr analyses of metasedimentary whole-rock samples	359
XII	Pb and U isotopic compositions of metasedimentary rocks sampled in the vicinity of the Dartmoor granite	363

Addendum I

Reproducibility of δD analyses, S W England palæo-hydrothermal waters thermally extracted *in vacuo* from quartz

Sample reference	Sample location	Laboratory (date)	δD (‰ _{SMOW-SLAP})
<i>Examples associated with early hydrothermal mineralisation of the Dartmoor granite</i>			
SW-89-160	Golden Dagger mine	KW (21.06.91)	-23.7
		"	-24.3
SW-89-161	Golden Dagger mine	KW (08.07.91)	-30.4
		"	-29.3
SW-89-162	Golden Dagger mine	KW (18.06.91)	-25.0
		"	-23.6
SW-89-163	Golden Dagger mine	KW (19.06.91)	-33.8
		"	-27.3
		KW (08.07.91)	-31.0
SW-89-154	East Vitifer mine	KW (13.06.91)	-34.5
		"	-31.7
SW-89-155	East Vitifer mine	KW (13.06.91)	-25.9
		"	-22.9
SW-89-156	East Vitifer mine	KW (14.06.91)	-28.1
		"	-26.4
SW-89-157	Great Rock mine	KW (20.06.91)	-30.1
		"	-28.5
<i>Examples associated with early W±Sn oxide assemblages</i>			
HEM-80-44	Hemerdon	GIR (28.10.88)	-30.1
		GIR (25.04.89)	-28.2
CD-88-1	Castle-an-Dinas mine	KW (09.07.91)	-10.8
		KW (09.09.91)	-10.1
		"	-9.4
SW-84-18	Old Gunnislake mine	GIR (11.05.89)	-17.1
		WL (15.01.85)	-15.1
SW-84-27	Prince of Wales mine	GIR (25.04.89)	-12.7
		GIR (11.05.89)	-15.1
		WL (15.01.85)	-16.7
SC-88-3	South Crofty mine	GIR (10.10.88)	-16.4
		"	-18.2

Key to laboratories:

GIR: NERC Isotope Geosciences Laboratory, 64 Gray's Inn Road, London (closed December 1989)

KW: NERC Isotope Geosciences Laboratory, Kingsley Dunham Centre, Keyworth

WL: British Geological Survey, Hydrogeology Division, Wallingford, Oxon.

Addendum II

Reproducibility of $\delta^{18}\text{O}$ analyses, S W England hydrothermal quartz

Sample reference	Sample location	Date of analysis	$\delta^{18}\text{O}$ (‰ _{SMOW})
SW-81-14	Birch Tor & Vitifer	11.11.88	14.03
		11.11.88	14.03
SW-84-15	Drakewalls mine	11.11.88	13.73
		11.11.88	13.61
		19.11.88	13.52
HEM-80-1	Hemerdon mine	15.11.88	14.66
			14.60
OG-88-1	Old Gunnislake mine	19.11.88	9.67
		19.11.88	9.85
CD-88-1	Castle-an-Dinas mine	22.11.88	9.35
		22.11.88	9.57
SW-88-8	South Tamar Consols	09.01.89	15.26
		09.01.89	15.22
SW-84-20	South Bedford mine	11.01.89	12.01
		11.01.89	12.38
SW-88-5	North Hooe mine	09.01.89	22.43
		09.01.89	22.87
		13.01.89	22.84
		13.01.89	23.09
SW-84-17	Wheal Emma mine	18.01.89	14.92
		18.01.89	15.33

All analyses undertaken by the author, at the NERC Isotope Geosciences Laboratory, 64 Gray's Inn Road, London (closed December 1989). $\delta^{18}\text{O}$ values were determined on the basis of the procedure described in Section 2.4.3 of the present work.

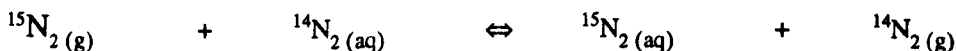
Oxygen isotope raw data were initially related to the PDB standard, then converted to the corresponding values relative to SMOW. Following the standard practice of the NERC Isotope Geosciences Laboratory, the conversion factors recommended by Friedman and O'Neil (1977) were used, rather than the more recent values recommended by Coplen (1988).

Addendum III

Nitrogen equilibrium isotope effects: ^{15}N - ^{14}N fractionation factors

1) Experimental determinations:

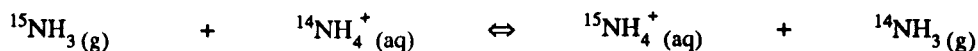
Solution of nitrogen gas:



Enrichment factor ϵ (defined as $10^3\alpha - 1$, where α is the fractionation factor) = 0.85 ± 0.10 for distilled water at 0°C (Klots and Benson, 1963).

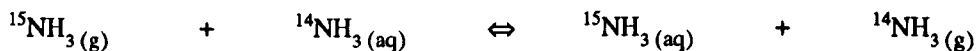
For aerobic seawater (down to about 4400m depth), $\epsilon = +0.13 \pm 0.13\text{‰}$ (Benson and Parker, 1961).

Ammonia volatilization:



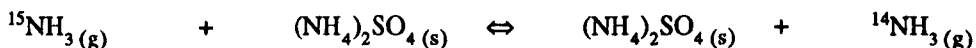
$$\alpha = 1.034 \text{ at } 25^\circ\text{C} \text{ (Kirschenbaum } et al., 1947)$$

Solution of ammonia gas:



$$\alpha = 1.005 \text{ at } 25^\circ\text{C} \text{ (Kirschenbaum } et al., 1947)$$

Ammonia/ammonium sulphate nitrogen exchange:



$\alpha = 1.0143$ at 250°C ; 1.0128 at 350°C (Nitzsche and Stiehl, 1984). The data from these experiments were reported subsequently by Haendel *et al.* (1986).

References:

Benson B. B. and Parker P. D. M. (1961) Nitrogen/argon and nitrogen isotope ratios in aerobic sea water. *Deep-Sea Research* 7, 237-253.

Kirshenbaum I., Smith J. S., Crowell T., Graff J. and McKee R. (1947) Separation of the nitrogen isotopes by the exchange reaction between ammonia and solutions of ammonium nitrate. *J. Chem. Phys.* 15, 440-446.

Klots C. E. and Benson B. B. (1963) Isotope effect in the solution of oxygen and nitrogen in distilled water. *J. Chem. Phys.* 38, 890-893.

2) Equilibrium fractionation factors (α), as a function of temperature, of the following gas phase isotope exchange reactions, as determined theoretically from spectroscopic data:



Urey, 1947:

T (K)	$\alpha(1)$	$\alpha(2)$	$\alpha(3)$
273.1	1.039	1.025	1.013
298.1	1.035	1.023	1.012
400	1.024	1.015	1.008
500	1.017	1.012	1.006
600	1.013	1.010	1.004

Scalan, 1958:

T (K)	$\alpha(1)$	$\alpha(2)$	$\alpha(3)$
273.1	1.0341	1.0182	1.0159
298.1	1.0311	1.0167	1.0143
303.1	1.0292	1.0159	1.0131
400	1.0216	1.0117	1.0099
500	1.0136	1.0069	1.0066
600	1.0104	1.0056	1.0048
800	1.0077	1.0049	1.0028
1000	1.0042	1.0037	1.0005
1200	1.0035	1.0032	1.0008

Hanschmann, 1981:

T (K)	$\alpha(1)$	$\alpha(2)$	$\alpha(3)$
298.16	1.0300	1.0124	1.0174
400	1.0204	1.0064	1.0139
500	1.0150	1.0047	1.0103
600	1.0115	1.0038	1.0077
800	1.0073	1.0023	1.0049
1000	1.0051	1.0022	1.0030

Richet *et al.*, 1977:

T(°C)	$\alpha(3)$
0	1.0115
10	1.0110
20	1.0105
30	1.0101
40	1.0097
50	1.0092
75	1.0083
100	1.0075
125	1.0069
150	1.0061
175	1.0056

T(°C)	$\alpha(3)$
200	1.0051
250	1.0041
300	1.0032
350	1.0026
400	1.0021
450	1.0015
500	1.0011
600	1.0003
700	0.9999
800	0.9994
900	0.9992

Note that Richet *et al.* (1977) tabulated theoretically-determined β factors for nitrogen exchange as a function of temperature; these were used to calculate the fractionation factors presented here.

Physically, the β factor for equilibrated isotopic exchange of element Y is the fractionation factor between $X_m Y_n$ and Y, where $X_m Y_n$ is the compound of interest:

$$\beta = [Y^*/Y^\dagger]_{X_m Y_n} / [Y^*/Y^\dagger] \quad \text{where } Y^* \text{ is the rare isotope and } Y^\dagger \text{ the abundant isotope of element Y.}$$

Addendum IV

The equilibrium speciation of nitrogen in hydrothermal fluids (*as illustrated in Figure 4.3a*)

The relative mole fractions of nitrogen and ammonia under equilibrium conditions, as a function of temperature and initial ($N_2 + NH_3$) mole fraction in the reactant mixture, under isobaric conditions of total pressure 500 or 1000 atm, as predicted by thermodynamic modelling using the computational procedure of Gordon and McBride (1971). Ideal mixing of ideal gases is assumed. (X_i is the mole fraction of component i).

a) Total pressure: 500 atm.

Reactant mixture 1: $X(CH_4) = X(H_2O) = 0.50$; $X(N_2) + X(NH_3) = 0.0002$

Temperature (°C)	$\log_{10}[X(N_2)]$	$\log_{10}[X(NH_3)]$	$\log_{10}[X(N_2)/X(NH_3)]$
300	-3.907	-3.821	-0.086
400	-3.924	-3.801	-0.123
500	-3.936	-3.794	-0.142
600	-3.947	-3.798	-0.149
700	-3.960	-3.809	-0.151

Reactant mixture 2: $X(CH_4) = X(H_2O) = 0.40$; $X(N_2) + X(NH_3) = 0.20$

Temperature (°C)	$\log_{10}[X(N_2)]$	$\log_{10}[X(NH_3)]$	$\log_{10}[X(N_2)/X(NH_3)]$
300	-0.704	-2.418	1.714
400	-0.706	-2.333	1.627
500	-0.711	-2.298	1.587
600	-0.718	-2.287	1.569
700	-0.729	-2.291	1.562

b) Total pressure: 1000 atm.

Reactant mixture 1: $X(CH_4) = X(H_2O) = 0.50$; $X(N_2) + X(NH_3) = 0.0002$

Temperature (°C)	$\log_{10}[X(N_2)]$	$\log_{10}[X(NH_3)]$	$\log_{10}[X(N_2)/X(NH_3)]$
300	-3.969	-3.734	-0.235
400	-3.992	-3.713	-0.279
500	-4.007	-3.705	-0.302
600	-4.019	-3.705	-0.313
700	-4.031	-3.712	-0.319

Reactant mixture 2: $X(CH_4) = X(H_2O) = 0.40$; $X(N_2) + X(NH_3) = 0.20$

Temperature (°C)	$\log_{10}[X(N_2)]$	$\log_{10}[X(NH_3)]$	$\log_{10}[X(N_2)/X(NH_3)]$
300	-0.704	-2.341	1.637
400	-0.707	-2.240	1.533
500	-0.711	-2.190	1.479
600	-0.716	-2.169	1.452
700	-0.724	-2.163	1.439

Addendum V

Equilibrium compositions, as a function of reactant stoichiometry, predicted by thermodynamic modelling using the computational procedures of Gordon and McBride (1971), for initial reactants N_2 and O_2 under isothermal, isobaric conditions. Total pressure: 0.01 atm. (X_i is the mole fraction of component i)

Reaction temperature: 850°C

$10^3 \times (pO_2/pN_2)_{\text{initial}}$	$\log_{10}[X(\text{NO})/X(N_2)]$	$\log_{10}[X(\text{NO}_2)/X(N_2)]$	$\log_{10}[X(N_2O)/X(N_2)]$	$\log_{10}[X(O)/X(N_2)]$
1	-2.044	-4.316	-8.693	-4.357
5	-1.693	-3.966	-8.693	-3.656
10	-1.542	-3.814	-8.694	-3.355
15	-1.453	-3.725	-8.693	-3.175
20	-1.390	-3.662	-8.693	-3.049

Reaction temperature: 1150°C

$10^3 \times (pO_2/pN_2)_{\text{initial}}$	$\log_{10}[X(\text{NO})/X(N_2)]$	$\log_{10}[X(\text{NO}_2)/X(N_2)]$	$\log_{10}[X(N_2O)/X(N_2)]$	$\log_{10}[X(O)/X(N_2)]$
1	-1.150	-3.993	-7.864	-1.859
5	-0.792	-3.634	-7.864	-1.142
10	-0.634	-3.477	-7.864	-0.827
15	-0.541	-3.384	-7.864	-0.640
20	-0.474	-3.317	-7.864	-0.506

The above data were used to construct Figure 4.7

Addendum VI

Predicted equilibrium compositions (mole fractions) of the major products resulting from the reaction between reactants $8\text{NH}_3 + 3\text{CO}_2$ under a range of temperatures and pressures corresponding to crustal environments. The computational procedure of Gordon and McBride (1971) was used for the modelling, adapted for $P > 1$ atm., to incorporate fugacity coefficients (calculated using the equation of state of Holloway, 1981) for all components except ammonia, which was assumed to behave ideally under all conditions.

(These data were used to construct Figure 4.10)

(i) $P = 1$ atm.

Temperature (°C)	$\log_{10}[X(\text{CH}_4)]$	$\log_{10}[X(\text{CO})]$	$\log_{10}[X(\text{CO}_2)]$	$\log_{10}[X(\text{H}_2)]$	$\log_{10}[X(\text{H}_2\text{O})]$
300	-0.6746	-4.4019	-1.8800	-1.2824	-0.3735
400	-0.7515	-2.9282	-1.4494	-0.8384	-0.4491
500	-0.9126	-1.8834	-1.2133	-0.5474	-0.5890
600	-1.2688	-1.2292	-1.2070	-0.3716	-0.7781
700	-2.0547	-0.9670	-1.3566	-0.3015	-0.9013
800	-3.1088	-0.9070	-1.4749	-0.2963	-0.9016
900	-4.0580	-0.8835	-1.5675	-0.3006	-0.8829

Temperature (°C)	$\log_{10}[X(\text{NH}_3)]$	$\log_{10}[X(\text{N}_2)]$	Z
300	-3.3574	-0.5236	1
400	-3.4016	-0.5451	1
500	-3.5139	-0.5818	1
600	-3.6921	-0.6324	1
700	-3.9410	-0.6692	1
800	-4.2126	-0.6760	1
900	-4.4501	-0.6766	1

(ii) $P = 250$ atm.

Temperature (°C)	$\log_{10}[X(\text{CH}_4)]$	$\log_{10}[X(\text{CO})]$	$\log_{10}[X(\text{CO}_2)]$	$\log_{10}[X(\text{H}_2)]$	$\log_{10}[X(\text{H}_2\text{O})]$
300	-0.6426	-6.1620	-2.5670	-2.3036	-0.3416
400	-0.6511	-4.7672	-2.2375	-1.7839	-0.3500
500	-0.6677	-3.6970	-1.9444	-1.4087	-0.3664
600	-0.6959	-2.8664	-1.7113	-1.1257	-0.3934
700	-0.7406	-2.2231	-1.5486	-0.9054	-0.4324
800	-0.8107	-1.7363	-1.4638	-0.7299	-0.4845
900	-0.9191	-1.3851	-1.4578	-0.5897	-0.5494

Temperature (°C)	$\log_{10}[X(\text{NH}_3)]$	$\log_{10}[X(\text{N}_2)]$	Z
300	-2.4072	-0.5153	1.055
400	-2.3464	-0.5182	1.059
500	-2.3282	-0.5234	1.059
600	-2.3323	-0.5317	1.057
700	-2.3496	-0.5440	1.054
800	-2.3760	-0.5616	1.050
900	-2.4121	-0.5848	1.046

(iii) P = 500 atm.

Temperature (°C)	$\log_{10}[X(\text{CH}_4)]$	$\log_{10}[X(\text{CO})]$	$\log_{10}[X(\text{CO}_2)]$	$\log_{10}[X(\text{H}_2)]$	$\log_{10}[X(\text{H}_2\text{O})]$
300	-0.6422	-6.3344	-2.5598	-2.4738	-0.3412
400	-0.6485	-4.9757	-2.2893	-1.9378	-0.3475
500	-0.6607	-3.9254	-2.0290	-1.5505	-0.3596
600	-0.6814	-3.1007	-1.8065	-1.2586	-0.3795
700	-0.7135	-2.4520	-1.6379	-1.0307	-0.4085
800	-0.7625	-1.9490	-1.5323	-0.8476	-0.4474
900	-0.8361	-1.5708	-1.4934	-0.6981	-0.4966

Temperature (°C)	$\log_{10}[X(\text{NH}_3)]$	$\log_{10}[X(\text{N}_2)]$	Z
300	-2.2915	-0.5157	1.151
400	-2.2199	-0.5180	1.143
500	-2.1928	-0.5220	1.134
600	-2.1892	-0.5282	1.124
700	-2.1985	-0.5374	1.115
800	-2.2153	-0.5505	1.106
900	-2.2382	-0.5682	1.097

(iv) P = 1000 atm.

Temperature (°C)	$\log_{10}[X(\text{CH}_4)]$	$\log_{10}[X(\text{CO})]$	$\log_{10}[X(\text{CO}_2)]$	$\log_{10}[X(\text{H}_2)]$	$\log_{10}[X(\text{H}_2\text{O})]$
300	-0.6423	-6.4852	-2.5194	-2.6769	-0.3413
400	-0.6469	-5.1648	-2.3103	-2.1217	-0.3459
500	-0.6557	-4.1442	-2.0957	-1.7177	-0.3546
600	-0.6704	-3.3340	-1.8967	-1.4131	-0.3688
700	-0.6931	-2.6867	-1.7327	-1.1755	-0.3897
800	-0.7268	-2.1744	-1.6161	-0.9840	-0.4180
900	-0.7764	-1.7770	-1.5534	-0.8260	-0.4540

Temperature (°C)	$\log_{10}[X(\text{NH}_3)]$	$\log_{10}[X(\text{N}_2)]$	Z
300	-2.1764	-0.5164	1.397
400	-2.0953	-0.5184	1.348
500	-2.0570	-0.5214	1.310
600	-2.0449	-0.5260	1.278
700	-2.0474	-0.5327	1.251
800	-2.0565	-0.5421	1.227
900	-2.0700	-0.5551	1.207

Notes: (1) The 'compressibility factor' Z ($=PV/nRT$) is a measure of the departure of the system from ideal gas behaviour.

(2) The mole fraction of graphite was $<10^{-25}$ for all P,T conditions considered.

Addendum VII

Experimental procedures adopted for the extraction and chemical analysis of fluid inclusion leachates.

VII. 1 *Declaration of analytical work undertaken by the author*

The preparation of fluid inclusion leachate solutions for investigating the palæofluid chemistry associated with specific paragenetic stages of hydrothermal mineralisation of the Dartmoor granite was undertaken by the author, under the guidance of Dr D A Banks at the Department of Earth Sciences, University of Leeds. Analysis of the leachates for minor cations, using graphite furnace atomic absorption spectrometry (GFAAS), was undertaken by the author. The prepared solutions were subsequently submitted to the Department of Chemistry, University of Leeds, for analysis by inductively-coupled plasma atomic emission spectrometry (ICP-AES) of major and minor cations. Flame emission spectrometry (FES) determinations of the Na and K concentrations in the leachate solutions were made by Dr D A Banks.

Replicate leachate solutions, but with doubly-distilled water (DDW) as the leaching agent rather than acidified lanthanum chloride, were subsequently prepared by Dr D A Banks, who determined the F^- , Cl^- , Br^- , I^- and SO_4^{2-} contents of the leachates by ion chromatography on the author's behalf. FES was used to measure Na concentrations in the same solutions and hence permit the relative abundance of individual halogens and sulphate to be determined with respect to Na. Isotope dilution analyses for Rb and U ionic concentrations, also Sr and Pb isotopic analyses, were undertaken by Dr D M Wayne, also at the Department of Earth Sciences, University of Leeds, using leachate solutions subsequently prepared from 'splits' of the same quartz samples.

A second batch of hydrothermal quartz samples, representative of association with $W \pm Sn$ oxide occurrences in the Cornubian region, was submitted to Dr D A Banks, who performed crush-leach analyses for fluid inclusion electrolyte composition on the author's behalf, using the same analytical procedures as reported herein for the vein quartz samples hosted by the Dartmoor granite.

VII. 2 *Preparation of quartz samples*

An essential requirement of fluid inclusion electrolyte analysis by crush-leach techniques is that no extraneous mineral grains are present whatsoever. The quartz samples used in the present investigation were originally prepared by the author for stable isotope ratio analysis of various palæofluid components. Quartz grain size 0.5-1.0 mm was used throughout. Samples were cleaned of extraneous material by hand-picking individual grains with the aid of a binocular microscope, followed by purification in boiling 6M HCl. The use of halogenated alkane 'heavy liquid' separation for the initial preparation of quartz concentrates was avoided throughout. For fluid inclusion leachate preparation, further purification of the quartz was undertaken by Dr D A Banks, based on the recommendations of Bottrell *et al.* (1988). These included boiling the quartz grains in concentrated HNO_3 (quartz-distilled), followed by electrolytic cleaning for 2-3 weeks to strip the quartz surfaces of adsorbed ions.

VII. 3 *Sample extraction procedure*

All work was undertaken in a purpose-built 'clean' laboratory. Quartz samples were crushed and leached in a laminar flow fume cupboard, with standard precautions taken against the ingress of contamination. All water used in the experimental procedures was doubly-distilled in silica glass stills.

For each of a batch of 15 samples, approximately 2g of quartz grains were finely crushed (dry) with an agate pestle and mortar and the resulting powder transferred into a screw-topped PTFE centrifuge tube (volume 30ml). 10ml of leaching solution, consisting of either (a) DDW or (b) 0.13M HNO₃ containing 200µg/ml La³⁺ (as LaCl₃), depending on the elements to be analysed, was added to each tube, which was subsequently sealed and shaken vigorously two or three times over a 15 minute period (approximately). After being allowed to stand for 5 minutes, the tubes were spun at 5000 rpm in a centrifuge for 10 minutes. The solutions were then decanted through a Buchner-type vacuum funnel, with the reduced pressure being provided by a hand pump (allowing a fine degree of control). A glass sinter in the funnel tube was overlain by a 0.45µm Whatman® membrane filter (cellulose nitrate); this was pre-washed with leaching solution (~5ml) then DDW (~10ml) prior to filtering of the sample solution. Filtered solutions were collected for storing in 10ml Savalex® beakers. At the end of each filtration, the membrane filter was replaced and the funnel thoroughly rinsed, first with 5-10ml of leachate solution and then with DDW.

For the batch of Dartmoor granite-hosted quartz samples (8) crushed and leached by the author for fluid inclusion cation analysis, three were prepared in duplicate (SW-89-161, SW-89-162 and SW-89-164 respectively) and the samples interspersed at regular intervals with a quartz 'blank' (gem quality, inclusion-free Brazil quartz). Four such 'blanks' were prepared, for this batch.

A further two quartz samples associated with mineralisation of the Dartmoor granite (SW-89-157 and SW-89-160) were visibly contaminated by intergrowths of hæmatite, in the case of the former sample, and orthoclase in the case of the latter. These samples were therefore excluded from that batch and analysed at a later stage (but not for As, Bi or Be) by Dr D A Banks on behalf of the author, after respective treatments with boiling HNO₃ (to minimise hæmatite contamination) and H₂SiF₆ at ambient temperature overnight, to remove orthoclase (both samples).

VII. 4 *Instrumentation and associated detection limits*

VII. 4.1 *FES and GFAAS:*

A Varian® Spectra AA-10 atomic absorption spectrometer was used (in conjunction with a GTA-96 graphite furnace in the case of GFAAS measurements). The detection limit for Na was ~10ppb. GFAAS was used for the determination of Cu, Bi, Pb, As, and Be; the approximate detection limits were 2, 2, 1, 0.3 and 0.05 ppb respectively.

VII. 4.2 *ICP-AES:*

An ARL 3580-B instrument was used for the analyses. The detection limits, as measured using acidified LaCl₃ leaching solution, are given in Table VII-A.

VII. 4.3 *Ion chromatography:*

DDW was used as the leaching solution. A Dionex® 4500i instrument was used for anion analyses (halogens and sulphate) in the leachates. The system incorporated post-column suppression, a 50µl sample loop volume, and an electrical conductivity detector linked directly to an Intel® 386-based Elonex® computer, running AI-450 data acquisition software. With the exception of iodide analyses, a PAX-100 column was used, in conjunction with a CG-1 guard column.

For iodide measurements, the retention time would be ~25 minutes under these conditions. This was shortened to ~3.5 minutes (thereby increasing the magnitude of the associated peaks and hence improving measurement capabilities) by using a trace anion concentrator (2ml solution used) and removing the PAX-100 column; anion separation was thus effected by the CG-1 guard column.

In both cases, the eluant used was DDW containing NaHCO₃ and Na₂CO₃ (both 3.2mM) and methanol (to a total concentration of 5%). Detection limits of the Dionex® system were: F⁻ ~5ppb, Cl⁻ ~10ppb, Br⁻ ~0.5ppb, I⁻ ~0.1ppb and SO₄²⁻ ~2ppb.

VII. 5 *Procedural blanks*

VII. 5.1 *ICP-AES measurements:*

Table VII-B gives the results of element blank concentrations (ppb in leachate solutions) associated with inclusion-free quartz leachates; also element blanks associated with the leaching solution (200ppm La³⁺ as LaCl₃ in 0.13M HNO₃). The inclusion-free quartz was included in the batch of Dartmoor granite-hosted samples prepared by the author. Note that for some elements, negative values were obtained; this is because the corresponding regression line used for calibration did not pass through zero. This is particularly apparent for the aluminium data. Also, the sensitivity of the ICP-AES method for aluminium analysis is relatively low.

VII. 5.2 *GFAAS measurements:*

For trace cations as measured using GFAAS, the following procedural blank values were obtained by the author, from leaching inclusion-free quartz: As~5ppb, Bi~2ppb, Cu~2ppb, Pb~1ppb, Be<0.1ppb. A 20µl injection was used for each analysis.

VII. 5.3 *Ion chromatography measurements:*

Anion procedural blanks, as recorded using the Dionex® system, were: F⁻ ~10ppb, Cl⁻ ~250ppb, SO₄²⁻ ~30ppb; Br⁻ and I⁻ were not detected. Data obtained by Dr D A Banks.

VII. 6 *Analysis of reference synthetic fluid inclusions for Cl, Br and I concentrations:*

Quartz samples containing synthetic fluid inclusions, supplied by the Centre de Recherches sur la Géologie de l'Uranium (CREGU) at Nancy, France, were used to verify the analytical procedures adopted for the determination of fluid inclusion halogen ion ratios. The results of the analyses, together with the corresponding 'true' values, are presented in Table VII-C. The data were obtained by Dr D A Banks.

VII.7 *Raw analytical data, Dartmoor mineralising fluid inclusion leachates:*

The results of ICP-AES analysis of cations and boron (determined as borate) concentrations in fluid inclusion leachate solutions (acidified LaCl_3 used as the leaching solution) are presented in Table VII-D. Minor cation concentrations, as measured using GFAAS, are reported in Table VII-E. The results of anion (halogen and sulphate) analysis of leachates prepared from separate 'splits' of the same quartz samples are shown in Table VII-F.

Table VII- A

Detection limits (at the 3σ level), as measured using ICP-AES on acidified LaCl₃ leaching solution:

Element	Concentration (ppb)	Element	Concentration (ppb)
Li	2	Ba	2
Na	19	B	4
K	146	Al	17
Mg	0.1	Mn	0.5
Ca(1)	7	Fe	3
Ca(2)	0.4	Cu	3
Sr	11	Zn	5

- Notes: (i) The two calcium values refer to different spectral lines.
(ii) The LaCl₃ spike solution used for these determinations was subsequently discovered to have been more concentrated by a factor of 10x than intended; the actual limits of detection were thus probably better than the values quoted here.
(iii) The relatively poor value for Sr probably reflects interference by La and/or a high Sr blank, rather than low sensitivity of the instrumentation, for which the Sr detection limit is ~ 0.1ppb.

Table VII- B

Element blank concentrations (ppb in leachate solutions) associated with inclusion-free quartz 'leachates' and also of the leaching solution (200ppm La³⁺ as LaCl₃ in 0.13M HNO₃), determined using ICP-AES:

	Li	Na	K	Mg	Ca ₍₁₎	Ca ₍₂₎	Sr	Ba	B	Al	Mn	Fe	Cu	Zn
Leachates of inclusion-free quartz: element blanks (ppb), uncorrected for leaching solution blanks:														
(1)	-3	25	36	3	31	52	46	-3	3	-111	-12	-21	-51	-21
(2)	0	24	38	5	72	91	44	-3	9	-108	-11	-14	-51	-23
(3)	-1	55	41	4	99	109	48	-2	12	-104	-10	-12	-51	-17
(4)	-2	20	45	1	32	51	41	-2	5	-119	-11	-18	-52	-22
<i>Mean:</i>	-2	31	40	3	58	76	45	-2	7	-110	-11	-16	-51	-21
Leaching solution (acidified LaCl ₃) element blanks (ppb):														
(1)	-5	2	13	-1	-32	-14	44	-2	6	-132	-12	-26	-50	-24
(2)	-5	-16	-20	-2	-38	-15	52	-3	2	-143	-12	-28	-51	-24
<i>Mean:</i>	-5	-7	-4	-2	-35	-15	48	-3	4	-136	-12	-27	-51	-24
Leachates of inclusion-free quartz: mean blanks (ppb), corrected for leaching solution blanks:														
<i>Blank (ppb):</i>	3	38	44	5	94	91	-3	1	3	26	1	11	0	3

Table VII-C

Anion analyses of synthetic fluid inclusions, as measured in the same laboratory and using the same experimental procedures as adopted for the present study of palæo-hydrothermal fluids

(D A Banks, unpublished data)

Sample		Concentration in leachate solution (ppb)			Weight ratio		Mole ratio	
		Cl	Br	I	Br/Cl	I/Cl	Br/Cl	I/Cl
47	As analysed:	17007	274	148	0.0161	0.0087	0.0071	0.0024
	'True' value:	-	-	-	0.0163	0.0120	0.0072	0.0034
48	As analysed:	4701	31	5.2	0.0066	0.0011	0.0029	0.0003
	'True' value:	-	-	-	0.0071	0.0011	0.0032	0.0003
	Detection limit:	10	0.5	0.1	-	-	-	-

Table VII-D

Cation (and boron as borate) concentrations (ppb) in fluid inclusion leachate solutions, Dartmoor granite-associated hydrothermal quartz, as determined using ICP-AES.
Data corrected for procedural blanks.

Locality (mine) :	Golden Dagger		Barracott	East Vitifer		Golden Dagger		East Vitifer	Golden Dagger	Great Rock			
Paragenetic stage :	I		II	II	II	II (III)	II (III)	Stage III (II)	Stage III	Stage III			
Sample reference :	SW-89-159	SW-89-160	SW-89-164	SW-89-155	SW-89-156	SW-89-162	SW-89-163	SW-89-154	SW-89-161	SW-89-157			
Li	110	26	45	66	141	92	146	133	64	83	9	15	8
Na	27,690	10,278	12,810	18,670	35,610	27,650	17,640	16,060	18,190	12,250	357	512	1,752
K	6,200	2,468	2,419	3,608	6,658	6,419	2,746	2,518	3,843	2,382	(153)	(186)	370
Ca	12,144	4,538	5,032	7,593	14,654	10,954	7,132	6,430	10,154	5,022	459	703	1,130
Mg	65	29	52	64	91	55	63	57	178	71	52	73	13
Sr	222	83	94	138	258	198	119	107	165	84	11	15	9
Ba	62	24	35	52	75	75	22	23	39	26	4	7	10
B	496	206	169	212	490	388	448	410	660	220	5	12	11
Al	538	208	199	282	441	297	457	436	630	414	177	312	196
Mn	1,606	208	776	1,179	1,765	1,385	785	686	1,213	573	(12)	(24)	222
Fe	2826	1062	587	881	3,020	2,848	876	747	1,760	1,130	(8)	(22)	390
Cu	13	6	4	9	19	23	21	19	35	34	(22)	(31)	2
Zn	320	122	163	234	350	257	155	140	258	114	(7)	(5)	34

Notes: (1) Analytical results in parentheses are of relatively low precision.

(2) Quartz samples SW-89-157 and SW-89-160 were treated with fluorosilicic acid (H_2SiF_6) in an attempt to remove feldspar. Residual feldspar in SW-89-157 probably responsible for anomalously high Al, Ca and Mg values.

(3) The predominant paragenetic stage is given in all cases. In some cases, secondary veining by later stage fluids will be of significance; for these samples, the minor stage is indicated in parentheses.

(4) Duplicate analyses of Sample SW-89-161 gave very low ion yields. Consequently, multiplication factors required to express elemental yields as a ratio to Na (on a weight or molar basis) would be very large and thus be likely to incorporate significant errors.

Table VII-E

Trace cation concentrations (ppb) in fluid inclusion leachate solutions, Dartmoor granite-associated hydrothermal quartz, as determined using GFAAS

Sample	Cu	Pb	As	Bi	Be
Barracott mine					
SW-89-164	4	37	20	<1	0.44
<i>duplicate</i>	9	56	23	<1	0.43
East Vitifer mine					
SW-89-155	20	(95)	50	1.4	0.57
SW-89-156	21	61	38	1.5	0.42
SW-89-154	25	30	30	1.6	0.67
Golden Dagger mine					
SW-89-159	13	(97)	70	1.5	0.66
SW-89-162	19	35	46	nd	2.46
<i>duplicate</i>	17	33	40	nd	2.10
SW-89-163	27	(99)	48	1.8	1.34
SW-89-161	22	nd	7	nd	1.42
<i>duplicate</i>	29	nd	20	1.5	2.52

- Notes: (i) All data corrected for procedural blanks.
(ii) Numbers in parentheses are extrapolations beyond calibration curves.
(iii) nd indicates *not detected*.
(iv) Analytical errors are in the region of ~5 to 10%, except for As, where the errors may be significantly greater.

Table VII-F

Fluid inclusion leachates from hydrothermal quartz associated with early mineralisation of the Dartmoor granite: anion concentrations (ppb), corrected for procedural blanks. Na⁺ concentrations (ppb), determined on the same leachates using FES, are reported for comparison. (Analyses undertaken on the author's behalf by Dr D A Banks at the University of Leeds.)

Sample	Na ⁺	Cl ⁻	F ⁻	Br ⁻	I ⁻	SO ₄ ²⁻
Barracott mine						
SW-89-164	5,300	13,209	-	23	-	71
		12,771	-	-	1.14	-
<i>duplicate</i>	12,000	30,063	-	-	1.61	-
		2,598*	39* (451)	4* (46)	-	-
East Vitifer mine						
SW-89-155	12,610	30,996	-	55	-	158
		31,191	-	-	2.59	175
<i>duplicate</i>	11,320	27,829	-	-	4.76	-
		6,451*	155* (669)	13* (56)	-	-
SW-89-156	10,000	25,218	-	47	-	51
		25,420	-	-	0.52	76
<i>duplicate</i>	11,050	27,879	-	-	1.92	-
		8,705*	82* (263)	15* (48)	-	-
SW-89-154	8,750	20,793	-	35	-	58
		20,561	-	-	0.79	73
<i>duplicate</i>	10,100	24,095	-	-	0.74	-
		2,502*	74* (713)	4* (39)	-	-
Golden Dagger mine						
SW-89-159	10,800	27,797	-	51	-	86
		28,290	-	-	2.06	137
<i>duplicate</i>	11,020	28,443	-	-	5.04	-
		7,388*	144* (554)	13* (50)	-	-
SW-89-160	14,400	36,119	-	57	4.0	336
SW-89-162	5,850	12,856	-	19	-	25
		12,556	-	-	1.08	31
<i>duplicate</i>	8,150	17,935	-	-	0.99	-
		2,579*	53* (369)	-	-	-
SW-89-163	7,550	20,727	-	40	-	80
		20,584	-	-	0.61	102
<i>duplicate</i>	9,050	24,929	-	-	1.40	-
		4,289*	73* (424)	9* (52)	-	-
SW-89-161	450	1,346	-	2	-	23 (?)
		284*	-	-	-	48* (227)
<i>duplicate</i>	1,000	3,111	-	-	0.18	-
		1,184*	22* (58)	-	-	-
Great Rock mine						
SW-89-157	3,550	8,857	na	16	0.3	-

Notes: (i) Values marked by an asterisk indicate a dilution of the leachate solution referred to in the immediately preceding row. In these cases, element concentrations in the undiluted leachates, as calculated from applying the appropriate dilution factor (given by the ratio of the corresponding sodium concentrations) are given in parentheses.

(ii) Samples SW-89-157 and SW-89-160 were treated with fluorosilicic acid.

Addendum VIII

a) Rb-Sr data obtained from fluid inclusion leachate analysis of early hydrothermal vein quartz hosted by the Dartmoor granite

(Data produced by Dr D M Wayne at the University of Leeds, using samples supplied by the author)

Sample	Rb (ppb)	Sr (ppb)	$^{87}\text{Rb}/^{86}\text{Sr}$	$^{87}\text{Sr}/^{86}\text{Sr}$	$^{87}\text{Sr}/^{86}\text{Sr}$ @ 280Ma
<i>Golden Dagger mine - pegmatitic quartz</i>					
SW-89-159	112	197	1.64	0.71884 (6)	0.7123
SW-89-160 (C)	30	50	1.74	0.71936 (4)	0.7124
<i>Golden Dagger mine - Stage II</i>					
SW-89-162 (A)	56	101	1.60	0.71927 (6)	0.7129
SW-89-162 (B)	46	84	1.59	0.71924 (7)	0.7129
SW-89-162 (C)	28	50	1.67	0.71928 (12)	0.7126
SW-89-163	59	121	1.40	0.71968 (5)	0.7141
<i>Barracott mine - Stage II</i>					
SW-89-164 (B)	61	126	1.41	0.71814 (6)	0.7125
SW-89-164 (C)	26	50	1.61	0.71816 (18)	0.7118
<i>East Vitifer mine - Stage II</i>					
SW-89-155 (A)	93	258*	-	0.71948 (3)	-
SW-89-155 (C)	27	49	1.62	0.71956 (4)	0.7131
SW-89-156	109	183	1.72	0.71935 (5)	0.7125
<i>East Vitifer mine - Stage III</i>					
SW-89-154 (A)	37	84*	-	0.71870 (3)	-
SW-89-154 (C)	47	85	1.61	0.71877 (7)	0.7123
<i>Golden Dagger mine - Stage III</i>					
SW-89-161 (A)	1	6	0.67	0.71619 (10)	0.7135
<i>Great Rock mine - Stage III</i>					
SW-89-157 (C)	11	23	1.33	0.71668 (10)	0.7114

Notes: (i) An asterisk (*) denotes that the Sr concentration was determined by ICP-AES. All other Sr concentration data were obtained by isotope dilution.

(ii) All sample splits denoted by a 'C' suffix were leached in La-free 0.13M HNO₃; others were La spiked (200 ppm), as recommended by Bottrell *et al.* (1988).

(iii) Stages II and III refer to the paragenetic classification by Scrivener (1982).

b) The isotopic composition of Pb and U in fluid inclusion leachates of early hydrothermal vein quartz hosted by the Dartmoor granite.
(Data produced by Dr D M Wayne at the University of Leeds, using samples supplied by the author.)

Sample	Pb (ppb)	U (ppb)	²⁰⁶ Pb/ ²⁰⁴ Pb	²⁰⁷ Pb/ ²⁰⁴ Pb	²⁰⁸ Pb/ ²⁰⁴ Pb	²³⁸ U/ ²⁰⁴ Pb	²⁰⁶ Pb/ ²⁰⁴ Pb @ 280 Ma	²⁰⁷ Pb/ ²⁰⁴ Pb @ 280 Ma
<i>Golden Dagger mine, pegmatitic quartz</i>								
SW-89-159	72	12.4	18.902 (17)	15.681 (18)	38.552 (61)	11.0	18.41	15.66
SW-89-160 (A)	28	-	18.615 (21)	15.673 (20)	38.444 (91)	-	-	-
SW-89-160 (C)	18	1.6	18.485 (13)	15.667 (17)	38.399 (50)	5.6	18.24	15.65
<i>Golden Dagger mine - Stage II</i>								
SW-89-162 (B)	24	3.8	18.577 (31)	15.632 (28)	38.220 (110)	10.1	18.13	15.61
SW-89-162 (C)	15	1.7	18.514 (13)	15.682 (16)	38.426 (51)	7.0	18.21	15.67
SW-89-163	60	4.6	18.629 (14)	15.646 (16)	38.381 (61)	4.9	18.41	15.63
<i>Barracott mine - Stage II</i>								
SW-89-164 (A)	38	0.7	18.310 (14)	15.637 (16)	38.326 (71)	1.2	18.26	15.63
SW-89-164 (B)	47	0.5	18.324 (16)	15.642 (17)	38.340 (67)	0.6	18.30	15.61
SW-89-164 (C)	21	nd	18.317 (12)	15.638 (16)	38.325 (50)	-	-	-
<i>East Vitifer mine - Stage II</i>								
SW-89-155 (A)	73	2.0	18.349 (13)	15.636 (16)	38.330 (57)	1.7	18.27	15.63
SW-89-155 (C)	30	0.9	18.361 (12)	15.646 (15)	38.356 (50)	1.9	18.28	15.64
SW-89-156	61	7.7	18.545 (16)	15.668 (17)	38.392 (62)	8.0	18.19	15.65
<i>East Vitifer mine - Stage III</i>								
SW-89-154 (A)	33	1.6	18.553 (17)	15.642 (18)	38.349 (80)	3.2	18.41	15.63
SW-89-154 (C)	16	0.6	18.437 (14)	15.657 (16)	38.320 (53)	2.6	18.32	15.65
<i>Great Rock mine - Stage III</i>								
SW-89-157 (A)	8	nd	18.381 (32)	15.665 (19)	38.596 (243)	-	-	-
SW-89-157 (C)	16	nd	18.303 (13)	15.630 (16)	38.309 (52)	-	-	-

Notes: The large range of ²⁰⁸Pb/²⁰⁴Pb recorded from sample SW-89-157 is in part due to the relatively large blank correction on SW-89-157(A); the result from sample SW-89-157(C) is probably more representative. nd indicates not detected.

All sample splits denoted by a 'C' suffix were leached in La-free 0.13M HNO₃; others were La spiked (200 ppm), as recommended by Bottrell *et al.* (1988).

Addendum IX

The time-dependant variation of $^{87}\text{Sr}/^{86}\text{Sr}$ in Rb-bearing systems: application to the age determination of early hydrothermal fluids hosted by the Dartmoor granite

In system closed to loss or gain of strontium or rubidium, increase in the $^{87}\text{Sr}/^{86}\text{Sr}$ ratio since closure of the system is attributable solely to the decay of ^{87}Rb . The decay constant $\lambda = 1.42 \times 10^{-11} \text{ a}^{-1}$ (Steiger and Jäger, 1977). In terms of present-day $^{87}\text{Sr}/^{86}\text{Sr}$ and $^{87}\text{Rb}/^{86}\text{Sr}$ ratios, the $^{87}\text{Sr}/^{86}\text{Sr}$ value at time t before present is given by

$$(^{87}\text{Sr}/^{86}\text{Sr})_t = (^{87}\text{Sr}/^{86}\text{Sr})_p - (^{87}\text{Rb}/^{86}\text{Sr})_p(e^{\lambda t} - 1)$$

where the p subscript refers to the present-day ratios. Using this equation, palaeofluid data given in Addendum VIII[†] and the whole-rock Rb-Sr data set (fourteen samples) of Darbyshire and Shepherd (1985) for the Dartmoor granite were used to construct the $^{87}\text{Sr}/^{86}\text{Sr}$ evolution curves shown in Figure IX-A. Assuming that the strontium in the fluids was derived exclusively from the granite, Figure IX-A permits age limits of the hydrothermal system to be estimated, on the basis of the time at which the $^{87}\text{Sr}/^{86}\text{Sr}$ value of the granite coincided with that of the fluids. The age corresponding to individual intersection points between the palaeofluid curves and those of the granite whole-rock samples may be calculated from:

$$t' = \frac{1}{\lambda} \log_e \left[\frac{(^{87}\text{Sr}/^{86}\text{Sr})_{p,\text{granite}} - (^{87}\text{Sr}/^{86}\text{Sr})_{p,\text{fluid}}}{(^{87}\text{Rb}/^{86}\text{Sr})_{p,\text{granite}} - (^{87}\text{Rb}/^{86}\text{Sr})_{p,\text{fluid}}} + 1 \right]$$

By taking the data in entirety, the age of the fluids is poorly constrained to between *ca.* 246 and 279Ma before present. It is, however, apparent from Figure IX-A(a) that if the (eight) poorly-megacrystic Dartmoor granite samples of Darbyshire and Shepherd (1985) are more representative of that pluton than the coarsely-megacrystic examples, for present purposes, the age limits of the associated early hydrothermal systems are much more tightly constrained, to *ca.* 273-279Ma. The corresponding mean is 276.6Ma ($2\sigma = 2.7\text{Ma}$). This latter value is in accord with a ^{40}Ar - ^{39}Ar (total gas) age of 277.2 ($2\sigma = 1.0\text{Ma}$) for early mineralisation hosted by the Dartmoor granite, as reported by Chesley *et al.* (1993) for biotite from a fine-grained biotite-granite dyke.

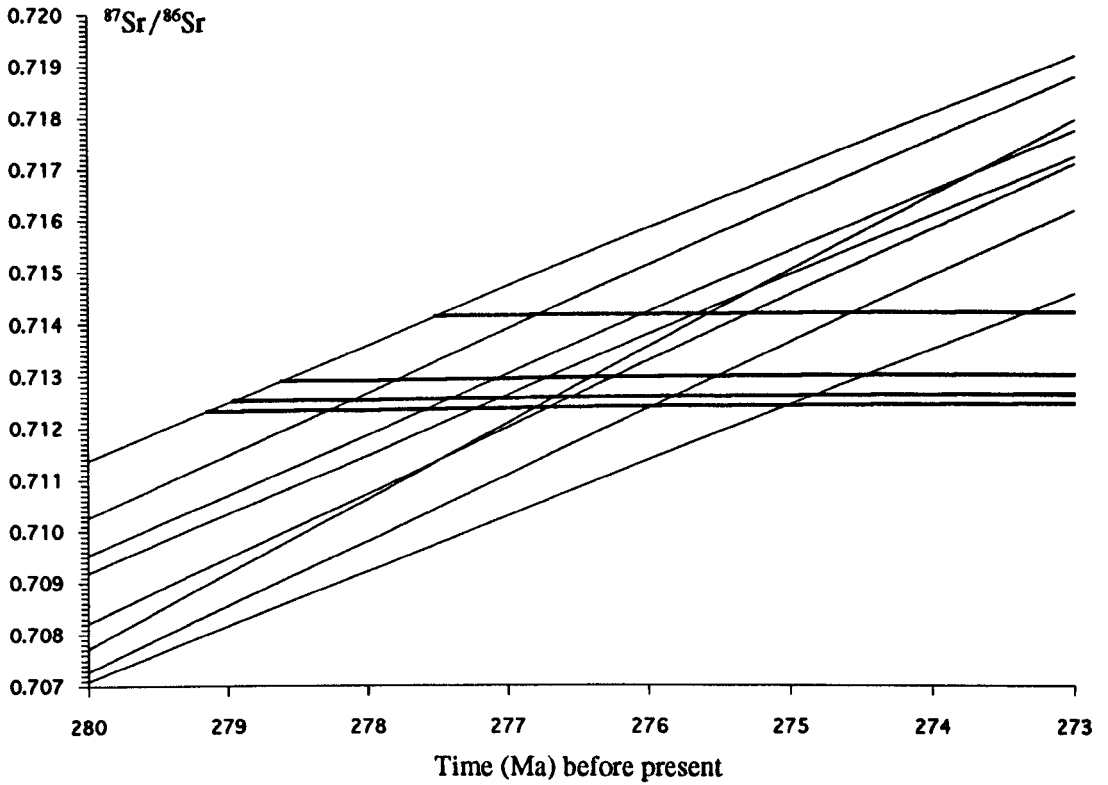
Conversely, if the set of (six) coarsely-megacrystic Dartmoor granite whole-rock samples of Darbyshire and Shepherd (1985) are used to constrain the palaeofluid age estimate (Figure IX-A(b)), the corresponding mean age is 258.6Ma, with 2σ error of 9.6Ma.

[†] With reference to Addendum VIII, only quartz samples leached using 0.13M HNO_3 spiked with 200ppm La^{3+} (as LaCl_3) are considered here; those leached with La-free acid invariably gave lower Sr yields. Furthermore, sample SW-89-161 is also excluded, on the basis of anomalously low concentrations of electrolytes in the inclusion fluids (see Chapter 5).

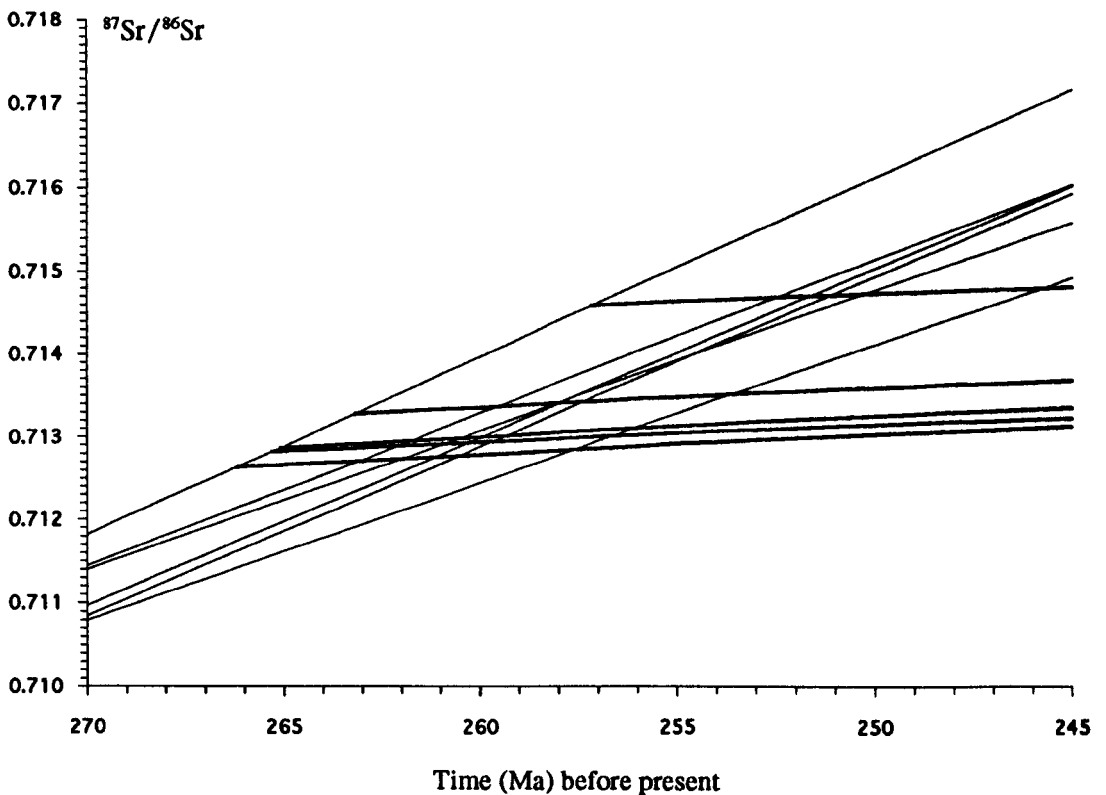
Figure IX-A

$^{87}\text{Sr}/^{86}\text{Sr}$ evolution in early hydrothermal fluids hosted by the Dartmoor granite:
comparison with the granite whole-rock samples of Darbyshire and Shepherd (1985).
(*Bold curves refer to the fluids*)

(a) Comparison with poorly-megacrystic Dartmoor granite samples



(b) Comparison with coarsely-megacrystic Dartmoor granite samples



Addendum X

Petrographic descriptions of metasedimentary rock samples collected in the vicinity of the Dartmoor granite.

The following notes were compiled for the present author by Dr N J Fortey of the British Geological Survey, following his petrographic examination, in transmitted light, of supplied thin sections of two suites of slaty metasedimentary rocks sampled across the thermal aureole of the Dartmoor granite. Details of the sample locations are given in Appendix A. The samples are listed in order of increasing distance from the granite contact, in each case. (Note that samples SW-87-S7 and SW-87-S8 were located virtually equidistant from the contact; sample SW-87-S13 was probably located closer, although this was difficult to assess with certainty.)

Upper Devonian metasediments from an area south-west of the Dartmoor granite

SW-87-S13

Retrogressive chlorite-sericite alteration of a schistose hornfels, very similar to sample SW-87-8 (see below).

SW-87-S7

Contact metamorphism of a pelitic rock has resulted in a foliated (schistose) hornfels consisting largely of muscovite, biotite and quartz with porphyroblasts of muscovite, andalusite and possibly K-feldspar. Minute prisms of yellow schorl are common, and microgranules of opaque mineral/s and likely rutile are ubiquitous. Retrogressive hydrothermal alteration has resulted in chloritisation of biotite and andalusite, and also sericitic alteration of muscovite and likely feldspar.

SW-87-S8

Schistose semi-pelitic hornfels with a strongly foliated fabric of muscovite grains is accompanied by relict silt-grade quartz and a few conformable minute quartz lenses. Fine-grained prograde biotite is also present, but no tourmaline was located. Retrogressive hydrothermal alteration has caused chloritisation of biotite and sericitic alteration of once abundant porphyroblasts of possible andalusite and cordierite. Also, films of iron oxide material along grain boundaries indicate either late hæmatitic alteration or, more probably, penetrative weathering during Permian redbed conditions penecontemporaneous with emplacement of the granite.

SW-87-S9

Metamorphism of a weakly-banded silty mudstone has resulted in development of a strongly foliated (lepidoblastic) bedding-parallel fabric composed of very fine-grained muscovite and quartz overgrown by non-oriented micro-porphyroblasts of biotite. Minute granules of opaque mineral/s and likely rutile are very common. A hairline veinlet of chlorite cuts the foliation at about 90°.

SW-87-S10

Much of the fabric of this metamorphosed mudstone is a very fine grained, poorly foliated mat of white mica, chlorite and quartz. This fabric is patchily interwoven with areas of strongly foliated (lepidoblastic) fabric composed of muscovite and quartz accompanied by very fine grained biotite flakes. The rock carries slender veinlets and lenses of quartz micro-mosaic (with rare pyrite cubes, now goethite-altered) developed sub-parallel with the foliated fabric possibly on syn-metamorphic shears. These pre-date a quartz-chlorite veinlet which cuts about perpendicular to the fabric, and is accompanied by areas of chloritisation of the host rock.

SW-87-S11

Mudstone converted in metamorphism to a lepidoblastic muscovite fabric, with probable minor quartz and abundant overgrowing fine-grained biotite. Minute granules of opaque mineral/s and likely rutile are common throughout. Penetrative iron staining has picked out numerous mm-scale patches rich in very fine-grained quartz and white mica, in which regularly spaced parallel films of iron oxide suggest relict cleavage preserved in altered former porphyroblasts of uncertain identity. Quartz veinlets occur at a high angle to the foliation and quartz lenses occupy minute gashes sub-parallel to the foliation. It is interesting to note deflexion of the muscovite fabric around the relict porphyroblasts, indicating that the schistose fabric is a product of the contact metamorphism rather than a regional fabric that has been inherited and overgrown. Contact metamorphism is not just a static process of recrystallisation. This sample appears to be the last in this sequence in which metamorphic biotite was located, and so lies close to the biotite isograd of the Dartmoor contact aureole.

SW-87-S12

A massive, very fine-grained silty mudstone, carrying a pervasive schistose fabric composed of tenuous muscovite laminæ separated by slender lithons of quartz-muscovite-chlorite, some of which preserve an early fabric lying at a high angle to the prevalent fabric. Chlorite forms minute lenses within the dominant fabric. The rock is crossed by a slender veinlet at a high angle to the main fabric of quartz; traces of chlorite and grains of possible topaz or apatite.

SW-87-S6

Massive silty mudstone similar to SW-87-12 (above) in which muscovite laminæ separated by slender lithons of unfoliated rock define a strong schistose fabric.

SW-87-S5

Mudstone in which very fine-scale sedimentary lamination is strongly contorted with development of a closely-spaced crenulation fabric on which schistose laminæ of new white mica have begun to grow. The crenulation fabric is also highlighted by films of dark, possibly organic, residue. A bedding parallel fabric is preserved in the lithons between the crenulation planes.

SW-87-S4

Massive mudstone in which trails of minute quartz grains indicate bedding. A pronounced bedding white mica foliation is crossed at about 30° (in the thin section) by a metamorphic fabric in which white mica laminæ 10-20 microns thick are separated by layer 30-50 microns thick of undisturbed material. (The mica laminæ display simultaneous optical extinction at an acutely oblique orientation to the laminæ, which indicates the mica flakes within the laminæ are oriented at this acute angle to the plane of the laminæ.)

SW-87-S3

Homogeneous mudstone, much darkened by a pervasive opaque pigmentation of probably organic material; lacks metamorphic features but is intersected by an interconnecting network of replacement veinlets of pale (?) quartz-illite alteration of hydrothermal origin.

SW-87-S2

In this mudstone, the fine-scale sedimentary silty laminæ have been contorted into a crenulated fabric on which a strong oblique crenulation cleavage has developed. The cleavage takes the form of dense packets of pressure-solution films of dark residue separated by slender lithons of mudstone in which the relict bedding-parallel fabric is preserved. In comparison with SW-87-5, this sample is marked by the absence of new mica growth along the crenulation fabric. This raises the question of the origin of the fabric: does it increase in development towards the granite (*i.e.* is it of contact origin), or is the change part of the underlying pattern of regional metamorphism?

SW-87-S1

Massive mudstone in which a strong pressure solution cleavage is seen as parallel films of opaque residue. The opaque laminæ tend to occur in dense packets about 20 microns thick, separated by laminæ of host mudstone 20-40 microns thick; a pattern reminiscent of the fabric in SW-87-2.

Carboniferous metasediments (Crackington Formation) from north-east of the Dartmoor granite

SW-87-S14

Interbedded mudstone and fine-grained sandstone: the former component contains ovoid, mm-scale patches of muscovite-quartz-goethite which suggest iron staining of proto-porphyroblasts of possible cordierite. The host mudstone carries a subtle fabric due to foliated alignment of white-mica flakes. An additional schistose fabric composed of closely-spaced, locally coalescing white mica laminæ picked out by iron staining is developed in the mudstone component.

SW-87-S15

Mudstone in which contact metamorphism has produced a strong foliation in the abundant white mica, which is overgrown by disoriented biotite flakes, and is accompanied by porphyroblasts of andalusite with iron-stained rims. The rock is cut at a high angle to the foliation by undeformed veinlets of quartz and chlorite.

SW-87-S16

Massive silty mudstone with little bedding visible at the thin section level, except for a weak fabric which displays microcrenulations related to the strong pressure-solution cleavage which is expressed principally by closely-spaced planar films of goethitic material.

SW-87-S17

Semi-pelitic andalusite and biotite-bearing hornfels has undergone strong regressive hydrothermal muscovite-chlorite alteration.

SW-87-S18

This massive silty mudstone is darkened by abundant organic matter. Where the pigmentation is weakest, the rock is seen to be quartz rich, but not apparently rich in mica or clays.

SW-87-S19

Thinly-bedded sandy mudstone, darkened by organic matter. An oblique, weak, spaced pressure-solution cleavage is present.

Discussion

- (1) Despite the enormous bulk of the adjacent granite pluton, it appears that contact metamorphism has not developed extensive high-grade hornfels. Although andalusite and possibly cordierite were formed, and fine grained biotite is abundant close to the granite, there is evidence of extensive retrogressive chloritic overprinting. This can be interpreted as encroachment by convective migration of heated fluids before coarse hornfels had time to develop fully.
- (2) Rocks from sites remote from the granite display strong crenulation and pressure-solution cleavage fabrics. Presumably, these belong to the pattern of regional deformation and very low grade (sub-greenschist) metamorphism.
- (3) Lepidoblastic or schistose foliations seen in several samples from sites within the biotite isograd may well have developed during the contact metamorphism. This may merely be mimetic intensification of pre-existing bedding or regional metamorphic fabrics, but it raises the question of whether granite emplacement entailed significant deformation and development of new fabrics.

Addendum XI

Analytical procedures used for Rb-Sr analyses of metasedimentary whole-rock samples

X.1 Rb and Sr concentrations

Rb and Sr concentrations, together with Rb/Sr atomic ratios, were determined by X-ray fluorescence analysis, using a Philips® PW1450 automated spectrometer. 20g pellets were prepared for these analyses from -200 mesh rock powder mixed with 2ml of Mowiol® solution (aqueous polyvinyl alcohol) and pressed at 7 tonnes for 1 minute. Both sides of the powder pellets were measured (except in the case of sample SW-87S-18, where visible contamination on one side was noted) and the average taken. The batch of samples included international reference standards and appropriate corrections were made for instrumental dead time, background and line interferences, following the recommendations of Pankhurst and O'Nions (1973). Errors on the Rb/Sr atomic ratios were generally $\pm 0.5\%$ at the 1σ level; the data are given in full in Table XI-A. In contrast, the Rb and Sr concentrations were determined from the molybdenum Compton scatter peak (Pankhurst and O'Nions, 1973); the associated error is about $\pm 5\%$ (1σ).

From the Rb/Sr atomic ratio, the corresponding $^{87}\text{Rb}/^{86}\text{Sr}$ isotopic ratio may be obtained by multiplying by a factor comprising the isotopic abundance of ^{87}Rb as a proportion of the atomic weight of this element (which, in turn, depends on the isotopic composition and is therefore sample dependant), then dividing the result by the corresponding value for ^{86}Sr (see *e.g.* Faure, 1986). The following algorithm relates the $^{87}\text{Rb}/^{86}\text{Sr}$ and Rb/Sr data reported in the present work, in terms of the $^{87}\text{Sr}/^{86}\text{Sr}$ as measured by mass spectrometry:

$$^{87}\text{Rb}/^{86}\text{Sr} = (2.6218 + (0.283 \times (^{87}\text{Sr}/^{86}\text{Sr}))) \times \text{Rb/Sr}$$

X.2 Sr isotopic composition

Preparation of strontium for isotopic composition was undertaken following total dissolution of 0.2g of whole-rock powder in 10ml HF and 2ml HNO₃. After evaporation to dryness on a hot block at $\sim 60^\circ\text{C}$, another 2ml HNO₃ was added and the solution similarly evaporated to dryness. The residue was then converted to chloride by the addition of 10ml of 6M HCl, before evaporation to dryness. After dissolution of the residue in 3ml of 2.5M HCl, the resulting solution was centrifuged to remove any particulate matter; 1ml was then transferred to a Dowex® -X8 cation exchange column. Following elution of the column with 28ml of 2.5M HCl, Sr was then obtained (as the chloride) by elution with a further 12ml of 2.5M HCl. This fraction was then evaporated to dryness and stored until required.

The hydrochloric acid was quartz-distilled; others were Merck® 'Suprapur' reagents. All chemical procedures were undertaken in a purpose-built 'clean' laboratory, with laminar flow of filtered air; the usual precautions against ingress of contamination were followed. For isotopic analysis, the Sr chloride residue was dissolved in a small quantity of water, for loading (~2µl) onto single tantalum filaments, together with (immediately after) a drop of 7% phosphoric acid. $^{87}\text{Sr}/^{86}\text{Sr}$ ratios were determined to six decimal places, using a VG® 354 thermal ionisation multi-collector mass spectrometer.

To correct for the variable amount of mass-dependant fractionation that occurs during the volatilisation of strontium from the mass spectrometer filament, a fractionation factor for each analysis was determined from a comparison of the measured ratio of two stable isotopes, ^{86}Sr to ^{88}Sr , to a standard value of 0.1194. This fractionation factor was then applied to the measured $^{87}\text{Sr}/^{86}\text{Sr}$ ratio.

During the period of this study, two batches of samples were analysed for Sr isotopic composition; one each during July and November 1989 respectively. The second batch of samples comprised all (three) Devonian metasediment samples prepared from borehole drill core material obtained from localities to the west of the St Austell granite, together with six samples of Kate Brook Slate from a traverse across the thermal aureole of the Dartmoor granite (samples SW-87-S1 to SW-87-S5, together with SW-87-S7 respectively). All other samples (14 in total) were analysed in the earlier batch. The average $^{87}\text{Sr}/^{86}\text{Sr}$ ratio, determined on 10 analyses of the international standard NBS 987 during the earlier period, was 0.710248 ± 23 ppm (1σ); during the second period, a similar number of analyses gave a value of 0.7102238 ± 46 ppm (1σ).

X.3 Data analysis - regression procedure

For a suite of igneous whole-rock or mineral samples of the same age, and which have remained closed with respect to gain or loss of Sr or Rb since emplacement, linear regression procedures of $^{87}\text{Sr}/^{86}\text{Sr}$ against $^{87}\text{Rb}/^{86}\text{Sr}$ may be used to determine the age of emplacement (from the slope of the regression 'isochron'); the corresponding $^{87}\text{Sr}/^{86}\text{Sr}$ (initial) ratio is given by the intercept ($^{87}\text{Rb}/^{86}\text{Sr}$ ratio = 0). Similar procedures have also been applied, with varying degrees of success, to the dating of metamorphic events in mudrocks. To examine the feasibility of obtaining geochronological information from the metasedimentary examples studied during the present investigation, these regression procedures were applied to the respective data sets relating to samples collected across the thermal metamorphic aureole of the Dartmoor granite.

The regression lines were calculated using a York-Williamson least-squares fit (York, 1969), incorporating errors assigned to both axes and with the mean square of weighted deviates (MSWD) describing the measure of fit of the data points (Brookes *et al.*, 1972). The error assigned to the $^{87}\text{Sr}/^{86}\text{Sr}$ data was 0.01% (1σ); the corresponding assignment for the $^{87}\text{Rb}/^{86}\text{Sr}$ ratios was 0.5% (1σ). The value of the ^{87}Rb decay constant used in the calculations was as recommended by the IUGS Subcommittee for Geochronology (Steiger and Jäger, 1977), *i. e.* $1.42 \times 10^{-11} \text{a}^{-1}$. When the MSWD value is less than a limiting value (2 in the case of modern, high precision analyses - Harland *et al.*, 1990; 3 in earlier data sets), the data scatter can be accounted for entirely by random analytical errors and it is conventional to describe the plot as an isochron. Where the MSWD value exceeds the limiting value, the resulting plot is termed an 'errorchron'; such plots can convey useful information, although the data must be interpreted with due caution. In such cases (as in the examples presented in this work), the errors on the age and initial $^{87}\text{Sr}/^{86}\text{Sr}$ ratio have been 'enhanced' by multiplying them by the square root of the MSWD, even though the geological factors responsible for the degree of scatter probably cannot be described by a Gaussian distribution. 'Enhanced' errors are those which would have been obtained if the analytical errors had been large enough to mask precisely the errors due to geological scatter at the 95% confidence level.

References

- Brookes C., Hart S. R. and Wendt I. (1972) Realistic use of two error regression treatment as applied to rubidium-strontium data. *Rev. Geophys. Space Phys.* **10**, 551-557.
- Pankhurst R. J. and O'Nions R. K. (1973) Determination of Rb/Sr and $^{87}\text{Sr}/^{86}\text{Sr}$ ratios of some standard rocks and evaluation of X-ray fluorescence spectrometry in Rb-Sr geochemistry. *Chem. Geol.* **12**, 127-136.
- York D. (1969) Least squares fitting of a straight line with correlated errors. *Earth Planet. Sci. Lett.* **5**, 320-324.

Table XI-A

Averages of X-ray fluorescence analyses of Rb and Sr in metasedimentary rock samples from
S W England

Sample	Rb _(average)	Sr _(average)	Rb/Sr ₍₁₎	Rb/Sr ₍₂₎	Rb/Sr _(average)	$\sigma_{(1)}$ %	$\sigma_{(2)}$ %	$\sigma_{(average)}$ %
SW-87-S1	4.77	120.63	0.04162	0.03954	0.04058	3.43	3.61	3.52
SW-87-S2	169.26	53.77	3.23152	3.22327	3.22740	0.52	0.52	0.52
SW-87-S3	184.27	187.50	1.00643	1.00870	1.00756	0.35	0.35	0.35
SW-87-S4	202.52	40.64	5.09355	5.12567	5.10961	0.61	0.61	0.61
SW-87-S5	251.89	62.26	4.15777	4.13768	4.14773	0.49	0.50	0.50
SW-87-S6	207.73	101.56	2.09647	2.09733	2.09690	0.41	0.41	0.41
SW-87-S7	210.95	108.12	1.99969	2.00094	2.00031	0.41	0.41	0.41
SW-87-S8	212.69	99.64	2.19827	2.17892	2.18859	0.41	0.41	0.41
SW-87-S9	199.91	71.25	2.88159	2.87143	2.87651	0.47	0.47	0.47
SW-87-S10	234.55	96.62	2.49299	2.48454	2.48877	0.42	0.42	0.42
SW-87-S11	232.74	95.92	2.48245	2.49250	2.48747	0.42	0.42	0.42
GSP1	251.15	227.94	1.12830	1.13095	1.12963	0.34	0.34	0.34
SW-87-S12	264.03	55.63	4.85057	4.88082	4.86569	0.52	0.52	0.52
SW-87-S13	351.92	35.39	10.30838	10.08555	10.19697	0.67	0.67	0.67
SW-87-S14	341.53	46.35	7.53374	7.57585	7.55480	0.56	0.55	0.55
SW-87-S15	287.35	76.08	3.88552	3.85856	3.87204	0.45	0.45	0.45
SW-87-S16	247.29	82.50	3.07991	3.06594	3.07293	0.44	0.44	0.44
G2	165.90	467.84	0.36309	0.36402	0.36355	0.34	0.34	0.34
SW-87-S17	273.22	49.02	5.72530	5.70414	5.71472	0.56	0.56	0.56
SW-87-S18	112.06	254.67	0.45006	0.45219	0.45112	0.39	0.39	0.39
SW-87-S19	142.55	53.34	2.74621	2.73355	2.73988	0.53	0.53	0.53
HF1	209.28	68.32	3.13192	3.14883	3.14038	0.48	0.48	0.48
HF2	118.11	188.72	0.64304	0.64028	0.64166	0.43	0.43	0.43
HF3	234.95	224.24	1.07798	1.07034	1.07416	0.35	0.35	0.35

Notes: (1) Rb_(average) and Sr_(average) values are in ppm by weight

(2) GSP1 and G2 are international calibration standards, supplied by the US Geological Survey

(3) The internal standard (to correct for instrumental drift) was P450 phonolite:

Rb = 2.436 µg/g, Sr = 1.706 µg/g, Rb/Sr = 1.428

(4) A Philips® PW 1450 machine was used for the measurements

Addendum XII

Whole-rock Pb and U isotopic data obtained from examples of metasedimentary rocks sampled in the vicinity of the Dartmoor granite

(Data produced by Dr D M Wayne at the University of Leeds, using samples supplied by the author)

Sample	Pb (ppm)	U (ppm)	$^{206}\text{Pb}/^{204}\text{Pb}$	$^{207}\text{Pb}/^{204}\text{Pb}$	$^{208}\text{Pb}/^{204}\text{Pb}$	$^{238}\text{U}/^{204}\text{Pb}$	$^{206}\text{Pb}/^{204}\text{Pb}$ @ 280Ma	$^{207}\text{Pb}/^{204}\text{Pb}$ @ 280Ma	$^{208}\text{Pb}/^{204}\text{Pb}$ @ 280Ma
<i>Upper Devonian metasediments (Kate Brook slate) from south-west of the Dartmoor granite</i>									
SW-87-S10	11.7	2.3	19.239 (20)	15.703 (15)	39.916 (81)	4.9	18.41	15.63	39.09
SW-87-S13	18.5	2.3	18.647 (19)	15.561 (15)	38.873 (78)	10.1	18.13	15.61	38.36
<i>Carboniferous (Crackington formation) metasediment from north-east of the Dartmoor granite</i>									
SW-87-S17	14.3	2.1	18.878 (19)	15.691 (15)	38.988 (78)	7.0	18.21	15.67	38.37

Notes: (i) All isotope ratios were corrected for procedural blanks and mass fractionation.

(ii) $^{206}\text{Pb}/^{204}\text{Pb}$ @ 280Ma and $^{207}\text{Pb}/^{204}\text{Pb}$ @ 280Ma data were corrected for *in situ* decay of U over the same period.

(iii) $^{208}\text{Pb}/^{204}\text{Pb}$ @ 280Ma data were corrected for *in situ* decay of ^{232}Th , based on an estimated Th concentration of 12ppm (the value of the North American Shale Composite).